Transfer of Alkyl Groups in Novel Amidine Dications and other Superelectrophiles

A thesis submitted to the University of Strathclyde in part fulfilment of regulations for the degree of Doctor of Philosophy in Chemistry

by

Luka Stefan Kovacevic

Department of Pure and Applied Chemistry,
University of Strathclyde, Thomas Graham Building,
295 Cathedral Street, G11XL Glasgow, UK

2014

This thesis is the result of the author's original research except where otherwise stated. It has been composed by the author and has not been previously submitted for examination which has led to the award of a degree.

Signed: 

Date: 31.01.14

Acknowledgments

First and foremost I want to express my utmost gratitude to my supervisor Prof John A. Murphy not only for his guidance and patience through all my work but also for promoting my personal skills and development and encouraging me to take on responsibilities. To my group co-workers, past and current, I pay tribute for making our lab and office such a vibrant and joyful place to work. The presence of and the interaction with each of you was always colourful, sometimes bubbly and now and then energetic. It is an experience I wouldn't like to miss.

Special thanks I owe to Craig Irving, who did not only spent hours on helping me with the low-temperature and kinetic NMR studies, but also impressed me by the high standards by which he runs the NMR facilities.

I sincerely thank Dr Alan Kennedy for obtaining crystallographic data from my compounds, for which the sensitivity of the crystals demanded the best of his skills and Dr Tell Tuttle, Dr Chris Idziak and Greg Anderson for computational calculations on my substrates.

For your constant patience, support, care, encouragment and love I feel the deepest appreciation. Jasmin, you are wonderful!

Hugs and kisses for Mom, Dad and my brother Mark who have always wanted the best for me and supported me in every way.

Lastly I want to thank all the people, that made my stay in Scotland one of the most interesting, precious and memorable periods of my life.

Abstract

This thesis explores the synthesis and the reactivity of novel amidine salts resulting from various *N*-methylformamides and *N*-methylbenzamides **I** and **II**.

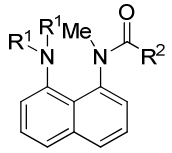

I

R^1 = Alkyl
R^2 = H, Ph

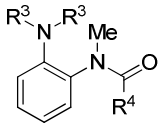

II

R^3 = Alkyl, Aryl
R^4 = H, Ph

Treatment of these compounds with triflic anhydride under mild conditions led to extremely facile alkyl transfer from an sp^3-hybridised nitrogen centre to very weakly nucleophilic triflate anions. For the reaction pathway of substrates **III** and **VII**, *in silico* studies propose an equilibrium between the more stable tetrahedral triflate intermediate **IV** and the superelectrophilic amidinium disalt **V** from which dealkylation takes place. The unprecedented α-aminotriflate **IV** was characterised by low-temperature ^{1}H- and ^{13}C-NMR spectra and the rate of alkyl transfer for substrates **III** and **VII** determined.

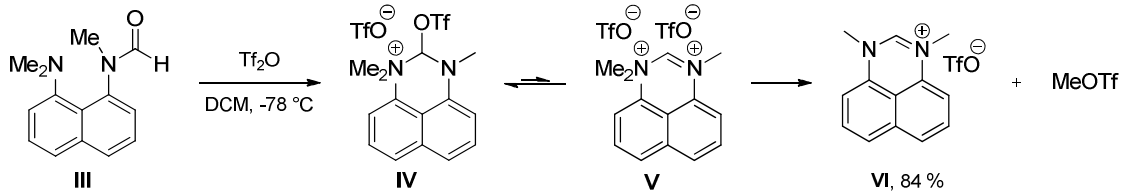

III **IV** **V** **VI**, 84 %

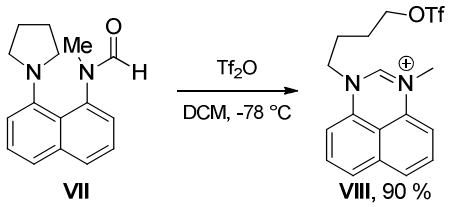

VII **VIII**, 90 %

Unlike formamides **III** and **VII**, *in silico* and low-temperature NMR studies of the reaction of benzamide **IX** with triflic anhydride showed amidinium disalt intermediate **XI** to be more stable than tetrahedral triflate **X** due to steric factors.

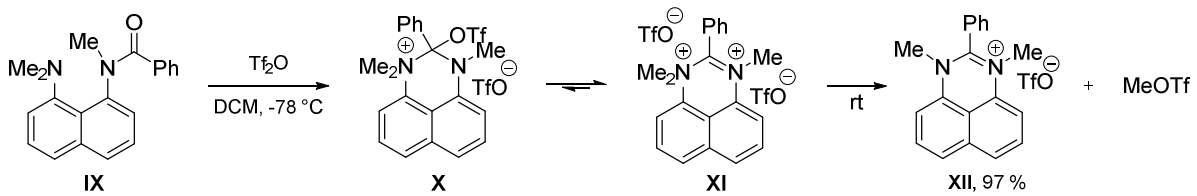

IX **X** **XI** **XII**, 97 %

Due to the enhanced alkyl transfer activity of amidinium disalt **XV** derived from benzene-based formamide **XIII**, low temperature NMR studies did not allow for observation of intermediates **XIV** or **XV**. However, the benzamide analogue **XVII** with phenyl residues on the tertiary amine allowed for isolation and characterisation of amidinium dication **XVIII**.

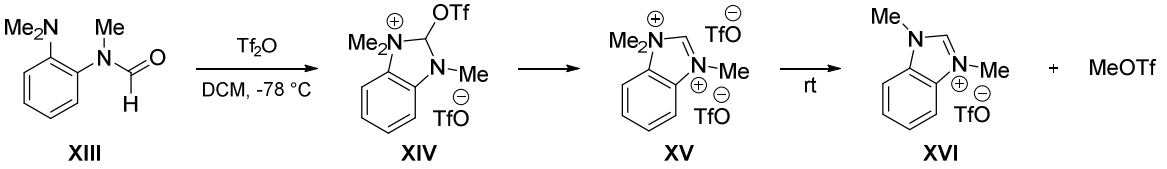

XIII **XIV** **XV** **XVI**

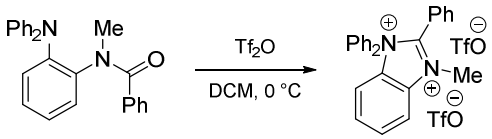

XVII **XVIII**, 82 %

The reaction protocol was subsequently applied to derivatives of 2-(alkylthio)phenylformamides **XIX** which underwent alkyl transfer to yield benzothiazolium salt **XXII**. Interestingly, benzamide analogue **XXIII** afforded benzthiazolium disalt **XXIV** upon addition of triflic anhydride, but gradually dephenylated to monocation **XXV**.

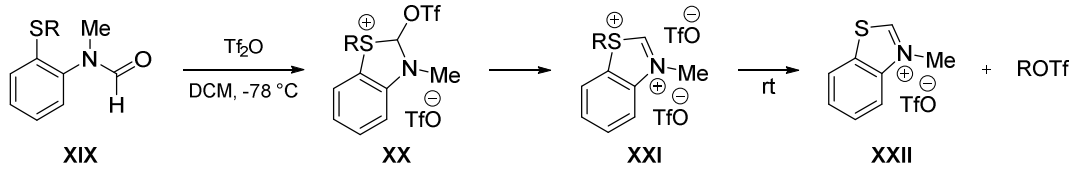

XIX
R = alkyl,
allyl, benzyl

XX **XXI** **XXII**

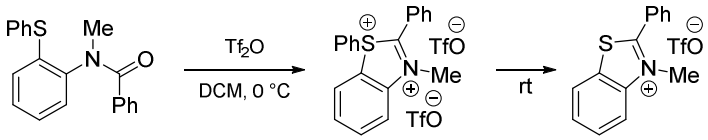

XXIII **XXIV**, 82 % **XXV**, 61 %

Abbreviations

A	Adenine
Ac	Acetyl
ACC	1-Aminocyclopropanecarboxylic acid
ACP	Acyl carrier protein
Acp^3U	3-(3-amino-3-carboxypropyl)uridine
Alk	Alkyl
aq.	Aqueous
Ar	Aryl
$ASAP^+$	Atmospheric solids analysis probe
Asp	Aspartic acid
ATP	Adenosine triphosphate
ATR	Attenuated total reflectance
avg	Average
Bn	Benzyl
bp	Boiling point
calcd	calculated
CAN	Cerium(IV) ammonium nitrate
CFA	Cyclopropane fatty acid
c-*hex*	Cyclohexyl
CI	Chemical ionisation
Clpy	chloropyridine
Cl_2py	dichloropyridine
cm	Centimetre(s)
COT	Cyclooctatetraene
Cys	Cysteine
DAPA	7,8- diaminopelargonic acid
DCM	Dichloromethane
DEAD	Diethyl azodicarboxylate
Decomp.	Decomposition
DFT	Density functional theory
DMA	Dimethylacetamide
DMAP	Dimethylaminopyridine
DMF	Dimethylformamide

DMSO	Dimethyl sulfoxide
e.g.	*Exempli gratia*
EIP^+	Electron ionisation positive mode
EPR	Electron paramagnetic resonance
EtOAc	Ethyl acetate
eq.	Equivalents
ESI	Electrospray ionisation
Et	Ethyl
GC	Gas chromatography
gem	geminal
Glu	Glutamic acid
iPr	Isopropyl
h	Hours
H_0	Hammett acidity
Hcy	Homocysteine
hex.	Hexane
His	Histidine
Hmd	N^5,N^{10}-methenyltetrahydromethanopterin hydrogenase
HRMS	High resolution mass spectrometry
i.e.	*Id est*
IM	Intermediate
IR	Infrared
ism	Isomer
J	Joule
k	Kilo
KAPA	7-Keto-8-aminopelargonic acid
LDA	Lithium diisopropylamide
LRMS	Low resolution mass spectrometry
LUMO	Lowest unoccupied molecular orbital
M	Molar (mol/L) or metal
m	Metre(s)
m.p.	Melting point
Me	Methyl
Met	Metal or methionine (depending on context)

min	Minute(s)
mL	Millilitre
mmol	Millimole(s)
MO	Molecular orbital
MS	Mass spectrometry
NMR	Nuclear magnetic resonance
NSI	Nanospray ionisation
oQ	Epoxyqueuosine
Pet ether	Petroleum Ether (40-60 °C)
ppm	Parts per million
Ph	Phenyl
Pv	Pivaloyl
py	Pyridine
rds	Rate-determining step
RNA	Ribonucleic acid
r.t.	Room temperature
SAM	*S*-adenosylmethionine
SAH	*S*-adenosylhomocysteine
sat.	Saturated
Ser	Serine
SM	Starting material
Sol	Solution
Std	Standard
tert	tertiary
TFA	Trifluoroacetic acid
THF	Tetrahydrofolate or tetrahydrofuran (depending on context)
TLC	Thin layer chromatography
Tp	Trispyrazolylborate
tRNA	Transfer ribonucleic acid
tol	Toluene
TS	Transition state
UV	Ultra-violet
vs.	Versus
Vis	Visible

Contents

1 Introduction

The novel work presented within this thesis covers different areas and aspects of organic chemistry including the generation of highly electrophilic species through reaction of amides with triflic anhydride. These electrophiles are excellent alkylating agents. The following introduction provides not only an overview of the achievements reported prior to this work, but also selected examples that connect the different sections of the research presented in this thesis in order to obtain an overall picture.

1.1 The concept of superelectrophiles

Although research on carbocations has had a long history and associated terms such as nucleophiles and electrophiles had been defined by Ingold[1] in the late 1920s, it was almost 50 years later that Olah expanded[2] the existing concepts by introduction of superelectrophiles, which would account for the unprecedented reactivity of some exceptionally electron-deficient systems. Superelectrophiles were defined as a class of multiply-charged electron-deficient compounds. Olah divided these superelectrophiles into two classes, namely the distonic dications, which have their charged centres separated by two or more carbon or heteroatoms and generally show the same reactivity as their monocationic counterparts. The gitonic superelectrophiles, however, have their charge-bearing centres in close proximity and distinction can be drawn between gitonic geminal superelectrophiles with multiple charges on the same atom, gitonic vicinal superelectrophiles, where the charged centres are direct neighbours and gitonic 1,3-superelectrophiles including one formally neutral carbon or heteroatom between the charged centres.[3]

The chemistry of superelectrophiles has always been inseparably connected to superacids, which were first referred to, when Conant[4,5] found perchloric acid $HClO_4$ to readily protonate the oxygen atom in carbonyl compounds and afford salts in non-aqueous solvents. Superacids have been shown to react with the n-electrons in *e.g.* carbonyl groups or the π-electrons in alkenes, arenes and alkynes, and even with σ-electrons of some alkanes as will be described shortly. A more elaborate and widely accepted description of superacids was given by Gillespie[6] and applies to Brønsted acids that are stronger than 100 % sulfuric acid ($H_0 \leq -12$). Equally, Lewis acids belong to the category of superacids, if they are stronger than anhydrous aluminium chloride, $AlCl_3$, according to Olah.[7] Chemists in the field of superacids and superelectrophiles usually refer to acid strength by the Hammett acidity function H_0, as the study of superelectrophiles and superacid-catalysed reactions

requires concentrated conditions for which the pH scale is not valid any more due to its simple approximations. The Hammett acidity function H_0 avoids the presence of water in its equation and hence eliminates the limiting effect of water. Due to this fact, the Hammett acidity function is not only valid for very strong and concentrated acids, but also extends the acidity range beyond the pH scale. Now, H_0 is usually equal to pH in aqueous dilute solutions as the predominant species is H_3O^+, however with changing concentrations the acid species can change as well. In the case of sulfuric acid, at high concentrations the predominant species is $H_3SO_4^+$, which is a much stronger acid than H_3O^+. Hence, H_0 = -12 for pure sulfuric acid does not stand for the concentration of H_3O^+, which would imply an impossible H_3O^+ concentration of 10^{12} mol/L in ideal solution, but rather describes the acidic strength of the active species $H_3SO_4^+$ as a fictional H_3O^+ concentration equivalent.

Although pure sulfuric acid H_2SO_4 (H_0 = -12) and oleum H_2SO_4-SO_3 (H_0 = -14.5) are deemed superacids, their use for synthetic applications involving superacid catalysis is only sparse, as they themselves are not inert to the superacidic conditions and can lead to sulfonation or oxidation of the intermediates.[8] More commonly used superacids are, for example, magic acid (FSO_3H-SbF_5), which can, depending on the stoichiometry of Brønsted acid to Lewis acid, reach acidities from H_0 = -12 to -27, with the latter number for a 9:1 mixture of Brønsted to Lewis acid. Superacids are media of low nucleophilicity and have allowed the study of long-lived highly electrophilic systems such as carbocations, acyl and carboxonium ions and other onium cations, including oxonium, sulfonium, azonium ions etc.

In pursuit of highly electron-deficient systems, chemists have simultaneously been referring to “non-coordinating” solvents or anions, a terminology that was first criticised by Rosenthal and later replaced by “weakly coordinating” by Olah as anions are by definition electron donors.[3,9] From the early beginning of superacid chemistry conjugate bases of superacids have been used as weakly coordinating anions, which would delocalise the negative charge over the entire anion structure. Later on, chemists started looking into more exotic anions, generally bearing hydrogens or fluorides on the structure’s outer sphere. Typical weakly coordinating anions are the tetrahedral tetrafluoroborate BF_4^- or the octahedral hexafluoroantimonate SbF_6^-, being the conjugate bases of the superacids HF-BF_3 and HF-SbF_5, respectively, but recently more complex anionic borate structures have been reported.[10,11] The latter notation HF-BF_3 and HF-SbF_5 instead of HBF_4 and $HSbF_6$, respectively, illustrates what superacids most often consist of. The strong Lewis acid BF_3 ionises the strong Brønsted acid HF making the acidic proton even more electrophilic. The “naked proton” which is not obtainable in solution is, according to Olah, the limiting case, for which an acidity between H_0 = -50 and -60 has been estimated. This concept of ionisation has also been used

to generate and study a number of carbocation electrophiles. Scheme 1.1 depicts ionisation of alkyl fluorides **1.1** by antimony pentafluoride.[3]

Scheme 1.1 The Lewis acid SbF_5 polarises and abstracts fluoride from alkyl fluorides to create carbocations.

Although Kiffen and Brouwer were the first to report[12-14] hydride transfer from isobutane to the acetyl cation under superacidic conditions, it was Olah who realised that an unprecedented mechanism for the reaction was in play. Based on his own studies, in which this kind of hydride transfer from alkanes was not seen when treated with acetyl salts in aprotic media, he proposed[2] protosolvated superelectrophile **1.5**, which must have formed upon the reaction between the n-electrons of acetyl cation **1.4** and superacid HF-BF_3. This superelectrophile was believed to be powerful enough to react with isobutane **1.6** and form complex **1.7** enabling the hydride transfer *via* a 2-electron-3-centre (2e3c) configuration.

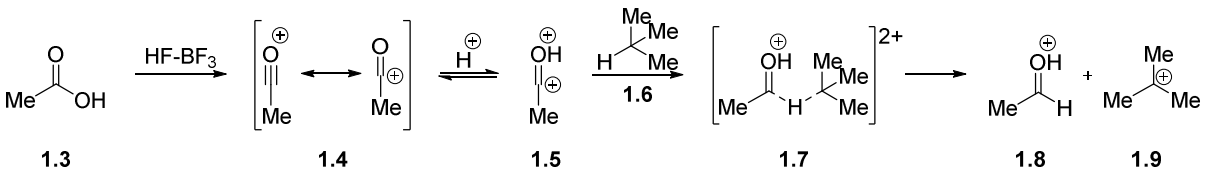

Scheme 1.2 Olah's findings about the superelectrophilic activation of acetyl cation to **1.5** formed in superacids paved the way for the world of superelectrophiles.[2]

Dicationic structure **1.5** might however be the limiting case. An alternative hydrogen bonded intermediate as seen in **1.10** might also account for the proposed transformation (Scheme 1.3).

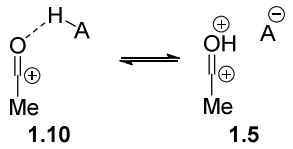

Scheme 1.3 Dicationic structure **1.5** might be the limiting case of superacid-bonded structure **1.10**.

It was after this finding that Olah introduced a new class of electrophiles, which account for the extraordinary reactivity of such multiply charged systems.

Due to the electrostatic repulsion between the charged centres in gitonic superelectrophiles, the species are rarely stable and undergo rapid rearrangements. For instance, 2,4-dichloro-2,4-

dimethylpentane **1.11** is believed to form a 1,3-dication **1.12**, which spontaneously releases a proton to minimise the electrostatic repulsion.

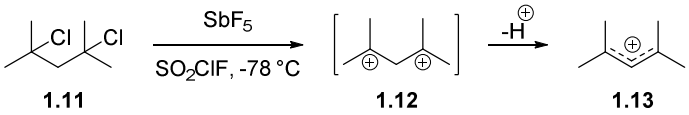

Scheme 1.4 Superelectrophiles are rarely stable species due to electrostatic repulsion and they usually undergo fast rearrangements such as loss of a proton in this gitonic 1,3-superelectrophile.

Many superelectrophiles are impossible to characterise spectroscopically, either because they are short-lived or are present in low concentrations or because they occur as non-persistent transition states. Where spectroscopic methods fail to characterise superelectrophiles, indirect methods such as kinetic experiments have provided a viable way to study superelectrophiles. Furthermore, kinetic studies also allow determination of and ranking of the reactivity of the superelectrophiles examined. For instance, an intramolecular superacid-catalysed Houben-Hoesch reaction was reported[15] involving diprotonation of a nitrile group. Phenylbutyronitrile **1.14** cyclises to intermediate **1.17** in solutions more acidic than H_0 = -10, which ultimately affords product **1.18** upon hydrolysis. Kinetic studies showed the rate of the superacid-catalysed reaction to be linearly proportional to the acid strength and increased 100-fold over a range of H_0 = -10.5 to -13.0. At an acidity of H_0 = -10.0, nitrile **1.14** is estimated to be half-protonated as **1.15**, however almost no cyclisation is observed at this point. The latter finding together with the kinetic data proposed formation of a superelectrophilic intermediate **1.16** in a stronger acidic medium as the rate-determining step.[3]

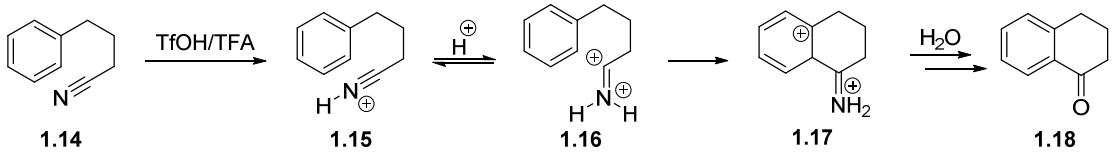

Scheme 1.5 Kinetic data suggests presence of superelectrophile **1.16** in this superacid-catalyses intramolecular Houben-Hoesch cyclisation.[3]

Although the electrostatic repulsion in most cases does not allow for isolation of stable superelectrophiles, some examples have been reported that make use of various factors to stabilise the superelectrophilic species. Stang reported[16] the first isolation of biscarbenium ions linked by a single atom by reaction of trifluoromethanesulfonic anhydride (triflic anhydride) with activated carbonyls. In these cases the stabilisation of the dication ether salts resulted from formation of a Hückel aromatic state and delocalisation of the positive charge. Cyclopropenone **1.19** was reacted with triflic anhydride and first afforded the triflated monocation **1.20**, which the authors could

isolate in some cases, before addition of another equivalent of carbonyl compound led to the ether disalt **1.21** at elevated temperatures.

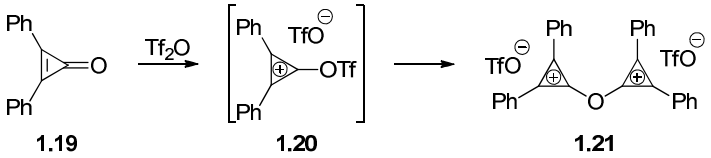

1.19 **1.20** **1.21**

Scheme 1.6 Hückel aromaticity delocalises the charges in this ether disalt **1.21** and allows for isolation and characterisation.

The authors also reported isolation of disalts, whose stabilisation, being acyclic doubly charged species, did not benefit from Hückel aromaticity. The centres of charge in the disalt **1.24**, generated by the addition of triflic anhydride to urea compound **1.22**, were stabilised by neighbouring group effects, that is the nitrogen atoms with their n-electrons donating electron density to the carbenium centre over the π-system (Scheme 1.7). In this example, the triflated monocation **1.23** could be isolated and characterised, before thermal activation afforded the ether dication **1.24**.

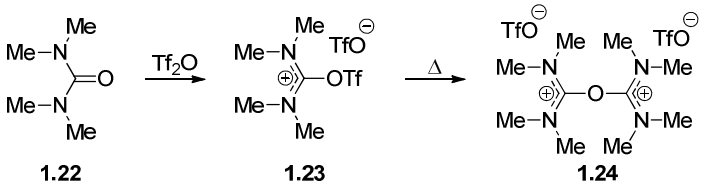

1.22 **1.23** **1.24**

Scheme 1.7 Neighbouring group effects are the stabilising factors in ether disalt **1.24**.[16]

Where delocalisation of the charges is not possible, sometimes a rigid backbone can hold the charge-bearing centres close together and prevent charge separation that can be referred to as a "coulombic explosion"[17] (spontaneous charge separation). Kilian and co-workers[18] isolated and fully characterised 1,2-diphosphaacenaphthene 1,2-dication **1.27** as a by-product from the oxidation of **1.25** with diphosphorus tetraiodide **1.26**, that possesses kinetic stability.

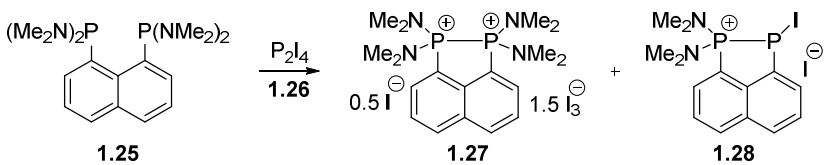

1.25 **1.27** **1.28**

Scheme 1.8 Rigid backbone structures such as the 1,8-naphthyl residue in this case can increase the overall stability of superelectrophiles**.**

Based on computational calculations on this 1,2-disalt **1.27**, the authors emphasised not only the buttressing role of the rigid 1,8-naphthyl backbone for the stability of the system but also revealed

the aromatic 10π electron ring system to donate electron density and compensate for the charged phosphorus centres, when comparing the energy of the structure with aliphatic analogues.

Synthetic chemists have also been looking for stable and isolable superelectrophiles in the absence of superacids and to achieve this goal, interest has simultaneously grown in the synthesis of very weakly coordinating anions. A particular class of large and spherical weakly coordinating anions are termed carboranes (Figure 1.1) and this class has been widely explored by Reed and co-workers.[19,20] Mainly consisting of boron, these clusters form polyhedral structures, in which one or more positions are substituted by carbon atoms. Related compounds, namely alkyl carboranes, were found to be alkylating agents even stronger than methyl triflate.

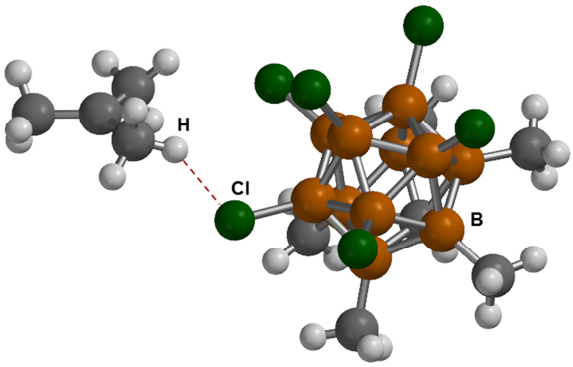

Figure 1.1 X-ray crystal structure of the *tert*-butyl cation hydrogen-bonded to the carborane $(CHB_{11}Me_5Cl_6)^-$ anion.

With these ions in hand the authors achieved isolation of structures like hexamethylhydrazonium as a $CHB_{11}Cl_{11}^-$ salt **1.29**.[21] This dication had previously been calculated to be unstable towards "coulombic explosion" due to the two positively charged nitrogen atoms being adjacent and hence experiencing great electrostatic repulsion.

Less challenging heavy atom analogues of **1.29**, such as **1.30** and **1.31**, which can disperse the positive charges over broader space, had previously been accessed *via* alkylating reactions with methyl triflate (Figure 1.2).[22,23]

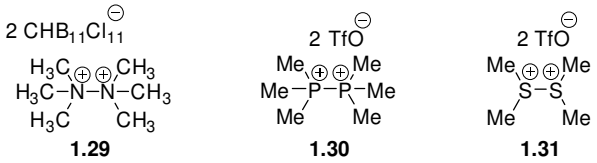

Figure 1.2 Unlike hydrazinium dication **1.29**, the phosphorus and sulfur dication analogues **1.30** and **1.31** are accessible *via* direct alkylation with methyl triflates.

However, applied to acyclic hydrazines, methyl triflate only afforded monomethylated pentamethylhydrazinium salt **1.32**. The authors[21] rationalised this through the higher localisation and proximity of the positive charge supressing the nucleophilicity of the neighbouring nitrogen atom.

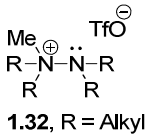

Figure 1.3 Treatment of tetraalkylhydrazines with methyl triflate affords only monocationic hydrazinium triflates **1.32**.

Only methyl carborane reagents, $CH_3(CHB_{11}R_5X_6)$, (R = Me, Cl; X = Cl, Br) were able to methylate weakly basic molecules that are inert to methyl triflate. In this case, the $(CHB_{11}Cl_{11})^-$ anion, as one of the least basic carborane ions known, was chosen as the counterion for the synthesis of the dicationic hydrazinium ion. However, the direct route *via* methyl carborane $CH_3(CHB_{11}Cl_{11})$ was not accessible, as it presented a problematic procedure. This carborane compound was found to readily react with the solvent DCM at dry ice temperature or with hexane to produce methane and methylcyclopentyl carbocation. Hence, a strategy was developed to form methylating carborane $CH_3(CHB_{11}Cl_{11})$ *in situ via* silylated tetramethylhydrazine **1.35** (Scheme 1.9). First, treatment of tetramethylhydrazine **1.33** with two equivalents of $Et_3Si(CHB_{11}Cl_{11})$ **1.34** in *o*-dichlorobenzene afforded the corresponding disilylated carborane **1.35**, which was characterised at -40 °C in sulfur dioxide. A subsequent reaction with methyl triflate then gave the desired hexamethylhydrazonium carborane **1.29**, which was precipitated with hexane. Even though the $[(Me_3NNMe_3)(CHB_{11}Cl_{11})_2]$ salt was found stable at room temperature, low solubility and limited thermal stability in solution have prevented isolation of single crystals for X-ray analysis.

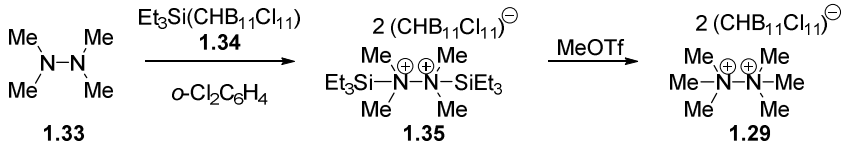

Scheme 1.9 Synthesis of hexamethylhydrazinium **1.29** *via* disilylated dication **1.35**.

1.2 A short review of chemical transformations induced by triflic anhydride

The novel work presented in this thesis deals with the synthesis and properties of reactive amidinium disalts and related structures, whose preparation in all examples made use of the particular reaction between the highly electron-deficient and reactive trifluoromethanesulfonic anhydride (triflic anhydride) and an amide functional group to create a highly electrophilic iminium triflate species. Trifluoromethanesulfonic acid or triflic acid is one of the strongest Brønsted acids, hence the triflate anion is, with the exception of the nitrogen molecule in diazonium species and the phenyl iodide in iodonium salts, the best leaving group in organic synthesis. The triflate anion is a better leaving group by a factor of 10^4 to 10^5 than the tosylate leaving group.[24] Furthermore, the Hammett constants have also been determined and show the triflate residue to be the strongest inductively withdrawing functional group.[25] All these aspects also make alkyl triflates among the most powerful alkylating agents mostly for N-, O- and S-nucleophiles. In contrast to trialkyloxonium ions (Meerwein salts), alkyl triflates are much more convenient to use due to better solubility in organic media, although 5-12 times less reactive than the oxonium species.[3,24,26]

Mainly over the past 50 years, organic chemists have achieved a wide scope of chemical transformations due to the exceptional features of the trifluoromethanesulfonic ester group, which had not been described by means of other reagents before. It is impossible to review all the various reactions on a few pages and the outcome of the interaction between the nucleophilic feature of the carbonyl bond (with the amide functionality in particular) and triflic anhydride shall briefly be mentioned. A few selected examples of different functional groups reacting with triflic anhydride will then be highlighted, as they relate more or less to the work carried out and described in this thesis.

The first step in the nucleophilic attack of the oxygen of a nucleophilic carbonyl group onto triflic anhydride affords a reactive species called a trifloxy carbenium ion **1.37** as an intermediate. Three different pathways can be described by which this intermediate can react further.

The first is defined by proton abstraction to afford vinyl triflates **1.38** and **1.39** and here the trifloxy carbenium ion **1.37** is generated from ketones **1.36** and aldehydes **1.40**. In case of aldehydes however, another intermediate called *gem*-bistriflate **1.42** is first generated by triflate counterion trapping, which can sometimes be isolated and decomposes preferentially to *E*-vinyl triflates upon thermal activation. If the carbonyl compound is a carboxylic acid **1.45**, then mixed anhydrides **1.47** are afforded, which are often employed as highly efficient acylating reagents even for unactivated arenes and without a catalyst in Friedel-Crafts transformations.[24]

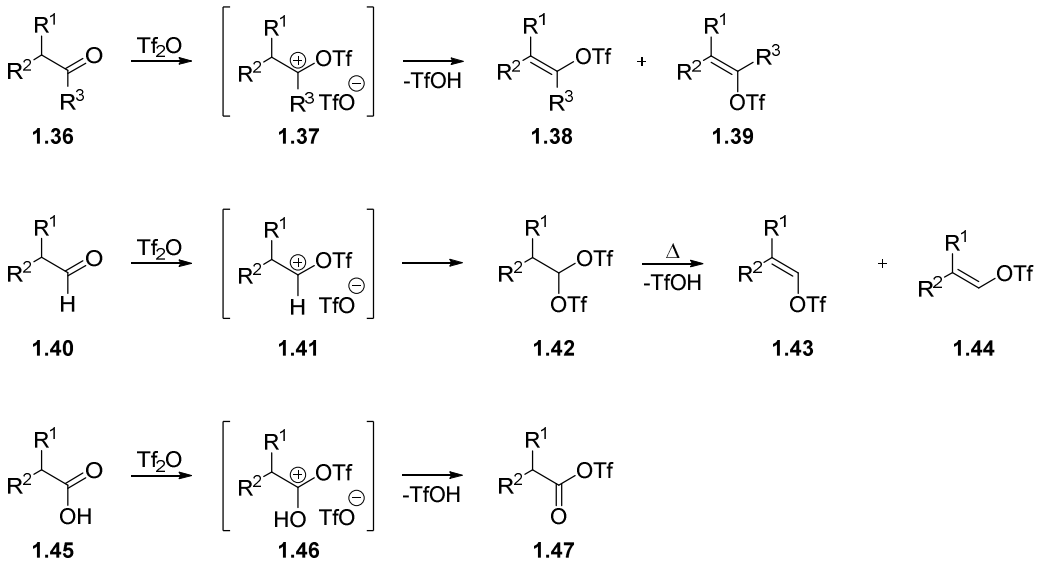

Scheme 1.10 The reaction of triflic anhydride with carbonyl compounds usually affords vinyl triflates (**1.38** and **1.39**), but sometimes *gem*-bistriflates **1.42** can be isolated. The reaction of triflic anhydride with carboxylic acids leads to mixed anhydrides **1.47** as highly efficient acylating agents.

Originally, vinyl triflates were used to prepare alkylidene carbenes *via* α-elimination or allow for the study of vinyl cations.[24] Nowadays, vinyl triflates and aryl triflates are most important in cross coupling reactions with organometallic reagents, a topic widely covered by reviews from Ritter and Stang.[26,27] With strong bases such as potassium *tert*-butoxide or LDA, vinyl triflates can also be dehydrated to alkynes.[24]

A second category is defined by trifloxycarbenium ions undergoing cationic rearrangements, most seen in bicyclic ketones **1.48** in the terpene series. The Wagner-Meerwein rearranged triflate products result from release of ring strain or the tendency to form a better stabilised carbocation. However, for these 1,2-migrations to occur the presence of an apical substituent and steric incapability to form vinyl triflates are a precondition. The Wagner-Meerwein rearrangement can be followed by methyl migrations in certain terpenes also known as Nametkin or retropinacol rearrangements to form a more stable carbocation as seen in **1.52** (Scheme 1.11).[28-30]

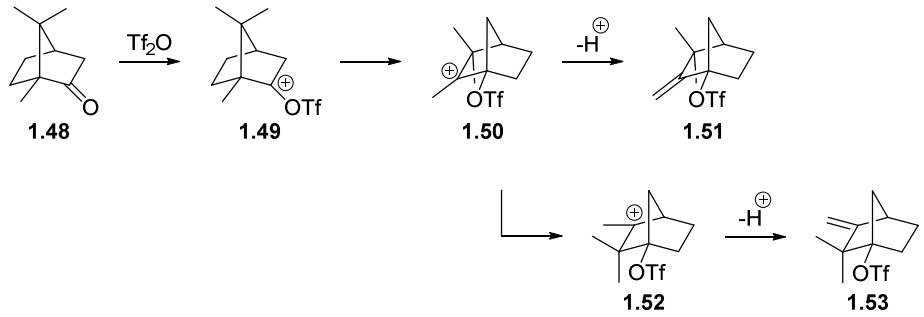

Scheme 1.11 Ketone **1.48** affords Wagner-Meerwein rearranged triflate products upon reaction with Tf_2O.

Ketones usually produce vinyl triflates upon reactions with triflic anhydride, although some ketone derivatives of the latter structures *e.g.* **1.54** and **1.56** allow, if they are non-enolisable or difficultly enolisable, for isolation of *gem*-bistriflates **1.55** and **1.57**. The solvolysis of **1.55** and **1.57** in 50:50 MeOH/H_2O at room temperature affords the starting material.[31]

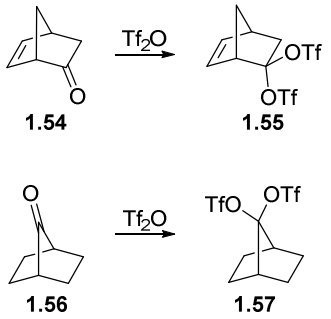

Scheme 1.12 Difficultly or non-enolisable ketones sometimes allow for isolation of *gem*-bistriflates.

The last group describes the reaction of external nucleophiles with the trifloxy carbenium ion. For instance, an elegant route to substituted pyrimidines **1.64** can be followed by the reaction of triflic anhydride with ketones in the presence of nitriles **1.60** (Scheme 1.13).[32]

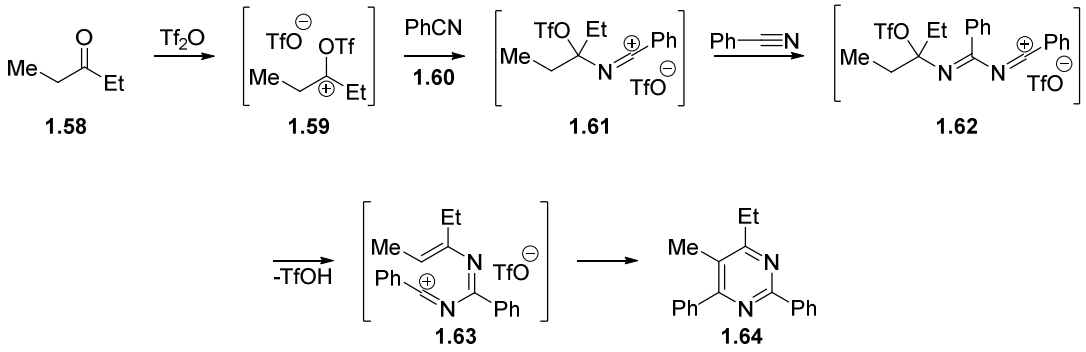

Scheme 1.13 The carbenium triflate intermediates **1.59** can form nitrilium cations **1.61** and **1.62** in the presence of nitriles, which then cyclise to afford pyrimidine derivatives.

The same mechanistic route also applies if esters are used instead of ketones as the carbonyl compound. From Scheme 1.14 it can be seen that with 2-arylesters (R^1 = aryl) as the starting material the intermediate **1.65** can undergo intramolecular electrophilic aromatic substitution to cyclise to isoquinoline structure **1.68**.[33,34]

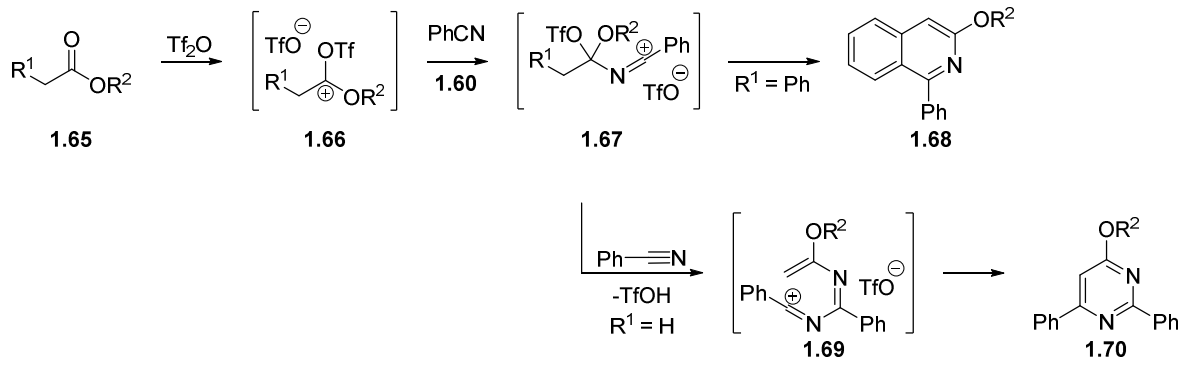

Scheme 1.14 Synthesis of isoquinolines **1.68** from 2-arylethanoate esters.

In the absence of nitriles, however, esters have been reported to react in a similar way to carboxylic acids. They produce alkyl triflates **1.74** and mixed anhydrides **1.73**, which are very efficient acylating agents in Friedel-Crafts transformations.[24]

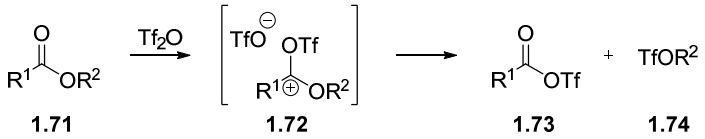

Scheme 1.15 Reaction of triflic anhydride with carboxylic esters afford mixed anhydrides **1.73** and alkyl triflates **1.74**.

The most diversity of all carbonyl groups upon reaction with triflic anhydride is provided by the amide bond, however. The first species generated in this case is the highly electrophilic iminium triflate species **1.76**, which can, depending on whether it is generated from primary, secondary or tertiary amides, follow different pathways. Scheme 1.16 depicts the first example of nitriles being produced upon reaction of triflic anhydride with primary amides. The mechanism proposed[35] is analogous to the mechanism of reactions of primary amides with other acid anhydrides. These reactions had also produced nitriles. After the expulsion of triflic acid from the iminium triflate intermediate **1.76** affording imido triflate **1.77**, the species eliminates triflic acid again to afford the corresponding nitrile **1.78**.

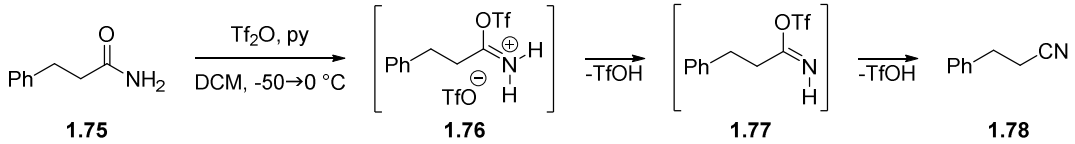

Scheme 1.16 The first species generated in the reaction of amides with triflic anhydride is a highly electrophilic iminium cation **1.76**. In the case of primary amides the reaction with Tf_2O affords nitriles **1.78** as products.

With secondary amides or tertiary amides, the respective imido (**1.77**) or iminium species (**1.76**) formed and underwent reactions with various nucleophiles such as alcohols, azides, cyanides, thiols

etc. For instance, Charette, a pioneer in the study of reactions between amides and triflic anhydride, reported[35] the efficient synthesis of orthoesters from iminium and imido triflate species with alcohols. The reaction shown in Scheme 1.17 is the first example of iminium and imido triflate species undergoing multiple nucleophile additions. The reaction was first kept below 0 °C to prevent elimination of triflic acid and production of ketiminium species, which will be discussed shortly. The method presented is a very efficient way to cleave the usually strong amide bond under mild conditions and produce carboxylic esters **1.82**, which are afforded from mild acidic hydrolysis of the orthoesters **1.81**.

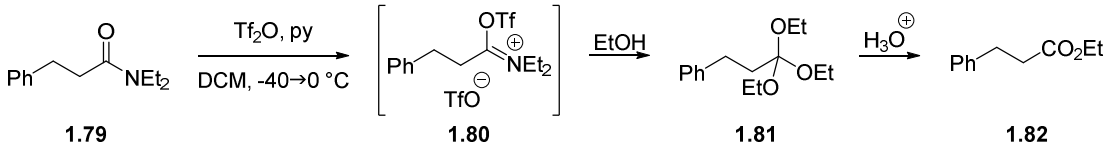

1.79 1.80 1.81 1.82

Scheme 1.17 Addition of ethanol to the iminium triflate intermediate **1.80**, formed from Tf_2O and secondary or tertiary amides, affords orthoesters **1.81**.

Applying the same methodology for secondary and tertiary amides, the same research group reported[36] triols such as trimethylolethane **1.86** to produce rigid bridged orthoesters **1.87** as good protecting groups for the carboxylic group. Although the entropic barrier for the generation of the bridged orthoesters is lowered compared to the formation of acyclic orthoesters and stoichiometric amounts of the triol should lead to full conversion, it was found that more equivalents of the triol afforded a better yield.

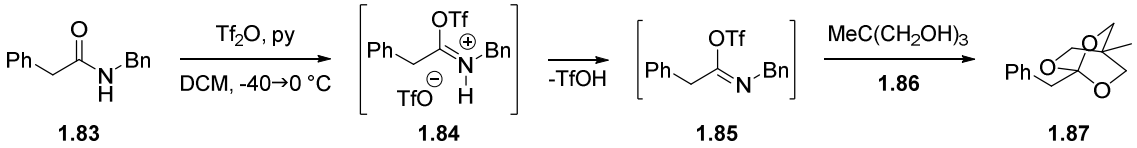

1.83 1.84 1.85 1.87

Scheme 1.18 Reactions of iminium or imido triflates with triols afford bridged orthoesters **1.87** as stable protecting groups for carboxylic acids.

The authors believed that this could be explained by the excess alcohol making the reaction medium more polar, thus stabilising the charged intermediates. The proposal was supported by the fact, that addition of only 1.5 eq. of triol followed by addition of ethanol or acetonitrile to the reaction mixture produced significantly higher yields (Table 1.1).

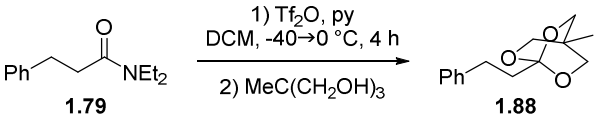

Table 1.1 Addition of polar solvents to the reaction mixture is believed to stabilise the iminium triflate intermediate **1.84**.

Equivalents of triol	additive	Yield of **1.88**
1.5	none	58 %
7.0	none	86 %
1.5	EtOH	88 %
1.5	MeCN	85 %

Similar to the last example with triols intercepting the iminium species to form bridged orthoesters, Charette also reported[37] preparation of heterocyclic thiazolines **1.91** from 2-aminoethanethiol (cysteamine) **1.89** reacting with intermediate iminium triflate species generated from secondary or tertiary amides upon reaction with triflic anhydride.

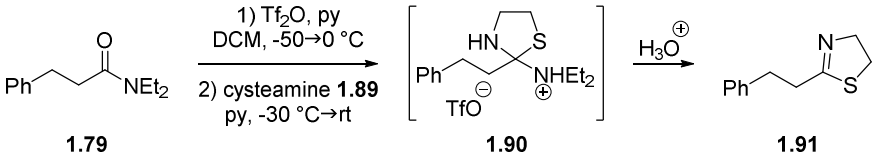

Scheme 1.19 Synthesis of thiazolines from the interception of iminium triflates with 2-aminoethanethiol (cysteamine) **1.89**.

Imido nitriles **1.94** have been synthesised from secondary α,β-unsaturated amides **1.92** *via in situ* formed *O*-triflyl imidates **1.93** using lithium cyanide in the presence of Hünig's base (diisopropylethylamine) and 12-crown-4 ether. This route has proved to be efficient and important as 2-cyano-1-azabutadienes **1.94** are very good precursors for a variety of tetrahydropyridines or other heterocycles, that can be obtained in Diels-Alder reactions with a suitable dienophile or in an intramolecular version.[38-40]

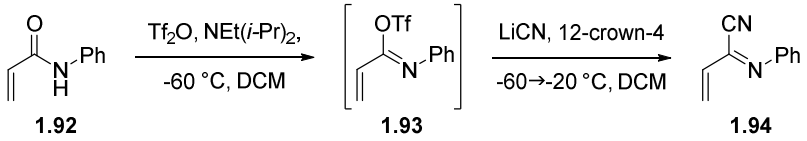

Scheme 1.20 Synthesis of stable imido nitriles.

When azides as nucleophiles were added to secondary amides **1.95** in the presence of triflic anhydride, the synthesis of tetrazoles **1.97** was achieved. With cyanoethyl protecting groups on the amide functionality even 1*H*-substituted tetrazoles **1.98** are formed.[41]

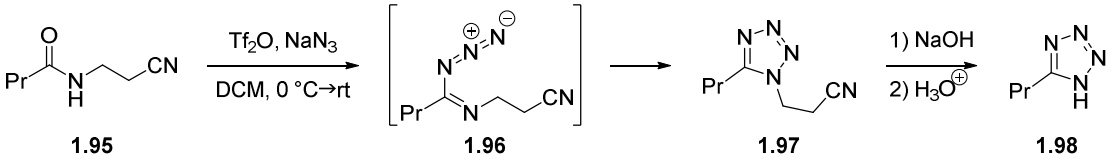

Scheme 1.21 Azides also intercept the intermediate formed iminium and imido triflates to form imido azides **1.96**, which subsequently cyclise to tetrazoles **1.97**.

Banwell and co-workers discovered[42] that $POCl_3$ can be substituted by a mixture of 4-dimethylaminopyridine (4-DMAP) and triflic anhydride in the Bischler-Napieralski cyclisation (Scheme 1.22). The latter reaction generally requires not only activated arenes but also high temperatures and aggressive reagents, which often clash with the sensitivity of other functional groups within the molecule, but here the temperatures applied were below room temperature and the methodology worked even for substrates where $POCl_3$ failed to effect the reaction although temperatures were raised up to 200 °C.

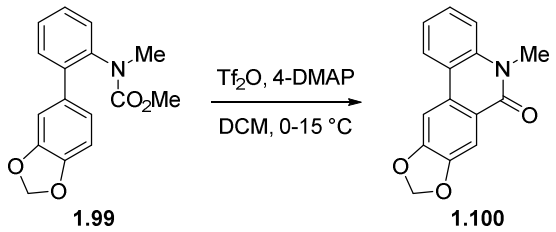

Scheme 1.22 An intramolecular Bischler-Napieralski cyclisation.

The reaction mechanism for the carbamate however, which was not discussed in the paper, must be somewhat different to that of the original Bischler-Napieralski cyclisation of β-phenethylamides **1.101** to produce 3,4-dihydroisoquinolines **1.106** shown below (Scheme 1.23), as Fodor and Nagubandi showed in a detailed study that secondary amides first dehydrate to imidoyl compounds **1.103**, which then form nitrilium salts **1.104** prior to cyclisation to the dihydroisoquinolines **1.106**.[43]

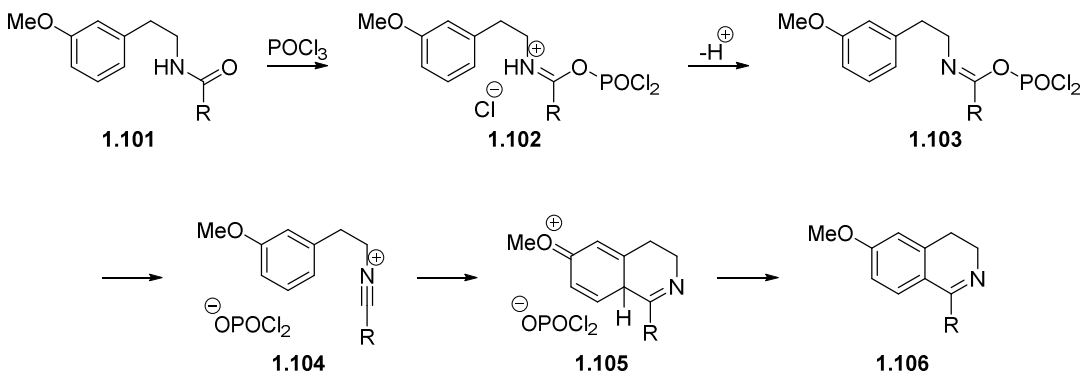

Scheme 1.23 Fodor and Nagubandi propose a detailed mechanism for their extensive studies on Bischler-Napieralski cyclisation using $POCl_3$.[43]

In an intermolecular analogue of the latter reaction, the combination of DMF and triflic anhydride has been used as a very efficient substitute for the classical Vilsmeier-Haack reaction, which works even for less nucleophilic arenes such as naphthalene.[44]

From reactions of tertiary amides including an enolisable α-proton and the base 2,4,6-trimethylpyridine (collidine) with triflic anhydride in the presence of alkenes or alkynes, Ghosez proposed[45-47] formation of keteniminium intermediates **1.111**. Such cumulative double bond species as **1.111** explained the formation of cyclobutanones and cyclobutenones *via* [2+2] cycloadditions, as seen in the formation of cyclobutanone **1.113** from styrene **1.112**.

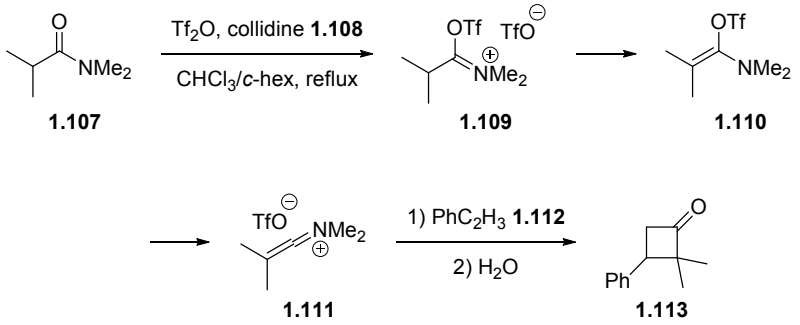

Scheme 1.24 Styrene **1.112** reacts with keteniminium intermediate **1.111** in a [2+2] cycloaddition to afford cyclobutanone **1.113**.

Lastly, a few special cases of triflic anhydride reacting with substrates shall be introduced, in which the generated triflate counterion acted as a nucleophile, as this usually means, that a highly reactive and strongly electrophilic intermediate had been formed. Acyclic bistriflates are usually afforded from triflic anhydride and the corresponding diols,[48,49] although Baum and co-workers showed[50] that they can be efficiently synthesised from cyclic ethers such as tetrahydrofuran **1.114** under very mild conditions as seen in Scheme 1.25. In terms of a mechanistic pathway, they referred to a similar study by Mazur,[51] in which, instead of triflic anhydride, mixed carboxylic-sulfonic anhydrides were

used for the cleavage of different ethers. Analogous to the initial acylation proposed by Mazur, in this example sulfonylation in **1.115** is believed to activate the cyclic ether followed by cleavage of one of the adjoining carbon-oxygen bonds in an S_N2 reaction for primary and in an S_N1 reaction for secondary and tertiary ethers.

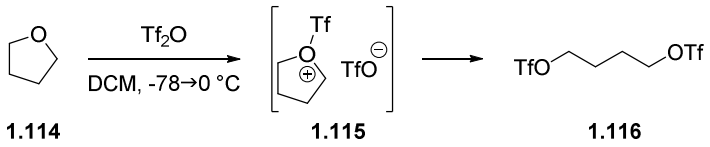

Scheme 1.25 Acylation as seen in **1.115** prior to ring cleavage is proposed for the reaction of tetrahydrofuran with triflic anhydride.

Cleavage of an ethyl group in triethylamine **1.117** upon addition of triflic anhydride, in which triflate anions react as nucleophiles, has been reported by Netscher and Bohrer in their study[52] on standard procedures for the synthesis of triflate esters from alcohols. They describe formation of triflate salt **1.118**, which is stable below -30 °C for months, but decomposes rapidly above 0 °C. This is somewhat controversial, as the authors also report a melting point between 52 and 54 °C for this triflate salt. They propose ethyl triflate **1.120** and sulfonamide **1.119** as products from this decomposition to explain the formation of ethyl ethers **1.121**, which have been observed as side-products in the formation of triflate esters from alcohols in the presence of triethylamine. Another side-route was proposed, in which triethylamine first abstracts a proton from salt **1.118** to form triflyl salt **1.122**, which can then react with triflic anhydride to afford a mixed (sulfinic-sulfonic) anhydride **1.123**. This mixed anhydride would explain the observed sulfinate products **1.124**, which can amount to significant yields, if the base, the reaction conditions or the order of reactants added is unsuitable.

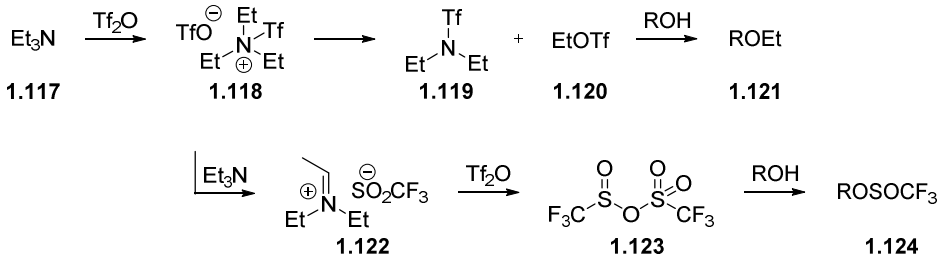

Scheme 1.26 Netscher and Bohrer proposed[52] different pathways for the reaction of Tf_2O with triethylamine to explain the formation of the observed products.

Triflic anhydride has also been employed to carry out synthetically useful but unusual transformations. Dimethyl sulfoxide **1.125** has been shown to form a highly reactive but isolable intermediate **1.126** upon reaction with triflic anhydride. This dimethyl(trifloxy)sulfonium ion **1.126** has been widely used as an agent to oxidise alcohols to aldehydes and ketones or generate sulfimines from moderately nucleophilic amines. It can also react with non-activated arenes, alkenes

and alkynes, in which the dimethyl(trifloxy)sulfonium ion **1.126** is considered as a superelectrophilic S^{2+} synthon sometimes rendering a triflate anion nucleophilic and to undergo addition with alkyne 1,2-diphenylethyne **1.127** as shown in Scheme 1.27.[24,53]

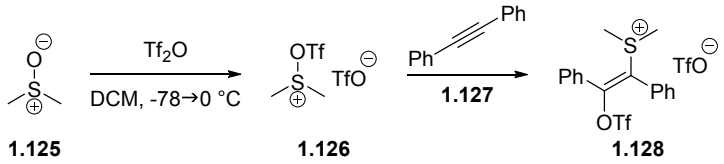

Scheme 1.27 Conjugate addition of dimethyl(trifloxy)sulfonium ion **1.126** onto 1,2-diphenylethyne **1.127**.

In the reaction of dimethylcyanamide **1.129** with triflic anhydride Martinez and co-workers proposed[54] formation of 2,3-bistriflate-1,1-dimethylisourea **1.131** which should result from triflate trapping of a nitrilium species **1.130**. Species **1.131** could not be isolated as it gradually forms urea **1.133** *via* a 4-membered heterocyclic Chapman rearrangement,[55] but in the presence of suitable nucleophiles such as alcohols, amines, ketones and thiols, the corresponding products can be obtained.

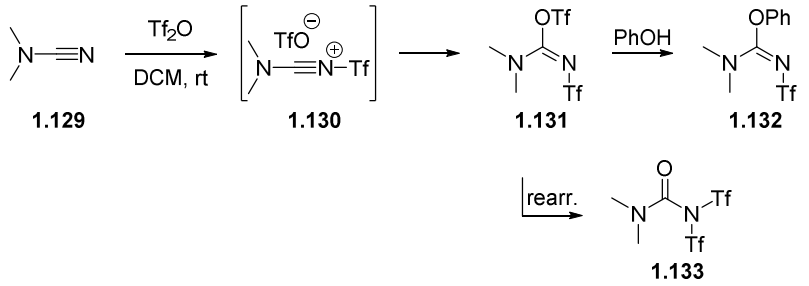

Scheme 1.28 Species **1.131** is afforded from the reaction of dimethylcyanamide **1.129** with triflic anhydride which can undergo substitution with phenol or rearrange *via* a Chapman pathway to urea **1.133**.

Furukawa and co-workers reported[56] alkyl transfer to very weakly nucleophilic triflate anions upon triflic anhydride addition to monooxides of 2,2'-bis(alkylthio)biphenyl under mild conditions and proposed from the NMR data superelectrophilic dithia disalt structure **1.135** as the reactive species, which gradually decomposed to thiasulfonium salt **1.136** and ethyl triflate **1.120** (Scheme 1.29).

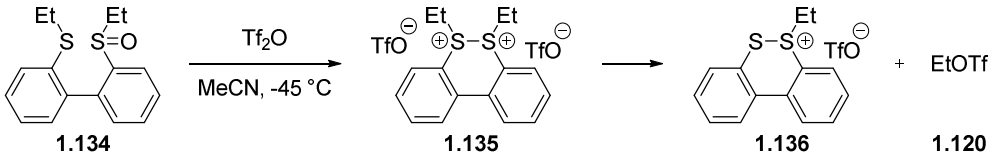

Scheme 1.29 Furukawa reports formation of dithia disalt **1.135** at -45 °C that undergo facile alkyl transfer to weakly coordinating triflate anions.

In a subsequent study with alkyl-2-(methylthiomethyl)phenyl sulfoxides they determined not only the rate of alkyl transfer but found this rate-determining step for substrates bearing a secondary alkyl residue on the sulfoxide moiety to proceed *via* an S_N1 mechanism. This was suggested after chiral phenethyl sulfoxide **1.137** was first subjected to triflic anhydride and then hydrolysed in a Ritter-type reaction to produce nearly racemised *N*-phenylethylacetamide **1.141**.[57]

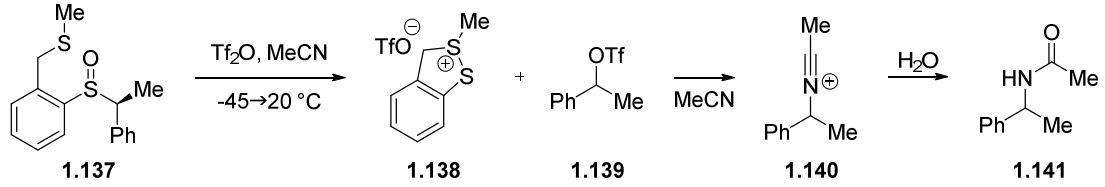

Scheme 1.30 A chiral alkyl group on the sulfinyl moiety leads to racemic product **1.141** suggesting an S_N1 displacement from the dithia disalt.

1.3 The interest in amidinium dications

Although the first formation of an amidinium disalt was proposed in the early 60s, it took almost 50 years until this superelectrophilic species was again reported as the active species being generated in the synthesis of some important heterocyclic compounds. Hammond was the first to propose[58,59] formation of amidinium disalt intermediates to explain the rates of C-N bond rotation within amidinium ions (Scheme 1.31).

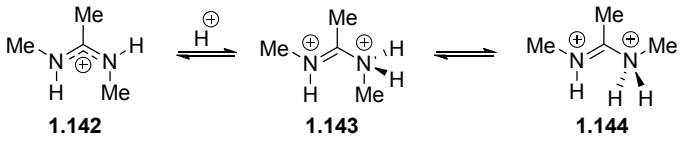

Scheme 1.31 Protonation of amidinium cation **1.142** allows formation of disalt **1.143** and rotation around the central C-N bond.

A few years later Watson studied[60,61] the kinetics of the acid-catalysed hydrolysis of alkyl-substituted amidines and imidazolines and found the lysidinium ion **1.145** being half-diprotonated in 102 % sulfuric acid (H_0 = -13.2) when the chemical shifts of the methyl and methylene groups were plotted against H_0. Furthermore, the rate of hydrolysis was observed to be linearly dependent on acid concentration up to 10 M sulfuric acid, which also supports the formation of the amidinium disalt intermediate, as in acidic solutions lysidine (2-methyl-2-imidazoline) is already completely converted to monoprotonated lysidinium ion **1.145**.

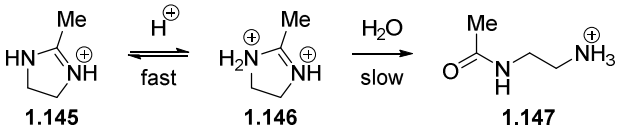

1.145 1.146 1.147

Scheme 1.32 The rate of acidic hydrolysis of lysidinium ion **1.145** is linearly dependent on acid concentration, thus suggesting diprotonation to lysidinium disalt intermediate **1.146**.

For completeness, Curphey and Prasad[62] need to be mentioned who were first to report the synthesis of pyrimidine-based 1,3-superelectrophiles containing the amidinium disalt structural element. These compounds were generated by reaction of pyrimidine with trialkyloxonium salts (Scheme 1.33). However, much of the reactivity of the amidinium disalt structural entity is diminished by incorporation into an aromatic ring and no applications have been reported for these structures since.

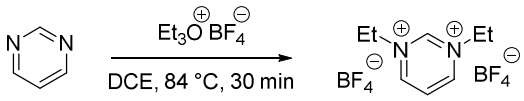

1.148 1.149

Scheme 1.33 Prasad and Curphey were the first to report[62] synthesis and characterisation of 1,3-superelectrophile **1.149** incorporating the amidinium disalt structural element into an aromatic ring.

Before synthetic applications were developed, a pioneering study[63] was conveyed by Charette and Grenon, in which they took a very close look by NMR spectroscopy at what was happening during addition of triflic anhydride to a mixture of pyridine and secondary or tertiary amides. They found that it was actually the base pyridine **1.150** that acted as a nucleophilic catalyst and was transformed to *N*-(trifluoromethylsulfonyl)-pyridinium triflate **1.151**, which is sufficiently electrophilic to react further with amides.

1.150 1.151

Scheme 1.34 Charette found pyridine to be a nucleophilic catalyst for reactions of amides with triflic anhydride.

From their study with secondary and tertiary amides, with the latter ones bearing enolisable and non-enolisable protons, they proposed different pathways depending on the reacting species. For tertiary amides **1.152** including an enolisable proton, the first generated species is *O*-triflyliminium triflate **1.153**. This intermediate can then either first expel triflic acid to afford keteniminium species **1.154** before it forms pyridinium adduct **1.156**, or it can first be attacked by pyridine producing amidinium disalt **1.155**, before the latter structure tautomerises to pyridinium compound **1.156**.

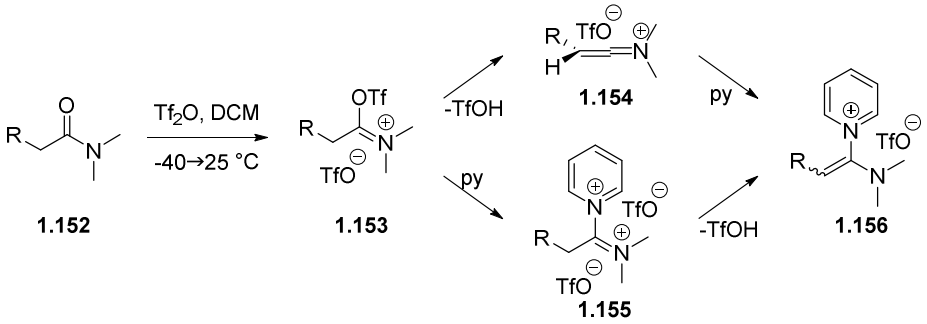

Scheme 1.35 Pyridinium product **1.156** can either form *via* keteniminium salt **1.154** or superelectrophilic disalt **1.155**.

The latter pathway was confirmed by low-temperature NMR studies, in which amidinium disalt **1.159** arising from non-enolisable tertiary amides was identified as well as pyridinium triflate **1.151** in the reaction mixture (Scheme 1.36). Interestingly, the amidinium disalt **1.159** showed a six-fold increased rate of alcoholysis compared to previously described pyridinium species **1.156** (Scheme 1.35) when subjected to deuterated ethanol.

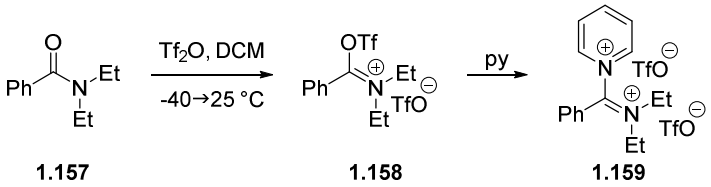

Scheme 1.36 Charette spectroscopically observed amidinium disalt intermediate **1.159** in solution.

The first synthetic application relating to this finding followed shortly by the same authors in 2005, in which, using their previous protocol, they described[64] a one-pot synthesis of a series of the natural alkaloids, tetraponerines, isolated from the venom of the New Guinean ant *Tetraponera sp*. In their synthetic route they proposed electrophilic activation of lactam **1.160** *via* pyridinium imidate **1.164**, which can possibly form from *O*-triflyl imidate **1.162**, as described in their preliminary publication, although the mechanism involving superelectrophilic amidinium disalt **1.163** is a viable route, too.

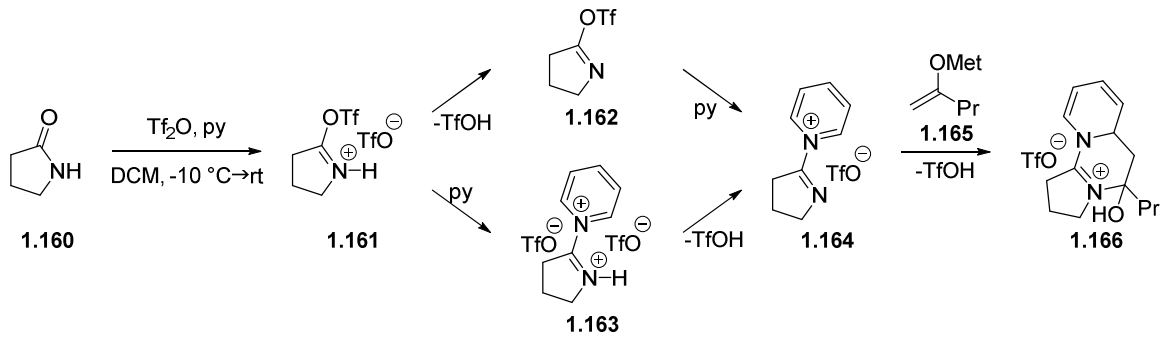

Scheme 1.37 Formation of imido pyridinium salt **1.164** can arise either from imido triflate **1.162** or amidinium disalt intermediate **1.163**.

This mechanism involving formation of a superelectrophilic amidinium disalt was also postulated[65] shortly afterwards by Movassaghi and Hill, when they reported highly efficient and versatile synthesis of pyrimidine derivatives **1.172** from nitriles **1.170** and non-enolisable secondary benzamides **1.167** upon reaction with triflic anhydride in the presence of 2-chloropyridine **1.168** (2-Clpy). From ^{13}C-NMR labelling experiments and React-IR studies they ruled out a possible imidoyl triflate as the reactive intermediate but proposed that it is the amidinium disalt species **1.169** instead, which allows addition of a suitable nitrile derivative to form the nitrilium compound **1.171** prior to cyclisation to the pyrimidine product **1.172**.

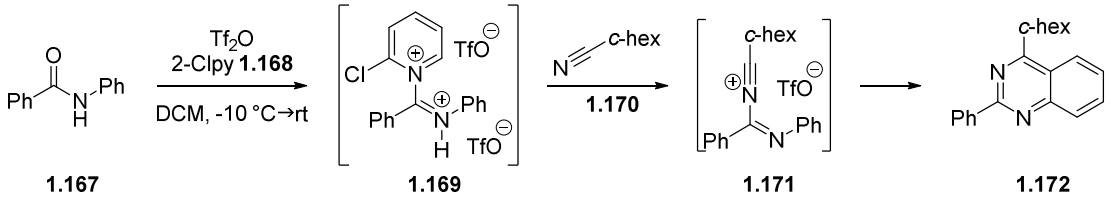

Scheme 1.38 Synthesis of pyrimidine **1.172** involves formation of amidinium disalt intermediate **1.169**.

The authors successfully applied their methodology to the synthesis of pyridine derivatives[66] not long after their first publication. Again, the initial step is the proposed formation of the amidinium disalt intermediate **1.174**, which is then reacted, not with σ-nucleophiles such as nitriles, but with π-nucleophiles such as alkoxy **1.175** and silyloxy acetylenes or enolethers **1.178** to form oxonium intermediates **1.176** and **1.179**, respectively, before they cyclise to the respective annulated products.

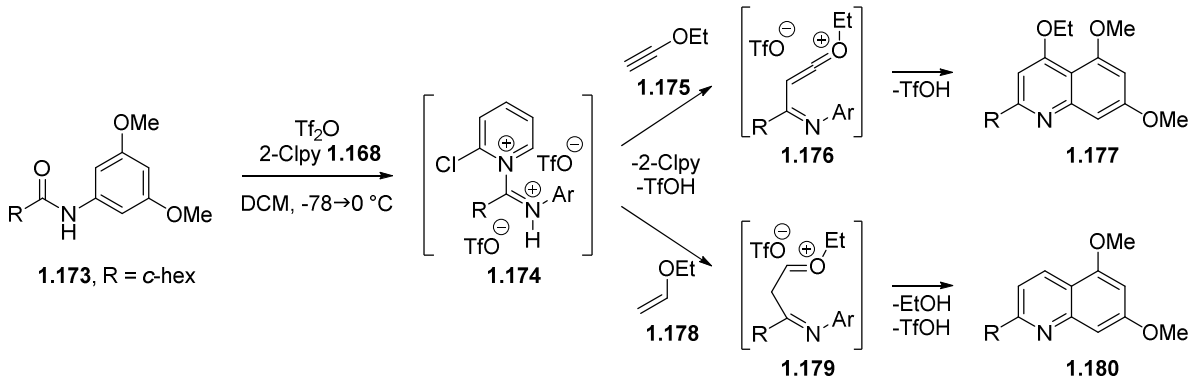

Scheme 1.39 The reactions of amidinium disalt **1.174** with π-nucleophiles such as alkoxy acetylene **1.175** or enolether **1.178** afford the respective quinoline products.

Very recently Wang applied a domino reaction of *N*-aryl amides **1.167** and ethyl diazoacetate **1.183** for the synthesis of a remarkable number of substituted indoles *e.g.* **1.186**. In a screening with different base additives they found that addition of 2,6-dichloropyridine (2,6-Cl_2Py) **1.181** in the presence of monosubstituted 2-chloropyridine (2-Clpy) **1.168** were crucial for the reaction as now an

even more electron-deficient amidinium disalt intermediate **1.182** could be generated which reacted with the only moderately nucleophilic diazo compound **1.183**.[67] However, direct evidence for these highly activated amidinium disalts is yet to emerge.

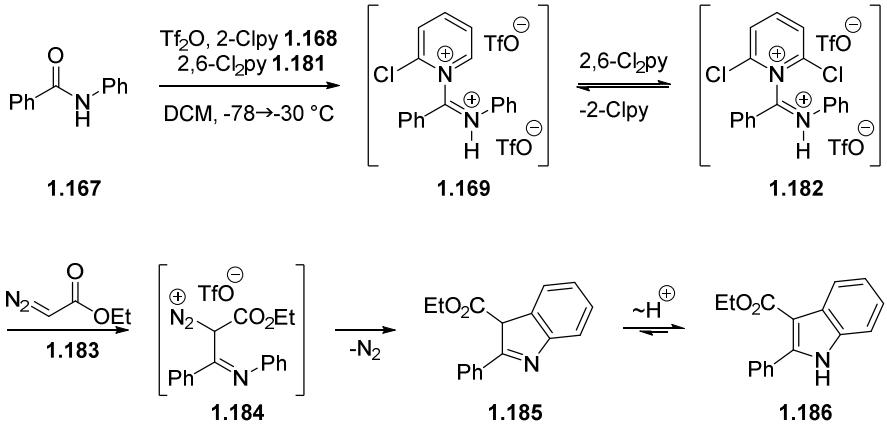

Scheme 1.40 Addition of 2,6-dichloropyridine (2,6-Cl_2Py) **1.181** to the reaction mixture affords an even more electron-deficient amidinium disalt intermediate **1.182**, which reacts with moderately nucleophilic azo compound **1.183.**

1.4 Superelectrophilic amidinium substrate activation in methanogenesis

Although the importance of the highly activated amidinium moiety in synthetic applications has only recently been highlighted, the interest of our research group in this reactive species arises from a mechanistic proposal that was communicated almost 20 years ago and which involves superelectrophilic amidinium activation for the reversible cleavage of molecular hydrogen performed within some methanogenic archaea. These microorganisms contain an enzyme, which, when first isolated from *methanobacterium thermoautotrophicum* in 1990, was believed to be metal-free and therefore was named the "iron sulfur cluster-free hydrogenase" or "H_2-forming methylene-tetrahydromethanopterin dehydrogenase" (Hmd). In a number of experiments then, including substrate labelling, kinetic isotope effect studies and others, it was shown that the key reaction in the reduction of carbon dioxide to methane is expressed in N^5,N^{10}-methenyltetrahydro-methanopterin ($CH{\equiv}H_4MPT^+$) **1.187** being reversibly and diastereoselectively reduced by hydrogen gas to N^5,N^{10}-methylenetetrahydromethanopterin ($CH_2{=}H_4MPT$) **1.188**. Scheme 1.41 depicts the reduction of the carbon centre in the amidinium moiety, which originally derives from carbon dioxide and is formally at the formic acid oxidation level, to the formaldehyde oxidation level in substrate **1.188**. The equilibrium for this hydride delivery was also found to be pH-dependent.[68-70]

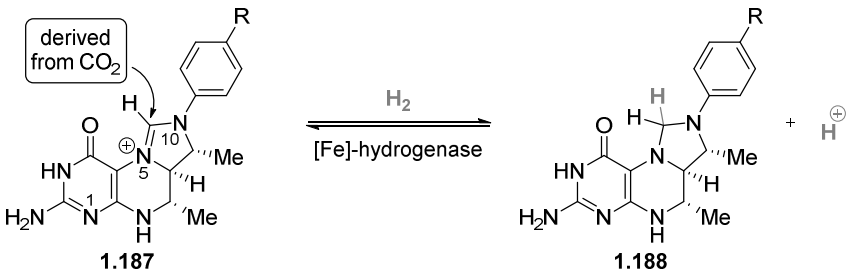

Scheme 1.41 The key reaction in methanogenesis involves the reversible reduction of N^5,N^{10}-methenyltetrahydromethanopterin ($CH{\equiv}H_4MPT^+$) **1.187** to methylenetetrahydromethanopterin ($CH_2{=}H_4MPT$) **1.188** by molecular hydrogen.

In 2004 Thauer and co-workers,[71] the same authors who isolated Hmd first, discovered that the active enzyme does indeed contain an essential iron cofactor and hence the enzyme's name was changed to [Fe]-hydrogenase. Again, a number of experiments enlightened the nature of the cofactor. Along with cyanide inhibition, enzymatic activity was also found to be reversibly inactivated by carbon monoxide, a finding contrary to earlier experiments. From these results along with EPR measurements showing the iron to be EPR-silent, the metal centre was proposed to be a low-spin complex containing an $Fe^{II}(CO)_2$ substructure most likely having a octahedral geometry. Changes of IR bands upon addition of $CH{\equiv}H_4MPT^+$ **1.187** or $CH_2{=}H_4MPT$ **1.188** to the enzyme, which were even more distinct in the presence of H_2, indicated binding of the substrates at the active centre or close by. However, no evidence for a Fe-H bond could be observed in the IR. UV-A/blue light-inactivation allowed for isolation of a compound, for which structure **1.189** was assigned and proposed to be derived from the active cofactor.[71-73]

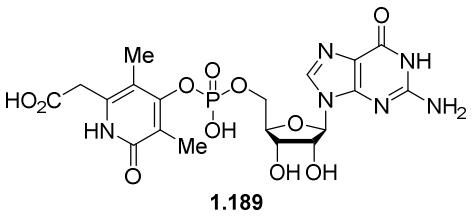

Figure 1.4 Compound **1.189** was isolated after UV-A/blue light-inactivation of the enzyme and was proposed to be derived from the active cofactor.

All these results elucidated that the active centre was most likely an iron(II) guanylyl pyridone cofactor (FeGP) **1.190**, which was finally confirmed in 2008 when Shima published[74] the first crystal structure of [Fe]-hydrogenase including FeGP as the cofactor, although the ligation sphere of the metal centre was first misassigned, as the authors could not imagine the electron density to match with a biologically unprecedented acyl-iron complex. After a crystal structure was obtained from a Cys176 mutant with $CH{\equiv}H_4MPT^+$ **1.187** bound to the enzyme, Hiromoto revised[75] the model **1.190** to

furnish, besides this novel acyl-ligation, two CO ligands at 90° to each other, Cys176, anchoring the cofactor to the apoenzyme, and an unknown (U) ligand.

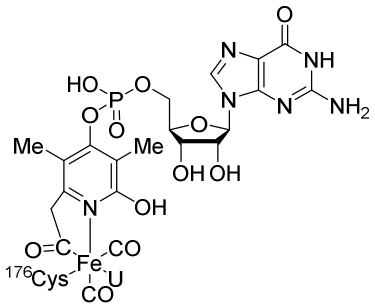

Figure 1.5 Model structure of the FeGP cofactor within the enzyme.

The crystal structure showed a metal-ligand conformation called "open" and involves a distance of 9.3 Å between the metal centre and the carbon centring the amidinium moiety, a distance far too long for a hydride transfer to occur from a possible iron hydrogen complex to the $CH{\equiv}H_4MPT^+$ substrate. Hence, the authors proposed an active "closed" conformation, in which the iron centre and the substrate come as close as 3 Å to one another, to allow hydride transfer from a hydrogen molecule held at the unknown ligand site of the FeGP cofactor.[75]

In 1995, long before the existence of the cofactor essential for the activity of the enzyme was known, Berkessel and Thauer proposed a unique mode of activation for $CH{\equiv}H_4MPT^+$, which might allow heterolytic cleavage of molecular hydrogen and reduction of the substrate. As seen from examples in superelectrophile chemistry at the beginning of the introduction to this thesis, the authors believed that protonation at N^5 or N^{10} would form superelectrophilic species such as **1.191** and **1.192**, respectively, which might be powerful enough to abstract a hydride from H_2.[76]

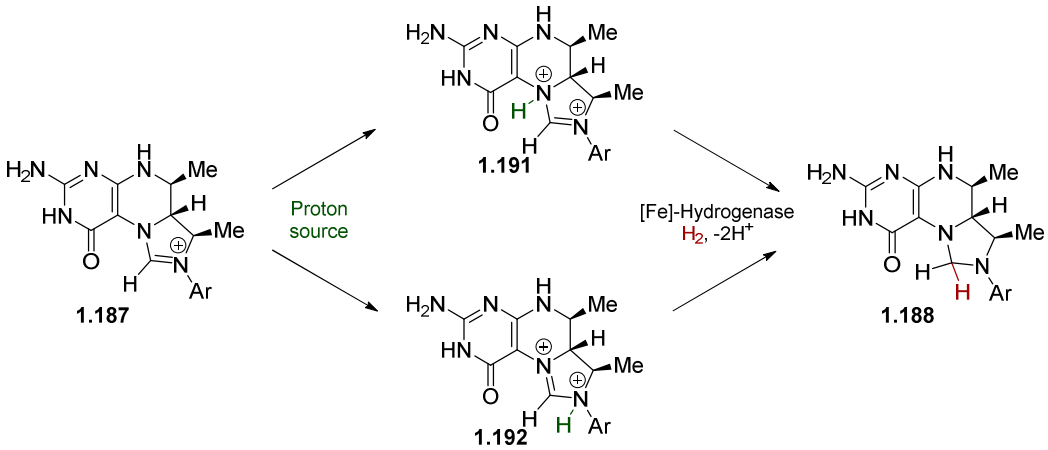

Scheme 1.42 Superelectrophilic activation *via* **1.191** or **1.192** was proposed[76] to allow reduction of the amidinium substrate **1.187** by molecular hydrogen.

As protonation of an amidinium cation would require an activating group of unprecedented acidity for a biological system the question arises, whether this activation of **1.187** would require full protonation as depicted in Scheme 1.42 or if a looser hydrogen-bonding network provided by acidic groups within the enzyme might provide the required boost in electrophilicity.

Inspired by this proposal and at a time, when it had been established that the substrate $CH{\equiv}H_4MPT^+$ and the iron centre do not become bonded, Corr and Murphy started investigations in the preparation and study of amidinium disalts and reported isolation of an amidinium disalt **1.194**, synthesised from 2-dimethylaminopyridine (2-DMAP) **1.193** and propane-1,3-ditriflate.[77] As mentioned before, Curphey and Prasad were the first to report synthesis and isolation of an amidinium disalt species (Scheme 1.33), but this compound was not very representative in terms of electrophilic reactivity, as the amidinium disalt structural entity was incorporated into an aromatic ring and the charges delocalised. Amidinium disalt species bearing the structural element exocyclic have only recently been proposed and even assigned as components of a mixture in NMR solutions but none have been isolated. Hence, the isolation and full characterisation of amidinium disalt **1.194** in the absence of superacidic media and which consists of an sp^2- and an sp^3-hybridised nitrogen centre is an important milestone in the characterisation of the superelectrophilic amidinium disalt entity.

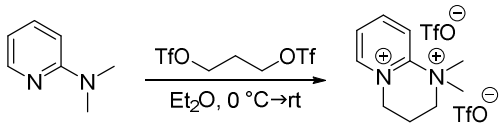

1.193 **1.194**

Scheme 1.43 Murphy and Corr reported isolation of an amidinium disalt **1.194** from the reaction of 2-DMAP **1.193** with propane-1,3-ditriflate.

Further studies[78,79] on this compound led to remarkable results, where it showed unusual sensitivity to hydrogenation. By treating amidinium dication **1.194** with hydrogen in the presence of palladium on charcoal under moderate pressure, fragmentation of the amidine core was observed (Scheme 1.44). From reduction experiments with deuterium, reversible, regioselective H_2/D_2 additions on the pyridinium ring were excluded, as the reaction gave specifically labelled compound **1.197**, and intermediates shown in Scheme 1.44 were suggested for the mechanistic pathway. The authors emphasised that the compound should be less susceptible to reduction compared to [Fe]-hydrogenase substrates **1.191/92** as hydride abstraction from H_2 would disrupt the aromaticity of the pyridinium moiety as in **1.195** or **1.196**. The enhanced reactivity of the dication was seen in the fact that the pyridinium ring in the product **1.197** was not reduced by H_2 under the conditions of the

experiments. Thus although not able to abstract hydride from H_2 in the absence of a catalyst as Berkessel and Thauer proposed, it showed an interesting reactivity. Development of alternative amidine disalts that could undergo hydrogenation without disruption of aromaticity was undertaken by a colleague, Callum Scullion[80], in a parallel project.

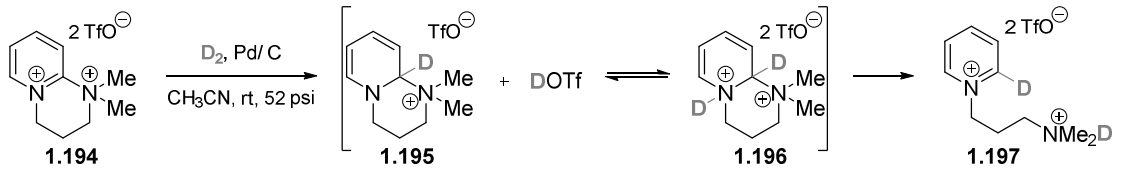

Scheme 1.44 Reduction of amidinium disalt **1.194** with molecular deuterium and a palladium catalyst.

However, the amidinium disalt isolated was not only shown to readily undergo reduction with hydrogen, but was also found to be a good methylating agent towards nucleophiles such as triphenylphosphine or triethylamine. This was quite a surprising finding, as sp^3-hybridised nitrogen centres, from which the methyl group comes in this case, are known to require not only aggressive reagents, but usually harsh reaction conditions as well to undergo cleavage of an N(sp^3)-alkyl bond. In competition reactions (Scheme 1.45) with common alkylating agents such as methyl iodide, dimethyl sulfate and methyl triflate, the disalt **1.194** was found to be as strong a methyl donor as dimethyl sulfate. The amidine dication **1.198**, incorporating an additional nitrogen atom in the aromatic ring, making the compound more electron-deficient, showed even higher activity.

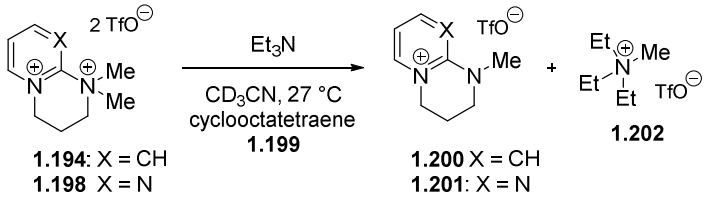

Scheme 1.45 Alkylating strength of the **1.194** and **1.198** was examined in competition experiments against some common methylating agents using Et_3N as the nucleophile and cyclooctatetraene as an internal NMR standard.

Table 1.2 Alkylating strength of the amidine dications **1.194** and **1.198** was found to be as strong as of dimethyl sulfate.

			amount remaining %	
entry	disalt	methylating agent	disalt	methylating agent
1	**1.194**	MeI	0	100
2	**1.194**	Me_2SO_4	53	59
3	**1.194**	MeOTf	94	0
4	**1.198**	Me_2SO_4	23	70

However, in competition with methyl triflate, no methyl-donating activity was seen for amidine dication **1.194**. This outcome is not surprising as methyl bisulfate $MeOSO_3H$ has an acidity of $H_0 = -3$ while triflic acid has $H_0 = -13$.[3] Hence, the triflate anion is 10^{10} times more reactive as a leaving group.

1.5 Alkyl transfers in Nature

The finding that our isolated amidinium disalt readily transferred a methyl group from a sp^3-hybridised nitrogen centre was not only interesting from a synthetic point of view, but had also drawn our attention as methyl transfers are ubiquitous in biological systems, including some where the cleavage of an N(sp^3)-C bond is also required but not very well understood.

1.6 *S*-Adenosylmethionine (SAM) – Nature's primary source of methyl groups

On a molecular basis, one of the most common processes in biological systems is the transfer of a methyl group. Methyl transfers are involved in many biochemical reactions leading to bioactive substrates.[81-88] Nature's most frequently used methyl-donating substrate is *S*-adenosylmethionine (SAM or AdoMet) **1.203**, which is also the second most widely used enzyme substrate after ATP.[89] Hence it is not surprising that SAM is involved in many other bioorganic transformations and provides more chemical groups than methyl. Scheme 1.46 gives an impression of the large scope of SAM. SAM is known for delivering amino groups *e.g.* to form 7,8-diaminopelargonic acid **1.208** (DAPA), which is an important intermediate in the biosynthetic pathway to biotin, a coenzyme in the synthesis of fatty acids.[89-91]

Transferring its ribosyl group, SAM is capable of modifying tRNAs such as **1.212** to epoxyqueuosine **1.213**, which is a precursor to queuosine **1.214**, a hypermodified tRNA nucleoside.[92] SAM is also a source of aminoalkyl groups, as seen in the creation of spermidine **1.206**, a polyamine involved in cellular metabolism.[93] In a review, Fontecave *et al.* consequently state that from *S*-adenosylmethionine "nothing goes to waste".

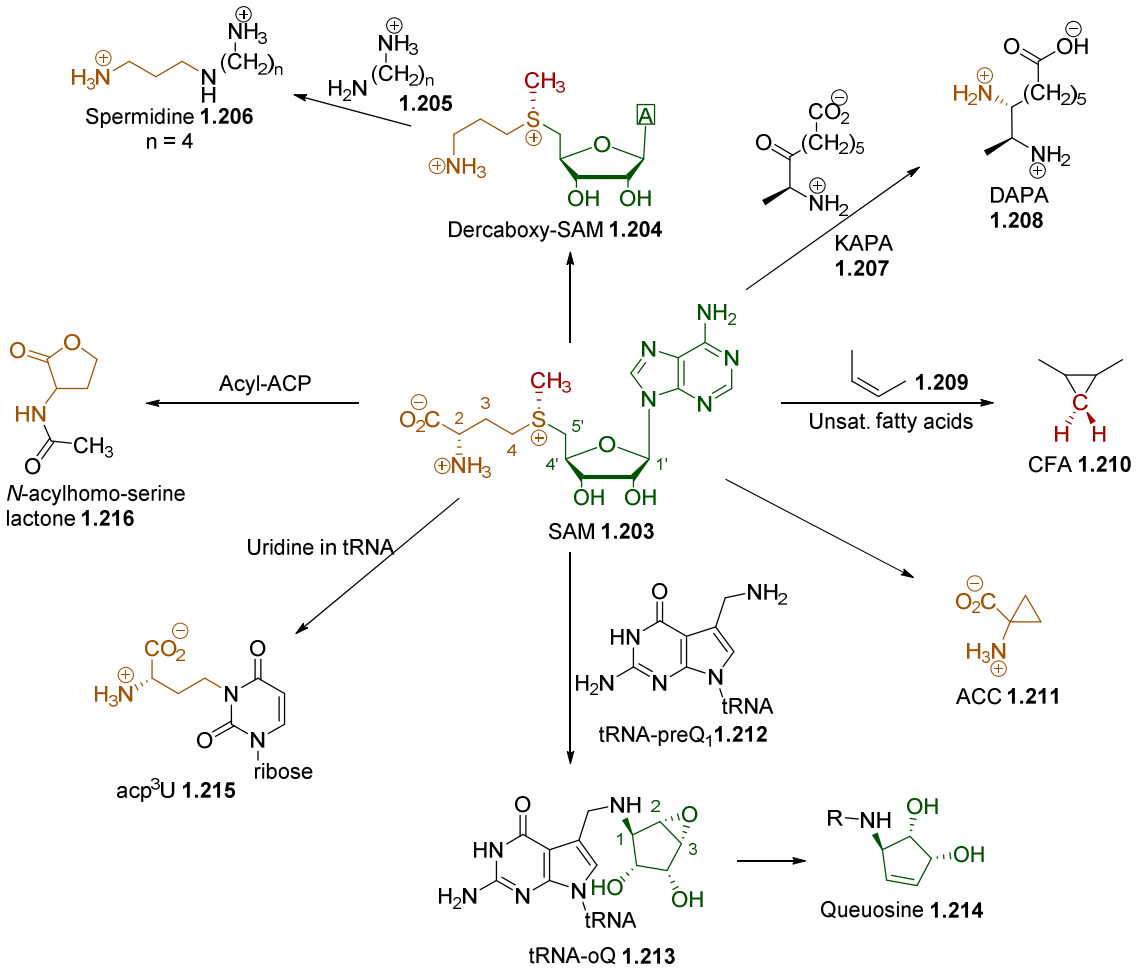

Scheme 1.46 SAM **1.203** as a source of various bioactive substrates.[89]

The enzyme that generates SAM **1.203** is called SAM synthetase and utilises ATP and methionine **1.222** (Scheme 1.47). This transformation is enantioselective and SAM is formed only in the *S*-configuration on the sulfur.[94] The methyl group on the sulfur atom is that which is transferred to various substrates with the reaction being catalysed by methylases. Even though not all questions arising about this process have been solved, it is accepted that the driving force for the methyl transfer results from the electrophilic nature of the carbon atom attached to the positively charged sulfur. In the SAM cycle, after the methyl group has been transferred, *S*-adenosyl homocysteine **1.217** (SAH) is expelled, which then is hydrolysed to homocysteine **1.219**.

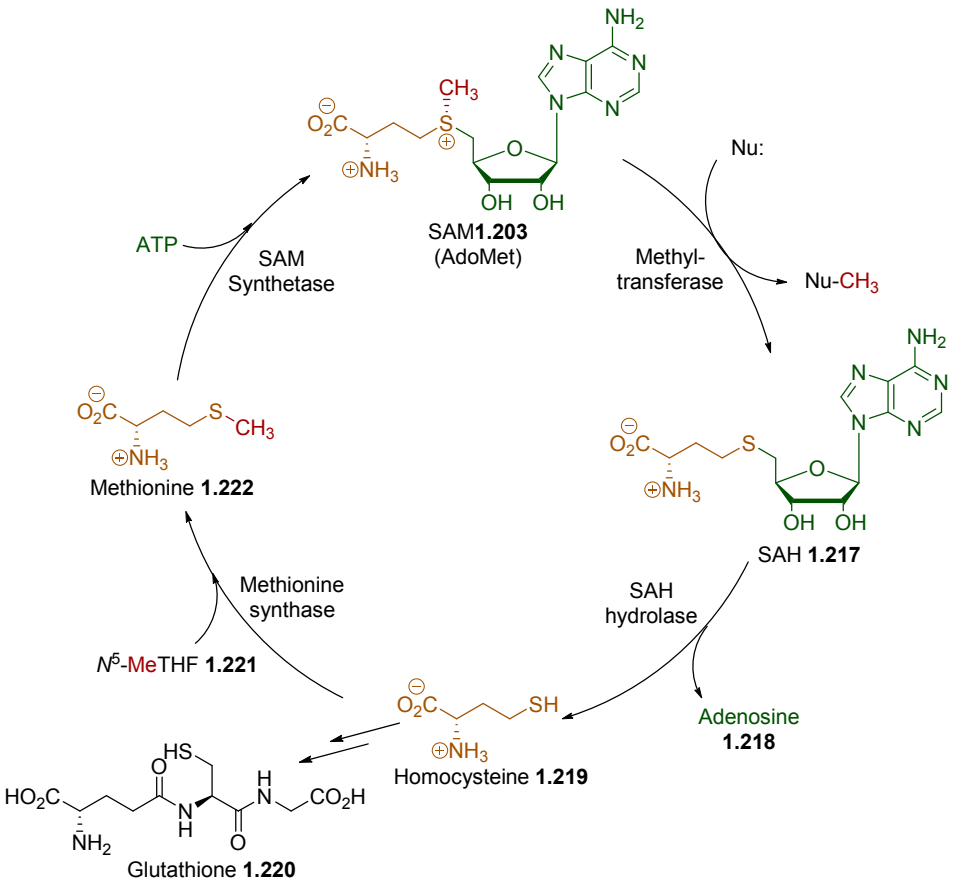

Scheme 1.47 The SAM cycle. Nu represents a general nucleophile for transmethylation from SAM **1.203**. In the last step of the cycle SAM synthetase utilises Met **1.221** and ATP to produce SAM.[89]

Finally homocysteine **1.219** can either be transformed to the cellular antioxidant glutathione **1.220**[95,96] (*via* transsulfuration with serine to cysteine as a direct precursor) or it can be converted to methionine **1.222**[97] in a remarkable reaction to close the cycle.

1.7 N^5-Methyltetrahydrofolate (N^5-MeTHF) as a methyl group donor

Methionine **1.222**, an essential amino acid and the precursor of SAM, is generated from homocysteine by methionine synthase (Scheme 1.48). In Nature, two classes of methionine synthase are known. One is cobalamin-dependent while the other one is not.[98] They both use a glutamate derivative of N^5-methyltetrahydrofolate **1.221** as the donor of the methyl group, but while the cobalamin-dependent enzyme (MetH) mediates the methyl group transfer first to a supernucleophilic cob(I)alamin cofactor before attachment to homocysteine (Hcy) **1.219**, in the cobalamin-independent enzyme (MetE) direct attack by the homocysteine's sulfur atom on the methyl group appears to happen. Another minor difference between these enzymes is that MetH uses Me-THF derivatives with one or more glutamate residues incorporated into the R group in **1.221**, whereas MetE requires three or more glutamate residues.

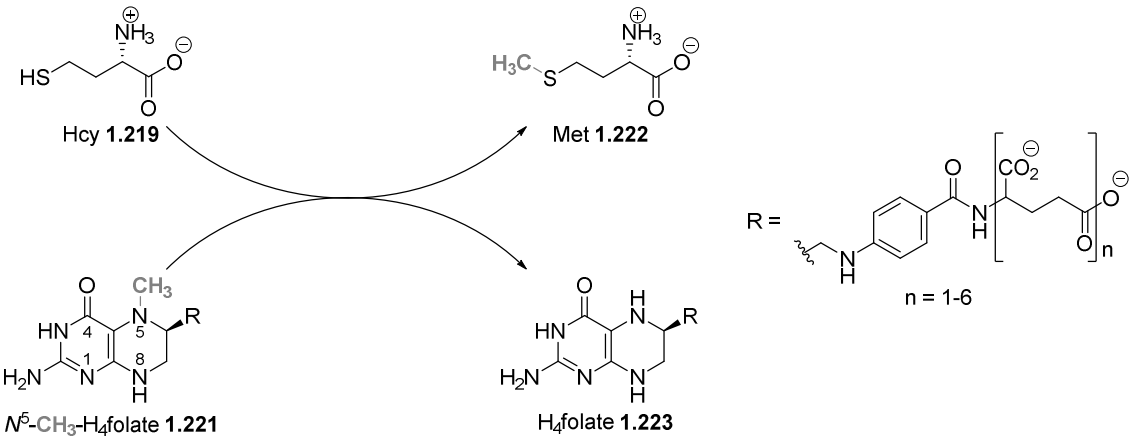

Scheme 1.48 Transmethylation from MeTHF **1.221** to homocysteine **1.223** catalysed by cobalamin-dependent (MetH) and cobalamin-independent (MetE) methyltransferase.

Looking more closely at the cobalamin-independent enzyme, the catalysed reaction is a fascinating transformation. On one hand, thiols *e.g.* **1.219** are only moderate nucleophiles as the pK_A of their functional group usually lies around 10, making them neutral under physiological pH. On the other hand, the methyl group in the donor **1.221** comes from a tertiary amine, making a potential anionic tetrahydrofolate an exceptionally bad leaving group with an estimated pK_A > 30 for the corresponding N-H of the folate.[99] Therefore, homocysteine **1.219** and N^5-methyl-tetrahydropteridine **1.221**, brought together in the cobalamin-independent MetE, are expected to be completely unreactive for methyl transfer and it is strongly believed that some sort of activation of the substrates has to occur prior to this reaction.

Before crystal structures of the enzyme became available, studies[100-102] had identified zinc in the active site and assigned its role in the binding and activation of Hcy. It was believed that the binding goes along with a deprotonation of the thiol functionality in order to make it a better nucleophile for the transfer of a methyl group from MeTHF **1.221**. This proposal was supported by structural investigations on pH dependence of the catalytic activity, which found the optimum range to be between pH = 6 and 8. Beyond this range, the catalytic activity decreases rapidly with the enzyme at pH = 4.6 being only 7 % as active as at pH = 7.5. In the last couple of years, structures of MetE from different organisms were obtained, giving more information about coordination and the nearby environment of the metal.[102-106] It was found that zinc is coordinated in tetrahedral fashion by two Cys, one His and one Glu residues. From crystal structures of zinc-replete *T. maritima* MetE with and without bound Hcy,[103] it was revealed that binding of Hcy does not proceed *via* a dissociative mechanism, being very common for zinc-containing active sites in enzymes and in which the Glu oxygen would be replaced by the substrate sulfur. Instead attack of Hcy occurs at the backside of the metal opposite to the Glu residue effecting inversion of the zinc geometry (Scheme 1.49) and hence

two models for this conversion were proposed.[104] In the Induced-Fit model, Hcy binding effects conformational rearrangement and Glu displacement, while the Dynamic Equilibrium model assumes oscillation between two tetrahedral geometries of the zinc going through a trigonal bipyramidal transition state even in the absence of Hcy.

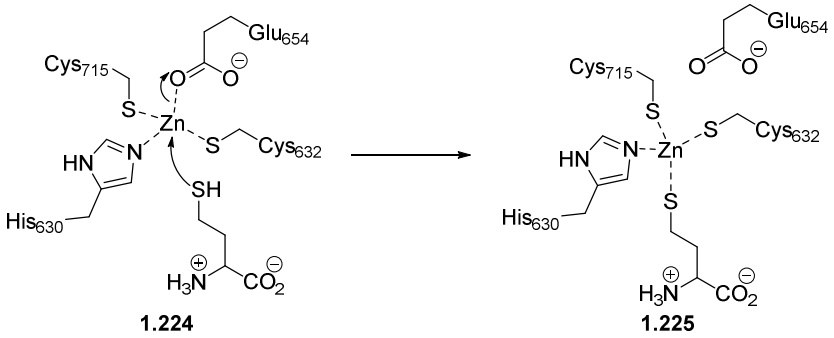

Scheme 1.49 Binding of Hcy to zinc and associative displacement of the Glu654 residue

Even before Ferrer *et al.* published[106] the first crystal structures of MetE from *Arabidopsis thaliana* and confirmed Hcy as being tightly ligated to a zinc ion, Matthews *et al*. had suggested an important role for zinc in the activation of Hcy to address the problem with the low nucleophilicity of thiols towards tertiary amines. Her group showed not only that wild-type MetE from *E. coli* contains 1.02 eq. of Zn^{2+} but also used extended X-ray absorption fine-structure analysis (EXAFS) studies[100,101] to indicate the metal being ligated by two N- or O- and two S-atoms. From these findings it was proposed that zinc acts as a Lewis acid, lowering the pK_A of Hcy, such that the substrate is present in its more nucleophilic thiolate form at neutral pH.

Addressing the second problem, that amines are very poor electrophiles (as an amide anion would be the leaving group), the relevant scientific community has agreed that activation of MeTHF **1.221** also has to occur to make the transfer of the methyl group feasible. It has been long suggested[107-110] that coordination of N^5 with an electrophilic species such as a proton or a coordinating amino acid residue in the active site of the enzyme, would generate an electron-deficient centre at N^5 resulting in a more susceptible attack by the thiolate (Scheme 1.50). Moreover, in this way a secondary amine (tetrahydrofolate THF **1.223**) would be expelled, which would present a much better leaving group rather than an amide anion. The required proton source has yet not been identified but in rapid reaction studies Matthews[109] found changes in the Me-H_4PteGlu$_3$ absorbance spectrum which are consistent with protonation at N^5 in the ternary complex and support an acid-catalysed S_N2 mechanism.

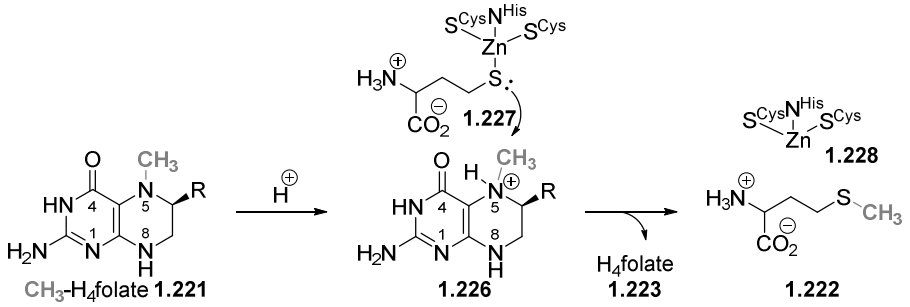

Scheme 1.50 The proposed acid-catalysed S_N2 mechanism for the methyl transfer from MeTHF **1.221** to zinc-bound Hcy **1.227**.

The proposal for the activation of MeTHF **1.221** by coordination on N^5 was modelled by Pandit *et al.*[108] more than 15 years ago. His group examined reactions between various substituted quaternary ammonium salts and thiolates of thiophenol and homocysteine. They also prepared a model of the cofactor N^5-MeTHF which was then quaternised at N^5 (**1.230**), using methyl iodide to produce an additional methyl group to mimic electrophilic activation on this position. This salt **1.230** was first reacted with potassium thiophenolate **1.229** under assistance of 18-crown-6 in acetonitrile at 70 °C over 24 h to yield 57 % of thioanisole **1.231** (Scheme 1.51).

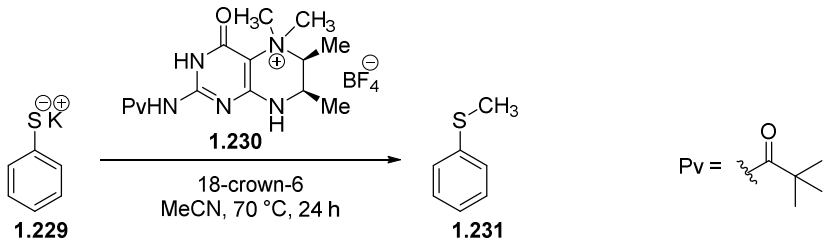

Scheme 1.51 Methylation of potassium thiophenolate by pterin salt **1.230**.

In a second experiment (Scheme 1.52), the pterin salt **1.230** was reacted with homocysteine **1.219** in the presence of sodium hydroxide as a base in aqueous ethanol at 70 °C for 24 h. The NMR spectrum of the mixture showed “clearly recognisable” signals for methionine **1.222** but also for the demethylated pterin derivative of **1.230** and the disulfide corresponding to homocysteine. From the proton integrals they observed a 1:1 ratio of methionine **1.222** and tetrahydrofolate and estimated the reaction to yield 40 % methionine from the methyl transfer from pterin salt **1.230** to homocysteine **1.219**.

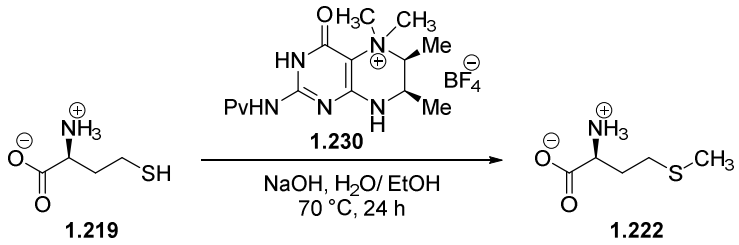

Scheme 1.52 Pandit's model reaction for methyl transfer catalysed by MetE.

The essential need for substrate activation of the MetE-catalysed methyl transfer reaction was shown by studies which were done almost 50 years ago when Schrauzer and Windgassen[111] employed simple model substrates to examine alkyl transfer from nitrogen to sulfur. Preliminary studies with quaternary ammonium salts and thiols in polar neutral or weakly alkaline solution at temperatures up to 60 °C did not lead to reaction, although the reaction was energetically reasonable from a thermodynamic perspective. Also, they noticed that cationic sp^2 hybridised nitrogen centres as in **1.232** and **1.234** (Scheme 1.53) – unlike tertiary amines - readily transferred methyl groups to thiophenolates **1.233** in ethanol at room temperature. In a test series, relative reaction rates for *N*-methylpyridinium **1.232**, *N*-methyl-8-hydroxyquinolinium **1.234** and methylaquocobaloxime **1.236** (3600:1:0.1) were determined.

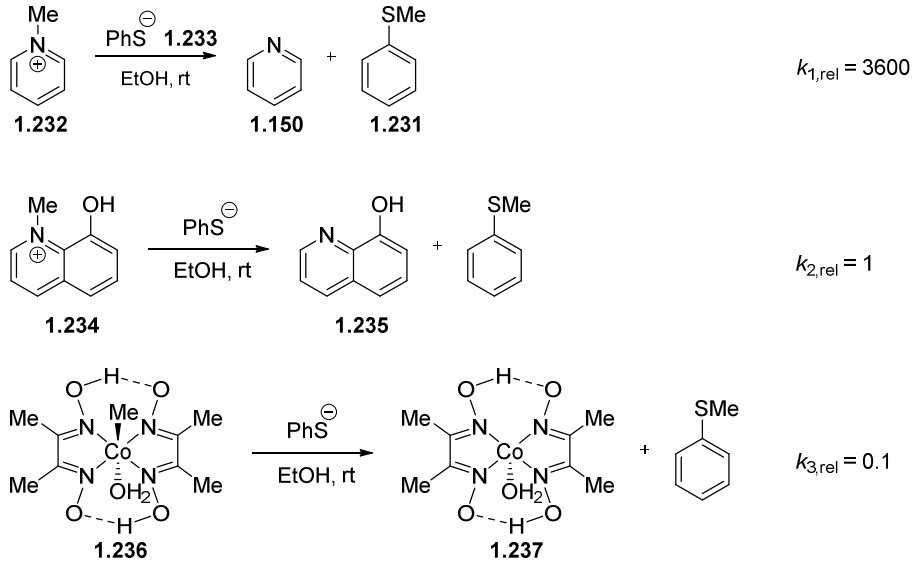

Scheme 1.53 Relative rates for methyl transfer to thiophenolate.

However, focussing on tertiary amines as model substrates for N^5-methyltetrahydrofolate, attempts with various simple trialkylamines and thiols were not successful, even when applying kinetic activation up to 100 °C. Using the *N*-methyl derivative of tetrahydro-8-hydroxyquinoline **1.238** as a simple model for the cofactor, significant conversion for the reaction with thiophenol **1.239** could

only be observed under very harsh conditions at 170 °C for 24 h, yielding only 7 % phenyl methyl sulfide **1.231**.

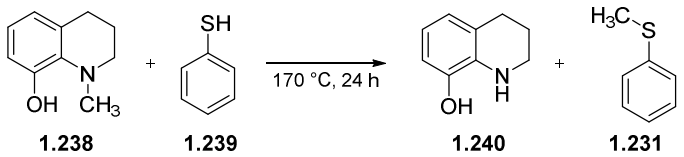

1.238 **1.239** **1.240** **1.231**

Scheme 1.54 Simple substrate used by Schrauzer and Windgassen[111] to model the reaction catalysed by MetH and MetE.

The ideas around the activation of homocysteine and Me-THF resulting from model studies summarised above, that is binding of Hcy to zinc in its thiolate form and activation of N^5 by protonation, have been accepted and are the current working hypothesis. However, many problems and unsolved questions are connected with this idea. The greatest obstacle for the activation of the substrates is their compatibility with neutral pH. To be in the right activation mode, the homocysteine has to be present in the thiolate form, with MeTHF being protonated at N^5. These postulates are contradictory as protonation of the pterin at N^5 occurs below pH 5. On the other hand thiols have a pK_A of 10. Matthews declares[99] that in aqueous solution protonated Me-THF would transfer its proton rather than the methyl group to a thiolate; hence proton transfer must be avoided. Nature would have to bypass this incompatibility by lowering homocysteine's pK_A below 7 while raising the pterin's pK_A above 7 at the same time and/ or by controlling the approach pathway for reaction.

It has been said that nature lowers the pK_A of Hcy's functional group by binding the homocysteine in its thiolate form to a zinc centre within the enzyme. Even though this move appears quite elegant, binding to an electrophilic metal centre does not only lower the pK_A but can also decrease the nucleophilicity of the functional group dramatically. Therefore the question arises of whether a zinc-bound thiolate would be strong enough to attack the methyl group of protonated MeTHF. Several attempts have been made modelling the activation of Hcy by zinc and looking into the nucleophilic strength of zinc-bound thiolates. Wilker and Lippard studied[112] the kinetics of $Zn(SPh)_4^{2-}$ complexes **1.241** reacting with the mild methylating agent trimethyl phosphate **1.243** at 25 °C and concluded that an S_N1 pathway at the zinc centre for the formation of methylthiophenyl ether **1.131** was reasonable (Scheme 1.55). The obtained data were consistent with a dissociated thiolate **1.233** being the active species and the liberation of this intermediate as the rate-determining step (rds). Interestingly, the counter-ion for $Zn(SPh)_4^{2-}$ was represented by tetramethyl ammonium but no methyl transfer between anion and cation was observed under the given reaction conditions.

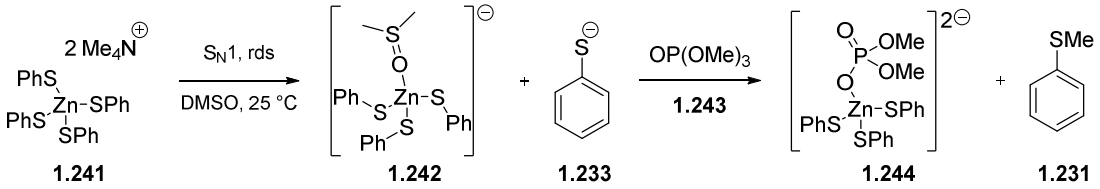

Scheme 1.55 Wilker and Lippard's probe[112] for testing the nucleophilic strength of zinc-bound thiolates. In this case "free thiolates" **1.223** are the active species.

Closer models of the enzyme's active centre have been presented[113-115] by Vahrenkamp's tetragonal coordinated pyrazolylborate-zinc-thiolate **1.245**, which reacts with various methylating agents such as methyl iodide, dimethyl sulfate and trimethylsulfonium iodide at room temperature and neutral pH in non-polar chloroform over 24 h to give the methylthioethers in quantitative yield. To use methylating agents which would be closer to the reaction with MeTHF or SAM, complex **1.245** was treated with the less powerful methyl donor trimethylsulfonium iodide **1.246** and *N*-methyl pyridinium iodide. The nature of these reactants required acetonitrile as a more polar solvent to dissolve them. While trimethylsulfonium iodide **1.246** performed clean transmethylation at higher temperature to yield ethylmethyl sulfide **1.247**, the *N*-methylpyridinium salt could not transfer its methyl group to the thiolate even at elevated temperature.

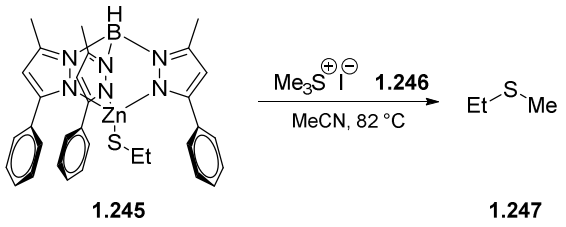

Scheme 1.56 The successful methylation of zinc-bound thiolate as a simple model for the reaction catalysed by the cobalamin-independent MetE.

Transalkylations from phosphotriesters to zinc-bound thiolates under mild and non-polar conditions have not been achieved in the laboratory as yet. Only by switching to polar solvents (MeOH, DMSO) and elevated temperatures, where zinc-unbound thiolates are the active species, are such reactions known to proceed. This is still far away from the level of reactivity which would be needed for methyl abstraction from tertiary amines and it is becoming clear that the methyl donor, MeTHF, also has to undergo some kind of activation to enable catalysis within methionine synthase.

Dealkylations of amines have been known in the literature for more than 100 years. One of the well-known examples is the Von Braun reaction,[116,117] in which its discoverer achieved a two-step reaction of cyanogen bromide with tertiary amines (Scheme 1.57). The very first reactions were performed on *N,N*-methylpropylaniline **1.248** and it was realised that the smaller more accessible alkyl group is

that preferred for attack by the bromide. While benzylic and allylic groups are easiest to cleave, phenyl groups on the nitrogen remain untouched (and in fact, they slow the reaction down).

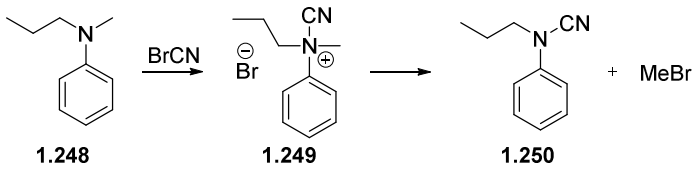

Scheme 1.57 The effect of cyanogen bromide on tertiary amines in the Von Braun reaction.

The driving force for all these reactions is the highly electrophilic nature of the carbon in the cyanogen bromide caused by the electronegative bromine and nitrogen atom and activating it towards nucleophiles. Chloroformates (benzyl chloroformate **1.252** in Scheme 1.58 have a reaction pattern similar to cyanogen bromide as shown here in the example of the demethylation of erythromycin **1.251**.[118,119]

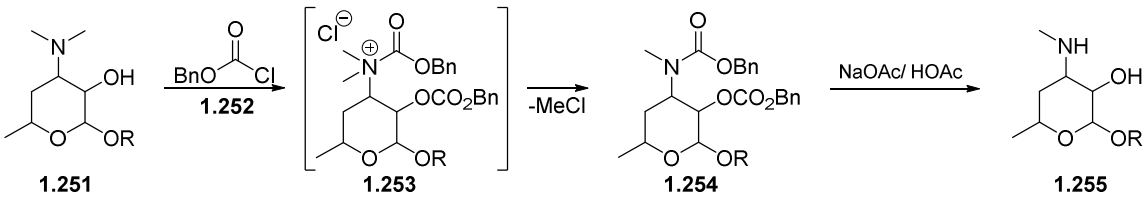

Scheme 1.58 Demethylation of tertiary amines with chloroformates.

Azodicarboxylic acid esters such as diethyl azodicarboxylate (DEAD) have been used for dealkylation reactions for many years, although the mechanism of this transformation had been subject to speculation at the beginning. Diels was the first to examine the reaction of these compounds with tertiary alkylamines.[120,121] With *N*,*N*-dimethylaniline he isolated an adduct, assigning structure **1.256** to it.

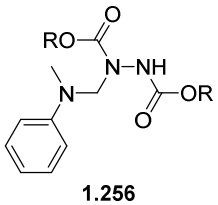

Figure 1.6 This structure was assigned to the addition product from DEAD and *N*,*N*-dimethylaniline by Diels.[120]

On treatment with Brønsted acids these compounds produced the corresponding monodemethylated amines along with formaldehyde. Kenner and Stedman[122] confirmed the structures of these adducts by IR techniques and suggested coordination of the amine nitrogen by

the electrophilic azo group (**1.258**) followed by ylide formation (**1.259**) and an aza-anionic 1,2-shift (**1.260**) (Scheme 1.59).[123]

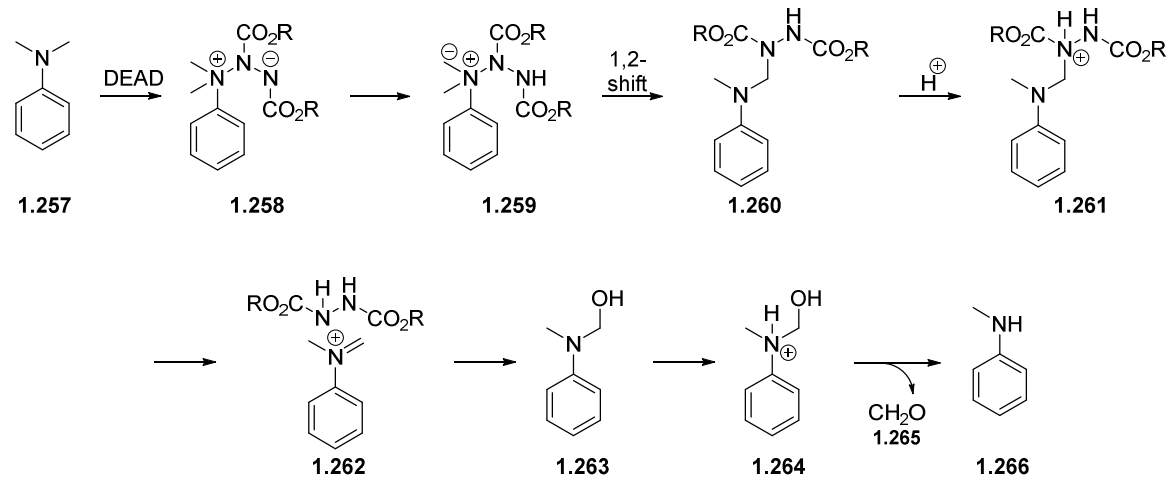

Scheme 1.59 The mechanism of the demethylation of DEAD applied to tertiary amines.

Other dealkylation reactions involving quaternisation of the tertiary amine (**1.269**) and an S_N2 pathway are reported by Allevi *et al.*[124] using sulfide as the alkyl displacing reagents (Scheme 1.60). However, harsh conditions (120 °C) and very polar solvents (sulfolane) were applied to obtain various alkyl substitutions on the tertiary amine in a one-pot synthesis.

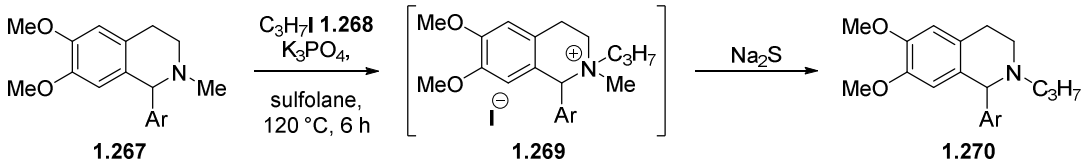

Scheme 1.60 *N*-Demethylation by quaternisation applying harsh conditions in a polar medium.

Electrophilic activation of the nitrogen atom in a tertiary amine followed by S_N2-type displacement of α-alkyl groups has been reported by Suckling and Waigh.[125] 2-Chloro derivatives of benzoxazole **1.271** and benzothiazole were reacted with tertiary amines leading to nucleophilic substitution of the chloride, which then displaced methyl and simple alkyl groups from the quaternised intermediate (Scheme 1.61).

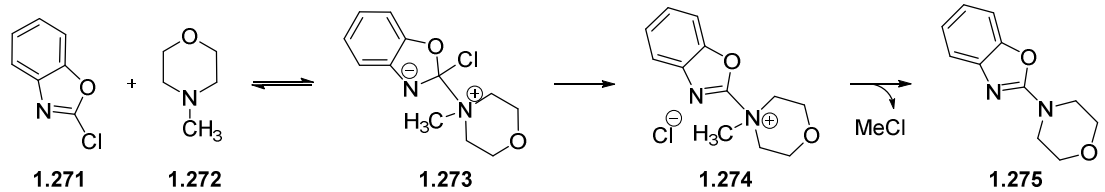

Scheme 1.61 Reaction of 2-chlorobenzoxazole **1.271** with *N*-methylmorpholine **1.272**.

Interestingly, when using *N*-methylpyrrolidine **1.276** or *N*-methylpiperidine as the tertiary amine, it was found out that a ring-opening reaction was preferred to methyl transfer (Scheme 1.62). Again polar media (tetrahydrofuran) and thermal activation (reflux or neat at 130 °C) were needed for these reactions to occur.

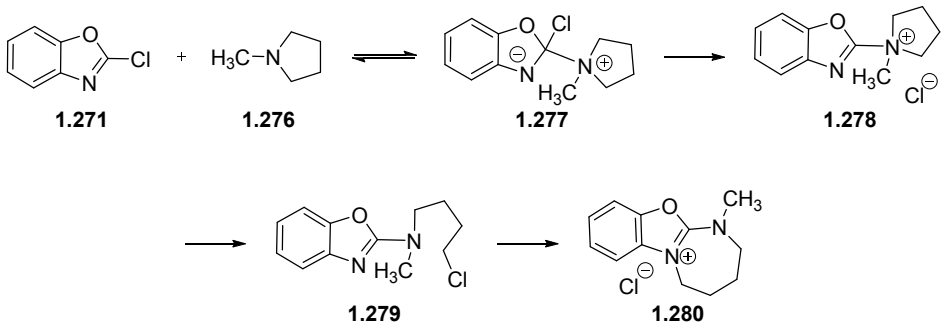

Scheme 1.62 Ring-opening of *N*-methylpyrrolidine through electrophilic aromatic substitution of 2-chloro benzoxazole.

A quite different dealkylation method for tertiary amines was presented by Ma *et al*.[126] His group reported a demethylation reaction by means of *N*-iodosuccinimide **1.282** (Scheme 1.63), which they claim to mimic the metabolism pathway mediated by cytochrome P450. The mechanistic route involves not only the presence of a base to abstract a proton from the alkyl group and form an iminium species, but also water for subsequent hydrolysis to an *O*,*N*-hemiacetal **1.286** and secondary amine **1.287**.

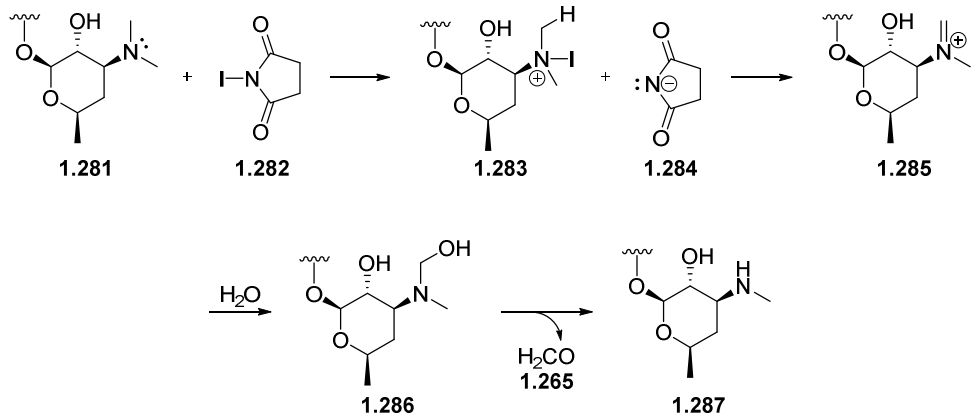

Scheme 1.63 Mimicking the oxidation reaction catalysed by cytochrome P450 with *N*-iodosuccinimide **1.282**.

In the literature there is little research on methyl migration from protonated tertiary amines, which is proposed to be the working mode of electrophilic activation in the enzyme. Only a couple of years ago, a major contribution addressing this question came from Callahan and Wolfenden.[127] When they had a closer look at the previously reported spontaneous decarboxylation of glycine in dilute aqueous solution at elevated temperature to form methylamine, they noticed small amounts of di-

and trimethylamine increasing with time. In kinetic studies they examined methyl group migration between aliphatic amines incubated with their conjugated acids at elevated temperature where competing water as a methyl acceptor was neglected. For example, in aqueous media with HCl half-titrated dimethylamine **1.288** led to methylamine **1.291** and trimethylamine in equimolar amounts (Scheme 1.64). This reaction was found to be of second order.

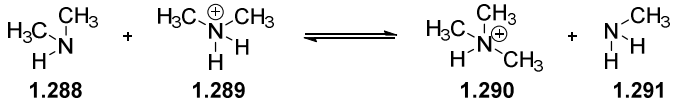

Scheme 1.64 Transmethylation from dimethylammonium ion to dimethylamine.

However, the rate constant *k* at 25 °C for the methyl transfer from tetramethylammonium ion **1.292** to dimethylamine **1.288** in aqueous media was determined to be 1.9 x 10^{-12} $M^{-1}s^{-1}$, a rather slow process (Scheme 1.65). Interestingly, under the same reaction conditions it was found that methyl transfer from trimethylsulfonium ion was 10^4-fold faster than from tetramethylammonium ion.

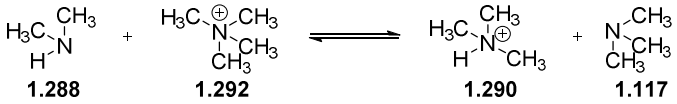

Scheme 1.65 Transmethylation from tetramethylammonium to trimethylamine.

All of the methods for dealkylation of tertiary amines shown so far, involve quaternisation or similar electrophilic activation of the amine nitrogen prior to alkyl transfer. The more electron-withdrawing the activating group the easier alkyl cleavage occurs. Furthermore, inorganic chemists modelling the active site of the enzyme MetE are still far away from a mimetic image of the reaction assumed in the enzyme. Their zinc-bond thiolates are clearly not strong enough to dealkylate tertiary amines under mild and non-polar conditions. Reasonable alkyl transfer results have only been shown in cases where polar and thermally activated conditions were applied, in which a stronger nucleophilic free thiolate is the active species. However, even with free thiolate species only phosphate esters have been dealkylated, known to be better alkyl donors than tertiary amines by far.

From the last literature examples presented, involving the synthetically challenging cleavage of an N(sp^3)-C(alkyl) bond but also the weakly nucleophilic strength of the most potent zinc-complexes mimicking the zinc-bound thiolate form of homocysteine, it can be seen that the current mechanistic hypothesis (Scheme 1.66) faces some open questions. Hence, in the literature other routes have been discussed for both the cobalamin-independent and the cobalamin-dependent methyl transferase.[128]

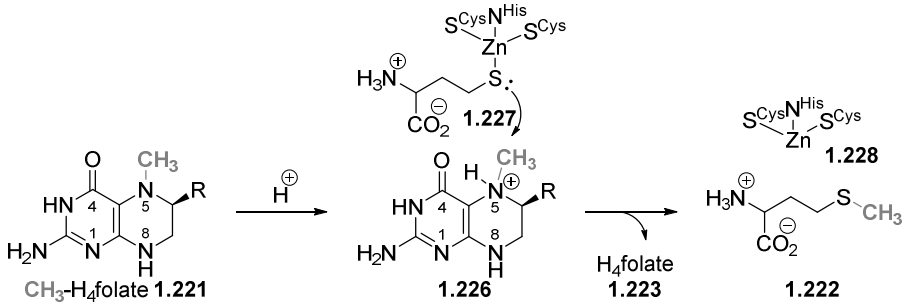

Scheme 1.66 An acid-catalysed S_N2 mechanism as the current mechanistic hypothesis for the methyl transfer in the enzyme MetE.

Focussing on the pterin substrate, the question arises as to what level of activation is really needed to activate MeTHF for alkyl transfer. As seen from the fascinating reactivities of some superelectrophiles introduced at the beginning of this chapter, one has to wonder if superelectrophilic activation of MeTHF could possibly exceed the level of activation needed for the methyl group transfer to Hcy. The redox systems of pteridines, dihydropterins and tetrahydropterins were extensively examined by Scrimgeour and co-workers[129,130] finding these compounds to be easily oxidised, hence one way of generating such an electron-deficient species would involve 2-electron oxidation to afford substrate activation as envisioned in **1.293**. This species would produce sp^2-hybridisation at N^5, which is expected to be even more susceptible to methyl transfer. Alternatively, another mode of superelectrophilic activation must be considered, that is closer to the current accepted mechanistic proposal and does not involve oxidation. A viable reactivity enhancement would be envisioned in a MeTHF substrate **1.294** that has not only encountered single electrophilic activation at the N^5-position but also a second electrophilic contact at N^1, possibly provided by nearby amino acid residues, that would boost the activation.

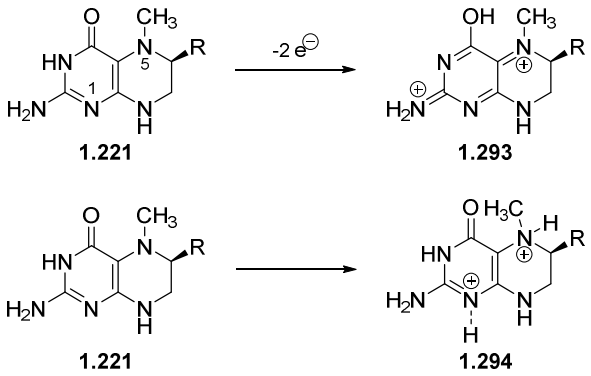

Scheme 1.67 Superelectrophilic activation of MeTHF *via* 2-electron oxidation in **1.293** or two-fold electrophilic coordination at the N^1- and N^5-position in **1.294**.

2 Aims

In the introduction section it has been shown that the scope of the reaction of triflic anhydride with the carbonyl group is of high synthetic interest. However, the highly reactive intermediates in most of these fascinating transformations cannot be observed and the exact mechanistic pathway remains vague. Within our laboratories, the isolation and full characterisation of these superelectrophilic species, which had previously only been observed as product mixtures in solution (except Curphey and Prasad's pyrimidine-based 1,3-superelectrophile), succeeded. Amidinium disalt compound **1.194** and **1.198** were shown to transfer methyl groups readily from their sp^3-hybridised nitrogen centre to moderate nucleophiles such as triethylamine and triphenylphosphine. The cleavage of the nitrogen-carbon bond is of great interest to the scientific world and especially in case of the cobalamin-independent methyl transferase, MetE, as the enzymatic alkyl transfer from nitrogen to sulfur remains mysterious.

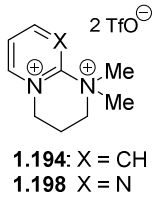

1.194: X = CH
1.198 X = N

Figure 2.1 Isolated and characterised amidinium disalts, synthesised within the Murphy research group.[77-79]

The alkylating strength of these new superelectrophilic amidinium disalts was shown to be comparable with dimethyl sulfate, a strong organic methyl donor. Their relevance to [Fe]-hydrogenase-catalysed fixation of hydrogen and carbon dioxide has also been highlighted and this aspect is discussed in the theses of colleagues. Hence, the main goal of my research was to study the reactivity of amidine disalts and in particular to explore the preparation of disalts that would be even more reactive in methyl transfer activity than **1.194** and **1.198**. Describing the factors that facilitate the cleavage of an N(sp^3)-C bond, determining the reactivity of the superelectrophilic species and examining the mechanistic pathway in which these highly electrophilic species are formed and react further is what this thesis deals with.

3 Results and Discussion

3.1 Synthetic and computational insights into naphthalene-based amidinium dications

Broadening the investigations on alkyl transfer and hydrogenation involving amidine disalts, synthesis of model compound **3.1** was attempted.

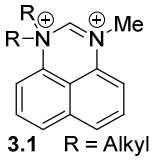

Figure 3.1 Generic amidine dication model.

Amidinium dication **3.1** should be an even more reactive species than salts **1.194** and **1.198**, as neither of the nitrogen atoms is incorporated into an aromatic ring, so no disruption of aromaticity is needed when a nucleophile adds to the amidinium centre (this would lead to studies on hydrogenation by a colleague, Callum Scullion). Moreover, no resonance delocalisation of the positive charges by the naphthalene π-system is possible in **3.1**.

Initial attempts at synthesising dication **3.2** by Markevicius[131] focused on retrosynthetic Scheme 3.1. Based on Charette's insights into reactions of formamides with triflic anhydride described earlier in the introduction, it was proposed that *N*-methylformamide **3.3** would first give rise to an iminium triflate species, which should instantaneously transform to the dication **3.2** by nucleophilic attack of the nearby tertiary amine residue. The details of this transformation will be discussed shortly.

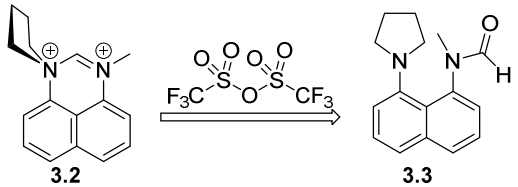

Scheme 3.1 Retrosynthetic route to amidine dication **3.2**.

The first synthetic step (Scheme 3.2) in the route to the desired *N*-methylformamide **3.3** was alkylation of 1,8-diaminonaphthalene **3.4** by 1,4-diiodobutane in anhydrous DMF at moderate temperature. The low yield (23 %) of product **3.5** is explained by the great amount of by-products

and the high tendency towards oxidation of 1,8-diamino derivatives, which was observed on air exposure during purification and led to discolouration of the product.

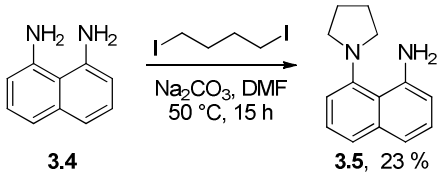

Scheme 3.2 Synthesis of 8-(pyrrolidin-1-yl)naphthalen-1-amine.

1,8-Diaminonaphthalene derivatives have been extensively reviewed[132,133] in the literature with 1,8-bis(dimethylamino)naphthalene as one of the most prominent exponents. This compound is also known as "proton sponge" for exhibiting characteristics of a strong base with its two nitrogen lone pairs which are capable of synergistic abstraction of a proton. Hence, an interesting finding in the ^{1}H-NMR spectrum for compound **3.5** can be explained, which indicates two different magnetic environments for the four α-protons on the pyrrolidine ring. Due to H-bonding between the amino functionalities, the pyrrolidine ring sits orthogonal to the aromatic system with one pair of α-protons (red in Figure 3.2) pointing towards the NH_2 group and with the other α-protons (green) facing away.

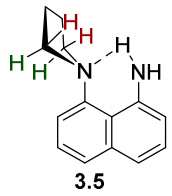

Figure 3.2 Different magnetic environments for the α-protons in the pyrrolidine residue in 8-(pyrrolidin-1-yl)naphthalen-1-amine **3.5**.

The next synthetic step required formylation of the free amine group, for which formic pivalic anhydride **3.7** was chosen. Although other formylation procedures are available, this reagent provides one of the highest reactivities and excellent selectivity, and hence mild reaction conditions for the modification of the free amino group can be applied. As this mixed anhydride is not commercially available, it was synthesised from cheap sources, sodium formate and pivaloyl chloride **3.6**, following the reported method by Vlietstra *et al.*[134] under neat conditions at temperatures between 0 and 10 °C. This compound showed good stability for several weeks in the refrigerator at -27 °C.

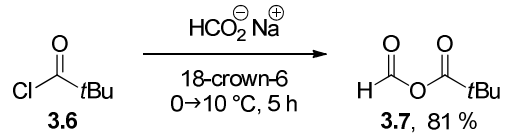

Scheme 3.3 Synthesis of formic pivalic anhydride.

8-Pyrrolidinyl-1-aminonaphthalene **3.5** was then reacted with formic pivalic anhydride **3.7** in DCM at 0 °C to yield the desired compound **3.8**.

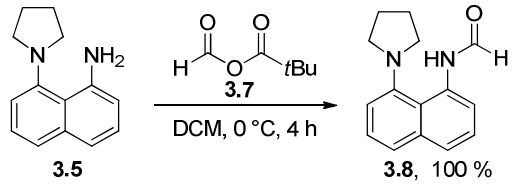

Scheme 3.4 Synthesis of 8-pyrroldin-1-yl-1-naphthylformamide **3.5**.

Interestingly for *N*-H formamide **3.8**, in deuterochloroform the ^{1}H-NMR spectrum showed the presence of a 2:1 mixture of rotameric isomers with the main rotamer bearing the carbonyl CO bond *cis* to the aromatic substituent (Figure 3.3).

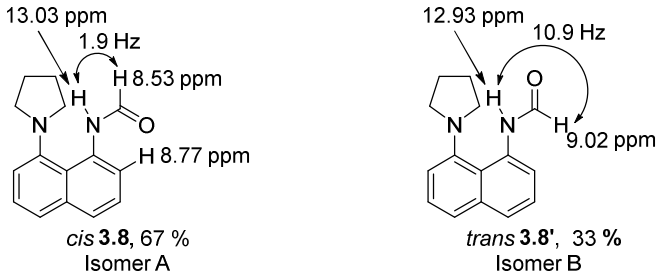

Figure 3.3 Selected chemical shifts and coupling constants for the two different rotamers of compound **3.8**.

In the ^{1}H-NMR spectrum (Figure 3.4) the most downfield signals correspond to the formamide nitrogen protons of the two isomers and lie at 13.03 ppm (major isomer) and 12.93 ppm (minor isomer) integrating to 0.60 and 0.31 protons, respectively. These chemical shifts in the downfield region are also consistent with strong H-bonding to the nitrogen incorporated in the pyrrolidine residue. The signal for the formyl proton in the major isomer is found more upfield (8.53 ppm, J = 1.9 Hz) than the minor one (9.02 ppm, J = 10.9 Hz) and exhibits a smaller coupling constant, which is consistent with the general rule of the *trans* vicinal coupling constant being greater than the *cis* coupling constant.[135,136] An interesting aspect is the chemical shift for the proton in the *ortho*-position to the formamide functional group. While in the minor *trans*-isomer the signal is found in the expected aromatic region between 7.0 and 8.0 ppm, the chemical shift for this proton appears at 8.77 ppm in the major *cis*-isomer. This finding is explained by the nearby carbonyl group exerting a

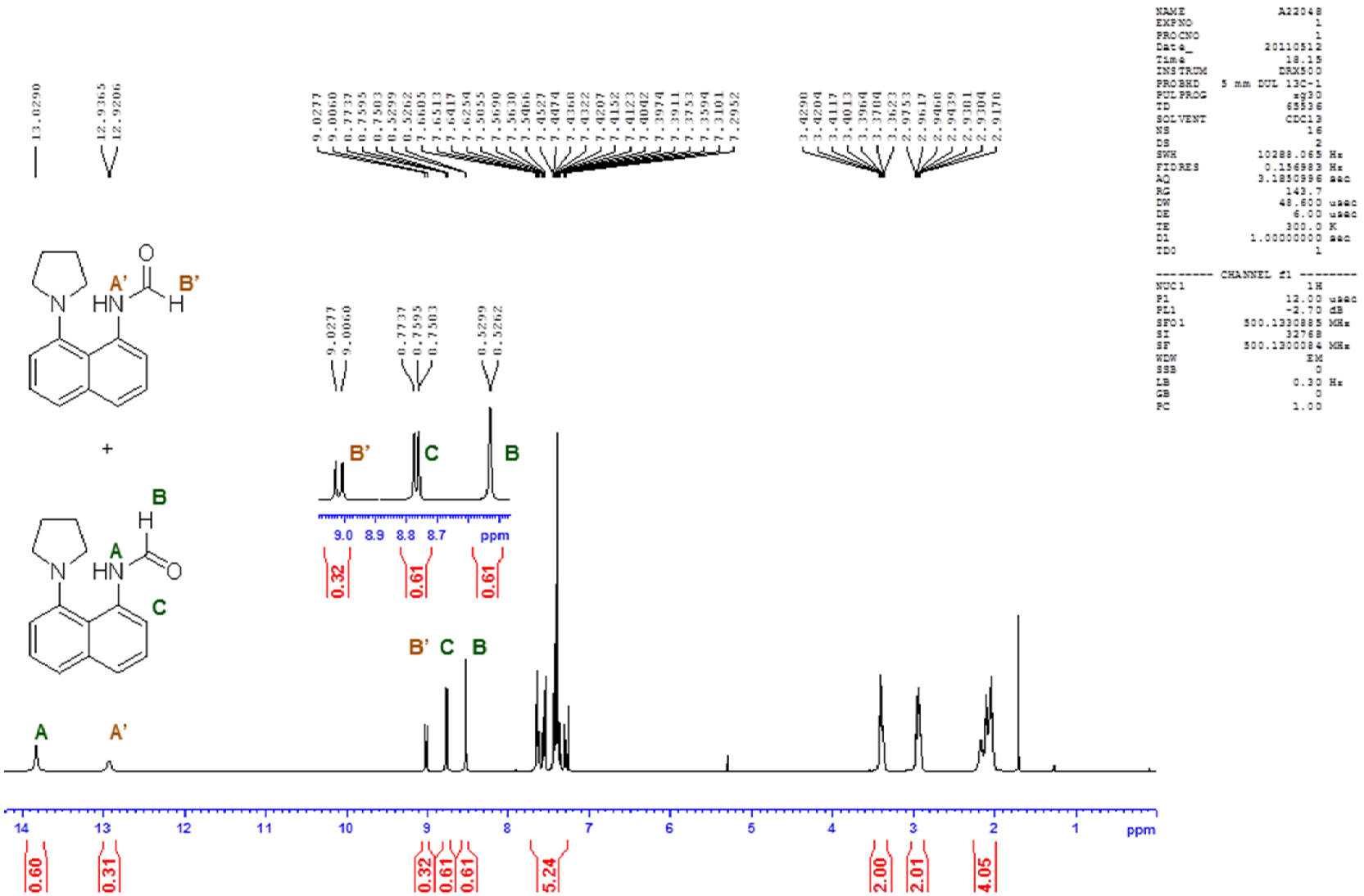

Figure 3.4 ^{1}H-NMR spectrum of *N*-pyrrolidyl-*N*'-formamidylnaphthalene **3.8**. In $CDCl_3$ the product is present as a 2:1 mixture of *cis*- (green) and *trans*-rotamers (orange).

strong magnetic anisotropy effect on the *ortho*-proton. The assignment of this signal to the *ortho*-proton is further confirmed by the overall integration of 5.24 H instead of 6.00 H in the normal aromatic region, indicating one proton from the major isomer being shifted.[137,138]

The finding that the major rotamer exhibits the carbonyl group *cis* to the aryl residue ((*Z*)-isomer) appears surprising as literature suggests[139-141] that the more stable conformation in acylanilides ArNRCOR' should be when aromatic groups are *trans* ((*E*)-isomer) to the carbonyl group. The centres of electron density, *i.e.* the electronegative carbonyl oxygen on one hand and the electron-rich phenyl residue on the other, are then separated the most. However, DFT calculations with the B3LYP functional and 6-31G* basis set for this substrate predicted a lower energy (3.6 kJ/mol difference) for the rotamer with the carbonyl and aromatic group *cis* ((*Z*)-isomer) to each other, being consistent with the experimental findings. This illustrates the difference between secondary and tertiary acyl anilides. As stated above, the proton in the *ortho*-position to the formamide residue experiences a great downfield shift induced by the anisotropy of the carbonyl group.[142-148] Here the term anisotropy describes magnetic fields, which derive from regions of high electron density of chemical bonds. These magnetic fields can vary depending on the direction of the chemical bond. Figure 3.5 depicts how the magnetic field of the carbonyl group deshields the *ortho*-proton so that its resonance frequency is found further downfield in the ^{1}H-NMR spectrum. This anisotropy effect was encountered in all later *N*-H formamide structures.

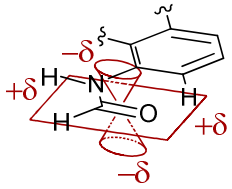

Figure 3.5 Electric shielding (-δ) and deshielding (+δ) fields induced by the carbonyl group in *N*-H formamides.

In the next step of the synthetic route, *N*-H formamide **3.8** was reduced with $LiAlH_4$ in THF at 0 °C over 4 h. Unlike the starting material, the product **3.9** was observed to be unstable due to oxidation, which was expressed in gradual discolouration inside a sealed flask over days. This enhanced tendency for discharging electrons can be explained by the electron-donating secondary amine group in **3.9** (mesomeric effect +M), having substituted a formamide residue in **3.8** by a more electron-rich alkylamino group.

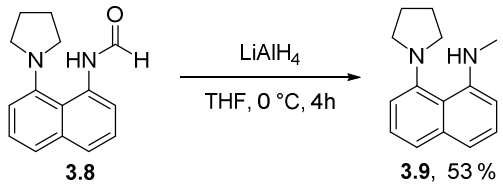

Scheme 3.5 Synthesis of *N*-methyl-8-(pyrrolidin-1-yl)-naphthalene-1-amine.

Formylation of the *N*-pyrrolidinyl-*N´*-methylnaphthalene **3.9** with the formic pivalic anhydride gave the desired *N*-methylformamide product **3.3**, for which the ^{1}H-NMR spectrum showed the (*E*)-isomer to be the more stable rotamer, as no aromatic signals appeared downfield-shifted from their normal chemical shift unlike for the *ortho*-proton in previously described secondary acylanilide **3.8**. Furthermore, the ratio between (*Z*)- and (*E*)-compounds appeared quite different than for the *N*-H formamide **3.8**, as from the ratio of integrals in the ^{1}H-NMR spectrum it was determined that approximately 95 % of the product had the carbonyl group and the naphthalene ring *trans* ((*E*)-isomer) to each other.[141]

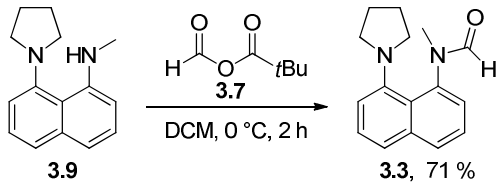

Scheme 3.6 Synthesis of methyl(8-pyrrolidin-1-yl-1naphthyl)formamide **3.3**.

Following the procedures which had been applied for synthesis of superelectrophilic species within our laboratories, the *N*-methylformamide **3.3** substrate was added to trifluoromethanesulfonic anhydride (triflic anhydride) in DCM at -78 °C using an electric syringe pump (0.254 mL/h). After 4.5 h of reaction time and upon removal of the solvent and excess triflic anhydride under reduced pressure, the ^{1}H-NMR spectrum did not indicate the presence of dication, and instead clean formation of a product was observed, for which structure **3.10** was assigned.

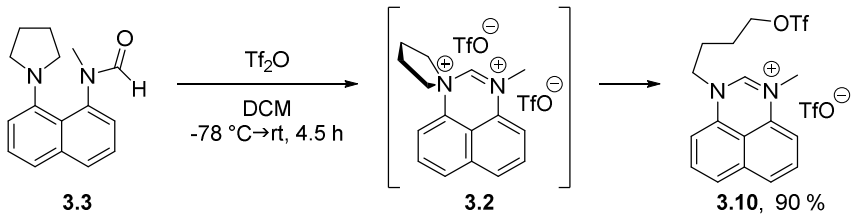

Scheme 3.7 Unexpected ring cleavage upon treatment of *N*-methylformamide **3.3** with triflic anhydride.

The possibility of having the desired dication **3.2** present was excluded, as the ^{1}H-NMR spectrum (Figure 3.6) showed the most downfield signal at 8.39 ppm, representing the proton of an amidinium

moiety as a singlet. From previous results within our research group[80] the proton shift for a dicationic amidine species would be expected further downfield in the region > 10 ppm. The two triplet signals (J = 5.8 and 7.5 Hz) in the aliphatic upfield region (signals F and G in Figure 3.6) together with the multiplet signal around 2.00 ppm indicate cleavage of the pyrrolidinyl ring in the starting material.

To confirm the unprecedented and fascinating outcome of this reaction, the product was subjected to nuclear Overhauser experiments (nOe) after the ^{1}H-NMR spectrum was obtained. The results from the homonuclear nOe experiments are shown in Figure 3.7. The bottom spectrum again shows the normal ^{1}H-NMR spectrum. Irradiation with the resonance frequency of protons G (red spectrum) results in spin polarisation transfer to protons A, D and J due to their physical proximity. However, protons F attached at the end of the carbon chain, which derives from the pyrrolidine ring lack proximity to other protons apart from those next to them in the chain. Therefore, irradiation of protons F only leads to expected spin polarisation to these nearby protons J (green spectrum).

The identity of this compound was finally confirmed by high resolution mass spectrometry. However, it presented a remarkable piece of chemistry, since a triflate anion, which is generally regarded as an extremely weak nucleophilic counterion, acted as a nucleophile to cleave the strong C-N bond originating in a tertiary amine.

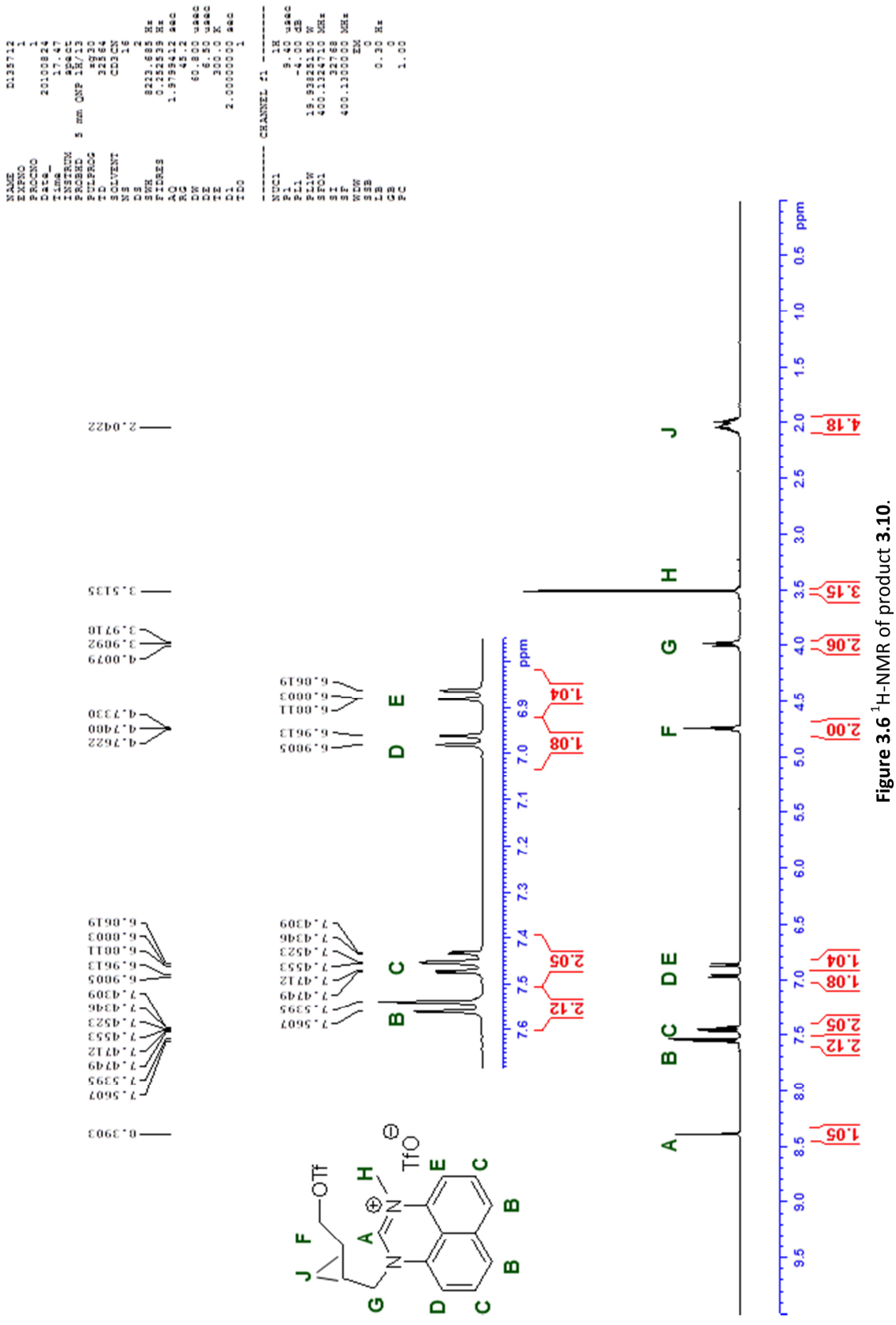

Figure 3.6 ^{1}H-NMR of product **3.10**.

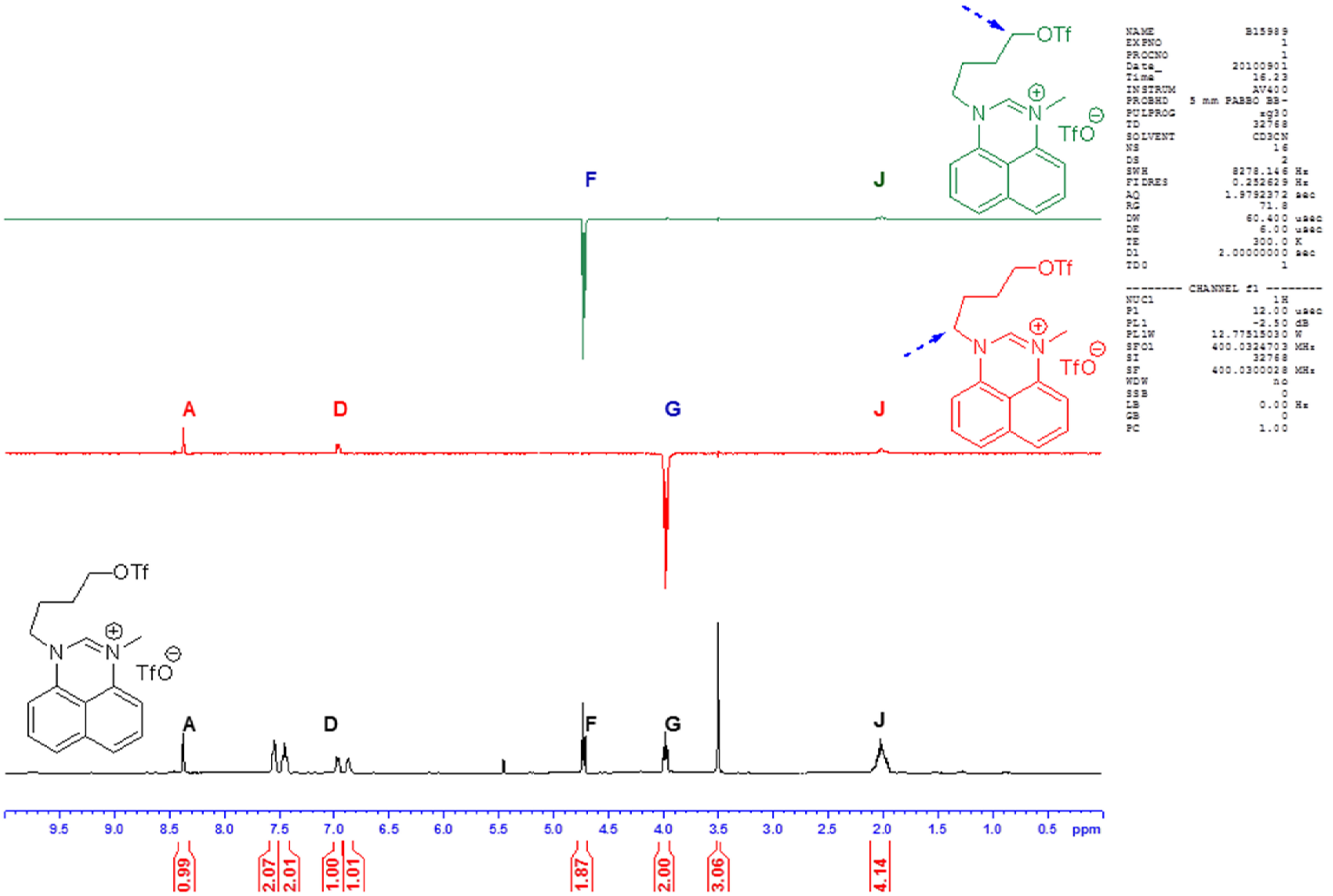

Figure 3.7 NOE experiments for compound **3.10**.

Two simple analogues were prepared to expand the scope of this intriguing reaction. The first slight amendment to the parent substrate was achieved by substituting the pyrrolidine ring for a piperidine ring. The synthetic route to this compound did not differ from the first one apart from the step creating the cyclic tertiary amine. Here, instead of 1,4-diiodobutane, 1,5-dibromopentane was used to synthesise the piperidine residue on one of the free naphthalene amines (Scheme 3.8).

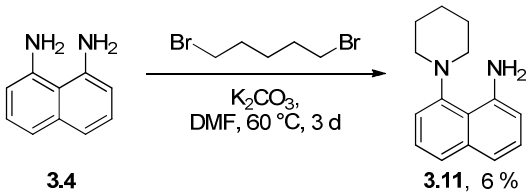

Scheme 3.8 Synthesis of 8-(piperidin-1-yl)naphthalen-1-amine **3.11**.

The corresponding *N*-methylformamide **3.14** was again prepared by formylation with formic pivalic anhydride, reduction with lithium aluminium hydride and formylation anew. Unlike the introduction of the cyclic tertiary amine, all synthetic steps proceeded with good yields from 76-95 % (Scheme 3.9).

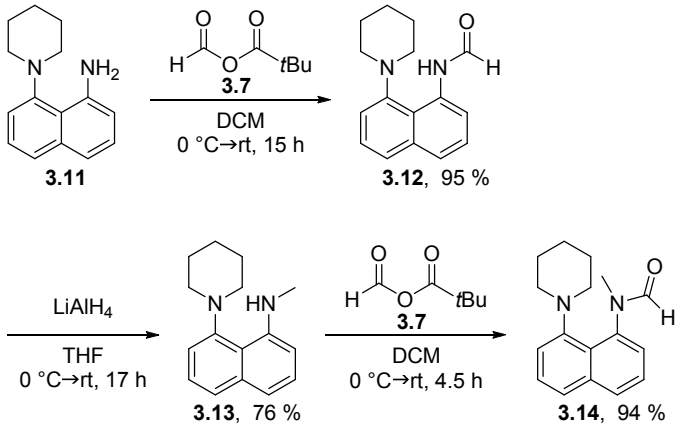

Scheme 3.9 Synthetic route to formamide **3.14**.

Treatment of this methyl(8-pyrrolidin-1-yl-1naphthyl)formamide **3.14** with triflic anhydride in DCM at -78 °C, again led to clean cleavage of the piperidine ring, forming product **3.15**.

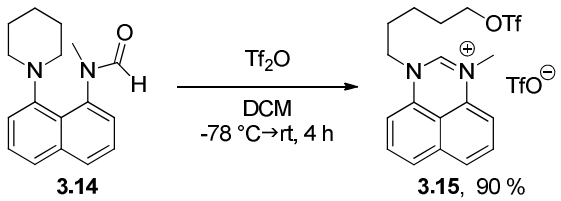

Scheme 3.10 Observed ring cleavage upon treatment of *N*-methylformamide **3.15** with triflic anhydride.

For the second analogue, the cyclic tertiary amine was substituted for a dimethylamino group. Following a procedure by Lloyd-Jones and Harvey,[132] 1,8-diaminonaphthalene **3.4** was reacted with two equivalents of methyl iodide and the desired *N*,*N*,*N*′-trimethylnaphthalene-1,8-diamine **3.16** was isolated from the by-products by flash chromatography (48 % yield). Again, being structurally close to proton-sponge [1,8-(bisdimethylamino)naphthalene] this substrate was unstable towards light and air, which was displayed in discolouration over days.

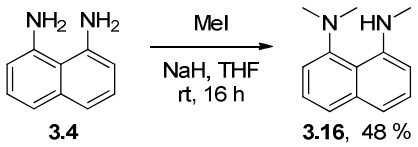

Scheme 3.11 Synthesis of *N,N,N*'-trimethylnaphthalene-1,8-diamine **3.16**.

Reaction of this naphthalene derivative with the formylation agent **3.7** afforded the *N*-methyl derivative **3.17** in excellent yield (96 %).

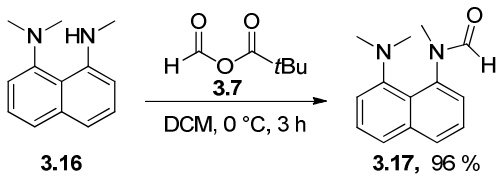

Scheme 3.12 Synthesis of *N*-methylformamide **3.17**.

Based upon our experience with the previous substrates, here the attack of a triflate anion was expected to demethylate the compound **3.17** from the dimethylamino residue. However, reaction of this derivative with triflic anhydride did not lead to complete demethylation. Although in the complex ^{1}H-NMR spectrum the signals for the symmetric demethylated monocationic product could be seen among others, no presence of starting material was observed. The reaction was repeated applying longer reaction times and/or with increased equivalents of triflic anhydride, but no clean product formation could be produced.

At first, it was assumed that if the reaction was to proceed *via* a dicationic intermediate **3.18** that this species would be much less soluble in organic media, due to lack of an aliphatic carbon ring and only small residues standing out of the plane of the naphthalene structure. In this case, the dicationic intermediate **3.18**, once precipitated out of solution, might not easily be accessible to subsequent attack by a triflate anion.

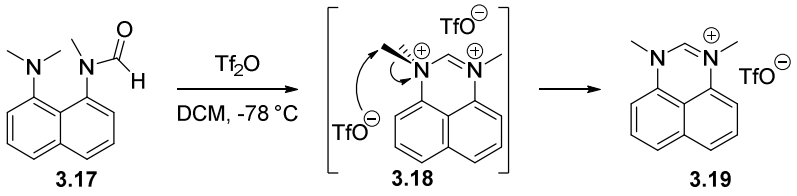

Scheme 3.13 The dicationic intermediate **3.18** is a nearly flat and highly charged intermediate, which was at first assumed to have low solubility in DCM.

This assumption was supported by ^{1}H-NMR spectra of the crude product, which showed a higher yield of the product **3.19** next to some unidentified impurities after the reaction conditions had been changed to involve stirring at 30 °C for 5 h followed by stirring for a further 15 h at room temperature. This heating was believed to render the intermediate disalt **3.18** more soluble and therefore susceptible to nucleophilic attack by the triflate anion.

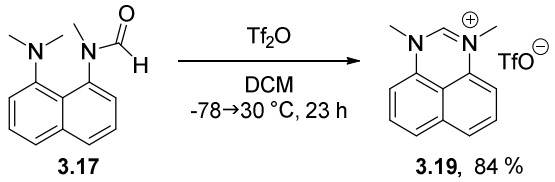

Scheme 3.14 Observed demethylation of *N*-methylformamide **3.19** upon treatment with triflic anhydride.

However, retrospectively and in regard to the kinetic studies of the alkyl transfer from this compound, which will be discussed later on, it is now believed that the poor solubility of the monocationic product **3.19** in deuterated DCM and chloroform has made the amount of by-products formed in course of the reaction look greater in the ^{1}H-NMR spectrum than it actually was. The enhanced signals of the impurities in the ^{1}H-NMR spectrum compared to the signals observed for product **3.19** led to the assumption that the reaction had not gone to completion. In this respect, a reported[149] work-up procedure, in which this compound was extracted from a saturated bicarbonate solution into DCM and then recrystallised from ethanol, was found unreproducible. This procedure was adopted but found ineffective for isolation of product **3.19**, as the compound, once dissolved in a solution of saturated bicarbonate, could not be extracted into DCM or any other commonly used organic medium (Et_2O, $CHCl_3$, EtOAc). Hence, the crude product was first triturated in diethyl ether and then recrystallised from ethanol to afford the perimidinium salt **3.19** in 84 % yield.

3.2 *In silico* studies of the alkyl transfer mechanism

Regarding the reaction mechanism for the small set of dealkylation reactions, the following route as seen in Scheme 3.15 was proposed. From well-explored reactions of formamides with triflic anhydride[142] it was suggested that in the first step an iminium triflate **3.20E** is generated. As the

starting material, formamide **3.17**, was found almost completely present in the (*E*)-conformation in NMR experiments, the reaction with triflic anhydride is believed to exclusively lead to an iminium triflate species **3.20E**, which is also in the (*E*)-configuration. Subsequently, intramolecular attack of the nearby tertiary amine on this species is proposed to form tetrahedral intermediate **3.21**.

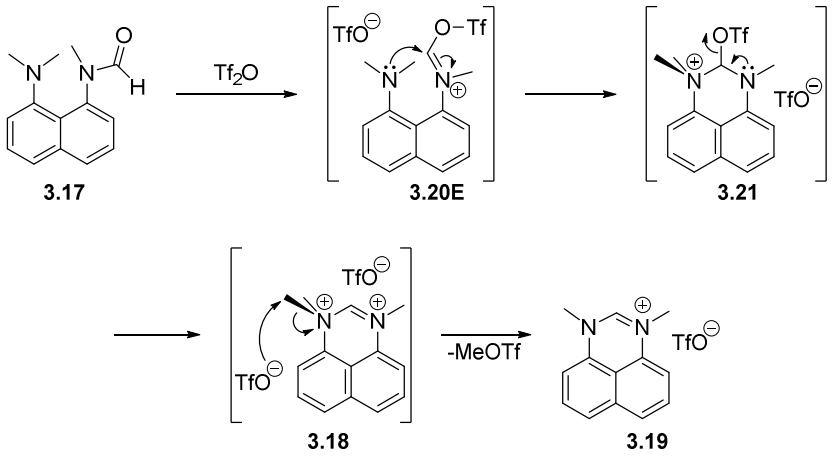

Scheme 3.15 Proposed mechanism for the reaction of *N*-methylformamide **3.17** with triflic anhydride.

For intermediate **3.21** two possible conformations can be described. As the carbon atom between the two nitrogen atoms is sp^3-hybridised in this intermediate, the attached triflate substituent can either be in the *pseudo*-axial position (**3.21a**) or in the *pseudo*-equatorial position (**3.21e**) to the naphthalene plane, as seen in Figure 3.8. However, as iminium triflate species **3.20E** should be exclusively formed in the (*E*)-configuration, intramolecular nucleophilic attack by the neighbouring tertiary amine group can only afford the tetrahedral intermediate **3.21e** with the triflate group equatorial to the ring plane.

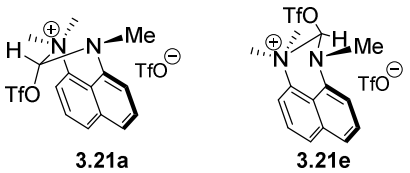

Figure 3.8 *Pseudo*-axial and *pseudo*-equatorial positions for the triflate residue in intermediate **3.21**.

The lone pair of electrons on the nitrogen atom can then flip within the tetrahedral intermediate **3.21e** to expel the triflate group and form the superelectrophilic disalt species **3.18**, which is now sufficiently electrophilic and reactive for alkyl transfer to only weakly nucleophilic triflate anions (Scheme 3.15). In the final step of the proposed pathway, the attack on the methyl group bonded to sp^3-hybridised nitrogen rather than the methyl group bonded to the sp^2-hybridised nitrogen can be explained by kinetic factors. Looking at the final product **3.19**, it is evident, that the stabilisation gained results from delocalisation of the newly formed electron lone pair over the π-system

including the amidinium moiety as well as the aromatic naphthalene backbone. Now, in the dicationic intermediate **3.18** the N(sp^3)-C bond aligns well with the π-system of the amidinium moiety and naphthalene plane, meaning that the process of bond breakage at this position should have a much lower energy transition state than for the N(sp^2)-Me bond.

In collaborations with Dr. Tell Tuttle, computational studies for the latter reaction were carried out by students Christopher Idziak and Greg Anderson to validate the mechanistic proposal and to explore any other routes to the formation of the observed product.[150] All calculations were performed using density functional theory on the Gaussian 09[151] software package. With the exception of structures **3.20E**, **3.20Z**, **3.21a** and **3.21e** all minima (reactants, intermediates, products) and maxima (transition states) were optimised using the M06 functional with a 6-311G(d,p) basis set. Structures **3.20E**, **3.20Z**, **3.21a** and **3.21e** were optimised using the M06L functional with a 6-311G(d,p) basis set. Single point calculations at the M06/6-311G(d,p) level of theory were then performed to obtain the corresponding M06 free energies. All reactant and product structures were optimised as their respective complexes. Solvation was modelled implicitly using the Conductor-like Polarizable Continuum Model (CPCM) for dichloromethane. Frequency calculations were performed on all optimized structures in order to characterise minima (zero imaginary frequencies) and maxima (single imaginary frequency). All profiles were plotted using the Gibbs free energy values and are depicted in Figure 3.9.

The *N*-methylformamide **3.17** was confirmed by ^{1}H-NMR studies to be almost exclusively present in the (*E*)-configuration, from which only the iminium triflate species **3.20E** and subsequently the tetrahedral species **3.21e** with the triflate group equatorial should arise. However, the energies and transition states of the opposite case involving the (*Z*)-configured iminium triflate species **3.20Z** and tetrahedral intermediate **3.21a** were also modelled and mechanisms examined which might allow crossover from one mechanistic path to the other. These two pathways afforded slightly different energies for disalt species **3.18**, with the two pathways giving distinctive and different positioning of the anions. As the energies for intermediate **3.18** did not differ significantly the two different mechanistic pathways, which were obtained from calculations for species **3.21a** on one hand and for intermediate **3.21e** on the other, were aligned at the stage of disalt **3.18** for a clearer illustration.

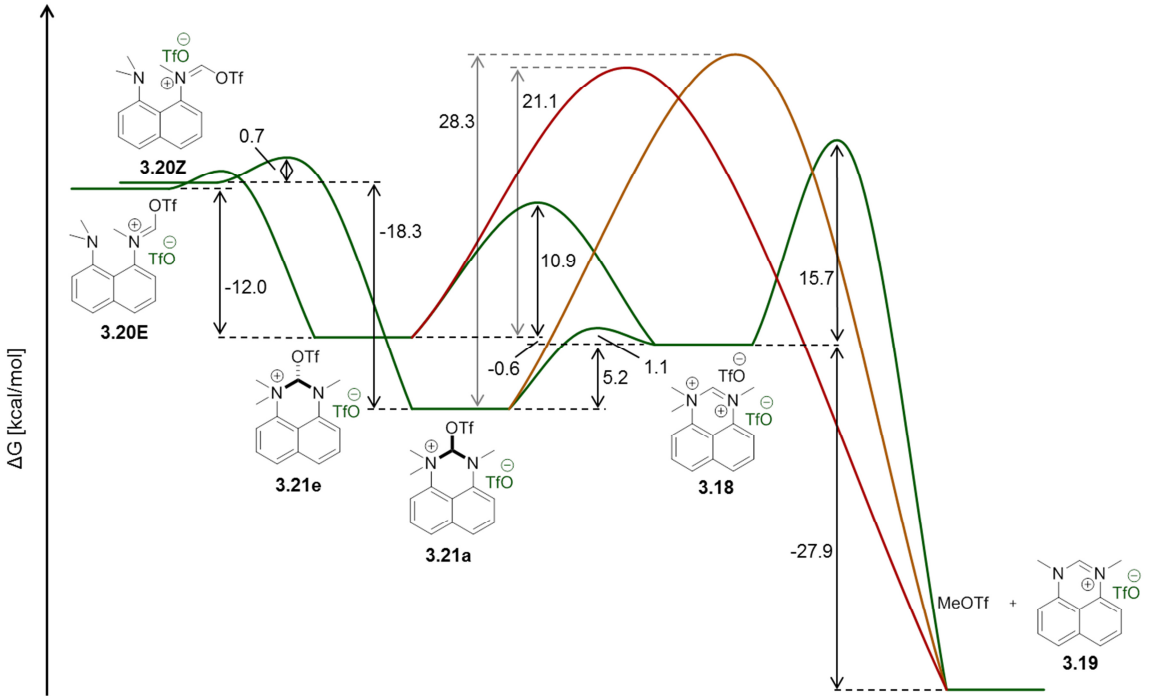

Figure 3.9 Calculated energy profile for the reaction of *N*-methylformamide **3.17** with triflic anhydride.

The first intermediate in the diagram is the (*E*)-configured iminium species **3.20E**, which results from an exothermic reaction (-3.5 kcal/mol) between triflic anhydride and the (*E*)-*N*-methylformamide **3.17**. It is believed that from the iminium ion only a small activation barrier has to be overcome for the thermodynamically favoured transformation to the tetrahedral intermediate **3.21e** bearing the triflate residue equatorial. In fact, so far our computational collaborators have not been able to model the mechanistic step from the (*E*)-configured iminium species **3.20E** to the tetrahedral triflate intermediate **3.21e**, but the same instance for the oppositely configured mechanism *i.e.* the (*Z*)-configured iminium triflate **3.20Z** going to species **3.21a** with the bound triflate group axial was shown to require only a minimal barrier (0.7 kcal/mol). Dissociation of the equatorial triflate group from the tetrahedral intermediate **3.21e** to form the dication species **3.18** requires only a small activation barrier and the resulting dication is more stable than the precursor species **3.21e** by only 0.6 kcal/mol. However, computational studies suggest that at this stage the interconversion is possible to the more stable tetrahedral species **3.21a**, with triflate group axial. This tetrahedral intermediate **3.21a** requires only a minimal barrier (1.1 kcal/mol) and is 5.2 kcal/mol more stable than the disalt species **3.18**. It is imaginable, that the relative energies and energy barriers at this point allow an equilibrium between the latter three intermediates (**3.18**, **3.21a** and **3.21e**) in which the most energetically favoured species **3.21a** has the longest lifetime. Hence, in line with the experimental results, which will be discussed shortly, the disalt **3.18** cannot be observed. Once the superelectrophilic disalt **3.18** is formed in this equilibrium, an additional activation energy of 15.7

kcal/mol is required for the dication to undergo dealkylation and proceed to the final perimidinium product **3.19** in an exothermic fashion (-27.9 kcal/mol).

As the isomerisation of species **3.21e** to **3.21a** can in principle occur through flipping of the 6-membered heterocycle (Figure 3.10), this proposal was also modelled. The activation barrier for this step was found to be slightly higher than the activation barrier for species **3.21e** to dissociate the equatorial triflate substituent and become the disalt intermediate **3.18**.

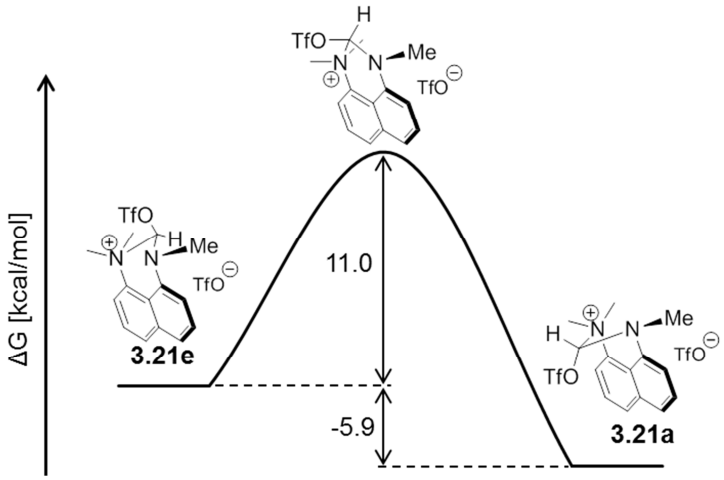

Figure 3.10 Isomerisation of intermediate **3.21** *via* flip of the 6-membered heterocycle.

Alternative demethylation pathways for both the tetrahedral intermediates **3.21a** and **3.21e**, in which the first triflate anion would attack the methyl group and expel the triflate substituent *via* a concerted E2 elimination mechanism were also modelled (Scheme 3.16), but the energies (red and orange line in Figure 3.9) of the transition states for this step were shown to be too high (21.1 and 28.3 kcal/mol, respectively) to play any role in this reaction.

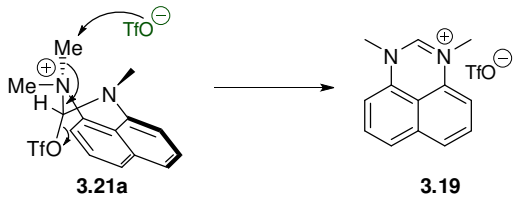

Scheme 3.16 The energetic barrier for an E2-based demethylation by the pre-existing triflate anion (green) was calculated to be too high to be involved in the reaction mechanism.

Another alternative dealkylation mechanism by a 6-centre rearrangement (Scheme 3.17) in which the oxygen of the triflate residue centring the amidinium moiety would attack the methyl group was also rejected. Computational investigations on both tetrahedral isomers **3.21a** and **3.21e** showed that the geometry needed for such a rearrangement cannot be adopted; hence, a transition state could not be modelled.

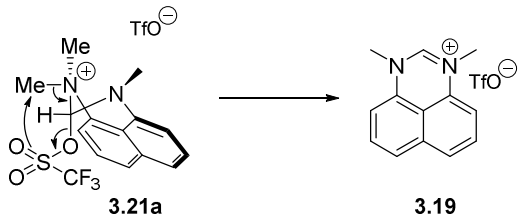

Scheme 3.17 The possibility of intramolecular demethylation *via* rearrangement was excluded by computational calculations.

3.3 Kinetic insights into the alkyl transfer from naphthalene-based amidinium disalts to triflate anions

As the calculated energy profile (Figure 3.9) for the mechanistic proposal suggested the amidinium dication **3.18** to be in an equilibrium with tetrahedral species **3.21a** and **3.21e**, though not being the most energetically favoured intermediate, it was clear that neither isolation nor observation of the superelectrophilic dicationic intermediate was possible. Upon addition of triflic anhydride to formamide **3.17** ^{1}H-NMR experiments at -35 °C in d_2-DCM indeed showed a tetrahedral triflate species **3.21** as the only species in solution, which was proposed to be isomer **3.21a** with the triflate residue axial to the 6-membered ring as *in silico* studies predicted this isomer to be more stable over the other. The proposed existence of isomer **3.21a** over the other is supported by the fact that in ^{1}H-NMR kinetic studies at higher temperatures neither the disalt species nor the other tetrahedral isomer **3.21e** have been observed at any time.

Figure 3.11 shows the low temperature ^{1}H-NMR spectrum of **3.21** including three different peaks for the methyl groups (at 3.18, 3.24 and 3.73 ppm), being in agreement with the structural proposal of a tetrahedral intermediate **3.21a** or **3.21e**. The singlet peak corresponding to the methine proton bonded to both nitrogen atoms is found at 6.94 ppm. The species was also characterised by ^{13}C-NMR in which the carbon atom of this methine moiety resonates at 100.9 ppm.

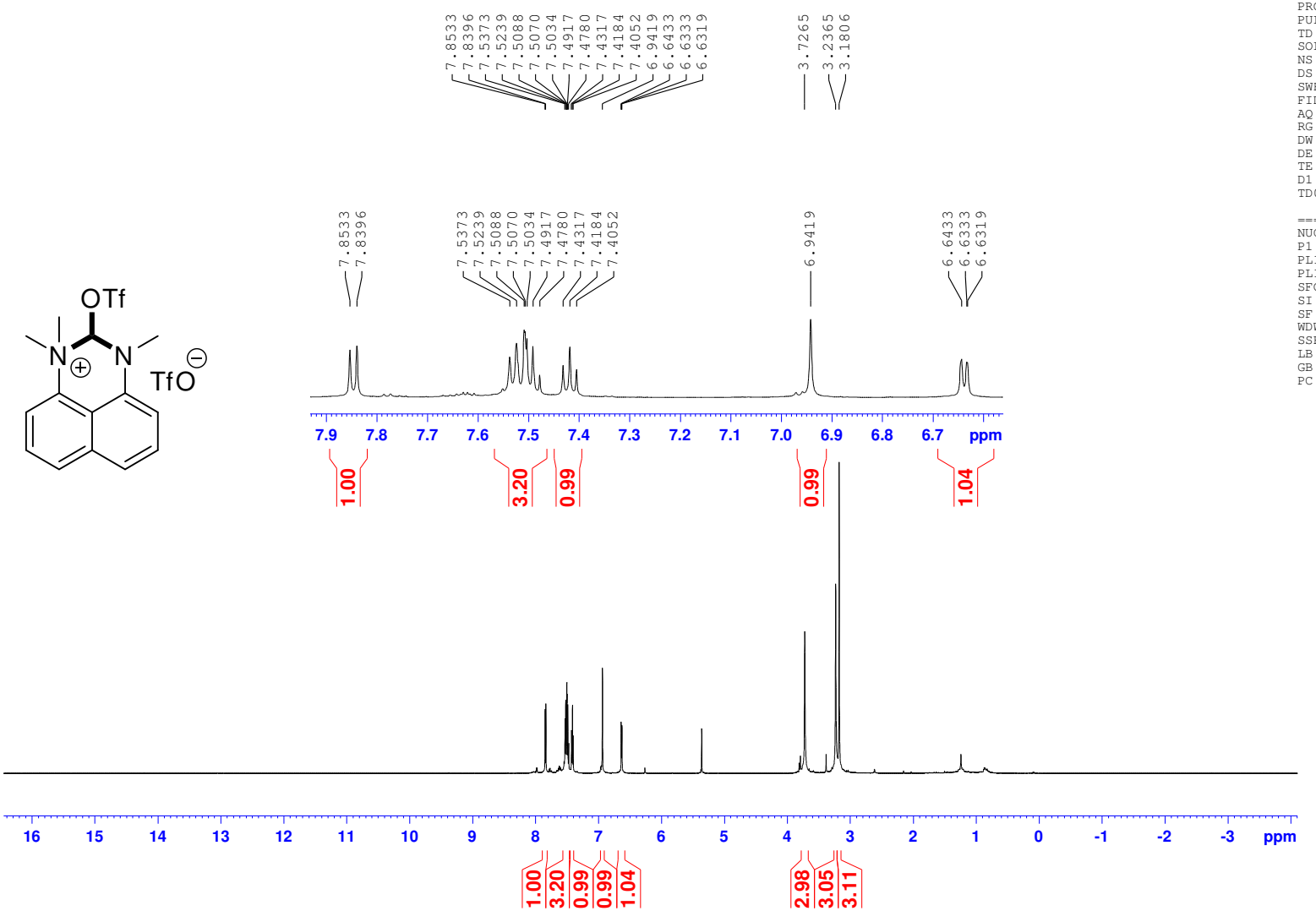


```
NAME                C02340
EXPNO                    1
PROCNO                   1
Date_             20130321
Time                 11.51
INSTRUM              spect
PROBHD    5 mm PABBO BB-
PULPROG               zg30
TD                   65536
SOLVENT              CD2Cl2
NS                       16
DS                        2
SWH              12335.526 Hz
FIDRES           0.188225 Hz
AQ               2.6564426 sec
RG                      101
DW                 40.533 usec
DE                  6.50 usec
TE                 236.9 K
D1              1.00000000 sec
TD0                      1

======== CHANNEL f1 ========
NUC1                    1H
P1                  12.00 usec
PL1                 -2.20 dB
PL1W          23.76155472 W
SFO1         600.1337060 MHz
SI                   32768
SF           600.1300000 MHz
WDW                     EM
SSB                      0
LB                  0.30 Hz
GB                       0
PC                    1.00
```

Figure 3.11 ^{1}H-NMR of intermediate **3.21**.

Interestingly, low temperature ^{1}H-NMR (-20 °C) spectra (Figure 3.13) of pyrrolidine substrate **3.3** upon triflic anhydride addition revealed both possible isomers **3.23a** and **3.23e** of the tetrahedral triflate intermediate in a 1:0.83 ratio in d_2-DCM solution (Scheme 3.18).

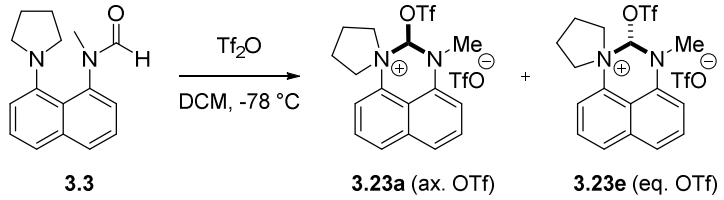

Scheme 3.18 Upon addition of triflic anhydride to *N*-methylformamide **3.3**, ^{1}H-NMR spectra reveal the presence of both tetrahedral triflate isomers **3.23a** and **3.23e** at low temperature.

Previously, low-temperature ^{1}H-NMR studies on the dimethylamino substrate **3.17** showed only one tetrahedral triflate isomer, which was assumed to be the one with the triflate group axial (**3.21a**) due to the relative energy difference between the two isomeric species and the favourable energetic barriers for the interconversion (Figure 3.9). Hence, at first the presence of both tetrahedral isomers **3.23a** and **3.23e** stemming from pyrrolidino substrate **3.3** suggested that the energy difference as well as the energetic barrier for interconverion between the two isomers was smaller than in the previously calculated dimethylamino formamide **3.17** to allow both tetrahedral isomers to be seen at low temperature. The assignment of the isomers to the major and the minor species was supported by two-dimensional proton-proton correlated NOESY experiments. From Figure 3.12 it can be seen, that for the isomer **3.23a** with the triflate residue in the axial position, two spin polarisation transfer events are expected between the N-C*H*-OTf methine proton and the two α-protons on the pyrrolidine ring. In the comparative case for the isomer **3.23e** with the triflate residue in the equatorial position, only one nOe event is expected.

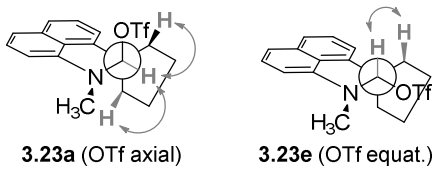

Figure 3.12 The possible spin polarisation effects between the α-protons on the pyrrolidine ring and the amidinium proton in the two conformers are indicated by grey curly arrows.

Indeed, the major species in solution was confirmed to be the isomer with the triflate residue in the axial position. The two-dimensional NOESY spectrum (Figure 3.14) showed spin polarisation transfer events between the methine proton at 6.68 ppm and two α-protons on the pyrrolidine; one at 3.01 and 4.16 ppm (green circles) for the major compound.

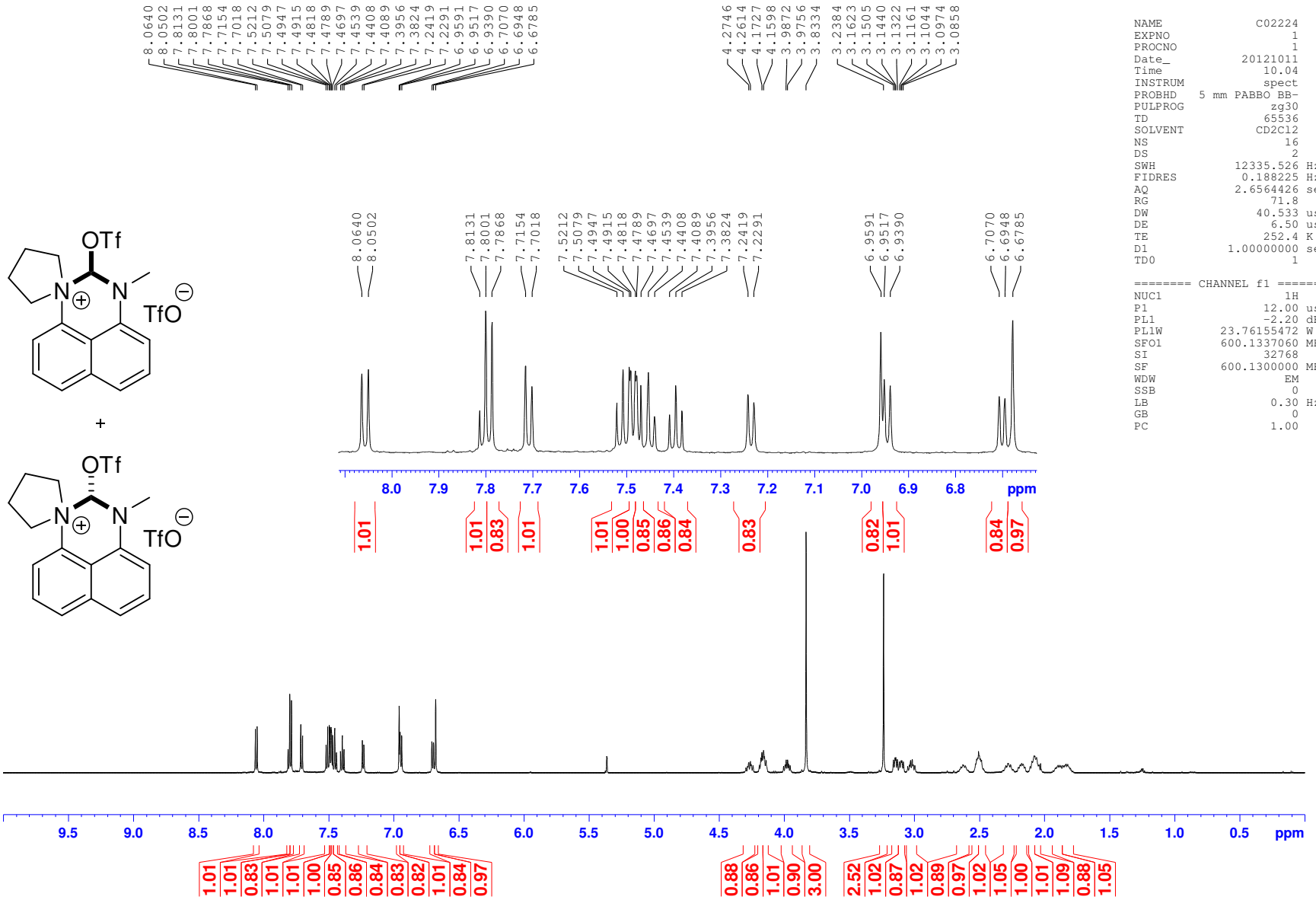


```
NAME                C02224
EXPNO                    1
PROCNO                   1
Date_             20121011
Time                 10.04
INSTRUM              spect
PROBHD    5 mm PABBO BB-
PULPROG               zg30
TD                   65536
SOLVENT           CD2Cl2
NS                       16
DS                        2
SWH             12335.526 Hz
FIDRES              0.188225 Hz
AQ                2.6564426 sec
RG                     71.8
DW                   40.533 usec
DE                     6.50 usec
TE                   252.4 K
D1              1.00000000 sec
TD0                      1

======== CHANNEL f1 ========
NUC1                    1H
P1                   12.00 usec
PL1                  -2.20 dB
PL1W           23.76155472 W
SFO1           600.1337060 MHz
SI                   32768
SF             600.1300000 MHz
WDW                     EM
SSB                      0
LB                    0.30 Hz
GB                       0
PC                    1.00
```

Figure 3.13 ^{1}H-NMR spectrum of intermediate **3.23a** and **3.23e**.

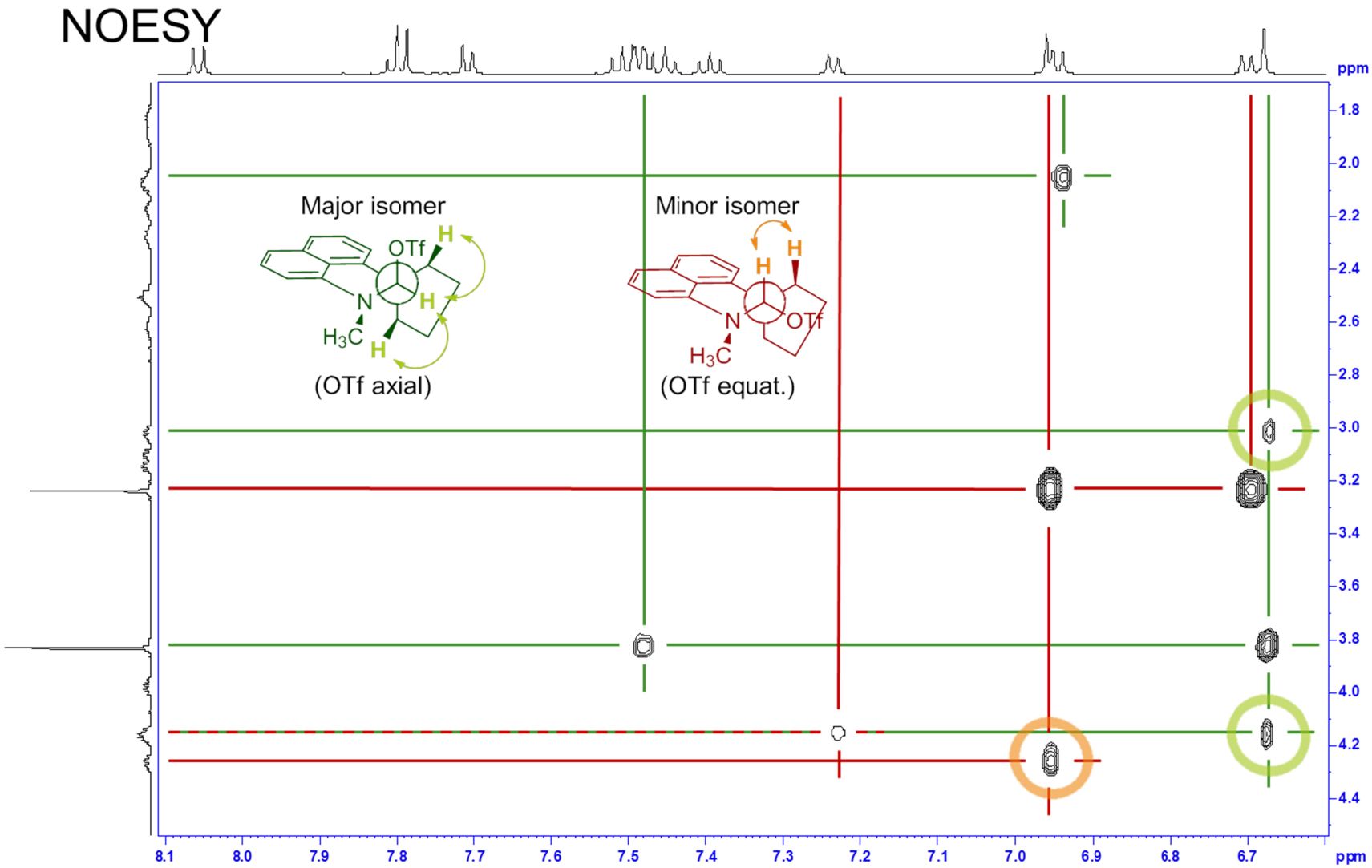

Figure 3.14 2-Dimensional NOESY spectrum of intermediate **3.23a** and **3.23e**.

For the minor isomer only one polarisation transfer event was seen between the methine proton at 6.96 and one α-proton at 4.29 ppm (orange circle).

For kinetic studies of the dealkylation process from the tetrahedral triflate intermediates, two stock solutions of dimethylamino formamide **3.17** and pyrrolidino substrate **3.3** in d_2-DCM were prepared with cyclooctatetraene as an internal standard that would not interfere with the reaction itself. By observing the decrease of a suitable proton peak of the intermediate in the ^{1}H-NMR spectrum and correlating the integral to the known concentration of the internal standard, the concentrations of the tetrahedral triflate intermediates **3.21a**, **3.23a** and **3.23e** were monitored against time. In case of the tetrahedral dimethylamino intermediate **3.21a**, in the ^{1}H-NMR spectrum, the decrease of the integral of the methine proton peak at 6.94 ppm, which directly correlates with the intermediate concentration, was observed over time.

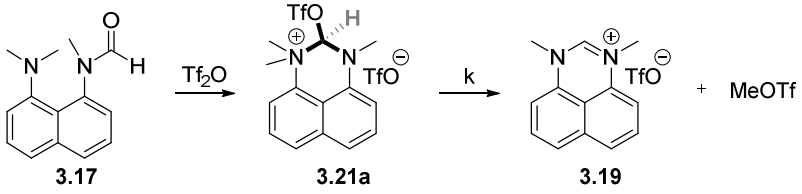

Scheme 3.19 For kinetic studies of the dealkylation process the decrease of the integral of the amidinium proton (grey) in intermediate **3.21a** was observed over time.

Below (Figure 3.15) is shown one out of six kinetic runs, where the concentration of the intermediate **3.21a** is plotted against time.

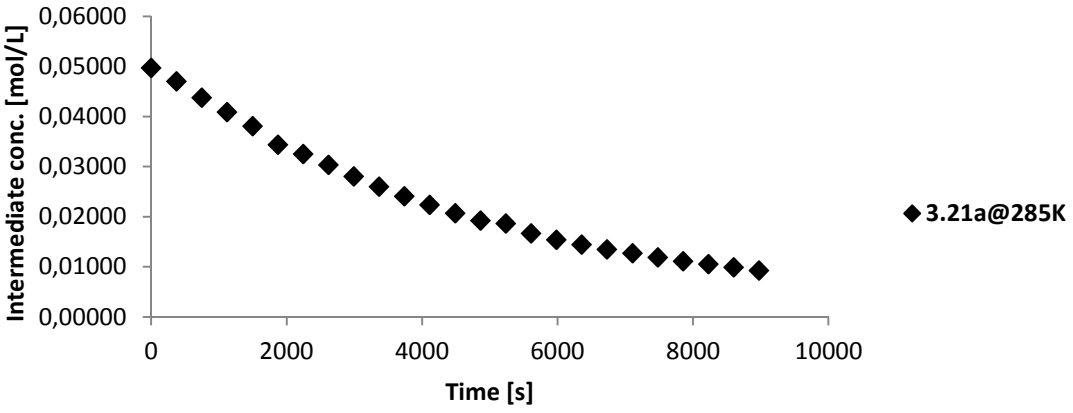

Figure 3.15 The plot visualises the concentration of intermediate **3.21a** against time during the reaction.

For a first order reaction the plot of the natural logarithm of the concentration of the intermediate **3.21a** against time should give a straight line with the slope as its rate constant. Figure 3.16 indeed

shows for the observed reaction a unimolecular reaction with a rate constant of 1.91 x 10^{-4} s^{-1} at 12 °C.

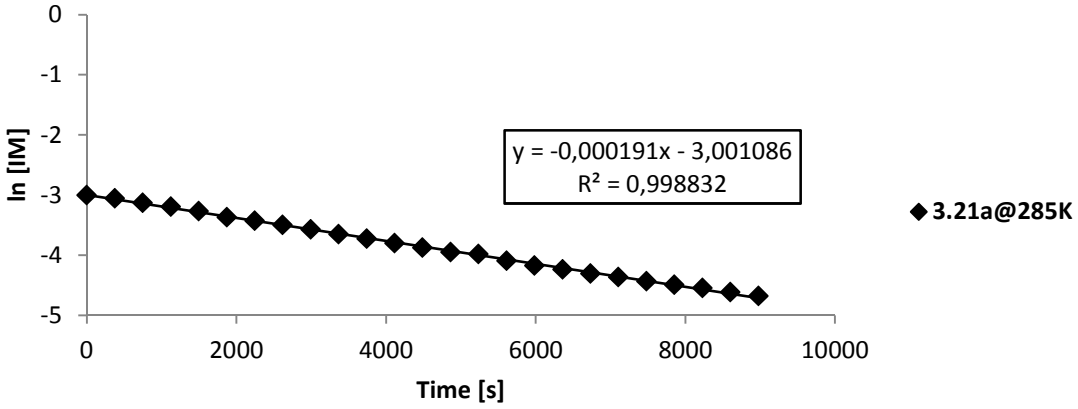

Figure 3.16 The plot of the natural logarithm of the concentration of intermediate **3.21a** against time allows for determination of the rate constant k from the slope of the graph.

To obtain temperature-dependent rate constants, the kinetic runs were recorded at different temperatures (279, 282, 285, 288, 291 and 294 K), but starting concentrations of the reagents in the NMR tube were kept constant.

For the kinetic investigation into the dealkylation process from the two tetrahedral pyrrolidino isomers **3.23a** and **3.23e**, this time the decrease of the integral of each methyl signal was monitored instead of the integrals of the N-C*H*-OTf methine protons as the singlet peaks of the latter methine protons were overlapping with aromatic proton peaks in the ^{1}H-NMR spectrum.

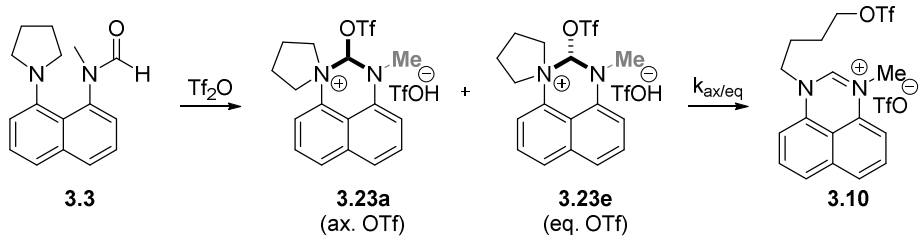

Scheme 3.20 For kinetic studies of the dealkylation process the decrease of the integral of the methyl groups (grey) in intermediate **3.23a** and **3.23e** were observed over time.

Again, below is first shown a plot (Figure 3.17) of the concentration of each isomer **3.23a** and **3.23e** and the arising monocationic product **3.10** against time.

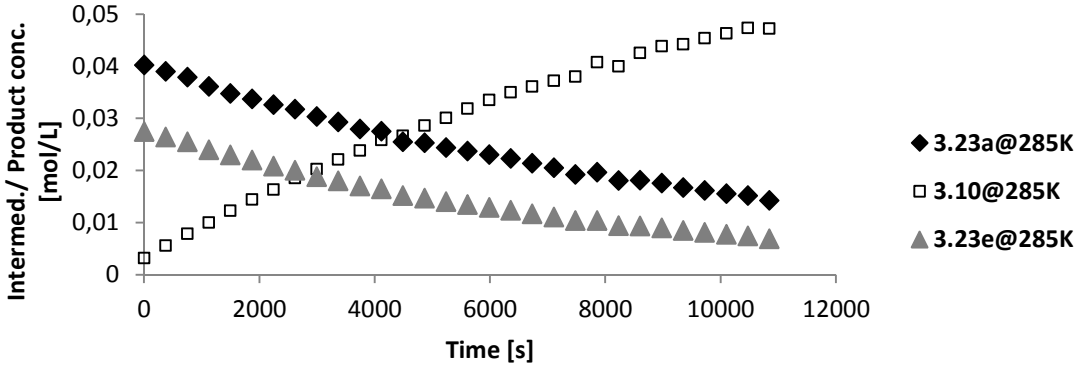

Figure 3.17 Plotted is the concentration of intermediates **3.23a** and **3.23e** and product **3.10** against time.

Interestingly, when the natural logarithm of the concentrations of the tetrahedral intermediates **3.23a** and **3.23e** were plotted against time, they gave straight lines as expected for first order kinetics, but their slope was not the same.

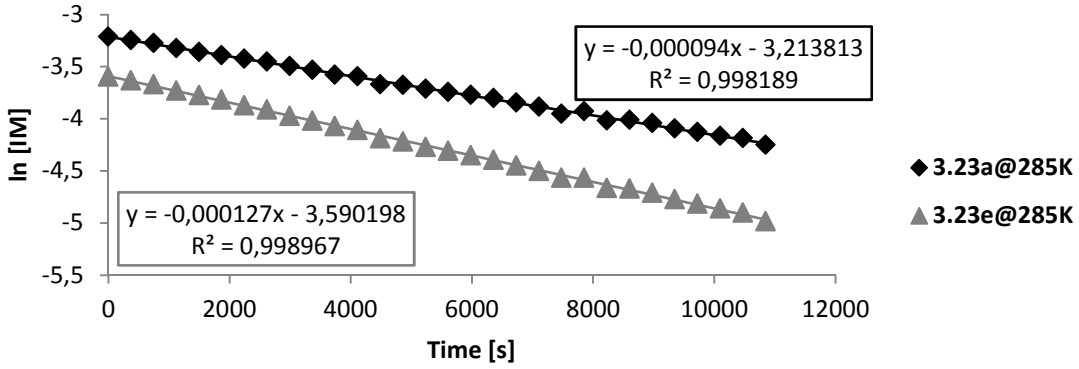

Figure 3.18 The plot of the natural logarithm of the concentrations of intermediates **3.23a** and **3.23e** against time shows two independent rate constants for the dealkylation process.

The presence of two independent rates of dealkylation suggested that there was no dynamic equilibrium, neither by inversion nor by going through the disalt intermediate **3.2**, between the isomers **3.23a** and **3.23e**. If the ratio between the isomers stayed constant during the course of the kinetic studies due to quick equilibration, then the plots in Figure 3.18 would run parallel.

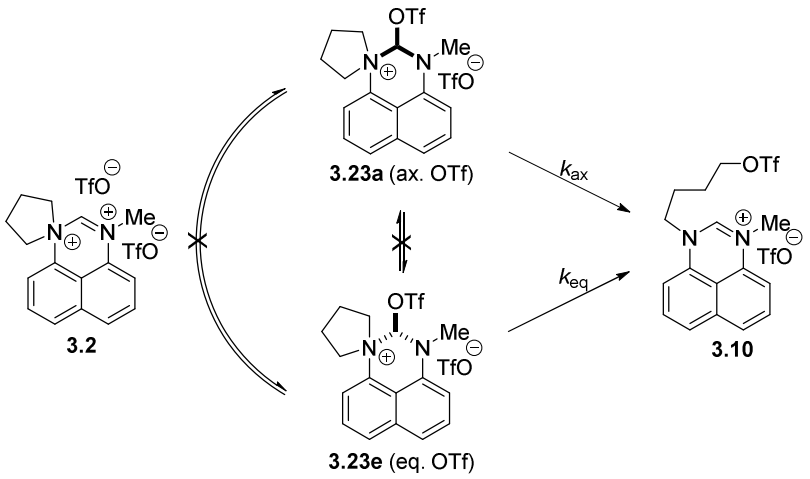

Scheme 3.21 The two independent dealkylation rates for intermediates **3.23a** and **3.23e** shows that there is no equilibrium between the two species, neither by inversion of the 6-membered ring nor *via* the dicationic intermediate **3.2**.

Obtaining the temperature-dependent rate constants k for the dimethylamino intermediate **3.21a** and the two pyrrolidino isomers **3.23a** and **3.23e** allow the Arrhenius plot to be drawn in which the natural logarithm of the rate constants is plotted against 1/T [K^{-1}]. The Arrhenius equation (1) can also be written in its graphical form (2), in which the data points of ln k should ideally lie on a straight line in the Arrhenius plot with the slope correlating to the activation energy E_A of the observed reaction. The intercept of the line at the point 1/T = 0 K allows determination of the pre-exponential factor A, also known as the frequency factor, which is a measure of how often molecules collide and if the molecules are orientated properly towards each other for reaction.

$$k = A \cdot e^{E_A/RT} \qquad (1)$$

$$\ln k = \frac{-E_A}{RT} + \ln A \qquad (2)$$

In the scientific literature some cases[145] have been reported in which the Arrhenius plot shows a curvature. This happens, if the reaction mechanism changes at a particular temperature. Figure 3.19 depicts Arrhenius plots including the kinetics for the three tetrahedral triflate intermediates **3.21a**, **3.23a** and **3.23e**.

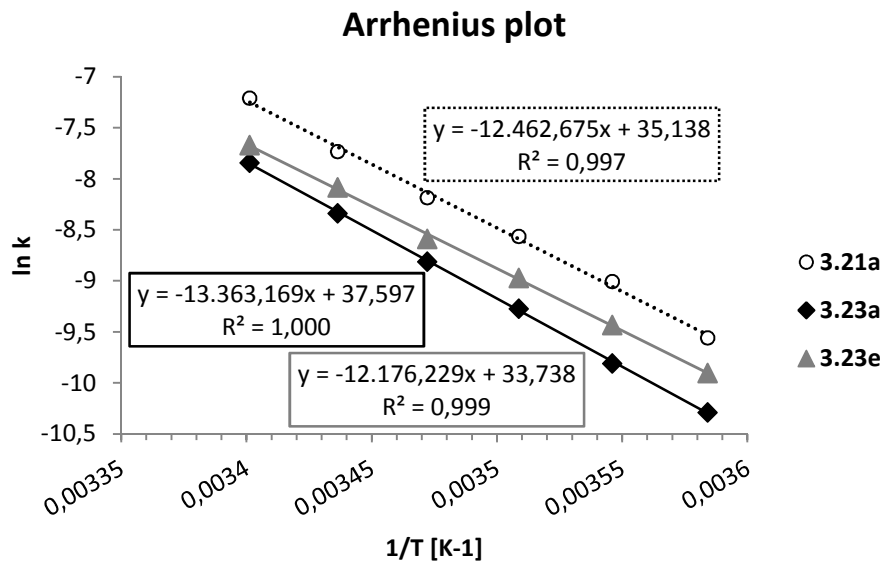

Figure 3.19 The Arrhenius plot allows for determination of the activation energy E_A and the pre-exponential factor A.

If the natural logarithm of the rate constant over temperature ln (k/T) is plotted against 1/T [K^{-1}] then the Eyring plot (Figure 3.20) can be drawn, which allows for determination of the entropy and enthalpy of activation $\Delta S^{\ddagger}$ and $\Delta H^{\ddagger}$ as being the respective difference of entropy and enthalpy between the tetrahedral triflate intermediates **3.21a**, **3.23a** and **3.23e** and the transition states towards the final product **3.19** and **3.10**, respectively. The Eyring equation (3) somewhat resembles the Arrhenius equation and can also be rearranged to solve for graphical form (4), where k_B and *h* are the Boltzmann and Planck's constant, respectively. Similar to the Arrhenius plot, here the slope of the graph correlates to the enthalpy of activation and the intercept at 1/T = 0 K is $\frac{\Delta S^{\ddagger}}{R} + \ln\frac{k_B}{h}$.

$$k = \frac{k_B T}{h}\, e^{-\Delta G^{\ddagger}/RT} \qquad (3)$$

$$\ln\left(\frac{k}{T}\right) = \frac{-\Delta H^{\ddagger}}{RT} + \ln\left(\frac{k_B}{h}\right) + \frac{\Delta S^{\ddagger}}{R} \qquad (4)$$

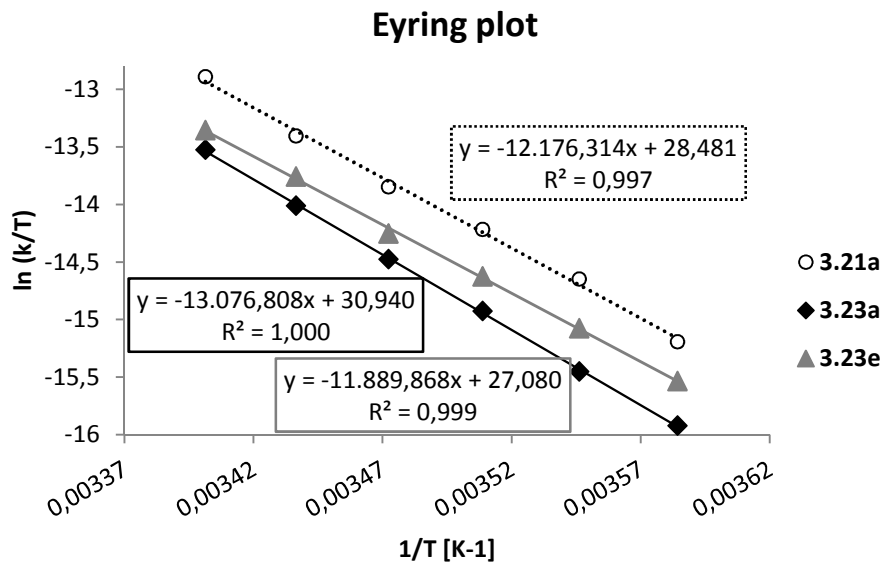

Figure 3.20 The Eyring plot allows for determination of the enthalpy and entropy of activation $\Delta H^{\ddagger}$ and $\Delta S^{\ddagger}$ for the observed dealkylation process from intermediates **3.21a**, **3.23a** and **3.23e**.

Below the table summarises the temperature-dependent rate constants, the entropy and enthalpy of activation $\Delta S^{\ddagger}$ and $\Delta H^{\ddagger}$ for the rate-determining step.

Table 3.1 Rate constants k, activation energy E_A, enthalpy and entropy of activation $\Delta H^{\ddagger}$ and $\Delta S^{\ddagger}$, respectively, for intermediates **3.21a**, **3.23a** and **3.23e**.

Dimethylamino intermediate **3.21a**				
T (K)	k x 10^{-4} (s^{-1})	E_A (kcal/mol)	$\Delta H^{\ddagger}$ (kcal/mol)	$\Delta S_{298K}{}^{\ddagger}$ (kcal/mol)
294	7.378 ± 0.124	24.8 ± 0.7	24.2 ± 0.7	2.8 ± 0.7
291	4.500 ± 0.097			
288	2.791 ± 0.035			
285	1.907 ± 0.014			
282	1.247 ± 0.013			
279	0.706 ± 0.014			
Pyrrolidino intermediate **3.23a** (OTf axial)				
T (K)	k_{ax} x 10^{-4} (s^{-1})	E_A (kcal/mol)	$\Delta H^{\ddagger}$ (kcal/mol)	$\Delta S_{298K}{}^{\ddagger}$ (kcal/mol)
294	3.933 ± 0.039	26.6 ± 0.2	26.0 ± 0.2	4.2 ± 0.2
291	2.393 ± 0.023			
288	1.491 ± 0.014			
285	0.942 ± 0.008			
282	0.547 ± 0.011			
279	0.341 ± 0.017			
Pyrrolidino intermediate **3.23e** (OTf equat.)				
T (K)	k_{eq} x 10^{-4} (s^{-1})	E_A (kcal/mol)	$\Delta H^{\ddagger}$ (kcal/mol)	$\Delta S_{298K}{}^{\ddagger}$ (kcal/mol)
294	4.658 ± 0.032	24.2 ± 0.4	23.6 ± 0.6	1.9 ± 0.4
291	3.078 ± 0.037			
288	1.863 ± 0.012			
285	1.270 ± 0.008			
282	0.800 ± 0.009			
279	0.496 ± 0.015			

The rate constants of alkyl transfer are of similar magnitude as for dithia disalts **1.137** generated from sulfoxides and discussed in the introduction section. For instance, there, the transfer of a primary ethyl group to the triflate anion was found to have a rate constant of 1.89×10^{-3} s^{-1} at 278 K. Compared to dimethylamino substrate **3.21a**, this is a 3-fold faster reaction. It is noteworthy that the two gitonic superelectrophiles afford a similar rate constant, although the dithia species are vicinal disalts, while the proposed amidinium intermediate **3.18** is a 1,3-disalt. The comparability of the two kinetic studies is however somewhat complicated as the kinetic studies on Furukawa's dithia disalts were performed[57] in acetonitrile, a solvent much more polar than dichloromethane, which was used in this study.

The computational data for dimethylamino formamide **3.17** can be seen in agreement with the low-temperature and the kinetic ^{1}H-NMR studies. The *in silico* studies proposed the tetrahedral isomer **3.21e** to be generated first from the (*E*)-configured *N*-methylformamide **3.17**, which then formed an equilibrium with the disalt **3.18** and the other tetrahedral isomer **3.21a**, with the latter species being the most stable intermediate and exhibiting the longest lifetime in this equilibrium. The low-temperature ^{1}H-NMR experiment indeed found a tetrahedral isomer as a single intermediate and, according to the dynamic equilibrium proposed from the computational calculations, structure **3.21a** with the triflate residue axial was assigned to the compound observed. The calculation also proposed formation of the superelectrophilic disalt **3.18** from the tetrahedral triflate intermediate **3.21a** as a prerequisite to the rate-determining dealkylation step. During the kinetic studies the ^{1}H-NMR spectra only showed the decay of the tetrahedral compound with the supposed structure of **3.21a** and the appearance of the final product **3.19**. However, the positive value of the entropy of activation ($\Delta S_{298K}^{\ddagger}$ = 2.8 ± 0.7 kcal/mol) indicated an S_N1 process,[152,153] exhibiting a less ordered transition state and hence being in agreement with the tetrahedral species **3.21a** to undergo transformation to the amidinium disalt **3.18** with more particles prior to demethylation. Additionally, the activation energy obtained from *in silico* studies (E_A = 5.2 + 15.7 = 20.9 kcal/mol) is close to the activation energy obtained from the kinetic studies (24.8 kcal/mol). Direct evidence for amidinium disalt formation however has yet to emerge.

Looking at the experimental results for the pyrrolidino substrate **3.3** obtained from low-temperature ^{1}H-NMR experiments and kinetic studies it becomes evident that there is a discrepancy between these data and the general idea of *N*-methylformamides reacting with triflic anhydride proposed from computational calculations.

Upon reaction of dimethylamino formamide **3.17** with triflic anhydride, low-temperature ^{1}H- and ^{13}C-NMR experiments revealed the presence of a single compound for which the tetrahedral

structure of **3.21a** with the triflate residue axial was proposed according to the relative energies and barriers from *in silico* studies. This structure was assumed to be in a dynamic equilibrium with the other isomer **3.21e** bearing the triflate residue equatorial and the disalt species **3.18** with the latter two intermediates being energetically higher than compound **3.21a**.

At low temperature and upon reaction of the pyrrolidino substrate **3.3** with triflic anhydride, the ^{1}H- and the ^{13}C-NMR spectra showed the presence of both tetrahedral isomers **3.23a** and **3.23e,** for which first a dynamic equilibrium, analogue to dimethylamino substrate **3.17**, was assumed involving a very small energy difference between the two isomers to explain the relative ratio of 1:0.83. However, the kinetic studies revealed two independent rates of dealkylation for these intermediates. This finding clearly excluded a dynamic equilibrium between the two isomers and proposed the barrier for interconversion to be too high to be overcome at these temperatures. The most interesting question then concerned how both isomers **3.23a** and **3.23e** can be afforded by reaction of the almost completely (*E*)-configured formamide **3.3** with triflic anhydride.

One way to explain these different observations would highlight crucial lifetimes of iminium triflate species **3.20E** (dimethylamino species) and **3.22E** (pyrrolidino species), being generated from almost exclusively (*E*)-configured formamide substrates **3.17** and **3.3**, respectively. While iminium species **3.20E**, produced from dimethylamino substrate **3.17** would have a rather short lifetime, instantly react intramolecularly and proceed to tetrahedral species **3.21e**, iminium species **3.22E**, derived from pyrrolidino substrate **3.3** might have a longer lifetime.

This extended lifetime might result due to steric bulk of the pyrrolidine ring, which could delay the intramolecular attack of the neighbouring tertiary amine onto the carbon of the iminium residue and allow for intermolecular attack of the triflate counter-ion to form *gem*-bistriflate **3.24** as depicted in Scheme 3.22. Formation of such a species would not be unusual, as the introduction to this thesis has presented a few examples of a similar kind. The subsequent dissociation of a triflate residue from *gem*-bistriflate **3.24** could then form the (*Z*)-configured iminium triflate intermediate **3.22Z**, from which tetrahedral species **3.23a** with the triflate residue axial could result. At the first glance, the finding of two independent rates of dealkylation for the tetrahedral triflate isomers **3.23a** and **3.23e** suggests that in the process of dealkylation at least one of the isomers does not afford an amidinium disalt intermediate. If both tetrahedral triflate isomers **3.23a** and **3.23e** were to give the same amidinium disalt intermediate **3.2** and dealkylation from the latter species was the rate determining step, then one would observe only one rate of dealkylation.

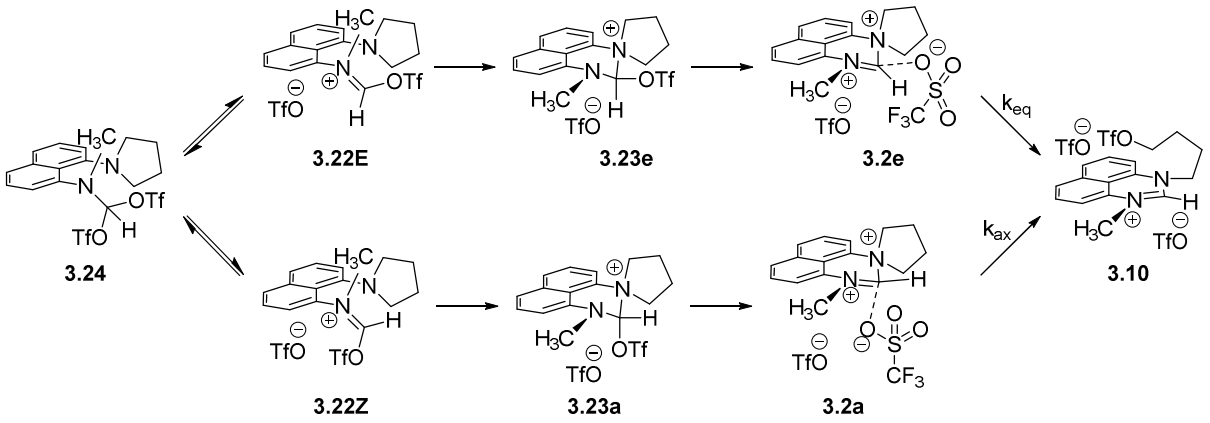

Scheme 3.22 Conversion *via gem*-bistriflate **3.24** might account for the presence of both tetrahedral isomers **3.23a** and **3.23e** in the low-temperature NMR spectra. From the latter species two diastereomeric tight ion pairs, **3.2a** and **3.2e**, might be formed explaining the two rates of dealkylation to **3.10** (k_{ax} and k_{eq}).

However, a different approach must be considered which accounts for both tetrahedral isomers **3.23a** and **3.23e** giving an amidinium disalt intermediate prior to dealkylation. Both values for the entropy of activation, obtained from the kinetic studies of pyrrolidino isomers **3.23a** and **3.23e**, are positive and indicate an S_N1 mechanism. This is in agreement with the previously calculated proposal for dimethylamino formamide **3.17** involving formation of an amidinium disalt as a less ordered intermediate composed of three particles. Additionally, the plots still showed characteristics of first order reactions when the concentration of the pyrrolidino amide **3.3** was increased from 0.031 mmol/L to 0.062 mmol/L at 288 K, but the rate of dealkylation did not follow proportionally (0.046 mmol/L: $k_{ax} = 1.767 \pm 0.019 \times 10^{-4}$ s^{-1}, $k_{eq} = 2.383 \pm 0.016 \times 10^{-4}$ s^{-1}; 0.062 mmol/L: $k_{ax} = 1.818 \pm 0.035 \times 10^{-4}$ s^{-1}, $k_{eq} = 2.680 \pm 0.028 \times 10^{-4}$ s^{-1}). Now, for both isomers, **3.23a** and **3.23e**, to go through an amidinium disalt species **3.2** and afford two independent rates of alkyl transfer, the superelectrophilic species emerging from each tetrahedral isomer must be chemically non-equivalent. This would be the case if each tetrahedral isomer would produce the respective disalt species as the respective diastereomeric contact ion pair, which would be rigid in structure and lack the ability for isomerisation. As seen from Scheme 3.22, dissociation of the equatorial triflate residue from isomer **3.23e** might result in a tight ion pair **3.2e** bearing the triflate ion beside the heterocyclic plane, while isomer **3.23a** might produce a contact ion pair **3.2a** with the counter-ion under the heterocyclic plane. This is repeatedly seen in computational investigations.

Ion-pairs have previously been reported as the stereocontrolling element in organic synthetic S_N1 reactions,[154,155] nevertheless this proposal would be somewhat novel in the field of superelectrophiles. Computational calculations together with experimental kinetic parameters predicted that in the reaction of *N*-methylformamides with triflic anhydride superelectrophilic

amidinium ions are formed, from which dealkylation took place by attack of weakly nucleophilic triflate anions. However, calculations on organic salts can be tricky to perform,[156] as the relative energy of the intermediates and transition states can significantly depend on the orientation and the distance between cation and anions and becomes even more complicated when multiple counter-ions are in play. Hence, the direct evidence for the presence of amidinium disalts in the dealkylation of the previously discussed *N*-methylformamides has yet to be observed, especially since recent NMR and kinetic experiments were not able to find direct evidence for amidinium disalt participation.

Although computational calculations on organic salts have to be handled with care for the reasons mentioned above, the next subchapter will show how they became useful by determining the relative energetic trends when going from one intermediate to another and in this way showed how to stabilise and obtain direct evidence for amidinium disalt species.

3.4 Pushing the equilibrium from the tetrahedral triflate intermediate species to the amidinium disalt species

The question arose by what means it would become possible to isolate or at least observe the dicationic intermediate rather than the tetrahedral triflate intermediate. From computational calculations by our co-worker Greg Anderson on the relative energies of tetrahedral species **3.27** and amidinium disalt **3.28** that would be formed along the pathway proposed in Scheme 3.23, it was predicted that the energy profile should look somewhat different from that found for the previously described *N*-methylformamide substrate **3.17**.

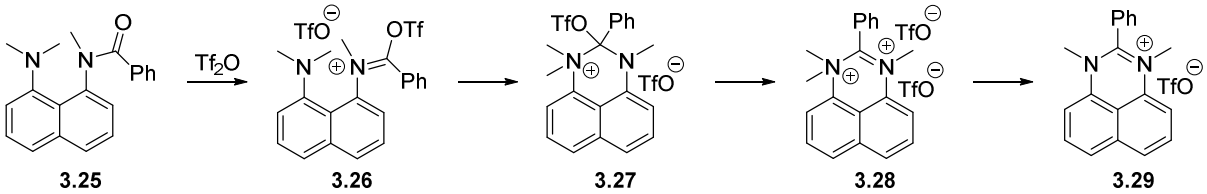

Scheme 3.23 Computational calculations predicted for the demethylation pathway of benzamide **3.25** that observation of dicationic intermediate **3.28** might be possible, as it is lower in energy than tetrahedral triflate intermediate **3.27**.

The relative energies of the intermediates relating to benzamide substrate **3.25** are shown below in Figure 3.21. Both tetrahedral triflate species **3.27a** and **3.27e** were calculated to have a higher relative energy than amidinium species **3.28** involving very low activation barriers towards the latter superelectrophilic intermediate. Hence, at low temperature ^{1}H-NMR experiments should show the

dication structure **3.28**. As the calculation of the equilibrium geometry of the dication **3.28** showed the phenyl group in the centre of the amidinium moiety to be perpendicular to the naphthalene plane, electronic effects can be ruled out as a reason for the stabilisation of the superelectrophile **3.28** and destabilisation of the tetrahedral intermediates **3.27a** and **3.27e** are more likely to be of a steric nature, which pushes the intermediate's energy above that of the dicationic intermediate **3.28**.

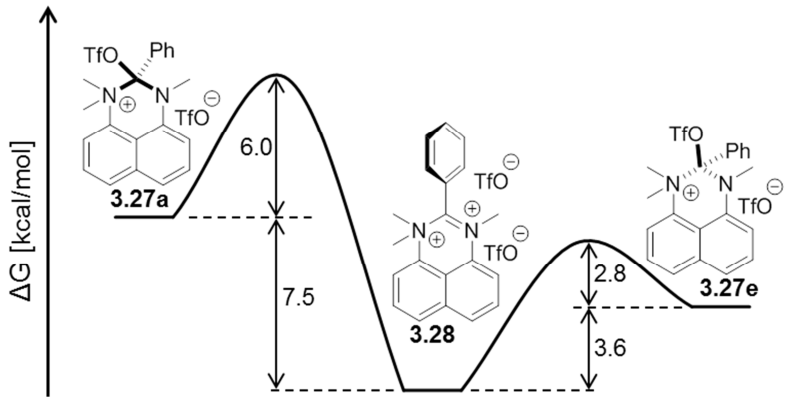

Figure 3.21 *In silico* studies predict tetrahedral intermediates **3.27a** and **3.27e** to be destabilised and higher in energy than dicationic intermediate **3.28**, due to steric crowding at the amidinium centre.

The synthesis of the naphthalene-based benzamide **3.25** was achieved by reacting *N*,*N*,*N*'-trimethylnaphthalene-1,8-diamine **3.16** with a slight excess of benzoyl chloride in a 1:1 mixture of DCM and pyridine at room temperature, providing a very good yield (94 %).

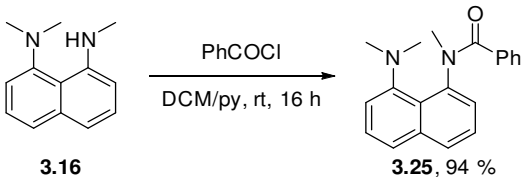

3.16 **3.25**, 94 %

Scheme 3.24 Synthesis of benzamide **3.25**.

For mechanistic studies, this product was now reacted with triflic anhydride in d_2-DCM at -78 °C inside an NMR-tube and analysed by NMR experiments at -35 °C. As predicted from computational calculations, the ^{1}H-NMR spectrum showed the formation of a stable compound that could clearly be assigned to a dicationic amidinium structure **3.28**, although the spectrum was of disappointing quality as the compound was hardly soluble in d_2-DCM and had precipitated inside the NMR-tube. Hence, the reaction (Scheme 3.25) was repeated in d_3-MeCN at -40 °C in an acetonitrile/dry ice bath, despite the fact that alkyl triflates and triflic anhydride had been reported[157] to afford nitrilium compounds upon reaction with nitriles. As triflic acid has an acidity of H_0 = -14.1 and protonated

acetonitrile H_0 = -10, acetonitrile is a 10^4-fold better nucleophile than the triflate anion, accounting for the reported attack on alkyl triflates.

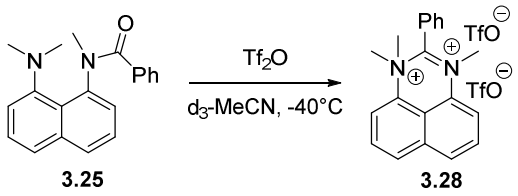

Scheme 3.25 Low temperature NMR studies at -40 °C in d_3-acetonitrile allow for observation and characterisation of dicationic intermediate **3.28**.

Indeed, this time the ^{1}H-NMR spectrum was of good quality and showed (Figure 3.22), in agreement with the structural proposal for amidinium dication **3.28**, only two different kinds of peaks for the methyl groups at 4.18 and 4.10 ppm with the relative integrals of 6:3, respectively. Compared to tetrahedral triflate structure **3.21a**, for which the low temperature NMR experiments found the three non-equivalent methyl signals at 3.18, 3.24 and 3.73 ppm, this is a significant downfield shift illustrating the highly electron-deficient character of the intermediate. The aromatic proton signals for superelectrophile **3.28** were all shifted downfield and found between 7.90 and 8.50 ppm, whereas the aromatic proton signals for intermediate **3.21a** appeared between 6.63 and 7.75 ppm. Warming the same sample to room temperature and analysing it by ^{1}H- and ^{13}C-NMR experiments again, the compound was found to be demethylated by the triflate anion. The ^{1}H-NMR spectrum now showed only one methyl peak at 3.27 ppm for the symmetric monosalt **3.29** and the aromatic proton signals were found more upfield in a region between 7.5 and 8.0 ppm. To obtain an accurate yield for this transformation, the reaction was repeated at 0 °C in DCM as solvent. Upon addition of triflic anhydride to the benzamide, the cooling bath was taken away to bring the reaction to room temperature and after 3 hours the product was triturated with an 1:2 DCM/Et_2O mixture to obtain the pure product **3.29** in 94 % yield.

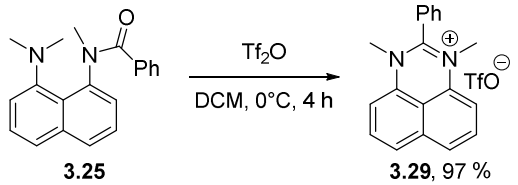

Scheme 3.26 Synthesis of monocationic product **3.29**.

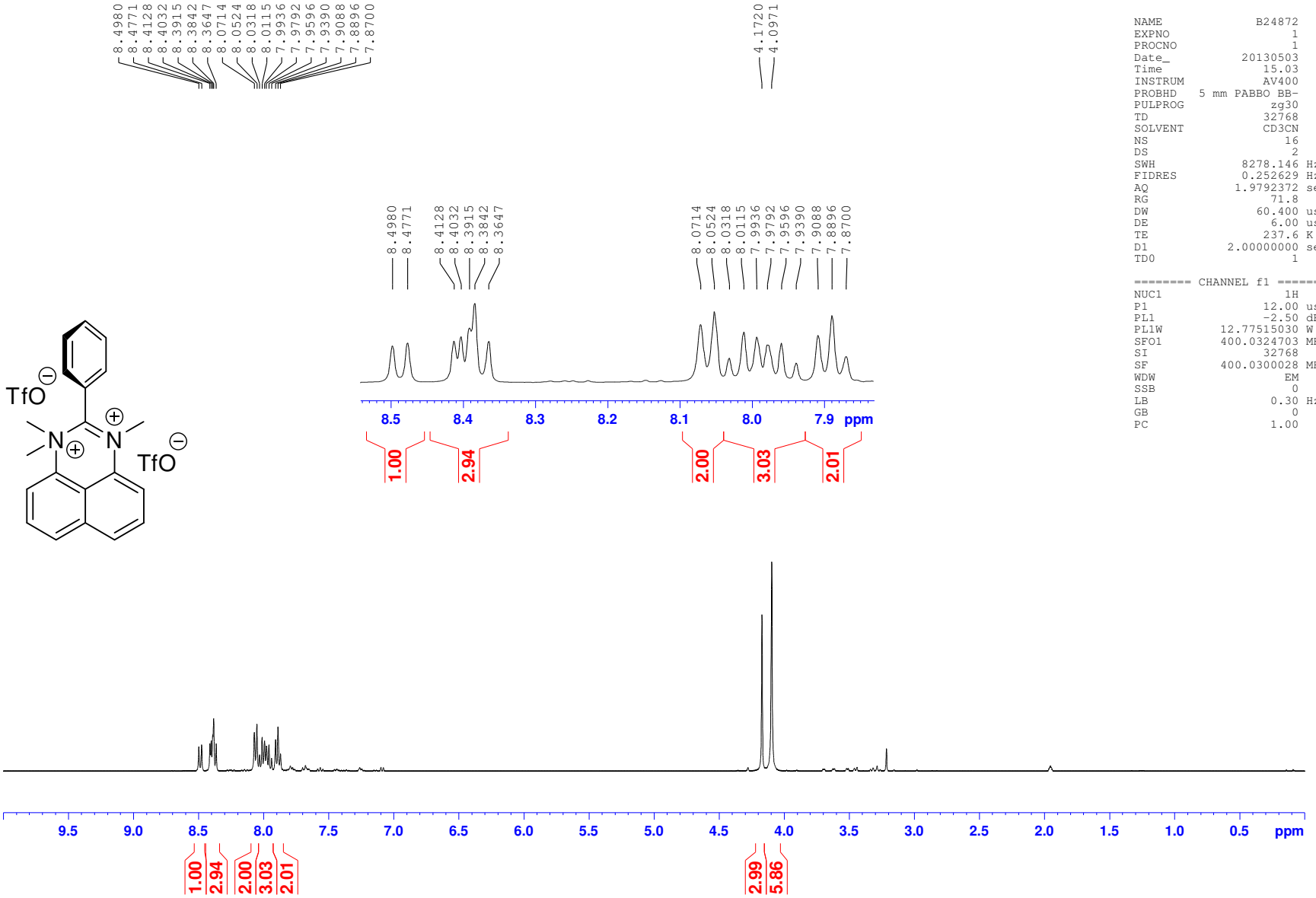

Figure 3.22 ^{1}H-NMR spectrum of disalt **3.28**.

3.5 Synthetic and computational investigations into benzene-based amidinium dications

Subsequently, these explorations were to be transferred to another family of diamine structures. For derivatives of *ortho*-diaminobenzene **3.32** it was assumed that the aromatic stabilisation gained in the imidazolium products **3.34** derived from dealkylation would be even higher than for the perimidinium disalt products **3.1** originating from the naphthalene-based formamides (Scheme 3.27), as in benzene-based formamides a new genuinely aromatic five-membered ring is synthesised upon dealkylation of disalt **3.33** to produce a benzimidazolium heterocycle **3.34**. Conversely, even though the perimidinium structure **3.31** meets most of the Hückel conditions for aromaticity, the aromaticity of this compound is restricted only to the naphthalene core structure and does not incorporate the newly formed pyrimidinium moiety due to cross-conjugation.

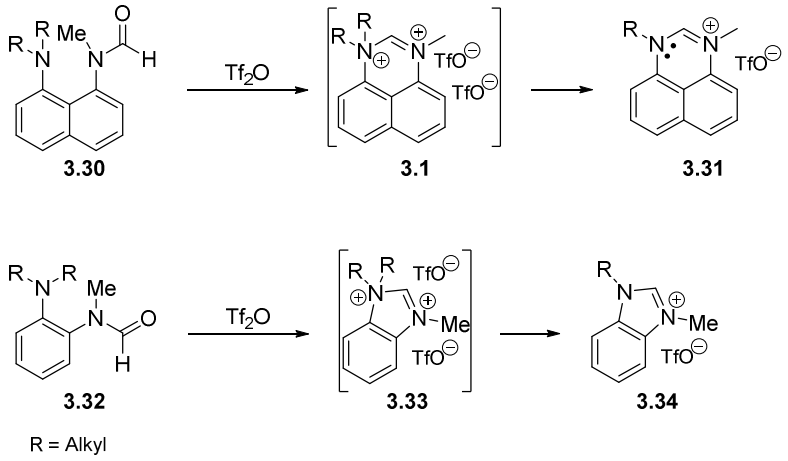

3.30 3.1 3.31

3.32 3.33 3.34

Scheme 3.27 Unlike benzimidazolium product **3.34**, the perimidinium product **3.31** is not a completely aromatic compound due to cross-conjugation.

As with the naphthalene-based compounds, the first formamide example was started with the synthesis of the pyrrolidine derivative. 1,2-Phenylenediamine **3.35** was first reacted with 1,4-diiodobutane to attach the aliphatic carbon chain. Interestingly, the yield for this product **3.36** (77 %) was significantly higher than for the previously described 1,8-diaminonaphthalene substrate (23 %).

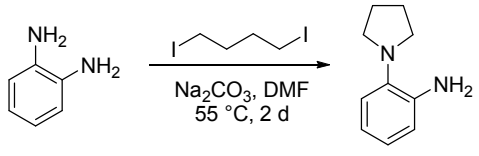

3.35 **3.36**, 77 %

Scheme 3.28 Synthesis of 2-pyrrolidin-1-ylaniline **3.36**.

Subsequent formylation, reduction and, again, formylation were carried out as in the previous cases to obtain the *N*-methylformamide structure **3.39**. All these synthetic steps provided product in good yield. Furthermore, as encountered in the *N*-H formamides based on the naphthalene core, the NMR spectra showed compound **3.37** to be present as a mixture of rotamers. Again, the rotamer with the substituents *cis* to each other was found to be the major isomer with an isomer ratio of 2:1.

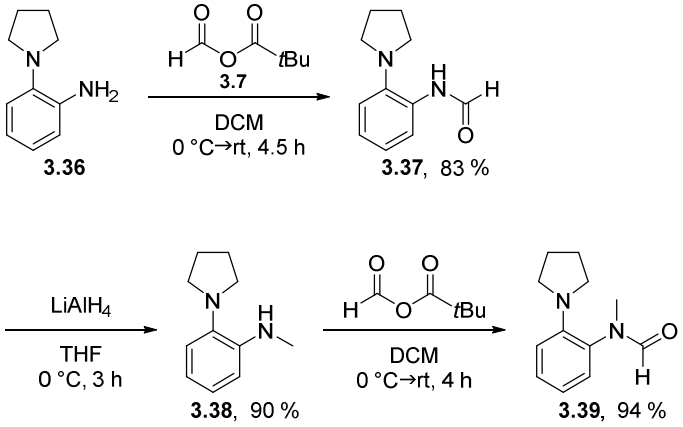

Scheme 3.29 Synthetic route to methyl(2-pyrrolidin-1-ylphenyl)formamide **3.39**.

Addition of the *N*-methylformamide **3.39** to a solution of triflic anhydride in DCM at -78 °C followed by warming to room temperature led to cleavage of the pyrrolidine ring leaving a pure single product **3.40** with a triflate attached to the aliphatic chain, which was isolated in 70 % yield.

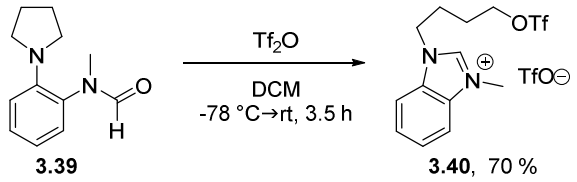

Scheme 3.30 Treatment of compound **3.39** with triflic anhydride leads to ring cleavage.

Bearing methyl groups on the tertiary amine, the next member in this *o*-phenylenediamine series, **3.42**, was prepared, using only two equivalents of methyl iodide on 1,2-phenylendiamine first and affording the expected product **3.41** in moderate yield (47 %). Formylation provided the desired *N*-methylformamide compound **3.42** in 87 % yield.

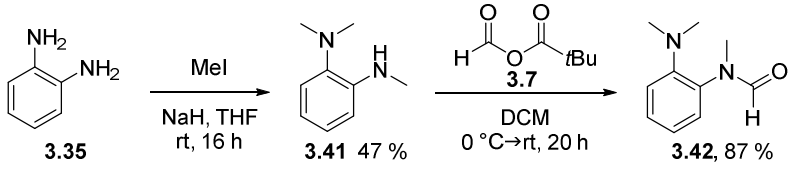

Scheme 3.31 Synthesis of 2-(dimethylamino)phenyl(methyl)formamide **3.42**.

While for the naphthalene analogue with the dimethylamino residue complete demethylation was only achieved when the temperature was elevated to 30 °C upon addition of the substrate to the reaction mixture, here thermal activation was not required to produce the symmetric product **3.43**.

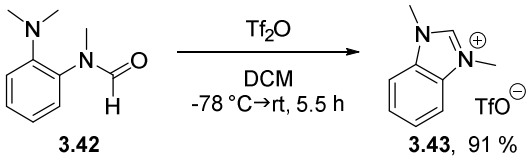

Scheme 3.32 Demethylation of *N*-methylformamide **3.42** upon treatment with triflic anhydride.

The scope of the dealkylation reactions was further broadened by substituting the tertiary amine with the aromatic pyrrole residue. For this, the bond between pyrrole **3.45** and the 2-bromoaniline **3.44** as the starting material was made in an Ullman-type reaction using (1*S*,2*S*)-*trans*-diaminocyclohexane **3.46** as a ligand for the copper catalyst (Scheme 3.33) previously reported by Buchwald *et al*.[147] As usually expected for this type of reaction, the yield was rather moderate, providing 35 % product **3.47**.

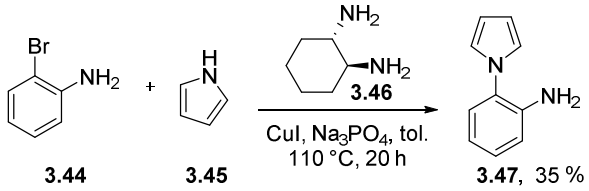

Scheme 3.33 Ullman-type coupling of pyrrole **3.45** and 2-bromoaniline **3.44** for the synthesis of compound **3.47** using a copper catalyst.

Again, formylation, reduction and formylation led to the *N*-methylformamide derivative **3.50**, with each step providing good to excellent yields.

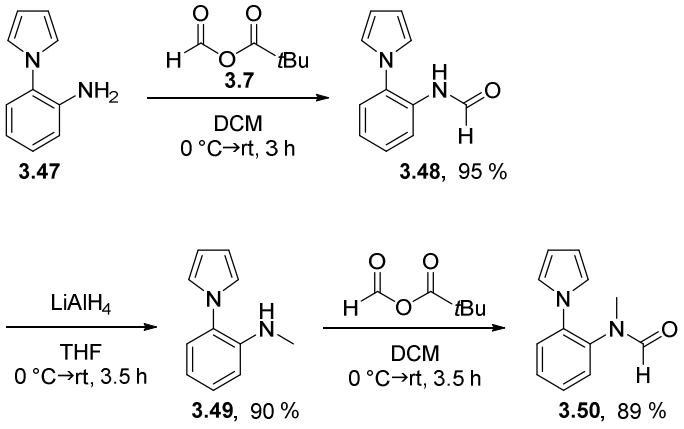

Scheme 3.34 Synthesis of methyl[2-(1*H*-pyrrol-1-yl)phenyl]formamide **3.50**.

Pyrroles are known to have their most reactive nucleophilic site in the 2-position and, as expected, when reacting this substrate with triflic anhydride, the intermediates were intercepted by the pyrrole's 2-position to afford compound **3.51**, which was fully characterised by ^{1}H-, ^{13}C-NMR, IR spectroscopy and high resolution mass spectrometry. This reaction was first stirred at -78 °C upon addition of the triflic anhydride and then warmed to 30 °C to allow better stirring, as the mixture appeared as a slurry.

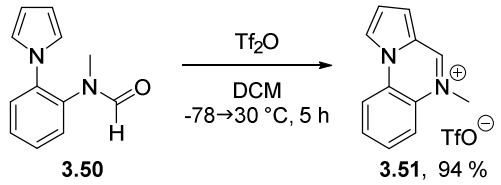

Scheme 3.35 Treatment of *N*-methylformamide **3.50** with triflic anhydride.

The proposed mechanism (Scheme 3.36) involves intramolecular aromatic electrophilic substitution on the pyrrole once the iminium triflate **3.52** is generated.

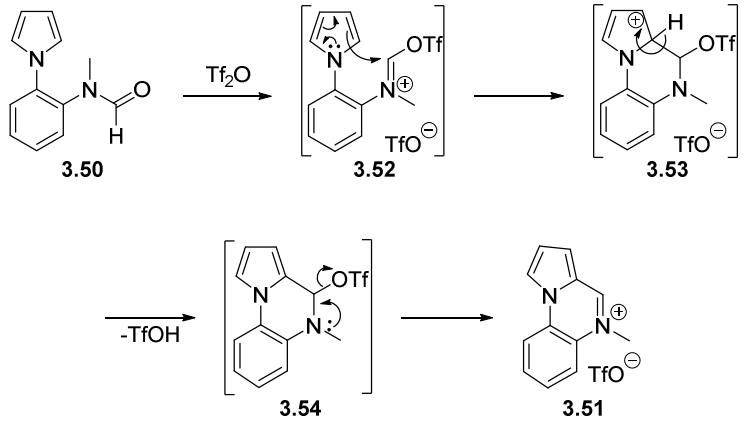

Scheme 3.36 Proposed mechanism for the reaction of compound **3.50** with triflic anhydride.

The previously described mechanistic study on benzamide substrate **3.25** indicated that steric factors can allow for observation of amidinium disalt species at low temperature. Hence, it was wondered if, through wise selection of substituents, a more stable dication could be obtained. Therefore, the next task aimed at an *N*-methylformamide compound with the tertiary amine bearing purely aromatic residues.

At the start of this synthesis an Ullman-type reaction was applied to prepare 2-nitro-*N*,*N*-diphenylaniline **3.57** from 1-bromo-2-nitrobenzene **3.55** and diphenylamine **3.56** in dimethylacetamide (DMA). Again, only a moderate yield (28 %) was obtained from this reaction.

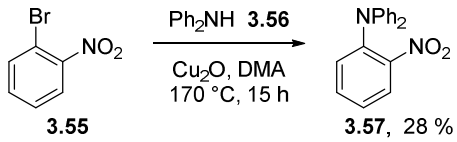

Scheme 3.37 Ullman-type coupling of diphenylamine **3.56** with 1-bromo-2-nitrobenzene **3.55**.

For reduction of the nitro substituent in **3.57** to an amine functionality a standard hydrogenation procedure was carried out using palladium on charcoal as catalyst in methanol. The reaction yield was quantitative (Scheme 3.38).

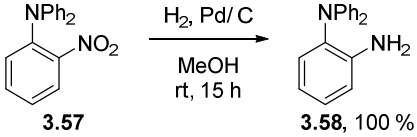

Scheme 3.38 Reduction of nitro-compound **3.57** to *N*,*N*-diphenylbenzene-1,2-diamine **3.58**.

Formylation, reduction and formylation again led to the desired compound, in this case **3.61**.

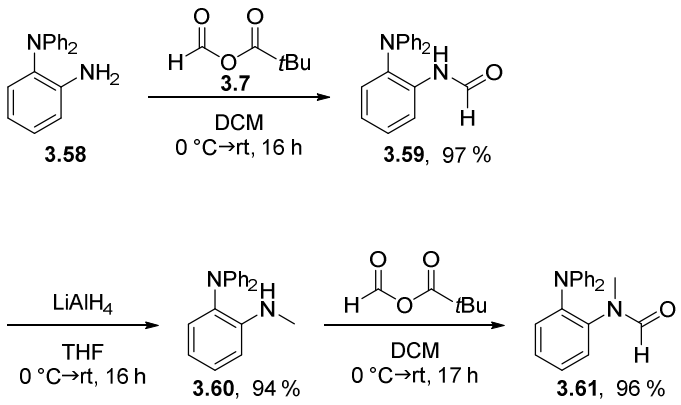

Scheme 3.39 Synthesis of 2-(diphenylamino)phenyl(methyl)formamide **3.61**.

This compound **3.61**, when treated with triflic anhydride, did not show a stable dication in the NMR spectra. However, the benzodiazepinium product **3.62**, which was formed from this reaction, indicated that an intriguing transformation had occurred with the mechanistic route to be examined. The structure of this single product was confirmed by ^{1}H-, ^{13}C-NMR, IR spectroscopy and high resolution mass spectrometry.

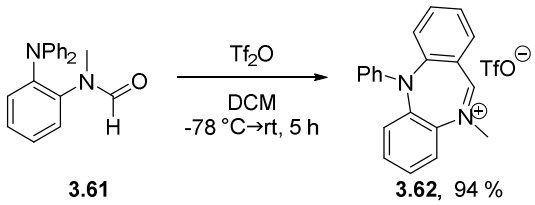

3.61 **3.62**, 94 %

Scheme 3.40 Unexpected rearrangement product **3.62** upon treatment of compound **3.61** with triflic anhydride.

As seen for the pyrrole containing derivative, the most favourable route to this outcome is explained by an electrophilic aromatic substitution of one of the phenyl residues. The lone pair of the nearby nitrogen in **3.63** could facilitate this step by donating sufficient electron density through the π-system. The resulting positive charge in **3.64** would also be well delocalised within the intermediate.

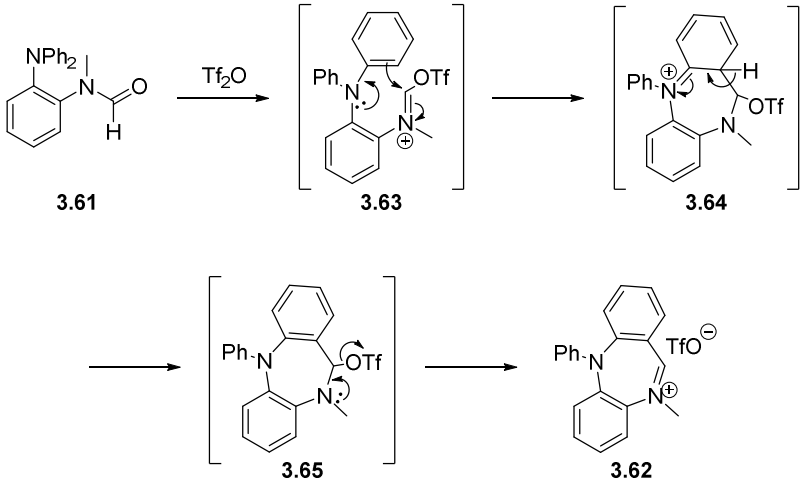

3.61 **3.63** **3.64** **3.65** **3.62**

Scheme 3.41 Postulated mechanism for the reaction of compound **3.61** with triflic anhydride.

However, at least two other possible mechanisms have to be considered with both leading through dicationic intermediates. The first one (Scheme 3.42) involves intramolecular nucleophilic attack of the tertiary amine onto the iminium carbon, generating the tetrahedral intermediate **3.66** prior to formation of the dication **3.67**. The highly positive character of the carbon centering the amidinium moiety then experiences nucleophilic attack by the *ortho*-position of one of the phenyl rings in an intramolecular electrophilic aromatic substitution. Lastly, rearomatisation and ring expansion occurs to afford the observed product **3.62**.

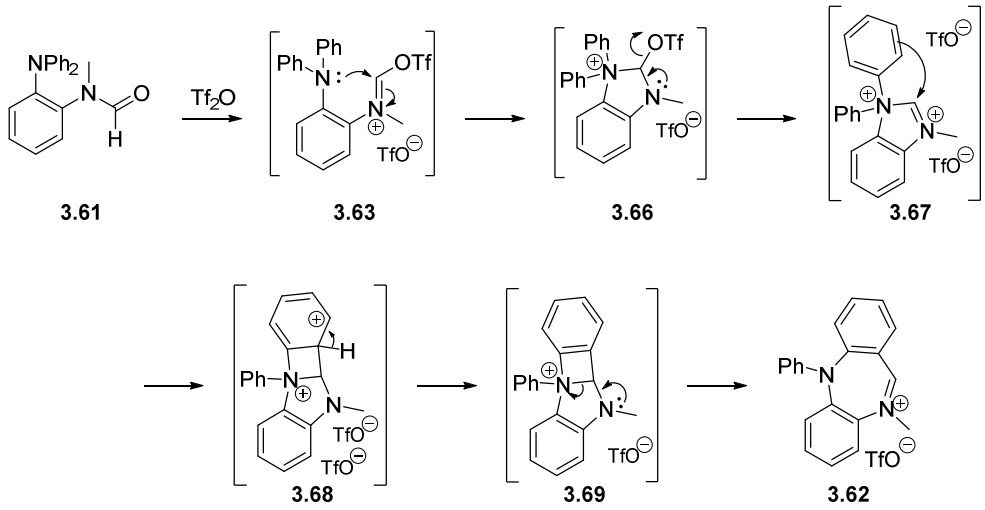

Scheme 3.42 Alternative mechanism for the reaction of triflic anhydride with compound **3.61** involving a 4-membered ring intermediate **3.69**.

Another pathway has to be considered involving intramolecular electrophilic aromatic substitution, which could also lead to product **3.62**. Attack from the *ortho*-position of one of the phenyl residues on the carbon centering the amidinium moiety would result in a concerted substitution with expulsion of the triflate substituent and direct formation of 4-membered ring intermediate **3.68** (Scheme 3.43).

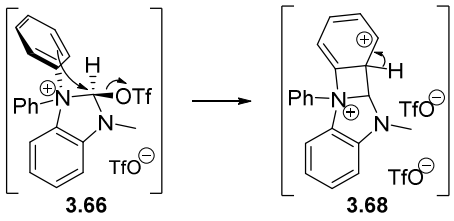

Scheme 3.43 Hypothetic E2-based formation of the 4-membered ring intermediate **3.68**.

The second proposal (Scheme 3.44) includes these initial steps until formation of the dication **3.67**, but then electrophilic aromatic substitution on one of the phenyl rings occurs on the *ipso*-position producing a three-membered ring intermediate **3.70**. This route would be identical with the latter one until the point where the tetrahedral species **3.66** is formed. Now, this time the *ipso*-position of one of the phenyl residues would attack the amidinium carbon centre forming a 3-membered ring intermediate **3.70** which would be followed by breakage of the bond between the sp^3-hybridised nitrogen centre and the carbon atom in the amidine moiety. Migration of the bond between the latter nitrogen centre and the cyclohexadienylium residue could form the 6-membererd pyrazinium ring. The pathway would be completed by proton loss and rearomatisation of the positively charged cyclohexadienyl moiety.

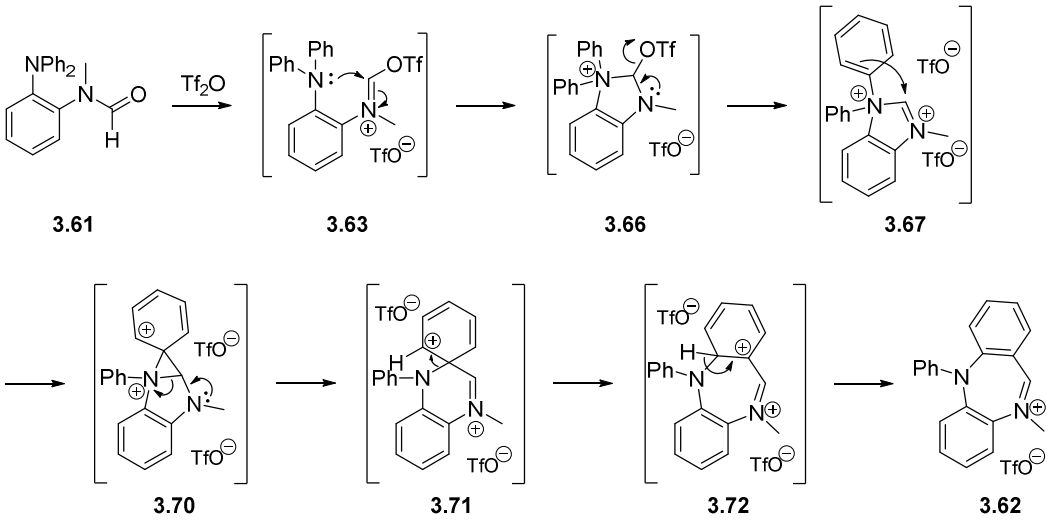

Scheme 3.44 Alternative mechanism for the reaction of triflic ahydride with compound **3.61** involving a 3-membered ring intermediate **3.70**.

The likelihood of one of these proposals could be further explored by *in silico* studies; however, the synthetic route to this product formed in this initial reaction might be of particular interest for pharmaceutical research as the structure is closely related to the core structure of the drugs Librium **3.74** and well-known Valium **3.75**. Librium, also known as chlordiazepoxide, was actually the first discovered member of a family of psychoactive compounds named benzodiazepines, including Valium **3.75** and Clozapine **3.76**. Until today a huge range of different derivatives and analogues have entered the market and research on efficient and economical synthetic approaches still leads to high profile publications (Figure 3.23).[158]

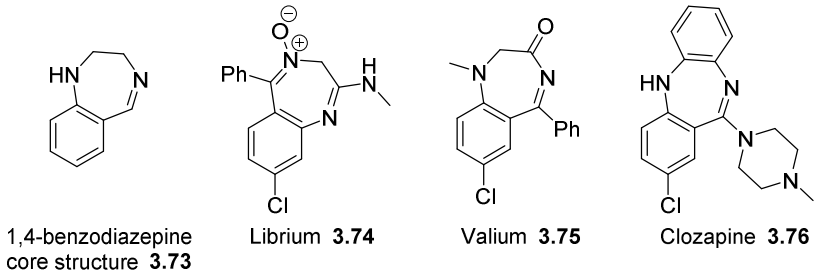

Figure 3.23 The benzodiazepine core structure **3.73** some derived selected bioactive compounds.

A comparison between the geometry optimised (DFT, B3LYP/6-31G*, vacuum) models of structure **3.62** and Clozapine **3.76** (Figure 3.24) reveals the newly presented formamide-derived compounds could indeed be highly interesting analogues for the long-known benzodiazepines.

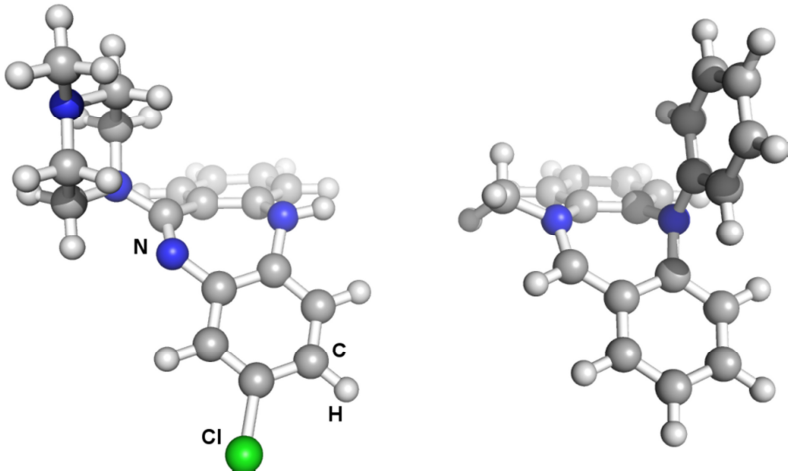

Figure 3.24 Geometry-optimised structures of the psychoactive drug Clozapine **3.76** (left) and rearrangement product **3.62**.

3.6 Mechanistic aspects of the reaction of triflic anhydride with benzene-based formamides and benzamides

At the beginning of the last subchapter it was predicted that benzene-based formamides should exhibit greater reactivity than the naphthalene-based derivatives. The reason for this was found in the greater aromatic stabilisation gained in the benzene-based products upon treatment with triflic anhydride, whereas the naphthalene-based formamides produced perimidinium products, which did not exhibit aromatisation over the entire structure due to cross-conjugation. Indeed, when the benzene-based formamides with alkyl residues on the tertiary amine were subjected to low temperature NMR studies, neither the dicationic nor the tetrahedral triflate intermediate could be observed upon triflic anhydride addition. Even when temperatures were lowered to -50 °C in d_2-DCM, only alkyl-cleaved product was observed.

Nevertheless, it was chosen to examine **3.77**, the benzamide analogue of *N*-methylformamide **3.61**. The chance of stabilising the dicationic intermediate in this case was most promising, as the tertiary amine residue was substituted with phenyl groups, which previously did not dealkylate. Therefore, the benzamide substrate **3.77** was prepared by reacting amine **3.60** with benzoyl chloride in a mixture of DCM and pyridine at room temperature over 15 h.

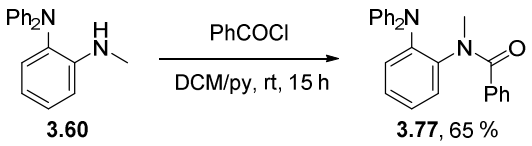

3.60 **3.77**, 65 %

Scheme 3.45 Synthesis of benzamide **3.77**.

This benzamide was now reacted with triflic anhydride in DCM at 0 °C and after 17 h of reaction time, the precipitate formed was first triturated with DCM to afford the disalt **3.78** in 82 % yield (Scheme 3.46). Although the dication **3.78** showed sufficient solubility in DCM, for NMR characterisation deuterated acetonitrile was used. The sample inside the NMR spectroscopic probe had to be cooled to 0 °C, as the dication reacted with the solvent within minutes at room temperature. The ^{1}H-NMR spectrum (Figure 3.25) shows not only a large downfield shift for the aromatic protons (7.50-8.50 ppm), which is in agreement with an highly electron-deficient system, but the methyl group as well is found strongly downfield-shifted and resonates at 4.56 ppm.

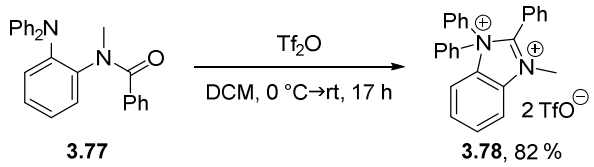

3.77 **3.78**, 82 %

Scheme 3.46 Synthesis of amidinium disalt **3.78**.

The exceptional reactivity of the novel amidinium disalts has been demonstrated on the previous pages. However, by suitable selection of residues on the tertiary amine and through substitution of the formamide residue for a benzamide group, isolation and characterisation of the amidinium disalt becomes possible. Furthermore, this finding also supports the formation of an amidinium disalt intermediate **3.67** from *N*-methylformamide analogue **3.61** for the speculated mechanism *en route* to benzodiazepine structure **3.62**.

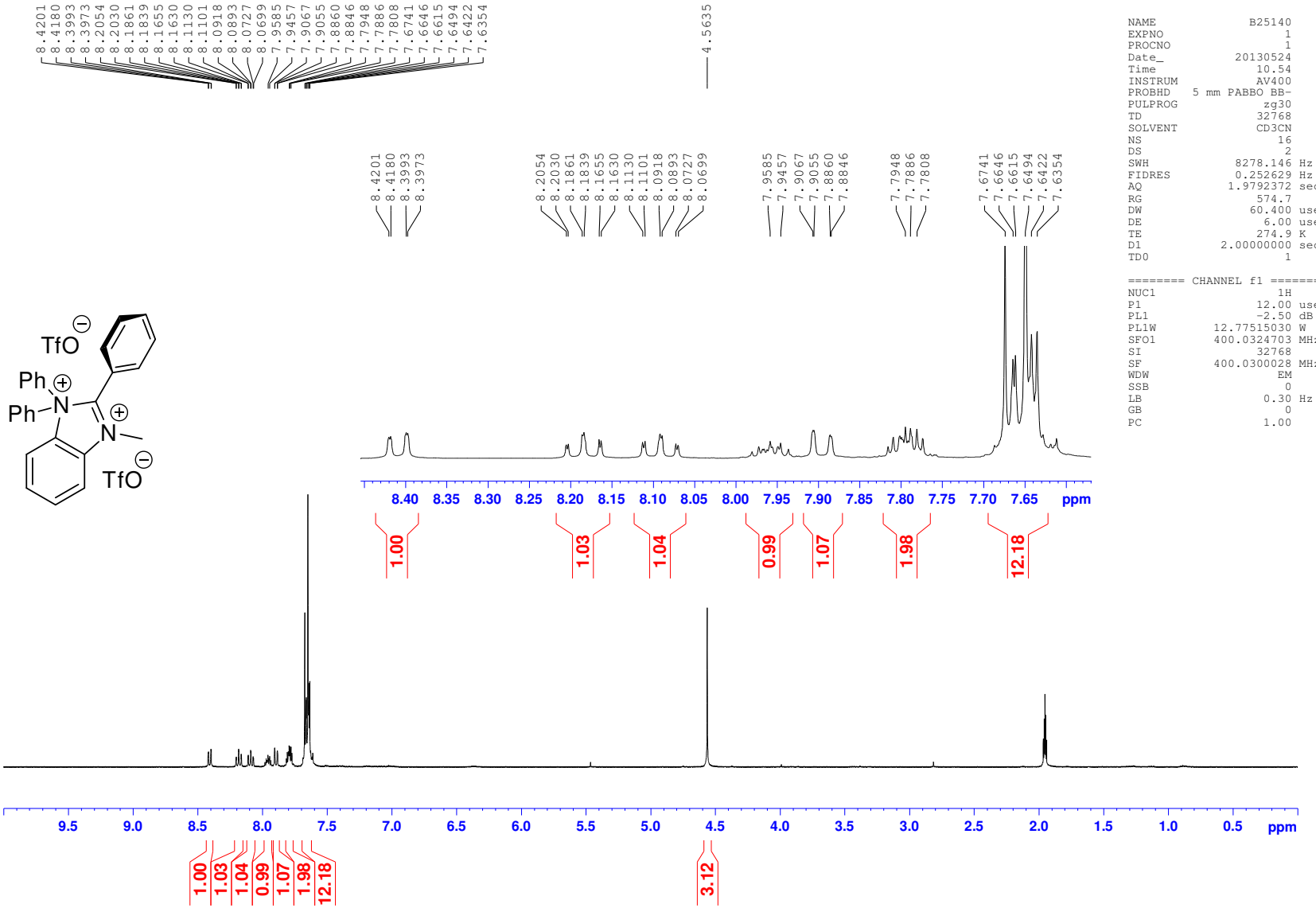

Figure 3.25 ^{1}H-NMR spectrum of dication **3.78**.

3.7 Control experiments for alkyl transfer from aromatic amines

Even though computational studies supported involvement of superelectrophilic species in these alkyl transfer reactions, test reactions were done to exclude the possibility that demethylations arise from the reactive nature of the triflic anhydride itself. Therefore, under the same conditions as for the previous studies, triflic anhydride was reacted with dimethylaniline **1.257** (Scheme 3.47). The reaction mixture was first stirred at -78 °C for 2 h, then warmed to room temperature and stirred for a further 15 h in DCM to form an orange precipitate. As almost all previous reactions of this type gave clean product formation, which did not need any sort of purification, the solvent was removed under reduced pressure and a ^{1}H-NMR spectrum of the crude material recorded in d_3-MeCN. As the spectrum appeared very complex and indicated the presence of several compounds as well as the starting material, the crude product was triturated in DCM, filtered and washed with DCM. Despite the precipitate being washed with DCM extensively, the ^{1}H-NMR spectrum showed that the obtained dication *N*,*N*,*N*',*N*'-tetramethylbenzidinium **3.79** could not be purified completely. It was assumed that these impurities originated from oxidised *ortho*-/*para*-coupled bisanilines, which were also not soluble in DCM, hence difficult to provide an accurate yield. Additional to the ^{1}H-NMR information, high resolution mass spectrometry supported dication **3.79** as the main compound in the orange precipitate. Attempts were carried out to obtain this salt in pure form, but were unsuccessful. The organic phases of the washings were collected and separation by flash chromatography afforded dimethylaniline, with *N*,*N*,*N*',*N*'-tetramethylbenzidine **3.80** and *N*,*N*-dimethyl-4-((trifluoromethyl)-sulfonyl)aniline **3.81** in small quantities.

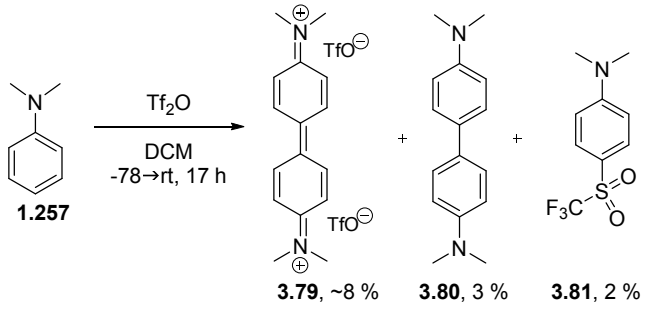

Scheme 3.47 A control reaction of *N*,*N*-dimethylaniline with triflic anhydride did not show demethylation.

From this control experiment it was shown that demethylation did not occur on tertiary amines lacking a neighbouring formamide group. This finding also supports the proposal that an amidinium disalt intermediate or a species such as the tetrahedral intermediate **3.21** is a prerequisite for the dealkylation process, which clearly cannot form in a reaction of triflic anhydride with dimethylaniline. Interestingly, the products obtained indicate an oxidation reaction for the substrate

and, in fact, literature shows many examples in which triflic anhydride was used as an oxidising agent in organic synthesis.[159,160]

The mechanisms to the products described above are proposed in Scheme 3.48. In the main pathway an electron is transferred from the electron-rich dimethylamine **1.257** to the triflic anhydride, which fragments to the triflate anion and a triflyl radical **3.82**. The radical cation **3.83** is then attacked by a second equivalent of amine to afford radical species **3.84**. Hydrogen abstraction, rearomatisation to benzidine **3.80** and twofold oxidation by two equivalents of triflic anhydride complete the proposed pathway to benzidinium dication **3.79**. The reduced species **3.80**, also known as benzidine, can simply evolve by reduction of the latter species.

Simultaneously, another independent pathway towards the observed *para*-triflyl aniline derivative **3.81** could possibly be explained by electrophilic aromatic attack from the *para*-position of *N*,*N*-dimethylaniline **1.257** onto triflic anhydride. The σ-complex can then loose a proton to the triflate anion to rearomatise again and become the final product **3.81**.

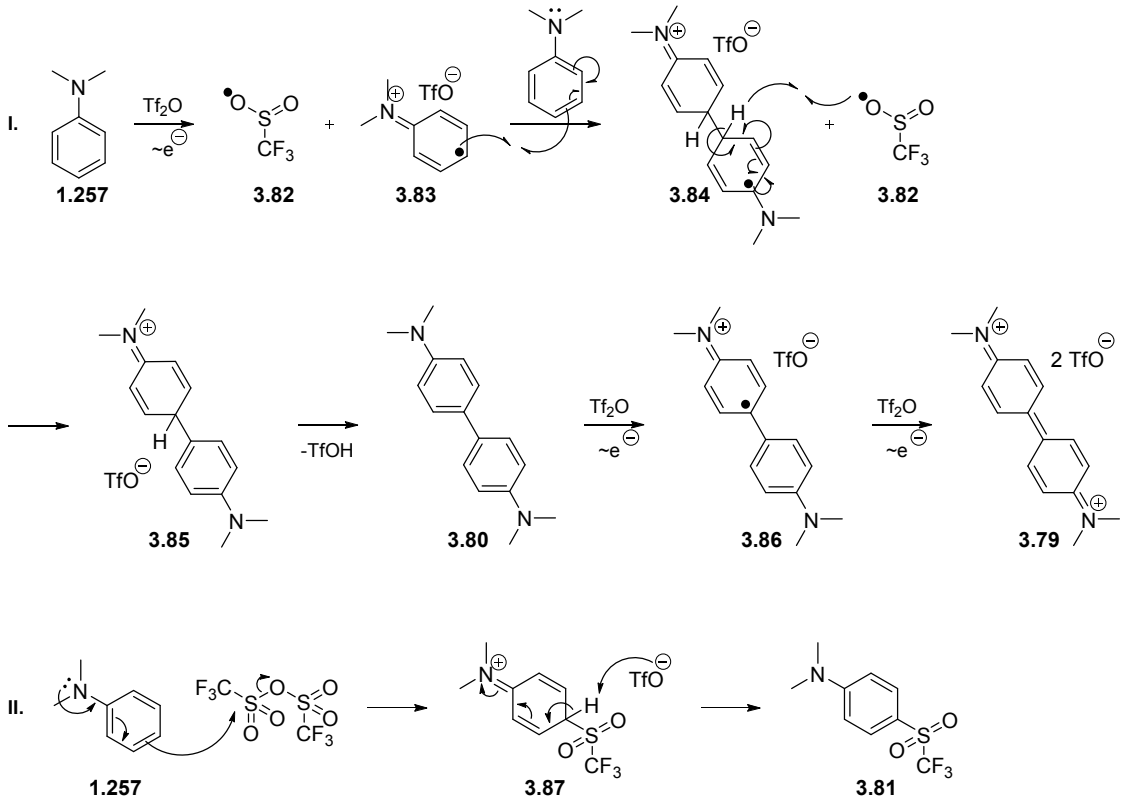

Scheme 3.48 Proposed oxidative (**I.**) and electrophilic aromatic substitution (**II.**) mechanism for the reaction of *N*,*N*-dimethylaniline **1.257** with triflic anhydride.

3.8 Synthesis and reactivity of benzothiazolium and benzoxazolium dications

By substitution of the tertiary amine residue for alkoxy or alkylthio groups in the formamide and benzamide substrates, exploration of superelectrophilic benzthiazolium and benzoxazolium dicationic species become available. These compounds do not only present an interesting synthetic challenge, but the benzthiazolium dications also have relevance to (*S*)-adenosylmethionine. As seen in the introduction chapter, transalkylation from this biologically most important alkylating agent is still of great interest, therefore benzthiazolium dications would be interesting in terms of comparing alkylating strength. On the other hand, benzoxazolium dications are interesting from a synthetic point of view, as one of the chemist's favourite class of methylating agents for reactions that cannot be achieved by methyl iodide or dimethyl sulfate is still alkyloxonium salts, better known as Meerwein salts. Initially, computational calculations (DFT, B3LYP/6-31G*, vacuum) were performed on three hypothetical superelectrophilic models **3.88**, **3.89** and **3.90**, which might have formed from the corresponding *N*-methylformamides analogous to the previously introduced reaction pattern. As expected, the results of the geometry optimisation (Figure 3.26) for the benzoxazolium dication **3.89** show sp^2-hybridisation for the oxygen atom, indicating that its electron lone pair resides in a p-orbital allowing delocalisation over the benzene and the imidinium moiety and therefore rendering the structure aromatic. This suggests that alkyl cleavage from this kind of superelectrophile might be a lot more difficult than from a benzimidazolium dication **3.88**.

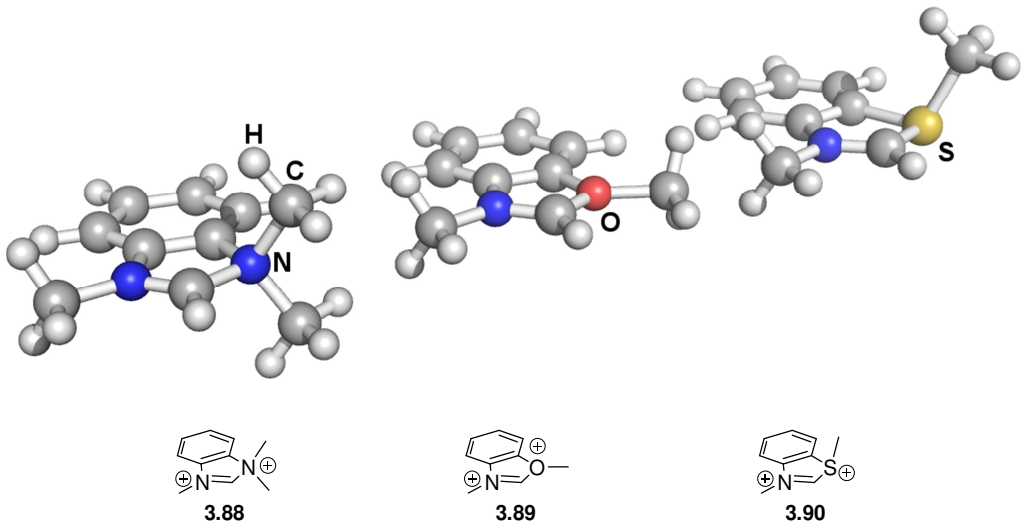

Figure 3.26 The geometry-optimised models of the disalts **3.88**, **3.89** and **3.90**.

Interestingly, for the next heavier homologue in the sixth main group, the hybridisation of the sulfur atom in **3.90** is again sp^3. This can be explained with the greater diameter of the sulfur atom, leading to larger bond lengths and subsequently less overlap of the p-orbitals. Therefore, compared with the benzoxazolium dication **3.89**, enhanced reactivity is expected for the benzthiazolium dication **3.90**.

For studies of the benzoxazolium dications reference is made to the work from Callum Scullion.[146] The following discussion only deals with investigations into the synthesis and features of benzthiazolium dications.

The synthetic preparation of the formamides in general followed the previously described routes to *ortho*-*N*-alkylamino formamides. The first methylation step in Scheme 3.49 though required deprotonation of the thiol group in 2-aminothiophenol **3.91** not only because it is a poor nucleophile and the reaction would be very slow, but also to prevent alkylation of the more nucleophilic amino functional group. This was achieved by adding one equivalent of sodium to a solution of 2-aminothiophenol **3.91** in ethanol generating a base which deprotonated the thiol functional group. The base also prevented generation of the strong acid hydrogen iodide. Compound **3.92** was subsequently formylated with formic pivalic anhydride to afford *N*-H formamide **3.93** and then reduced with lithium aluminium hydride again to yield *N*-methyl-2-(methylthio)aniline **3.94** whose isolation required much care as it oxidised extremely quickly on exposure to air due to being a very electron-rich compound. Hence, the whole work-up procedure was carried out under oxygen-free conditions with degassed solvents. The compound's sensitivity towards oxygen didn't allow for purification by flash chromatography. Despite all difficulties, the compound was obtained in a good yield. For the same reasons, the next formylation step was performed in dry and deoxygenated DCM to produce the desired *N*-methylformamide **3.95** in an almost quantitative yield.

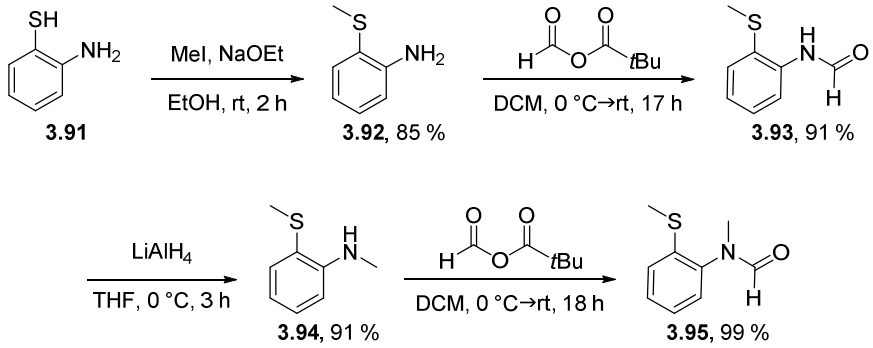

Scheme 3.49 Synthetic route to *N*-methylformamide **3.95**.

Compound **3.95** was reacted with triflic anhydride to afford the demethylated benzothiazolium triflate **3.96**. Small amounts of impurities required the product to be purified by flash chromatography with a highly polar solvent system (10 % MeOH/DCM) due to it being a charged species.

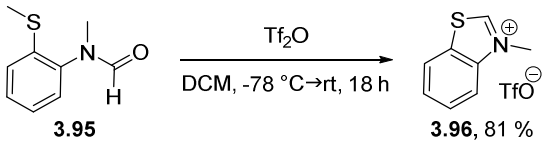

Scheme 3.50 Demethylation of **3.96** upon addition of triflic anhydride.

The second substrate in this series was synthesised to bear a benzyl residue instead of a methyl group on the sulfur. For this, 2-aminothiophenol **3.91** was reacted with benzyl chloride with sodium methoxide as a base in anhydrous DMF.

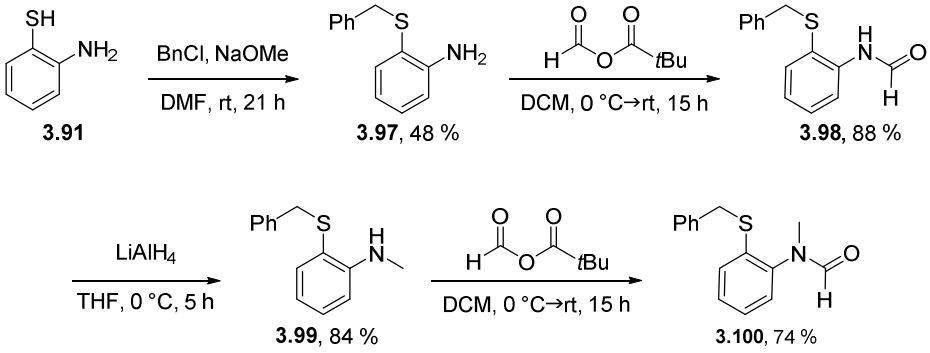

Scheme 3.51 Synthetic route to formamide **3.100**.

The compound was then reacted with formic pivalic anhydride to afford the *N*-H formamide **3.98** in a good yield. Reduction with lithium aluminium hydride again provided a very air-sensitive compound **3.99** that had to be worked-up in the absence of oxygen.

When *N*-methyl formamide **3.100** was reacted with triflic anhydride, unlike for substrate **3.95** with the methylthioether residue, simple trituration of the monocationic product **3.96** with diethyl ether was sufficient for purification.

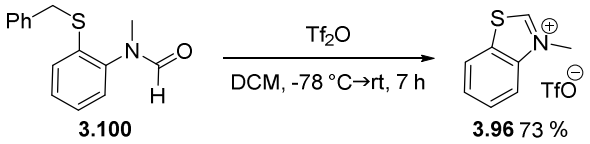

Scheme 3.52 Debenzylation upon reaction of formamide **3.100** with triflic anhydride.

The fact that the thioalkyl derivatives worked as well as the previously studied *N*-methylformamides with tertiary amine residues inspired the investigation of a well-known biosynthetic transformation of terpenoids. Geranyl pyrophosphate **3.101** is an important starting point in the biosynthesis of a huge number of natural products such as limonene **3.105**. Expulsion of the pyrophosphate first leads to a delocalised geranyl carbocation **3.102** which is then converted enzymatically to the analogous

neryl carbocation **3.103**, which upon cyclisation and proton abstraction affords the final product **3.105**.[161-164]

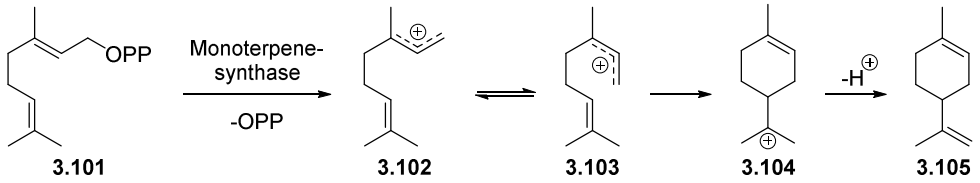

Scheme 3.53 Geranyl pyrophosphate is enzymatically cyclised to limonene **3.105**.

In the terpene case, the pyrophosphate is the leaving group. By synthesising a thioether **3.111** incorporating the neryl chain (Scheme 3.56), we could now explore whether upon addition of triflic anhydride, the allyl cation analogously to **3.102** would form and undergo further reaction.

The first synthetic step towards the desired formamide involved transformation of the hydroxyl group of nerol into a good leaving group. By reacting nerol **3.106** with acetic anhydride under nucleophilic catalysis by means of 4-DMAP under mild conditions, neryl acetate **3.107** was obtained in a rapid and high yielding transformation.

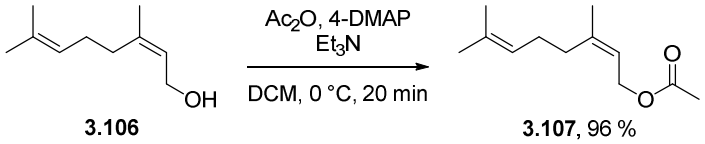

Scheme 3.54 Synthesis of neryl acetate **3.107**.

Formation of the thioether was achieved by reaction of the neryl acetate **3.107** with 2-aminothiophenol **3.91** in DMF at 90 °C producing **3.108** in a rather poor yield (31 %).[165]

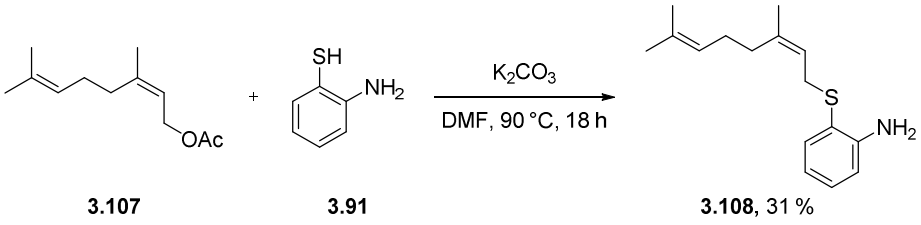

Scheme 3.55 Synthesis of amine **3.108**.

Subsequently, the three familiar synthetic steps involving formylation, reduction and again formylation were applied providing the respective products in good to excellent yield (Scheme 3.56).

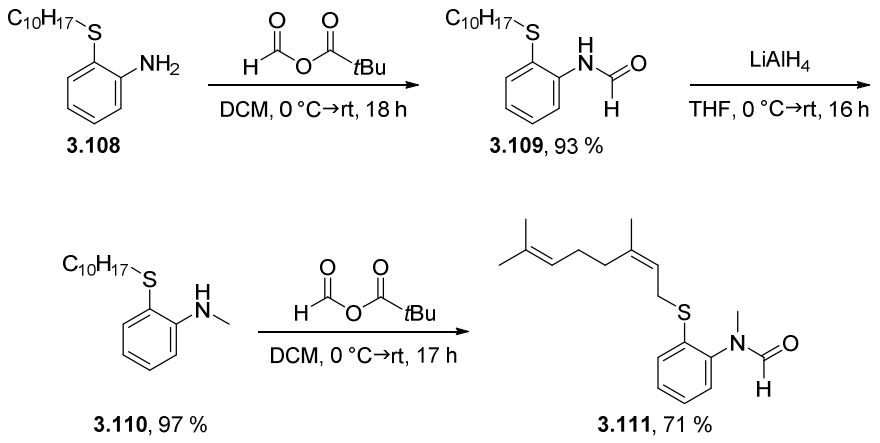

Scheme 3.56 Synthetic route to *N*-methylformamide **3.111**.

The *N*-methylformamide compound **3.111** was now reacted with triflic anhydride at 0 °C, and as expected, the demethylated monosalt was obtained by trituration in excellent yield. However, when the organic washings from the trituration were evaporated under reduced pressure a colourless viscous oil was first afforded, for which analysis by ^{1}H-NMR spectroscopy was attempted, but the spectrum showed no characteristic signals due to the insolubility of the compound. Therefore the oil was stirred in a 1M sodium hydroxide solution overnight, then neutralised with an aqueous sodium hydrogen carbonate solution and lastly extracted with DCM. Again, after removing the organic solvent under reduced pressure, an oil was afforded which was soluble neither in organic solvent nor in water. In a mass spectrometer using (ESI^{+}) mode, ions were found at *m/z* = 254 (100) and 287 (30), which could not be assigned to a possible structure resulting from a proposed S_N1 mechanism.

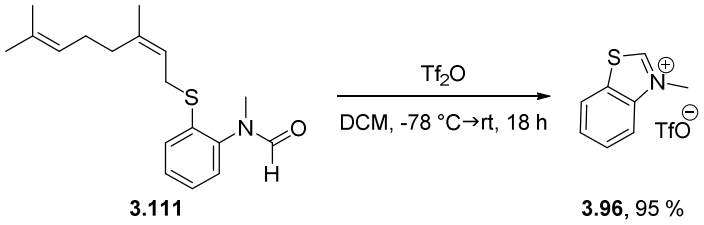

Scheme 3.57 Dealkylation of substrate **3.111**.

These investigations into the thioether derivatives of the *N*-methylformamides were followed up with coupling aromatic residues to the thiol functionality of 2-aminothiol. For that, a 1-fluoro-2-nitrobenzene **3.112** solution in toluene was stirred vigorously with an aqueous basic solution of thiophenol. In this phase transfer reaction, tetrabutylammonium iodide was used as a catalyst that allowed migration of the thiophenolate into the organic phase to react with the 1-fluoro-2-nitrobenzene in a nucleophilic aromatic substitution. Subsequent reduction of the nitro group in compound **3.113** to a primary amine **3.114** by hydrogen gas and palladium over charcoal worked very efficiently.

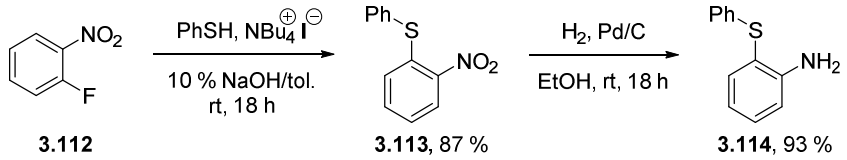

3.112 **3.113**, 87 % **3.114**, 93 %

Scheme 3.58 Synthetic route to amine **3.114**.

Nitro compound **3.113** and the reduced amine product **3.114** do not differ a lot in terms of NMR analysis. Hence, the latter reaction provides an excellent opportunity to recall some fundamental principles and insights of infrared spectroscopy, an analytical method that has been more and more neglected in times of modern NMR spectroscopy. For compound **3.113** two distinct and strong bands are found for the nitro group at 1497 and 1333 cm^{-1} (Figure 3.28). As the asymmetric N-O stretch requires more energy for vibration, the corresponding band is usually found around 1550 cm^{-1} band, while the weaker symmetric N-O stretch comes around 1350 cm^{-1}. Similar instance is then given for reduced compound **3.114** in which the band for the asymmetric N-H stretch is found at 3466 cm^{-1} and the band for the symmetric N-H stretch at 3364 cm^{-1} (Figure 3.28).

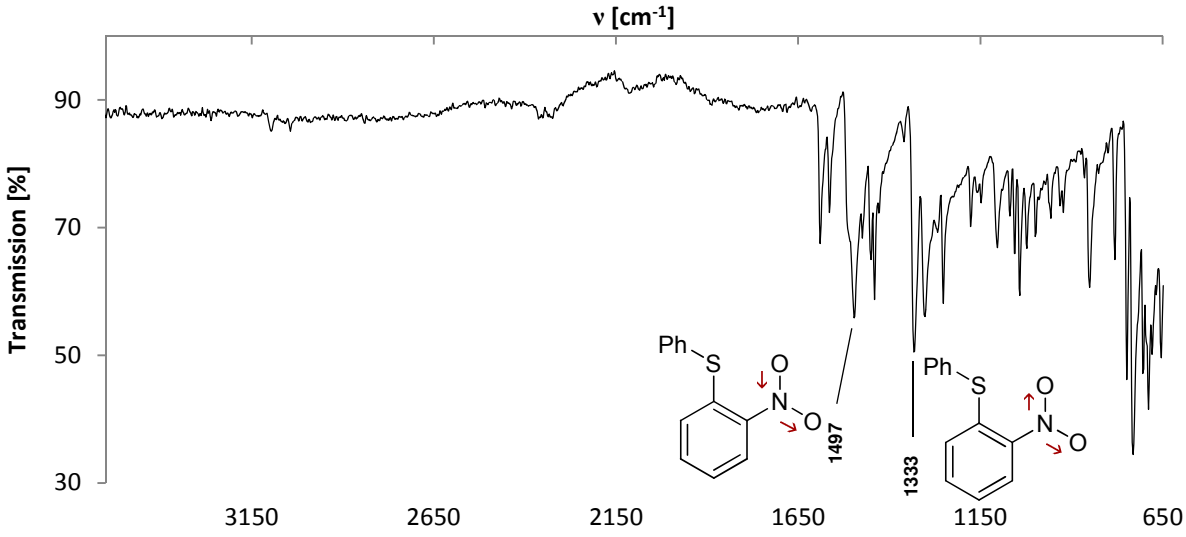

Figure 3.27 IR spectrum of nitro compound **3.113**.

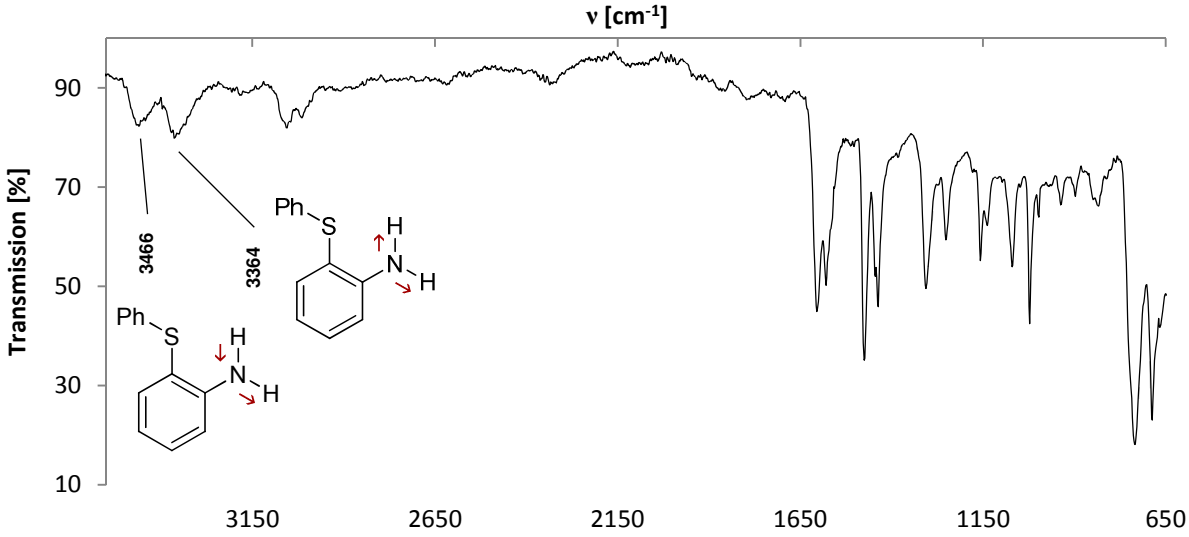

Figure 3.28 IR spectrum of aniline **3.114**.

Again, the three synthetic steps formylation, reduction and formylation followed to provide the desired *N*-methylformamide **3.117** in a good yield.

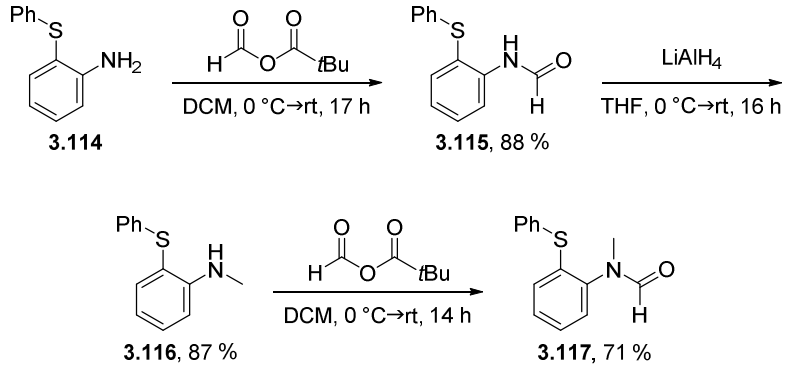

Scheme 3.59 Synthetic route to *N*-methylformamide **3.117**.

Analogously to the reaction of *N*-methylformamide **3.61** with a *N,N*-diphenylamine residue, phenylthioether **3.117** led to formation of a 7-membered heterocyclic product **3.118** exclusively. This compound is also structurally related to a class of psychoactive drugs known as benzothiazepines.

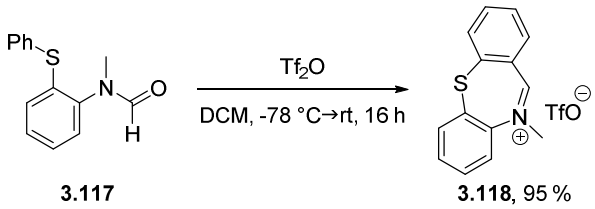

Scheme 3.60 Formation of benzothiazepine **3.118** from formamide **3.117** and triflic anhydride.

Again as in the case of the benzodiazepine structure **3.62**, comparison between the geometry optimised models of compound **3.118** with quetiapine[166] **3.119** (Figure 3.29) revealed high structual analogy worth further exploration.

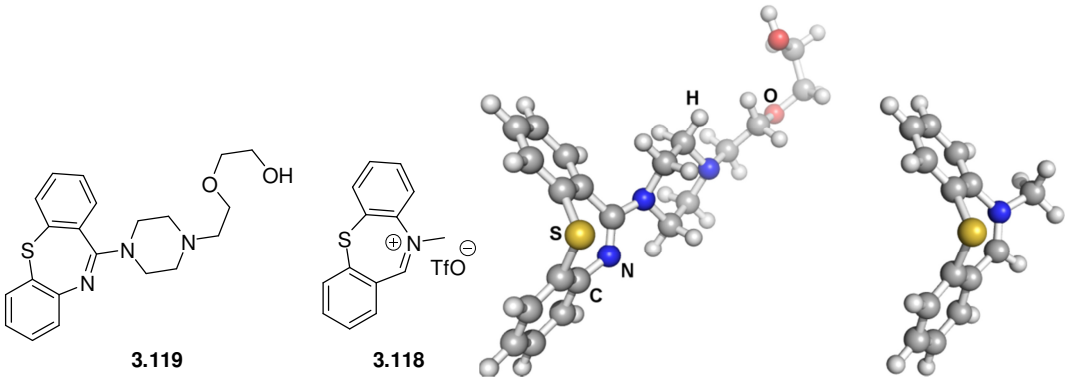

Figure 3.29 Geometry-optimised structures of the psychoactive drug quetiapine **3.119** (left) and benzothiazepine product **3.118**.

Subsequently, synthesis and investigation of a benzamide derivative followed, which bore the potential of affording a stable dication. For this, secondary amine **3.116** was reacted with benzoyl chloride in a mixture of DCM and pyridine at room temperature to yield the desired benzamide **3.120** in very good yield (94 %).

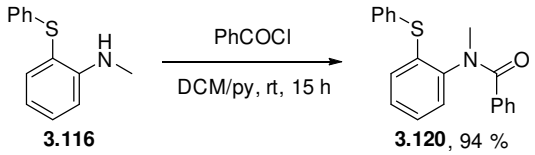

Scheme 3.61 Synthetic route to benzamide **3.120**.

Benzamide **3.120** was then reacted with triflic anhydride at 0 °C for 18 h. Interestingly, although highly polar, this chiral compound did not precipitate from the product mixture dissolved in DCM. Therefore, the compound was then concentrated under reduced pressure and the solid washed with small amounts of DCM to yield 61 % of disalt **3.121**. This novel superelectrophile was successfully characterised, but NMR experiments revealed that this highly electrophilic species was so reactive that it even reacted with d_3-acetonitrile, which was used for NMR analysis, within minutes. Hence, the NMR spectra were recorded at 0 °C.

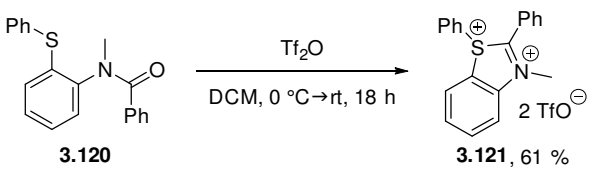

Scheme 3.62 Formation of thiazinium dication **3.121**.

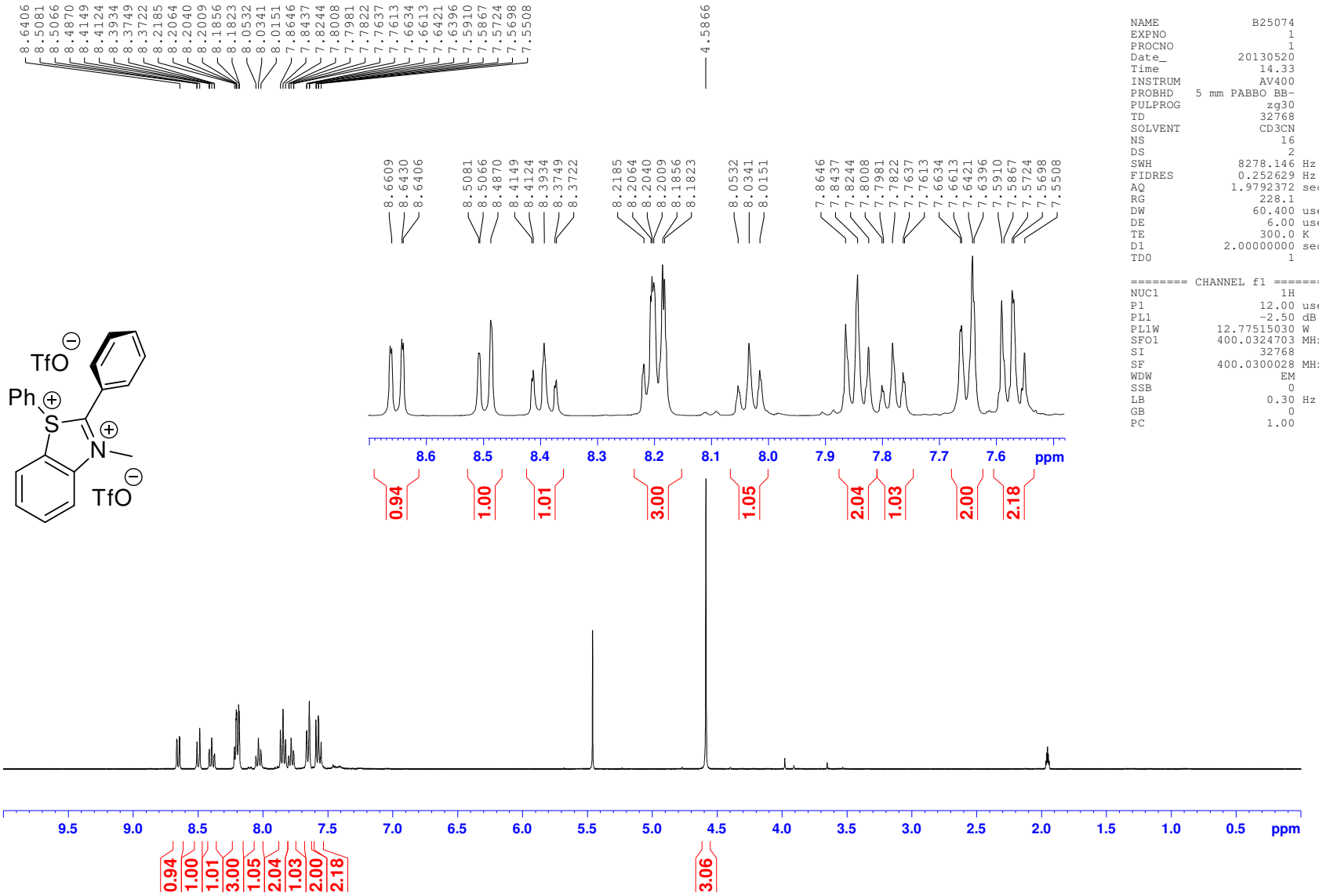

Figure 3.30 ^{1}H-NMR spectrum of disalt **3.121**.

Geometry optimisation predicted the phenyl group attached to the carbon centre between the sulfur and the nitrogen atom to be perpendicular to the heterocyclic ring plane. Hence, the stability of the dication can be explained due to steric reasons rather than electronic reasons preventing an intramolecular electrophilic substitution from the sulfur's phenyl residue onto the carbon atom of the thiazolium moiety. The ^{1}H-NMR spectrum above (Figure 3.30) shows the only aliphatic residue, *i.e.* the methyl group, shifted downfield to 4.59 ppm. Furthermore, the aromatic protons of the benzothiazolium core are most deshielded and found between 8.1 and 8.7 ppm, reflecting the highly electrophilic character of the disalt species.

A recrystallisation from DCM and diethyl ether was attempted for structural analysis by X-ray crystallography, but the crystals produced revealed a compound (Figure 3.31) in which the phenyl residue attached to the sulfonium atom had cleaved to produce monocation **3.122**.

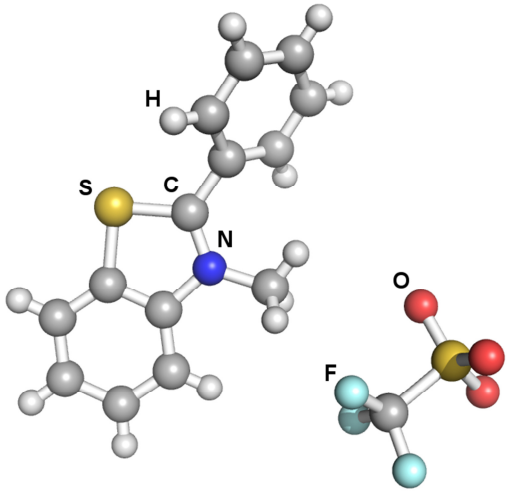

Figure 3.31 Crystal structure of dephenylated monocation **3.122**.

A mechanistic proposal for this transformation involves loss of a phenyl cation followed by nucleophilic attack of a triflate anion (Scheme 3.63). Isolation of phenyl triflate **3.124** should provide further proof for the proposed mechanism. The loss of a phenyl cation associated with the interception by a nucleophile *i.e.* triflate anion in this case, is always an S_N1 displacement, as the geometry of the phenyl residue does not allow for a back-side attack in an S_N2 reaction.

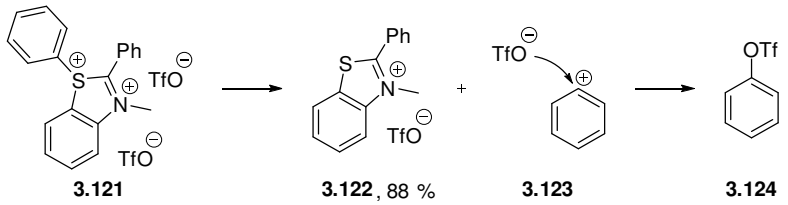

Scheme 3.63 Proposed dephenylation mechanism for benzothiazolium disalt **3.124**.

Formation of a phenyl cation is an unusual process as the species is very high in energy and usually only encountered in the dediazoniation of arenediazonium ions where the strong driving force needed is provided by generation of a molecule of dinitrogen gas (Scheme 3.64).[167,168] More often the dediazoniation involves an electron transfer induction step to form a phenyl radical intermediate instead of a phenyl cation. The latter electron transfer induces homolytic dediazoniation and has not only been achieved with chemical induction, but also with electrochemical and radiolytic methods. The aryl radical **1.127** is a starting point for a larger number for synthetic transformation including some popular named reactions such as the Sandmeyer,[169] Gomberg-Bachmann[170] reaction or the Meerwein arylation.[171]

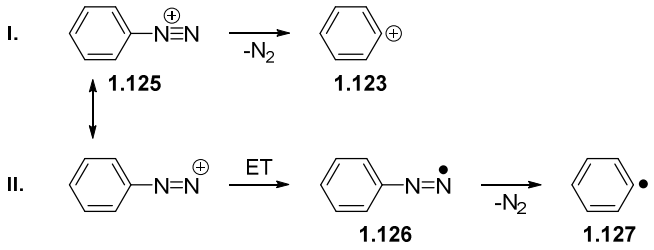

Scheme 3.64 Heterolytic (I.) and homolytic (II.) dediazoniation pathways.

However, an alternative dephenylation mechanism must be considered in which diethyl ether would act as the nucleophile instead of the triflate anion, as under dry conditions the dication was stable for weeks. Thus, the next recrystallisation attempt should be carried out with DCM and pentane.

Herein, it has been demonstrated that superelectrophilic disalts resulting from the reaction of the amide bond with triflic anhydride can be produced in pure form and spectroscopically observed and characterised at low temperature. The introduction of this thesis refers to Charette *et al.* as the first group to attempt ^{1}H-NMR characterisation of these highly electrophilic species in the cold. However, isolation and full characterisation was only achieved recently by our group and the results reported within this thesis describe the synthesis, isolation and the reactive features of even more electron-deficient systems. The exceptional reactivity of these compounds is lastly seen in the unusual dephenylation reaction. Similarly to the well-known stabilisation effect of weakly-coordinating anions (such as tetrafluoroborates) on diazonium salts, introduction of even less nucleophilic counter-ions compared to triflates might produce better stabilised superelectrophiles.

3.9 Substituting the formamide group for carbamate and urethane groups

As most of the superelectrophilic disalts did not allow for isolation, introduction of electron density to the amidinium moiety by suitable residues was considered, that might decrease electrophilicity. It has been shown that by replacing the formamide residue by a benzamide group, stabilisation of the dicationic species resulted for steric reasons. The task was to probe how electronic effects would come into play by substituting the formamide group for carbamate (Figure 3.32).

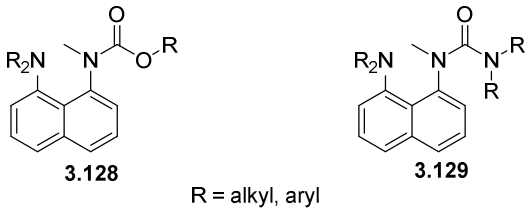

Figure 3.32 Generic structure of carbamates **3.128** and urethanes **3.129**.

For this, it was logical to start the investigations with the less reactive naphthalene-based substrates. First amine **3.16** was reacted with isobutyl chloroformate **3.130** to afford the corresponding carbamate **3.131** in good yield (75 %).

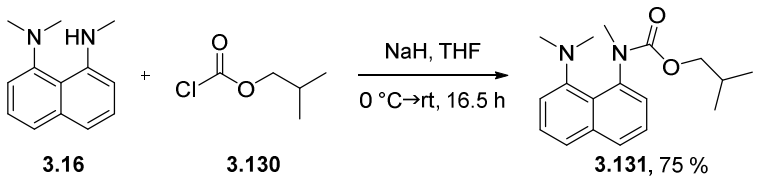

Scheme 3.65 Synthesis of carbamate **3.131**.

This substrate was now reacted with triflic anhydride, but upon completion of the reaction two different compounds had formed in a 1:1 ratio, as NMR experiments on the crude product revealed. The product mixture was therefore completely dissolved in DCM and now diethyl ether was successively added until the more polar product **3.132** of the two started to precipitate. In this way the two compounds were separated by means of a 1:2 Et_2O/DCM mixture to afford the protonated starting material **3.133** as the less polar product.

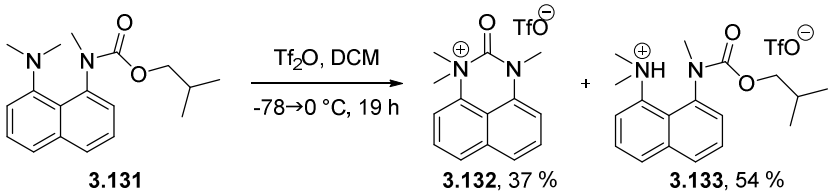

Scheme 3.66 The reaction of triflic anhydride and urethane substrate **3.131** produces a 1:1 mixture of 2-oxo-perimidinium salt **3.132** and protonated starting material **3.133**.

The other compound was identified as the product **3.132**, which although not doubly charged can also be regarded as highly electrophilic, as the positively charged sp^3-hybridised nitrogen centre is next to a strongly electron-withdrawing carbonyl group. For both compounds from the product mixture, isolation and recrystallisation was achieved and their structures solved by X-ray crystallography (Figure 3.33).

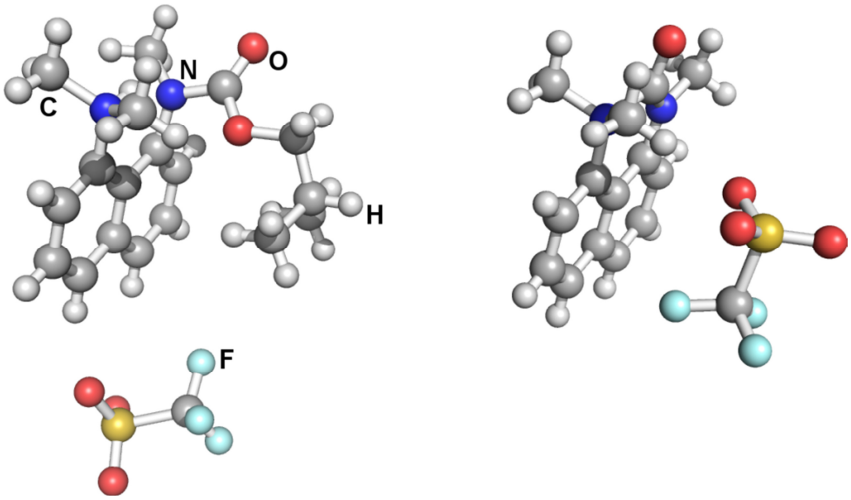

Figure 3.33 Crystal structures of **3.133** (left) and **3.132** (right).

In fact, the highly increased reactivity of electrophile **3.132** was first encountered when NMR analysis was attempted with d_6-DMSO as solvent. Although the spectra produced had not been interpretable, crystals had grown within a couple of days inside the NMR tube, which were then analysed by x-ray crystallography. Apparently, the d_6-DMSO, as an NMR solvent, had been a too good nucleophile that dealkylated the compound to give a symmetric perimidinone product **3.136**.

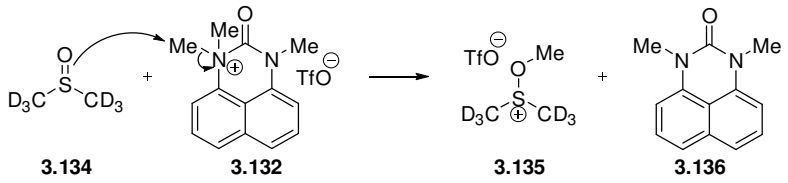

3.134 **3.132** **3.135** **3.136**

Scheme 3.67 Proposed mechanism of demethylation of electrophile **3.132** by d_6-DMSO.

The crystal structures of both the electrophilic monocation **3.132** and the demethylated neutral perimidinone **3.136** allow for comparison of the structural features to give an idea of what factors drive the dealkylation. Shown below (Figure 3.34) is the neutral perimidinone **3.136**, whose crystallographic data were published a few years ago.[172] The amide bond (N-CO) in the neutral molecule is 1.369 Å long, which is just the length of an average nitrogen-carbonyl C bond in *e.g.* tetramethylurea (1.371 Å),[164] although one would expect the amide bond in the perimidinone to be a bit shorter, as in this compound all centres are sp^2-hybridised and electron density well-delocalised,

while the geometry of the nitrogen centres in the urea derivative is somewhat between an sp^2- and an sp^3-hybridisation and the crystal structure shows the urea derivative to be not at all planar.

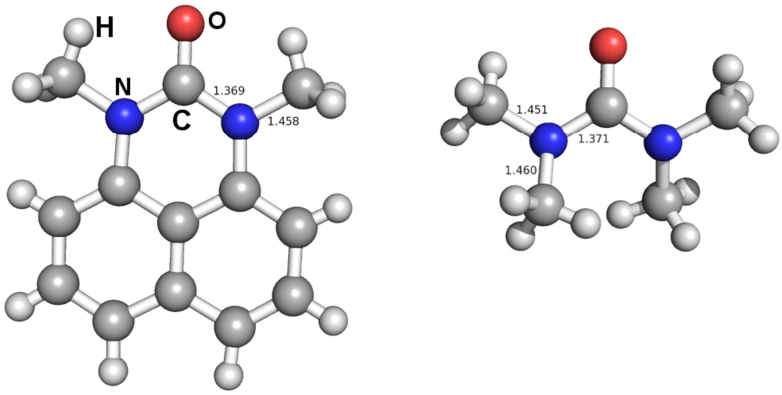

Figure 3.34 Crystal structures of the neutral demethylated perimidinone **3.136** (left) and tetramethylurea (right).[172,173]

In the monocationic perimidinone structure **3.132**, it is remarkable that the two N(sp^3)-Me bonds have not only quite different bond lengths (1.527 vs. 1.515 Å) but also different geometric environments. While the shorter bond is almost in plane with the aromatic π-system, the longer bond is almost perpendicular to the ring plane, thus nucleophilic attack on this site should be more likely. Furthermore, in the cation **3.132**, the N(sp^3)-CO bond is anomalous 1.542 Å long, and thus very electron-deficient and highly destabilised.

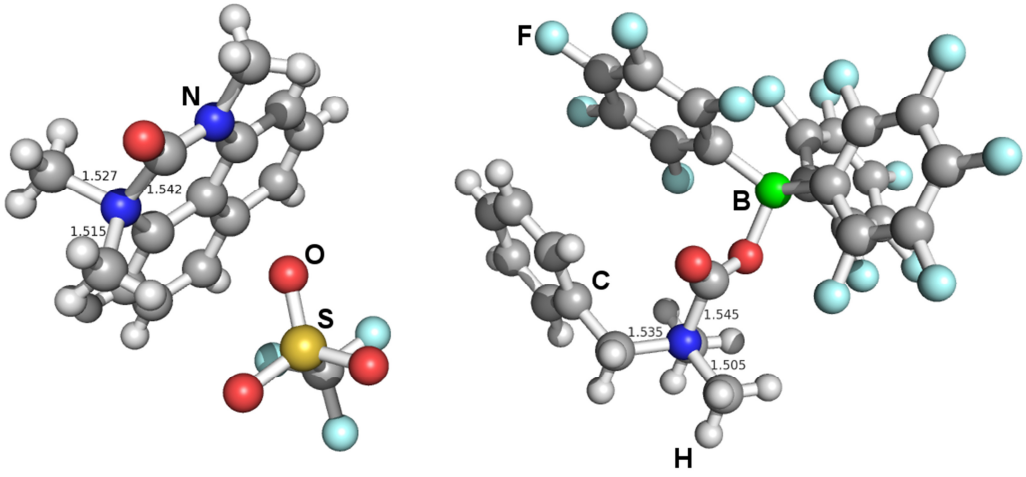

Figure 3.35 Crystal structures of electrophile **3.132** (left) and **3.138** (right).

To emphasise how exceptional such a N(sp^3)-carbonyl C bond length is, the crystal structure of a urethane compound **3.138** is shown on the right hand side of Figure 3.35, which Stephan and co-workers recently reported.[174] The temperature-labile species shown was formed, when they treated frustrated Lewis pair **3.137**, which was initially generated from dimethylbenzylamine and tris(perfluorophenyl)-borane, with carbon dioxide at temperatures below -32 °C. The highly electron-

deficient species **3.138**, in which the N(sp^3)-carbonyl C bond expands to 1.545 Å undergoes the reverse reaction above -20 °C.

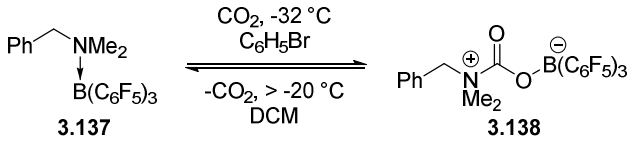

Scheme 3.68 Carbon dioxide activation by the frustrated Lewis pair **3.137**.

Looking back at the outcome of the reaction in Scheme 3.66, it is likely that the loss of the isobutyl group in the 2-oxo-perimidinium species **3.132** involves formation of isobutene allowing release of a proton used in the generation of protonated starting urethane **3.133**. Furthermore, the ^{1}H-NMR spectrum of the product mixture displays a 1:1 ratio of the two compounds **3.132** and **3.133** indicating, that one mechanism in the reaction is at play to afford two different compounds. The most probable mechanism for the transformation seen, however, comes with some problems. The first species generated in this pathway should be the iminium triflate species **3.139** (Scheme 3.69), which is subsequently attacked by the nearby tertiary amine residue to afford the tetrahedral intermediate **3.140**. Now, this species can expel the triflate residue in a rearrangement reaction as shown, which is most likely not concerted and can afford the 2-oxoperimidinium ion **3.132**. The triflic acid generated by the formation of isobutene instantaneously protonates an equivalent of starting material (SM) **3.131**. This pathway and similar mechanisms that involve formation of isobutene and a proton leave one equivalent of unreacted triflic anhydride, which in theory could further react with ammonium compound **3.133**. However, observation of such a species not been made in the NMR spectrum.

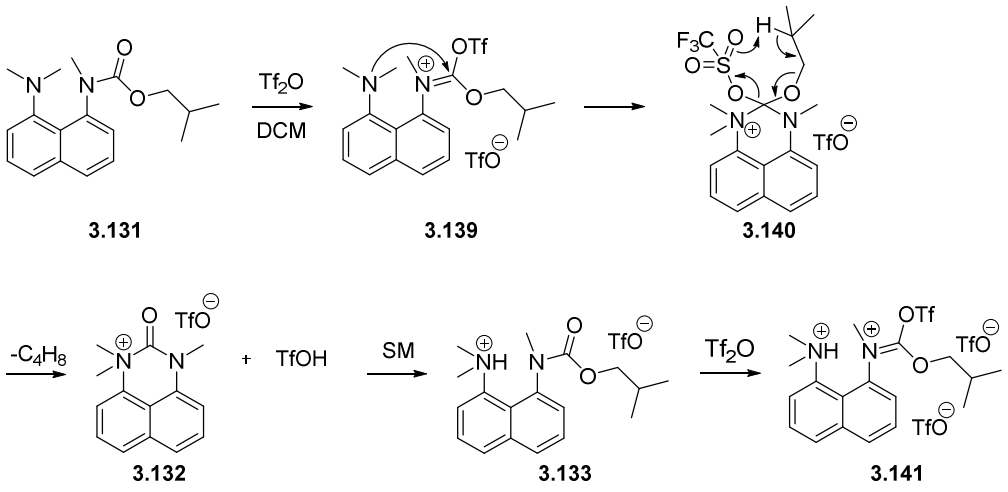

Scheme 3.69 Proposed pathway for the reaction between urethane **3.131** and triflic anhydride.

However, inspecting the crystal structure (Figure 3.36) of the protonated carbamate **3.133**, we see that the amide bond in the *N*-methylformamide residue is not planar but the nitrogen atom tetrahedral. Furthermore, both the orientation of this sp^3-hybridised nitrogen centre and the orientation of the protonated tertiary amine residue indicate strong H-bonding between the two nitrogen atoms. Hence, the nucleophilic feature of the amide bond is extinguished and not available for attack on the excess triflic anhydride to form **3.141**.

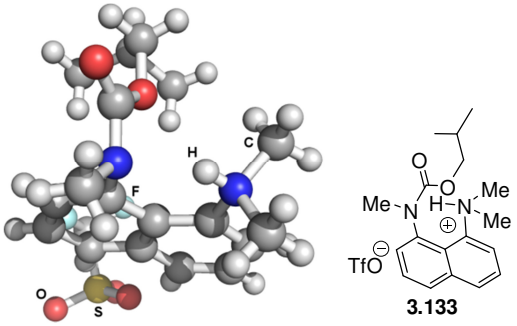

Figure 3.36 The crystal structure of **3.133** shows H-bonding between the protonated tertiary amine and the nitrogen centre in the carbamate residue.

The same outcome was seen when the pyrrolidine analogue **3.142** was synthesised by the previously described method and reacted with triflic anhydride (Scheme 3.70). Again, the ^{1}H-NMR spectrum of the product mixture showed a 1:1 ratio of perimidinium species **3.143** and protonated starting material (not shown). The different solubility features of the products were again used to isolate the perimidinium species **3.143** in a good 41 % from an expected 50 % yield by trituration. The protonated starting material was not isolated.

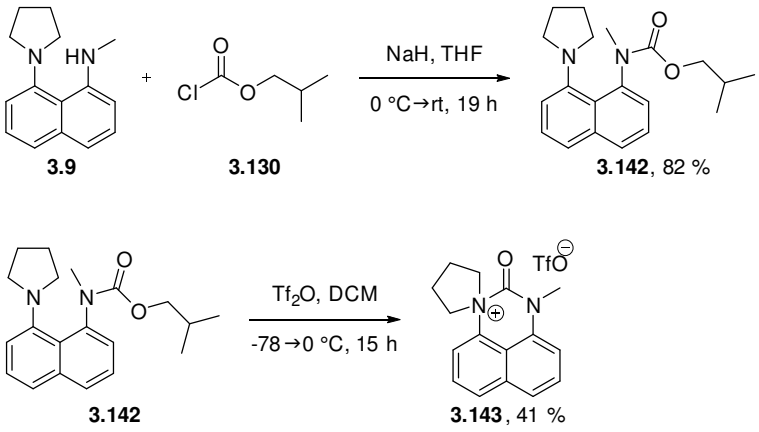

Scheme 3.70 Synthesis of salt **3.143**.

This urethane substitution pattern was also applied to the benzene-based backbone, producing compound **3.144**, when isobutyl chloroformate was reacted with amine **3.38** at 0 °C. Reaction of urethane species **3.144** with triflic anhydride gave, as determined by ^{1}H-NMR spectroscopy, a 1:1

mixture of a 2-oxo-imidazolium salt **3.145** and the protonated starting material, from which the imidazolium compound **3.145** was isolated by trituration with a 1:1 Et_2O/DCM solvent system.

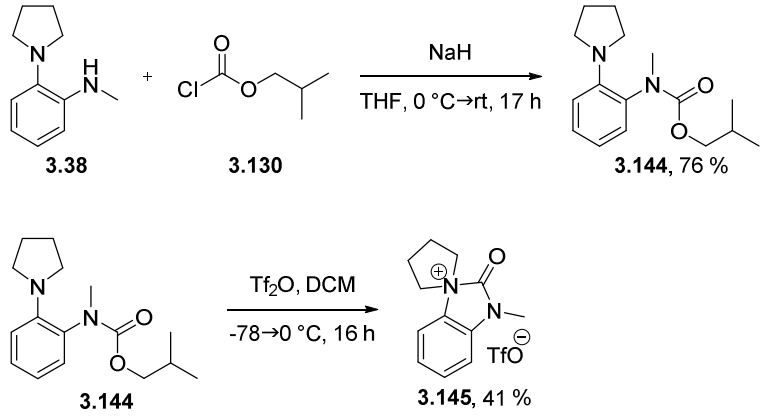

Scheme 3.71 Synthesis of urethane **3.144** and electrophile **3.145**.

In order to see if the aliphatic residue on the carbamate moiety had any effect on the observed outcome of the reaction, a slight modification was undertaken. A carbamate compound similar to **3.144** was synthesised in which the isobutyl residue was replaced by a methyl group. Instead of isobutyl chloroformate, amine **3.38** was reacted with methyl chloroformate **3.146** to give rise to urethane species **3.147**. When this compound was reacted with triflic anhydride the ^{1}H-NMR spectrum showed a highly complex mixture of different products. Nevertheless, trituration with a 1:1 Et_2O/DCM solvent system afforded the product **3.148**, this time however in a much lower yield (25 %).

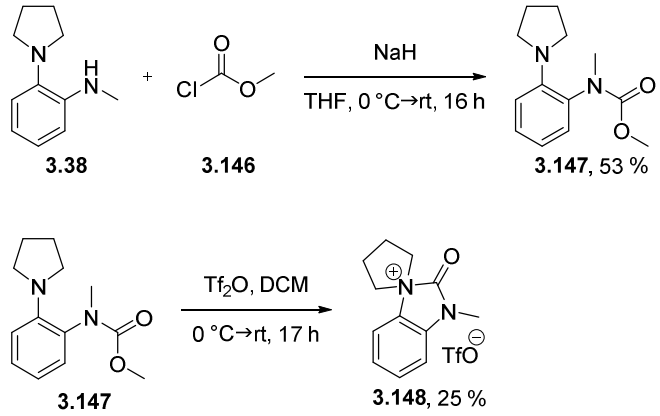

Scheme 3.72 Synthesis of urethane **3.147** and monosalt **3.148**.

3.10 Exploring the reactivity of the oxidised dicationic form of tetramethylphenylenediamine

Looking back at the proposal for the activation of N^5-methyltetrahydrofolate involving 2-electron oxidation (Scheme 3.73), it can be concluded that superelectrophilic species described on the previous pages indeed bear a strong capability of transferring alkyl groups.

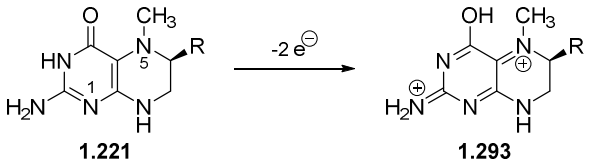

1.221 **1.293**

Scheme 3.73 Hypothetical superelectrophilic activation of MeTHF **1.221** involving 2-electron oxidation.

With the *N*-methylformamides, alkyl transfer had exclusively been observed from the sp^3-hybridised nitrogen atom in the dication species and not from the sp^2-hybridised nitrogen. However, in the superelectrophilic proposal for the MeTHF activation depicted in Scheme 3.73, the methyl group in the dicationic MeTHF would come from a sp^2-hybridised nitrogen centre in **1.293**. Further investigations exploring alkyl transfers from sp^2-hybridised nitrogen atoms in superelectrophiles therefore need to be carried out and the reactivity compared with the sp^3-nitrogen substrates. Furthermore, a modified proposal for the currently accepted acid-catalysed S_N2 mechanism should be considered, which still involves superelectrophilic activation but not 2-electron oxidation. The alternative proposal is depicted in Scheme 3.74. Here, additionally to the protonated N^5-position, coordination of the N^1-position by electrophilic contacts could lead to a dicationic superelectrophilic species **1.294**, which could be sufficiently activated for methyl transfer.

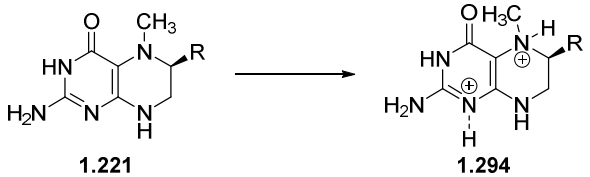

1.221 **1.294**

Scheme 3.74 Hypothetic superelectrophilic activation of MeTHF involving coordination by suitable electrophiles.

Returning to methyl groups attached to sp^2-hybridised nitrogen atoms, another compound had drawn attention for investigations into alkyl transfer by superelectrophilic activation, *i.e. N*,*N*,*N*',*N*'-tetramethyl-*p*-phenylendiamine (TMPD). The properties of TMPD **3.149** and its radical cation (Wurster's blue) have been widely explored for different purposes.[175,176] It has gained interest as a quencher of excited singlet states in aromatic compounds, as radicals and radical ions may regulate the emission of chemiluminescent systems.[177] Due to the intense blue colour of the radical cation, it

has found use in other applications as a redox indicator.[178] In aqueous solutions TMPD has been found to undergo 2-electron oxidation with selected oxidising agents and, interestingly, as a dication it is not stable.[179] Krieger and co-workers[180] even achieved isolation of the dication **3.150** after having oxidised TMPD with bromine in acetonitrile at 0 °C (Scheme 3.75), but stated that decomposition in solution, already seen with other counter-ions, can be suppressed in the presence of silver triflate as an oxidant.[181,182]

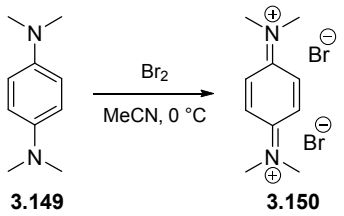

3.149 **3.150**

Scheme 3.75 Attempted oxidation of TMPD **3.149** with bromine.

It was decided to follow up Krieger's investigations and explore the nature of the decomposition seen with the dication of TMPD **3.150**. Repeating the published experimental procedure, it was not possible to obtain the desired product in pure form. Attempts were also made with ceric ammonium nitrate (CAN) as an oxidising agent under the same reaction conditions, but again, clean product formation could not be achieved. To exclude the possibility of acetonitrile acting as a nucleophile and a source of decomposition, the dimethylamino functionalities were replaced by piperidine moieties. By this it was hoped to increase the compound's solubility in organic solvents in order to avoid use of acetonitrile. The substrate was synthesised by reacting 1,4-phenylendiamine **3.151** with 1,5-dibromopentane in DMF over 2 d. This compound **3.152** was unstable towards oxidation by oxygen and was observed to decompose on TLC strips very quickly. Nevertheless, a yield of 47 % was obtained by flash chromatography.

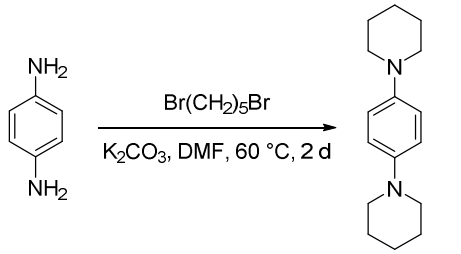

3.151 **3.152**, 47 %

Scheme 3.76 Synthesis of 1,4-di(piperidin-1-yl)benzene **3.152**.

Surprisingly, compared to TMPD this compound showed less solubility in organic solvents and hardly any solubility in MeCN. Calculations on geometry equilibrium rationalised this behaviour by the flatness of the substrate.

However, 1,4-dipiperidinylbenzene **3.152** was reacted with bromine in DCM at 0 °C, but again clean product formation could not be achieved as seen from ^{1}H-NMR experiments. Using CAN as an oxidising agent instead of bromine did not succeed either.

What had been seen in the test reaction of triflic anhydride with dimethylaniline (Scheme 3.47) now came to mind in which the triflic anhydride acted as an oxidising agent. Therefore, TMPD **3.149** was reacted with 3 equivalents of triflic anhydride in DCM at -78 °C for 2 h and then for a further 24 h at room temperature (Scheme 3.77). The white precipitate which had formed was triturated, filtered and extensively washed with DCM. Analysis by ^{1}H- and ^{13}C-NMR spectroscopy confirmed the structure to be the oxidised dication derivative of TMPD **3.153**. For NMR analysis, d_3-MeCN turned out to be a bad solvent, as it reacted with the substrate rapidly leading to an inseparable complex product mixture as seen from ^{1}H-NMR spectra. So did every other common NMR solvent apart from deuterated trifluoroacetic acid (d-TFA), which was chosen as the solvent as it proved to be sufficiently polar and non-nucleophilic to dissolve the compound without reacting with it.

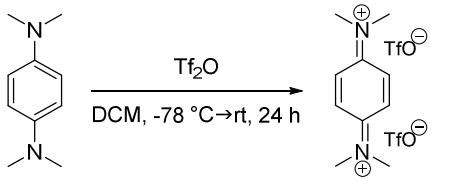

3.149 **3.153**, 87 %

Scheme 3.77 Oxidation of TMPD **3.149** with triflic anhydride.

The same oxidising behaviour was observed when 1,4-dipiperidinylphenylene **3.152** was reacted with triflic anhydride in DCM in the same way. The dication was triturated, filtered and extensively washed with DCM to afford **3.154** in 85 % yield.

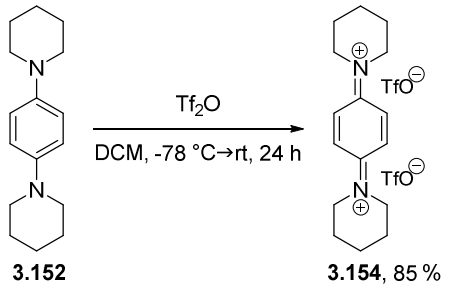

3.152 **3.154**, 85 %

Scheme 3.78 Oxidation of 1,4-di(piperidin-1-yl)benzene **3.152** with triflic anhydride.

Again, characterisation by NMR spectroscopy was only possible when d-TFA was used as a solvent. It was evident, that doing chemistry with the latter two dications proved to be extremely difficult. Finding a suitable solvent, which would dissolve the disalts without reacting with them, was not the

only requirement. Although using d-TFA for characterisation of the dications seems uncomplicated it is still unsuitable as a reaction medium as, being a rather strong acid, it would protonate almost every nucleophile. The only other solvent, that the dications did not seem to react with but that dissolved the electrophilic species was thioacetic acid, but again, being a strong acid (pK_A = 3.33)[183] it would react with most nucleophiles. Furthermore, during the reaction with triethylamine as a potential nucleophile for dealkylation an intense blue colour was observed indicating that triethylamine had possibly acted as an electron-donor to transform the disalt back to a Wurster's blue derivative, affording a complex inseparable product mixture as seen from the ^{1}H-NMR spectrum. Triethylamine has previously been reported[184,185] to act as an electron donor under certain reaction conditions, hence it was concluded that electron-rich nucleophiles might complicate the reaction with these kinds of disalts even further due to radical side-reactions. Surprisingly, it was realised that in d-TFA the dication **3.154** was not absolutely stable when it was characterised by NMR. Slowly over days, a transformation in the NMR sample appeared to occur which gave clean formation of a compound for which structure **3.155** was tentatively assigned.

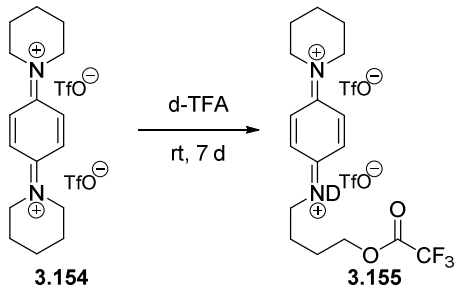

3.154 **3.155**

Scheme 3.79 The tentatively assigned structure **3.155** to the product from reaction of dication **3.154** with d-TFA.

High resolution mass spectrometry found peaks at m/z = 245.2002, 275.2107 and 485.3619. These peaks can be assigned as seen below in Figure 3.37. It has to be remarked, that the mass peak at *m/z* = 275.2107 can correspond to structure **3.157**, which might have emerged from S_N2 displacement of the trifluoroacetate residue by the mass spectrometry solvent methanol.

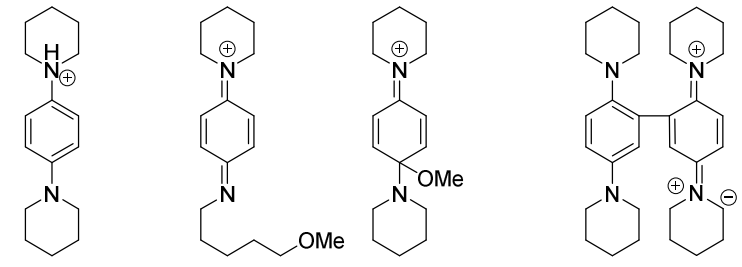

3.156 *m/z* = 245 **3.157** *m/z* = 275 **3.158** *m/z* = 275 **3.159** *m/z* = 485

Figure 3.37 Possible structure assignments for the peaks found in the high resolution mass spectrometry.

4 Conclusions and Future Work

The research on the chemistry of amidinium disalts and related species is novel. This work demonstrates the exceptional reactivity of these intermediates seen in their transfer of alkyl groups to very weakly nucleophilic triflate anions or their loss of a phenyl cation to become less electrophilic monosalts. Their ability to rearrange to benzodiazepine or benzothiazepine structures also emphasises this enhanced electrophilic potential. It has also been shown that where isolation of the superelectrophilic species is not possible, stabilisation and spectroscopic observation is achieved at low temperature. This fact is helpful for further explorations of the reactivity of the superelectrophilic species *e.g.* the intermolecular mode of amidinium disalt formation.

Iminium triflate species **4.2**, formed from the reaction of DMF with triflic anhydride, has been characterised spectroscopically and, unlike the classical Vilsmeier-Haack reaction, was shown to readily formylate unactivated aromatic systems. With aliphatic alcohols **4.3** and aliphatic primary or secondary amines as nucleophiles the respective formates and formamides were produced upon basic hydrolysis.[44,186]

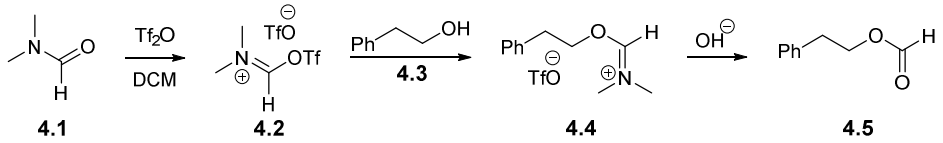

Scheme 4.1 Iminium triflate **4.2** reacts readily with aliphatic amines and alcohols to produce the respective formamides and formates upon basic hydrolysis.

However, the intermolecular mode of alkyl transfer to weakly nucleophilic triflate anions from the reaction of tertiary amines with species **4.2** has not been reported and is available for investigations.

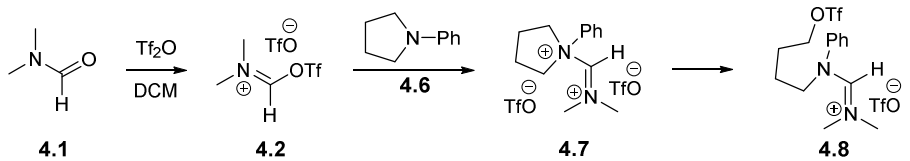

Scheme 4.2 Reaction of iminium triflate **4.2** with tertiary amines might result in alkyl transfer to triflate anions.

Furthermore, the reaction of iminium triflate species **4.2** with anilines or phenols affording rearrangement products **4.12** (analogous to the intramolecular formation of benzodiazepine **3.62** presented in this thesis) has not been reported and can also be studied.

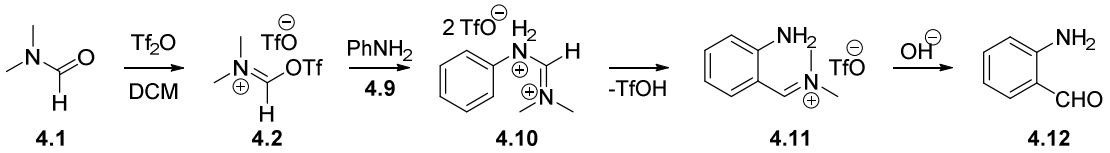

Scheme 4.3 Reaction of iminium triflate **4.2** with anilines or phenols might lead to rearranged products as seen in the formation of benzodiazepine **3.62**.

The new disalts isolated or stabilised at low temperature are viable candidates for activation of molecular hydrogen, which has gained high interest in recent times. The heterolytic fission of hydrogen has been accomplished by means of frustrated Lewis pairs and has been extensively covered by Stephan[187] and Powers.[188] For the formation of frustrated Lewis pairs, both, the Lewis base and the Lewis acid need to be sterically hindered to avoid the reaction between each other. Initial attempts in this regard were made by bubbling hydrogen gas through a solution of amidinium disalt **3.28** and the sterically hindered base 2,6-lutidine **4.13** at -35 °C, but ^{1}H-NMR spectroscopy indicated on methyl transfer from the superelectrophile to the base.

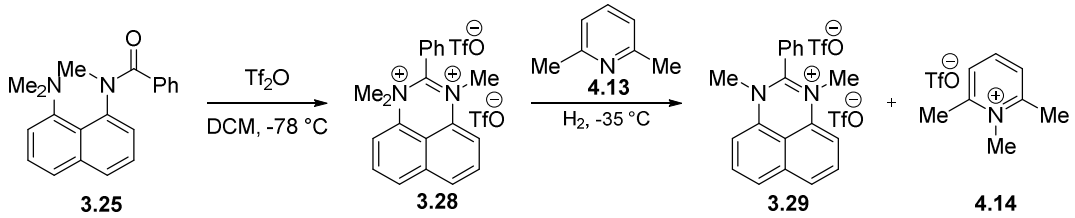

Scheme 4.4 ^{1}H-NMR of initial attempts in hydrogen activation with disalt **3.28** indicated on demethylation of the superelectrophile and formation of pyridinium derivative **4.14**.

Hence, a more sterically shielded base must be applied to avoid alkyl transfer and this route tested with the other isolated superelectrophiles **3.78** and **3.121**. An alternative less nucleophilic and sterically more shielded base might be triphenylphosphine, which could abstract a proton while the hydride might reduce the carbon centre in the amidinium moiety (Scheme 4.5).

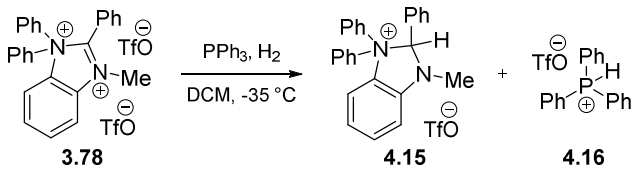

Scheme 4.5 A frustrated Lewis pair involving hydrogen activation might be achieved by bubbling hydrogen gas through a solution of the amidinium disalt **4.15** and triphenylphosphine as the Lewis base.

It has been shown that the stabilisation of the amidinium disalt moiety on the naphthalene or the benzene core can only be achieved if the more energetically favoured tetrahedral precursory intermediate is destabilised by steric factors *i.e*. a phenyl group on the central carbon between the

two nitrogen atoms. However, stabilisation of the disalt species without inclusion of this equilibrium-determining phenyl group would not only be highly interesting in terms of testing the susceptibility to dihydrogen. It has been shown that formamides with phenyl groups on the tertiary amine do not dealkylate, but undergo rearrangement to diazepinium structures possibly by intramolecular electrophilic aromatic substitution on the *ortho*-position of the phenyl rings. This attack onto the carbon centre might be prevented by steric factors such as methyl groups on the *ortho*- and *para*-position of the phenyl residues and make isolation of the corresponding disalt **4.19** possible. However, the increased steric environment might also complicate the nucleophilic attack of the tertiary amine onto the iminium triflate residue in the precursory intermediate **4.18**. The route presented is still worth exploring as successful isolation of such a species might also be a promising starting point for the synthesis of an unprecedented type of carbene with a sterically hindered non-nucleophilic base such as LDA as seen in structure **4.20**.

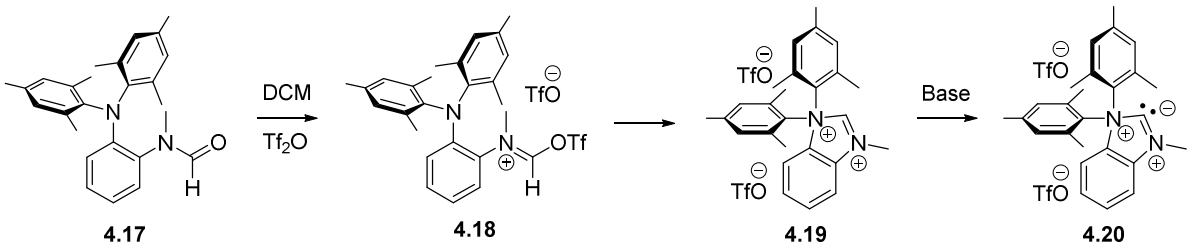

Scheme 4.6 Methyl groups on the phenyl residues might not only prevent rearrangement to benzodiazepine structures but also favour the amidinium disalt species over the tetrahedral triflate intermediate.

The step from formamides with a naphthalene core to formamides with a benzene ring as the rigid backbone is associated with increased reactivity of the corresponding tetrahedral triflate intermediates and disalt species. As described earlier, the increased reactivity can be explained due to the amount of aromatic stabilisation gained in the products. While in the perimidinium products derived from the naphthalene-based substrates the aromaticity does not spread over the entire ring system, the benzimidazolium products emerging from the benzene-based substrates exhibit aromaticity over the entire core structure. This enhanced reactivity, however, can still be further increased by synthesising structures in which the formamide or benzamide residue and the tertiary amine functionality are bridged by an ethene fragment in (*Z*)-configuration. As an aromatic imidazolium heterocycle **4.23** results from the starting substrate **4.21** containing no aromaticity at all, the energetic stabilisation gained must be higher than for the previously discussed systems. Unlike the naphthalene- and benzene-based formamides however, these systems might require a different and more difficult synthetic approach, as enamine-isomerisation during the course of synthesis might yield the opposite, energetically more favoured (*E*)-configured precursors.

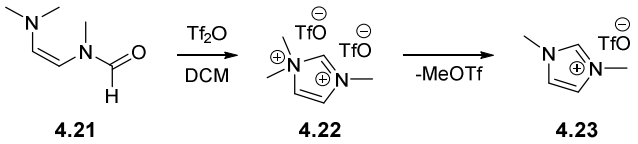

Scheme 4.7 For ethane-based formamides the aromatic stabilisation gained in the imidazolium products must be higher than for the previously discussed systems.

Chapter 3.9 deals with the possibility of stabilising the dicationic species by introducing electron-donating residues in the centre of the amidinium moiety to reduce the electrophilic nature of the compound and delocalise the positive charge over a more extended π-system. However, when the appropriate carbamate was reacted with triflic anhydride, salt **3.132** was isolated, whose crystal structure revealed an exceptionally long N(sp^3)-CO bond representing the strong electrophilic character of this compound.

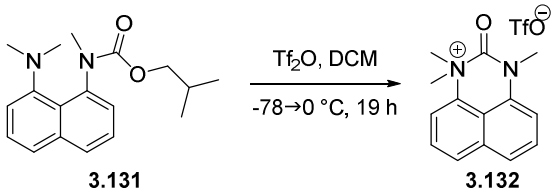

Scheme 4.8 The electrophilic character of salt **3.132** is envisioned in the exceptionally long N(sp^3)-CO bond.

Computational models of this compound and the related benzimidazolium structure **4.24**, predicted for the latter salt an even longer N(sp^3)-CO bond. Hence, a crystal structure of compound **4.24** might set a new record for this kind of nitrogen-carbon bond.

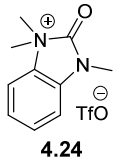

Figure 4.1 Computational calculations predict the length of the N(sp^3)-CO bond to be even longer than in monosalt **3.132**.

For all further attempts in forming superelectrophilic species from the reaction with triflic anhydride it should be considered to substitute the triflate anions for tetrakis(triflate) boronate. This could be achieved by the addition of boron tris(triflate) to the reaction mixture at low temperature to capture the forming free triflate anions. Interception of triflate anions by $B(OTf)_3$ would then give tetrakis(triflate) boronate anions which are even less nucleophilic than triflate anions (pK_A of conjugated acid $HB(OTf)_4$ is -18.5 compared to -14.1 of triflic acid).[189] In the example shown below (Scheme 4.9) the substitution of triflate anions for tetrakis(triflate) boronates might prevent alkyl transfer and render the amidinium disalt stable at room temperature.

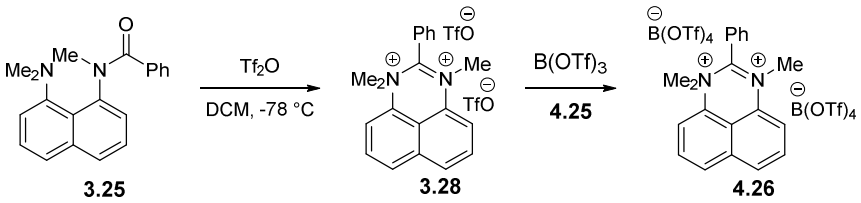

Scheme 4.9 Tetrakis(triflate) boronates instead of triflate counter-ions might prevent methyl transfer to the anion and render amidinium disalt **4.26** stable at room temperature.

5 Experimental

^{1}H-NMR spectra were recorded at 400.03 MHz (Bruker DPX 400 or Bruker AV 400), 500.13 MHz (Bruker AV 500) or 600.13 MHz (Bruker AV 600). ^{13}C-NMR spectra were recorded at 100.59, 125.76 and 150.92 MHz, respectively, using a broadband decoupled mode on the same spectrometers. Experiments were carried out using deuterated chloroform ($CDCl_3$) except where otherwise stated. Deuterated acetonitrile and deuterated trifluoroacetic acid were distilled over P_2O_5 and the solvents deoxygenated by bubbling a stream of argon through the solutions. Chemical shifts are reported in parts per million (ppm) and coupling constants *J* are reported in Hertz (Hz). The following abbreviations are used for the multiplicities; s, singlet; d, doublet; t, triplet; q, quartet; qui, quintet; m, multiplet; dd, doublet of doublets; dt, doublet of triplets; bs, broad singlet.

Infrared spectra were recorded on a Perkin Elmer "Spectrum One FT-IR Spectrometer" or A_2 Technologies "ML FTIR". Melting points were recorded using a Gallenkamp "Griffin Melting Point Apparatus".

High resolution mass spectrometry analysis was performed by the EPSRC National Mass Spectrometry facility in Swansea.

Column chromatography using silica gel employed Prolabo 35-70 μm particle sized silica gel 60 (200-400 mesh). Reactions were followed using thin layer chromatography (TLC) carried out on Merck silica gel 60 F_{254} precoated aluminium plates. Visualisation was achieved under UVP mineralight UVG-11 lamp or by developing plates with methanolic vanillin, potassium permanganate or phosphomolybdic acid solution.

All reagents were obtained from commercial suppliers. Tetrahydrofuran, dichloromethane, hexane, diethyl ether and toluene were dried and deoxygenated with a Pure-Solv 400 solvent purification system (by Innovative Technology Inc.; USA). Flash chromatography eluent mixtures are stated as percentages of the total volume. The 40-60 °C distillation fraction of petrol ether exclusively was used as a flash chromatography eluent. Other solvents were deoxygenated by bubbling a stream of argon through the solutions prior to use. *N*,*N*-Dimethylformamide was obtained from commercial suppliers as anhydrous (99.98 %) and used directly. Sodium hydride was supplied as a 60 % suspension in mineral oil and was not further purified prior to use. All reactions were carried out under argon unless otherwise stated. Reactions involving addition of triflic anhydride were all worked-up inside a glovebox using deoxygenated and specially dried solvents unless otherwise stated.

Computational calculations were carried out by Dr. Tell Tuttle and his researchers Greg Anderson and Christopher Idziak applying density functional theory (DFT) to characterise the minima and first order saddle points (transition states) on the potential energy surface for the reactants and intermediates. The structures were optimised in the solvent phase (DCM, Conductor-like Polarizable Continuum CPCM) using MO6(L)/6-311G level of theory.[190,191] Frequency calculations on each structure determined the stationary points either as minima or transition states. The calculations were carried out on the Gaussian 09 package.[151]

Simpler calculations were carried out with the molecular modelling program Spartan 04[192] or Spartan 10[193] applying Hartree-Fock or DFT B3LYP each with the 6-31G* basis set in vacuum.

Crystallographic measurements were carried out and interpreted by Alan R. Kennedy using an Oxford Diffraction Xcalibur and Gemini instruments with graphite monochromated radiation. Samples were mounted in an oil droplet frozen in a cold nitrogen stream. Structural solution and refinement against F^2 to convergence used programmes from the SHELX suit.[194] Hydrogen atoms bound to carbon were placed in idealised positions and refined in riding modes, but those bound to nitrogen were placed as found in difference syntheses and refined isotropically.

Images of the crystallographic or the geometry-optimised structures were created using the molecular graphics system PyMOL.[195]

Formic pivalic anhydride[134]

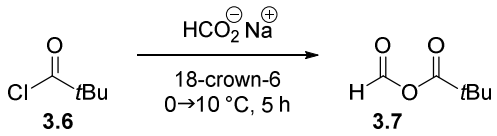

3.6 **3.7**

A mixture of sodium formate (4.00 g, 58.8 mmol, 1.0 eq.) and 18-crown-6 (1.55 g, 5.9 mmol, 0.1 eq.) was dried under argon for 1 h under reduced pressure at 60 °C. The flask containing the mixture was then cooled to 0 °C and trimethylacetyl chloride **3.6** (7.3 mL, 58.8 mmol, 1.0 eq.) was added dropwise. After 1 h, the reaction mixture was warmed to 10 °C and stirred for a further 4 h. The product was purified by distillation under high vacuum (10^{-3} mbar) at room temperature and trapped into a flask cooled to -78 °C to yield formic pivalic anhydride **3.7** as a colourless liquid (6.23 g, 47.9 mmol, 81 %); ν_{max}(ATR)/cm^{-1} 2980, 2876, 1782, 1757, 1701, 1086, 1019, 894; ^{1}H-NMR (500 MHz, $CDCl_3$): δ= 1.31 (9H, s, CH_3), 9.11 (1H, s, C*H*O); ^{13}C-NMR (125 MHz, $CDCl_3$): δ= 26.3 (*C*H$_3$), 27.0 (*C*), 156.7 (*C*), 175.4 (*C*H).

8-(Pyrrolidin-1-yl)naphthalen-1-amine

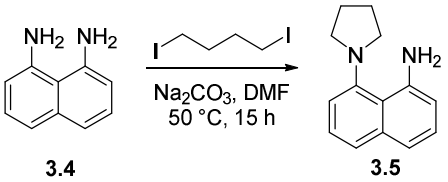

3.4 **3.5**

A mixture of 1,8-diaminonaphthalene **3.4** (3.16 g, 20.0 mmol, 1.0 eq.) and sodium carbonate (4.45 g, 42.0 mmol, 2.1 eq.) was dissolved in anhydrous DMF (40 mL) under argon. 1,4-Diiodobutane (2.6 mL, 20.0 mmol, 1.0 eq.) was then added and the reaction mixture heated to 50 °C and stirred for 15 h. The reaction mixture was partitioned between DCM and water and extracted with DCM (3 x 100 mL). The combined organic layers were washed with water (3 x 125 mL), brine (2 x 75 mL), dried over sodium sulfate, filtered and concentrated *in vacuo*. The crude product was purified by flash chromatography (8 % EtOAc/Pet ether) to afford the *title compound* **3.5** as an off-white solid (955 mg, 4.5 mmol, 23 %); mp: 58-60 °C; ν_{max}(ATR)/cm^{-1} 3433, 3290, 2968, 2839, 1579, 1399, 1315, 817; ^{1}H-NMR (500 MHz, $CDCl_3$): δ= 1.95-2.05 (4H, m, C*H*$_2$), 2.75-2.88 (2H, m, C*H*$_2$), 3.42-3.50 (2H, m, C*H*$_2$), 6.14 (2H, bs, N*H*$_2$), 6.59 (1H, dd, *J* = 7.4, 1.2 Hz, Ar*H*), 7.12-7.18 (2H, m, Ar*H*), 7.20-7.24 (1H, m, Ar*H*), 7.28-7.32 (1H, m, Ar*H*), 7.49 (1H, dd, *J* = 8.2, 1.0 Hz, Ar*H*); ^{13}C-NMR (125 MHz, $CDCl_3$): δ= 24.2 (*C*H$_2$), 54.5 (*C*H$_2$), 109.6 (*C*H), 114.8 (*C*H), 117.0 (*C*H), 119.7 (*C*), 125.1 (*C*H), 125.6 (*C*H), 126.7 (*C*H), 137.1 (*C*), 146.0 (*C*), 148.4 (*C*); HRMS (NSI$^+$) ([M+H]$^+$) calcd for $C_{14}H_{17}N_2$ 213.1386, found 213.1385.

N-(8-(Pyrrolidin-1-yl)naphthalen-1-yl)formamide

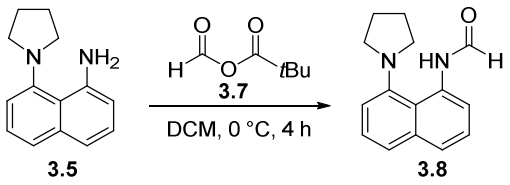

3.5 **3.8**

A solution of formic pivalic anhydride **3.7** (465 mg, 3.6 mmol, 1.3 eq.) in dry DCM (5 mL) was added under argon to a solution of 8-(pyrrolidin-1-yl)naphthalen-1-amine **3.5** (584 mg, 2.8 mmol, 1.0 eq.) in dry DCM (5 mL) at 0 °C. The reaction mixture was stirred for 4 h, before it was diluted with DCM (75 mL) and washed with 2 M NaOH (2 x 50 mL), brine (40 mL) and dried over sodium sulfate. The solvent was removed *in vacuo* to give the *title compound* **3.8** as a green oil (660 mg, 2.8 mmol, 100 %); ν_{max}(ATR)/cm^{-1} 2949, 2926, 2821, 1683, 1539, 1431, 1286, 1195, 824, 765; in the NMR the compound appeared as an isomer mixture (isomer ratio A:B = 2:1) ^{1}H-NMR (500 MHz, $CDCl_3$): δ= 2.00-2.22 (4H, m, C*H*$_2$), 2.88-3.01 (2H, m, C*H*$_2$), 3.34-3.47 (2H, m, C*H*$_2$), 7.29-7.67 [m, ism A+B] and 8.77 [dd, *J* = 7.7, 0.8 Hz, ism A] (6H, Ar*H*), 8.53 [d, *J* = 1.9 Hz, ism A] and 9.02 (d, *J* = 10.9 Hz, ism B]

(1H, C*H*O), 12.94 [bs, ism B] and 13.03 [bs, ism A] (1H, N*H*); ^{13}C-NMR (125 MHz, $CDCl_3$): δ= 24.2 (*C*H_2), 24.3 (*C*H_2), 54.9 (*C*H_2), 55.0 (*C*H_2), 110.6 (*C*H), 116.9 (*C*H), 118.9 (*C*H), 120.2 (*C*), 120.4 (*C*), 123.9 (*C*H), 124.2 (*C*H), 125.7 (*C*H), 125.8 (*C*H), 126.0 (*C*H), 126.3 (*C*H), 126.6 (*C*H), 135.7 (*C*), 135.8 (*C*), 135.8 (*C*), 136.4 (*C*), 146.5 (*C*), 147.2 (*C*), 158.6 (*C*O), 162.5 (*C*O); HRMS (NSI$^+$) ([M+H]$^+$) calcd for $C_{15}H_{17}N_2O$ 241.1335, found 241.1334.

N-Methyl-8-(pyrrolidin-1-yl)naphthalen-1-amine

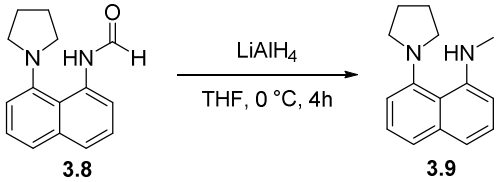

3.8 **3.9**

A solution of *N*-(8-(pyrrolidin-1-yl)naphthalen-1-yl)formamide **3.8** (1138 mg, 6.1 mmol, 1.0 eq.) in THF (7 mL) was slowly added under argon to a stirred suspension of $LiAlH_4$ (557 mg, 14.7 mmol, 2.4 eq.) in THF (10 mL) *via* cannula at 0 °C. The reaction mixture was stirred for 4 h, before it was quenched with 2 M NaOH carefully. The reaction mixture was diluted with DCM (150 mL) and washed with 2 M NaOH (2 x 200 mL), brine (100 mL) and dried over sodium sulfate. The solvent was removed *in vacuo*. Flash chromatography (20 % tol/Pet ether + 1% Et_3N) afforded the *title compound* **3.9** as a red oil (737 mg, 3.3 mmol, 53 %); ν_{max}(NaCl disc)/cm^{-1} 3287, 3049, 2959, 2924, 2853, 2814, 1582, 1537, 1420, 1376, 1308, 1122, 1099, 816, 758; ^{1}H-NMR (400 MHz, $CDCl_3$): δ= 1.95-2.05 (4H, m, CH_2), 2.75-2.85 (2H, m, CH_2), 2.95 (3H, d, *J* = 5.0 Hz, CH_3), 3.35-3.45 (2H, m, CH_2), 6.42 (1H, d, *J* = 7.7 Hz, Ar*H*), 7.05 (1H, dd, *J* = 8.0, 0.8 Hz, Ar*H*), 7.16 (1H, dd, *J* = 7.4, 1.1 Hz, Ar*H*), 7.27-7.33 (2H, m, Ar*H*), 7.49 (1H, dd, *J* = 8.1, 1.1 Hz, Ar*H*), 8.91 (1H, bs, N*H*); ^{13}C-NMR (100 MHz, $CDCl_3$): δ= 23.6 (*C*H_2), 29.8 (*C*H_3) 53.6 (*C*H_2), 101.8 (*C*H), 114.3 (*C*H), 114.4 (*C*H), 118.6 (*C*), 124.7 (*C*H), 124.8 (*C*H), 126.4 (*C*H), 136.3 (*C*), 147.5 (*C*), 147.8 (*C*); HRMS (NSI$^+$) ([M+H]$^+$) calcd for $C_{15}H_{19}N_2$ 227.1543, found 227.1544.

N-Methyl-N-(8-(pyrrolidin-1-yl)naphthalen-1-yl)formamide

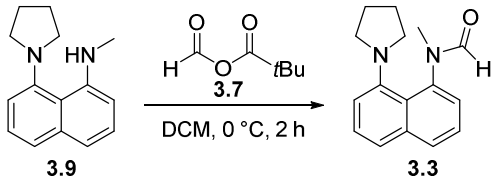

3.9 **3.3**

A solution of formic pivalic anhydride **3.7** (413 mg, 3.2 mmol, 1.3 eq.) in dry DCM (5 mL) was added under argon to a solution of *N*-methyl-8-(pyrrolidin-1-yl)naphthalen-1-amine **3.9** (551 mg, 2.4 mmol, 1.0 eq.) in dry DCM (5 mL) at 0 °C. The reaction mixture was stirred for 2 h, before it was diluted with DCM (75 mL) and washed with 2 M NaOH (2 x 75 mL), brine (75 mL) and dried over sodium sulfate.

The solvent was removed *in vacuo*. Flash chromatography (80 % DCM/Pet ether) afforded the *title compound* **3.3** as an off-white solid (44 mg, 1.7 mmol, 71 %); mp: 86-89 °C; ν_{max}(ATR)/cm^{-1} 3687, 2951, 2819, 1660, 1572, 1377, 1347, 1034, 826, 766; ^{1}H-NMR (400 MHz, $CDCl_3$): δ= 1.85-2.00 (4H, m, CH_2), 2.75-3.20 (4H, m, CH_2), 3.37 (3H, s, CH_3), 7.16-7.19 (2H, m, Ar*H*), 7.36-7.43 (2H, m, Ar*H*), 7.52 (1H, dd, *J* = 8.1, 0.8 Hz, Ar*H*), 7.73 (1H, dd, *J* = 8.2, 1.0 Hz, Ar*H*), 8.29 (1H, s, C*H*O); ^{13}C-NMR (100 MHz, $CDCl_3$): δ= 23.2 (*C*H_2), 33.6 (*C*H_3), 52.4 (*C*H_2), 115.2 (*C*H), 122.5 (*C*), 122.9 (*C*H), 122.9 (*C*H), 124.89 (*C*H), 126.09 (*C*H), 127.69 (*C*H), 136.6 (*C*), 137.9 (*C*), 145.6 (*C*), 162.8 (*C*O); HRMS (NSI$^+$) ([M+H]$^+$) calcd for $C_{16}H_{19}N_2O$ 255.1492, found 255.1495, ([2M+Na]$^+$) calcd for $C_{32}H_{36}N_4NaO_2$ 531.2730, found 531.2727.

3-Methyl-1-(4-(((trifluoromethyl)sulfonyl)oxy)butyl)-1H-perimidin-3-ium triflate

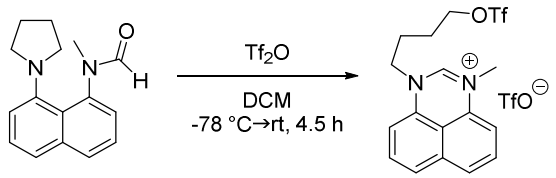

3.3 **3.10**

A solution of *N*-methyl-*N*-(8-(pyrrolidin-1-yl)naphthalen-1-yl)-formamide **3.3** (127 mg, 0.5 mmol, 1.0 eq.) in dry DCM (0.5 mL) was added under argon to a flask containing trifluoromethanesulfonic anhydride (0.1 mL, 0.6 mmol, 1.2 eq.) in dry DCM (0.5 mL) *via* syringe pump (0.254 mL/h) at -78 °C. After 3.5 h, the reaction mixture was warmed to room temperature and stirred for a further hour. The solvent was removed *in vacuo* to give the *title compound* **3.10** as a yellow solid (241 mg, 0.45 mmol, 90 %); mp: 120-122 °C (decomp.); ν_{max}(ATR)/cm^{-1} 1667, 1607, 1408, 1257, 1201, 1141, 1030, 925, 817, 767; ^{1}H-NMR (400 MHz, d_3-MeCN): δ= 1.90-2.10 (4H, m, CH_2), 3.51 (3H, s, CH_3), 3.99 (2H, t, *J* = 7.5 Hz, CH_2), 4.75 (2H, t, *J* = 5.7 Hz, CH_2), 6.87 (1H, d, *J* = 7.6 Hz, Ar*H*), 6.97 (1H, d, *J* = 7.6 Hz, Ar*H*), 7.42-7.48 (2H, m, Ar*H*), 7.53-7.56 (2H, m, Ar*H*), 8.39 (1H, s, C*H*); ^{13}C-NMR (100 MHz, d_3-MeCN): δ= 21.6 (*C*H_2), 25.2 (*C*H_2), 38.5 (*C*H_2), 50.5 (*C*H_3), 77.9 (*C*H_2), 107.4 (*C*H), 107.6 (*C*H), 118.2 (q, $J_{C\text{-}F}$ = 317 Hz, *C*F_3SO_3), 120.4 (q, $J_{C\text{-}F}$ = 318 Hz, *C*F_3SO_3), 120.7 (*C*), 123.6 (*C*H), 123.8 (*C*H), 127.8 (*C*H), 127.8 (*C*H), 130.9 (*C*), 132.1 (*C*), 134.1 (*C*), 152.0 (*C*H); HRMS (NSI$^+$) ([M-TfO]$^+$) calcd for $C_{17}H_{18}F_3N_2O_3S$ 387.0985, found 387.0980, ([2M-TfO]$^+$) calcd for $C_{35}H_{36}F_9N_4O_9S_3$ 923.1490, found 923.1482.

8-(Piperidin-1-yl)naphthalen-1-amine

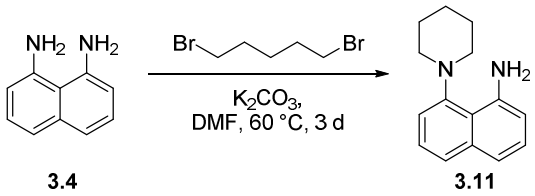

3.4 **3.11**

A mixture of 1,8-diaminonaphthalene **3.4** (3.00 g, 19.0 mmol, 1.0 eq.) and potassium carbonate (5.51 g, 39.9 mmol, 2.1 eq.) was dissolved under argon in anhydrous DMF (15 mL). 1,5-Dibromopentane (3.3 mL, 19.0 mmol, 1.0 eq.) was then added and the reaction mixture heated to 60 °C and stirred for 3 d. The reaction mixture was partitioned between diethyl ether and water and extracted with diethyl ether (3 x 75 mL). The combined organic layers were washed with water (3 x 100 mL), brine (100 mL), dried over sodium sulfate, filtered and concentrated *in vacuo*. The crude product was adsorbed onto silica gel and purified by flash chromatography (15 % Et_2O/hex.) to afford the *title compound* **3.11** as a colourless oil (274 mg, 1.2 mmol, 6 %); ν_{max}(ATR)/cm^{-1} 3451, 3276, 3051, 2929, 2805, 1582, 1394, 994, 755; ^{1}H-NMR (500 MHz, $CDCl_3$): δ= 1.35-1.45 (1H, m, CH_2), 1.79-1.92 (5H, m, CH_2), 2.67-2.73 (2H, m, CH_2), 3.29-3.33 (2H, m, CH_2), 6.36 (2H, bs, NH_2), 6.60 (1H, dd, *J* = 7.5, 1.2 Hz, Ar*H*), 7.13-7.16 (2H, m, Ar*H*), 7.21-7.25 (1H, m, Ar*H*), 7.30-7.34 (1H, m, Ar*H*), 7.52 (1H, dd, *J* = 8.2, 0.9 Hz, Ar*H*); ^{13}C-NMR (125 MHz, $CDCl_3$): δ= 24.2 (*C*H_2), 26.6 (*C*H_2), 55.6 (*C*H_2), 109.5 (*C*H), 115.7 (*C*H), 117.0 (*C*H), 118.9 (*C*), 125.4 (*C*H), 125.4 (*C*H), 126.5 (*C*H), 137.2 (*C*), 146.1 (*C*), 152.1 (*C*); HRMS (NSI$^+$) ([M+H]$^+$ calcd for $C_{15}H_{19}N_2$ 227.1543, found 227.1545.

N-(8-(Piperidin-1-yl)naphthalen-1-yl)formamide

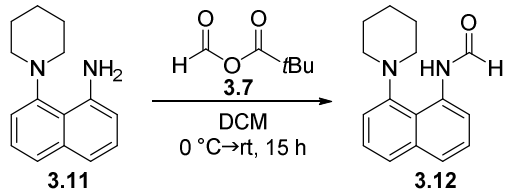

3.11 **3.12**

A solution of formic pivalic anhydride **3.7** (186 mg, 1.4 mmol, 1.3 eq.) in dry DCM (5 mL) was added under argon to a solution of *N*-methyl-8-(piperidin-1-yl)naphthalen-1-amine **3.11** (249 mg, 1.1 mmol, 1.0 eq.) in dry DCM (10 mL) at 0 °C. The reaction mixture was stirred for 3 h, the ice bath then taken away and the solution stirred for a further 12 h at room temperature. The solution was partitioned between DCM and 2 M NaOH and extracted with DCM (3 x 50 mL). The combined organic phases were washed with brine (50 mL), dried over sodium sulfate and filtered. The solvent was removed *in vacuo*. Flash chromatography (15 % EtOAc/Pet ether) afforded the *title compound* **3.12** as a colourless oil (267 mg, 1.1 mmol, 95 %); ν_{max}(ATR)/cm^{-1} 3058, 2934, 2850, 2816, 1675, 1580, 1537,

1489, 1429, 1338, 1312, 1273, 822, 762; in the NMR the compound appeard as an isomer mixture (isomer ratio A:B = 2:1) ^{1}H-NMR (500 MHz, $CDCl_3$): δ= 1.35-1.50 (1H, m, C*H*$_2$), 1.74-2.10 (5H, m, C*H*$_2$), 2.77-2.86 (2H, m, C*H*$_2$), 3.19-3.26 (2H, m, C*H*$_2$), 7.29-7.67 [m, ism A+B] and 8.76-8.79 [m, ism A] (6H, Ar*H*), 8.61 [d, *J* = 2.1 Hz, ism A] and 9.03 [d, *J* = 10.8 Hz, ism B] (1H, C*H*O), 13.35 [bs, ism B] and 14.22 [bs, ism A] (1H, N*H*); ^{13}C-NMR (125 MHz, $CDCl_3$): δ= 23.8 (*C*H$_2$), 23.9 (*C*H$_2$), 26.0 (*C*H$_2$), 26.5 (*C*H$_2$), 55.2 (*C*H$_2$), 55.6 (*C*H$_2$), 110.4 (*C*H), 116.8 (*C*H), 119.1 (*C*), 119.2 (*CH*), 124.0 (*CH*), 124.2 (*C*H), 125.6 (*C*H), 125.8 (*C*H), 126.2 (*C*H), 126.3 (*C*H), 126.8 (*C*H), 135.8 (*C*), 136.0 (*C*), 136.5 (*C*), 149.8 (*C*), 150.7 (*C*), 158.6 (*C*O), 162.1 (*C*O). HRMS (NSI$^+$) [M+H] calcd for $C_{16}H_{19}N_2O$ 255.1492, found 255.1499.

N-Methyl-8-(piperidin-1-yl)naphthalen-1-amine

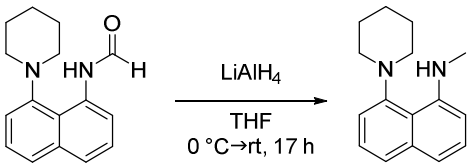

3.12 **3.13**

A solution of *N*-(8-(piperidin-1-yl)naphthalen-1-yl)formamide **3.12** (260 mg, 1.02 mmol, 1.0 eq.) in THF (7 mL) was slowly added under argon to a stirred suspension of $LiAlH_4$ (93 mg, 2.45 mmol, 2.4 eq.) in THF (8 mL) *via* cannula at 0 °C. The reaction mixture was stirred for 2 h, the ice bath then taken away and the reaction mixture stirred for further 15 h at room temperature, before it was quenched with 2 M NaOH (10 mL) carefully. The reaction mixture was diluted with DCM (50 mL) and washed with 2 M NaOH (2 x 50 mL), brine (50 mL), dried over sodium sulfate and filtered. The solvent was removed *in vacuo*. Flash chromatography (25% DCM/Pet ether + 1% Et_3N) afforded the *title compound* **3.13** as an off-white solid (187 mg, 0.78 mmol, 76 %); mp: 80-82 °C; ν_{max}(ATR)/cm^{-1} 3245, 3146, 3051, 2932, 2848, 2824, 1582, 1537, 1416, 1330, 1316, 1101, 816, 762; ^{1}H-NMR (500 MHz, $CDCl_3$): δ= 1.35-1.45 (1H, m, C*H*$_2$), 1.75-1.95 (5H, m, C*H*$_2$), 2.71 (2H, m, C*H*$_2$), 2.99 (3H, d, *J* = 4.8 Hz, C*H*$_3$), 3.25 (2H, m, C*H*$_2$), 6.42 (1H, d, *J* = 7.6 Hz, Ar*H*), 7.04-7.08 (1H, m, Ar*H*), 7.12-7.16 (1H, m, Ar*H*), 7.29-7.34 (2H, m, Ar*H*), 7.51-7.54 (1H, m, Ar*H*), 9.37 (1H, bs, N*H*); ^{13}C-NMR (125 MHz, $CDCl_3$): δ= 24.1 (*C*H$_2$), 26.8 (*C*H$_2$), 30.0 (*C*H$_3$), 55.3 (*C*H$_2$), 102.3 (*C*H), 115.0 (*C*H), 115.8 (*C*H), 118.3 (*C*), 125.3 (*C*H), 125.6 (*C*H), 126.9 (*C*H), 137.0 (*C*), 148.5 (*C*), 151.8 (*C*); HRMS (NSI$^+$) ([M+H]$^+$)calcd for $C_{16}H_{21}N_2$ 241.1699, found 241.1701.

N-Methyl-N-(8-(piperidin-1-yl)naphthalen-1-yl)formamide

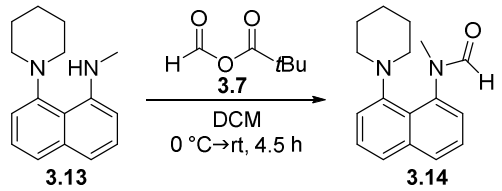

3.13 3.14

A solution of *N*-methyl-8-(piperidin-1-yl)naphthalen-1-amine **3.13** (820 mg, 3.4 mmol, 1.0 eq.) in dry DCM (7 mL) was added under argon to a solution of formic pivalic anhydride (622 mg, 4.8 mmol, 1.4 eq.) **3.7** in dry DCM (10 mL) at 0 °C. The reaction mixture was stirred for 4.5 h, before it was diluted with DCM (150 mL) and washed with 2 M NaOH (2 x 100 mL), brine (100 mL) and dried over sodium sulfate. The solvent was removed *in vacuo*. Flash chromatography (20 % EtOAc/Pet ether) afforded the *title compound* **3.14** as a brown solid (861 mg, 3.2 mmol, 94 %); mp: 120-122 °C; ν_{max}(ATR)/cm^{-1} 2937, 1664, 1571, 1329, 1282, 1036, 1008, 829, 767; ^{1}H-NMR (400 MHz, $CDCl_3$): δ= 1.22-1.37 (1H, m, C*H*$_2$), 1.57-1.92 (5H, m, C*H*$_2$), 2.55 (1H, dt, *J* = 11.6, 2.8 Hz, C*H*$_2$), 2.73 (1H, dt, *J* = 11.6, 2.8 Hz, C*H*$_2$), 3.10 (1H, d, *J* = 11.3 Hz, C*H*$_2$), 3.17 (1H, d, *J* = 11.3 Hz, C*H*$_2$), 3.40 (3H, s, C*H*$_3$), 7.21 (1H, dd, *J* = 7.3, 1.2 Hz, Ar*H*), 7.27-7.31 (1H, m, Ar*H*), 7.44-7.51 (2H, m, Ar*H*), 7.61-7.65 (1H, m, Ar*H*), 7.83 (1H, dd, *J* = 8.2, 1.1 Hz, Ar*H*), 8.40 (1H, s, C*H*O); ^{13}C-NMR (100 MHz, $CDCl_3$): δ= 23.8 (*C*H$_2$), 24.9 (*C*H$_2$), 25.3 (*C*H$_2$), 34.2 (*C*H$_3$), 53.4 (*C*H$_2$), 55.8 (*C*H$_2$), 117.0 (*C*H), 123.0 (*C*), 123.9 (*C*H), 124.6 (*C*H), 124.7 (*C*H), 126.1 (*C*H), 128.5 (*C*H), 136.8 (*C*), 137.5 (*C*), 150.1 (*C*), 163.0 (*C*O); HRMS (NSI$^+$) ([M+H]$^+$) calcd for $C_{17}H_{21}N_2O$ 269.1648, found 269.1651, ([2M + Na]$^+$) calcd for $C_{34}H_{40}N_4NaO_2$ 559.3043, found 559.3039.

3-Methyl-1-(5-(((trifluoromethyl)sulfonyl)oxy)pentyl)-1H-perimidin-3-ium triflate

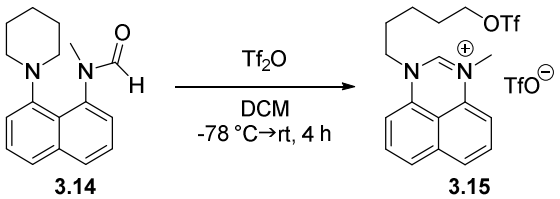

3.14 3.15

A solution of *N*-methyl-*N*-(8-(piperidin-1-yl)naphthalen-1-yl)formamide **3.14** (125 mg, 0.47 mmol, 1.0 eq.) in dry DCM (0.5 mL) was added under argon to a flask containing trifluoromethanesulfonic anhydride (0.12 mL, 0.70 mmol, 1.5 eq.) in dry DCM (0.5 mL) at -78 °C *via* syringe pump (0.254 mL/h). After 3.5 h, the reaction mixture was warmed to room temperature and stirred for a further half hour. The solvent was removed *in vacuo* and the residue stirred in Et_2O (15 mL) for 3 h. The product was washed with Et_2O (3 x 20 mL), filtered and dried under reduced pressure to give the *title compound* **3.15** as a yellow solid (230 mg, 0.42 mmol, 90 %); mp: 70-72 °C (decomp.);

ν_{max}(ATR)/cm^{-1} 1667, 1410, 1246, 1147, 1028, 934, 819; ^{1}H-NMR (400 MHz, d_3-MeCN): δ= 1.55-1.65 (2H, m, CH_2), 1.85-2.00 (4H, m, CH_2), 3.49 (3H, s, CH_3), 3.91 (2H, t, *J* = 7.7 Hz, CH_2), 4.69 (2H, t, *J* = 6.3 Hz, CH_2), 6.83 (1H, d, *J* = 7.6 Hz, Ar*H*), 6.92 (1H, d, *J* = 7.7 Hz, Ar*H*), 7.39-7.45 (2H, m, Ar*H*), 7.49-7.54 (2H, m, Ar*H*), 8.36 (1H, s, C*H*); ^{13}C-NMR (100 MHz, d_3-MeCN): δ= 21.2 (*C*H$_2$), 25.1 (*C*H$_2$), 28.0 (*C*H$_2$), 38.6 (*C*H$_3$), 51.2 (*C*H$_2$), 78.7 (*C*H$_2$), 107.5 (*C*H), 107.8 (*C*H), 118.4 (q, $J_{C\text{-}F}$ = 317 Hz, *C*F$_3$SO$_3$), 120.4 (q, $J_{C\text{-}F}$ = 317 Hz, *C*F$_3$SO$_3$), 120.8 (*C*), 123.7 (*C*H), 123.9 (*C*H), 128.0 (*C*H), 128.0 (*C*H), 131.1 (*C*), 132.3 (*C*), 134.3 (*C*), 152.0 (*C*H); HRMS (NSI$^+$) ([M-TfO]$^+$) calcd for $C_{18}H_{20}F_3N_2O_3S$ 401.1141, found 401.1134.

N,*N*,*N*'-Trimethylnaphthalene-1,8-diamine[132]

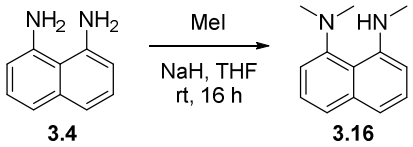

3.4 **3.16**

Sodium hydride (60 %, 776 mg, 19.4 mmol, 1.02 eq.) was added under argon to a solution of 1,8-diaminonaphthalene **3.4** (3.0 g, 19.0 mmol, 1.00 eq.) in dry THF (40 mL) at room temperature. After the effervescence ceased, methyl iodide (1.2 mL, 19.0 mmol, 1.00 eq.) was added and the reaction mixture was stirred for 20 min, before another portion of sodium hydride (776 mg, 19.4 mmol, 1.02 eq.) was introduced, followed by addition of methyl iodide (1.2 mL, 19.0 mmol, 1.00 eq.). The reaction mixture was stirred for 16 h. The reaction mixture was quenched with water (50 mL) carefully and extracted with EtOAc (3 x 75 mL). The combined organic layers were dried over sodium sulfate, filtered and the solvent was removed *in vacuo*. Flash chromatography (20 % DCM/Pet ether + 1% Et$_3$N) afforded the title compound **3.16** as a colourless oil (1.21 g, 6.1 mmol, 48 %); ν_{max}(ATR)/cm^{-1} 3249, 3051, 2865, 1580, 1532, 1302, 1153, 1025, 816, 756; ^{1}H-NMR (400 MHz, $CDCl_3$): δ= 2.77 (6H, s, CH_3), 2.99 (3H, s, CH_3), 6.45 (1H, d, *J* = 7.7 Hz, Ar*H*), 7.06 (1H, dd, *J* = 8.0, 0.6 Hz, Ar*H*), 7.15-7.19 (1H, m, Ar*H*), 7.29-7.36 (2H, m, Ar*H*), 7.50 (1H, dd, *J* = 8.1, 1.0 Hz, Ar*H*), 8.98 (1H, bs, N*H*); ^{13}C-NMR (100 MHz, $CDCl_3$): δ= 30.0 (*C*H$_3$), 45.6 (*C*H$_3$), 102.1 (*C*H), 114.5 (*C*H), 114.6 (*C*H), 117.8 (*C*), 124.8 (*C*H), 125.1 (*C*H), 126.5 (*C*H), 136.4 (*C*), 147.6 (*C*), 151.4 (*C*); HRMS (NSI$^+$) ([M+H]$^+$) calcd for $C_{13}H_{17}N_2$ 201.1386, found 201.1385.

N-(8-(Dimethylamino)naphthalen-1-yl)-N-methylformamide

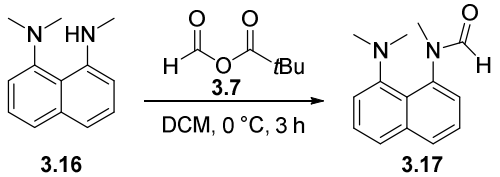

3.16 **3.17**

A solution of formic pivalic anhydride **3.7** (1742 mg, 13.4 mmol, 1.4 eq.) in dry DCM (10 mL) was added under argon to a solution of *N*,*N*,*N*'-trimethylnaphthalene-1,8-diamine **3.16** (1915 mg, 9.6 mmol, 1.0 eq.) in dry DCM (10 mL) at 0 °C. The reaction mixture was stirred for 3 h, before it was diluted with DCM (250 mL) and washed with 2 M NaOH (2 x 200 mL), brine (150 mL) and dried over sodium sulfate. The solvent was removed *in vacuo*. Flash chromatography (30 % EtOAc/Pet ether) afforded the *title compound* **3.17** as a pale yellow solid (2.10 g, 9.2 mmol, 96 %); mp: 73-75 °C; ν_{max}(ATR)/cm^{-1} 2930, 2900, 2833, 2783, 1662, 1575, 1332, 1280, 1034, 825, 766; ^{1}H-NMR (400 MHz, $CDCl_3$): δ= 2.69 (3H, s, CH_3), 2.70 (3H, s, CH_3), 3.38 (3H, s, CH_3), 7.19-7.25 (2H, m, Ar*H*), 7.42-7.48 (2H, m, Ar*H*), 7.59 (1H, dd, *J* = 8.1, 0.9 Hz, Ar*H*), 7.80 (1H, dd, *J* = 8.2, 1.1 Hz, Ar*H*), 8.33 (1H, s, C*H*O); ^{13}C-NMR (100 MHz, $CDCl_3$): δ= 33.9 (*C*H$_3$), 43.7 (*C*H$_3$), 45.0 (*C*H$_3$), 116.1 (*C*H), 122.5 (*C*), 123.3 (*C*H), 124.0 (*C*H), 124.9 (*C*H), 125.9 (*C*H), 128.1 (*C*H), 136.8 (*C*), 137.8 (*C*), 149.4 (*C*), 162.9 (*C*O); HRMS (NSI$^+$) ([M+H]$^+$) calcd for $C_{14}H_{17}N_2O$ 229.1335, found 229.1336, ([M+Na]$^+$) calcd for $C_{14}H_{16}N_2NaO$ 251.1155, found 251.1156.

1,3-Dimethyl-1*H*-perimidin-3-ium triflate[149]

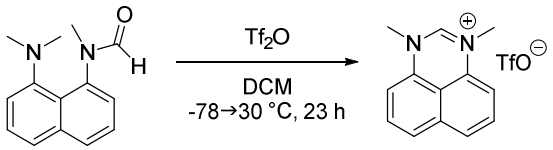

3.17 **3.19**

A solution of *N*-(8-(dimethylamino)naphthalen-1-yl)-*N*-methyl-formamide **3.17** (100 mg, 0.44 mmol, 1.0 eq.) in dry DCM (0.5 mL) was added under argon to a flask containing trifluoromethanesulfonic anhydride (0.10 mL, 0.61 mmol, 1.4 eq.) in dry DCM (0.5 mL) at -78 °C *via* syringe pump (0.508 mL/h). After 3 h, the reaction mixture was warmed to 30 °C and stirred for a further 5 h. The reaction mixture was then stirred at room temperature for additional 15 h. The solvent was removed *in vacuo* and the product stirred in diethyl ether (10 mL) for 16 h. The solvent was decanted and the product recrystallised from ethanol to give the title compound **3.19** as yellow needles (128 mg, 0.37 mmol, 84 %); mp: 257-258 °C (decomp.) (lit.[149]: 275-276 °C); ν_{max}(ATR)/cm^{-1} 1669, 1608, 1504, 1254, 1157, 1024, 754; ^{1}H-NMR (400 MHz, d_6-DMSO): δ= 3.53 (6H, s, CH_3), 7.05 (2H, d, *J* = *7*.4 Hz, Ar*H*), 7.52-7-57 (2H, m, Ar*H*), 7.58 (2H, d, *J* = 8.4 Hz, Ar*H*), 8.96 (1H, s, C*H*); ^{13}C-NMR (100 MHz, d_6-DMSO): δ= 38.7 (*C*H$_3$), 107.7 (*C*H), 120.4 (*C*), 120.7 (q, $J_{C\text{-}F}$ = 320 Hz, *C*F_3SO_3), 123.6 (*C*H), 128.4 (*C*H), 132.8 (*C*), 133.9 (*C*), 153.4 (*C*H); HRMS (NSI$^+$) ([M-TfO]$^+$) calcd for $C_{13}H_{13}N_2$ 197.1073, found 197.1071, ([2M-TfO]$^+$) calcd for $C_{27}H_{26}F_3N_4O_3S$ 543.1667, found 543.1665.

1,1-Dimethyl-2-(((trifluoromethyl)sulfonyl)oxy)-2,3-dihydro-1H-perimidin-1-ium triflate

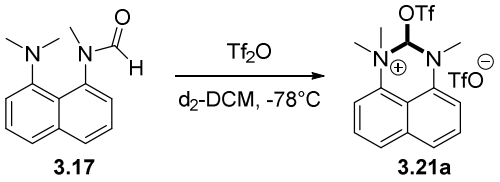

3.17 **3.21a**

N-(8-(Dimethylamino)naphthalen-1-yl)-*N*-methylformamide **3.17** (23 mg, 0.1 mmol, 1.0 eq.) was dissolved under nitrogen in d_2-DCM (0.7 mL) inside an NMR tube and the sample was sealed with a rubber septum. The NMR sample was cooled to -78 °C in a Dewar cooling bath and freshly distilled triflic anhydride (25 µL, 0.15 mmol, 1.5 eq.) was added through the rubber septum *via* syringe. The NMR tube was quickly taken out of the cooling bath, inverted once to allow the solution to mix thoroughly and then put back into the Dewar cooling bath. The *title compound* **3.21a** was characterised by NMR experiments at -35 °C. ^{1}H-NMR (600 MHz, d_2-DCM, -35 °C): δ = 3.18 (3H, s, C*H*$_3$), 3.24 (3H, s, C*H*$_3$), 3.73 (3H, s, C*H*$_3$), 6.64 (1H, dd, *J* = 6.8, 0.8 Hz, Ar*H*), 6.94 (1H, s, C*H*OTf), 7.42 (1H, dd, *J* = 8.0, 7.9 Hz, Ar*H*), 7.48-7.54 (3H, m, Ar*H*), 7.85 (1H, d, *J* = 8.2 Hz, Ar*H*); ^{13}C-NMR (150 MHz, d_2-DCM, -35 °C): δ = 37.8 (*C*H$_3$), 49.3 (*C*H$_3$), 53.6 (*C*H$_3$), 100.9 (*C*HOTf), 111.2 (*C*), 113.0 (*C*H), 116.4 (*C*H), 118.0 (q, $J_{C\text{-}F}$ = 321.2 Hz, *C*F$_3$SO$_3$), 120.4 (q, $J_{C\text{-}F}$ = 319.4 Hz, *C*F$_3$SO$_3$), 121.4 (*C*H), 125.9 (*C*), 128.2 (*C*), 130.4 (*C*), 132.4 (*C*H), 133.3 (*C*H), 135.5 (*C*H).

3-Methyl-2-(((trifluoromethyl)sulfonyl)oxy)-2,3-dihydrospiro[*perimidine-1,1'-pyrrolidin*]*-1-ium triflate*

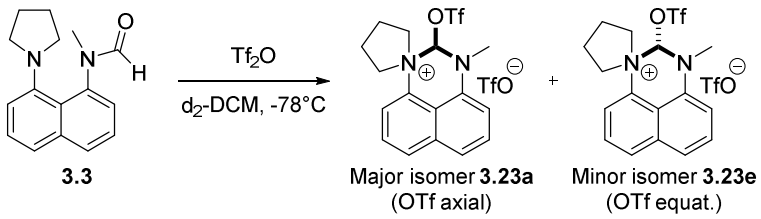

3.3 Major isomer **3.23a** (OTf axial) Minor isomer **3.23e** (OTf equat.)

N-Methyl-*N*-(8-(pyrrolidin-1-yl)naphthalen-1-yl)formamide **3.3** (25 mg, 0.1 mmol, 1.0 eq.) was dissolved under nitrogen in d_2-DCM (0.7mL) inside an NMR tube and the sample was sealed with a rubber septum. The NMR sample was cooled to -78 °C in a Dewar cooling bath and freshly distilled triflic anhydride (25 µL, 0.15 mmol, 1.5 eq.) was added through the rubber septum *via* syringe. The NMR tube was quickly taken out of the Dewar cooling bath, inverted once to allow the solution to mix thoroughly and then put back into the Dewar cooling bath. The ^{1}H-NMR spectrum was recorded at -20 °C showing two isomers **3.23a** and **3.23e** present in solution with a ratio of 1:0.8, respectively. By nOesy experiments (see discussion and Figure 3.14 in chapter 3.3) it was determined that the major isomer (**3.23a**) was bearing the bound triflate residue in an axial position on the six-membered ring, while in the minor isomer (**3.23e**) the triflate residue was equatorial. ^{1}H-NMR

(600 MHz, d_2-DCM, -20 °C): δ= 1.78-1.85 (1H, m, CH_2, **3.23a**), 1.85-1.93 (1H, m, CH_2, **3.23e**), 2.04-2.08 (1H, m, CH_2, **3.23a**), 2.08-2.12 (1H, m, CH_2, **3.23e**), 2.14-2.22 (1H, m, CH_2, **3.23e**), 2.24-2.31 (1H, m, CH_2, **3.23a**), 2.45-2.51 (1H, m, CH_2, **3.23a**), 2.51-2.55 (1H, m, CH_2, **3.23e**), 2.57-2.67 (1H, m, CH_2, **3.23e**), 2.99-3.04 (1H, m, CH_2, **3.23a**), 3.09-3.12 (1H, dd, *J* = 11.2, 7.0 Hz, CH_2, **3.23e**), 3.12-3.3.18 (1H, dd, *J* = 11.0, 7.1 Hz, CH_2, **3.23a**), 3.24 (3H, s, CH_3, **3.23e**), 3.83 (3H, s, CH_3, **3.23a**), 3.95-3.01 (1H, m, CH_2, **3.23a**), 4.12-4.17 (1H, m, CH_2, **3.23a**), 4.17-4.20 (1H, m, CH_2, **3.23e**), 4.23-4.30 (1H, m, CH_2, **3.23e**), 6.68 (1H, s, C*H*OTf, **3.23a**), 6.70 (1H, d, *J* = 7.3 Hz, Ar*H*, **3.23a**), 6.95 (1H, d, *J* = 7.6 Hz, Ar*H*, **3.23e**), 6.96 (1H, s, C*H*OTf, **3.23e**), 7.24 (1H, d, *J* = 7.7 Hz, Ar*H*, **3.23e**), 7.40 (1H, dd, *J* = 8.0, 7.9 Hz, Ar*H*, **3.23e**), 7.43-7.46 (1H, m, Ar*H*, **3.23e**), 7.46-7.48 (1H, m, Ar*H*, **3.23e**), 7.48-7.50 (1H, m, Ar*H*, **3.23a**), 7.50-7.53 (1H, m, Ar*H*, **3.23a**), 7.71 (1H, d, *J* = 8.2 Hz, Ar*H*, **3.23a**), 7.78-7.80 (1H, m, Ar*H*, **3.23e**), 7.80-7.82 (1H, m, Ar*H*, **3.23a**), 8.06 (1H, d, *J* = 8.3 Hz, Ar*H*, **3.23a**); ^{13}C-NMR (150 MHz, d_2-DCM, -20 °C): δ= 20.3 (*C*H_2), 20.6 (*C*H_2), 23.5 (*C*H_2), 23.7 (*C*H_2), 37.6 (*C*H_3), 38.2 (*C*H_3), 62.2 (*C*H_2), 62.7 (*C*H_2), 64.8 (*C*H_2), 65.3 (*C*H_2), 99.4 (*C*HOTf), 100.9 (*C*HOTf), 111.0 (*C*H), 112.7 (*C*), 113.0 (*C*H), 113.2 (*C*), 116.8 (*C*H), 117.5 (*C*H), 118.0 (q, $J_{C\text{-}F}$ = 321 Hz, *C*F_3SO_3), 120.6 (q, $J_{C\text{-}F}$ = 318 Hz, *C*F_3SO_3), 121.2 (*C*H), 121.4 (*C*H), 125.3 (*C*H), 125.4 (*C*H), 128.2 (*C*H), 129.1 (*C*H), 130.2 (*C*H), 130.9 (*C*H), 133.0 (*C*), 133.1 (*C*), 133.2 (*C*), 133.5 (*C*), 134.0 (*C*), 134.4 (*C*).

N-(8-(Dimethylamino)naphthalen-1-yl)-*N*-methylbenzamide[196]

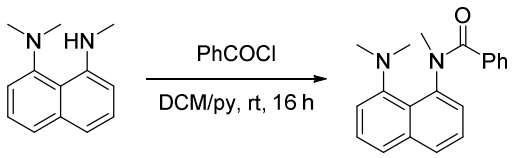

3.16 **3.25**

Benzoyl chloride (1.04 mL, 9.0 mmol, 1.2 eq.) was added to *N*,*N*,*N*'-trimethylnaphthalene-1,8-diamine **3.16** (1.5 g, 7.5 mmol, 1.0 eq.) dissolved in a DCM/pyridine mixture (15 ml/15 mL). The reaction mixture was stirred at room temperature for 16 h. The product mixture was then partitioned between DCM and water and extracted with DCM (2 x 50 mL). The combined organic phases were washed with water (2 x 50 mL), brine (50 mL) and dried over sodium sulfate. The crude product was concentrated under reduced pressure. Flash chromatography (20 % EtOAc/Pet ether) afforded the title compound **3.25** as a yellow solid (2.14 g, 7.0 mmol, 94 %); mp: 111-114 °C; ν_{max}(ATR)/cm^{-1} 1626, 1570, 1373, 1047, 1024, 829 789, 770, 712 667; The ^{1}H-NMR spectrum showed two isomers present in solution with a ratio of 0.8:0.2. In the following only the peaks of the major isomer are quoted. ^{1}H-NMR (400 MHz, $CDCl_3$): δ = 2.68 (3H, s, CH_3), 2.73 (3H, s, CH_3), 3.85 (3H, s, CH_3), 6.82-6.89 (3H, m, Ar*H*), 6.95-7.01 (1H, m, Ar*H*), 7.01-7.05 (2H, m, Ar*H*), 7.19 (1H, t, *J* = 7.7 Hz, Ar*H*), 7.40 (1H, dd, *J* = 8.0, 0.9 Hz, Ar*H*), 7.44-7.48 (2H, m, Ar*H*), 7.70-7.73 (1H, m, Ar*H*); ^{13}C-NMR

(100 MHz, $CDCl_3$): δ= 40.0 (*C*H_3), 43.2 (*C*H_3), 46.8 (*C*H_3), 115.2 (*C*H), 122.9 (*C*H), 124.3 (*C*H), 124.6 (*C*H), 125.4 (*C*H), 126.1 (*C*H), 127.7 (*C*H), 128.3 (*C*H), 128.5 (*C*H), 129.1 (*C*), 135.1 (*C*), 136.2 (*C*), 140.9 (*C*), 149.5 (*C*), 169.2 (*C*O); HRMS (NSI^+) ([M+H]$^+$) calcd for $C_{20}H_{21}N_2O$ 305.1648, found 305.1649.

1,1,3-Trimethyl-2-phenyl-1H-perimidine-1,3-diium triflate

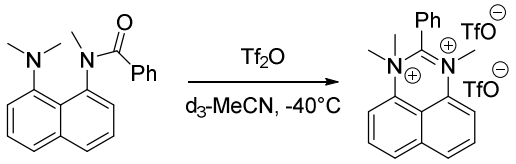

3.25 **3.28**

N-(8-(Dimethylamino)naphthalen-1-yl)-*N*-methylbenzamide **3.25** (30 mg, 0.1 mmol, 1.0 eq.) was dissolved under nitrogen in d_3-MeCN (0.7mL) inside an NMR tube and the sample was sealed with a rubber septum. The NMR sample was cooled to -40 °C in a Dewar cooling bath and freshly distilled triflic anhydride (25 µL, 0.15 mmol, 1.5 eq.) was added through the rubber septum *via* syringe. The NMR tube was quickly taken out of the Dewar cooling bath, inverted once to allow the solution to mix thoroughly and then put back into the Dewar cooling bath. The *title compound* **3.28** was characterised by NMR experiments at -35 °C. ^{1}H-NMR (600 MHz, d_3-MeCN, -35 °C): δ= 4.10 (6H, s, C*H*$_3$), 4.18 (3H, s, C*H*$_3$), 7.89 (2H, dd, *J* = 8.0, 7.5 Hz, Ar*H*), 7.93-8.04 (3H, m, Ar*H*), 8.05-8.09 (2H, m, Ar*H*), 8.36-8.42 (3H, m, Ar*H*), 8.49 (1H, d, *J* = 8.4 Hz, Ar*H*); ^{13}C-NMR (150 MHz, d_3-MeCN, -35 °C): δ= 48.1 (*C*H_3), 61.1 (*C*H_3), 115.2 (*C*), 118.0 (q, $J_{C\text{-}F}$ = 320 Hz, *C*F_3SO_3), 121.5 (*C*H), 122.4 (*C*), 123.7 (*C*H), 127.1 (*C*), 128.3 (*C*H), 129.6 (*C*H), 130.2 (*C*H), 130.4 (*C*H), 131.5 (*C*H), 132.8 (*C*), 134.3 (*C*), 135.1 (*C*H), 135.3 (*C*H), 164.1 (*C*).

1,1,3-Trimethyl-2-phenyl-1H-perimidine-1,3-diium triflate

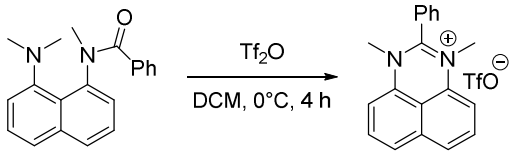

3.25 **3.29**

To a solution of *N*-(8-(dimethylamino)naphthalen-1-yl)-*N*-methylbenzamide **3.25** (152 mg, 0.5 mmol, 1.0 eq.) in DCM (0.5 mL) was added under argon triflic anhydride (0.1 mL, 0.6 mmol, 1.2 eq.) dropwise *via* syringe at 0 °C. After the addition, the reaction mixture was stirred for 1 h, before it was warmed to room temperature and stirred for a further 3 h. The product mixture was triturated with a 1:2-mixture of DCM/Et_2O (3 x 6 mL) and the organic washings were decanted. The precipitate was dried under reduced pressure to afford the *title compound* **3.29** as a yellow solid (205 mg,

4.9 mmol, 97 %); mp: 220-222 °C; ν_{max}(ATR)/cm^{-1} 1643 1572, 1485, 1263, 1250, 1223, 1144, 1030, 986, 820, 766, 702; ^{1}H-NMR (400 MHz, d_3-MeCN): δ = 3.27 (6H, s, CH_3), 7.12 (2H, d, *J* = 7.8 Hz, Ar*H*), 7.61 (2H, dd, *J* = 8.4, 7.8 Hz, Ar*H*), 7.66-7.71 (2H, m, Ar*H*), 7.73 (2H, dd, *J* = 8.4, 0.5 Hz, Ar*H*), 7.78-7.87 (3H, m, Ar*H*); ^{13}C-NMR (100 MHz, d_3-MeCN): δ = 39.0 (*C*H$_3$), 108.5 (*C*H), 116.9 (*C*H), 120.5 (*C*), 120.7 (q, $J_{C\text{-}F}$ = 320 Hz, *C*F$_3$SO$_3$), 123.7 (*C*H), 126.9 (*C*H), 127.7 (*C*), 127.9 (*C*H), 130.0 (*C*H), 132.2 (*C*), 133.6 (*C*), 160.7 (*C*); HRMS (NSI$^+$) ([M-OTf]$^+$) calcd for $C_{19}H_{17}N_2$ 273.1386, found 273.1386.

2-(Pyrrolidin-1-yl)aniline[197]

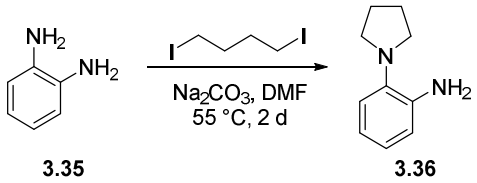

3.35 **3.36**

1,2-Phenylenediamine **3.35** (3.0 g, 27.7 mmol, 1.0 eq.) and sodium carbonate (6.2 g, 58.3 mmol, 2.1 eq.) were dissolved in dry DMF (30 mL) under argon. 1,4-Diiodobutane (3.7 mL, 27.7 mmol, 1.0 eq.) was added and the reaction mixture stirred for 2 days at 55 °C. The reaction mixture was partitioned between DCM (50 mL) and water (400 mL) and extracted with DCM (3 x 100 mL). The combined organic phases were washed with water (2 x 100 mL), 2 M NaOH (2 x 100 mL), brine (50 mL) and dried over sodium sulfate. The solvent was removed *in vacuo*. Flash chromatography (10 % EtOAc/Pet ether) afforded the title compound **3.36** as a colourless oil (3.467 g, 21.4 mmol, 77 %); ν_{max}(ATR)/cm^{-1} 3428, 3338, 2963, 2874, 2811, 1608, 1500, 1455, 1286, 1258, 1192, 1120, 950, 738; ^{1}H-NMR (400 MHz, $CDCl_3$): δ = 1.85-2.00 (4H, m, CH_2), 3.00-3.10 (4H, m, CH_2), 3.86 (2H, bs, NH_2), 6.73-6.78 (2H, m, Ar*H*), 6.88-6.93 (1H, m, Ar*H*), 6.99-7.03 (1H, m, Ar*H*); ^{13}C-NMR (100 MHz, $CDCl_3$): δ = 23.6 (*C*H$_2$), 50.3 (*C*H$_2$), 114.9 (*C*H), 118.0 (*C*H), 118.1 (*C*H), 122.9 (*C*H), 137.3 (*C*), 140.8 (*C*); HRMS (NSI$^+$) ([M+H]$^+$) calcd for $C_{10}H_{15}N_2$ 163.1230, found 163.1222.

N-(2-(Pyrrolidin-1-yl)phenyl)formamide[198]

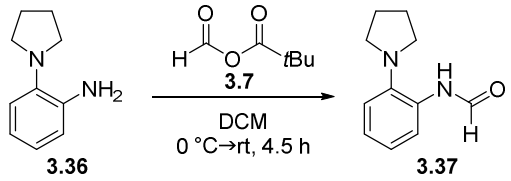

3.36 **3.37**

A solution of 2-(pyrrolidin-1-yl)aniline **3.36** (1.5 g, 9.3 mmol, 1.0 eq.) in dry DCM (10 mL) was added under argon to a solution of formic pivalic anhydride **3.7** (1.56 mg, 12.0 mmol, 1.3 eq.) in dry DCM (15 mL) at 0 °C. The reaction mixture was stirred for 4 h, then for a further half hour at room temperature before it was diluted with DCM (50 mL) and washed with 2 M NaOH (2 x 50 mL), brine

(75 mL) and dried over sodium sulfate. The solvent was removed *in vacuo*. Flash chromatography (20 % EtOAc/Pet ether) afforded the title compound **3.37** as a colourless oil (1.472 g, 7.7 mmol, 83 %); ν_{max}(ATR)/cm^{-1} 3264, 2965, 2874, 2826, 1668, 1593, 1515, 1446, 1295, 743; in the NMR spectra the compound appeared as an isomer mixture (isomer ratio A:B = 2:1) ^{1}H-NMR (500 MHz, $CDCl_3$): δ= 1.90-2.05 (4H, m, CH_2), 3.00-3.06 (2H, m, CH_2), 3.06-3.12 (2H, m, CH_2), 6.97-7.19 [m, ism A+B] and 8.26-8.31 [m, ism A] (4H, Ar*H*), 7.77 [bs, ism B] and 8.26-8.31 [bs, ism A] (1H, N*H*), 8.51 [d, *J* = 1.5 Hz, ism A] and 8.70 [d, *J* = 11.9 Hz, ism B] (1H, C*H*O); ^{13}C-NMR (125 MHz, $CDCl_3$): δ= 24.5 and 24.6 (*C*H_2), 51.8 and 52.6 (*C*H_2), 119.2 and 119.5 (*C*H), 119.8 and 120.8 (*C*H), 122.7 and 125.8 (*C*H), 124.3 and 124.6 (*C*H), 129.8 and 132.4 (*C*), 140.2 and 142.0 (*C*), 158.8 and 161.9 (*C*O); HRMS (NSI$^+$) ([M+H]$^+$) calcd for $C_{11}H_{15}N_2O$ 191.1179, found 191.1174, ([M+Na]$^+$) calcd for $C_{11}H_{14}N_2NaO$ 213.0998, found 213.0992, ([2M+Na]$^+$) calcd for $C_{22}H_{28}N_4NaO_2$ 403.2110, found 403.2093.

N-Methyl-2-(pyrrolidin-1-yl)aniline

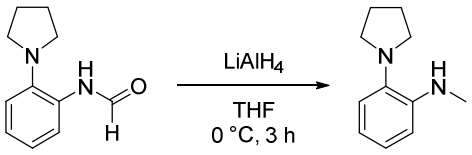

3.37 **3.38**

A solution of *N*-(2-(pyrrolidin-1-yl)phenyl)formamide **3.37** (1.472 g, 7.6 mmol, 1.0 eq.) in THF (10 mL) was slowly added under argon to a stirred suspension of $LiAlH_4$ (656 mg, 17.3 mmol, 2.3 eq.) in THF (15 mL) *via* cannula at 0 °C. The reaction mixture was stirred for 3 h, before it was quenched with 2 M NaOH carefully. The reaction mixture was diluted with DCM (150 mL), washed with 2 M NaOH (2 x 300 mL), brine (200 mL) and dried over sodium sulfate. The solvent was removed *in vacuo*. Flash chromatography (40 % DCM/Pet ether) afforded the title compound **3.38** as a colourless oil (1.204 g, 6.8 mmol, 90 %); ν_{max}(ATR)/cm^{-1} 3375, 2963, 2809, 1597, 1506, 1276, 1165, 1127, 948, 736; ^{1}H-NMR (500 MHz, $CDCl_3$): δ= 1.90-2.00 (4H, m, CH_2), 2.88 (3H, d, *J* = 3.2 Hz, CH_3), 2.95-3.10 (4H, m, CH_2), 4.50 (1H, s, N*H*), 6.63-6.67 (1H, m, Ar*H*), 6.70 (1H, dt, *J* = 7.6, 1.5 Hz, Ar*H*), 7.02-7.06 (2H, m, Ar*H*); ^{13}C-NMR (125 MHz, $CDCl_3$): δ= 24.1 (*C*H_2), 30.9 (*C*H_3), 51.2 (*C*H_2), 109.6 (*C*H), 116.6 (*C*H), 118.3 (*C*H), 124.2 (*C*H), 137.2 (*C*), 144.8 (*C*); HRMS (NSI$^+$) ([M+H]$^+$) calcd for $C_{11}H_{17}N_2$ 177.1386, found 177.1387.

N-Methyl-N-(2-(pyrrolidin-1-yl)phenyl)formamide

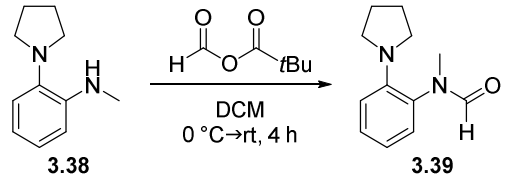

3.38 **3.39**

A solution of *N*-methyl-2-(pyrrolidin-1-yl)aniline **3.38** (1.200 g, 6.8 mmol, 1.0 eq.) in dry DCM (10 mL) was added under argon to a solution of formic pivalic anhydride (1.150 g, 8.9 mmol, 1.3 eq.) in dry DCM (15 mL) at 0 °C. The reaction mixture was stirred for 3.5 h, then at room temperature for a further half hour, before it was diluted with DCM (50 mL), washed with 2 M NaOH (2 x 75 mL), brine (100 mL) and dried over sodium sulfate. The solvent was removed *in vacuo*. Flash chromatography (25 % EtOAc/Pet ether) afforded the *title compound* **3.39** as a colourless oil (1.308 g, 6.4 mmol, 94 %); ν_{max}(ATR)/cm^{-1} 2965, 2872, 1673, 1597, 1498, 1452, 1332, 1299, 1116, 952, 745; ^{1}H-NMR (500 MHz, $CDCl_3$): δ= 1.90-2.00 (4H, m, CH_2), 3.14 (3H, s, CH_3), 3.15-3.17 (4H, m, CH_2), 6.81-6.85 (1H, m, Ar*H*), 6.88 (1H, dd, *J* = 8.3, 1.2 Hz, Ar*H*), 7.01-7.04 (1H, m, Ar*H*), 7.21-7.25 (1H, m, Ar*H*), 8.25 (1H, s, C*H*O); ^{13}C-NMR (125 MHz, $CDCl_3$): δ= 25.3 (*C*H_2), 32.3 (*C*H_3), 50.1 (*C*H_2), 116.2 (*C*H), 118.3 (*C*H), 128.7 (*C*H), 129.4 (*C*H), 129.8 (*C*), 146.5 (*C*), 163.6 (*C*O); HRMS (NSI$^+$) ([M-H]$^+$) calcd for $C_{12}H_{15}N_2O$ 203.1179, found 203.1176, ([M+Na]$^+$) calcd for $C_{12}H_{16}N_2NaO$ 227.1155, found 227.1153, ([2M+Na]$^+$) calcd for $C_{24}H_{32}N_4NaO_2$ 431.2417, found 431.2411.

3-Methyl-1-(3-(((trifluoromethyl)sulfonyl)oxy)propyl)-1H-benzo[*d*]*imidazol-3-ium triflate*

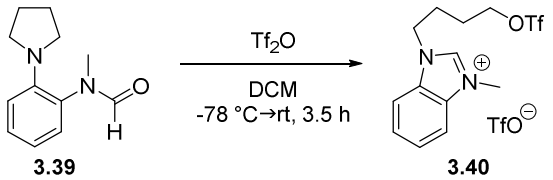

3.39 **3.40**

A solution of *N*-methyl-*N*-(2-(pyrrolidin-1-yl)phenyl)formamide **3.39** (102 mg, 0.5 mmol, 1.0 eq.) in dry DCM (0.5 mL) was added under argon to a flask containing trifluoromethanesulfonic anhydride (0.12 mL, 0.7 mmol, 1.4 eq.) in dry DCM (0.5 mL) *via* syringe pump (0.508 mL/h) at -78 °C. After 3 h, the reaction mixture was warmed to room temperature and stirred for a further half hour. The solvent was removed *in vacuo* to give the *title compound* **3.40** as a brown oil (169 mg, 0.35 mmol, 70 %); ν_{max}(ATR)/cm^{-1} 3083, 1574, 1410, 1198, 1127, 1026, 926, 748; ^{1}H-NMR (500 MHz, $CDCl_3$): δ= 1.98-2.04 (2H, m, CH_2), 2.17-2.24 (2H, m, CH_2), 4.17 (3H, s, CH_3), 4.60 (2H, t, *J* = 7.4 Hz, CH_2), 4.62 (2H, t, *J* = 6.2 Hz, CH_2), 7.68-7.72 (2H, m, Ar*H*), 7.73-7.79 (2H, m, Ar*H*), 9.79 (1H, s, C*H*); ^{13}C-NMR (125 MHz, $CDCl_3$): δ= 25.2 (*C*H_2), 26.2 (*C*H_2), 33.6 (*C*H_3), 46.7 (*C*H_2), 76.7 (*C*H_2), 112.8 (*C*H), 113.0 (*C*H),

118.5 (q, $J_{C\text{-}F}$ = 318 Hz, CF_3SO_3), 120.4 (q, $J_{C\text{-}F}$ = 319 Hz, CF_3SO_3), 127.5 (*C*H), 127.6 (*C*H), 131.1 (*C*), 132.1 (*C*), 142.6 (*CH*); HRMS (NSI$^+$) ([M-TfO]$^+$) calcd for $C_{13}H_{16}F_3N_2O_3S$ 337.0828, found 337.0825, ([2M-TfO]$^+$) calcd for $C_{27}H_{32}F_9N_4O_9S_3$ 823.1177, found 823.1166.

N,*N*,*N*'-Trimethylbenzene-1,2-diamine[199]

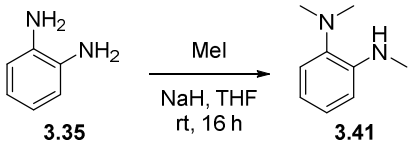

3.35 **3.41**

Sodium hydride (60 %, 776 mg, 19.4 mmol, 1.02 eq.) was added under argon to a solution of 1,2-phenylenediamine **3.35** (2.05 g, 19.0 mmol, 1.00 eq.) in dry THF (50 mL) at room temperature. After the effervescence ceased, methyl iodide (1.2 mL, 19.0 mmol, 1.00 eq.) was added and the reaction mixture was stirred for 20 min, before another portion of sodium hydride (776 mg, 19.4 mmol, 1.02 eq.) was introduced followed by addition of methyl iodide (1.2 mL, 19.0 mmol, 1.00 eq.). The reaction mixture was stirred for 16 h. The reaction mixture was quenched with water (200 mL) carefully and then extracted with DCM (3 x 100 mL). The combined organic layers were dried over sodium sulfate, filtered and the solvent was removed *in vacuo*. Flash chromatography (45 % DCM/Pet ether) afforded the title compound **3.41** as an orange oil (891 mg, 6.1 mmol, 47 %); ν_{max}(ATR)/cm^{-1} 3374, 2937, 2865, 2824, 2785, 1599, 1509, 1289, 1146, 1040, 939, 738; ^{1}H-NMR (400 MHz, $CDCl_3$): δ= 2.66 (6H, s, CH_3), 2.88 (3H, s, CH_3), 4.69 (1H, bs, N*H*), 6.61-6.65 (1H, m, Ar*H*), 6.70 (1H, dt, *J* = 7.6, 1.4 Hz, Ar*H*), 7.01-7.08 (2H, m, Ar*H*); ^{13}C-NMR (100 MHz, $CDCl_3$): δ= 30.7 (*C*H$_3$), 43.9 (*C*H$_3$), 109.5 (*C*H), 116.4 (*C*H), 118.8 (*C*H), 124.7 (*C*H), 140.2 (*C*), 144.3 (*C*); HRMS (NSI$^+$) ([M+H]$^+$) calcd for $C_9H_{15}N_2$ 151.1230, found 151.1226.

N-(2-(Dimethylamino)phenyl)-*N*-methylformamide[200]

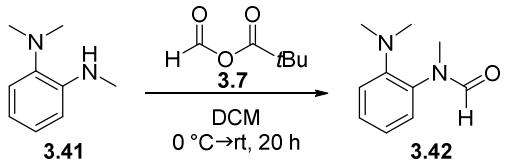

3.41 **3.42**

A solution of *N*,*N*,*N*'-trimethylbenzene-1,2-diamine **3.41** (825 mg, 5.5 mmol, 1.0 eq.) in dry DCM (5 mL) was added under argon to a solution of formic pivalic anhydride **3.7** (1.0 g, 7.7 mmol, 1.4 eq.) in dry DCM (15 mL) at 0 °C. The reaction mixture was stirred for 4 h and then at room temperature for a further 16 h. The solution was diluted with DCM (100 mL), washed with 2 M NaOH (2 x 75 mL), brine (75 mL) and dried over sodium sulfate. The solvent was removed *in vacuo*. Flash chromatography (22 % EtOAc/Pet ether) afforded the title compound **3.42** as a colourless oil

(854 mg, 4.8 mmol, 87 %); ν_{max}(ATR)/cm^{-1} 2945, 2867, 2835, 2786, 1673, 1595, 1498, 1453, 1338, 1088, 978, 754; ^{1}H-NMR (500 MHz, $CDCl_3$): δ= 2.71 (6H, s, CH_3), 3.24 (3H, s, CH_3), 6.97-7.02 (1H, m, Ar*H*), 7.03-7.07 (2H, m, Ar*H*), 7.25-7.29 (1H, m, Ar*H*), 8.30 (1H, s, C*H*O); ^{13}C-NMR (125 MHz, $CDCl_3$): δ= 31.4 (*C*H$_3$), 42.7 (*C*H$_3$), 119.3 (*C*H), 122.1 (*C*H), 127.9 (*C*H), 128.3 (*C*H), 134.3 (*C*), 149.1 (*C*), 163.6 (*C*O); HRMS (NSI$^+$) ([M+H]$^+$) calcd for $C_{10}H_{15}N_2O$ 179.1179, found 179.1177, ([M+Na]$^+$) calcd for $C_{10}H_{14}N_2NaO$ 201.0998, found 201.0998, ([2M+Na]$^+$) calcd for $C_{20}H_{28}N_4NaO_2$ 379.2104, found 379.2107.

1,3-Dimethyl-1H-benzo[d]imidazol-3-ium triflate

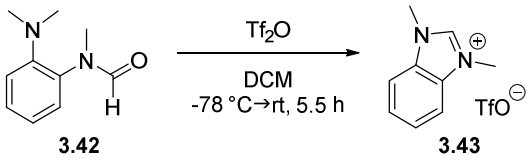

3.42 **3.43**

A solution of *N*-(2-(dimethylamino)phenyl)-*N*-methylformamide **3.42** (89 mg, 0.5 mmol, 1.0 eq.) in dry DCM (0.5 mL) was added under argon to a flask containing trifluoromethanesulfonic anhydride (0.1 mL, 0.6 mmol, 1.2 eq.) in dry DCM (0.5 mL) *via* syringe pump (0.508 mL/h) at -78 °C. After 2.5 h, the reaction mixture was warmed to room temperature and stirred for a further 3 h. The product was precipitated by addition of diethyl ether (5 mL). The solvent was decanted and the precipitate was washed with diethyl ether (2 x 15 mL), filtered and dried under reduced pressure to give the *title compound* **3.43** as a white solid (134 mg, 0.45 mmol, 91 %); mp: 111-114 °C; ν_{max}(ATR)/cm^{-1} 3109, 1577, 1261, 1222, 1150, 1025, 756; ^{1}H-NMR (500 MHz, d_3-MeCN): δ= 4.07 (6H, s, CH_3), 7.68-7.71 (2H, m, Ar*H*), 7.84-7.87 (2H, m, Ar*H*), 9.07 (1H, s, C*H*); ^{13}C-NMR (125 MHz, d_3-MeCN): δ= 33.2 (*C*H$_3$), 113.2 (*C*H), 121.1 (q, $J_{C\text{-}F}$ = 319 Hz, *C*F$_3$SO$_3$), 126.9 (*C*H), 132.1 (*C*), 142.3 (*C*H); HRMS (NSI$^+$) ([M-TfO]$^+$) calcd for $C_9H_{11}N_2$ 147.0917, found 147.0912, ([2M-TfO]$^+$) calcd for $C_{19}H_{22}F_3N_4O_3S$ 443.1359, found 443.1353.

2-(1*H*-Pyrrol-1-yl)aniline[201]

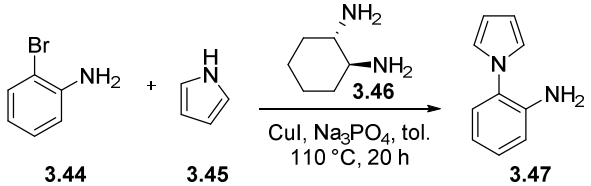

3.44 **3.45** **3.47**

A mixture of 2-bromoaniline **3.44** (1.5 g, 8.7 mmol, 1.20 eq.), copper(I) iodide (76 mg, 0.4 mmol, 0.05 eq.), and sodium phosphate (3.0 g, 15.3 mmol, 2.10 eq.) was dissolved in dry toluene (40 mL) under argon. (1*S*)-*trans*-1,2-diaminocyclohexane **3.46** (0.18 mL, 1.5 mmol, 0.20 eq.) and pyrrole **3.45**

(0.5 mL, 7.3 mmol, 1.00 eq.) were added and the reaction mixture was heated to 110 °C and stirred for 20 h. The reaction mixture was cooled to room temperature and the volume decreased *in vacuo*. The crude product was filtered through a plug of silica and the plug was flushed thoroughly with EtOAc (100 mL). The filtrate was concentrated under reduced pressure. Flash chromatography (40 % DCM/Pet ether) afforded the title compound **3.47** as a white solid (407 mg, 2.6 mmol, 35 %); mp: 93-95 °C (lit.[201]: 96-97 °C); ν_{max}(ATR)/cm^{-1} 3374, 3303, 3206, 1621, 1588, 1508, 1299, 1069, 1014, 924, 753, 726; ^{1}H-NMR (500 MHz, $CDCl_3$): δ= 3.72 (2H, bs, N*H*$_2$), 6.36 (2H, t, *J* = 2.1 Hz, Ar*H*), 6.78-6.84 (2H, m, Ar*H*), 6.85 (2H, t, *J* = 2.1 Hz, Ar*H*), 7.15-7.20 (2H, m, Ar*H*); ^{13}C-NMR (125 MHz, $CDCl_3$): δ= 109.4 (*C*H), 116.1 (*C*H), 118.4 (*C*H), 121.7 (*C*H), 127.2 (*C*H), 127.5 (*C*), 128.5 (*C*H), 142.1 (*C*); HRMS (NSI$^+$) ([M+H]$^+$) calcd for $C_{10}H_{11}N_2$ 159.0917, found 159.0914.

N-(2-(1*H*-Pyrrol-1-yl)phenyl)formamide[202]

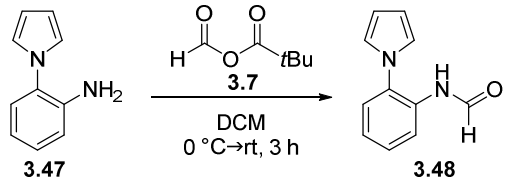

A solution of 2-(1*H*-pyrrol-1-yl)aniline **3.47** (373 mg, 2.4 mmol, 1.0 eq.) in dry DCM (10 mL) was added under argon to a solution of formic pivalic anhydride **3.7** (435 mg, 3.4 mmol, 1.4 eq.) in dry DCM (10 mL) at 0 °C. The reaction mixture was stirred for 2.5 h, then at room temperature for a further half hour, before it was diluted with DCM (100 mL) and washed with 2 M NaOH (2 x 150 mL), brine (100 mL) and dried over sodium sulfate. The solvent was removed *in vacuo*. Flash chromatography (20 % EtOAc/Pet ether) afforded the title compound **3.48** as a white solid (418 mg, 2.3 mmol, 95 %); mp: 111-112 °C (lit.[202]: 123-124 °C); ν_{max}(ATR)/cm^{-1} 3256, 1660, 1595, 1521, 1480, 1452, 1403, 1297, 1068, 922, 766, 719; in the NMR the compound appeard as an isomer mixture (isomer ratio A:B = 2:1) ^{1}H-NMR (400 MHz, $CDCl_3$): δ= 6.41 (2H, t, *J* = 2.1 Hz, Ar*H*), 6.80 (2H, t, *J* = 2.1 Hz, Ar*H*), 7.11 [bs, ism A] and 7.17-7.44 [bs, ism B] (1H, N*H*), 7.17-7.60 [m, ism A+B] and 8.47 [dd, *J* = 8.3, 1.0 Hz, ism A] (4H, Ar*H*), 8.32 [d, *J* = 1.5 Hz, ism A] and 8.66 [d, *J* = 11.2 Hz, ism B] (1H, C*H*O); ^{13}C-NMR (100 MHz, $CDCl_3$): δ= 110.6 and 110.8 (*C*H), 118.1 and 121.7 (*C*H), 121.8 and 122.1 (*C*H), 124.7 and 125.4 (*C*H), 127.1 and 128.0 (*C*H), 128.6 and 130.4 (*C*), 128.9 and 128.9 (*C*H), 130.8 and 132.9 (*C*), 158.9 and 161.3 (*C*O); HRMS (NSI$^+$) ([M+Na]$^+$) calcd for $C_{11}H_{10}N_2NaO$ 209.0685, found 209.0683, ([2M + Na)$^+$) calcd for $C_{22}H_{20}N_4NaO_2$ 395.1478, found 395.1477.

N-Methyl-2-(1*H*-pyrrol-1-yl)aniline[203]

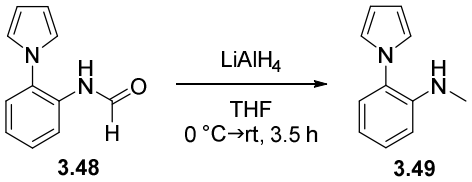

3.48 **3.49**

A solution of *N*-(2-(1*H*-pyrrol-1-yl)phenyl)formamide **3.48** (400 mg, 2.2 mmol, 1.0 eq.) in THF (10 mL) was slowly added under argon to a stirred suspension of $LiAlH_4$ (196 mg, 5.2 mmol, 2.3 eq.) in THF (10 mL) *via* cannula at 0 °C. The reaction mixture was stirred for 3 h, then warmed to room temperature and stirred for a further half hour. The solution was quenched with 2 M NaOH carefully, diluted with DCM (250 mL) and washed with 2 M NaOH (2 x 200 mL), brine (150 mL) and dried over sodium sulfate. The solvent was removed *in vacuo*. Flash chromatography (25 % DCM/Pet ether) afforded the title compound **3.49** as a colourless oil (341 mg, 2.0 mmol, 90 %); ν_{max}(ATR)/cm^{-1} 3424, 2919, 2818, 1606, 1517, 1483, 1317, 1168, 1066, 924; ^{1}H-NMR (400 MHz, $CDCl_3$): δ= 2.81 (3H, d, *J* = 5.1 Hz, C*H*$_3$), 3.85 (1H, bs, N*H*), 6.36 (2H, t, *J* = 2.1 Hz, Ar*H*), 6.71-6.77 (2H, m, Ar*H*), 6.81 (2H, t, *J* = 2.1 Hz, Ar*H*), 7.13-7.17 (1H, m, Ar*H*), 7.27-7.33 (1H, m, Ar*H*); ^{13}C-NMR (100 MHz, $CDCl_3$): δ= 30.3 (*C*H$_3$), 109.3 (*C*H), 110.5 (*C*H), 116.3 (*C*H), 121.9 (*C*H), 126.9 (*C*H), 127.2 (*C*), 129.0 (*C*H), 144.8 (*C*); HRMS (NSI$^+$) ([M+H]$^+$) calcd for $C_{11}H_{13}N_2$ 173.1073, found 173.1071.

N-(2-(1H-Pyrrol-1-yl)phenyl)-N-methylformamide

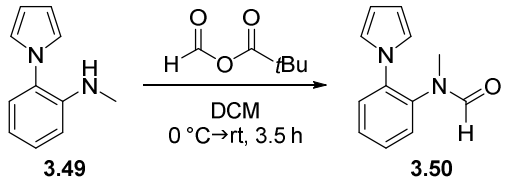

3.49 **3.50**

A solution of *N*-methyl-2-(1*H*-pyrrol-1-yl)aniline **3.49** (335 mg, 2.0 mmol, 1.0 eq.) in dry DCM (10 mL) was added under argon to a solution of formic pivalic anhydride (329 mg, 2.5 mmol, 1.3 eq.) in dry DCM (10 mL) at 0 °C. The reaction mixture was stirred for 3 h, then warmed to room temperature and stirred for a further half hour. The solution was diluted with DCM (200 mL), washed with 2 M NaOH (2 x 150 mL), brine (100 mL) and dried over sodium sulfate. The solvent was removed *in vacuo*. Flash chromatography (25 % EtOAc/Pet ether + 1 % Et_3N) afforded the *title compound* **3.50** as a brown solid (348 mg, 1.7 mmol, 89 %); mp: 73-76 °C; ν_{max}(ATR)/cm^{-1} 3120, 3094, 2876, 1677, 1509, 1332, 1071, 974, 777, 736; ^{1}H-NMR (500 MHz, $CDCl_3$): δ= 2.83 (3H, d, *J* = 0.4 Hz, C*H*$_3$), 6.35 (2H, t, *J* = 2.2 Hz, Ar*H*), 6.77 (2H, t, *J* = 2.2 Hz, Ar*H*), 7.24-7.27 (1H, m, Ar*H*), 7.38-7.46 (3H, m, Ar*H*), 8.21 (1H, s, C*H*O); ^{13}C-NMR (125 MHz, $CDCl_3$): δ= 31.9 (*C*H$_3$), 110.6 (*C*H), 121.3 (*C*H), 127.3 (*C*H), 128.0 (*C*H), 128.1

(*C*H), 128.7 (*C*H), 136.6 (*C*), 137.2 (*C*), 162.5 (*C*O); HRMS (NSI$^+$) ([M+H]$^+$) calcd for $C_{12}H_{13}N_2O$ 201.1022, found 201.1023, ([M+Na]$^+$) calcd for $C_{12}H_{12}N_2NaO$ 223.0847, found 223.0842, ([2M+H]$^+$) calcd for $C_{24}H_{25}N_4O_2$ 401.1977, found 401.1976, ([2M+Na]$^+$) calcd for $C_{24}H_{24}N_4NaO_2$ 423.1797, found 423.1792.

5-Methylpyrrolo[1,2-a]quinoxalin-5-ium triflate

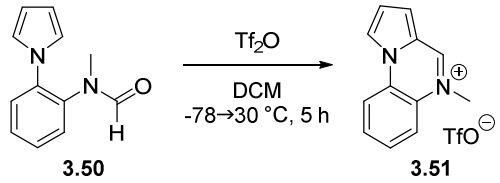

3.50 **3.51**

A solution of *N*-(2-(1*H*-pyrrol-1-yl)phenyl)-*N*-methylformamide **3.50** (100 mg, 0.5 mmol, 1.0 eq.) in dry DCM (0.5 mL) was added under argon to a flask containing trifluoromethanesulfonic anhydride (0.12 mL, 0.7 mmol, 1.4 eq.) in dry DCM (0.5 mL) *via* syringe pump (0.508 mL/h) at -78 °C. After 2 h, the reaction mixture was warmed to 30 °C and stirred for a further 3 h. The solvent was removed *in vacuo* to give the *title compound* **3.51** as a brown oil (156 mg, 0.47 mmol, 94 %); ν_{max}(ATR)/cm^{-1} 1640, 1573, 1498, 1301, 1175, 1116, 1014, 756; ^{1}H-NMR (500 MHz, d$_3$-MeCN): δ= 4.28 (3H, s, C*H*$_3$), 7.35-7.38 (1H, m, Ar*H*), 7.78-7.83 (2H, m, Ar*H*), 7.90-7.95 (1H, m, Ar*H*), 8.07-8.11 (1H, m, Ar*H*), 8.35-8.39 (1H, m, Ar*H*), 8.72-8.72 (1H, m, Ar*H*), 9.10 (1H, s, Ar*H*); ^{13}C-NMR (125 MHz, d$_3$-MeCN): δ= 43.8 (*C*H$_3$), 116.7 (*C*H), 119.6 (q, $J_{C\text{-}F}$ = 316 Hz, *C*F$_3$SO$_3$) 119.6 (*C*H), 119.9 (*C*H), 120.7 (*C*H), 123.8 (*C*), 125.3 (*C*H), 126.5 (*C*), 127.4 (*C*), 128.0 (*C*H), 131.0 (*C*H), 143.8 (*C*H); HRMS (NSI$^+$) ([M-TfO]$^+$) calcd for $C_{12}H_{11}N_2$ 183.0917, found 183.0913, ([2M-TfO]$^+$) calcd for $C_{25}H_{22}F_3N_4O_3S$ 515.1359, found 515.1352.

2-Nitro-*N*,*N*-diphenylaniline[204]

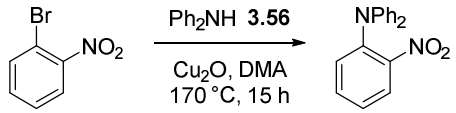

3.55 **3.57**

A mixture of 1-bromo-2-nitrobenzene **3.55** (1.0 g, 5.9 mmol, 1.0 eq.), diphenylamine **3.56** (995 mg, 5.9 mmol, 1.0 eq.) and copper(I)oxide (421 mg, 2.9 mmol, 0.5 eq.) was dissolved under argon in *N,N*-dimethylacetamide (25 mL) and stirred at 170 °C for 15 h. The reaction mixture was let to cool and then partitioned between diethyl ether and water. The product was extracted with diethyl ether (3 x 50 mL) and the combined organic phases were dried over sodium sulfate. Flash chromatography (20 % DCM/Pet ether) afforded the title compound **3.57** as an orange solid (472 mg, 1.6 mmol, 28 %); mp: 96-98 °C (lit.[204]: 100-101 °C); ν_{max}(ATR)/cm^{-1} 2924, 1588, 1522, 1487, 1355, 1275, 741, 605; ^{1}H-NMR (500 MHz, CDCl$_3$): δ= 7.01-7.07 (6H, m, Ar*H*), 7.19-7.30 (6H, m, Ar*H*), 7.47-7.52 (1H, m, Ar*H*),

7.79 (1H, dd, *J* = 8.2, 1.6 Hz, Ar*H*); ^{13}C-NMR (125 MHz, $CDCl_3$): δ= 123.2 (*C*H), 123.6 (*C*H), 124.2 (*C*H), 126.0 (*C*H), 129.4 (*C*H), 129.8 (*C*H), 133.5 (*C*H), 141.1 (*C*), 125.7 (*C*), 146.5 (*C*); HRMS (NSI$^+$) ([M+H]$^+$) calcd for $C_{18}H_{15}N_2O_2$ 291.1128, found 291.1127.

N,*N*-Diphenylbenzene-1,2-diamine[205]

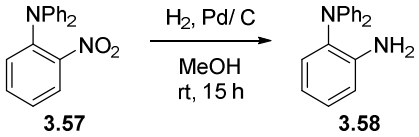

3.57 **3.58**

2-Nitro-*N*,*N*-diphenylaniline **3.57** (2.026 g, 7.0 mmol) was dissolved in methanol (30 mL) and the reaction mixture was degassed from oxygen. Palladium on charcoal (10 %, 150 mg) was added, the flask flushed with hydrogen and a balloon filled with hydrogen applied to the reaction vessel. The mixture was stirred vigorously at room temperature for 15 h. The crude product was filtered through celite and flash chromatography (40 % DCM/Pet ether) afforded the title compound **3.58** as a white solid (1.927 g, 7.0 mmol, 100 %); mp: 146-149 °C (lit.[205]: 146 °C); ν_{max}(ATR)/cm^{-1} 3472, 3379, 1584, 1487, 1289, 1273, 1247, 741, 695; ^{1}H-NMR (500 MHz, $CDCl_3$): δ= 3.74 (2H, bs, N*H*$_2$), 6.75-6.79 (1H, m, Ar*H*), 6.79-6.81 (1H, m, Ar*H*), 6.94-6.98 (2H, m, Ar*H*), 7.04-7.07 (5H, m, Ar*H*), 7.08-7.12 (1H, m, Ar*H*), 7.21-7.26 (4H, m, Ar*H*); ^{13}C-NMR (125 MHz, $CDCl_3$): δ= 116.7 (*C*H), 119.3 (*C*H), 121.2 (*C*H), 121.8 (*C*H), 127.3 (*C*H), 129.2 (*C*H), 130.3 (*C*H), 132.2 (*C*), 143.6 (*C*), 146.8 (*C*); HRMS (NSI$^+$) ([M+H]$^+$) calcd for $C_{18}H_{17}N_2$ 261.1386, found 261.1389.

N-(2-(Diphenylamino)phenyl)formamide

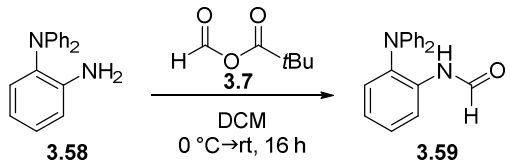

3.58 **3.59**

A solution of *N*,*N*-diphenylbenzene-1,2-diamine **3.58** (800 mg, 3.1 mmol, 1.0 eq.) in dry DCM (10 mL) was added under argon to a solution of formic pivalic anhydride **3.7** (560 mg, 4.3 mmol, 1.4 eq.) in dry DCM (10 mL) at 0 °C. The reaction mixture was stirred for 1 h, then warmed to room temperature and stirred for a further 15 h. The solution was diluted with DCM (50 mL) and washed with 2 M NaOH (2 x 50 mL), brine (75 mL) and dried over sodium sulfate. The solvent was removed *in vacuo*. Flash chromatography (18 % EtOAc/Pet ether) afforded the *title compound* **3.59** as a white solid (464 mg, 3.0 mmol, 97 %); mp: 120-121 °C; ν_{max}(ATR)/cm^{-1} 3265, 3040, 2870, 1683, 1588, 1524, 1487, 1444, 1267, 747, 736, 695; in the NMR spectra the compound appeared as an isomer mixture (isomer ratio A:B = 2:1) ^{1}H-NMR (500 MHz, $CDCl_3$): δ= 6.97-7.27 [m, ism A+B] and 8.44 [dd, *J* = 8.2,

1.1 Hz, ism A] (14H, Ar*H*), 7.84 [bs, ism B] and 8.13 [bs, ism A] (1H, N*H*), 8.02 [d, *J* = 1.8 Hz, ism A] and 8.45 [d, *J* = 11.2 Hz, ism B] (1H, C*H*O); ^{13}C-NMR (125 MHz, $CDCl_3$): δ = 120.5 and 122.6 (*C*H), 121.9 and 122.2 (*C*H), 122.8 and 123.0 (*C*H), 125.6 and 126.6 (*C*H), 126.9 and 127.1 (*C*H), 129.5 and 129.6 (*C*H), 129.8 and 130.3 (*C*H), 134.0 and 134.6 (*C*), 136.1 and 137.9 (*C*), 146.8 and 147.0 (*C*), 159.6 and 162.1 (*C*O); HRMS (NSI$^+$) ([M+H]$^+$) calcd for $C_{19}H_{17}N_2O$ 289.1335, found 289.1328.

N-Methyl-N',N'-diphenylbenzene-1,2-diamine

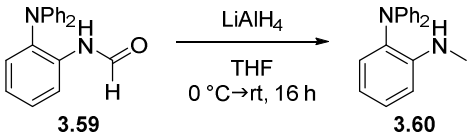

3.59 **3.60**

A solution of *N*-(2-(diphenylamino)phenyl)formamide **3.59** (812 mg, 2.7 mmol, 1.0 eq.) in THF (10 mL) was slowly added under argon to a stirred suspension of $LiAlH_4$ (245 mg, 6.5 mmol, 2.4 eq.) in THF (10 mL) *via* cannula at 0 °C. The reaction mixture was stirred for 1 h, then warmed to room temperature and stirred for a further 15 h. The solution was quenched with 2 M NaOH carefully and partitioned between diethyl ether and water. It was extracted with diethyl ether (3 x 100 mL) and the combined organic layers were washed with brine (100 mL) and dried over sodium sulfate. The solvent was removed *in vacuo*. Flash chromatography (35 % DCM/Pet ether) afforded the *title compound* as a white solid **3.60** (699 mg, 2.6 mmol, 94 %); mp: 77-78 °C; ν_{max}(ATR)/cm^{-1} 3416, 3025, 2908, 2812, 1586, 1491, 1269, 1165, 739, 691; ^{1}H-NMR (500 MHz, $CDCl_3$): δ = 2.79 (3H, d, *J* = 3.6 Hz, CH_3), 4.18 (1H, bs, N*H*), 6.70-7.75 (2H, m, Ar*H*), 6.93-6.98 (2H, m, Ar*H*), 7.03-7.07 (5H, m, Ar*H*), 7.20-7.25 (5H, m, Ar*H*); ^{13}C-NMR (125 MHz, $CDCl_3$): δ = 30.5 (*C*H_3), 111.1 (*C*H), 117.3 (*C*H), 121.1 (*C*H), 121.8 (*C*H), 127.7 (*C*H), 129.2 (*C*H), 130.1 (*C*H), 131.8 (*C*), 146.3 (*C*), 147.0 (*C*); HRMS (NSI$^+$) ([M+H]$^+$) calcd for $C_{19}H_{19}N_2$ 275.1543, found 275.1546.

N-(2-(Diphenylamino)phenyl)-N-methylformamide

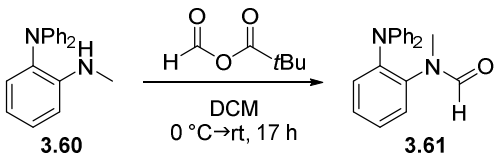

3.60 **3.61**

A solution of *N*-methyl-*N*',*N*'-diphenylbenzene-1,2-diamine **3.60** (694 mg, 2.5 mmol, 1.0 eq.) in dry DCM (10 mL) was added under argon to a solution of formic pivalic anhydride (428 mg, 3.3 mmol, 1.3 eq.) in dry DCM (10 mL) at 0 °C. The reaction mixture was stirred for 2 h, then warmed to room temperature and stirred for a further 15 h. The solution was partitioned between DCM and 2 M NaOH and extracted with DCM (3 x 75 mL). The combined organic layers were washed with brine

(75 mL) and dried over sodium sulfate. The solvent was removed *in vacuo*. Flash chromatography (25 % EtOAc/Pet ether) afforded the *title compound* **3.61** as a white solid (732 mg, 2.4 mmol, 96 %); mp: 107-108 °C; ν_{max}(ATR)/cm^{-1} 3051, 2874, 1675, 1584, 1487, 1282, 782, 749, 693; ^{1}H-NMR (500 MHz, $CDCl_3$): δ= 2.84 (3H, s, CH_3), 6.96-7.00 (6H, m, Ar*H*), 7.13-7.15 (1H, m, Ar*H*), 7.19-7.24 (5H, m, Ar*H*), 7.29-7.32 (2H, m, Ar*H*), 7.90 (1H, s, C*H*O); ^{13}C-NMR (125 MHz, $CDCl_3$): δ= 31.9 (*C*H$_3$), 122.3 (*C*H), 122.9 (*C*H), 125.9 (*C*H), 129.0 (*C*H), 129.1 (*C*H), 129.4 (*C*H), 129.4 (*C*H), 138.5 (*C*), 143.9 (*C*), 146.8 (*C*), 162.7 (*C*O); HRMS (NSI$^+$) ([M+H]$^+$) calcd for $C_{20}H_{19}N_2O$ 303.1492, found 303.1495, ([2M+H]$^+$) calcd for $C_{40}H_{37}N_4O_2$ 605.2911, found 605.2910, ([2M+Na]$^+$) calcd for $C_{40}H_{36}N_4NaO_2$ 627.2730, found 627.2724.

10-Methyl-5-phenyl-5H-dibenzo[b,e] [1,4]diazepin-10-ium triflate

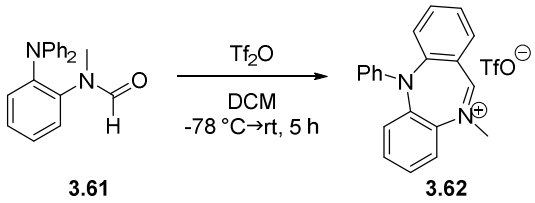

3.61 **3.62**

A solution of *N*-(2-(diphenylamino)phenyl)-*N*-methylformamide **3.61** (100 mg, 0.33 mmol, 1.0 eq.) in dry DCM (0.5 mL) was added under argon to a flask containing trifluoromethanesulfonic anhydride (0.08 mL, 0.46 mmol, 1.4 eq.) in dry DCM (0.5 mL) *via* syringe pump (0.508 mL/h) at -78 °C. After 3 h, the reaction mixture was warmed to room temperature and stirred for a further 2 h. The solvent was removed *in vacuo* to give the *title compound* **3.62** as a dark red oil (135 mg, 0.31 mmol, 94 %); ν_{max}(ATR)/cm^{-1} 1627, 1591, 1560, 1496, 1446, 1291, 1174, 1023, 747; ^{1}H-NMR (500 MHz, d_3-MeCN): δ= 4.23 (3H, d, *J* = 1.1 Hz, CH_3), 6.70-6.74 (2H, m, Ar*H*), 6.92-6.96 (1H, m, Ar*H*), 7.18-7.22 (2H, m, Ar*H*), 7.64-7.70 (2H, m, Ar*H*), 7.73 (1H, dd, *J* = 8.1, 1.5 Hz, Ar*H*), 7.76 (1H, d, *J* = 8.2 Hz, Ar*H*), 7.83-7.88 (1H, m, Ar*H*), 7.89-7.96 (2H, m, Ar*H*), 8.03-8.07 (1H, m, Ar*H*), 9.32 (1H, s, C*H*); ^{13}C-NMR (100 MHz, d_6-DMSO): δ= 50.2 (*C*H$_3$), 112.2 (*C*H), 119.7 (q, $J_{C\text{-}F}$ = 320 Hz, *C*F$_3$SO$_3$), 120.5 (*C*H), 125.0 (*C*H), 127.1 (*C*), 128.3 (*C*H), 129.1 (*C*H), 129.3 (*C*H), 129.3 (*C*H), 130.7 (*C*H), 133.8 (*C*H), 135.9 (*C*H), 138.0 (*C*), 138.9 (*C*H), 141.0 (*C*), 145.1 (*C*), 148.6 (*C*), 173.0 (*C*H); HRMS (NSI$^+$) ([M-TfO]$^+$) calcd for $C_{20}H_{17}N_2$ 285.1386, found 285.1388.

N-(2-(Diphenylamino)phenyl)-N-methylbenzamide

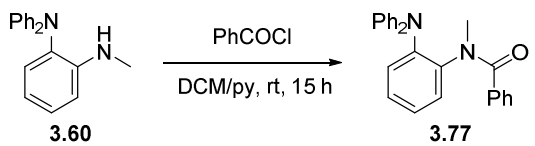

3.60 **3.77**

Benzoyl chloride (0.46 mL, 3.99 mmol, 1.2 eq.) was added under argon to *N*-methyl-*N*',*N*'-diphenylbenzene-1,2-diamine **3.60** (912 mg, 3.32 mmol, 1.0 eq.) dissolved in a mixture of DCM/pyridine (10 mL/2 mL) at room temperature and the solution was stirred for 15 h. The reaction mixture was partitioned between water and DCM and extracted with DCM (2 x 75 mL). The combined organic phases were washed with water (2 x 75 mL), brine (50 mL), dried over sodium sulfate and concentrated under reduced pressure. The crude product was purified by flash chromatography (15 % EtOAc/Pet ether) to afford the *title compound* **3.77** as a white solid (818 mg, 2.16 mmol, 65 %); mp: 172-174 °C; ν_{max}(ATR)/cm^{-1} 1634, 1587, 1485, 1366, 1298, 1279, 1074, 766, 750, 718; ^{1}H-NMR (400 MHz, $CDCl_3$): δ= 2.66 (3H, s, CH_3), 6.39-6.56 (3H, m, Ar*H*), 6.90-7.45 (16H, m, Ar*H*); ^{13}C-NMR (100 MHz, $CDCl_3$): δ= 36.2 (*C*H_3), 122.5 (*C*H), 122.7 (*C*H), 124.8 (*C*H), 127.4 (*C*H), 127.6 (*C*H), 128.5 (*C*H), 128.6 (*C*H), 129.0 (*C*H), 129.1 (*C*H), 135.7 (*C*H), 135.7 (*C*), 139.9 (*C*), 144.6 (*C*), 146.6 (*C*), 169.3 (*C*O); HRMS (NSI$^+$) ([M+H]$^+$) calcd for $C_{26}H_{23}N_2O$ 379.1805, found 379.1805.

3-Methyl-1,1,2-triphenyl-1H-benzo[d]imidazole-1,3-diium triflate

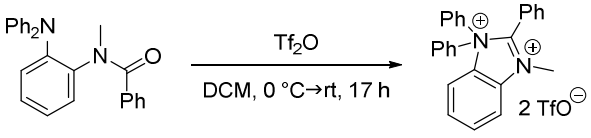

3.77 **3.78**

A solution of *N*-(2-(diphenylamino)phenyl)-*N*-methylbenzamide **3.77** (190 mg, 0.5 mmol, 1.0 eq.) in DCM (1.5 mL) was added under argon to a solution of triflic anhydride (0.10 mL, 0.60 mol, 1.2 eq.) in DCM (1.5 mL) at 0 °C using a syringe pump (6.0 mL/h). After 2 h upon addition, the reaction mixture was warmed to room temperature and stirred for a further 15 h. The precipitate was triturated with DCM (4 x 2 mL) to afford the *title compound* **3.78** as a white solid (292 mg, 0.41 mmol, 82 %); mp: 88-90 °C (decomp.); ν_{max}(ATR)/cm^{-1} 1591, 1481, 1256, 1225, 1146, 1028, 1028, 995, 762, 743, 691; ^{1}H-NMR (400 MHz, d_3-MeCN): δ= 4.56 (3H, s, CH_3), 7.60-7.71 (12H, m, Ar*H*), 7.76-7.82 (2H, m, Ar*H*), 7.90 (1H, dd, *J* = 8.6, 1.1 Hz, Ar*H*), 7.93-7.99 (1H, m, Ar*H*), 8.09 (1H, ddd, *J* = 8.4, 7.7, 1.1 Hz, Ar*H*), 8.19 (1H, ddd, *J* = 8.6, 7.7, 1.0 Hz, Ar*H*), 8.41 (1H, dd, *J* = 8.4, 1.0 Hz, Ar*H*); ^{13}C-NMR (100 MHz, d_3-MeCN): δ= 41.5 (*C*H_3), 116.4 (*C*), 120.4 (q, $J_{C\text{-}F}$ = 318 Hz, *C*F_3SO_3), 120.8 (*C*H), 121.2 (*C*H), 123.0 (*C*H), 130.1 (*C*H), 131.6 (*C*H), 132.1 (*C*H), 133.0 (*C*), 133.6 (*C*H), 134.2 (*C*H), 135.2 (*C*H), 138.0 (*C*H), 139.4 (*C*), 142.0 (*C*), 169.9 (*C*); HRMS (NSI$^+$) ([M-H]$^+$) calcd for $C_{26}H_{21}N_2$ 361.1699, found 361.1697.

Attempted reaction of *N,N-dimethylaniline* with triflic anhydride

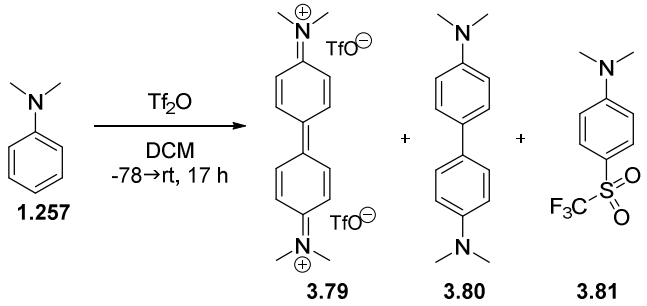

A solution of *N*,*N*-dimethylaniline **1.257** (240 mg, 2.0 mmol, 1.0 eq.) in dry DCM (1.5 mL) was added under argon to a flask containing trifluoromethanesulfonic anhydride (0.48 mL, 2.8 mmol, 1.4 eq.) in dry DCM (1.5 mL) *via* syringe pump (0.508 mL/h) at -78 °C. After 2 h, the reaction mixture was warmed to room temperature and stirred for a further 15 h. An orange precipitate, which had formed, was triturated (3 x 5 mL), filtered and washed with DCM (3 x 10 mL). The solvent was removed *in vacuo* to give *N,N,N',N'-tetramethylbenzidinium triflate* **3.79** as an orange solid (87 mg, 0.16 mmol, ~8 %); ^{1}H-NMR (400 MHz, d_3-MeCN): δ= 3.80 (12H, s, CH_3), 7.36 (4H, d, *J* = 10.1 Hz, Ar*H*), 8.36 (4H, d, *J* = 10.1 Hz, Ar*H*); HRMS (NSI$^+$) ([M+H]$^+$) calcd for $C_{16}H_{21}N_2$ 241.1699, found 241.1700 (mass of the reduced neutral species **3.79** + H).

The DCM washing phase was added to a sat. sodium bicarbonate solution (40 mL) and extracted with DCM (2 x 50 mL), washed with brine (50 mL) and dried over sodium sulfate. Purification by gradient-flash chromatography (10 % DCM/Pet ether rising to 100 % DCM) afforded *N*,*N*,*N*',*N*'-tetramethylbenzidine **3.80** as a brown solid (14 mg, 0.06 mmol, 3 %); mp: 190-191 °C (lit.[206]: 194-196 °C); ^{1}H-NMR (400 MHz, $CDCl_3$): δ= 3.00 (12H, s, CH_3), 6.84 (4H, d, *J* = 8.9 Hz, Ar*H*), 7.49 (4H, d, *J* = 8.9 Hz, Ar*H*); ^{13}C-NMR (100 MHz, $CDCl_3$): δ= 40.8 (*C*H$_3$), 113.2 (*C*H), 127.0 (*C*H), 129.9 (*C*), 149.3 (*C*); LRMS (ESI$^+$) ([M+H]$^+$) 241.07.

Furthermore, *N*,*N*-dimethyl-4-((trifluoromethyl)sulfonyl)aniline **3.81** was obtained from the gradient-flash chromatography as a white solid (10 mg, 0.04 mmol, 2 %); mp: 136-137 °C (lit.[207]: 144-145 °C); ν_{max}(ATR)/cm^{-1} 2926, 1587, 1348, 1178, 1132, 1072, 822, 775; ^{1}H-NMR (400 MHz, $CDCl_3$): δ= 3.14 (6H, s, CH_3), 6.76 (2H, d, *J* = 9.2 Hz, Ar*H*), 7.80 (2H, d, *J* = 9.2 Hz, Ar*H*); ^{13}C-NMR (100 MHz, $CDCl_3$): δ= 40.1 (*C*H$_3$), 111.3 (*C*H), 114.1 (*C*), 120.2 (q, $J_{C\text{-}F}$ = 325 Hz, *C*F$_3$SO$_3$), 132.6 (*C*H), 155.1 (*C*); LRMS (ESI$^+$) ([M+H]$^+$) 253.87.

2-(Methylthio)aniline[208]

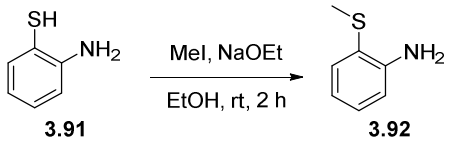

3.91 **3.92**

Sodium (0.90 g, 39.2 mmol, 0.97 eq.) was added in small portions under argon to a solution of 2-aminothiophenol **3.91** (4.31 mL, 40.0 mmol, 1.00 eq.) in ethanol (225 mL). After all the sodium had dissolved, methyl iodide (0.86 mL, 13.77 mmol, 0.97 eq.) was slowly added and it was stirred for 2 h. The reaction mixture was poured into an equal volume of water causing an oil to separate. The oil was extracted into diethyl ether (3 x 75 mL), dried over calcium chloride and distilled under reduced pressure (bp. 114 °C/5 mm) to afford the title compound **3.92** as a colourless oil (4.64 g, 33.3 mmol, 85 %); ν_{max}(ATR)/cm^{-1} 3439, 3344, 2921, 1604, 1477, 1446, 1298, 743; ^{1}H-NMR (400 MHz, $CDCl_3$): δ= 2.38 (1H, s, C*H*$_3$), 4.28 (2H, bs, N*H*$_2$), 6.71-6.76 (2H, m, Ar*H*), 7.11 (1H, ddd, *J* = 8.0, 7.4, 1.0 Hz, Ar*H*), 7.37 (1H, dd, *J* = 8.0, 1.4 Hz, Ar*H*); ^{13}C-NMR (100 MHz, $CDCl_3$): δ= 17.2 (*C*H$_3$), 114.4 (*C*H), 118.3 (*C*H), 119.8 (*C*), 128.4 (*C*H), 133.0 (*C*H), 146.6 (*C*); HRMS (GC-EIP$^+$) ([M]$^+$) calcd for C_7H_9NS 139.0450, found 139.0449.

2-(Methylthio)phenylformamide[209]

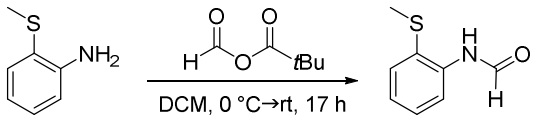

3.92 **3.93**

A solution of 2-(methylthio)aniline **3.92** (2.00 g, 14.4 mmol, 1.0 eq.) in DCM (10 mL) was added under argon to a solution of formic pivalic anhydride (2.43 g, 18.7 mmol, 1.3 eq.) in DCM (10 mL) at 0 °C and it was stirred for 17 h. The reaction mixture was partitioned between 2M NaOH and DCM and extracted with DCM (2 x 75 mL). The combined organic layers were washed with brine (50 mL), dried over sodium sulfate, filtered and the solvent was removed under reduced pressure. Flash chromatography (25 % EtOAc/Pet ether) afforded the title compound **3.93** as a pale yellow oil (2.20 g, 13.2 mmol, 91 %); ν_{max}(ATR)/cm^{-1} 3280, 2922, 2878, 1668, 1580, 1507, 1431, 1293, 1272, 749; in the NMR the compound appeard as an isomer mixture (isomer ratio A:B = 2:1) ^{1}H-NMR (500 MHz, $CDCl_3$): δ= 2.38 [s, ism A] and 2.39 [s, ism B] (3H, C*H*$_3$), 7.07-7.51 [m, ism A + B] and 8.35 [d, *J* = 8.1 Hz, ism A] (4H, Ar*H*), 8.06 [bs, ism B] and 8.34 [bs, ism A] (1H, N*H*), 8.50 [bs, ism A] and 8.71 [d, *J* = 11.2 Hz, ism B] (1H, C*H*O); ^{13}C-NMR (125 MHz, $CDCl_3$): δ= 17.8 and 19.0 (*C*H$_3$), 118.2 and 121.1 (*C*H), 124.9 and 125.7 (*C*H), 125.3 and 128.0 (*C*), 128.2 and 129.0 (*C*H), 131.9 and 133.1 (*C*H),

136.4 and 137.5 (*C*), 159.1 and 161.8 (*C*O); HRMS (NSI$^+$) ([M+H]$^+$) calcd for C_8H_9NOS 168.0478, found 168.0482.

N-Methyl-*N*-[2-(methylthio)phenyl]amine[210]

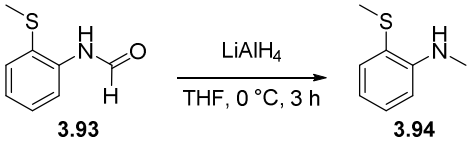

3.93 **3.94**

A solution of 2-(methylthio)phenylformamide **3.93** (1.5 g, 9.0 mmol, 1.0 eq.) in dry and deoxygenated THF (10 mL) was slowly added under argon to a stirred suspension of $LiAlH_4$ (805 mg, 21.2 mmol, 2.4 eq.) in dry and deoxygenated THF (10 mL) *via* cannula at 0 °C. The reaction mixture was stirred for 3 h, then deoxyg. ethanol (3 mL) was added carefully to quench the reaction. Under oxygen-free conditions, the reaction mixture was partitioned between deoxyg. diethyl ether and deoxygenated 2M NaOH and extracted with diethyl ether (3 x 75 mL). The combined organic phases were washed with deoxyg. 2M NaOH (2 x 75 mL), deoxyg. brine (75 mL) and dried over sodium sulfate. The solvent was removed under reduced pressure to afford the title compound **3.94** as a colourless oil (1.26 g, 8.2 mmol, 91 %); ν_{max}(ATR)/cm^{-1} 3377, 2919, 2812, 1591, 1500, 1455, 1425, 1315, 1285, 1166, 741; ^{1}H-NMR (400 MHz, $CDCl_3$): δ= 2.34 (3H, s, C*H*$_3$), 2.92 (3H, d, *J* = 4.0 Hz, C*H*$_3$), 4.94 (1H, bs, N*H*), 6.63 (1H, dd, *J* = 8.1, 0.7 Hz, Ar*H*), 6.68 (1H, ddd, *J* = 8.6, 7.6, 0.7 Hz, Ar*H*), 7.24 (1H, ddd, *J* = 8.6, 8.1, 1.5 Hz, Ar*H*), 7.41 (1H, dd, *J* = 7.6, 1.5 Hz, Ar*H*); ^{13}C-NMR (125 MHz, $CDCl_3$): δ= 18.0 (*C*H$_3$), 30.6 (*C*H$_3$), 109.5 (*C*H), 116.9 (*C*H), 119.7 (*C*), 129.5 (*C*H), 133.8 (*C*H), 149.3 (*C*); HRMS (GC-EIP$^+$) ([M]$^+$) calcd for $C_8H_{11}NS$ 153.0607, found 153.0605.

Methyl[*2-(methylthio)phenyl]formamide*

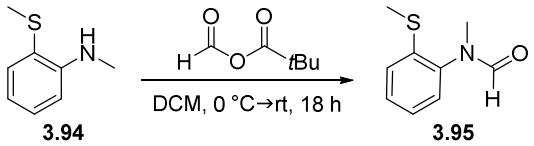

3.94 **3.95**

A solution of *N*-methyl-*N*-[2-(methylthio)phenyl]amine **3.94** (1.00 g, 6.53 mmol, 1.00 eq.) in DCM (10 mL) was added under argon to a solution of formic pivalic anhydride (1.1 g, 8.45 mmol, 1.30 eq.) in DCM (10 mL) at 0 °C and it was stirred for 18 h. The reaction mixture was partitioned between 2M NaOH and DCM and extracted with DCM (2 x 75 mL). The combined organic layers were washed with brine (50 mL), dried over sodium sulfate and the solvent was removed under reduced pressure. Flash chromatography (18 % EtOAc/Pet ether + 1 % Et_3N) afforded the *title compound* **3.95** as a pale yellow oil (1.17 g, 6.46 mmol, 99 %); ν_{max}(ATR)/cm^{-1} 2924, 2859, 1671, 1474, 1435, 1338, 1119, 1065,

758, 730; ^{1}H-NMR (400 MHz, $CDCl_3$): δ= 2.45 (3H, s, CH_3), 3.22 (3H, s, CH_3), 7.14 (1H, dd, *J* = 7.7, 1.3 Hz, Ar*H*), 7.21 (1H, ddd, *J* = 7.7, 7.6, 1.2 Hz, Ar*H*), 7.27 (1H, dd, *J* = 7.9, 1.2 Hz, Ar*H*), 7.38 (1H, ddd, *J* = 7.9, 7.6, 1.3 Hz, Ar*H*), 8.11 (1H, s, C*H*O); ^{13}C-NMR (100 MHz, $CDCl_3$): δ= 14.4 (*C*H_3), 32.0 (*C*H_3), 125.0 (*C*H), 125.3 (*C*H), 127.9 (*C*H), 128.6 (*C*H), 137.9 (*C*), 138.5 (*C*), 162.7 (*C*O); HRMS (NSI$^+$) ([M+H]$^+$) calcd for $C_9H_{12}NOS$ 182.0634, found 182.0636.

3-Methyl-1,3-benzothiazol-3-ium triflate[211]

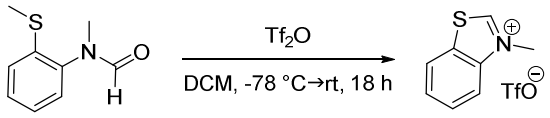

3.95 **3.96**

A solution of methyl[2-(methylthio)phenyl]formamide **3.95** (91 mg, 0.5 mmol, 1.0 eq.) in dry DCM (0.5 mL) was added under argon to a flask containing trifluoromethanesulfonic anhydride (0.12 mL, 0.7 mmol, 1.3 eq.) in dry DCM (0.5 mL) *via* syringe pump (0.508 mL/h) at -78 °C. After 2 h, the reaction mixture was warmed to room temperature and stirred for a further 16 h. The solvent was removed under reduced pressure and the crude product was triturated in diethyl ether (20 mL). The solvent was decanted and the crude product was purified by flash chromatography (10 % MeOH/DCM + 1.5 % HCO_2H) to afford the title compound **3.96** as a white solid (121 mg, 0.4 mmol, 81 %); mp: 190-192 °C (lit.[211] 191-192 °C); ν_{max}(ATR)/cm^{-1} 3070, 3040, 1248, 1222, 1144, 1024, 763; ^{1}H-NMR (400 MHz, d_6-DMSO): δ= 4.41 (3H, s, CH_3), 7.87 (1H, ddd, *J* = 8.2, 7.2, 0.9 Hz, Ar*H*), 7.95 (1H, ddd, *J* = 8.4, 7.2, 1.2 Hz, Ar*H*), 8.32 (1H, dd, *J* = 8.4, 0.9 Hz, Ar*H*), 8.50 (1H, dd, *J* = 8.2 Hz, 1.2 Hz, Ar*H*), 10.52 (1H, s, Ar*H*); ^{13}C-NMR (100 MHz, d_6-DMSO): δ= 39.3 (*C*H_3), 117.1 (*C*H), 123.6 (q, $J_{C\text{-}F}$ = 319 Hz, *C*F_3SO_3), 125.0 (*C*H), 128.4 (*C*H), 129.4 (*C*H), 131.2 (*C*), 141.0 (*C*), 164.9 (*C*H); HRMS (ASAP$^+$) ([M-TfO]$^+$) calcd for C_8H_8NS 150.0372, found 150.0371.

2-Benzylthioaniline[212]

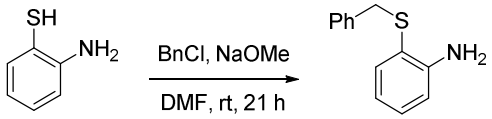

3.91 **3.97**

Sodium methoxide (1.43 g, 26.4 mmol, 1.1 eq.) was added under argon to a stirred solution of 2-aminothiophenol **3.91** (2.59 mL, 24.0 mmol, 1.0 eq.) in DMF (15 mL). After stirring for 0.5 h at room temperature, benzyl chloride (2.76 mL, 26.4 mmol, 1.0 eq.) was slowly added over a period of 5 min and the mixture was then stirred for a further 20 h. The reaction mixture was partitioned between water and diethyl ether and extracted with diethyl ether (2 x 75 mL). The combined organic layers

were washed with brine, dried over sodium sulfate, filtered and concentrated under reduced pressure. Flash chromatography (25 % DCM/Pet ether + 1 % Et_3N) afforded the title compound **3.97** as a yellow solid (2.47 g, 11.5 mmol, 48 %); mp: 42-45 °C (lit.[213]: 42-45 °C); ν_{max}(ATR)/cm^{-1} 3460, 3356, 3059, 3024, 1599, 1476, 1447, 1308, 1020, 745, 696; ^{1}H-NMR (500 MHz, $CDCl_3$): δ= 3.91 (2H, s, C*H*$_2$), 4.18 (2H, bs, N*H*$_2$), 6.64 (1H, ddd, *J* = 7.5, 7.5, 1.3 Hz, Ar*H*), 6.71 (1H, dd, *J* = 8.0, 1.2 Hz, Ar*H*), 7.12 (1H, ddd, *J* = 7.9, 7.4, 1.6 Hz, Ar*H*), 7.15-7.19 (2H, m, Ar*H*), 7.22-7.27 (4H, m, Ar*H*); ^{13}C-NMR (125 MHz, $CDCl_3$): δ= 39.7 (*C*H$_2$), 114.9 (*C*H), 117.5 (*C*), 118.5 (*C*H), 127.0 (*C*H), 128.4 (*C*H), 128.9 (*C*H), 130.1 (*C*H), 136.5 (*C*H), 138.3 (*C*), 148.6 (*C*); LRMS (ESI$^+$) ([M+H]$^+$) calcd for $C_{13}H_{14}NS$ 216.08, found 216.95.

N-(2-(Benzylthio)phenyl)formamide[214]

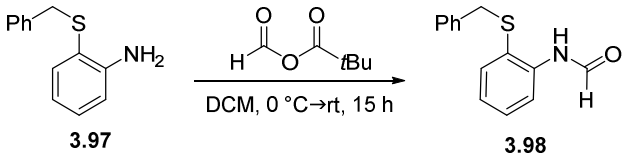

3.97 **3.98**

A solution of formic pivalic anhydride (1.57 g, 12.1 mmol, 1.3 eq.) in DCM (10 mL) was added under argon to a solution of 2-benzylthioaniline **3.97** (2.00 g, 9.3 mmol, 1.0 eq.) in DCM (10 mL) at 0 °C. The reaction mixture was stirred for 3 h, before it was warmed to room temperature and stirred for a further 12 h. The reaction mixture was partitioned between DCM and 2M NaOH and extracted with DCM (2 x 75 mL), washed with brine (75 mL) and dried over sodium sulfate. The solvent was removed under reduced pressure and flash chromatography (20 % EtOAc/Pet ether) afforded the title compound **3.98** as an off-white solid (1.98 g, 8.1 mmol, 88 %); mp: 57-59 °C (lit.[214]: 60-61 °C); ν_{max}(ATR)/cm^{-1} 3237, 1694, 1663, 1582, 1510, 1493, 1433, 1395, 750, 694; the compound appeard as an isomer mixture in the NMR spectra (isomer ratio A:B = 2:1) ^{1}H-NMR (500 MHz, $CDCl_3$): δ= 3.89 [s, ism A] and 3.90 [s, ism B] (2H, C*H*$_2$), 7.02-7.47 [m, ism A + B] and 8.36 [dd *J* = 8.2 Hz, *J* = 0.7 Hz, ism A] (9H, Ar*H*), 8.03 [bs, ism B] and 8.14 [bs, ism A] (1H, N*H*), 8.16 [s, ism A], and 8.58 [d, *J* = 11.4 Hz, ism A] (1H, C*H*O); ^{13}C-NMR (125 MHz, $CDCl_3$): δ= 41.0 and 41.7 (*C*H$_2$), 116.5 and 123.4 (*C*), 120.5 and 121.8 (*C*H), 124.5 and 125.0 (*C*H), 127.5 and 127.6 (*C*H), 128.6 and 128.6 (*C*H), 128.7 and 128.7 (*C*H), 130.1 and 130.4 (*C*H), 136.4 and 136.7 (*C*H), 137.1 and 137.6 (*C*), 139.0 and 139.4 (*C*), 158.6 and 161.0 (*C*O); HRMS (NSI$^+$) ([M+H]$^+$) calcd for $C_{14}H_{14}NOS$ 244.0791, found 244.0791.

2-(Benzylthio)-*N*-methylaniline[215]

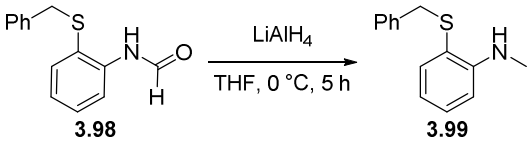

3.98 **3.99**

A solution of *N*-(2-(benzylthio)phenyl)formamide **3.98** (150 mg, 0.62 mmol, 1.0 eq.) in dry and deoxygenated THF (10 mL) was slowly added under argon to a stirred suspension of $LiAlH_4$ (56 mg, 1.48 mmol, 2.4 eq.) in dry and deoxygenated THF (10 mL) *via* cannula at 0 °C. The reaction mixture was stirred for 3 h, then warmed to room temperature and stirred for a further 2 h. Still under argon, the reaction mixture was quenched with some drops of a deoxygenated sat. sodium bicarbonate solution carefully and then partitioned between the bicarbonate solution and deoxygenated diethyl ether. It was extracted with diethyl ether (75 mL) once and the extract was washed with deoxygenated brine (35 mL) and dried over sodium sulfate. The solvent was removed under reduced pressure to afford the title compound **3.99** as a colourless oil (118 mg, 0.52 mmol, 84 %); ν_{max}(ATR)/cm^{-1} 3385, 3026, 2922, 2810, 1589, 1497, 1452, 1316, 1167, 743, 694; ^{1}H-NMR (400 MHz, $CDCl_3$): δ= 2.79 (3H, s, C*H*$_3$), 3.88 (2H, s, C*H*$_2$), 5.00 (1H, bs, N*H*), 6.58-6.63 (2H, m, Ar*H*), 7.24-7.39 (7H, m, Ar*H*); ^{13}C-NMR (100 MHz, $CDCl_3$): δ= 30.0 (*C*H$_3$), 39.5 (*C*H$_2$), 109.0 (*C*H), 116.0 (*C*H), 116.5 (*C*), 126.5 (*C*H), 127.8 (*C*H), 128.3 (*C*H), 130.0 (*C*H), 136.1 (*C*H), 137.9 (*C*), 150.0 (*C*); HRMS (NSI$^+$) ([M+H]$^+$) calcd for $C_{14}H_{16}NS$ 230.0998, found 230.0996.

2-(Benzylthio)phenyl(methyl)formamide

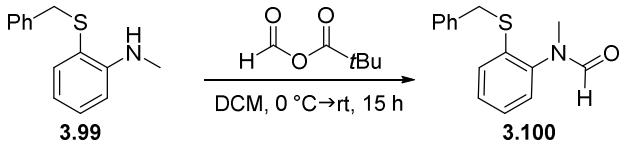

3.99 **3.100**

A solution of 2-(benzylthio)-*N*-methylaniline **3.99** (1.25 g, 5.45 mmol, 1.0 eq.) in DCM (10 mL) was added under argon to a solution of formic pivalic anhydride (922 mg, 7.09 mmol, 1.3 eq.) in DCM (10 mL) and it was stirred for 3 h at 0 °C, then warmed to room temperature and stirring was continued for a further 12 h. The reaction mixture was partitioned between 2M NaOH and DCM and extracted with DCM (2 x 75 mL). The combined organic layers were washed with brine (50 mL), dried over sodium sulfate and the solvent was removed under reduced pressure. Flash chromatography (30 % EtOAc/Pet ether + 1 % Et_3N) afforded the *title compound* **3.100** as a white solid (1.04 g, 4.04 mmol, 74 %); mp: 66-68 °C, ν_{max}(ATR)/cm^{-1} 3066, 2883, 1666, 1584, 1569, 1474, 1455, 1338, 1300, 1125, 980, 754, 717; ^{1}H-NMR (500 MHz, $CDCl_3$): δ= 3.13 (3H, s, C*H*$_3$), 4.08 (2H, s, C*H*$_2$), 7.12 (1H, dd, *J* = 7.7, 1.2 Hz, Ar*H*), 7.22-7.33 (7H, m, Ar*H*), 7.43 (1H, dd, *J* = 7.9, 1.1 Hz, Ar*H*), 7.97 (1H, s,

C*H*O); ^{13}C-NMR (125 MHz, $CDCl_3$): δ= 33.0 (*C*H_3), 38.2 (*C*H_2), 127.1 (*C*H), 127.5 (*C*H), 128.3 (*C*H), 128.6 (*C*H), 128.8 (*C*H), 128.9 (*C*H), 130.1 (*C*H), 135.9 (*C*), 136.4 (*C*), 141.0 (*C*), 163.1 (*C*O); HRMS (NSI$^+$) ([M+H]$^+$) calcd for $C_{15}H_{16}NOS$ 258.0947, found 258.0947.

3-Methylbenzo[d]thiazol-3-ium triflate[211]

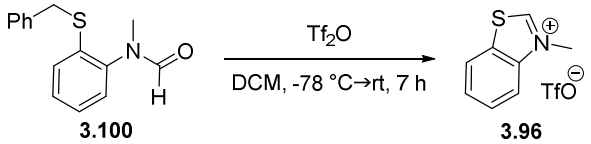

3.100 **3.96**

A solution of 2-(benzylthio)phenyl(methyl)formamide **3.100** (129 mg, 0.5 mmol, 1.0 eq.) in dry DCM (0.5 mL) was added under argon to a flask containing trifluoromethanesulfonic anhydride (0.12 mL, 0.7 mmol, 1.3 eq.) in dry DCM (0.5 mL) *via* syringe pump (0.508 mL/h) at -78 °C. After 2 h, the reaction mixture was warmed to room temperature and stirred for a further 5 h. The solvent was removed under reduced pressure and the crude product was triturated in dry diethyl ether (10 mL). The solvent was decanted, the product washed with diethyl ether (3 x 10 mL), filtered and dried under reduced pressure to afford the title compound **3.96** as a white solid (109 mg, 0.36 mmol, 73 %). (For analytical data see above)

Neryl acetate[216]

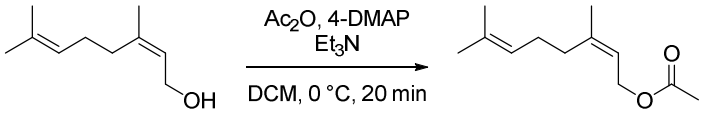

3.106 **3.107**

Acetic anhydride (3.24 mL, 34.3 mmol, 1.2 eq.) was added under argon to a solution of nerol **3.106** (5.0 mL, 28.6 mmol, 1.00 eq.), 4-dimethylaminopyridine (69 mg, 0.6 mmol, 0.02 eq.) and triethylamine (6.91 mL, 0.05 mmol, 1.72 eq.) in DCM (60 mL) *via* syringe at 0 °C. The reaction mixture was stirred for 20 min, then poured into water (50 mL) and extracted with DCM (3 x 75 mL). The combined organic phases were washed with a sat. $NaHCO_3$ solution (50 mL), brine (50 mL) and dried over sodium sulfate. The crude product was filtered through a plug of silica, the plug flushed with a EtOAc/Pet ether mixture (100/200 mL) and then concentrated *in vacuo* to afford the title compound **3.107** as a colourless oil (5.38 g, 27.4 mmol, 96 %); ν_{max}(ATR)/cm^{-1} 2969, 2924, 1737, 1442, 1381, 1226, 1021, 952; ^{1}H-NMR (500 MHz, $CDCl_3$): δ= 1.60 (3H, s, CH_3), 1.68 (3H, s, CH_3), 1.77 (3H, s, CH_3), 2.05 (3H, s, CH_3), 2.04-2.13 (4H, m, CH_2), 4.56 (2H, dd, *J* = 7.3, 0.6 Hz, CH_2), 5.07-5.11 (1H, m, C*H*), 5.33-5.38 (1H, m, C*H*); ^{13}C-NMR (125 MHz, $CDCl_3$): δ=17.6 (*C*H_3), 21.0 (*C*H_3), 23.5 (*C*H_3), 25.7 (*C*H_3),

26.6 (*C*H_2), 32.26 (*C*H_2), 61.16 (*C*H_2), 119.1 6 (*C*H), 123.66 (*C*H), 132.26 (*C*), 142.6 (*C*), 171.1 (CO); HRMS (GC-CI) ([M]$^+$) calcd for $C_{12}H_{20}O_2$ 196.1458, found 196.1459.

(*Z*)-2-((3,7-Dimethylocta-2,6-dien-1-yl)thio)aniline[165]

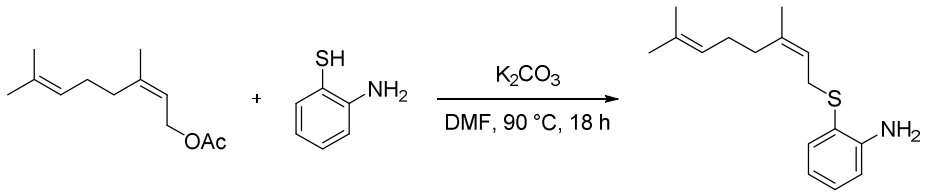

3.107 **3.91** **3.108**

Neryl acetate **3.107** (2.00 g, 10.2 mmol ,1.0 eq.) was added under argon to a suspension of 2-aminothiophenol **3.91** (1.10 mL, 10.2 mmol, 1.0 eq.) and potassium carbonate (2.11 g, 15.3 mmol, 1.5 eq.) in DMF (20 mL) and the reaction mixture was stirred at 90 °C for 18 h. The reaction mixture was then partitioned between 1 M NaOH and Et_2O and it was extracted with Et_2O (3 x 75 mL). The combined organic phases were dried over sodium sulfate filtered and the crude product was concentrated *in vacuo*. Flash chromatography (3 % Et_2O/Pet ether) on silica gel afforded the title compound **3.108** as a yellow oil (816 mg, 3.12 mmol, 31 %); ν_{max}(ATR)/cm^{-1} 2967, 2913, 2855, 1606, 1477, 1446, 1375 1304, 834, 745; ^{1}H-NMR (400 MHz, $CDCl_3$): δ= 1.62 (3H, s, C*H*$_3$), 1.71 (3H, s, C*H*$_3$), 1.72 (3H, s, C*H*$_3$), 1.94-2.04 (4H, m, C*H*$_2$), 1.70 (2H, dd, *J* = 8.0, 0.8 Hz, C*H*$_2$), 4.22 (2H, bs, N*H*$_2$), 5.06-5.12 (1H, m, C*H*), 5.31 (1H, dt, 8.0, 0.8 Hz, C*H*), 6.70 (1H, ddd, *J* = 8.0, 7.4, 1.5 Hz, Ar*H*), 6.74 (1H, dd, *J* = 8.0, 1.2 Hz, Ar*H*), 7.13 (1H, ddd, *J* = 7.6, 7.4, 1.2 Hz, Ar*H*), 7.38 (1H, dd, *J* = 7.6, 1.5 Hz, Ar*H*); ^{13}C-NMR (100 MHz, $CDCl_3$): δ= 17.2 (*C*H_3), 22.9 (*C*H_3), 25.2 (*C*H_3), 26.1 (*C*H_2), 31.1 (*C*H_2), 32.3 (*C*H_2), 114.2 (*C*H), 117.6 (*C*), 117.8 (*C*H), 119.9 (*C*H), 123.5 (*C*H), 129.2 (*C*H), 131.3 (*C*), 135.7 (*C*H), 139.3 (*C*), 147.9 (*C*); HRMS (NSI$^+$) ([M+H]$^+$) calcd for $C_{16}H_{24}NS$ 262.1624, found 262.1617.

(Z)-N-(2-((3,7-Dimethylocta-2,6-dien-1-yl)thio)phenyl)formamide

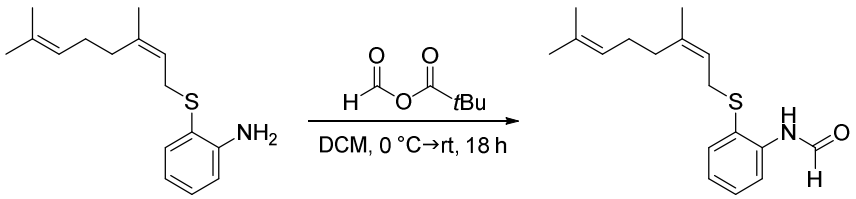

3.108 **3.109**

A solution of (*Z*)-2-((3,7-dimethylocta-2,6-dien-1-yl)thio)aniline **3.108** (750 mg, 2.9 mmol, 1.0 eq.) in DCM (10 mL) was added under argon to a flask containing formic pivalic anhydride (485 mg, 3.7 mmol, 1.3 eq.) in DCM (5 mL) at 0 °C. It was stirred for 3 h, before the solution was warmed to room temperature and stirred for a further 15 h. The reaction mixture was partitioned between 2 M

NaOH and DCM and extracted with DCM (3 x 50 mL). The combined organic phases were washed with brine (50 mL), dried over sodium sulfate and concentrated *in vacuo*. The crude product was purified by flash chromatography (10 % EtOAc/Pet ether) to afford the *title compound* **3.109** as a colourless oil (803 mg, 2.8 mmol, 93 %); ν_{max}(ATR)/cm^{-1} 2967, 2913, 1691, 1672, 1582, 1510, 1433, 1292, 750; in the NMR the compound appeared as an isomer mixture (isomer ratio A:B = 2:1) ^{1}H-NMR (500 MHz, $CDCl_3$): δ= 1.58 (3H, s, CH_3), 1.68 (3H, s, CH_3), 1.68 (3H, s, CH_3), 1.80-1.86 (2H, m, CH_2), 1.89-1.96 (2H, m, CH_2), 3.38 (2H, d, *J* = 8.0 Hz, CH_2), 4.99-5.06 (1H, m, C*H*), 5.24 (1H, t, *J* = 6.3 Hz, C*H*), 7.07 [ddd, *J* = 7.6, 7.6, 1.2 Hz, ism A] and 7.11 [dd, *J* = 7.6, 7.6 Hz, ism B] (1H, Ar*H*), 7.23 [d, *J* = 7.8 Hz, ism B] and 8.43 [dd, *J* = 8.2, 0.8 Hz, ism A] (1H, Ar*H*), 7.30 [dd, *J* = 7.8, 7.4 Hz, ism B] and 7.34 [ddd, *J* = 8.2, 7.6, 0.8 Hz, ism A] (1H, Ar*H*), 7.53 [dd, *J* = 7.6, 1.2 Hz, ism A + B] (1H, Ar*H*), 8.30 [bs, ism B] and 8.57 [bs, s, ism A] (1H, N*H*), 8.49 [d, *J* = 1.6 Hz, ism A] and 8.78 [d, *J* = 11.4 Hz, ism B] (C*H*O); ^{13}C-NMR (125 MHz, $CDCl_3$): δ= 17.7 (*C*H_3), 23.3 (*C*H_3), 25.7 (*C*H_3), 26.4 (*C*H_2), 31.5 (*C*H_2), 33.9 (*C*H_2) and 34.6 (*C*H_2), 116.4 (*C*), 119.5 and 119.5 (*C*H), 120.5 (*C*H), 122.6 and 123.7 (*C*H), 124.4 and 124.9 (*C*H), 129.6 and 129.9 (*C*H), 132.1 (*C*), 136.0 and 136.3 (*C*H), 138.6 and 139.1 (*C*), 140.7 and 140.8 (*C*), 158.8 and 161.2 (*C*O); HRMS (NSI$^+$) ([M+H]$^+$) calcd for $C_{17}H_{24}NOS$ 290.1573, found 290.1578.

(Z)-2-((3,7-Dimethylocta-2,6-dien-1-yl)thio)-N-methylaniline

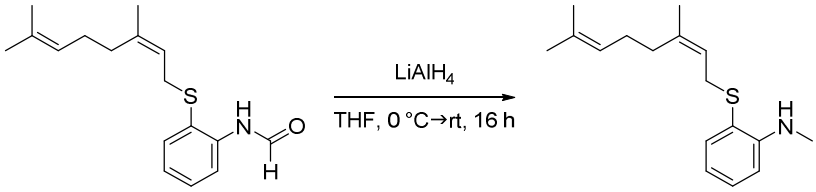

3.109 **3.110**

A solution of (*Z*)-*N*-(2-((3,7-dimethylocta-2,6-dien-1-yl)thio)phenyl)formamide **3.109** (780 mg, 2.7 mmol, 1.0 eq.) in deoxygenated THF (10 mL) was slowly added under argon to a flask containing a stirred suspension of lithium aluminium hydride (245 mg, 6.5 mmol, 2.4 eq.) in deoxygenated THF (10 mL) *via* cannula at 0 °C. It was stirred for 2 h, before the solution was warmed to room temperature and stirred for a further 14 h. The reaction mixture was partitioned between deoxygenated water and deoxygenated DCM and extracted with DCM (2 x 75 mL). The combined organic phases were washed with deoxygenated brine (50 mL), dried over sodium sulfate and the solvent was removed under reduced pressure to afford the *title compound* **3.110** as a colourless oil (721 mg, 2.6 mmol, 97 %); ν_{max}(ATR)/cm^{-1} 2967, 2913, 1591, 1502, 1457, 1427, 1375, 1317, 1285, 1168, 1034, 834, 743; ^{1}H-NMR (500 MHz, $CDCl_3$): δ= 1.61 (3H, s, CH_3), 1.70 (3H, s, CH_3), 1.71 (3H, s, CH_3), 1.89-1.85 (2H, m, CH_2), 1.93-1.99 (2H, m, CH_2), 2.89 (3H, s, CH_3), 3.34 (2H, dd, *J* = 8.0, 0.7 Hz,

CH_2), 5.06-5.09 (1H, m, C*H*), 5.13 (1H, bs, N*H*), 5.29 (1H, dt, *J* = 8.0, 0.7 Hz, C*H*), 6.59 (1H, dd, *J* = 8.2, 1.0 Hz, Ar*H*), 6.63 (1H, ddd, *J* = 7.5, 7.5, 1.0 Hz, Ar*H*), 7.23 (1H, ddd, *J* = 8.2, 7.5, 1.6 Hz, Ar*H*), 7.39, (1H, dd, *J* = 7.5, 1.6 Hz, Ar*H*); ^{13}C-NMR (125 MHz, $CDCl_3$): δ= 17.7 (*C*H_3), 23.3 (*C*H_3), 25.7 (*C*H_3), 26.6 (*C*H_2), 30.6 (*C*H_2), 31.7 (*C*H_2), 32.9 (*C*H_3), 109.4 (*C*H), 116.4 (*C*H), 117.6 (*C*), 120.4 (*C*H), 124.1 (*C*H), 130.1 (*C*H), 131.8 (*C*), 136.3 (*C*H), 139.8 (*C*), 150.3 (*C*); HRMS (NSI$^+$) ([M+H]$^+$) calcd for $C_{17}H_{26}NS$ 276.1780, found 276.1778.

(Z)-N-(2-((3,7-Dimethylocta-2,6-dien-1-yl)thio)phenyl)-N-methylformamide

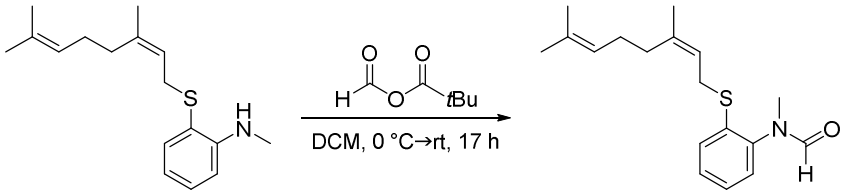

3.110 **3.111**

A solution of (*Z*)-2-((3,7-dimethylocta-2,6-dien-1-yl)thio)-*N*-methylaniline **3.110** (600 mg, 2.2 mmol, 1.0 eq.) in deoxygenated DCM (10 mL) was added under argon to a solution of formic pivalic anhydride (369 mg, 2.8 mmol, 1.3 eq.) in deoxygenated DCM (5 mL) at 0 °C. The solution was stirred for 2 h, before it was warmed to room temperature and stirred for a further 15 h. The reaction mixture was partitioned between 2M NaOH and DCM and extracted with DCM (2 x 75 mL). The combined organic phases were washed with brine (50 mL) and dried over sodium sulfate. The crude product was concentrated *in vacuo* and purified by flash chromatography (15 % EtOAc/Pet ether + 1 % Et_3N) to afford the *title compound* **3.111** as a colourless oil (475 mg, 1.6 mmol, 71 %); ν_{max}(ATR)/cm^{-1} 2926, 1680, 1472, 1335, 1119, 1063, 976, 822, 758, 731; ^{1}H-NMR (400 MHz, $CDCl_3$): δ= 1.61 (3H, s, CH_3), 1.70 (3H, s, CH_3), 1.74 (3H, s, CH_3), 2.06-2.08 (4H, m, CH_2), 3.22 (3H, s, CH_3), 3.54 (2H, d, *J* = 7.7 Hz, CH_2), 5.10-5.11 (1H, m, C*H*), 5.29 (1H, dt, *J* = 7.7, 1.2 Hz, C*H*), 7.15 (1H, dd, *J* = 7.6, 1.3 Hz, Ar*H*), 7.20-7.26 (1H, m, Ar*H*), 7.29-7.39 (2H, m, Ar*H*), 8.11 (1H, s, C*H*O); ^{13}C-NMR (100 MHz, $CDCl_3$): δ= 17.2 (*C*H_3), 28.9 (*C*H_3), 25.2 (*C*H_3), 26.0 (*C*H_2), 30.3 (*C*H_2), 31.5 (*C*H_3), 32.4 (*C*H_2), 118.2 (*C*H), 123.2 (*C*H), 125.8 (*C*H), 127.9 (*C*H), 128.2 (*C*H), 128.4 (*C*H), 131.7 (*C*), 136.7 (*C*), 139.6 (*C*), 140.7 (*C*), 162.7 (*C*O); HRMS (NSI$^+$) ([M+H]$^+$) calcd for $C_{18}H_{26}NOS$ 304.1730, found 304.1734.

3-Methyl-1,3-benzothiazol-3-ium triflate[211]

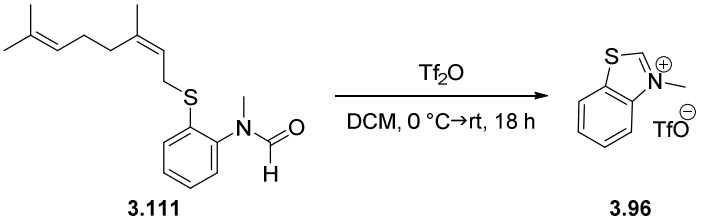

3.111 **3.96**

A solution of methyl[2-(methylthio)phenyl]formamide **3.111** (213 mg, 0.7 mmol, 1.0 eq.) in dry DCM (3 mL) was added under argon to a flask containing trifluoromethanesulfonic anhydride (0.12 mL, 0.7 mmol, 1.3 eq.) in dry DCM (10 mL) *via* syringe pump (0.508 mL/h) at 0 °C. After 4 h, the reaction mixture was warmed to room temperature and stirred for a further 14 h. The solvent was removed under reduced pressure and the crude product was triturated with a 1:1 Et_2O/DCM mixture (3 x 5 mL). The solvent was decanted and the product was dried under reduced pressure to afford the title compound **3.96** as a white solid (142 mg, 0.4 mmol, 95 %). (For data see above)

The organic washings were concentrated *in vacuo* to afford a colourless oil, which was analysed by ^{1}H-NMR spectroscopy. The oil was then stirred in 1M NaOH (50 mL) for 15 h. The reaction mixture was partitioned between a sat. $NaHCO_3$ solution and DCM and extracted with DCM (2 x 50 mL). The combined organic phases were washed with brine and dried over sodium sulfate. The crude product was concentrated under reduced pressure to afford a very viscous and colourless oil, which could not be analysed by NMR due to insolubility in organic and aqueous solvents.

(2-Nitrophenyl)(phenyl)sulfane[217]

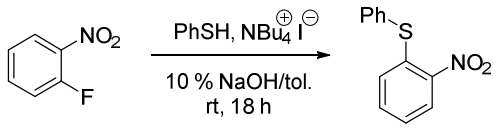

3.112 **3.113**

A solution of 1-fluoro-2-nitrobenzene **3.112** (3.92 mmol, 30.0 mmol, 1.00 eq.) in toluene (50 mL) was added under argon to a mixture of thiophenol (3.06 mL, 30.0 mmol, 1.00 eq.) and tetrabutylammonium iodide (554 mg, 1.5 mmol, 0.05 eq.) in 10 % NaOH (50 mL) over 20 min at room temperature. The reaction mixture was stirred for 18 h and the progress monitored by TLC strips. The reaction mixture was partitioned between EtOAc and 2M NaOH and extracted with EtOAc (2 x 100 mL). The combined organic phases were washed with 2M NaOH (2 x 75 mL), brine (50 mL), dried over sodium sulfate and concentrated under reduced pressure. The crude product was purified by flash chromatography (5 % EtOAc/Pet ether) and then recrystallized from EtOH to afford the title compound **3.113** as yellow needles (6.00 g, 25.9 mmol, 87 %); mp: 79-81 °C (lit.[218]: 78-81 °C); ν_{max}(ATR)/cm^{-1} 3096, 1589, 1497, 1441, 1333, 1302, 1252, 1042, 851 748, 731, 689; ^{1}H-NMR (400 MHz, d_6-DMSO): δ= 6.88 (1H, dd, *J* = 8.2, 1.2 Hz, Ar*H*), 7.38-7.42 (1H, m, Ar*H*), 7.54-7.64 (6H, m, Ar*H*), 8.24 (1H, dd, *J* = 8.2, 1.4 Hz, Ar*H*); ^{13}C-NMR (100 MHz, $CDCl_3$): δ= 125.7 (*C*H), 126.1 (*C*H), 128.2 (*C*H), 130.2 (*C*H), 130.2 (*C*), 130.4 (*C*H), 134.3 (*C*H), 135.3 (*C*H), 137.3 (*C*), 144.9 (*C*); HRMS (NSI$^+$) ([M+H]$^+$) calcd for $C_{12}H_{10}NO_2S$ 232.0427, found 232.0426.

2-(Phenylthio)aniline[219]

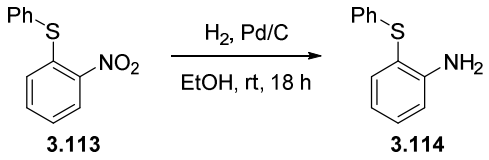

3.113 **3.114**

(2-Nitrophenyl)(phenyl)sulfane **3.113** (4.40 g, 19.0 mmol) was added under argon to a suspension of 10 % Pd/C (400 mg) in EtOH (60 mL). Under stirring, the suspension was first deoxygenated and then hydrogen applied at 3.5 bar at room temperature for 18 h. The reaction mixture was poured into a centrifuge tube and centrifuged. The upper liquids were decanted, the tubes refilled with EtOH, shaken, centrifuged and the upper liquid layer again decanted. The combined organic phases were concentrated under reduced pressure to give the title compound **3.114** as a yellow oil (3.5 g, 17.6 mmol, 93 %); ν_{max}(ATR)/cm^{-1} 3466, 3364, 3055, 1605, 1580, 1476, 1580, 1476, 1437, 1306, 1022, 733, 687; ^{1}H-NMR (400 MHz, d_6-DMSO): δ= 5.37 (2H, bs, N*H*$_2$), 6.61 (1H, ddd, *J* = 8.3, 7.7, 1.3 Hz, Ar*H*), 6.83 (1H, dd, *J* = 8.2, 1.3 Hz, Ar*H*), 7.05-7.08 (2H, m, Ar*H*), 7.11-7.16 (1H, m, Ar*H*), 7.19 (1H, ddd, *J* = 8.3, 8.2, 1.6 Hz, Ar*H*), 7.24-7.29 (2H, m, Ar*H*), 7.32 (1H, dd, *J* = 7.7, 1.6 Hz, Ar*H*); ^{13}C-NMR (100 MHz, $CDCl_3$): δ= 111.9 (*C*), 114.9 (*C*H), 116.7 (*C*H), 125.3 (*C*H), 126.3 (*C*H), 129.0 (*C*H), 131.0 (*C*H), 136.7 (*C*), 136.9 (*C*H), 150.3 (*C*); HRMS (NSI$^+$) ([M+H]$^+$) calcd for $C_{12}H_{12}NS$ 202.0685, found 202.0685.

N-(2-(Phenylthio)phenyl)formamide[220]

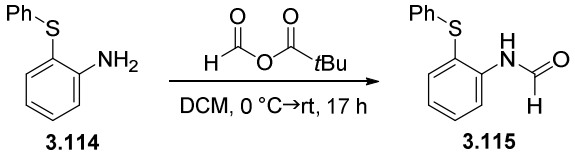

3.114 **3.115**

A solution of 2-(phenylthio)aniline **3.114** (2.38 g, 11.8 mmol, 1.0 eq.) in DCM (10 mL) was added under argon to a solution of formic pivalic anhydride (2.00 g, 15.4 mmol, 1.3 eq.) in DCM (10 mL) at 0 °C. It was stirred for 3 h, the reaction mixture then warmed to room temperature and stirred for a further 14 h. The mixture was partitioned between 2M NaOH and DCM and extracted with DCM (2 x 60 mL). The combined organic phases were washed with brine (50 mL), dried over sodium sulfate and concentrated *in vacuo.* The crude product was purified by flash chromatography (20 % EtOAc/Pet ether) to afford the title compound **3.115** as a yellow solid (2.37 g, 10.3 mmol, 88 %); mp: 76-78 °C; ν_{max}(ATR)/cm^{-1} 1667 1578, 1568, 1505, 1478, 1433, 1400, 1290, 1024, 754, 731, 687; in the NMR spectra the compound appeared as an isomer mixture (isomer ratio A:B = 2:1) ^{1}H-NMR (400 MHz, $CDCl_3$): δ=7.03-7.31 (6H, m, Ar*H*), 7.34 [d, *J* = 7.8 Hz, ism B] and 8.55 [dd, *J* = 8.3, 1.1 Hz,

ism A] (1H, Ar*H*), 7.40-7.52 (1H, m, Ar*H*), 7.60 [dd, *J* = 8.9, 1.2 Hz, ism B] and 7.62 [dd, *J* = 7.8, 1.5 Hz, ism A] (1H, Ar*H*), 8.12 [bs, ism B] and 8.33 [s, ism A] (1H, N*H*), 8.39 [d, *J* = 1.6 Hz, ism A] and 8.75 [d, *J* = 11.3 Hz, ism B] (C*H*O); ^{13}C-NMR (100 MHz, $CDCl_3$): δ= 116.9 and 120.8 (*C*H), 119.2 and 122.0 (*C*), 124.5 and 125.1 (*C*H), 125.8 and 126.3 (*C*H), 126.4 and 127.6 (*C*H), 128.9 and 129.0 (*C*H), 130.2 and 130.7 (*C*H), 134.5 and 135.2 (*C*), 136.4 and 136.5 (*C*H), 138.1 and 138.7 (*C*), 158.5 and 160.7 (*C*O); HRMS (NSI$^+$) ([M+H]$^+$) calcd for $C_{13}H_{12}NOS$ 230.0634, found 230.0635.

N-Methyl-2-(phenylthio)aniline[221]

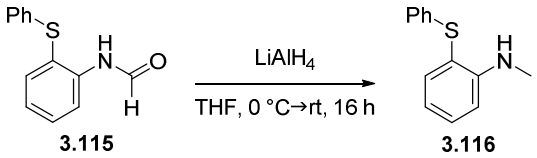

3.115 **3.116**

A deoxygenated solution of *N*-(2-(phenylthio)phenyl)formamide **3.115** (1.77 g, 7.72 mmol, 1.0 eq.) in THF (15 mL) was slowly added to a deoxygenated stirred suspension of lithium aluminium hydride (703 mg, 18.53 mmol, 2.4 eq.) in THF (15 mL) *via* cannula at 0 °C and it was stirred for 2 h. The reaction mixture was then warmed to room temperature and stirred for a further 14 h. The reaction mixture was carefully quenched with water (deoxyg.) at 0 °C and partitioned between water (deoxyg.) and Et_2O (deoxyg.) and extracted with Et_2O (200 mL). The organic phase was dried over sodium sulfate, filtered and concentrated under reduced pressure. The title compound **3.116** was obtained as a colourless oil (1.45 g, 6.71 mmol, 87 %); ν_{max}(ATR)/cm^{-1} 3391, 2812, 1589, 1501, 1476, 1316, 1289, 1167, 1022, 735, 687; ^{1}H-NMR (400 MHz, $CDCl_3$): δ= 2.86 (3H, s, CH_3), 5.00 (1H, bs, N*H*), 6.70-6.77 (2H, m, Ar*H*), 7.07-7.11 (2H, m, Ar*H*), 7.14 (1H, tt, *J* = 7.4, 1.5 Hz, Ar*H*), 7.22-7.27 (2H, m, Ar*H*), 7.39 (1H, ddd, *J* = 8.2, 7.4, 1.6 Hz, Ar*H*), 7.52 (1H, dd, *J* = 7.6, 1.6 Hz, Ar*H*); ^{13}C-NMR (100 MHz, $CDCl_3$): δ= 30.5 (*C*H$_3$), 110.1 (*C*H), 113.5 (*C*), 116.8 (*C*H), 125.3 (*C*H), 126.2 (*C*H), 129.0 (*C*H), 131.6 (*C*H), 137.1 (*C*), 137.7 (*C*H), 150.6 (*C*); HRMS (NSI$^+$) ([M+H]$^+$) calcd for $C_{13}H_{14}NS$ 216.0841, found 216.0837.

N-Methyl-N-(2-(phenylthio)phenyl)formamide

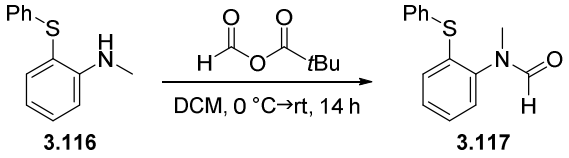

3.116 **3.117**

A deoxygenated solution of *N*-methyl-2-(phenylthio)aniline formamide **3.116** (600 mg, 2.79 mmol, 1.0 eq.) in DCM (10 mL) was added under argon to a deoxygenated solution of formic pivalic anhydride (472 mg, 3.62 mmol, 1.3 eq.) in DCM (10 mL) at 0 °C. The reaction mixture was stirred for

2 h, then warmed to room temperature and stirred for a further 12 h. The reaction mixture was partitioned between 2 M NaOH and DCM and extracted with DCM (2 x 75 mL). The combined organic phases were stirred over sodium sulfate and concentrated *in vacuo*. The crude product was purified by flash chromatography (30 % EtOAc/Pet ether) to afford the *title compound* **3.117** as a colourless oil (633 mg, 1.98 mmol 71 %); ν_{max}(ATR)/cm^{-1} 1672, 1580, 1472, 1439, 1331, 1292, 1119, 1059, 976, 822, 748, 731, 689; ^{1}H-NMR (400 MHz, $CDCl_3$): δ= 3.19 (3H, s C*H*$_3$), 7.18-7.37 (9H, m, Ar*H*), 8.12 (1H, s, C*H*O); ^{13}C-NMR (100 MHz, $CDCl_3$): δ= 32.3 (*C*H$_3$), 127.5 (*C*H), 127.7 (*C*H), 128.2 (*C*H), 128.5 (*C*H), 129.1 (*C*H), 131.3 (*C*H), 132.0 (*C*H), 132.7 (*C*), 135.7 (*C*), 140.3 (*C*), 162.5 (*C*O); HRMS (NSI$^+$) ([M+H]$^+$) calcd for $C_{14}H_{14}NOS$ 244.0791, found 244.0784.

10-Methyldibenzo[b,f] [1,4]thiazepin-10-ium triflate

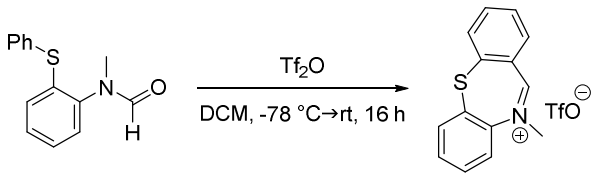

3.117 **3.118**

A solution of *N*-methyl-*N*-(2-(phenylthio)phenyl)formamide **3.117** (122 mg, 0.5 mmol, 1.0 eq.) in DCM (1.5 mL) was added under argon to a solution of triflic anhydride (0.11 mL, 0.65 mol, 1.3 eq.) in DCM (1.5 mL) at 0 °C using a syringe pump (4.5 mL/h). Upon addition, it was stirred for 2 h, before the reaction mixture was warmed to room temperature and stirred for a further 14 h. To the reaction mixture was added Et_2O (3.0 mL) and a red oil precipitated. The upper liquid was decanted and the precipitated oil triturated with a 1:2 DCM/Et_2O mixture (3 x 6 mL) until it turned to a white solid. The precipitate was dried under reduced pressure to afford the *title compound* **3.118** as a white solid (179 mg, 4.77 mmol, 95 %); mp: 146-148 °C; ν_{max}(ATR)/cm^{-1} 2363, 1445, 1254, 1223, 1144, 1026, 824, 754, 721, 694; ^{1}H-NMR (400 MHz, d_3-MeCN): δ= 4.25 (3H, s, C*H*$_3$), 7.77-7.83 (2H, m, Ar*H*), 7.86-7.94 (4H, m, Ar*H*), 8.02 (1H, ddd, *J* = 8.4, 7.4, 1.0 Hz, Ar*H*), 8.23 (1H, d, *J* = 8.6 Hz, Ar*H*), 8.37 (1H, d, *J* = 8.2 Hz, Ar*H*); ^{13}C-NMR (100 MHz, d_3-MeCN): δ= 37.5 (*C*H$_3$), 116.9 (*C*H), 120.7 (q, 320 Hz, $J_{C\text{-}F}$ = *C*F_3SO_3), 123.6 (*C*H), 124.7 (*C*), 128.6 (*C*H), 129.3 (*C*H), 129.4 (*C*H), 129.4 (*C*H), 129.8 (*C*H), 129.8 (*C*H), 129.9 (*C*H), 133.6 (*C*), 142.2 (*C*), 174.3 (*C*); HRMS (NSI$^+$) ([M-TfO]$^+$) calcd for $C_{14}H_{12}NS$ 226.0685, found 226.0679.

N-Methyl-*N*-(2-(phenylthio)phenyl)benzamide

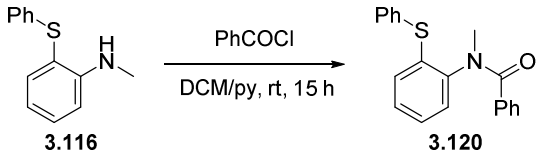

3.116 **3.120**

Benzoyl chloride (0.54 mL, 4.68 mmol, 1.2 eq.) was added to *N*-methyl-2-(phenylthio)aniline **3.116** (840 mg, 3.90 mmol, 1.0 eq.) dissolved in a mixture of DCM/pyridine (10 mL/2 mL) at room temperature and it was stirred for 15 h. The reaction mixture was partitioned between water and DCM and extracted with DCM (2 x 75 mL). The combined organic phases were washed with water (2 x 50 mL), brine (50 mL), dried over sodium sulfate and concentrated under reduced pressure. The crude product was purified by flash chromatography (25 % EtOAc/Pet ether) to afford the *title compound* **3.120** as a white solid (1172 mg, 3.67 mmol, 94 %); mp: 76-78 °C; ν_{max}(ATR)/cm^{-1} 1641, 1578, 1472, 1439, 1416, 1354, 1300, 1109, 1058, 731, 711, 691; ^{1}H-NMR (400 MHz, $CDCl_3$): δ= 3.41 (3H, s, C*H*$_3$), 6.89 (1H, d, *J* = 6.3 Hz, Ar*H*), 7.00-7.12 (3H, m, Ar*H*), 7.13-7.19 (2H, m, Ar*H*), 7.23 (1H, d, *J* = 7.1 Hz, Ar*H*), 7.30-7.38 (5H, m, Ar*H*), 7.45 (2H, d, *J* = 7.4 Hz, Ar*H*); ^{13}C-NMR (100 MHz, $CDCl_3$): δ= 37.2 (*C*H$_3$), 127.0 (*C*H), 127.6 (*C*H), 128.2 (*C*H), 128.3 (*C*H), 128.4 (*C*H), 129.4 (*C*H), 129.6 (*C*H), 129.7 (*C*H), 130.0 (*C*H), 132.7 (*C*), 133.3 (*C*H), 136.0 (*C*), 136.7 (*C*), 142.6 (*C*), 171.2 (*C*O); HRMS (NSI$^+$) ([M+H]$^+$) calcd for $C_{20}H_{18}NOS$ 320.1104, found 320.1103.

3-Methyl-1,2-diphenyl-1H-benzo[d]thiazole-1,3-diium triflate

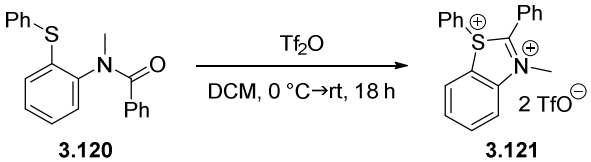

3.120 **3.121**

A solution of *N*-methyl-*N*-(2-(phenylthio)phenyl)formamide **3.120** (122 mg, 0.5 mmol, 1.0 eq.) in DCM (1.5 mL) was added under argon to a solution of triflic anhydride (0.11 mL, 0.65 mol, 1.3 eq.) in DCM (1.5 mL) at 0 °C using a syringe pump (4.5 mL/h). Upon addition, the reaction mixture was stirred for a 2 h, before it was warmed to room temperature and stirred for a further 16 h. The solvent was removed under reduced pressure and the precipitate was triturated with DCM (2 x 1 mL) to afford the *title compound* **3.121** as a yellow solid (270 mg, 0.45 mmol, 61 %); mp: 118-120 °C (decomp.); ν_{max}(ATR)/cm^{-1} 1586, 1564, 1451, 1267, 1242, 1223, 1194, 1150, 1024, 997, 756, 731, 679; ^{1}H-NMR (400 MHz, d_3-MeCN): δ= 4.59 (3H, s, C*H*$_3$), 7.54-7.60 (2H, m, Ar*H*), 7.63-7.68 (2H, m, Ar*H*), 7.78 (1H, ddd, *J* = 8.4, 7.4, 1.0 Hz, Ar*H*), 7.82-7.87 (2H, m, Ar*H*), 8.03 (1H, m, *J* = 7.6 Hz, Ar*H*), 8.17-8.23 (3H, m, Ar*H*), 8.39 (1H, ddd, *J* = 8.6, 8.5, 1.0 Hz, Ar*H*), 8.50 (1H, dd, *J* = 8.4, 0.6 Hz, Ar*H*),

8.65 (1H, dd, *J* = 8.1, 1.0 Hz, Ar*H*); ^{13}C-NMR (100 MHz, d_3-MeCN): δ= 42.4 (*C*H_3), 119.5 (*C*), 119.8 (*C*), 120.4 (*C*), 120.4 (q, $J_{C\text{-}F}$ = 318 Hz, *C*F_3SO_3), 122.1 (*C*H), 130.1 (*C*H), 130.9 (*C*H), 131.8 (*C*H), 132.3 (*C*H), 133.6 (*C*H), 134.2 (*C*H), 137.0 (*C*H), 137.3 (*C*H), 139.5 (*C*H), 145.3 (*C*), 176.4 (*C*); HRMS (NSI$^+$) ([M-2TfO-H]$^+$) calcd for $C_{20}H_{16}NS$ 302.0998, found 302.0996.

3-Methyl-2-phenylbenzo[d]thiazol-3-ium triflate

3.121 **3.122**

A solution of 3-methyl-1,2-diphenyl-1H-benzo[d]thiazole-1,3-diium triflate **3.121** (80 mg, 0.17 mmol) in DCM (1.0 mL) was under argon recrystallized by diffusion of diethyl ether into the substrate solution. After two days, colourless crystals formed, which were analysed by X-ray crystallography confirming the dephenylated *title compound* **3.122**. The crystalline product mixture was triturated with a 1:2 DCM/Et_2O mixture (3 x 5 mL) and the solvent removed under reduced pressure to afford the *title compound* as a white solid (55 mg, 0.15 mmol, 88 %); mp: 122-124 °C; ν_{max}(ATR)/cm^{-1} 1447, 1254, 1223, 1144, 1028, 754, 721, 694; ^{1}H-NMR (400 MHz, d_3-MeCN): δ= 4.25 (3H, s, C*H*$_3$), 7.77-7.83 (2H, m, Ar*H*), 7.86-7.93 (4H, m, Ar*H*), 8.01 (1H, ddd, *J* = 8.6, 7.3, 1.2 Hz, Ar*H*), 8.23 (1H, d, *J* = 8.6, Ar*H*), 8.37 (1H, d, *J* = 7.8 Hz, Ar*H*); ^{13}C-NMR (100 MHz, d_3-MeCN): δ=37.5 (*C*H_3), 116.9 (*C*H), 120.7 (q, $J_{C\text{-}F}$ = 321 Hz, *C*F_3SO_3), 123.6 (*C*H), 124.7 (*C*), 128.6 (*C*H), 129.3 (*C*), 129.4 (*C*H), 129.8 (*C*H), 129.9 (*C*H), 133.6 (*C*H), 142.2 (*C*), 174.3 (*C*); HRMS (NSI$^+$) ([M]$^+$) calcd for $C_{14}H_{12}NS$ 226.0683, found 226.0682.

Isobutyl (8-(dimethylamino)naphthalen-1-yl)(methyl)carbamate

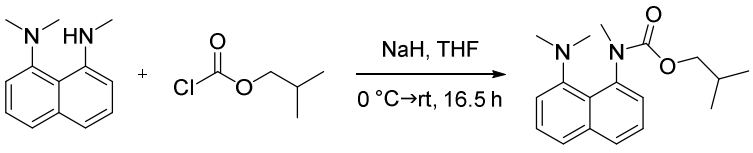

3.16 **3.130** **3.131**

Sodium hydride (60 %, 210 mg, 5.24 mmol, 1.5 eq.) was added under argon to a solution of *N*,*N*,*N*'-trimethylnaphthalene-1,8-diamine **3.16** (700 mg, 3.50 mmol, 1.0 eq.) in dry THF (20 mL) at room temperature. The reaction mixture was stirred for 0.5 h before isobutyl chloroformate **3.130** (0.55 mL, 4.20 mmol, 1.2 eq.) was added dropwise. The suspension was stirred for a further 16 h. The reaction mixture was partitioned between DCM and water and the product was extracted with DCM (3 x 50 mL). The combined organic phases were washed with brine (50 mL), dried over sodium sulfate and the solvent was removed under reduced pressure. Flash chromatography (10 %

EtOAc/Pet ether) afforded the *title compound* **3.131** as a brown oil (792 mg, 2.64 mmol, 75 %); ν_{max}(ATR)/cm^{-1} 2957, 2826, 2778, 1697, 1578, 1153, 1030, 988, 828, 764; in the NMR the compound appeared as an isomer mixture (isomer ratio A:B = 2.5:1) ^{1}H-NMR (400 MHz, $CDCl_3$): δ= 0.65 [d, *J* = 6.7 Hz, ism A] and 0.66 [d, *J* = 6.7 Hz, ism A] and 1.07 [d, *J* = 6.7 Hz, ism B] (6H, C*H*$_3$), 1.64-1.71 (1H, m, C*H*), 2.67 [s, ism B] and 2.70 [s, ism A] (3H, C*H*$_3$), 2.82 [s, ism A] and 2.86 [s, ism B] (3H, C*H*$_3$), 3.26 [s, ism B] and 3.33 [s, ism A] (3H, C*H*$_3$), 3.67 [dd, *J* = 10.3, 6.6 Hz, ism A] and 4.00-4.04 [m, ism B] (1H, C*H*$_2$), 3.97 [dd, *J* = 10.3, 6.6 Hz, ism A] and [d, *J* = 6.6 Hz, ism B] (1H, C*H*$_2$), 7.19-7.22 (1H, m, Ar*H*), 7.28-7.30 (1H, m, Ar*H*), 7.38-7.44 (2H, m, Ar*H*), 7.56-7.58 (1H, m, Ar*H*), 7.75-7.77 (1H, m, Ar*H*); ^{13}C-NMR (100 MHz, $CDCl_3$): δ= 18.4 and 18.5 and 18.7 (*C*H$_3$), 27.3 and 27.6 (*C*H), 38.4 and 38.5 (*C*H$_3$), 44.1 and 44.9 (*C*H$_3$), 45.3 and 46.3 (*C*H$_3$), 71.1 (*C*H$_2$), 116.1 (*C*H), 123.4 (*C*H), 124.3 and 124.6 (*C*H), 125.0 and 125.2 (*C*H), 125.7 (*C*H), 126.5 (*C*), 127.6 and 127.7 (*C*H), 136.5 (*C*), 138.4 (*C*), 150.3 (*C*), 155.5 (*C*O); HRMS (NSI$^+$) ([M+H]$^+$) calcd for $C_{18}H_{25}N_2O_2$ 301.1911, found 301.1911, ([M+Na]$^+$) calcd for $C_{18}H_{24}N_2NaO$ 323.1735, found 323.1727.

1,1,3-Trimethyl-2-oxo-2,3-dihydro-1H-perimidin-1-ium triflate

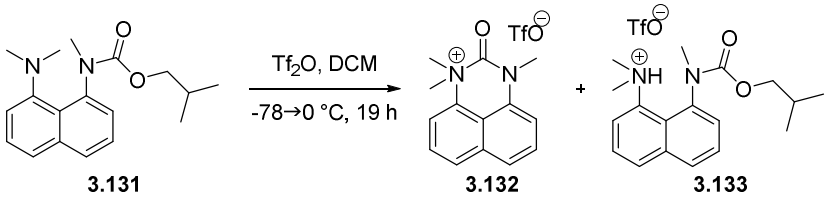

A solution of isobutyl (8-(dimethylamino)naphthalen-1-yl)(methyl)-carbamate **3.131** (570 mg, 1.9 mmol, 1.0 eq.) in dry DCM (1.0 mL) was added under argon to a flask containing trifluoromethanesulfonic anhydride (0.48 mL, 2.8 mmol, 1.4 eq.) in dry DCM (1.0 mL) *via* syringe pump (1.5 mL/h) at -78 °C. After 3 h, the reaction mixture was warmed to room temperature and stirred for a further 16 h. The solvent was removed under reduced pressure. At this stage, the ^{1}H-NMR of the crude product showed a 1:1 mixture of protonated starting material **3.133** and the title compound **3.132**. The product mixture was triturated with a 1:2 Et_2O/DCM mixture (6 mL), then filtered and further washed with the solvent mixture (4 x 10 mL) to afford the *title compound* **3.132** as a white solid (267 mg, 0.71 mmol, 37 %); mp: 145-148 °C; ν_{max}(ATR)/cm^{-1} 1759, 1262, 1225, 1155, 1146, 1028, 885, 820, 760; ^{1}H-NMR (400 MHz, d_3-MeCN): δ= 3.74 (3H, s, C*H*$_3$), 3.90 (6H, s, C*H*$_3$), 7.49 (1H, d, *J* = 7.8 Hz, Ar*H*), 7.75-7.79 (1H, m, Ar*H*), 7.82-7.86 (1H, m, Ar*H*), 7.93 (1H, d, *J* = 8.3 Hz, Ar*H*), 8.13 (1H, d, *J* = 7.9 Hz, Ar*H*), 8.21 (1H, d, *J* = 8.3 Hz, Ar*H*); ^{13}C-NMR (100 MHz, d_3-MeCN): δ= 33.8 (*C*H$_3$), 57.1 (*C*H$_3$), 112.3 (*C*H), 116.9 (*C*), 118.9 (*C*H), 120.7 (q, $J_{C\text{-}F}$ = 318 Hz, *C*F_3SO_3), 124.2 (*C*H), 127.1

(*C*H), 127.9 (*C*H), 129.9 (*C*H), 130.2 (*C*), 133.0 (*C*), 136.8 (*C*), 148.5 (*C*O); HRMS (NSI^+) ($[M\text{-}TfO]^+$) calcd for $C_{14}H_{15}N_2O$ 227.1179, found 227.1173.

Within 24 h, crystallisation of another product was observed in the washing phase, which was filtered and washed with Et_2O (3 x 10 mL) thoroughly. The solvent was removed under reduced pressure to yield the *compound* **3.133** as an off-white solid (462 mg, 1.03 mmol, 54 %); mp: 48-51 °C; ν_{max}(ATR)/cm^{-1} 2963, 1736, 1254, 1223, 1150, 1028, 976, 833, 764, 636; ^{1}H-NMR (400 MHz, $CDCl_3$): δ= 0.79 (3H, d, *J* = 6.4 Hz, CH_3), 0.81 (3H, d, *J* = 6.4 Hz, CH_3), 1.93 (1H, m, C*H*), 3.41 (3H, s, CH_3), 3.61 (3H, d, *J* = 5.0 Hz, CH_3), 3.67 (3H, d, *J* = 5.0 Hz, CH_3), 3.96-4.08 (2H, m, CH_2), 7.51-7.53 (1H, m, Ar*H*), 7.65-7.69 (1H, m, Ar*H*), 7.73-7.77 (1H, m, Ar*H*), 8.00 (1H, d, *J* = 7.6 Hz, Ar*H*), 8.08 (1H, d, *J* = 8.0 Hz, Ar*H*), 8.18 (1H, m, Ar*H*), 11.66 (1H, bs, N*H*); ^{13}C-NMR (100 MHz, $CDCl_3$): δ=17.6 (*C*H_3), 27.2 (*C*H), 39.2 (*C*H_3), 47.8 (*C*H_3), 48.3 (*C*H_3), 72.7 (*C*H_2), 120.3 (*C*), 120.9 (*C*H), 125.2 (q, $J_{C\text{-}F}$ = 323 Hz, *C*F_3SO_3) 126.0 (*C*H), 127.4 (*C*H), 127.5 (*C*H), 129.5 (*C*H), 131.4 (*C*H), 135.4 (*C*), 138.4 (*C*), 138.7 (*C*), 158.0 (*C*); HRMS (NSI^+) ($[M\text{-}TfO]^+$) calcd for $C_{18}H_{25}N_2O_2$ 301.1911, found 301.1912.

Isobutyl methyl(8-(pyrrolidin-1-yl)naphthalen-1-yl)carbamate

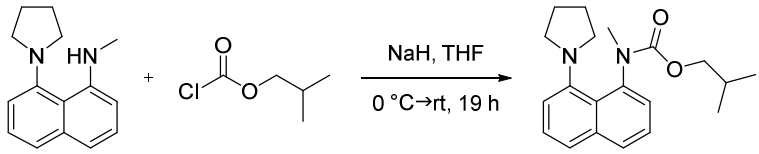

3.9 **3.130** **3.142**

A solution of *N*-methyl-8-(pyrrolidin-1-yl)naphthalen-1-amine **3.9** (731 mg, 3.23 mmol, 1.0 eq.) in THF (15 mL) was added under argon to a suspension of sodium hydride (60 %, 194 mg, 4.85 mmol, 1.5 eq.) in dry THF (20 mL) at room temperature. The reaction mixture was stirred for 1 h, before isobutyl chloroformate **3.130** (0.55 mL, 4.20 mmol, 1.2 eq.) was added dropwise to the suspension at 0 °C and stirring was continued for a further 2 h. The reaction mixture was then warmed to room temperature and stirred for a further 16 h. The reaction mixture was quenched with water carefully, then partitioned between DCM and sat. $NaHCO_3$ and extracted with DCM (3 x 40 mL). The combined organic phases were washed with brine (100 mL), dried over sodium sulfate and the solvent was removed under reduced pressure. Flash chromatography (10 % EtOAc/Pet ether + 1 %) afforded the *title compound* **3.142** as a colourless oil (861 mg, 2.63 mmol, 82 %); ν_{max}(ATR)/cm^{-1} 2957, 2801, 1697, 1576, 1383, 1289, 1155, 990, 826 762; in the NMR spectra the compound appeared as an isomer mixture (isomer ratio A:B = 2.3:1) ^{1}H-NMR (400 MHz, $CDCl_3$): δ= 0.67 [d, *J* = 6.7 Hz, ism A] and 1.06 [d, *J* = 6.7, ism B] and 1.07 [d, *J* = 6.7, ism B] (6H, CH_3), 1.64-1.74 [m, ism A] and 2.04-2.12 [m, ism B], (1H, C*H*), 1.90-2.01 (4H, m, CH_2), 2.68-3.04 [m, ism B] and 3.04-3.17 [m, ism A] (4H, CH_2), 3.23 [s, ism

B] and 3.33 [s, ism A] (3H, CH_3), 3.67 [d, *J* = 6.5 Hz, ism A] and 3.70 [d, *J* = 6.5 Hz, ism A] and 4.08 [d, *J* = 6.4 Hz, ism B] and 4.11 [d, 6.4 Hz, ism B] (1H, CH_2), 3.91 [d, *J* = 6.7 Hz, ism B] and 3.94 [d, *J* = 6.6 Hz, ism A] 3.94 [d, *J* = 6.7 Hz, ism B] and 3.96 [d, *J* = 6.6 Hz, ism A] (1H, CH_2), 7.21 [d, *J* = 7.1 Hz, ism B] and 7.22 [dd, *J* = 7.4, 1.0 Hz, ism A] (1H, Ar*H*), 7.28 [dd, *J* = 7.3, 1.2 Hz, ism A] and 7.36-7.46 [m, ism B] (1H, Ar*H*), 7.36-7.46 (2H, m, Ar*H*), 7.55 [d, *J* = 7.8 Hz, ism B] and 7.56 [dd, *J* = 8.0, 0.8 Hz, ism A] (1H, Ar*H*), 7.72-7.77 (1H, m, Ar*H*); ^{13}C-NMR (100 MHz, $CDCl_3$): δ= 18.5 and 18.5 and 18.8 (*C*H_3), 23.2 and 23.3 (*C*H_3), 27.3 and 27.6 (*C*H), 38.4 and 38.5 (*C*H_3), 53.3 (*C*H_2), 71.2 and 71.2 (*C*H_2), 115.1 and 115.6 (*C*H), 123.1 and 123.3 (*C*H), 124.3 and 124.7 (*C*), 124.5 and 124.9 (*C*H), 125.1 and 125.3 (*C*H), 125.3 and 126.1 (*C*H), 127.3 and 127.4 (*C*H), 136.3 and 136.5 (*C*), 138.6 and 138.9 (*C*), 146.2 and 146.6 (*C*), 155.4 and 155.6 (*C*O); HRMS (NSI$^+$) ([M+H]$^+$) calcd for $C_{20}H_{27}N_2O_2$ 327.2067, found 327.2071.

3-Methyl-2-oxo-2,3-dihydrospiro[*perimidine-1,1'-pyrrolidin]-1-ium triflate*

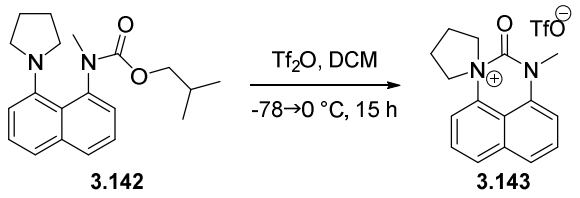

3.142 **3.143**

A solution of isobutyl (8-(dimethylamino)naphthalen-1-yl)(methyl)-carbamate **3.142** (140 mg, 0.43 mmol, 1.0 eq.) in dry DCM (1.5 mL) was added under argon to a flask containing trifluoromethanesulfonic anhydride (0.09 mL, 0.52 mmol, 1.2 eq.) in dry DCM (1.5 mL) *via* syringe pump (6 mL/h) at -78 °C. After 2 h, the reaction mixture was warmed to room temperature and stirred for a further 13 h. To the reaction mixture was added Et_2O (6 mL) to precipitate the product. The precipitate was triturated with a 1:2 mixture of DCM/Et_2O (3 x 6 mL). The product was dried under reduced pressure to afford the *title compound* **3.143** as a white solid (71 mg, 0.18 mmol, 41 %); mp: 59-61 °C; ν_{max}(ATR)/cm^{-1} 1641, 1574, 1532, 1258, 1142, 1030, 957, 816; ^{1}H-NMR (400 MHz, d_3-MeCN): δ= 2.05-212 (2H, m, CH_2), 2.19-2.25 (2H, m, CH_2), 3.53 (3H, s, CH_3), 4.16-4.89 (2H, m, CH_2), 4.87 (2H, m, CH_2), 7.05 (1H, dd, *J* = 7.6, 0.6 Hz, Ar*H*), 7.15 (1H, d, *J* = 7.6 Hz, Ar*H*), 7.53-7.59 (2H, m, Ar*H*), 7.62-7.67 (2H, m, Ar*H*); ^{13}C-NMR (100 MHz, d_3-MeCN): δ= 22.2 (*C*H_2), 26.6 (*C*H_2), 33.3 (*C*H_3), 52.1 (*C*H_2), 79.9 (*C*H_2), 108.7 (*C*H), 108.8 (*C*H), 119.4 (*C*), 123.0 (*C*H), 123.4 (*C*H), 128.0 (*C*H), 128.0 (*C*H), 133.8 (*C*), 133.8 (*C*), 134.2 (*C*), 158.2 (*C*O); HRMS (NSI$^+$) ([M-TfO]$^+$) calcd for $C_{16}H_{17}N_2O$ 253.1335, found 253.1332.

Isobutyl methyl(2-(pyrrolidin-1-yl)phenyl)carbamate

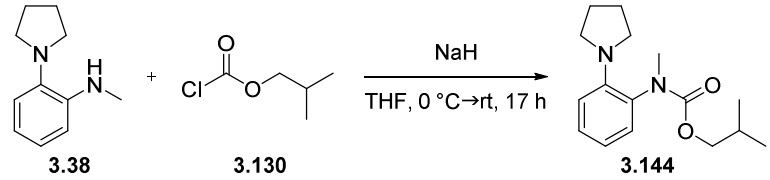

3.38 **3.130** **3.144**

Sodium hydride (60 %, 238 mg, 5.96 mmol, 1.5 eq.) was added under argon to a solution of *N*-methyl-2-(pyrrolidin-1-yl)aniline **3.38** (700 mg, 3.97 mmol, 1.0 eq.) in dry THF (20 mL) at room temperature. The reaction mixture was stirred for 1 h, before at 0 °C isobutyl chloroformate **3.130** (0.62 mL, 4.77 mmol, 1.2 eq.) was added and the reaction mixture stirred for 2 h. The solution was then warmed to room temperature and stirred for a further 14 h. The reaction mixture was quenched with water carefully, partitioned between water and DCM and extracted with DCM (3 x 50 mL). The combined organic phases were washed with brine (50 mL), dried over sodium sulfate and concentrated *in vacuo*. The crude product was purified by flash chromatography (10 % EtOAc/Pet ether) to afford the *title compound* **3.144** as a colourless oil (829 mg, 3.00 mmol, 76 %); ν_{max}(ATR)/cm^{-1} 2959, 1697, 1599, 1352, 334, 1306, 1146, 1003, 743; in the NMR spectra the compound appeared as an isomer mixture (isomer ratio A:B = 2.5:1) ^{1}H-NMR (400 MHz, $CDCl_3$): δ= 0.81 [d, *J* = 6.4 Hz, ism A] and 1.01 [d, *J* = 5.4 Hz, ism B] (6H, C*H*$_3$), 1.65-1.74 [m, ism B] and 1.78-1.90 [m, ism A] (1H, C*H*), 1.88-2.08 (4H, m, C*H*$_2$), 3.15 (3H, s, C*H*$_3$), 3.15-3.25 (2H, m, C*H*$_2$), 3.25-3.35 (2H, m, C*H*$_2$), 3.81-3.91 [m, ism A] and 3.92-4.03 [m, ism B] (2H, C*H*$_2$), 6.71-6.84 (2H, m, Ar*H*), 7.04 (1H, d, *J* = 7.6 Hz, Ar*H*), 7.09-7.19 (1H, m, Ar*H*); ^{13}C-NMR (100 MHz, $CDCl_3$): δ= 18.4 (*C*H$_2$), 25.1 (*C*H$_3$), 27.5 (*C*H), 36.4 (*C*H$_3$), 48.9 (*C*H$_2$), 71.2 (*C*H$_2$), 114.7 (*C*H), 117.2 (*C*H), 127.3 (*C*H), 129.2 (*C*H), 129.4 (*C*), 145.0 (*C*), 155.9 (*C*O); HRMS (NSI$^+$) ([M+H]$^+$) calcd for $C_{16}H_{25}N_2O_2$ 277.1911, found 277.1914.

3-Methyl-2-oxo-2,3-dihydrospiroimidazole-1,1'-pyrrolidin]-1-ium triflate

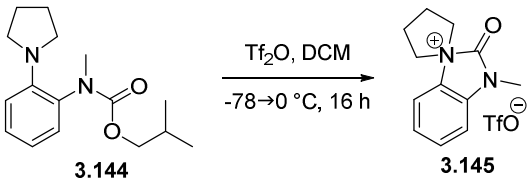

3.144 **3.145**

A solution of isobutyl methyl(2-(pyrrolidin-1-yl)phenyl)carbamate **3.144** (500 mg, 1.83 mmol, 1.0 eq.) in dry DCM (3.0 mL) was added under argon to a flask containing trifluoromethanesulfonic anhydride (0.43 mL, 2.56 mmol, 1.4 eq.) in dry DCM (2.0 mL) *via* syringe pump (1.5 mL/h) at -78 °C. After one hour, the reaction mixture was warmed to room temperature and stirred for a further 15 h. The solvent was removed under reduced pressure. The product mixture was triturated with a 1:1

Et_2O/DCM mixture (3 x 5 mL) and the washings were decanted. The product was dried under reduced pressure to afford the *title compound* **3.145** as a white solid (264 mg, 0.75 mmol, 41 %); mp: 120-122 °C; ν_{max}(ATR)/cm^{-1} 1813, 1495, 1373, 1260, 1225, 1144, 1132, 1030, 951, 768, 637; ^{1}H-NMR (400 MHz, $CDCl_3$): δ= 2.50-2.61 (4H, m, CH_2), 3.43 (3H, s, CH_3), 3.92-3.96 (2H, m, CH_2), 4.21-4.25 (2H, m, CH_2), 7.35 (1H, d, *J* = 8.0 Hz, Ar*H*), 7.44 (1H, ddd, *J* = 8.0, 8.0, 1.1 Hz, Ar*H*), 7.68 (1H, ddd, *J* = 8.2, 8.0, 1.0 Hz, Ar*H*), 7.72 (1H, d, *J* = 8.2 Hz, Ar*H*); ^{13}C-NMR (100 MHz, $CDCl_3$): δ= 24.1 (*C*H_2), 28.6 (*C*H_3), 67.8 (*C*H_2), 111.1 (*C*H), 117.5 (*C*H), 120.5 (q, $J_{C\text{-}F}$ = 319 Hz, *C*F_3SO_3), 124.9 (*C*H), 131.5 (*C*H), 132.8 (*C*), 135.0 (*C*), 156.3 (*C*O); HRMS (NSI$^+$) ([M-TfO]$^+$) calcd for $C_{12}H_{15}N_2O$ 203.1179, found 203.1180.

N-Methyl[o-(1-pyrrolidinyl)phenyl]amino acetate

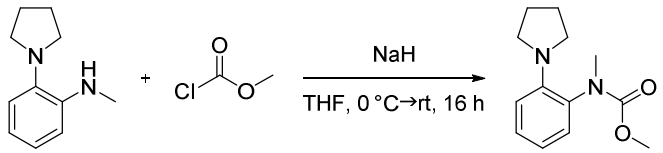

3.38 **3.146** **3.147**

Sodium hydride (60 %, 244 mg, 6.11 mmol, 1.5 eq.) was added under argon to a solution of *N*-methyl-2-(pyrrolidin-1-yl)aniline **3.38** (718 mg, 4.07 mmol, 1.0 eq.) in dry THF (10 mL) at room temperature. The reaction mixture was stirred for 2 h, before methyl chloroformate **3.146** (0.38 mL, 4.89 mmol, 1.2 eq.) was added at 0 °C and the reaction mixture stirred for 2 h. The solution was then warmed to room temperature and stirred for a further 12 h. The reaction mixture was quenched with water carefully, partitioned between water and DCM and extracted with DCM (3 x 50 mL). The combined organic phases were washed with brine (50 mL), dried over sodium sulfate and concentrated *in vacuo*. The crude product was purified by flash chromatography (8.5 % EtOAc/Pet ether + 1 % Et_3N) to afford the *title compound* **3.147** a colourless oil (503 mg, 2.15 mmol, 53 %); ν_{max}(ATR)/cm^{-1} 2951, 1697, 1599, 1445, 1354, 1304, 1150, 1119, 1003, 770, 743; ^{1}H-NMR (400 MHz, $CDCl_3$): δ= 1.82-2.04 (4H, m, CH_2), 3.12 (3H, s, CH_3), 3.12-3.24 (2H, m, CH_2), 3.24-3.35 (2H, m, CH_2), 3.68 (3H, s, CH_3), 6.73-6.80 (2H, m, Ar*H*), 7.03 (1H, d, *J* = 7.6 Hz, Ar*H*), 7.10-7.20 (1H, m, Ar*H*); ^{13}C-NMR (100 MHz, $CDCl_3$): δ=25.6 (*C*H_2), 36.9 (*C*H_3), 49.4 (*C*H_2), 52.9 (*C*H_3), 115.4 (*C*H), 117.8 (*C*H), 128.1 (*C*H), 129.6 (*C*), 129.9 (*C*H), 145.4 (*C*), 156.8 (*C*O); HRMS (NSI$^+$) ([M+H]$^+$) calcd for $C_{13}H_{19}N_2O_2$ 235.1441, found 235.1439.

3-Methyl-2-oxo-2,3-dihydrospiroimidazole-1,1'-pyrrolidin]-1-ium triflate

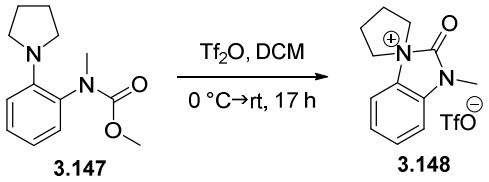

3.147 **3.148**

A solution of N-methyl[o-(1-pyrrolidinyl)phenyl]amino acetate **3.147** (234 mg, 1.0 mmol, 1.0 eq.) in dry DCM (1.5 mL) was added under argon to a flask containing trifluoromethanesulfonic anhydride (0.2 mL, 1.2 mmol, 1.2 eq.) in dry DCM (1.5 mL) *via* syringe pump (1.5 mL/h) at 0 °C. Upon addition, the reaction mixture was stirred for 2 h, before it was warmed to room temperature and stirred for a further 15 h. The solvent was removed under reduced pressure. The product mixture was triturated with a 1:1 Et_2O/DCM mixture (4 x 5 mL) and the washings were decanted. The product was dried under reduced pressure to afford the *title compound* **3.148** as a white solid (89 mg, 0.25 mmol, 25 %). (For analytical data see above)

1,4-Di(piperidin-1-yl)benzene[222]

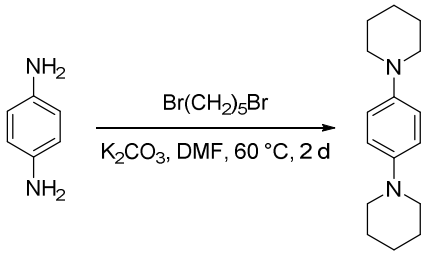

3.151 **3.152**

1,5-Dibromopentane (7.7 mL, 58.3 mmol, 2.1 eq.) was added under argon to a suspension of benzene-1,4-diamine **3.151** (3.0 g, 27.7 mmol, 1.0 eq.) and potassium carbonate (16.1 g, 166.5 mmol, 4.2 eq.) in DMF (5 mL) and the reaction mixture was stirred for 2 d at 60 °C. The suspension was partitioned between water and diethyl ether and extracted with diethyl ether (3 x 75 mL). The organic layer was washed with 2M NaOH (3 x 100 mL), dried over sodium sulfate and the solvent was removed under reduced pressure. The crude product was purified by flash chromatography (15% EtOAc/Pet ether + 1 % Et_3N) to give *the title compound* **3.152** as a white solid 3.15 g (12.9 mmol, 47 %); mp: 105-106 °C (lit.[213]: 104-106 °C); ν_{max}(ATR)/cm^{-1} 2930, 2795, 1510, 1441, 1317, 1209, 909, 826, 700; ^{1}H-NMR (400 MHz, $CDCl_3$): δ= 1.52-1.61 (4H, m, CH_2), 1.71-1.78 (8H, m, CH_2), 3.06 (8H, t, *J* = 5.4 Hz, CH_2), 6.92 (4H, s, C*H*); ^{13}C-NMR (100 MHz, $CDCl_3$): δ= 23.8 (*C*H_2), 25.7 (*C*H_2), 51.5 (*C*H_2), 117.7 (*C*H), 145.8 (*C*); HRMS (NSI$^+$) ([M+H]$^+$) calcd for $C_{16}H_{25}N_2$ 245.2012, found 245.2013.

N,N'-(Cyclohexa-2,5-diene-1,4-diylidene)bis(N-methylmethanaminium) triflate

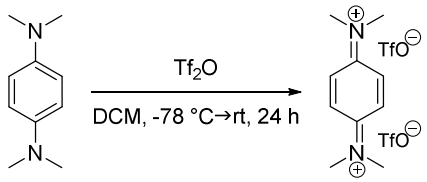

3.149 **3.153**

A solution of *N,N,N',N'*-tetramethyl-1,4-phenylenediamine **3.149** (0.7 g mL, 4.26 mmol, 1.0 eq.) in DCM (5 mL) was added under argon to a solution of triflic anhydride (2.5 mL, 14.8 mmol, 3.0 eq.) in DCM (10 mL) at -78 °C slowly. Upon addition, the reaction mixture was stirred for 2 h, then warmed to room temperature and stirred for a further 22 h. A precipitate had formed which was filtered, washed thoroughly with DCM (4 x 5 mL) and dried under reduced pressure to give the *title compound* **3.153** as a grey powder (1.71 g, 3.70 mmol, 87 %); mp: 121-123 °C (decomp.); ν_{max}(ATR)/cm^{-1} 3090, 1620, 1258, 1223, 1142, 1028, 847, 625; ^{1}H-NMR (400 MHz, d-TFA): δ= 4.35 (12H, s, C*H*$_3$), 8.22 (4H, s, C*H*); ^{13}C-NMR (100 MHz, d-TFA): δ= 46.2 (*C*H$_3$), 118.9 (q, $J_{C\text{-}F}$ = 282 Hz, *C*F$_3$SO$_3$), 123.0 (*C*), 130.4 (*C*H); HRMS (NSI$^+$) ([M-2TfO]$^+$) calcd for $C_{10}H_{16}N_2$ 164.1308, found 164.1305.

1,1'-(Cyclohexa-2,5-diene-1,4-diylidene)bis(piperidin-1-ium) triflate

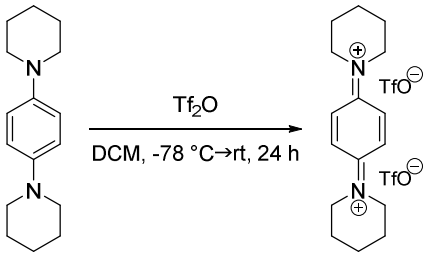

3.152 **3.154**

A solution of 1,4-di(piperidin-1-yl)benzene **3.152** (1.0 g, 4.09 mmol, 1.0 eq.) in DCM (5 mL) was added under argon to a solution of triflic anhydride (3.5 mL, 20.5 mmol, 5.0 eq.) in DCM (10 mL) at -78 °C slowly. Upon addition, the reaction mixture was stirred for 2 h and then warmed to room temperature and stirred for further 22 h. The precipitate was filtered, washed thoroughly with DCM (4 x 10 mL) and dried under reduced pressure to the give *title compound* **3.154** as an off-white powder (1.89 g, 3.48 mmol, 85 %); mp: 218-221 °C; ν_{max}(ATR)/cm^{-1} 3102, 1603, 1505, 1258, 1221, 1142, 1028, 845, 633; ^{1}H-NMR (500 MHz, d-TFA): δ= 2.22-2.29 (4H, m, C*H*$_2$), 2.45 (8H, m, C*H*$_2$), 4.76 (8H, t, *J* = 5.3 Hz, C*H*$_2$), 8.35 (4H, s, C*H*); ^{13}C-NMR (100 MHz, d-TFA): δ= 22.1 (*C*H$_2$), 28.8 (*C*H$_2$), 57.3 (*C*H$_2$), 119.1 (q, $J_{C\text{-}F}$ = 318 Hz, *C*F$_3$SO$_3$), 123.8 (*CH*), 130.1 (*C*); HRMS (NSI$^+$) ([M-2TfO-H]$^+$) calcd for $C_{16}H_{23}N_2$ 245.2012, found 245.2006.

Kinetic ^{1}H-NMR studies of the dealkylation process of formamides **3.3** and **3.17**

For ^{1}H-NMR kinetic studies of the *N*-methylformamides **3.3** and **3.17** reacting with triflic anhydride in DCM (shown below), two stock solutions were prepared, each containing 0.2 mol/L amide and 0.1 mol/L of the standard cyclooctatetraene (COT) in d_2-DCM. The solvent d_2-DCM was previously distilled over P_2O_5 and degassed by bubbling a stream of argon through the solution. The solutions were stored at -30 °C when not used. For each kinetic experiment 0.2 mL of the stock solution and 0.4 mL of d_2-DCM were pipetted into an NMR tube and sealed with a rubber cap.

The NMR tube was then cooled to -15 °C in a sodium chloride/ice bath and freshly distilled triflic anhydride (0.05 mL) was syringed into the NMR tube and the reaction solution mixed by inverting the NMR tube briefly, before putting it back into the ice bath.

The reactions were then recorded by ^{1}H-NMR at different temperatures (279, 282, 285, 288, 291 and 294 K) and with a fixed delay of 374 s (5:00 min set delay plus 1:14 min acquisition time) between each acquisition from a total of 30 experiments for the pyrrolidine-based substrate **3.3** and from a total of 25 experiments for the dimethylamino-based formamide **3.17**.

For analysis, the spectra of each kinetic run were processed using TOPSPIN's internal serial processing command, which ensured all spectra of each kinetic run to have the same phasing (sr, phc0, phc1 values).

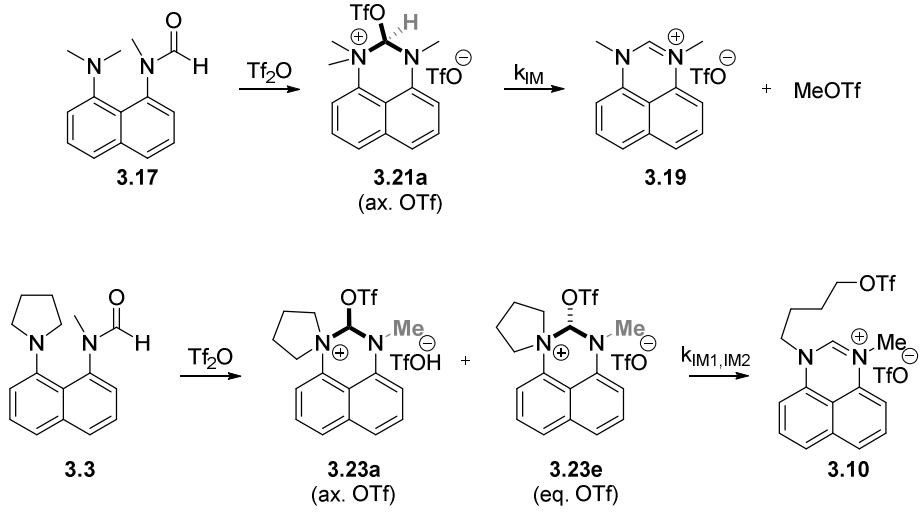

For substrate **3.17**, the concentration of intermediate **3.21a** vs. time was calculated by multiplying the integral of the methine proton NC*H*OTfN (at 7.05 ppm) with the concentration (0.03077mol/L) of the internal standard COT. However, for substrate **3.3**, the concentration of each intermediate

(**3.23a** and **3.23e**) vs. time was calculated by dividing the integral of the methyl group (at 3.90 and 3.30 ppm, respectively) by 3 (3 protons) and with the concentration of the internal standard.

	Rate constants *k* for the dealkylation x 10^{-4} [s^{-1}] at [COT] = 0.03077 mol/L		
Intermediate	**3.21a**	**3.23a**	**3.23e**
294 K	7.378 ± 0.124	3.933 ± 0.039	4.658 ± 0.032
291 K	4.500 ± 0.097	2.393 ± 0.023	3.078 ± 0.037
288 K	2.791 ± 0.035	1.491 ± 0.014	1.863 ± 0.012
285 K	1.907 ± 0.014	0.942 ± 0.008	1.270 ± 0.008
282 K	1.247 ± 0.013	0.547 ± 0.011	0.800 ± 0.009
279 K	0.706 ± 0.014	0.341 ± 0.017	0.496 ± 0.015

	Rate constants *k* for the dealkylation x 10^{-4} [s^{-1}] at T = 288 K	
Intermediate	**3.23a**	**3.23e**
[COT] = 0.03077 mol/L	1.491 ± 0.014	1.863 ± 0.012
[COT] = 0.04615 mol/L	1.767± 0.019	2.383 ± 0.016
[COT] = 0.03077 mol/L	1.818 ± 0.035	2.680 ± 0.028

6 References

(1) Ingold, C. K. *Recl. Trav. Chim. Pays-Bas* **1929**, *48*, 797.

(2) Olah, G. A.; Germain, A.; Lin, H. C.; Forsyth, D. A. *J. Am. Chem. Soc.* **1975**, *97*, 2928.

(3) Olah, G. A.; Klumpp, D. A. *Superelectrophiles and Their Chemistry*; Wiley: New Jersey, **2008**.

(4) Hall, N. F.; Conant, J. B. *J. Am. Chem. Soc.* **1927**, *49*, 3047.

(5) Conant, J. B.; Hall, N. F. *J. Am. Chem. Soc.* **1927**, *49*, 3062.

(6) Gillespie, R. J. *Acc. Chem. Res.* **1968**, *1*, 202.

(7) Olah, G. A.; Prakash, G. K. S.; Sommer, J. *Science* **1979**, *206*, 13.

(8) Kreevoy, M. M.; Baughman, E. H. *J. Am. Chem. Soc.* **1973**, *95*, 8178.

(9) Rosenthal, M. R. *J. Chem. Educ.* **1973**, *50*, 331.

(10) Zhdankin, V. V.; Tykwinski, R.; Berglund, B.; Mullikin, M.; Caple, R.; Zefirov, N. S.; Koz'min, A. S. *J. Org. Chem.* **1989**, *54*, 2609.

(11) Otto, M.; Scheschkewitz, D.; Kato, T.; Midland, M. M.; Lambert, J. B.; Bertrand, G. *Angew. Chem. Int. Ed.* **2002**, *41*, 2275.

(12) Brouwer, D. M.; Kiffen, A. A. *Recl. Trav. Chim. Pays-Bas* **1973**, *92*, 689.

(13) Brouwer, D. M.; Kiffen, A. A. *Recl. Trav. Chim. Pays-Bas* **1973**, *92*, 809.

(14) Brouwer, D. M.; Kiffen, A. A. *Recl. Trav. Chim. Pays-Bas* **1973**, *92*, 906.

(15) Sato, Y.; Yato, M.; Ohwada, T.; Saito, S.; Shudo, K. *J. Am. Chem. Soc.* **1995**, *117*, 3037.

(16) Stang, P. J.; Maas, G.; Smith, D. L.; McCloskey, J. A. *J. Am. Chem. Soc.* **1981**, *103*, 4837.

(17) Schröder, D. *Angew. Chem., Int. Ed.* **2004**, *43*, 1329.

(18) Somisara, D. M. U. K.; Bühl, M.; Lebl, T.; Richardson, N. V.; Slawin, A. M. Z.; Woollins, J. D.; Kilian, P. *Chem. Eur. J.* **2011**, *17*, 2666.

(19) Stasko, D.; Reed, C. A. *J. Am. Chem. Soc.* **2002**, *124*, 1148.

(20) Reed, C. A. *Acc. Chem. Res.* **2009**, *43*, 121.

(21) Zhang, Y.; Reed, C. A. *Dalton Trans.* **2008**, 4392.

(22) Alder, R. W.; Ganter, C.; Harris, C. J.; Orpen, A. G. *J. Chem. Soc., Chem. Commun.* **1992**, 1172.

(23) Weigand, J. J.; Riegel, S. D.; Burford, N.; Decken, A. *J. Am. Chem. Soc.* **2007**, *129*, 7969.

(24) Baraznenok, I. L.; Nenajdenko, V. G.; Balenkova, E. S. *Tetrahedron* **2000**, *56*, 3077.

(25) Stang, P. J.; Anderson, A. G. *J. Org. Chem.* **1976**, *41*, 781.

(26) Stang, P. J.; Hanack, M.; Subramanian, L. R. *Synthesis* **1982**, 85.

(27) Ritter, K. *Synthesis* **1993**, 735.

(28) Martinez, A. G.; Vilar, E. T.; Fraile, A. G.; Fernandez, A. H.; de la Moya Cerero, S.; Jimenez, F. M. *Tetrahedron* **1998**, *54*, 4607.

(29) Martinez, A. G.; Vilar, E. T.; Barcina, J. O.; Alonso, J. M.; Herrero, E. R; Hanack, M.; Subramanian, L. R. *Tetrahedron Lett.* **1992**, *33*, 607.

(30) Martinez, A. G.; Vilar, E. T.; Marin, M. G.; Franco, C. R. *Chem. Ber.* **1985**, *118*, 1282.

(31) Martinez, A. G.; Rios, I. E.; Vilar, E. T. *Synthesis* **1979**, 382.

(32) Martinez, A. G.; Fernandez, A. H.; Jimenez, F. M.; Fraile, A. G.; Subramanian, L. R.; Hanack, M. *J. Org. Chem.* **1992**, *57*, 1627.

(33) Martinez, A. G.; Fernandez, A. H.; Vilchez, D. M.; Gutierrez, M. L. L.; Subramanian, L. R. *Synlett* **1993**, 229.

(34) Martinez, A. G.; Fernandez, A. H.; Alvarez, R. M.; Vilchez, M. D. M.; Gutierrez, M. L. L.; Subramanian, L. R. *Tetrahedron* **1999**, *55*, 4825.

(35) Charette, A.; Chua, P. *Synlett* **1998**, 163.

(36) Charette, A.; Chua, P. *Tetrahedron Lett.* **1997**, *38*, 8499.

(37) Charette, A. B.; Chua, P. *J. Org. Chem.* **1998**, *63*, 908.

(38) Piers, E.; Fleming, F. F. *J. Chem. Soc., Chem. Commun.* **1989**, 756.

(39) Sisti, N. J.; Fowler, F. W.; Grierson, D. S. *Synlett* **1991**, 816.

(40) Sisti, N. J.; Zeller, E.; Grierson, D. S.; Fowler, F. W. *J. Org. Chem.* **1997**, *62*, 2093.

(41) Thomas, E. W. *Synthesis* **1993**, 767.

(42) Banwell, M. G.; Bissett, B. D.; Busato, S.; Cowden, C. J.; Hockless, D. C. R.; Holman, J. W.; Read, R. W.; Wu, A. W. *J. Chem. Soc., Chem. Commun.* **1995**, 2551.

(43) Fodor, G.; Nagubandi, S. *Tetrahedron* **1980**, *36*, 1279.

(44) Martinez, A. G.; Alvarez, R. M.; Barcina, J. O.; de la Moya Cerero, S.; Vilar, E. T.; Fraile, A. G.; Hanack, M.; Subramanian, L. R. *J. Chem. Soc., Chem. Commun.* **1990**, 1571.

(45) Hoornaert, C.; Hesbain-Frisque, A. M.; Ghosez, L. *Angew. Chem., Int. Ed.* **1975**, *14*, 569.

(46) Falmagne, J.-B.; Escudero, J.; Taleb-Sahraoui, S.; Ghosez, L. *Angew. Chem., Int. Ed.* **1981**, *20*, 879.

(47) Schmit, C.; Sahraoui-Taleb, S.; Differding, E.; Dehasse-De Lombaert, C. G.; Ghosez, L. *Tetrahedron Lett.* **1984**, *25*, 5043.

(48) Lindner, E.; von Au, G.; Eberle, H.-J. *Chem. Ber.* **1981**, *114*, 810.

(49) Lindner, E.; Schauß, E. *Chem. Ber.* **1985**, *118*, 4292.

(50) Beard, C. D.; Baum, K.; Grakauskas, V. *J. Org. Chem.* **1973**, *38*, 3673.

(51) Mazur, Y.; Karger, M. H. *J. Org. Chem.* **1971**, *36*, 532.

(52) Netscher, T.; Bohrer, P. *Tetrahedron Lett.* **1996**, *37*, 8359.

(53) Nenajdenko, V. G.; Vertelezkij, P. V.; Balenkova, E. S. *Synthesis* **1997**, 351.

(54) Martinez, A. G.; Fernandez, A. H.; Jimenez, F. M.; Ruiz, P. M.; Subramanian, L. R. *Synlett* **1995**, 161.

(55) Martinez, A. G.; Vilar, E. T.; Garcia Fraile, A.; de la Moya Cerero, S.; Oliva, C. D.; Subramanian, L. R.; Maichle, C. *Tetrahedron: Asymmetry* **1994**, *5*, 949.

(56) Shima, H.; Kobayashi, R.; Nabeshima, T.; Furukawa, N. *Tetrahedron Lett.* **1996**, *37*, 667.

(57) Naka, H.; Maruyama, T.; Sato, S.; Furukawa, N. *Tetrahedron Lett.* **1999**, *40*, 345.

(58) Hammond, G. S.; Neuman, R. C. *J. Phys. Chem.* **1963**, *67*, 1655.

(59) Neuman, R. C.; Hammond, G. S. *J. Phys. Chem.* **1963**, *67*, 1659.

(60) Haake, P.; Watson, J. *J. Org. Chem.* **1970**, *35*, 4063.

(61) Limatibul, S.; Watson, J. *J. Org. Chem.* **1971**, *36*, 3803.

(62) Curphey, T. J.; Prasad, K. S. *J. Org. Chem.* **1972**, *37*, 2259.

(63) Charette, A. B.; Grenon, M. *Can. J. Chem.* **2001**, *79*, 1694.

(64) Charette, A. B.; Mathieu, S.; Martel, J. *Org. Lett.* **2005**, *7*, 5401.

(65) Movassaghi, M.; Hill, M. D. *J. Am. Chem. Soc.* **2006**, *128*, 14254.

(66) Movassaghi, M.; Hill, M. D.; Ahmad, O. K. *J. Am. Chem. Soc.* **2007**, *129*, 10096.

(67) Cui, S.-L.; Wang, J.; Wang, Y.-G. *J. Am. Chem. Soc.* **2008**, *130*, 13526.

(68) Zirngibl, C.; Hedderich, R.; Thauer, R. K. *FEBS Lett.* **1990**, *261*, 112.

(69) Zirngibl, C.; Van Dongen, W.; Schwörer, B.; Von Bünau, R.; Richter, M.; Klein, A.; Thauer, R. K. *Eur. J. Biochem.* **1992**, *208*, 511.

(70) Schleucher, J.; Griesinger, C.; Schwörer, B.; Thauer, R. K. *Biochemistry* **1994**, *33*, 3986.

(71) Lyon, E. J.; Shima, S.; Buurman, G.; Chowdhuri, S.; Batschauer, A.; Steinbach, K.; Thauer, R. K. *Eur. J. Biochem.* **2004**, *271*, 195.

(72) Lyon, E. J.; Shima, S.; Boecher, R.; Thauer, R. K.; Grevels, F.-W.; Bill, E.; Roseboom, W.; Albracht, S. P. J. *J. Am. Chem. Soc.* **2004**, *126*, 14239.

(73) Shima, S.; Lyon, E. J.; Sordel-Klippert, M.; Kauß, M.; Kahnt, J.; Thauer, R. K.; Steinbach, K.; Xie, X.; Verdier, L.; Griesinger, C. *Angew. Chem., Int. Ed.* **2004**, *43*, 2547.

(74) Shima, S.; Pilak, O.; Vogt, S.; Schick, M.; Stagni, M. S.; Meyer-Klaucke, W.; Warkentin, E.; Thauer, R. K.; Ermler, U. *Science* **2008**, *321*, 572.

(75) Hiromoto, T.; Warkentin, E.; Moll, J.; Ermler, U.; Shima, S. *Angew. Chem., Int. Ed.* **2009**, *48*, 6457.

(76) Berkessel, A.; Thauer, R. K. *Angew. Chem., Int. Ed.* **1995**, *34*, 2247.

(77) Corr, M. J.; Gibson, K. F.; Kennedy, A. R.; Murphy, J. A. *J. Am. Chem. Soc.* **2009**, *131*, 9174.

(78) Corr, M. J.; Roydhouse, M. D.; Gibson, K. F.; Zhou, S.-Z.; Kennedy, A. R.; Murphy, J. A. *J. Am. Chem. Soc.* **2009**, *131*, 17980.

(79) Corr, M. J.; Murphy, J. A. *Chem. Soc. Rev.* **2011**, *40*, 2279.

(80) Scullion, C. *PhD Thesis*; University of Strathclyde: Glasgow, **2014**.

(81) Bird, A. P.; Taggart, M. H.; Smith, B. A. *Cell* **1979**, *17*, 889.

(82) Claudia, K. *Biochim. Biophys. Acta* **2005**, *1733*, 53.

(83) Aktas, M.; Wessel, M.; Hacker, S.; Klüsener, S.; Gleichenhagen, J.; Narberhaus, F. *Eur. J. Cell Biol.* **2010**, *89*, 888.

(84) Lister, R.; Pelizzola, M.; Dowen, R. H.; Hawkins, R. D.; Hon, G.; Tonti-Filippini, J.; Nery, J. R.; Lee, L.; Ye, Z.; Ngo, Q.-M.; Edsall, L.; Antosiewicz-Bourget, J.; Stewart, R.; Ruotti, V.; Millar, A. H.; Thomson, J. A.; Ren, B.; Ecker, J. R. *Nature* **2009**, *462*, 315.

(85) Cao, X.; Jacobsen, S. E. *Proc. Natl. Acad. Sci. U. S. A.* **2002**, *99*, 16491.

(86) Antequera, F.; Tamame, M.; Villanueva, J. R.; Santos, T. *J. Biol. Chem.* **1984**, *259*, 8033.

(87) Jones, P. A.; Taylor, S. M. *Cell* **1980**, *20*, 85.

(88) Udenfriend, S.; Dairman, W. *Adv. Enzyme Regul.* **1971**, *9*, 145.

(89) Fontecave, M.; Atta, M.; Mulliez, E. *Trends Biochem. Sci.* **2004**, *29*, 243.

(90) Pai, C. H. *J. Bacteriol.* **1971**, *105*, 793.

(91) Lin, S.; Cronan, J. E. *Mol. Biosyst.* **2011**, *7*, 1811.

(92) Miles, Z. D.; McCarty, R. M.; Molnar, G.; Bandarian, V. *Proc. Natl. Acad. Sci. U. S. A.* **2011**, *108*, 7368.

(93) Kaeberlein, M. *Nat. Cell Biol.* **2009**, *11*, 1277.

(94) Cornforth, J. W.; Reichard, S. A.; Talalay, P.; Carrell, H. L.; Glusker, J. P. *J. Am. Chem. Soc.* **1977**, *99*, 7292.

(95) Austin, R. C.; Lentz, S. R.; Werstuck, G. H. *Cell Death Differ.* **2004**, *11*, 56.

(96) Mosharov, E.; Cranford, M. R.; Banerjee, R. *Biochemistry* **2000**, *39*, 13005.

(97) Banerjee, R. V.; Matthews, R. G. *FASEB J.* **1990**, *4*, 1450.

(98) Gonzalez, J. C.; Banerjee, R. V.; Huang, S.; Sumner, J. S.; Matthews, R. G. *Biochemistry* **1992**, *31*, 6045.

(99) Matthews, R. G.; Smith, A. E.; Zhou, Z. S.; Taurog, R. E.; Bandarian, V.; Evans, J. C.; Ludwig, M. *Helv. Chim. Acta* **2003**, *86*, 3939.

(100) Gonzalez, J. C.; Peariso, K.; Penner-Hahn, J. E.; Matthews, R. G. *Biochemistry* **1996**, *35*, 12228.

(101) Goulding, C. W.; Matthews, R. G. *Biochemistry* **1997**, *36*, 15749.

(102) Peariso, K.; Goulding, C. W.; Huang, S.; Matthews, R. G.; Penner-Hahn, J. E. *J. Am. Chem. Soc.* **1998**, *120*, 8410.

(103) Pejchal, R.; Ludwig, M. L. *PLoS Biol.* **2004**, *3*, e31.

(104) Fu, T.-M.; Almqvist, J.; Liang, Y.-H.; Li, L.; Huang, Y.; Su, X.-D. *J. Mol. Biol.* **2011**, *412*, 688.

(105) Koutmos, M.; Pejchal, R.; Bomer, T. M.; Matthews, R. G.; Smith, J. L.; Ludwig, M. L. *Proc. Natl. Acad. Sci. U. S. A.* **2008**, *105*, 3286.

(106) Ferrer, J.-L.; Ravanel, S.; Robert, M.; Dumas, R. *J. Biol. Chem.* **2004**, *279*, 44235.

(107) Doukov, T. I.; Hemmi, H.; Drennan, C. L.; Ragsdale, S. W. *J. Biol. Chem.* **2007**, *282*, 6609.

(108) Hilhorst, E.; Chen, T. B. R. A.; Iskander, A. S.; Pandit, U. K. *Tetrahedron* **1994**, *50*, 7837.

(109) Taurog, R. E.; Matthews, R. G. *Biochemistry* **2006**, *45*, 5092.

(110) Smith, A. E.; Matthews, R. G. *Biochemistry* **2000**, *39*, 13880.

(111) Schrauzer, G. N.; Windgassen, R. J. *J. Am. Chem. Soc.* **1967**, *89*, 3607.

(112) Wilker, J. J.; Lippard, S. J. *Inorg. Chem.* **1997**, *36*, 969.

(113) Brand, U.; Rombach, M.; Vahrenkamp, H. *Chem. Commun.* **1998**, 2717.

(114) Brand, U.; Rombach, M.; Seebacher, J.; Vahrenkamp, H. *Inorg. Chem.* **2001**, *40*, 6151.

(115) Seebacher, J.; Ji, M.; Vahrenkamp, H. *Eur. J. Inorg. Chem.* **2004**, *2004*, 409.

(116) v. Braun, J. *Ber. Dtsch. Chem. Ges.* **1900**, *33*, 1438.

(117) v. Braun, J. *Ber. Dtsch. Chem. Ges.* **1907**, *40*, 3914.

(118) Flynn, E. H.; Sigal, M. V.; Wiley, P. F.; Gerzon, K. *J. Am. Chem. Soc.* **1954**, *76*, 3121.

(119) Flynn, E. H.; Murphy, H. W.; McMahon, R. E. *J. Am. Chem. Soc.* **1955**, *77*, 3104.

(120) Diels, O.; Fritzsche, P. *Ber. Dtsch. Chem. Ges.* **1911**, *44*, 3018.

(121) Diels, O.; Paquin, M. *Ber. Dtsch. Chem. Ges.* **1913**, *46*, 2000.

(122) Kenner, G. W.; Stedman, R. J. *J. Chem. Soc.* **1952**, 2089.

(123) Hauser, C. R.; Kantor, S. W. *J. Am. Chem. Soc.* **1951**, *73*, 1437.

(124) Anastasia, L.; Cighetti, G.; Allevi, P. *J. Chem. Soc., Perkin Trans. 1* **2001**, 2398.

(125) Khalaf, A. I.; Alvarez, R. G.; Suckling, C. J.; Waigh, R. D. *Tetrahedron* **2000**, *56*, 8567.

(126) Stenmark, H. G.; Brazzale, A.; Ma, Z. *J. Org. Chem.* **2000**, *65*, 3875.

(127) Callahan, B. P.; Wolfenden, R. *J. Am. Chem. Soc.* **2002**, *125*, 310.

(128) Matthews, R. G. *Acc. Chem. Res.* **2001**, *34*, 681.

(129) Archer, M. C.; Scrimgeour, K. G. *Can. J. Biochem.* **1970**, *48*, 278.

(130) Chippel, D.; Scrimgeour, K. G. *Can. J. Biochem.* **1970**, *48*, 999.

(131) Markevicius, A.; *M. Sc. Thesis;* University of Strathclyde: Glasgow, **2010**.

(132) Lloyd-Jones, G. C.; Harvey, J. N.; Hodgson, P.; Murray, M.; Woodward, R. L. *Chem. Eur. J.* **2003**, *9*, 4523.

(133) Charmant, J. P. H.; Lloyd-Jones, G. C.; Peakman, T. M.; Woodward, R. L. *Tetrahedron Lett.* **1998**, *39*, 4733.

(134) Vlietstra, E. J.; Zwikker, J. W.; Nolte, R. J. M.; Drenth, W. *Recl. Trav. Chim. Pays-Bas* **1982**, *101*, 460.

(135) LaPlanche, L. A.; Rogers, M. T. *J. Am. Chem. Soc.* **1964**, *86*, 337.

(136) Headley, A. D.; Nam, J. *J. Mol. Struct.* **2002**, *589–590*, 423.

(137) Quintanilla-Licea, R.; Colunga-Valladares, J.; Caballero-Quintero, A.; Rodriguez-Padilla, C.; Tamez-Guerra, R.; Gomez-Flores, R.; Waksman, N. *Molecules* **2002**, *7*, 662.

(138) Hess, F. K.; Pook, K. H. *Can. J. Chem.* **1969**, *47*, 1151.

(139) Skancke, P. N.; Thomson, C. *J. Mol. Struct.* **1980**, *69*, 241.

(140) Baliah, V.; Aparajithan, K. *Tetrahedron* **1963**, *19*, 2177.

(141) Mandel, J.; Pan, X.; Hay, E. B.; Geib, S. J.; Wilcox, C. S.; Curran, D. P. *J. Org. Chem.* **2013**, *78*, 4083.

(142) Gribble, G. W.; Bousquet, F. P. *Tetrahedron* **1971**, *27*, 3785.

(143) Brown, R. F. C.; Radom, L.; Sternhell, S.; Rae, I. D. *Can. J. Chem.* **1968**, *46*, 2577.

(144) Bartels-Keith, J. R.; Cieciuch, R. F. W. *Can. J. Chem.* **1968**, *46*, 2593.

(145) Ribera, A.; Rico, M. *Tetrahedron Lett.* **1968**, *9*, 535.

(146) Siddall III, T. H.; Stewart, W. E. *J. Mol. Spectrosc.* **1967**, *24*, 290.

(147) Zanger, M.; Simons, W. W.; Gennaro, A. R. *J. Org. Chem.* **1968**, *33*, 3673.

(148) Williams, D. H.; Fleming, I. *Spectroscopic Methods in Organic Chemistry*; 4. Ed. rev. ed.; McGraw-Hill Book Company: London, **1989**.

(149) Alder, R. W.; Blake, M. E.; Bufali, S.; Butts, C. P.; Orpen, A. G.; Schutz, J.; Williams, S. J. *J. Chem. Soc., Perkin Trans. 1* **2001**, 1586.

(150) Kovacevic, L. S.; Idziak, C.; Markevicius, A.; Scullion, C.; Corr, M. J.; Kennedy, A. R.; Tuttle, T.; Murphy, J. A. *Angew. Chem., Int. Ed.* **2012**, *124*, 8644.

(151) Frisch, M. J.; Trucks, G. W.; Schlegel, H. B.; Scuseria, G. E.; Robb, M. A.; Cheeseman, J. R.; Scalmani, G.; Barone, V.; Mennucci, B.; Petersson, G. A.; Nakatsuji, H.; Caricato, M.; Li, X.; Hratchian, H. P.; Izmaylov, A. F.; Bloino, J.; Zheng, G.; Sonnenberg, J. L.; Hada, M.; Ehara, M.; Toyota, K.; Fukuda, R.; Hasegawa, J.; Ishida, M.; Nakajima, T.; Honda, Y.; Kitao, O.; Nakai, H.; Vreven, T.; Montgomery, J., J. A.; Peralta, J. E.; Ogliaro, F.; Bearpark, M.; Heyd, J. J.; Brothers, E.; Kudin, K. N.; Staroverov, V. N.; Kobayashi, R.; Normand, J.; Raghavachari, K.; Rendell, A.; Burant, J. C.; Iyengar, S. S.; Tomasi, J.; Cossi, M.; Rega, N.; Millam, J. M.; Klene, M.; Knox, J. E.; Cross, J. B.; Bakken, V.; Adamo, C.; Jaramillo, J.; Gomperts, R.; Stratmann, R. E.; Yazyev, O.; Austin, A. J.; Cammi, R.; Pomelli, C.; Ochterski, J. W.; Martin, R. L.; Morokuma, K.; Zakrzewski, V. G.; Voth, G. A.; Salvador, P.; Dannenberg, J. J.; Dapprich, S.; Daniels, A. D.; Farkas, O.; Foresman, J. B.; Ortiz, J. V.; Cioslowski, J.; Fox, D. J.; Gaussian, Inc.: Wallingford, CT, 2009.

(152) Clayden, J.; Greeves, N.; Warren, S.; Wothers, P. *Organic Chemistry*; OUP: Oxford, 2001.

(153) Furukawa, N.; Kobayashi, K.; Sato, S. *J. Organomet. Chem.* **2000**, *611*, 116.

(154) Lu, C.; Su, X.; Floreancig, P. E. *J. Org. Chem.* **2013**, *78*, 9366.

(155) Kice, J. L.; Scriven, R. L.; Koubek, E.; Barnes, M. *J. Am. Chem. Soc.* **1970**, *92*, 5608.

(156) Karamertzanis, P. G.; Price, S. L. *J. Phys. Chem. B* **2005**, *109*, 17134.

(157) Booth, B. L.; Jibodu, K. O.; Proenca, M. F. J. R. P. *J. Chem. Soc., Perkin Trans. 1* **1983**, 1067.

(158) Tsvelikhovsky, D.; Buchwald, S. L. *J. Am. Chem. Soc.* **2011**, *133*, 14228.

(159) Maas, G.; Stang, P. J. *J. Org. Chem.* **1981**, *46*, 1606.

(160) Nenajdenko, V. G.; Vertelezkij, P. V.; Koldobskij, A. B.; Alabugin, I. V.; Balenkova, E. S. *J. Org. Chem.* **1997**, *62*, 2483.

(161) Lodeiro, S.; Xiong, Q.; Wilson, W. K.; Kolesnikova, M. D.; Onak, C. S.; Matsuda, S. P. T. *J. Am. Chem. Soc.* **2007**, *129*, 11213.

(162) Yoder, R. A.; Johnston, J. N. *Chem. Rev.* **2005**, *105*, 4730.

(163) Christianson, D. W. *Chem. Rev.* **2006**, *106*, 3412.

(164) Cori, O.; Chayet, L.; Perez, L. M.; Bunton, C. A.; Hachey, D. *J. Org. Chem.* **1986**, *51*, 1310.

(165) Saha, A.; Ranu, B. C. *Tetrahedron Lett.* **2010**, *51*, 1902.

(166) Pettersson, H.; Bülow, A.; Ek, F.; Jensen, J.; Ottesen, L. K.; Fejzic, A.; Ma, J.-N.; Del Tredici, A. L.; Currier, E. A.; Gardell, L. R.; Tabatabaei, A.; Craig, D.; McFarland, K.; Ott, T. R.; Piu, F.; Burstein, E. S.; Olsson, R. *J. Med. Chem.* **2009**, *52*, 1975.

(167) Galli, C. *Chem. Rev.* **1988**, *88*, 765.

(168) Patai, S. *The Chemistry of Amino, Nitroso, Nitro and Related Groups*; Wiley: New Jersey, **1996**.

(169) Beletskaya, I. P.; Sigeev, A. S.; Peregudov, A. S.; Petrovskii, P. V. *Synthesis* **2007**, 2534.

(170) Beadle, J. R.; Korzeniowski, S. H.; Rosenberg, D. E.; Garcia-Slanga, B. J.; Gokel, G. W. *J. Org. Chem.* **1984**, *49*, 1594.

(171) Molinaro, C.; Mowat, J.; Gosselin, F.; O'Shea, P. D.; Marcoux, J.-F.; Angelaud, R.; Davies, I. W. *The Journal of Organic Chemistry* **2007**, *72*, 1856.

(172) Claramunt, R. M.; Dotor, J.; Sanz, D.; Foces-Foces, C.; Llamas-Saniz, A. L.; Elguero, J.; Flammang, R.; Morizur, J. P.; Chapon, E.; Tortajada, J. *Helv. Chim. Acta* **1994**, *77*, 121.

(173) Frampton, C. S.; Parkes, K. E. B. *Acta Crystallogr., Sect. C: Cryst. Struct. Commun.* **1996**, *52*, 3246.

(174) Voss, T.; Mahdi, T.; Otten, E.; Fröhlich, R.; Kehr, G.; Stephan, D. W.; Erker, G. *Organometallics* **2012**, *31*, 2367.

(175) Wurster, C.; Sendtner, R. *Ber. Dtsch. Chem. Ges.* **1879**, *12*, 1803.

(176) Störle, C.; Eyer, P. *Chem.-Biol. Interact.* **1991**, *78*, 333.

(177) Phillies, G. D. J.; Stanley, H. E. *J. Am. Chem. Soc.* **1976**, *98*, 3892.

(178) Störle, C.; Eyer, P. *Chem.-Biol. Interact.* **1991**, *78*, 321.

(179) Michaelis, L.; Schubert, M. P.; Granick, S. *J. Am. Chem. Soc.* **1939**, *61*, 1981.

(180) Barth, T.; Krieger, G.; Staab, H. A.; Neugebauer, F. A. *J. Chem. Soc., Chem. Commun.* **1993**, 1129.

(181) Hünig, S.; Richters, P. *Chem. Ber.* **1958**, *91*, 442.

(182) Pott, G. T.; Kommandeur, J. *J. Chem. Phys.* **1967**, *47*, 395.

(183) Washburn, E. W.; *International Critical Tables of Numerical Data, Physics, Chemistry and Technology*; Knovel: New York, **1921**.

(184) Zhang, L.; Su, J.-H.; Wang, S.; Wan, C.; Zha, Z.; Du, J.; Wang, Z. *Chem. Commun.* **2011**, *47*, 5488.

(185) Hamanoue, K.; Nakayama, T.; Ibuki, K.; Otani, A. *J. Chem. Soc., Faraday Trans.* **1991**, *87*, 3731.

(186) Sforza, S.; Dossena, A.; Corradini, R.; Virgili, E.; Marchelli, R. *Tetrahedron Lett.* **1998**, *39*, 711.

(187) Stephan, D. W.; Erker, G. *Angew. Chem., Int. Ed.* **2010**, *49*, 46.

(188) Spikes, G. H.; Fettinger, J. C.; Power, P. P. *J. Am. Chem. Soc.* **2005**, *127*, 12232.

(189) Olah, G. A.; Farooq, O.; Farnia, S. M. F.; Olah, J. A. *J. Am. Chem. Soc.* **1988**, *110*, 2560.

(190) Zhao, Y.; Truhlar, D. *Theor. Chem. Acc.* **2008**, *120*, 215.

(191) Barone, V.; Cossi, M. *J. Phys. Chem. A* **1998**, *102*, 1995.

(192) Spartan `04, Wavefunction, Inc.: Irvine, CA.

(193) Spartan `10, Wavefunction, Inc.: Irvine, CA.

(194) Sheldrick, G. *Acta Crystallogr., Sect. A: Found. Crystallogr.* **2008**, *64*, 112.

(195) The PyMOL Molecular Graphics System, Version 1.5.0.4, Schrödinger, LLC.

(196) Cox, C.; Wack, H.; Lectka, T. *Angew. Chem., Int. Ed.* **1999**, *38*, 798.

(197) Nair, M. D.; Adams, R. *J. Am. Chem. Soc.* **1961**, *83*, 3518.

(198) Meth-Cohn, O.; Suschitzky, H. *J. Chem. Soc.* **1963**, 4666.

(199) Brunet, P.; Wuest, J. D. *Can. J. Chem.* **1996**, *74*, 689.

(200) Saito, I.; Abe, S.; Takahashi, Y.; Matsuura, T. *Tetrahedron Lett.* **1974**, *15*, 4001.

(201) Antilla, J. C.; Baskin, J. M.; Barder, T. E.; Buchwald, S. L. *The Journal of Organic Chemistry* **2004**, *69*, 5578.

(202) Kobayashi, K.; Irisawa, S.; Matoba, T.; Matsumoto, T.; Yoneda, K.; Morikawa, O.; Konishi, H. *Bull. Chem. Soc. Jpn.* **2001**, *74*, 1109.

(203) Raines, S.; Chai, S. Y.; Palopoli, F. P. *J. Heterocycl. Chem.* **1976**, *13*, 711.

(204) Bacon, R. G. R.; Stewart, O. J. *J. Chem. Soc.* **1969**, 301.

(205) Serve, D. *Bull. Soc. Chim. Fr.* **1976**, 1567.

(206) Kirai, N.; Yamamoto, Y. *Eur. J. Org. Chem.* **2009**, 1864.

(207) Mendel, A. *J. Org. Chem.* **1966**, *31*, 3445.

(208) Maji, M.; Chatterjee, M.; Chattopadhyay, S. K.; Ghosh, S. *Acta Chem. Scand.* **1999**, *53*, 253.

(209) Di Nunno, L.; Scilimati, A. *Tetrahedron* **1986**, *42*, 3913.

(210) Ainpour, P.; Heimer, N. E. *J. Org. Chem.* **1978**, *43*, 2061.

(211) Nadeem, S.; Munawar, M. A.; Ahmad, S.; Smiglak, M.; Drab, D. M.; Malik, K. I.; Amjad, R.; Ashraf, C. M.; Rogers, R. D. *ARKIVOC* **2010**, *2010*, 19.

(212) Hucher, N.; Decroix, B.; Daïch, A. *J. Org. Chem.* **2001**, *66*, 4695.

(213) Goetz, F. J. *J. Heterocycl. Chem.* **1967**, *4*, 80.

(214) Yale, H. L.; Beer, B.; Pluscec, J.; Spitzmiller, E. R. *J. Med. Chem.* **1970**, *13*, 713.

(215) Dowerah, D.; Spence, J. T.; Singh, R.; Wedd, A. G.; Wilson, G. L.; Farchione, F.; Enemark, J. H.; Kristofzski, J.; Bruck, M. *J. Am. Chem. Soc.* **1987**, *109*, 5655.

(216) Snyder, S. A.; Treitler, D. S. *Angew. Chem. Int. Ed.* **2009**, *48*, 7899.

(217) Reeves, W. P.; Bothwell, T. C.; Rudis, J. A.; McClusky, J. V. *Synth. Commun.* **1982**, *12*, 1071.

(218) Tercio, J.; Ferreira, B.; Simonelli, F.; Comasseto, J. V. *Synth. Commun.* **1986**, *16*, 1335.

(219) E.-Subbagh, H. I.; Abadi, A. H.; Al-Khawad, L. E.; Al-Rashood, K. A. *Arch. Pharm.* **1999**, *332*, 19.

(220) Hunziker, F.; Künzle, F.; Schindler, O.; Schmutz, J. *Helv. Chim. Acta* **1964**, *47*, 1163.

(221) Hisaoka, M.; Akiba, K.-y.; Inamoto, N. *Bull. Chem. Soc. Jpn.* **1975**, *48*, 3274.

(222) Christensen, J. B.; Schiodt, N.-C.; Bechgaard, K.; Buch-Rasmussen, T. *Acta Chem. Scand.* **1996**, *50*, 1013.

7 Appendices

In the following, for each kinetic run a table of raw data is first shown including temperature, NMR folder number and TOPSPIN's internal phasing values (sr, phc0, phc1). Furthermore, the first column contains the integrals and the range of the respective integral for the observed peaks. The peaks observed correspond to the NMR standard COT, the amide proton peak (methine proton in **3.21a** and methyl proton in **3.23a** and **3.23e**) and a background noise integral, which is subtracted from the intermediate's integral to produce a corrected integral.

A typical calculation for the concentration of the intermediate is shown for kinetic run A1 at 279 K at t = 0 sec: $\ln((I_H - E_{avg})/N_H \times C_{COT}) = \ln((1.18619-0.05202)/1 \times 0.03077\ mol/L) = -3.355316218$

I_H: Integral of the intermediate proton

E_{avg}: average error (background noise)

N_H: number of protons observed (methine proton in **3.21a**: 1; methyl protons in **3.23a**/**3.23e**: 3)

C_{COT}: concentration of the internal standard cyclooctatetraene (COT)

Note: Data points faded in the plots (ln [intermediate] vs. time) and shaded in the boxes of the tables were not used for calculations of the kinetic parameters.

Kinetic data for compound **3.21a** at 279K ([COT] = 0.03077 mol/L)

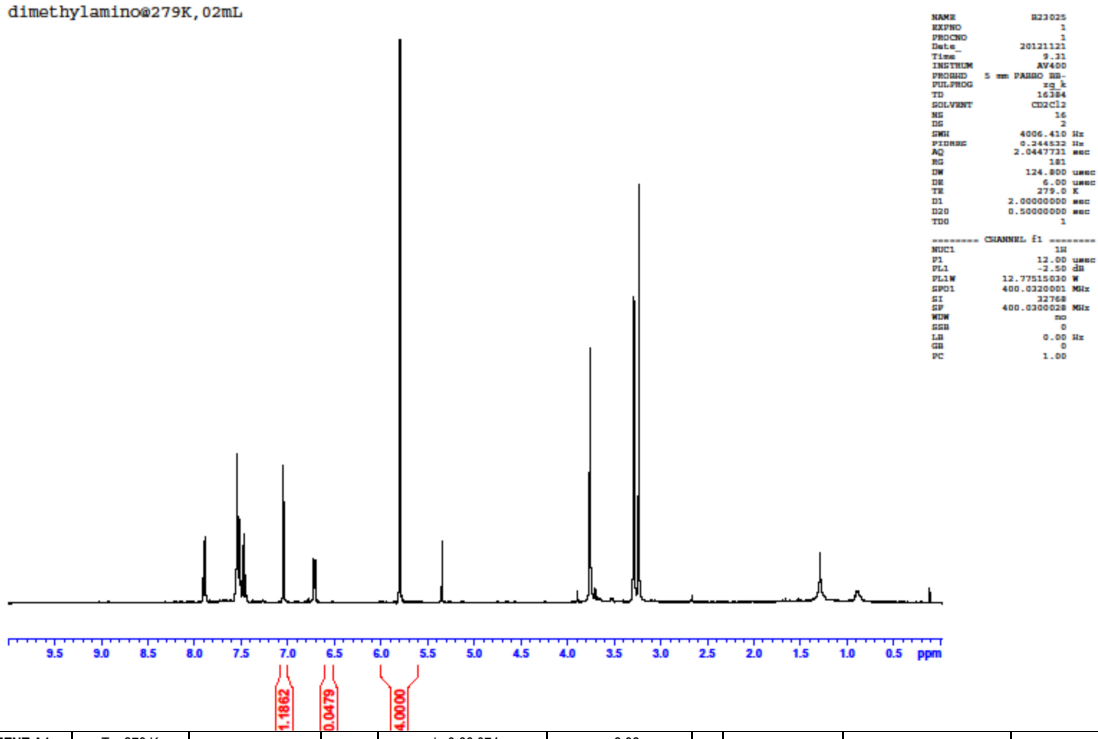

EXPERIMENT A1	T = 279 K			phc0 66.074	sr 2.82				
FOLDER 23025				phc1 -5.802					
INTEGRALS normalised				INTEGRALS			LN OF INTEGRALS		
NCHOTfN	error (noise)	standard (COT)		NCHOTfN	NCHOTfN		NCHOTfN	NCHOTfN	NCHOTfN
7.08-7.00 ppm	6.6-6.52 ppm	6.0-5.6 ppm	Time [sec]	corr. by variable error	corr. by avg. error		uncorrected	corr. by variable error	corr. by avg. error
1.18619	0.047931	4	0	1.138259	1.134167		0.17074649	0.129499902	0.125898872
1.119378483	0.044483501	4	374	1.074894981	1.067356		0.112773605	0.072222965	0.065184514
1.010384809	0.051414168	4	748	0.958970641	0.958362		0.010331258	-0.041894819	-0.042529414
1.050347538	0.045519299	4	1122	1.004828239	0.998325		0.049121098	0.00481662	-0.001676401
1.019694479	0.045888733	4	1496	0.973805746	0.967672		0.019503052	-0.026543434	-0.032862149
0.998686996	0.044978894	4	1870	0.953708102	0.946664		-0.001313867	-0.047397627	-0.054810566
0.971130835	0.046824056	4	2244	0.924306778	0.919108		-0.029294078	-0.078711251	-0.084351317
0.911936251	0.051844777	4	2618	0.860091475	0.859914		-0.092185191	-0.150716529	-0.150923223
0.923368106	0.049309946	4	2992	0.87405816	0.871346		-0.079727309	-0.134608361	-0.137716627
0.905648818	0.049106041	4	3366	0.856542777	0.853626		-0.099103666	-0.154851018	-0.158261787
0.873132688	0.05401884	4	3740	0.819113848	0.82111		-0.135667743	-0.199532196	-0.197098007
0.871289865	0.05067731	4	4114	0.820612555	0.819267		-0.137780562	-0.197704199	-0.199344837
0.85361452	0.052281443	4	4488	0.801333077	0.801592		-0.158275569	-0.221478591	-0.221155546
0.831076773	0.05398756	4	4862	0.777089213	0.779054		-0.185033102	-0.252200118	-0.249674608
0.79389669	0.056142345	4	5236	0.737754346	0.741874		-0.230801939	-0.304144375	-0.29857565
0.791941171	0.053203922	4	5610	0.738737249	0.739919		-0.233268169	-0.302812971	-0.301215049
0.772262962	0.054254364	4	5984	0.718008597	0.72024		-0.258430163	-0.331273736	-0.328170195
0.725884924	0.060246684	4	6358	0.66563824	0.673862		-0.320363784	-0.407008939	-0.394729358
0.726750126	0.055209501	4	6732	0.671540625	0.674728		-0.319172567	-0.398180766	-0.393446237
0.692510895	0.058911476	4	7106	0.633599419	0.640488		-0.367431308	-0.456338355	-0.445524329
0.690773092	0.055530429	4	7480	0.635242663	0.638751		-0.369943885	-0.453748207	-0.448241263
0.673943073	0.054424033	4	7854	0.61951904	0.621921		-0.394609634	-0.478811844	-0.474942946
0.65395383	0.054909205	4	8228	0.599044626	0.601931		-0.424718526	-0.512419184	-0.507611966
0.636472605	0.05483911	4	8602	0.581633495	0.58445		-0.451813902	-0.541914764	-0.537083923
0.618846294	0.054626709	4	8976	0.564219585	0.566824		-0.47989835	-0.572311769	-0.567706852
	average error								
	0.052022534								

Experiment A1	NMR entry	Time [sec]	Std COT 5.8 ppm, Integral=4	Integral NCHOTfN (7.0 ppm)	Time [sec]	[OTf IM]	LN[OTf IM]
Folder B23025	1	0	4	1.134167466	0	0.03490	-3.355316218
T = 279 K	2	374	4	1.067355949	374	0.03284	-3.416030575
0.2 mL Stk sol	3	748	4	0.958362275	748	0.02949	-3.523744504
0.05 mL Tf2O	4	1122	4	0.998325004	1122	0.03072	-3.48289149
0.4 mL d2-DCM	5	1496	4	0.967671945	1496	0.02978	-3.514077238
	6	1870	4	0.946664462	1870	0.02913	-3.536025655
V(sample) = 0.65 mL	7	2244	4	0.919108301	2244	0.02828	-3.565566407
n(COT) = 0.02 mmol	8	2618	4	0.859913718	2618	0.02646	-3.632138313
c(COT) = 0.03077	9	2992	4	0.871345573	2992	0.02681	-3.618931717
c(amide) = 0.06154	10	3366	4	0.853626284	3366	0.02627	-3.639476877
	11	3740	4	0.821110155	3740	0.02527	-3.678313097
	12	4114	4	0.819267331	4114	0.02521	-3.680559926
	13	4488	4	0.801591986	4488	0.02466	-3.702370635
	14	4862	4	0.77905424	4862	0.02397	-3.730889698
	15	5236	4	0.741874157	5236	0.02283	-3.77979074
	16	5610	4	0.739918637	5610	0.02277	-3.782430139
	17	5984	4	0.720240428	5984	0.02216	-3.809385284
	18	6358	4	0.67386239	6358	0.02073	-3.875944447
	19	6732	4	0.674727592	6732	0.02076	-3.874661327
	20	7106	4	0.640488361	7106	0.01971	-3.926739419
	21	7480	4	0.638750558	7480	0.01965	-3.929456353
	22	7854	4	0.621920539	7854	0.01914	-3.956158035
	23	8228	4	0.601931296	8228	0.01852	-3.988827055
	24	8602	4	0.584450072	8602	0.01798	-4.018299012
	25	8976	4	0.56682376	8976	0.01744	-4.048921942
slope	-7.05177E-05	-3.406313354	y-intercept				
slope uncertainty	1.36143E-06	0.007595067	y-intercept uncertainty				
R2 value	0.992600562	0.015151684	s(y)				
F	2682.908038	20	degrees of freedom				
regression ss	0.615924669	0.004591471	residual ss				
k_{LSK355}(279 K) [s-1]							
7.052 ± 0.136 x 10-5							

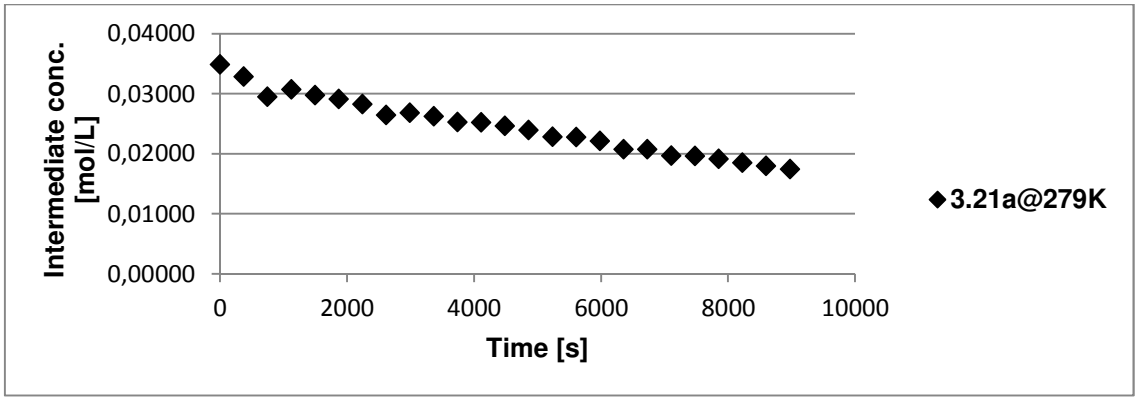

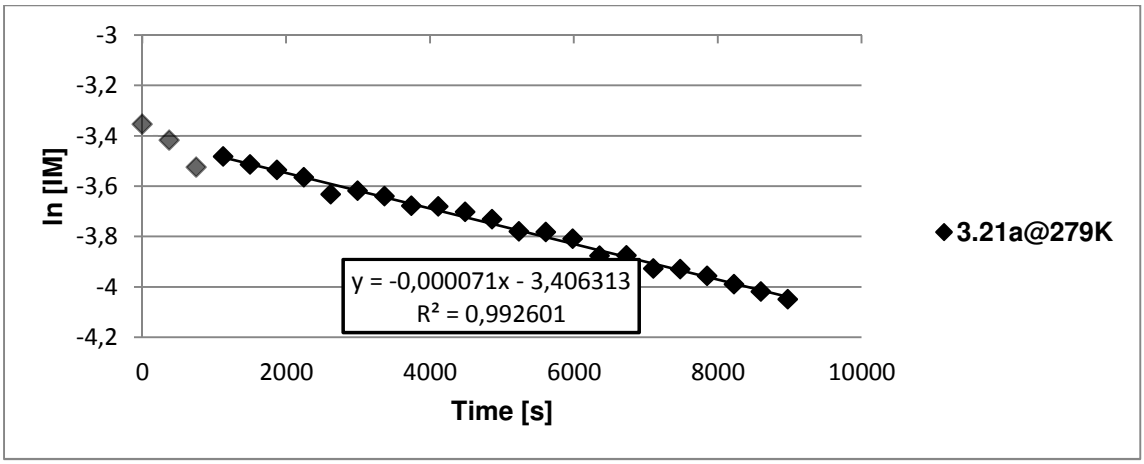

Kinetic data for compound **3.21a** at 282K ([COT] = 0.03077 mol/L)

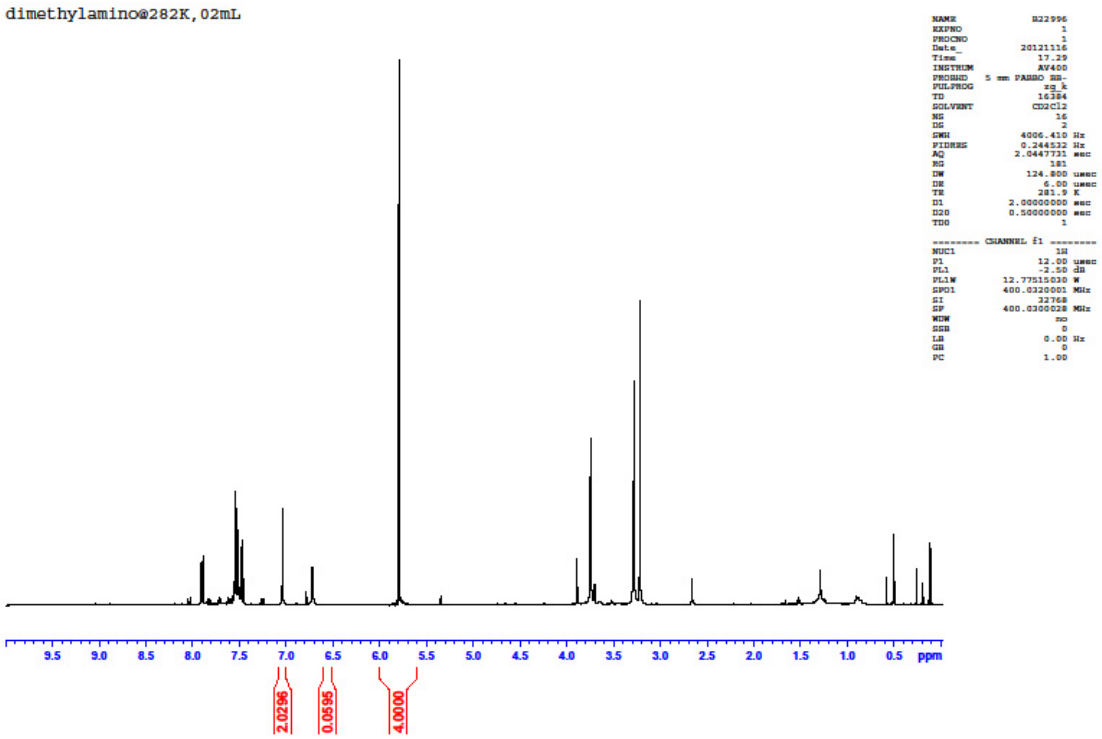

EXPERIMENT A2	T = 282 K			phc0 68.220	sr 2.82				
FOLDER 22996				phc1 -9.572					
INTEGRALS normalised				INTEGRALS			LN OF INTEGRALS		
NCHOTfN	error (noise)	standard (COT)		NCHOTfN	NCHOTfN		NCHOTfN	NCHOTfN	NCHOTfN
7.08-7.00 ppm	6.6-6.52 ppm	6.0-5.6 ppm	Time [sec]	corr. by variable error	corr. by avg. error		uncorrected	corr. by variable error	corr. by avg. error
2.02964	0.059491	4	0	1.970149	1.953185432		0.707858437	0.678109174	0.669461595
1.902795131	0.054694418	4	374	1.848100713	1.826340563		0.643323927	0.61415847	0.602314273
1.830357404	0.05504769	4	748	1.775309715	1.753902836		0.604511251	0.573974895	0.561843497
1.696070545	0.059964832	4	1122	1.636105713	1.619615976		0.528314131	0.492318853	0.48218907
1.649369729	0.061358612	4	1496	1.588011117	1.572915161		0.500393232	0.462482363	0.452930688
1.569979134	0.064218849	4	1870	1.505760285	1.493524565		0.451062329	0.409297943	0.401138807
1.488055236	0.070605051	4	2244	1.417450185	1.411600668		0.397470057	0.348859613	0.344724286
1.468273309	0.062520478	4	2618	1.405752831	1.391818741		0.384087091	0.340572982	0.330611338
1.364691176	0.066956602	4	2992	1.297734574	1.288236608		0.310928159	0.260620109	0.253274313
1.323128324	0.072306227	4	3366	1.250822097	1.246673756		0.279998875	0.223801013	0.220479009
1.244681433	0.076939359	4	3740	1.167742074	1.168226865		0.21887962	0.155072033	0.155487099
1.207431897	0.080552916	4	4114	1.126878982	1.130977329		0.188495705	0.119451848	0.123082152
1.154030872	0.084663206	4	4488	1.069367666	1.077576303		0.143260919	0.067067507	0.074714356
1.11714886	0.077319189	4	4862	1.03982967	1.040694291		0.110779779	0.039056921	0.039888078
1.05785568	0.080287688	4	5236	0.977567992	0.981401112		0.056243916	-0.022687432	-0.018774022
1.042032253	0.082366359	4	5610	0.959665894	0.965577685		0.041172896	-0.041170082	-0.035028719
0.963921933	0.084738848	4	5984	0.879183086	0.887467365		-0.03674497	-0.128762115	-0.11938353
0.922478133	0.086485012	4	6358	0.835993121	0.846023565		-0.080691607	-0.179134894	-0.167208065
0.895962017	0.08511261	4	6732	0.810849407	0.819507449		-0.109857258	-0.20967293	-0.199051791
0.84648501	0.090212474	4	7106	0.756272536	0.770030442		-0.166662786	-0.27935347	-0.26132523
0.829743909	0.089980808	4	7480	0.739763101	0.753289341		-0.186638169	-0.301425278	-0.283305874
0.805381857	0.090816972	4	7854	0.714564885	0.728927289		-0.216438757	-0.336081474	-0.316181293
0.76701595	0.090516401	4	8228	0.676499549	0.690561382		-0.265247683	-0.390823497	-0.370250415
0.742054952	0.093639279	4	8602	0.648415674	0.665600384		-0.298331979	-0.433223316	-0.407065812
0.731117338	0.090569325	4	8976	0.640548013	0.65466277		-0.313181315	-0.445431199	-0.423635031
	average error								
	0.076454568								

Experiment A2	NMR entry	Time [sec]	Std COT 5.8 ppm, Integral=4	Integral NCHOTfN (7.0 ppm)	Time [sec]	[OTf IM]	LN[OTf IM]
Folder B22996	1	0	4	1.95319	0	0.06010	-2.811753495
T = 282K	2	374	4	1.826340563	374	0.05620	-2.878900817
0.2 mL Stk sol	3	748	4	1.753902836	748	0.05397	-2.919371593
0.05 mL Tf2O	4	1122	4	1.619615976	1122	0.04984	-2.99902602
0.4 mL d2-DCM	5	1496	4	1.572915161	1496	0.04840	-3.028284402
	6	1870	4	1.493524565	1870	0.04596	-3.080076283
V(sample)= 0.65 mL	7	2244	4	1.411600668	2244	0.04343	-3.136490804
n(COT) = 0.02 mmol	8	2618	4	1.391818741	2618	0.04283	-3.150603751
c(COT) = 0.03077	9	2992	4	1.288236608	2992	0.03964	-3.227940777
c(amide) = 0.06154	10	3366	4	1.246673756	3366	0.03836	-3.260736081
	11	3740	4	1.168226865	3740	0.03595	-3.32572799
	12	4114	4	1.130977329	4114	0.03480	-3.358132938
	13	4488	4	1.077576303	4488	0.03316	-3.406500734
	14	4862	4	1.040694291	4862	0.03202	-3.441327011
	15	5236	4	0.981401112	5236	0.03020	-3.499989112
	16	5610	4	0.965577685	5610	0.02971	-3.516243809
	17	5984	4	0.887467365	5984	0.02731	-3.60059862
	18	6358	4	0.846023565	6358	0.02603	-3.648423155
	19	6732	4	0.819507449	6732	0.02522	-3.680266881
	20	7106	4	0.770030442	7106	0.02369	-3.74254032
	21	7480	4	0.753289341	7480	0.02318	-3.764520964
	22	7854	4	0.728927289	7854	0.02243	-3.797396382
	23	8228	4	0.690561382	8228	0.02125	-3.851465505
	24	8602	4	0.665600384	8602	0.02048	-3.888280902
	25	8976	4	0.65466277	8976	0.02014	-3.904850121
slope	-0.000122777	-2.845752912	y-intercept				
slope uncertainty	1.33455E-06	0.006987705	y-intercept uncertainty				
R2 value	0.99728992	0.017996091	s(y)				
F	8463.833971	23	degrees of freedom				
regression ss	2.741091351	0.007448764	residual ss				
k_{LSK355}(282 K) [s-1]							
1.228 ± 0.013 x 10-4							

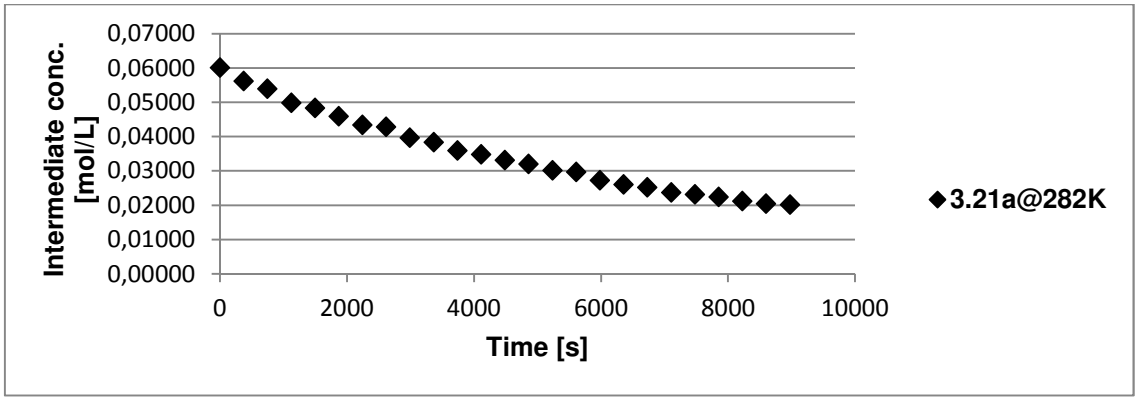

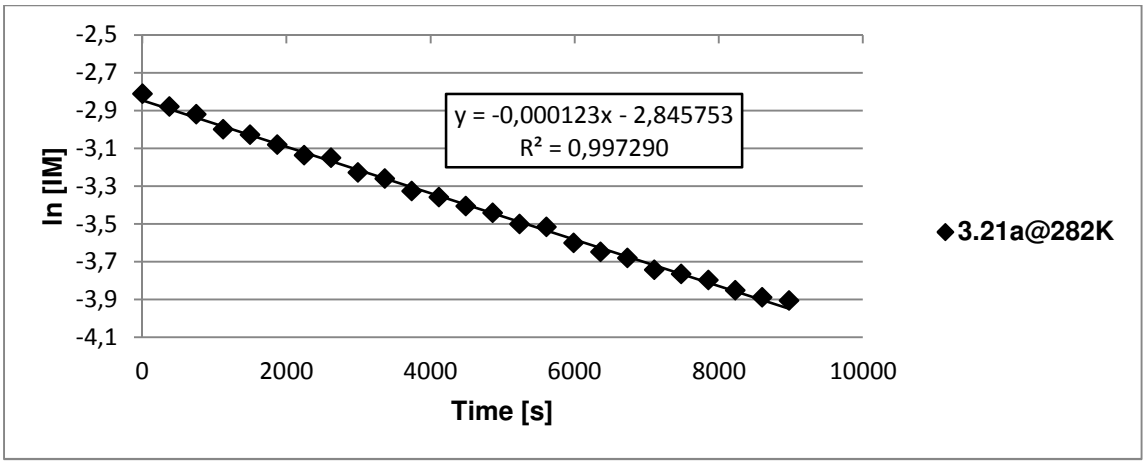

Kinetic data for compound **3.21a** at 285K ([COT] = 0.03077 mol/L)

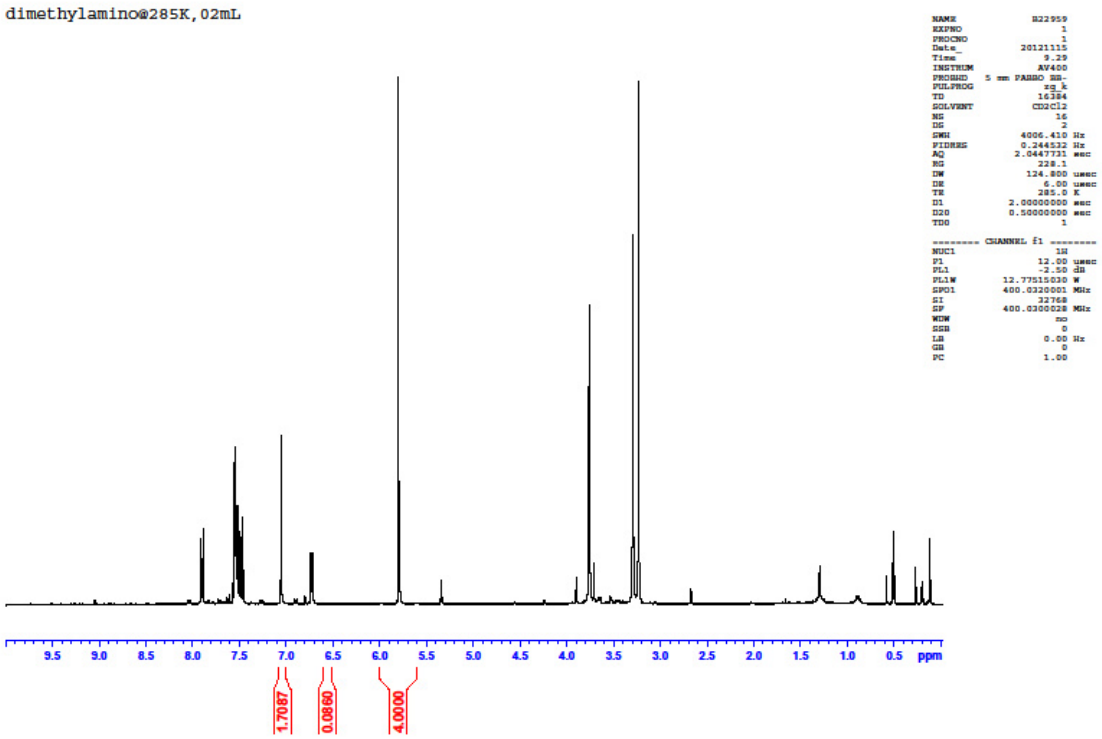

EXPERIMENT A3	T = 285 K			phc0 206.366	sr 2.82				
FOLDER 22959				phc1 -13.307					
INTEGRALS normalised				INTEGRALS			LN OF INTEGRALS		
NCHOTfN	error (noise)	standard (COT)		NCHOTfN	NCHOTfN		NCHOTfN	NCHOTfN	NCHOTfN
7.08-7.00 ppm	6.6-6.52 ppm	6.0-5.6 ppm	Time [sec]	corr. by variable error	corr. by avg. error		uncorrected	corr. by variable error	corr. by avg. error
1.70872	0.086029	4	0	1.622691	1.61496275		0.535744552	0.484085882	0.479311891
1.621653738	0.083738622	4	374	1.537915117	1.527896488		0.483446455	0.430427679	0.423891945
1.5161037	0.08681062	4	748	1.42929308	1.42234645		0.416143689	0.357179972	0.352307938
1.423745979	0.088418442	4	1122	1.335327537	1.329988729		0.353291412	0.289176608	0.285170468
1.331224904	0.087863614	4	1496	1.243361291	1.237467654		0.286099499	0.217818431	0.213067077
1.211031051	0.112517412	4	1870	1.09851364	1.117273801		0.191472105	0.093958029	0.110891612
1.150244352	0.097374168	4	2244	1.052870184	1.056487102		0.1399744	0.051519943	0.05494935
1.07977569	0.093519725	4	2618	0.986255965	0.98601844		0.076753325	-0.013839359	-0.014080223
1.006089454	0.09214941	4	2992	0.913940044	0.912332204		0.006070989	-0.089990307	-0.091751096
0.93807454	0.095270097	4	3366	0.842804443	0.84431729		-0.063925866	-0.171020325	-0.169226919
0.877017305	0.094060255	4	3740	0.78295705	0.783260055		-0.131228555	-0.244677438	-0.244290512
0.820095704	0.09607391	4	4114	0.724021793	0.726338454		-0.198334234	-0.322933786	-0.319739183
0.76700673	0.097041317	4	4488	0.669965413	0.673249481		-0.265259703	-0.40052919	-0.395639319
0.718584162	0.094371806	4	4862	0.624212355	0.624826912		-0.330472445	-0.471264656	-0.470280609
0.701121219	0.098536149	4	5236	0.60258507	0.607363969		-0.355074484	-0.506526429	-0.498627048
0.636722962	0.094058962	4	5610	0.542664	0.542965712		-0.451420629	-0.611264935	-0.610709106
0.594384397	0.096052249	4	5984	0.498332148	0.500627147		-0.520229035	-0.69648846	-0.691893672
0.563607528	0.095374202	4	6358	0.468233325	0.469850278		-0.573397142	-0.758788549	-0.755341193
0.532209402	0.093275343	4	6732	0.438934059	0.438452152		-0.630718254	-0.823406085	-0.82450459
0.50693393	0.092532901	4	7106	0.41440103	0.41317668		-0.679374599	-0.880921104	-0.88387998
0.479790629	0.094199967	4	7480	0.385590663	0.386033379		-0.734405459	-0.952978932	-0.951831438
0.456304658	0.092515136	4	7854	0.363789522	0.362547408		-0.784594584	-1.011179816	-1.014600034
0.437373325	0.094257708	4	8228	0.343115616	0.343616075		-0.826968159	-1.069687815	-1.068230307
0.415022034	0.0923284	4	8602	0.322693633	0.321264784		-0.879423667	-1.131051909	-1.135489624
0.395809645	0.095561831	4	8976	0.300247814	0.302052395		-0.926821877	-1.203147099	-1.197154782
	average error								
	0.09375725								

Experiment A3	NMR entry	Time [sec]	Std COT 5.8 ppm, Integral=4	Integral NCHOTfN (7.0 ppm)	Time [sec]	[OTf IM]	LN[OTf IM]
Folder B22959	1	0	4	1.61496	0	0.04969	-3.001903198
T = 285K	2	374	4	1.527896488	374	0.04701	-3.057323144
0.2 mL Stk sol	3	748	4	1.42234645	748	0.04377	-3.128907152
0.05 mL Tf2O	4	1122	4	1.329988729	1122	0.04092	-3.196044622
0.4 mL d2-DCM	5	1496	4	1.237467654	1496	0.03808	-3.268148012
	6	1870	4	1.117273801	1870	0.03438	-3.370323477
V(sample)= 0.65 mL	7	2244	4	1.056487102	2244	0.03251	-3.42626574
n(COT) = 0.02 mmol	8	2618	4	0.98601844	2618	0.03034	-3.495295313
c(COT) = 0.03077	9	2992	4	0.912332204	2992	0.02807	-3.572966186
c(amide) = 0.06154	10	3366	4	0.84431729	3366	0.02598	-3.650442009
	11	3740	4	0.783260055	3740	0.02410	-3.725505602
	12	4114	4	0.726338454	4114	0.02235	-3.800954273
	13	4488	4	0.673249481	4488	0.02072	-3.876854408
	14	4862	4	0.624826912	4862	0.01923	-3.951495699
	15	5236	4	0.607363969	5236	0.01869	-3.979842138
	16	5610	4	0.542965712	5610	0.01671	-4.091924196
	17	5984	4	0.500627147	5984	0.01540	-4.173108761
	18	6358	4	0.469850278	6358	0.01446	-4.236556282
	19	6732	4	0.438452152	6732	0.01349	-4.30571968
	20	7106	4	0.41317668	7106	0.01271	-4.36509507
	21	7480	4	0.386033379	7480	0.01188	-4.433046528
	22	7854	4	0.362547408	7854	0.01116	-4.495815123
	23	8228	4	0.343616075	8228	0.01057	-4.549445397
	24	8602	4	0.321264784	8602	0.00989	-4.616704714
	25	8976	4	0.302052395	8976	0.00929	-4.678369872
slope	-0.000190917	-3.001085678	y-intercept				
slope uncertainty	1.3614E-06	0.007128266	y-intercept uncertainty				
R2 value	0.998831851	0.018358091	s(y)				
F	19666.26307	23	degrees of freedom				
regression ss	6.62791399	0.007751448	residual ss				
k_{LSK355}(285 K) [s-1]							
1.909 ± 0.014x 10-4							

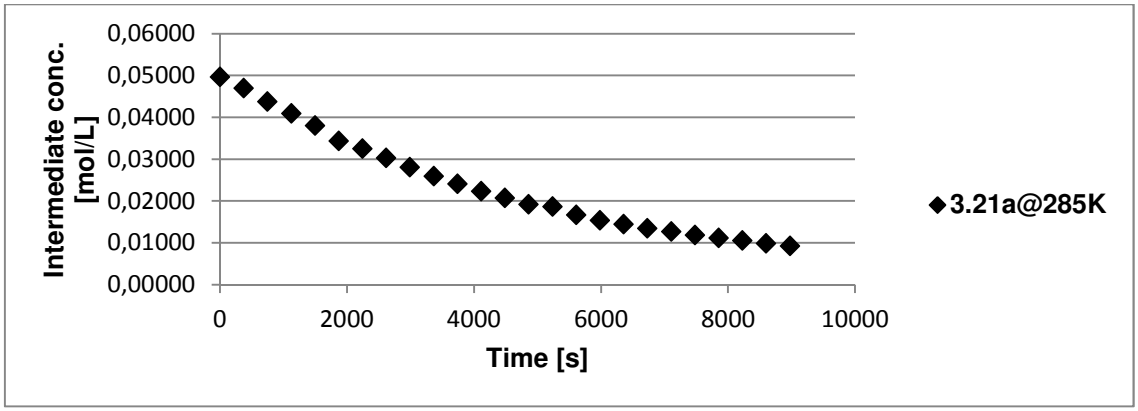

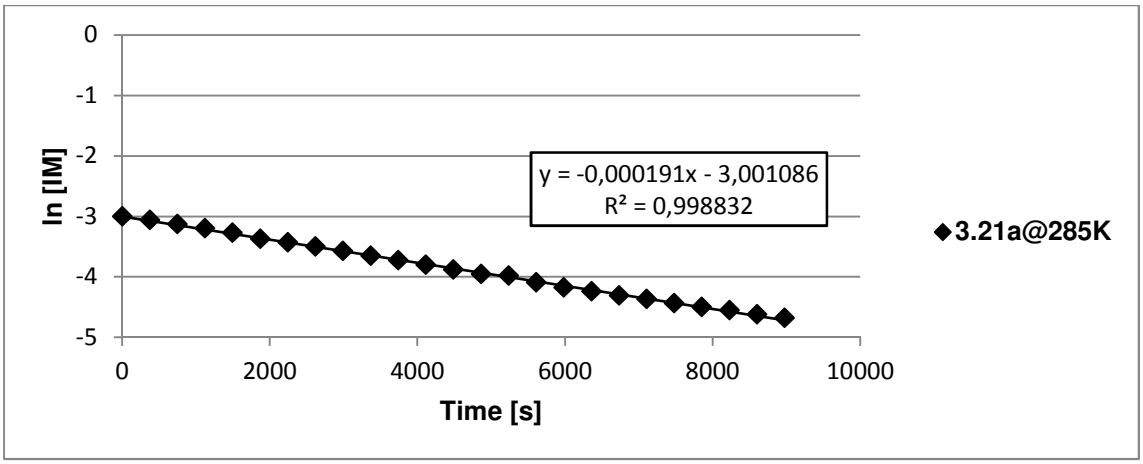

Kinetic data for compound **3.21a** at 288K ([COT] = 0.03077 mol/L)

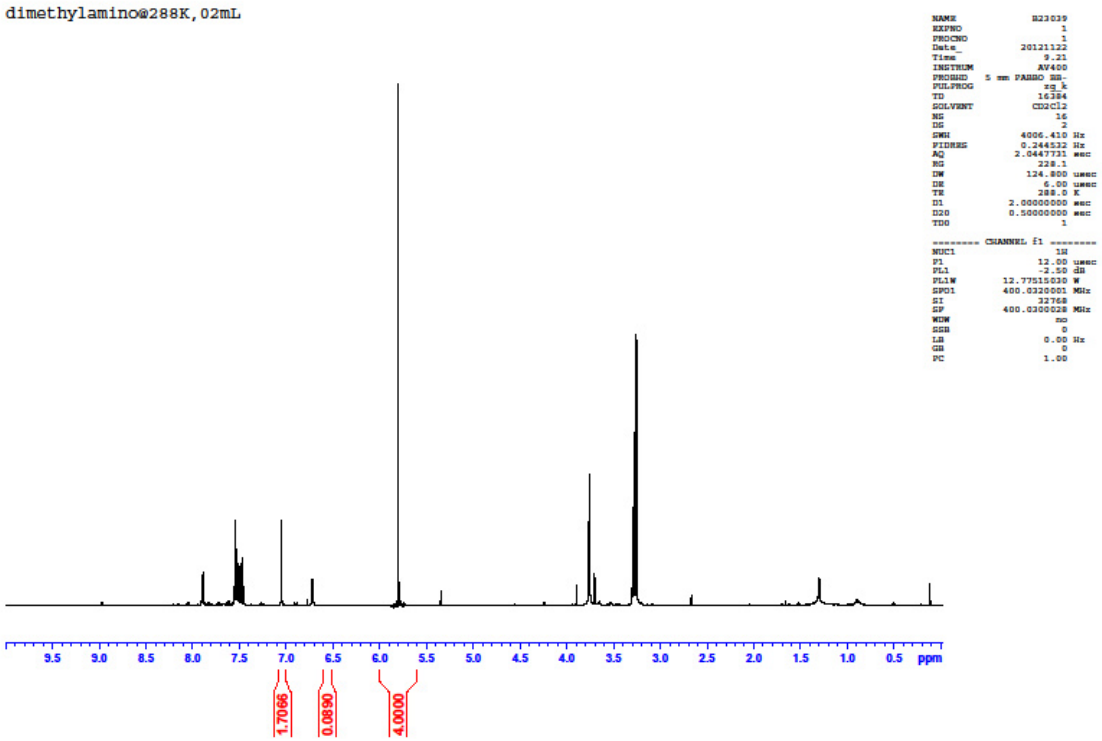

EXPERIMENT A4	T = 288 K			phc0 199.560	sr 2.82				
FOLDER 23039				phc1 -8.634					
INTEGRALS normalised				INTEGRALS			LN OF INTEGRALS		
NCHOTfN	error (noise)	standard (COT)		NCHOTfN	NCHOTfN		NCHOTfN	NCHOTfN	NCHOTfN
7.08-7.00 ppm	6.6-6.52 ppm	6.0-5.6 ppm	Time [sec]	corr. by variable error	corr. by avg. error		uncorrected	corr. by variable error	corr. by avg. error
1.70656	0.088985	4	0	1.617575	1.603747537		0.534479648	0.480928114	0.472343101
1.51828604	0.087767065	4	374	1.430518975	1.415473577		0.417582094	0.358037298	0.347464158
1.359253538	0.095078539	4	748	1.264174998	1.256441074		0.30693568	0.234419734	0.22828318
1.216068174	0.098216837	4	1122	1.117851337	1.113255711		0.195622846	0.111408394	0.107288795
1.102556765	0.099329972	4	1496	1.003226793	0.999744302		0.097631814	0.003221598	-0.000255731
1.004672248	0.102673399	4	1870	0.901998849	0.901859785		0.004661367	-0.103142035	-0.10329622
0.905531118	0.103504479	4	2244	0.802026639	0.802718655		-0.099233637	-0.220613456	-0.219750994
0.818236999	0.102528793	4	2618	0.715708206	0.715424536		-0.200603255	-0.334482729	-0.334879156
0.753748666	0.104294915	4	2992	0.649453752	0.650936203		-0.2826963	-0.431623652	-0.42934364
0.693644601	0.105468841	4	3366	0.58817576	0.590832137		-0.365795552	-0.530729464	-0.526223334
0.626996489	0.105440033	4	3740	0.521556456	0.524184026		-0.466814338	-0.650937753	-0.645912462
0.581583958	0.10580167	4	4114	0.475782288	0.478771495		-0.541999936	-0.742794907	-0.736531842
0.542422683	0.1061105	4	4488	0.436312183	0.439610219		-0.611709724	-0.829397276	-0.82186681
0.505909289	0.107287911	4	4862	0.398621378	0.403096825		-0.681397897	-0.91974324	-0.908578484
0.468972977	0.109460957	4	5236	0.35951202	0.366160513		-0.757210131	-1.023007668	-1.004683481
0.433622472	0.10490579	4	5610	0.328716682	0.330810009		-0.835581003	-1.112559048	-1.106211059
0.420296818	0.109911101	4	5984	0.310385718	0.317484355		-0.866794107	-1.169939505	-1.147326737
0.375775321	0.104487023	4	6358	0.271288298	0.272962858		-0.978763865	-1.304573195	-1.298419546
0.36919956	0.104070987	4	6732	0.265128572	0.266387096		-0.996417969	-1.327540393	-1.322804779
0.357791052	0.105691933	4	7106	0.252099119	0.254978588		-1.027806117	-1.377932939	-1.366575704
0.322777362	0.103498747	4	7480	0.219278616	0.219964899		-1.130792474	-1.51741214	-1.514287296
0.319169094	0.103608897	4	7854	0.215560197	0.216356631		-1.142034242	-1.534515072	-1.530827165
0.289609153	0.104969975	4	8228	0.184639178	0.186796689		-1.239223014	-1.689351746	-1.677734476
0.292015673	0.103734779	4	8602	0.188280894	0.18920321		-1.230947803	-1.669820312	-1.664933658
0.277530168	0.103483444	4	8976	0.174046724	0.174717705		-1.281825638	-1.748431488	-1.744583723
	average error								
	0.102812463								

Experiment A4	NMR entry	Time [sec]	Std COT 5.8 ppm, Integral=4	Integral NCHOTfN (7.0 ppm)	Time [sec]	[OTf IM]	LN[OTf IM]
Folder B23039	1	0	4	1.603747537	0	0.049347312	-3.008871989
T = 288 K	2	374	4	1.415473577	374	0.043554122	-3.133750931
0.2 mL Stk sol	3	748	4	1.256441074	748	0.038660692	-3.252931909
0.05 mL Tf2O	4	1122	4	1.113255711	1122	0.034254878	-3.373926295
0.4 mL d2-DCM	5	1496	4	0.999744302	1496	0.030762132	-3.481470821
	6	1870	4	0.901859785	1870	0.027750226	-3.58451131
V(sample)= 0.65 mL	7	2244	4	0.802718655	2244	0.024699653	-3.700966084
n(COT) = 0.02 mmol	8	2618	4	0.715424536	2618	0.022013613	-3.816094246
c(COT) = 0.03077	9	2992	4	0.650936203	2992	0.020029307	-3.91055873
c(amide) = 0.06154	10	3366	4	0.590832137	3366	0.018179905	-4.007438423
	11	3740	4	0.524184026	3740	0.016129142	-4.127127552
	12	4114	4	0.478771495	4114	0.014731799	-4.217746932
	13	4488	4	0.439610219	4488	0.013526806	-4.3030819
	14	4862	4	0.403096825	4862	0.012403289	-4.389793574
	15	5236	4	0.366160513	5236	0.011266759	-4.485898571
	16	5610	4	0.330810009	5610	0.010179024	-4.587426149
	17	5984	4	0.317484355	5984	0.009768994	-4.628541827
	18	6358	4	0.272962858	6358	0.008399067	-4.779634636
	19	6732	4	0.266387096	6732	0.008196731	-4.804019869
	20	7106	4	0.254978588	7106	0.007845691	-4.847790794
	21	7480	4	0.219964899	7480	0.00676832	-4.995502385
	22	7854	4	0.216356631	7854	0.006657294	-5.012042255
	23	8228	4	0.186796689	8228	0.005747734	-5.158949565
	24	8602	4	0.18920321	8602	0.005821783	-5.146148748
	25	8976	4	0.174717705	8976	0.005376064	-5.225798813
slope	-0.000279196	-3.053206265	y-intercept				
slope uncertainty	3.57279E-06	0.011763319	y-intercept uncertainty				
R2 value	0.997712656	0.02463874	s(y)				
F	6106.636184	14	degrees of freedom				
regression ss	3.707140346	0.008498945	residual ss				
k_{LSK355}(288 K) [s-1]							
2.792 ± 0.036 x 10-4							

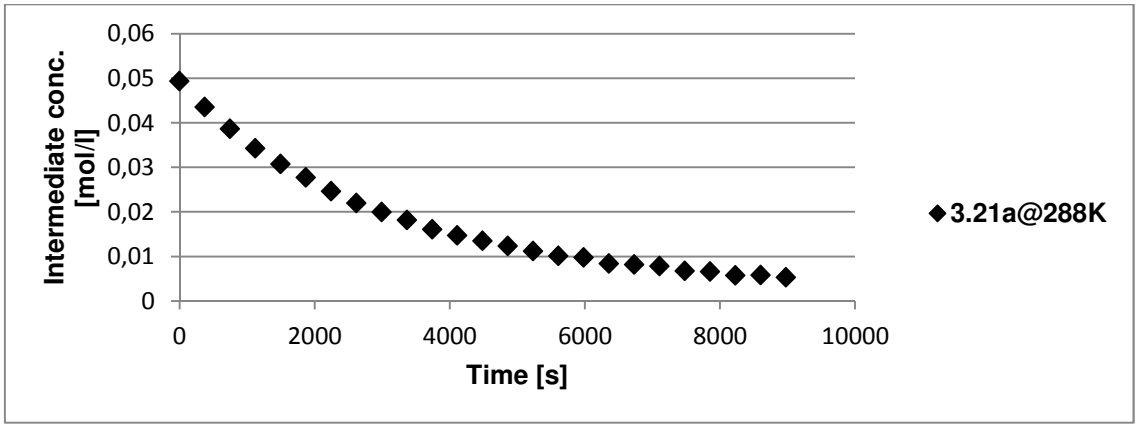

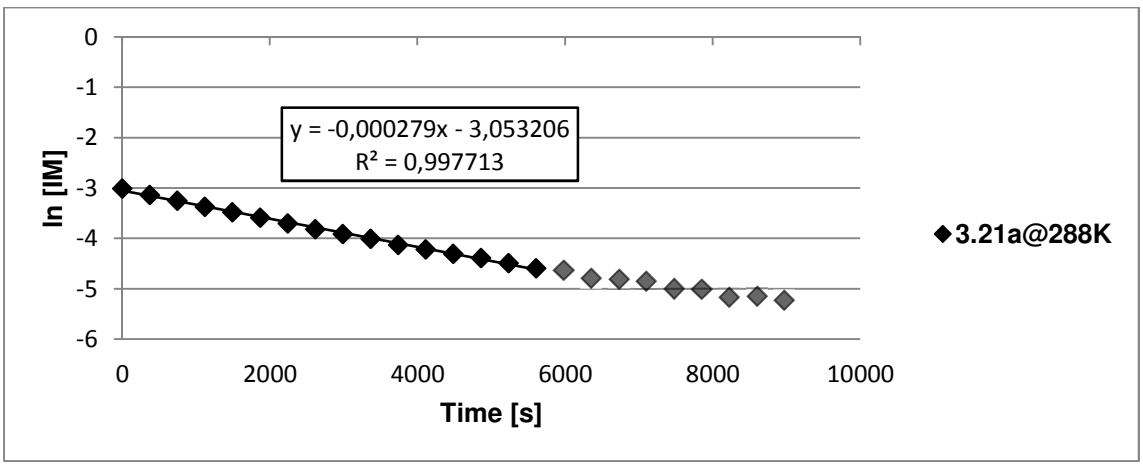

Kinetic data for compound **3.21a** at 291K ([COT] = 0.03077 mol/L)

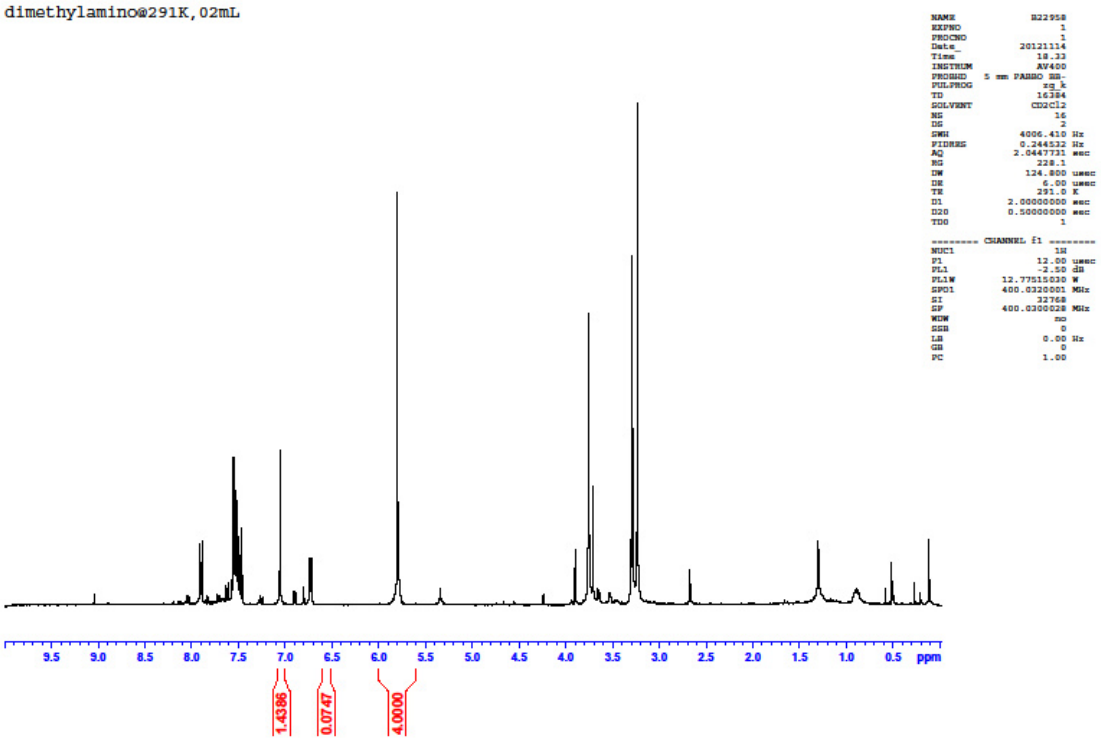

EXPERIMENT A5	T = 291 K			phc0 195.008	sr 2.82				
FOLDER 22958				phc1 3.731					
INTEGRALS normalised				INTEGRALS			LN OF INTEGRALS		
NCHOTfN	error (noise)	standard (COT)		NCHOTfN	NCHOTfN		NCHOTfN	NCHOTfN	NCHOTfN
7.08-7.00 ppm	6.6-6.52 ppm	6.0-5.6 ppm	Time [sec]	corr. by variable error	corr. by avg. error		uncorrected	corr. by variable error	corr. by avg. error
1.43864	0.07474	4	0	1.3639	1.355289322		0.363698223	0.310348243	0.304014953
1.261557762	0.072815293	4	374	1.188742469	1.178207084		0.232347277	0.172896	0.163993862
1.067522151	0.07590997	4	748	0.99161218	0.984171473		0.065340216	-0.008423195	-0.015955136
0.893727613	0.078652077	4	1122	0.815075537	0.810376935		-0.112354233	-0.204474487	-0.210255788
0.763168936	0.081490812	4	1496	0.681678123	0.679818257		-0.270275862	-0.383197693	-0.385929785
0.650890516	0.084371304	4	1870	0.566519212	0.567539838		-0.429413829	-0.568244286	-0.566444334
0.557019568	0.092770582	4	2244	0.464248986	0.473668889		-0.585154909	-0.767334263	-0.747246747
0.487583653	0.090302616	4	2618	0.397281037	0.404232975		-0.718293407	-0.923111347	-0.905763897
0.438625059	0.084669609	4	2992	0.35395545	0.35527438		-0.824110312	-1.038584221	-1.034864886
0.399869151	0.084541566	4	3366	0.315327585	0.316518472		-0.916617908	-1.154143228	-1.150373675
0.35892749	0.085358064	4	3740	0.273569425	0.275576811		-1.02463489	-1.296199849	-1.288888883
0.324871392	0.091699464	4	4114	0.233171928	0.241520713		-1.124325893	-1.455597921	-1.420800041
0.300339005	0.082879635	4	4488	0.21745937	0.216988326		-1.202843426	-1.52574325	-1.527911722
0.278091681	0.086172788	4	4862	0.191918892	0.194741002		-1.279804433	-1.650682431	-1.636084796
0.261288571	0.082446723	4	5236	0.178841848	0.177937893		-1.342129847	-1.721253393	-1.726320708
0.243881144	0.082323084	4	5610	0.16155806	0.160530466		-1.411074287	-1.822890698	-1.829271537
0.234013167	0.084859095	4	5984	0.149154072	0.150662488		-1.452377897	-1.902775466	-1.89271312
0.224761744	0.087494734	4	6358	0.13726701	0.141411066		-1.492714352	-1.985827272	-1.956084269
0.212649438	0.081559058	4	6732	0.13109038	0.12929876		-1.548110299	-2.031868266	-2.045629584
0.2104649	0.088544869	4	7106	0.121920031	0.127114221		-1.558436388	-2.104389933	-2.062669218
0.199636056	0.078306387	4	7480	0.121329669	0.116285377		-1.611259291	-2.109243902	-2.151707958
0.190889718	0.081004072	4	7854	0.109885646	0.10753904		-1.656059409	-2.208315033	-2.229901337
0.1894489	0.083743113	4	8228	0.105705787	0.106098222		-1.663635948	-2.247095637	-2.243389996
0.185776888	0.085838344	4	8602	0.099938544	0.10242621		-1.683208851	-2.303199839	-2.278612645
0.181452757	0.081273702	4	8976	0.100179055	0.098102078		-1.706759953	-2.300796148	-2.321746727
	average error								
	0.083350678								

Experiment A5	NMR entry	Time [sec]	Std COT 5.8 ppm, Integral=4	Integral NCHOTfN (7.0 ppm)	Time [sec]	[OTf IM]	LN[OTf IM]
Folder B22958	1	0	4	1.355289322	0	0.041702252	-3.177200137
T = 291 K	2	374	4	1.178207084	374	0.036253432	-3.317221227
0.2 mL Stk sol	3	748	4	0.984171473	748	0.030282956	-3.497170226
0.05 mL Tf2O	4	1122	4	0.810376935	1122	0.024935298	-3.691470877
0.4 mL d2-DCM	5	1496	4	0.679818257	1496	0.020918008	-3.867144875
	6	1870	4	0.567539838	1870	0.017463201	-4.047659423
V(sample)= 0.65 mL	7	2244	4	0.473668889	2244	0.014574792	-4.228461837
n(COT) = 0.02 mmol	8	2618	4	0.404232975	2618	0.012438249	-4.386978987
c(COT) = 0.03077	9	2992	4	0.35527438	2992	0.010931793	-4.516079976
c(amide) = 0.06154	10	3366	4	0.316518472	3366	0.009739273	-4.631588764
	11	3740	4	0.275576811	3740	0.008479498	-4.770103972
	12	4114	4	0.241520713	4114	0.007431592	-4.90201513
	13	4488	4	0.216988326	4488	0.006676731	-5.009126812
	14	4862	4	0.194741002	4862	0.005992181	-5.117299886
	15	5236	4	0.177937893	5236	0.005475149	-5.207535798
	16	5610	4	0.160530466	5610	0.004939522	-5.310486627
	17	5984	4	0.150662488	5984	0.004635885	-5.373928209
	18	6358	4	0.141411066	6358	0.004351218	-5.437299359
	19	6732	4	0.12929876	6732	0.003978523	-5.526844674
	20	7106	4	0.127114221	7106	0.003911305	-5.543884307
	21	7480	4	0.116285377	7480	0.003578101	-5.632923048
	22	7854	4	0.10753904	7854	0.003308976	-5.711116427
	23	8228	4	0.106098222	8228	0.003264642	-5.724605086
	24	8602	4	0.10242621	8602	0.003151654	-5.759827735
	25	8976	4	0.098102078	8976	0.003018601	-5.802961817
slope	-0.000438285	-3.192323129	y-intercept				
slope uncertainty	1.01261E-05	0.022405215	y-intercept uncertainty				
R2 value	0.995218826	0.039720201	s(y)				
F	1873.382932	9	degrees of freedom				
regression ss	2.955625704	0.014199249	residual ss				
k_{LSK355}(291 K) [s-1]							
4.383 ± 0.101 x 10-4							

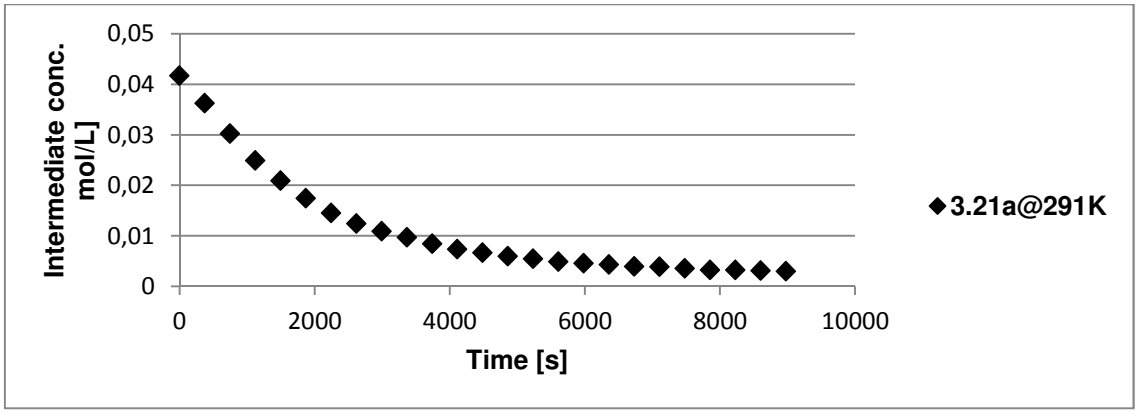

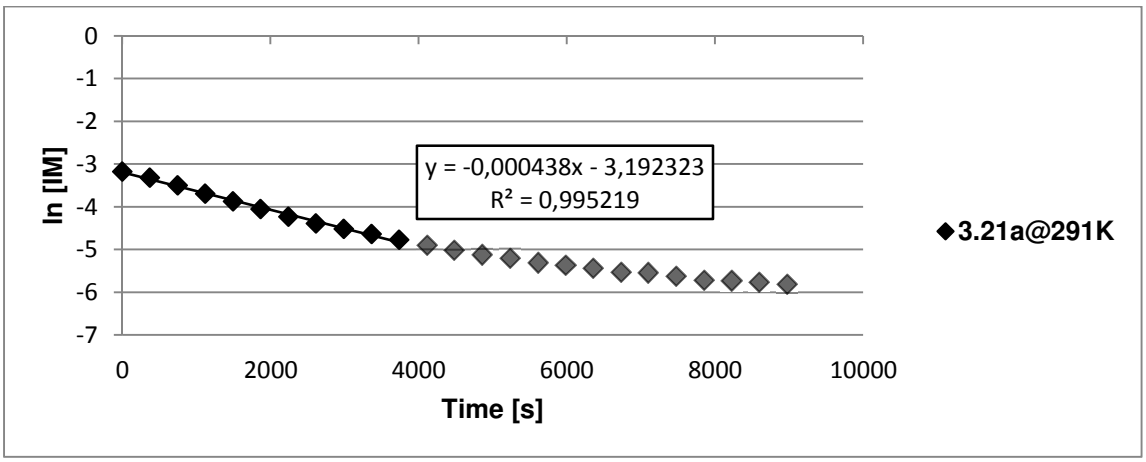

Kinetic data for compound **3.21a** at 294K ([COT] = 0.03077 mol/L)

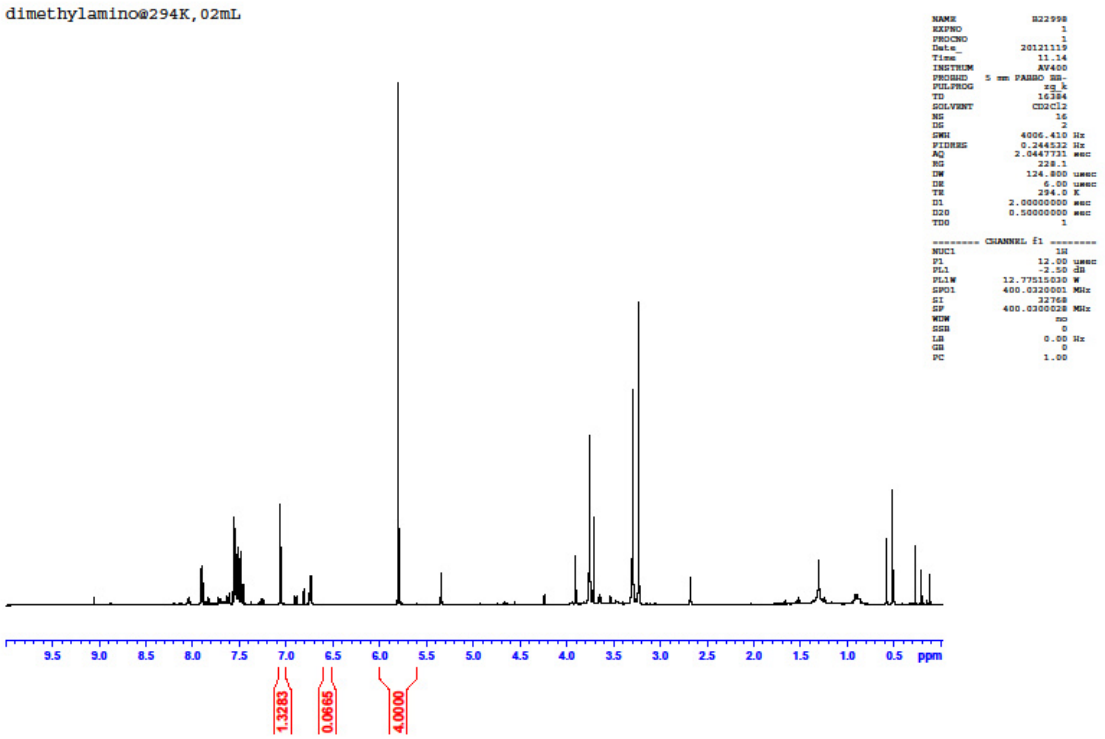

EXPERIMENT A6	T = 294 K			phc0 203.070	sr 2.82				
FOLDER 22998				phc1 -12.301					
INTEGRALS normalised				INTEGRALS			LN OF INTEGRALS		
NCHOTfN	error (noise)	standard (COT)		NCHOTfN	NCHOTfN		NCHOTfN	NCHOTfN	NCHOTfN
7.08-7.08 ppm	6.6-6.52 ppm	6.0-5.6 ppm	Time [sec]	corr. by variable error	corr. by avg. error		uncorrected	corr. by variable error	corr. by avg. error
1.32831	0.066469	4	0	1.261841	1.255664881		0.283907458	0.232571766	0.227665218
1.017359787	0.070856399	4	374	0.946503388	0.944714668		0.017210828	-0.054980729	-0.056872335
0.777848405	0.073054357	4	748	0.704794047	0.705203286		-0.251223627	-0.349849651	-0.349269169
0.609037998	0.073501206	4	1122	0.535536791	0.536392879		-0.49587462	-0.624485687	-0.622888404
0.490213664	0.071812377	4	1496	0.418401287	0.417568546		-0.712913933	-0.87131429	-0.873306567
0.40191203	0.078200313	4	1870	0.323711716	0.329266911		-0.911522046	-1.127901924	-1.110886578
0.341367828	0.072719019	4	2244	0.268648809	0.268722709		-1.074794709	-1.314350295	-1.314075252
0.300906095	0.072303541	4	2618	0.228602554	0.228260976		-1.20095704	-1.475770354	-1.477265673
0.272806756	0.075852487	4	2992	0.196954269	0.200161638		-1.298991587	-1.624783712	-1.608630051
0.24777664	0.073257944	4	3366	0.174518696	0.175131521		-1.395227584	-1.745723405	-1.742218038
0.230388233	0.072852957	4	3740	0.157535276	0.157743114		-1.467989423	-1.848105868	-1.846787428
0.215881458	0.072246272	4	4114	0.143635186	0.14323634		-1.533025826	-1.940478622	-1.943259289
0.202120306	0.071108599	4	4488	0.131011707	0.129475187		-1.598892184	-2.032468591	-2.044266021
0.194083158	0.074832668	4	4862	0.11925049	0.121438039		-1.639468563	-2.126529038	-2.108351113
0.183450268	0.072246206	4	5236	0.111204062	0.110805149		-1.69581167	-2.196388369	-2.199982037
0.17735521	0.074008683	4	5610	0.103346527	0.104710091		-1.729600721	-2.2696676	-2.256559783
0.172368168	0.07284007	4	5984	0.099528098	0.099723049		-1.758122577	-2.30731528	-2.305358441
0.169496004	0.073056655	4	6358	0.096439349	0.096850885		-1.774925928	-2.338840978	-2.33458275
0.165351624	0.071246768	4	6732	0.094104856	0.092706506		-1.799681016	-2.363345629	-2.378316631
0.164798037	0.073479874	4	7106	0.091318163	0.092152918		-1.803034572	-2.393405573	-2.384305926
0.163525978	0.071040313	4	7480	0.092485666	0.090880859		-1.810783413	-2.380701613	-2.398205868
0.160710519	0.073673959	4	7854	0.08703656	0.0880654		-1.828150551	-2.441427014	-2.429675557
0.161973235	0.070224718	4	8228	0.091748517	0.089328116		-1.820324175	-2.388703955	-2.415438993
0.163452561	0.072114475	4	8602	0.091338086	0.090807443		-1.811232475	-2.393187424	-2.399014031
0.159679591	0.073129111	4	8976	0.08655048	0.087034472		-1.834586031	-2.447027453	-2.441451012
	average error								
	0.072645119								

Experiment A6	NMR entry	Time [sec]	Std COT 5.8 ppm, Integral=4	Integral NCHOTfN (7.0 ppm)	Time [sec]	[OTf IM]	LN[OTf IM]
Folder B22958	1	0	4	1.255664881	0	0.038636808	-3.253549872
T = 291 K	2	374	4	0.944714668	374	0.02906887	-3.538087425
0.2 mL Stk sol	3	748	4	0.705203286	748	0.021699105	-3.830484259
0.05 mL Tf2O	4	1122	4	0.536392879	1122	0.016504809	-4.104103493
0.4 mL d2-DCM	5	1496	4	0.417568546	1496	0.012848584	-4.354521657
	6	1870	4	0.329266911	1870	0.010131543	-4.592101668
V(sample)= 0.65 mL	7	2244	4	0.268722709	2244	0.008268598	-4.795290342
n(COT) = 0.02 mmol	8	2618	4	0.228260976	2618	0.00702359	-4.958480762
c(COT) = 0.03077	9	2992	4	0.200161638	2992	0.006158974	-5.089845141
c(amide) = 0.06154	10	3366	4	0.175131521	3366	0.005388797	-5.223433127
	11	3740	4	0.157743114	3740	0.004853756	-5.328002517
	12	4114	4	0.14323634	4114	0.004407382	-5.424474378
	13	4488	4	0.129475187	4488	0.003983952	-5.52548111
	14	4862	4	0.121438039	4862	0.003736648	-5.589566202
	15	5236	4	0.110805149	5236	0.003409474	-5.681197127
	16	5610	4	0.104710091	5610	0.00322193	-5.737774873
	17	5984	4	0.099723049	5984	0.003068478	-5.786573531
	18	6358	4	0.096850885	6358	0.002980102	-5.81579784
	19	6732	4	0.092706506	6732	0.002852579	-5.85953172
	20	7106	4	0.092152918	7106	0.002835545	-5.865521015
	21	7480	4	0.090880859	7480	0.002796404	-5.879420957
	22	7854	4	0.0880654	7854	0.002709772	-5.910890646
	23	8228	4	0.089328116	8228	0.002748626	-5.896654083
	24	8602	4	0.090807443	8602	0.002794145	-5.88022912
	25	8976	4	0.087034472	8976	0.002678051	-5.922666102
slope	-0.000740096	-3.262557413	y-intercept				
slope uncertainty	1.23918E-05	0.011352269	y-intercept uncertainty				
R2 value	0.999159668	0.014655716	s(y)				
F	3567.01881	3	degrees of freedom				
regression ss	0.766160056	0.00064437	residual ss				
k_{LSK355}(294 K) [s-1]							
7.401 ± 0.124 x 10-4							

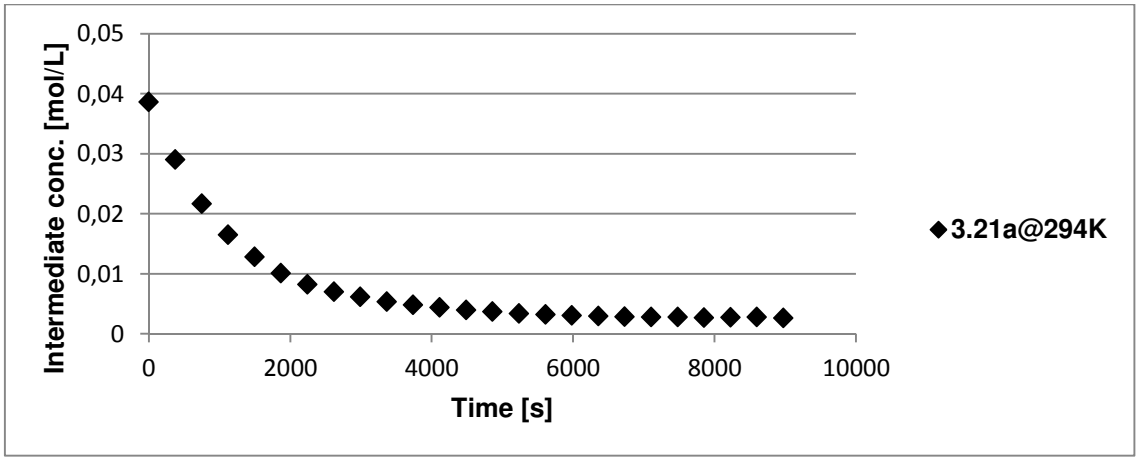

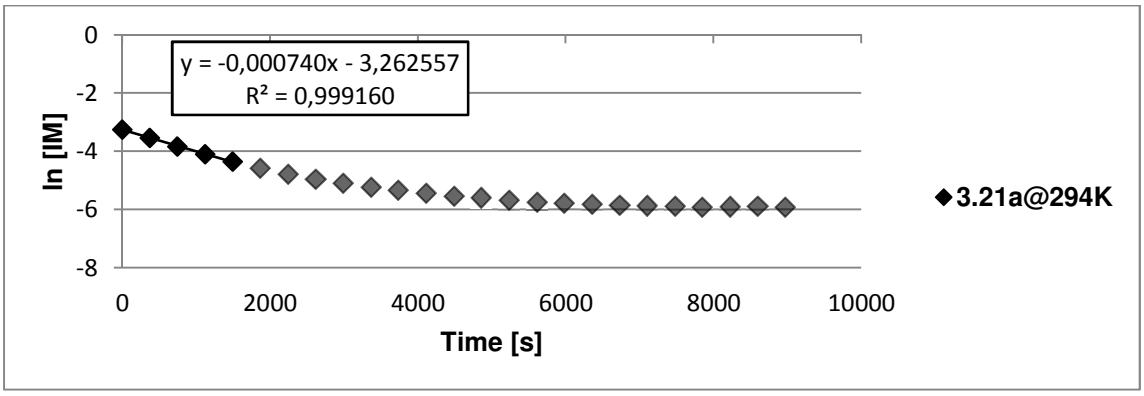

T [K]	1/T [K]	k	ln k	ln (k/T)	T [K]						
294	0.003401361	0.0007401	-7.208725246	-12.89230501	294						
291	0.003436426	0.0004383	-7.732606951	-13.40593022	291						
288	0.003472222	0.0002792	-8.183582187	-13.84654267	288						
285	0.003508772	0.0001909	-8.563760827	-14.21625001	285						
282	0.003546099	0.0001228	-9.004953542	-14.64686061	282						
slope	-12462.6751	35.13806977	y-intercept	**EA**	**ln A**		slope	-12176.31439	28.48065753	y-intercept	ΔH‡
slope uncertainty	331.1079659	1.156254476	y-intercept uncertainty	**103.6 ± 2.8 kJ/mol**	**35.1381**		slope uncertainty	330.9511639	1.155706912	y-intercept uncertainty	101.2 ± 2.8 kJ/mol
R^2 value	0.997184521	0.050658466	s(y)				R2 value	0.997053716	0.050634476	s(y)	
F	1416.717595	4	degrees of freedom	$\Delta S^{\ddagger}$ = R(ln A-ln (ek_B/h)-ln T			F	1353.642185	4	degrees of freedom	
regression ss	3.635694244	0.010265121	residual ss	**$\Delta S^{\ddagger}$(298K) = 11.5 ± 2.9 kJ/mol^{-1}**			regression ss	3.470535668	0.0102554	residual ss	

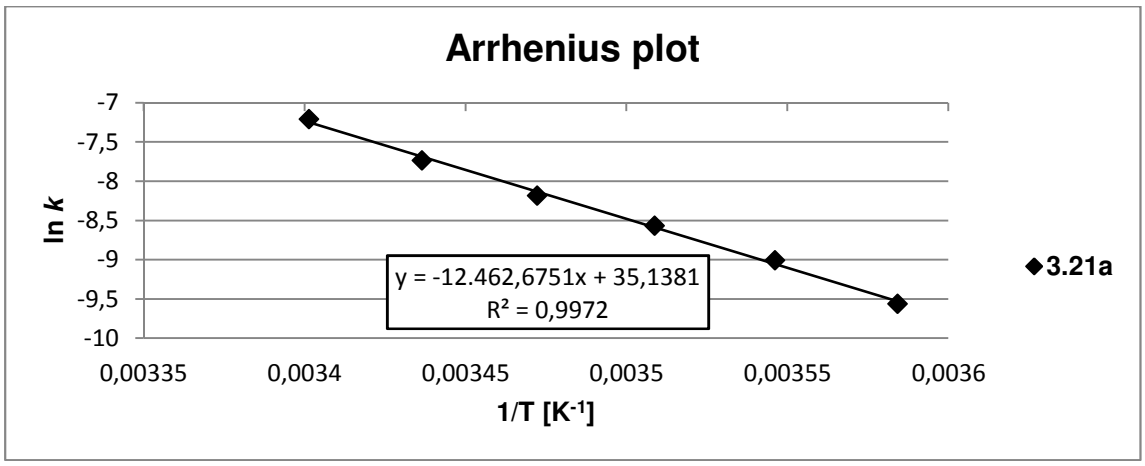

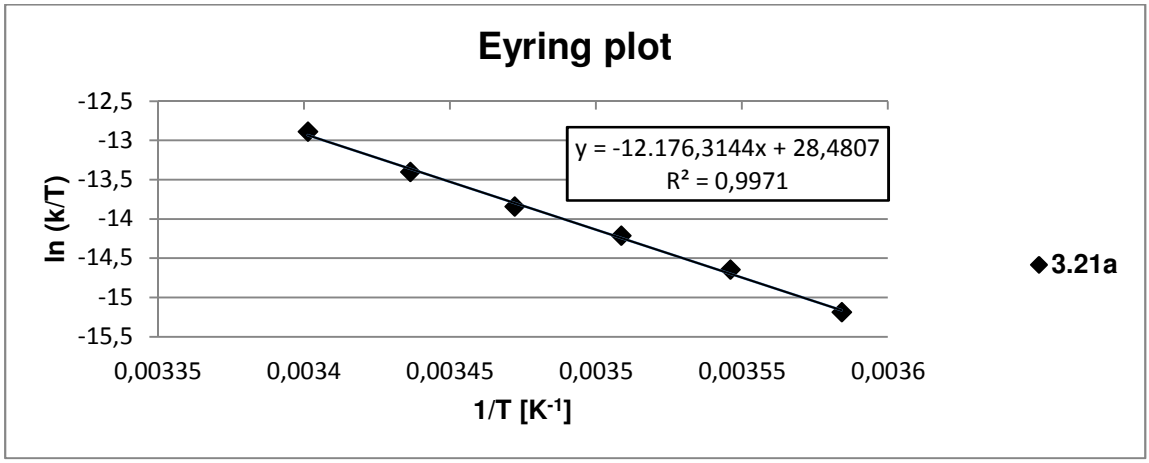

Kinetic data for compounds **3.23a** and **3.23e** at 279 K ([COT] = 0.03077 mol/L)

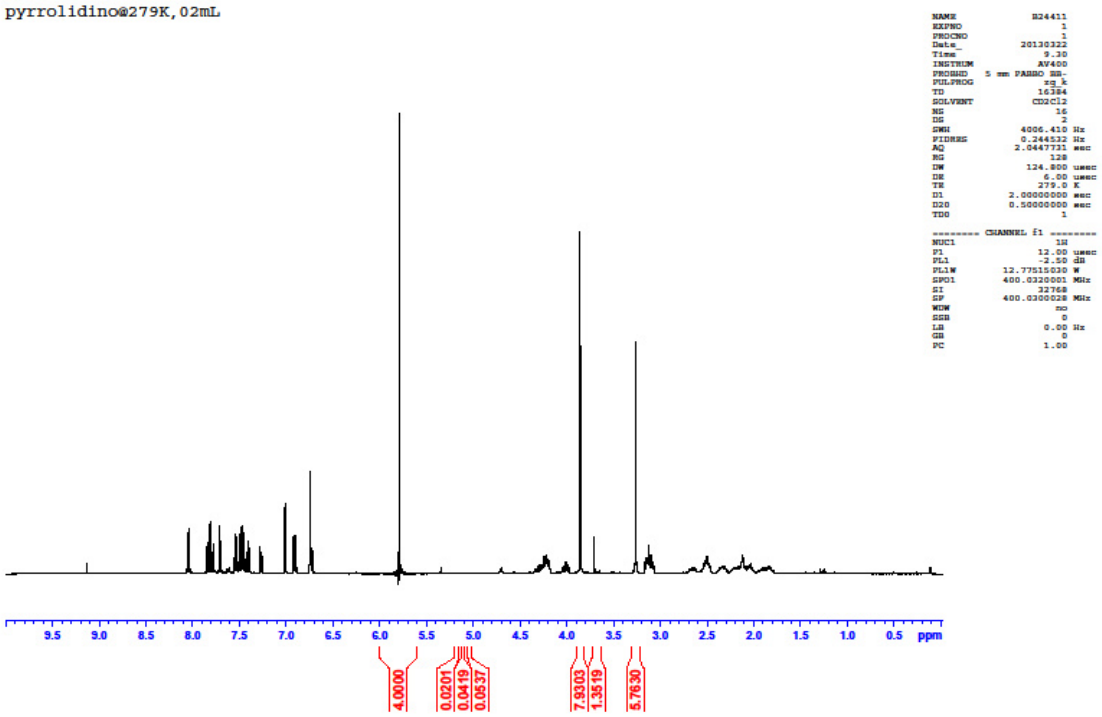

EXPERIMENT B1	T = 279 K			phc0 163.605	sr 2.82						
FOLDER B24411				phc1 -15.423							
INTEGRALS normalised							INTEGRALS			LN OF INTEGRALS	
standard (COT)	error IM1 (noise)	corrected by avg error	error IM2 (noise)	corrected by avg error	P-CH3	IM2-CH3 eq	corrected by avg error			corrected by avg error	
6.0-5.6 ppm	5.2-5.125 ppm	5.15-5.06 ppm	5.1-5.016 ppm	3.895-3.820 ppm	3.73-3.64 ppm	3.31-3.225 ppm	IM1-CH3	P-CH3	IM2-CH3	IM1-CH3 OTf ax	IM2-CH3 OTf eq
4	0.020083	0.041935	0.05368	7.93032	1.35192	5.76301	7.895770238	1.283711228	5.68586574	2.066327203	1.737983401
4	0.032510206	0.053033454	0.06487458	7.657274898	1.663026008	5.523766977	7.622725136	1.594817237	5.446622718	2.031133935	1.694995732
4	0.026033601	0.055406551	0.068049482	8.107699427	2.000145596	5.71412229	8.073149665	1.931936824	5.63697803	2.088543699	1.729348112
4	0.034124211	0.064019282	0.078193145	7.824991871	2.236695553	5.474376906	7.790442109	2.168486781	5.397232647	2.052897612	1.685886349
4	0.031844293	0.065529915	0.077143496	7.901705647	2.493946278	5.417802985	7.867155885	2.425737506	5.340658725	2.06269661	1.675349002
4	0.039065884	0.069525216	0.079997163	7.323340992	2.619871368	5.041338099	7.288791229	2.551662596	4.964193839	1.98633772	1.602250916
4	0.035351107	0.072599447	0.08605415	7.683024381	2.914722979	5.156296304	7.648474619	2.846514208	5.079152044	2.034506232	1.625144327
4	0.04345454	0.073294929	0.083352129	7.000152397	2.967183801	4.736281711	6.965602635	2.89897503	4.659137452	1.940984127	1.538830335
4	0.03837641	0.07676209	0.08754551	7.449994078	3.286502186	4.916034544	7.415444315	3.218293414	4.838890284	2.003564895	1.576685414
4	0.039210683	0.075009774	0.08718595	7.179972839	3.458034116	4.776394576	7.145423077	3.389825344	4.699250316	1.966472023	1.547402989
4	0.044893072	0.080327581	0.092452064	7.097684873	3.658649173	4.70017055	7.063135111	3.590440402	4.62302629	1.95488902	1.531049532
4	0.041595362	0.081618138	0.092130341	7.208561741	3.851168569	4.66114864	7.174011979	3.782959797	4.58400438	1.970465049	1.522572935
4	0.039627969	0.077757355	0.089070149	6.778342959	3.893550309	4.420488347	6.743793197	3.825341538	4.343344087	1.908622555	1.468644578
4	0.050449776	0.085120346	0.094673185	6.591561283	4.029921837	4.279386695	6.557011521	3.961713066	4.202242435	1.880534938	1.435618296
4	0.043216583	0.084157672	0.093899467	7.028396552	4.409306173	4.453067283	6.993846789	4.341097402	4.375923023	1.945030732	1.476117474
4	0.025839254	0.059311947	0.067371105	6.955323201	4.724628747	4.427847721	6.920773439	4.656419975	4.350703461	1.934527532	1.470337547
4	0.035804396	0.060204616	0.066790022	6.394824323	4.691346587	4.122790717	6.360274561	4.623137815	4.045646457	1.850071546	1.397641354
4	0.026180274	0.064715401	0.069271059	6.654698443	4.967841655	4.197087341	6.62014868	4.899632883	4.119943081	1.890117829	1.415839348
4	0.026520017	0.061950652	0.068820144	6.459002708	5.140024731	4.126745939	6.424452946	5.07181596	4.04960168	1.860111482	1.398618526
4	0.024576722	0.061736485	0.0680389	6.500079117	5.298075501	4.066759532	6.465529355	5.22986673	3.989615273	1.866484889	1.383694803
4	0.042821526	0.070606139	0.075900142	6.091644001	5.341719553	3.846878643	6.057094239	5.273510781	3.769734383	1.801230187	1.327004544
4	0.028567702	0.065795982	0.071097313	6.372491521	5.639144273	3.944659536	6.337941759	5.570935502	3.867515276	1.846554072	1.352612253
4	0.030746483	0.063879752	0.068725257	5.869935635	5.503145832	3.684003087	5.835385872	5.434937061	3.606858827	1.763940394	1.282837263
4	0.034145621	0.067470928	0.074585505	5.946601829	5.825708907	3.730342083	5.912052066	5.757500136	3.653197823	1.77699299	1.2956029
4	0.026625116	0.064887581	0.074408378	6.191691977	6.155245507	3.787638151	6.157142214	6.087036736	3.710493891	1.817612744	1.311164992
4	0.02886599	0.065070926	0.073498194	5.668126409	5.928066955	3.504030086	5.633576647	5.859858184	3.426885826	1.728744524	1.231651926
4	0.040784671	0.070328224	0.078166648	5.566368862	6.091724583	3.430887949	5.531819099	6.023515811	3.353743689	1.710516713	1.210077241
4	0.027687038	0.066699589	0.073155099	5.937451733	6.55522225	3.578994373	5.902901971	6.487013478	3.501850114	1.775444089	1.253291433
4	0.039046449	0.074842565	0.078971825	5.653179344	6.658903517	3.493841936	5.618629582	6.590694745	3.416697677	1.726087788	1.228674493
4	0.038444915	0.072665612	0.07722739	5.532864677	6.695350415	3.377839938	5.498314914	6.627141643	3.300695678	1.704441666	1.194133258
	average	average	average								
	0.034549762	0.068208772	0.07714426								

Experiment B1	NMR entry	Time [sec]	Std COT 5.8 ppm, Integral=4	Integral IM1-CH3 (3.9 ppm)	Integral P-CH3 (3.7 ppm)	Integral IM2-CH3 (3.3 ppm)	[OTf IM1]	[P]	[OTf IM2]	LN [OTf IM1]	LN [OTf IM2]
Folder B22331	1	0	4	7.895770238	1.283711228	5.68586574	0.080984283	0.013166598	0.05831803	-2.513500175	-2.841843978
T = 279 K	2	374	4	7.622725136	1.594817237	5.446622718	0.078183751	0.016357509	0.055864194	-2.548693443	-2.884831647
0.2 mL Stk sol	3	748	4	8.073149665	1.931936824	5.63697803	0.082803605	0.019815232	0.057816605	-2.491283679	-2.850479267
0.05 mL Tf2O	4	1122	4	7.790442109	2.168486781	5.397232647	0.079903968	0.022241446	0.055357616	-2.526929767	-2.893941029
0.4 mL d2-DCM	5	1496	4	7.867155885	2.425737506	5.34	0.080690796	0.024879981	0.054777356	-2.517130768	-2.904478376
	6	1870	4	7.288791229	2.551662596	4.964193839	0.074758702	0.026171553	0.050916081	-2.593489658	-2.977576463
V(sample)= 0.65 mL	7	2244	4	7.648474619	2.846514208	5.079152044	0.078447855	0.029195747	0.052095169	-2.545321147	-2.954683051
n(COT) = 0.02 mmol	8	2618	4	6.965602635	2.89897503	4.659137452	0.071443864	0.029733821	0.04778722	-2.638843252	-3.040997044
c(COT) = 0.03077	9	2992	4	7.415444315	3.218293414	4.838890284	0.076057741	0.033008963	0.049630885	-2.576262483	-3.003141964
c(amide) = 0.06154	10	3366	4	7.145423077	3.389825344	4.699250316	0.073288223	0.034768309	0.048198644	-2.613355356	-3.03242439
	11	3740	4	7.063135111	3.590440402	4.62302629	0.072444222	0.03682595	0.04741684	-2.624938359	-3.048777847
	12	4114	4	7.174011979	3.782959797	4.58400438	0.07358145	0.038800558	0.047016605	-2.609362329	-3.057254443
	13	4488	4	6.743793197	3.825341538	4.343344087	0.069168839	0.039235253	0.044548233	-2.671204823	-3.1111828
	14	4862	4	6.557011521	3.961713066	4.202242435	0.067253081	0.04063397	0.043101	-2.69929244	-3.144209082
	15	5236	4	6.993846789	4.341097402	4.375923023	0.071733555	0.044525189	0.044882384	-2.634796646	-3.103709904
	16	5610	4	6.920773439	4.656419975	4.350703461	0.070984066	0.047759348	0.044623715	-2.645299846	-3.109489831
	17	5984	4	6.360274561	4.623137815	4.045646457	0.065235216	0.047417984	0.041494847	-2.729755832	-3.182186024
	18	6358	4	6.62014868	4.899632883	4.119943081	0.067900658	0.050253901	0.042256883	-2.689709549	-3.16398803
	19	6732	4	6.424452946	5.07181596	4.04960168	0.065893472	0.052019926	0.041535415	-2.719715896	-3.181208853
	20	7106	4	6.465529355	5.22986673	3.989615273	0.066314779	0.053641	0.040920154	-2.713342489	-3.196132575
	21	7480	4	6.057094239	5.273510781	3.769734383	0.062125597	0.054088642	0.038664909	-2.778597192	-3.252822835
	22	7854	4	6.337941759	5.570935502	3.867515276	0.065006156	0.057139228	0.039667815	-2.733273306	-3.227215125
	23	8228	4	5.835385872	5.434937061	3.606858827	0.059851608	0.055744338	0.036994349	-2.815886984	-3.296990116
	24	8602	4	5.912052066	5.757500136	3.653197823	0.060637947	0.05905276	0.037469632	-2.802834388	-3.284224478
	25	8976	4	6.157142214	6.087036736	3.710493891	0.063151755	0.062432707	0.038057299	-2.762214635	-3.268662386
	26	9350	4	5.633576647	5.859858184	3.426885826	0.057781718	0.060102612	0.035148426	-2.851082854	-3.348175452
	27	9724	4	5.531819099	6.023515811	3.353743689	0.056738025	0.061781194	0.034398231	-2.869310666	-3.369750137
	28	10098	4	5.902901971	6.487013478	3.501850114	0.060544098	0.066535135	0.035917309	-2.804383289	-3.326535946
	29	10472	4	5.618629582	6.590694745	3.416697677	0.057628411	0.067598559	0.035043929	-2.853739591	-3.351152885
	30	10846	4	5.498314914	6.627141643	3.300695678	0.056394383	0.067972383	0.033854135	-2.875385712	-3.38569412
IM1-ax					IM2-eq						
slope	-3.40882E-05	2.496771035	y-intercept		slope	-4.9617E-05	-2.857385541	y-intercept			
slope uncertainty	1.73388E-06	0.010950643	y-intercept uncertainty		slope uncertainty	1.46575E-06	0.009257223	y-intercept uncertainty			
R2 value	0.932451744	0.030742565	s(y)		R2 value	0.976147629	0.025988499	s(y)			
F	386.5184739	28	degrees of freedom		F	1145.887478	28	degrees of freedom			
regression ss	0.36530066	0.026462949	residual ss		regression ss	0.77393476	0.018911258	residual ss			

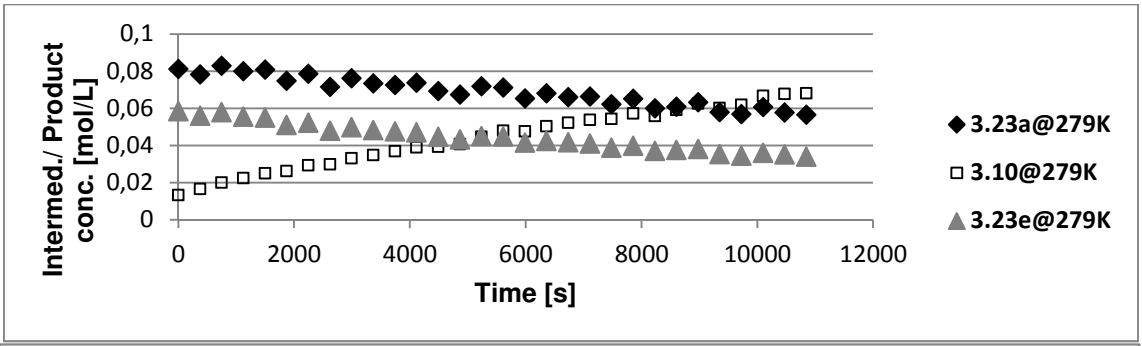

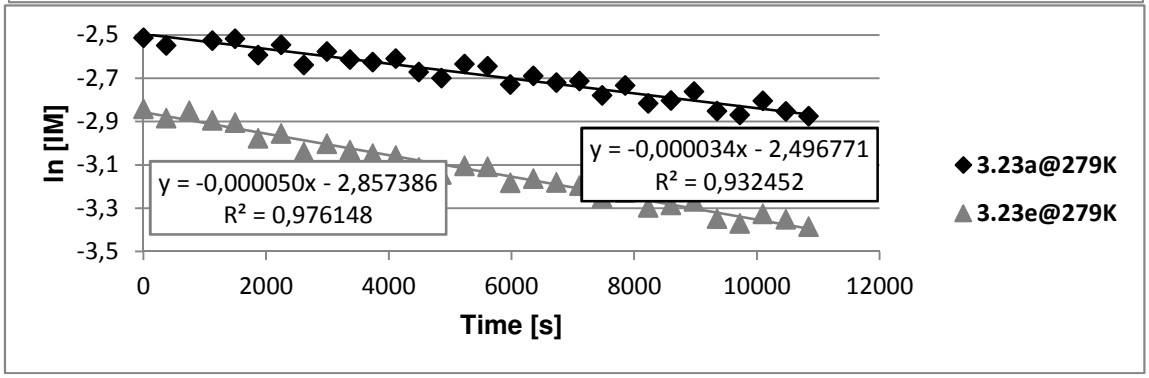

Kinetic data for compounds **3.23a** and **3.23e** at 282 K ([COT] = 0.03077 mol/L)

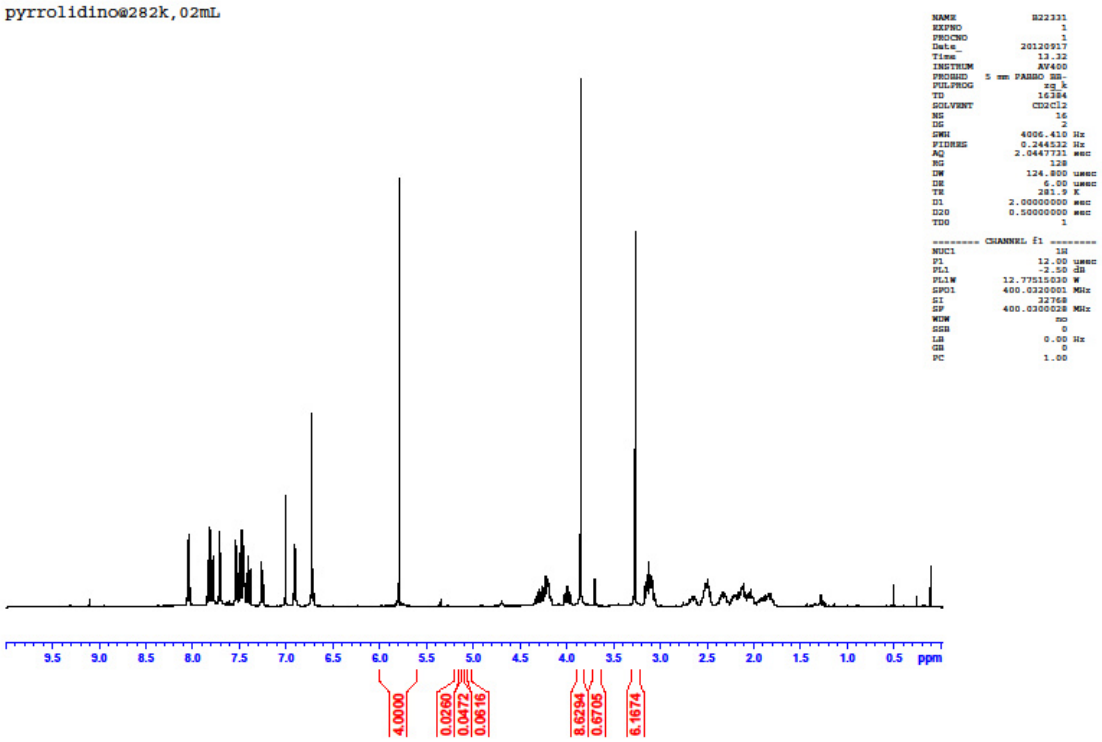

EXPERIMENT B2	T = 282 K			phc0 63.792	sr 2.82						
FOLDER B22331				phc1 -11.354							
INTEGRALS normalised							INTEGRALS			LN OF INTEGRALS	
standard (COT)	error IM1 (noise)	corrected by avg error	error IM2 (noise)	corrected by avg error	P-CH3	IM2-CH3 eq	corrected by avg error			corrected by avg error	
6.0-5.6 ppm	5.2-5.125 ppm	5.15-5.06 ppm	5.1-5.016 ppm	3.895-3.820 ppm	3.73-3.64 ppm	3.31-3.225 ppm	IM1-CH3	P-CH3	IM2-CH3	IM1-CH3 OTf ax	IM2-CH3 OTf eq
4	0.025986	0.047188	0.061645	8.62938	0.670487	6.16742	8.568931763	0.566496178	6.044124075	2.148143076	1.799086573
4	0.035043132	0.061482908	0.081398341	8.49382716	0.974401964	5.998184676	8.433378924	0.870411142	5.874888751	2.132197513	1.770687124
4	0.038970693	0.067974114	0.091082667	8.334411081	1.282062167	5.874372479	8.273962844	1.178071345	5.751076555	2.113113577	1.749387064
4	0.04063098	0.073597231	0.09248807	8.219923353	1.62681172	5.699938188	8.159475116	1.522820898	5.576642263	2.099179843	1.71858685
4	0.041013201	0.076281449	0.09606029	7.943214294	1.908593268	5.482187963	7.882766057	1.804602446	5.358892038	2.064678865	1.678757244
4	0.04514409	0.08121026	0.102183116	7.7532902	2.190772157	5.298564563	7.692841963	2.086781335	5.175268639	2.040290281	1.643891249
4	0.042900029	0.079340676	0.100305577	7.669585651	2.530942453	5.153260102	7.609137414	2.426951632	5.029964178	2.029349816	1.615412862
4	0.051542503	0.091045371	0.109507426	7.31364956	2.745094652	4.895482137	7.253201323	2.64110383	4.772186213	1.981442933	1.562804525
4	0.045048936	0.083385172	0.104223944	7.309796348	3.076787958	4.819469447	7.249348112	2.972797137	4.696173523	1.980911549	1.546748033
4	0.057659399	0.096597873	0.11559462	7.149944156	3.345758267	4.694604963	7.089495919	3.241767446	4.571309038	1.958614241	1.519799606
4	0.062912542	0.104022487	0.126650961	7.04080709	3.639539407	4.596755688	6.980358854	3.535548585	4.473459764	1.943100327	1.498162106
4	0.051080391	0.094204344	0.114941609	6.986478347	3.916846102	4.490993287	6.92603011	3.81285528	4.367697362	1.935286793	1.474235951
4	0.06181653	0.105268068	0.12578936	6.770335568	4.172892712	4.340421397	6.709887331	4.06890189	4.217125472	1.90358216	1.439153728
4	0.064529949	0.107762652	0.129458779	6.742237225	4.485579989	4.274449262	6.681788989	4.381589167	4.151153338	1.899385764	1.423386208
4	0.069999313	0.112001454	0.132814449	6.477337681	4.661729899	4.073236366	6.416889444	4.557739077	3.949940441	1.85893349	1.373700501
4	0.066120727	0.112591559	0.13066797	6.349540453	4.91882853	3.949544382	6.289092217	4.814837708	3.826248457	1.838816739	1.341884808
4	0.07058115	0.120147087	0.141270999	6.275410928	5.169624889	3.889851297	6.214962691	5.065634068	3.766555373	1.826959722	1.32616089
4	0.066079235	0.115202488	0.138537745	6.248804436	5.472103508	3.827066199	6.188356199	5.368112686	3.703770274	1.822669494	1.309351294
4	0.083427204	0.129720381	0.146883318	5.76108259	5.402741365	3.48502218	5.700634353	5.298750543	3.361726256	1.740577459	1.212454609
4	0.066810966	0.123906187	0.142236383	6.279761831	6.035933121	3.681029855	6.219313595	5.931942299	3.557733931	1.827659546	1.269123806
4	0.06939507	0.120958953	0.138805578	5.793124076	6.040798211	3.450533918	5.732675839	5.93680739	3.327237993	1.746182409	1.202142528
4	0.072270908	0.123703948	0.141877818	5.710273201	6.318183585	3.377963236	5.649824964	6.214192763	3.254667312	1.731624565	1.180090062
4	0.07586956	0.127849059	0.143049134	5.468006942	6.397866891	3.227335117	5.407558705	6.293876069	3.104039193	1.687797735	1.132704229
4	0.082608328	0.136844928	0.153226465	5.360785688	6.608946497	3.142189633	5.300337451	6.504955676	3.018893708	1.667770489	1.104890443
4	0.078923892	0.127403661	0.146085742	5.32517341	6.824633911	3.066676301	5.264725174	6.72064309	2.943380376	1.661028946	1.079558709
4	0.080393364	0.136352897	0.155657848	5.145836678	6.972958596	2.967849843	5.085388441	6.868967774	2.844553918	1.626371416	1.04540626
4	0.073963624	0.128383362	0.144327796	5.097465845	7.22178026	2.904118455	5.037017608	7.117789439	2.780822531	1.616814162	1.022746758
4	0.076859706	0.129956457	0.151373746	4.971046428	7.361053102	2.801962563	4.910598192	7.25706228	2.678666639	1.591395766	0.985319148
4	0.076338452	0.129481963	0.148771575	4.881700693	7.577110509	2.733971695	4.821252456	7.473119687	2.610675771	1.57303374	0.959609104
4	0.039527223	0.075859662	0.091961415	4.804999164	8.105352174	2.794635043	4.744550928	8.001361352	2.671339119	1.556996786	0.982579889
	average	average	average								
	0.060448237	0.103990822	0.123295925								

Experiment B2	NMR entry	Time [sec]	Std COT 5.8 ppm, Integral=4	Integral IM1-CH3 (3.9 ppm)	Integral P-CH3 (3.7 ppm)	Integral IM2-CH3 (3.3 ppm)	[OTf IM1]	[P]	[OTf IM2]	LN [OTf IM1]	LN [OTf IM2]
Folder B22331	1	0	4	8.568931763	0.566496178	6.044124075	0.087888677	0.005810362	0.061992566	-2.431684302	-2.780740805
T = 282K	2	374	4	8.433378924	0.870411142	5.874888751	0.086498356	0.008927517	0.060256776	-2.447629865	-2.809140254
0.2 mL Stk sol	3	748	4	8.273962844	1.178071345	5.751076555	0.084863279	0.012083085	0.058986875	-2.466713801	-2.830440314
0.05 mL Tf2O	4	1122	4	8.159475116	1.522820898	5.576642263	0.083689016	0.015619066	0.057197761	-2.480647535	-2.861240528
0.4 mL d2-DCM	5	1496	4	7.882766057	1.804602446	5.36	0.080850904	0.018509206	0.054964369	-2.515148514	-2.901070134
	6	1870	4	7.692841963	2.086781335	5.175268639	0.078902916	0.021403421	0.053081005	-2.539537097	-2.93593613
V(sample)= 0.65 mL	7	2244	4	7.609137414	2.426951632	5.029964178	0.078044386	0.024892434	0.051590666	-2.550477562	-2.964414516
n(COT) = 0.02 mmol	8	2618	4	7.253201323	2.64110383	4.772186213	0.074393668	0.027088922	0.048946723	-2.598384445	-3.017022853
c(COT) = 0.03077	9	2992	4	7.249348112	2.972797137	4.696173523	0.074354147	0.030490989	0.048167086	-2.598915829	-3.033079345
c(amide) = 0.06154	10	3366	4	7.089495919	3.241767446	4.571309038	0.072714596	0.033249728	0.046886393	-2.621213138	-3.060027773
	11	3740	4	6.980358854	3.535548585	4.473459764	0.071595214	0.036262943	0.045882786	-2.636727051	-3.081665273
	12	4114	4	6.92603011	3.81285528	4.367697362	0.071037982	0.039107186	0.044798016	-2.644540585	-3.105591428
	13	4488	4	6.709887331	4.06890189	4.217125472	0.068821078	0.04173337	0.04325365	-2.676245219	-3.14067365
	14	4862	4	6.681788989	4.381589167	4.151153338	0.068532882	0.0449405	0.042576996	-2.680441614	-3.15644117
	15	5236	4	6.416889444	4.557739077	3.949940441	0.065815896	0.04674721	0.040513222	-2.720893888	-3.206126878
	16	5610	4	6.289092217	4.814837708	3.826248457	0.064505123	0.049384185	0.039244555	-2.74101064	-3.23794257
	17	5984	4	6.214962691	5.065634068	3.766555373	0.063744801	0.05195652	0.038632303	-2.752867656	-3.253666489
	18	6358	4	6.188356199	5.368112686	3.703770274	0.063471907	0.055058942	0.037988337	-2.757157884	-3.270476085
	19	6732	4	5.700634353	5.298750543	3.361726256	0.058469506	0.054347518	0.034480106	-2.83924992	-3.36737277
	20	7106	4	6.219313595	5.931942299	3.557733931	0.063789426	0.060841955	0.036490491	-2.752167832	-3.310703572
	21	7480	4	5.732675839	5.93680739	3.327237993	0.058798145	0.060891854	0.034126371	-2.833644969	-3.37768485
	22	7854	4	5.649824964	6.214192763	3.254667312	0.057948371	0.063736904	0.033382038	-2.848202813	-3.399737316
	23	8228	4	5.407558705	6.293876069	3.104039193	0.055463527	0.064554189	0.031837095	-2.892029643	-3.44712315
	24	8602	4	5.300337451	6.504955676	3.018893708	0.054363794	0.066719162	0.030963786	-2.91205689	-3.474936936
	25	8976	4	5.264725174	6.72064309	2.943380376	0.053998531	0.068931396	0.030189271	-2.918798433	-3.50026867
	26	9350	4	5.085388441	6.868967774	2.844553918	0.052159134	0.070452713	0.029175641	-2.953455962	-3.534421118
	27	9724	4	5.037017608	7.117789439	2.780822531	0.051663011	0.073004794	0.02852197	-2.963013216	-3.55708062
	28	10098	4	4.910598192	7.25706228	2.678666639	0.050366369	0.074433269	0.027474191	-2.988431613	-3.59450823
	29	10472	4	4.821252456	7.473119687	2.610675771	0.049449979	0.076649298	0.026776831	-3.006793638	-3.620218275
	30	10846	4	4.744550928	8.001361352	2.671339119	0.048663277	0.082067296	0.027399035	-3.022830592	-3.597247489
IM1-ax					IM2-eq						
slope	-5.47057E-05	-2.429701659	y-intercept		slope	-7.99989E-05	-2.782151545	y-intercept			
slope uncertainty	1.05344E-06	0.006425742	y-intercept uncertainty		slope uncertainty	8.79822E-07	0.005366696	y-intercept uncertainty			
R2 value	0.99008726	0.017751314	s(y)		R2 value	0.996744868	0.014825666	s(y)			
F	2696.767655	27	degrees of freedom		F	8267.5941	27	degrees of freedom			
regression ss	0.849776115	0.008507947	residual ss		regression ss	1.817220187	0.00593461	residual ss			

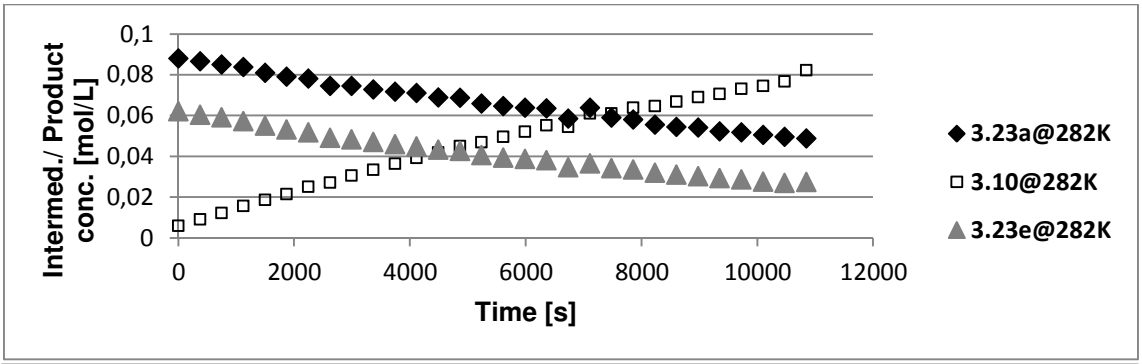

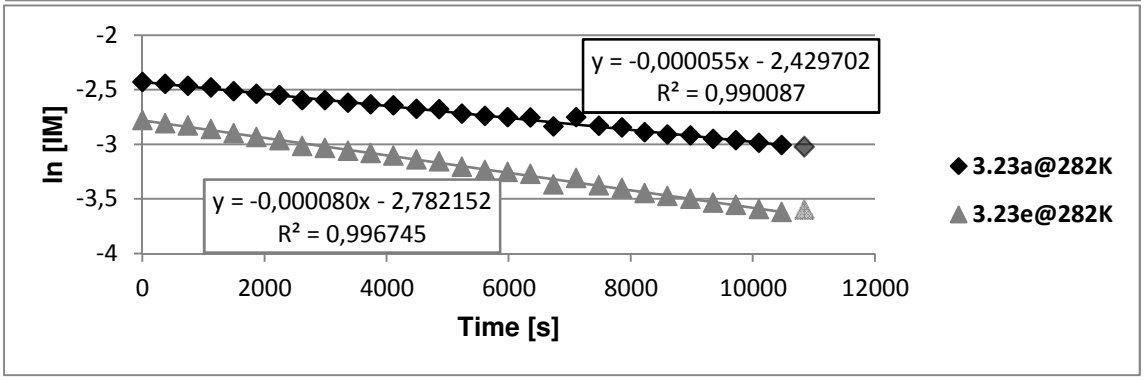

Kinetic data for compounds **3.23a** and **3.23e** at 285 K ([COT] = 0.03077 mol/L)

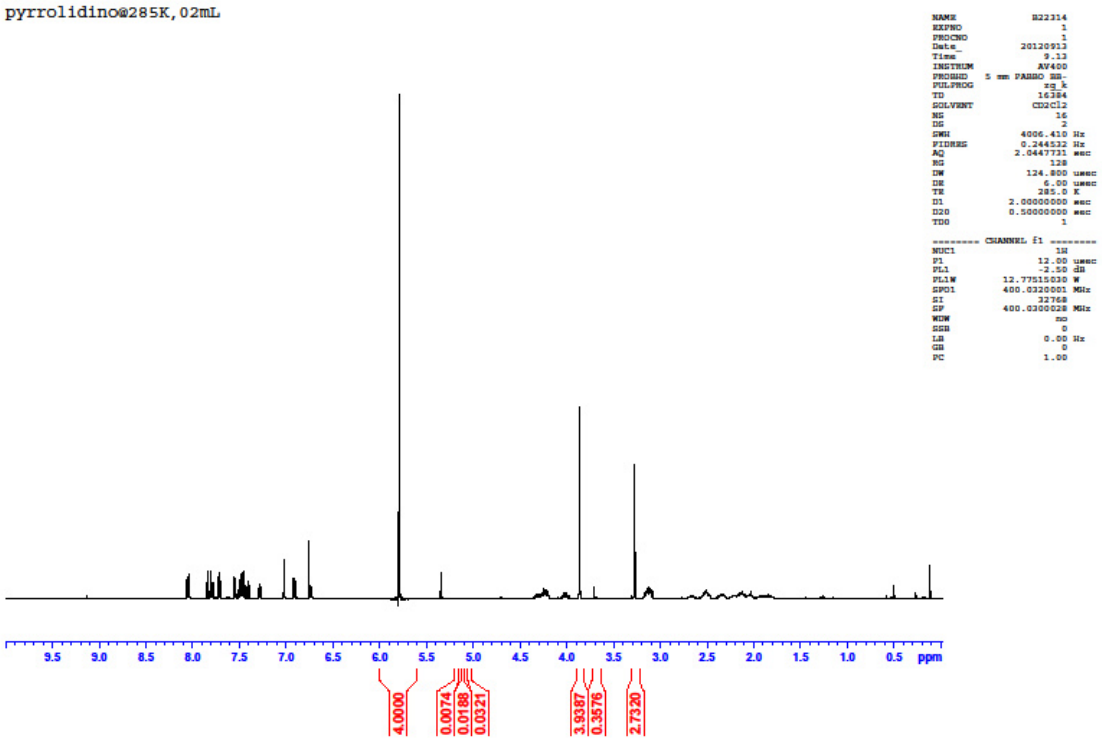

EXPERIMENT B3	T = 285K			phc0 69.929	sr 2.82						
FOLDER B22314				phc1 -12.889							
INTEGRALS normalised							INTEGRALS			LN OF INTEGRALS	
standard (COT)	error IM1 (noise)	corrected by avg error	error IM2 (noise)	corrected by avg error	P-CH3	IM2-CH3 eq	corrected by avg error			corrected by avg error	
6.0-5.6 ppm	5.2-5.125 ppm	5.15-5.06 ppm	5.1-5.016 ppm	3.895-3.820 ppm	3.73-3.64 ppm	3.31-3.225 ppm	IM1-CH3	P-CH3	IM2-CH3	IM1-CH3 OTf ax	IM2-CH3 OTf eq
4	0.0074	0.018765	0.032063	3.93871	0.35765	2.73199	3.923084871	0.313626692	2.677149793	1.366878301	0.984752719
4	0.010179264	0.027285263	0.042392781	3.817748511	0.586994884	2.632839042	3.802123382	0.542971576	2.577998835	1.335559696	0.947013453
4	0.0054306	0.026060256	0.044898778	3.708632065	0.810418684	2.538755237	3.693006936	0.766395376	2.48391503	1.306441014	0.909835956
4	0.006792923	0.02966253	0.04628427	3.536237332	1.019660601	2.390630178	3.520612203	0.975637293	2.335789971	1.258634896	0.848350151
4	0.010772392	0.031516215	0.047933437	3.406546038	1.240549346	2.296125507	3.390920909	1.196526038	2.241285301	1.221101539	0.807049496
4	0.010519687	0.033971104	0.050125942	3.305686535	1.451779309	2.200006045	3.290061407	1.407756002	2.145165838	1.190906229	0.763216863
4	0.007571243	0.034012779	0.04836859	3.197582658	1.639049073	2.08542726	3.181957529	1.595025766	2.030587053	1.157496583	0.70832494
4	0.012767686	0.037833636	0.052115911	3.110615164	1.854158099	2.006800606	3.094990035	1.810134791	1.951960399	1.129784686	0.6688342
4	0.010589852	0.038927148	0.050642074	2.971944464	2.017834971	1.886710807	2.956319335	1.973811663	1.831870601	1.083945027	0.605337631
4	0.010757819	0.038428089	0.050353675	2.872922959	2.201717709	1.807284032	2.85729783	2.157694402	1.752443825	1.049876364	0.561011285
4	0.015299452	0.043009835	0.053994661	2.743713562	2.36972695	1.717125022	2.728088433	2.325703642	1.662284815	1.003601156	0.508193051
4	0.014804246	0.045107277	0.056352639	2.698797688	2.568460475	1.658240076	2.683172559	2.524437168	1.603399869	0.986999885	0.472126293
4	0.017016513	0.044013191	0.055374731	2.50220616	2.644996897	1.534163229	2.486581031	2.600973589	1.479323022	0.910908687	0.391584566
4	0.013659902	0.043960952	0.054547937	2.482743488	2.837879482	1.487151481	2.467118359	2.793856175	1.432311274	0.903050813	0.359289415
4	0.015943797	0.045904385	0.056793568	2.395113841	2.97891152	1.418067007	2.379488712	2.934888212	1.3632268	0.866885638	0.309854537
4	0.018346852	0.048579153	0.058568344	2.325967433	3.154007368	1.365748197	2.310342304	3.109984061	1.31090799	0.837395697	0.270720019
4	0.019584195	0.05256831	0.05986982	2.261040352	3.312061112	1.312485504	2.245415223	3.268037805	1.257645297	0.808890459	0.229241161
4	0.019349262	0.051091127	0.059012723	2.19276446	3.460824209	1.259638842	2.177139331	3.416800901	1.204798635	0.778011782	0.186312445
4	0.018764918	0.050260788	0.060210987	2.099335016	3.564931684	1.195143752	2.083709887	3.520908377	1.140303546	0.734149905	0.131294495
4	0.0201521	0.051981967	0.058964167	2.01859539	3.672298446	1.13459765	2.002970261	3.628275138	1.079757443	0.694631209	0.076736426
4	0.021927205	0.050066055	0.058756375	1.890752825	3.748403468	1.070187596	1.875127697	3.70438016	1.015347389	0.628676762	0.015230809
4	0.019372264	0.05346906	0.06033393	1.934105103	4.019180958	1.0693812	1.918479974	3.97515765	1.014540993	0.651533192	0.014436287
4	0.022971862	0.05224452	0.060966689	1.774539897	3.943306912	0.974639446	1.758914768	3.899283605	0.919799239	0.56469701	-0.083599851
4	0.018953359	0.052191507	0.061058203	1.785578663	4.193151634	0.967076811	1.769953534	4.149128326	0.912236604	0.570953294	-0.091855888
4	0.018554145	0.052217778	0.057353265	1.727477252	4.320257974	0.93190281	1.711852124	4.276234666	0.877062603	0.537575898	-0.131176906
4	0.017845263	0.052796059	0.060094735	1.64239939	4.357674583	0.880124669	1.626774262	4.313651275	0.825284462	0.486599073	-0.192027149
4	0.018314482	0.050299235	0.060117318	1.59029775	4.467420736	0.844829344	1.574672621	4.423397428	0.789989137	0.454047391	-0.235736084
4	0.021110041	0.055541163	0.062780278	1.531894658	4.55785868	0.809271061	1.516269529	4.513835373	0.754430854	0.416253061	-0.28179165
4	0.020949402	0.053650082	0.060111048	1.49766889	4.663472321	0.779691125	1.482043762	4.619449014	0.724850918	0.393422055	-0.321789276
4	0.023053138	0.055284768	0.064766332	1.407483148	4.648163542	0.723246114	1.39185802	4.604140234	0.668405907	0.330639559	-0.402859644
	average	average	average								
	0.015625129	0.044023308	0.054840207								

Experiment B3	NMR entry	Time [sec]	Std COT 5.8 ppm, Integral=4	Integral IM1-CH3 (3.9 ppm)	Integral P-CH3 (3.7 ppm)	Integral IM2-CH3 (3.3 ppm)	[OTf IM1]	[P]	[OTf IM2]	LN [OTf IM1]	LN [OTf IM2]
Folder B22314	1	0	4	3.923084871	0.313626692	2.677149793	0.040237774	0.003216764	0.027458633	-3.212949077	-3.59507466
T = 285K	2	374	4	3.802123382	0.542971576	2.577998835	0.038997112	0.005569078	0.026441675	-3.244267683	-3.632813926
0.2 mL Stk sol	3	748	4	3.693006936	0.766395376	2.48391503	0.037877941	0.007860662	0.025476688	-3.273386364	-3.669991422
0.05 mL Tf2O	4	1122	4	3.520612203	0.975637293	2.335789971	0.036109746	0.010006787	0.023957419	-3.321192482	-3.731477227
0.4 mL d2-DCM	5	1496	4	3.390920909	1.196526038	2.241285301	0.034779545	0.012272369	0.022988116	-3.358725839	-3.772777882
	6	1870	4	3.290061407	1.407756002	2.145165838	0.033745063	0.014438884	0.022002251	-3.388921149	-3.816610515
V(sample)= 0.65 mL	7	2244	4	3.181957529	1.595025766	2.030587053	0.032636278	0.016359648	0.020827055	-3.422330796	-3.871502438
n(COT) = 0.02 mmol	8	2618	4	3.094990035	1.810134791	1.951960399	0.031744281	0.018565949	0.020020607	-3.450042692	-3.910993178
c(COT) = 0.03077	9	2992	4	2.956319335	1.973811663	1.831870601	0.030321982	0.020244728	0.018788886	-3.495882351	-3.974489747
c(amide) = 0.06154	10	3366	4	2.85729783	2.157694402	1.752443825	0.029306351	0.022130752	0.017974232	-3.529951015	-4.018816093
	11	3740	4	2.728088433	2.325703642	1.662284815	0.027981094	0.023853967	0.017049501	-3.576226222	-4.071634328
	12	4114	4	2.683172559	2.524437168	1.603399869	0.027520407	0.025892311	0.016445538	-3.592827493	-4.107701085
	13	4488	4	2.486581031	2.600973589	1.479323022	0.025504033	0.026677319	0.015172923	-3.668918691	-4.188242813
	14	4862	4	2.467118359	2.793856175	1.432311274	0.025304411	0.028655651	0.014690739	-3.676776565	-4.220537963
	15	5236	4	2.379488712	2.934888212	1.3632268	0.024405623	0.03010217	0.013982163	-3.712941741	-4.269972842
	16	5610	4	2.310342304	3.109984061	1.31090799	0.023696411	0.03189807	0.013445546	-3.742431681	-4.309107359
	17	5984	4	2.245415223	3.268037805	1.257645297	0.023030475	0.033519174	0.012899249	-3.77093692	-4.350586218
	18	6358	4	2.177139331	3.416800901	1.204798635	0.022330192	0.035044988	0.012357218	-3.801815597	-4.393514933
	19	6732	4	2.083709887	3.520908377	1.140303546	0.021371918	0.036112784	0.011695713	-3.845677474	-4.448532883
	20	7106	4	2.002970261	3.628275138	1.079757443	0.020543798	0.037214009	0.011074712	-3.885196169	-4.503090952
	21	7480	4	1.875127697	3.70438016	1.015347389	0.01923256	0.037994593	0.01041408	-3.951150616	-4.564596569
	22	7854	4	1.918479974	3.97515765	1.014540993	0.01967721	0.040771867	0.010405809	-3.928294186	-4.565391091
	23	8228	4	1.758914768	3.899283605	0.919799239	0.018040602	0.039993652	0.009434074	-4.015130369	-4.663427229
	24	8602	4	1.769953534	4.149128326	0.912236604	0.018153823	0.042556226	0.009356507	-4.008874084	-4.671683266
	25	8976	4	1.711852124	4.276234666	0.877062603	0.017557897	0.043859914	0.008995739	-4.042251481	-4.711004285
	26	9350	4	1.626774262	4.313651275	0.825284462	0.016685281	0.044243683	0.008464668	-4.093228305	-4.771854527
	27	9724	4	1.574672621	4.423397428	0.789989137	0.016150892	0.045369313	0.008102655	-4.125779987	-4.815563462
	28	10098	4	1.516269529	4.513835373	0.754430854	0.015551871	0.046296905	0.007737946	-4.163574317	-4.861619028
	29	10472	4	1.482043762	4.619449014	0.724850918	0.015200829	0.047380149	0.007434554	-4.186405323	-4.901616654
	30	10846	4	1.39185802	4.604140234	0.668405907	0.014275824	0.047223132	0.006855617	-4.249187819	-4.982687023
IM1-ax					IM2-eq						
slope	-9.41723E-05	-3.21381265	y-intercept		slope	-0.000126996	-3.590198161	y-intercept			
slope uncertainty	7.57956E-07	0.004787018	y-intercept uncertainty		slope uncertainty	7.71674E-07	0.004873658	y-intercept uncertainty			
R2 value	0.998189441	0.013438957	s(y)		R2 value	0.998967244	0.013682188	s(y)			
F	15436.83796	28	degrees of freedom		F	27083.90975	28	degrees of freedom			
regression ss	2.787978739	0.005056956	residual ss		regression ss	5.07016934	0.005241664	residual ss			

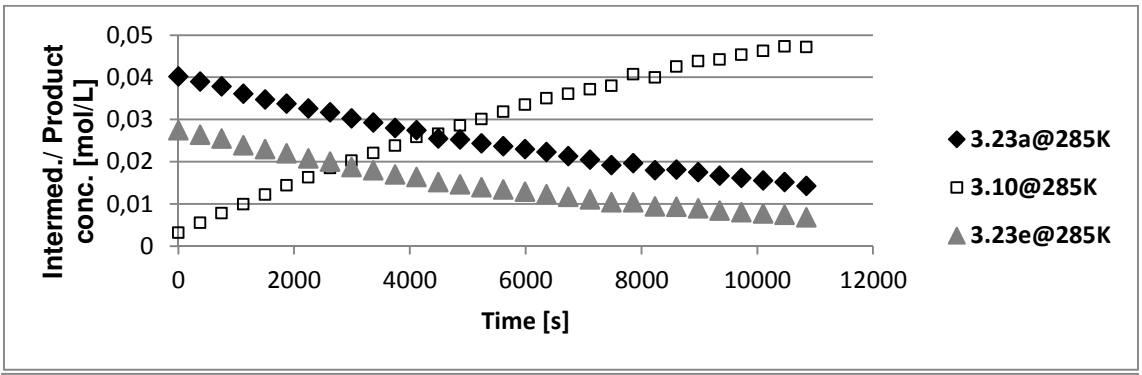

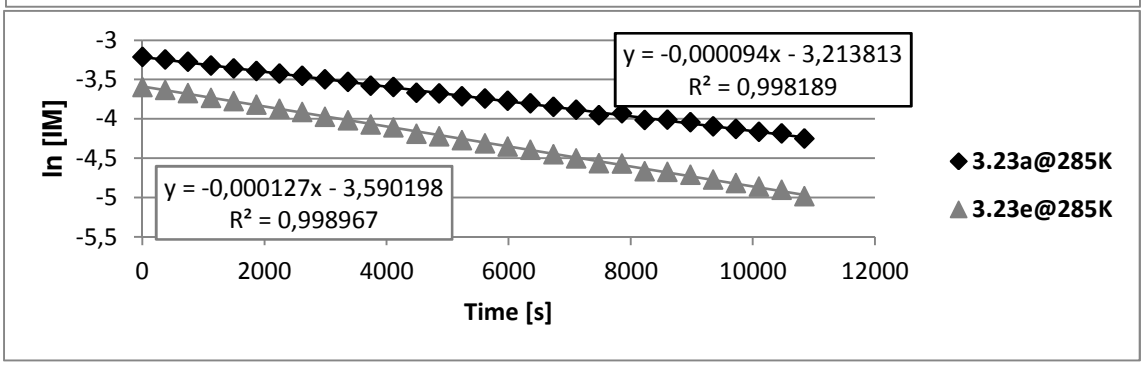

Kinetic data for compounds **3.23a** and **3.23e** at 288 K ([COT] = 0.03077 mol/L)

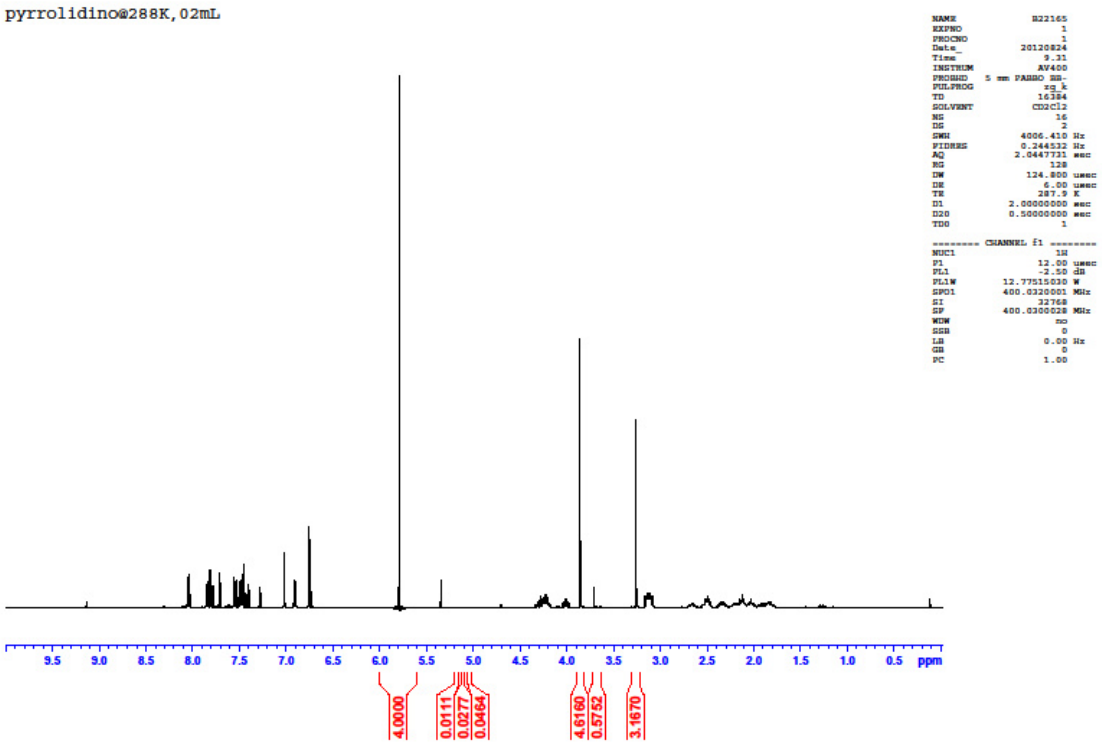

EXPERIMENT B4A	T = 288 K			phc0 54.847	sr 2.82						
FOLDER B22165				phc1 14.634							
INTEGRALS normalised							INTEGRALS			LN OF INTEGRALS	
standard (COT)	error IM1 (noise)	corrected by avg error	error IM2 (noise)	corrected by avg error	P-CH3	IM2-CH3 eq	corrected by avg error			corrected by avg error	
6.0-5.6 ppm	5.2-5.125 ppm	5.15-5.06 ppm	5.1-5.016 ppm	3.895-3.820 ppm	3.73-3.64 ppm	3.31-3.225 ppm	IM1-CH3	P-CH3	IM2-CH3	IM1-CH3 OTf ax	IM2-CH3 OTf eq
4	0.011114	0.027738	0.046353	4.61596	0.575241	3.16696	4.596866137	0.515963054	3.094509784	1.525374797	1.129629504
4	0.011162893	0.034954737	0.058314385	4.401862154	1.013625208	3.016066965	4.38276829	0.954347262	2.94361675	1.477680554	1.079639012
4	0.011577558	0.038675574	0.059821517	4.128114515	1.412902778	2.813158887	4.109020651	1.353624832	2.740708672	1.413184716	1.008216526
4	0.012676784	0.040949672	0.061299933	3.795898659	1.761345804	2.55695958	3.776804796	1.702067858	2.484509365	1.32887836	0.910075201
4	0.015391626	0.046282685	0.065454349	3.586116665	2.151328943	2.408287271	3.567022801	2.092050997	2.335837055	1.271731299	0.848370309
4	0.015866127	0.050849743	0.06821559	3.459461321	2.547574765	2.285586357	3.440367458	2.488296819	2.213136141	1.235578285	0.794410578
4	0.015133493	0.053125528	0.067160203	3.259342033	2.87653005	2.132019849	3.240248169	2.817252104	2.059569633	1.175649922	0.722497045
4	0.018864211	0.054990761	0.067578026	3.075900011	3.220834162	1.990003018	3.056806147	3.161556216	1.917552802	1.117370628	0.651049791
4	0.019344496	0.056664578	0.067433218	2.878959666	3.495883064	1.843162972	2.859865803	3.436605119	1.770712757	1.050774702	0.571382153
4	0.016458343	0.055670967	0.067020326	2.678830002	3.735718101	1.696952859	2.659736138	3.676440155	1.624502644	0.978226922	0.485201704
4	0.013734256	0.057003023	0.068122778	2.60485086	4.11115816	1.631488247	2.585756997	4.051880214	1.559038031	0.950018307	0.444068984
4	0.016575729	0.056492654	0.067797112	2.385771201	4.246116931	1.478852538	2.366677337	4.186838985	1.406402322	0.861487004	0.341034899
4	0.014842325	0.057584177	0.068185298	2.226670069	4.433835134	1.363913853	2.207576205	4.374557188	1.291463637	0.791895174	0.255776178
4	0.015945089	0.058453791	0.071404558	2.080015336	4.615332104	1.266190212	2.060921473	4.556054158	1.193739997	0.7231532	0.177091233
4	0.023717406	0.065928696	0.077738721	1.986182945	4.806556548	1.18609495	1.967089081	4.747278603	1.113644734	0.676554826	0.107638181
4	0.026515682	0.070522297	0.082316047	1.905358326	5.09304509	1.134632524	1.886264462	5.033767145	1.062182308	0.634598398	0.060325573
4	0.031212419	0.075698347	0.085670274	1.817913957	5.307896442	1.072687573	1.798820094	5.248618496	1.000237358	0.587130947	0.000237329
4	0.028128536	0.073357894	0.08441456	1.735357059	5.50478548	1.013619376	1.716263196	5.445507534	0.941169161	0.540149367	-0.060632389
4	0.026552463	0.073198867	0.084483762	1.670985504	5.774242888	0.972362072	1.651891641	5.714964942	0.899911856	0.50192108	-0.105458458
4	0.026539684	0.074142671	0.087052814	1.571423001	5.873588989	0.906148987	1.552329138	5.814311043	0.833698771	0.439756473	-0.181883127
4	0.026918472	0.075848069	0.085960357	1.503441548	6.061046211	0.858362937	1.484347684	6.001768265	0.785912721	0.394975406	-0.240909535
4	0.027585316	0.076023881	0.08692679	1.389891377	6.022174031	0.78613609	1.370797514	5.962896085	0.713685874	0.315392697	-0.337312365
4	0.023054268	0.070540755	0.081581666	1.317250823	6.173839095	0.743355034	1.298156959	6.114561149	0.670904818	0.260945535	-0.399128003
4	0.022654943	0.069136293	0.080190044	1.223315842	6.185307049	0.688465939	1.204221978	6.126029103	0.616015723	0.185833697	-0.484482792
4	0.026616079	0.072435163	0.083781665	1.159354251	6.262522036	0.646804324	1.140260388	6.20324409	0.574354108	0.131256647	-0.554509159
4	0.012537152	0.055958088	0.067885982	1.129854883	6.419025712	0.59537604	1.110761019	6.359747766	0.522925825	0.105045383	-0.648315652
4	0.016459686	0.059097372	0.070125183	1.10542591	6.784773249	0.582316327	1.086332046	6.725495304	0.509866112	0.082806926	-0.673607114
4	0.015584364	0.06034559	0.072428138	1.052786467	6.817835955	0.542848608	1.033692603	6.758558009	0.470398392	0.033137443	-0.754175301
4	0.013828609	0.058586378	0.070102471	0.992156436	6.913206465	0.516787007	0.973062573	6.853928519	0.444336791	-0.02730689	-0.811172465
4	0.016223894	0.058082118	0.068687706	0.931706185	7.022213125	0.498162094	0.912612321	6.96293518	0.425711878	-0.091444109	-0.853992503
	average	average	average								
	0.019093863	0.059277946	0.072450216								

Experiment B4A	NMR entry	Time [sec]	Std COT 5.8 ppm, Integral=4	Integral IM1-CH3 (3.9 ppm)	Integral P-CH3 (3.7 ppm)	Integral IM2-CH3 (3.3 ppm)	[OTf IM1]	[P]	[OTf IM2]	LN [OTf IM1]	LN [OTf IM2]
Folder B22165	1	0	4	4.596866137	0.515963054	3.094509784	0.047148524	0.005292061	0.031739355	-3.054452582	-3.450197874
T = 288 K	2	374	4	4.38276829	0.954347262	2.94361675	0.044952593	0.009788422	0.030191696	-3.102146824	-3.500188366
0.2 mL Stk sol	3	748	4	4.109020651	1.353624832	2.740708672	0.042144855	0.013883679	0.028110535	-3.166642663	-3.571610852
0.05 mL Tf2O	4	1122	4	3.776804796	1.702067858	2.484509365	0.038737428	0.017457543	0.025482784	-3.250949018	-3.669752177
0.4 mL d2-DCM	5	1496	4	3.567022801	2.092050997	2.335837055	0.036585764	0.02145747	0.023957902	-3.30809608	-3.731457069
	6	1870	4	3.440367458	2.488296819	2.213136141	0.035286702	0.025521631	0.0226994	-3.344249094	-3.7854168
V(sample)= 0.65 mL	7	2244	4	3.240248169	2.817252104	2.059569633	0.033234145	0.028895616	0.021124319	-3.404177456	-3.857330333
n(COT) = 0.02 mmol	8	2618	4	3.056806147	3.161556216	1.917552802	0.031352642	0.032427028	0.0196677	-3.46245675	-3.928777587
c(COT) = 0.03077	9	2992	4	2.859865803	3.436605119	1.770712757	0.02933269	0.035248113	0.018161611	-3.529052677	-4.008445225
c(amide) = 0.06154	10	3366	4	2.659736138	3.676440155	1.624502644	0.027280027	0.037708021	0.016661982	-3.601600457	-4.094625675
	11	3740	4	2.585756997	4.051880214	1.559038031	0.026521248	0.041558785	0.015990533	-3.629809071	-4.135758394
	12	4114	4	2.366677337	4.186838985	1.406402322	0.024274221	0.042943012	0.014425	-3.718340374	-4.238792479
	13	4488	4	2.207576205	4.374557188	1.291463637	0.022642373	0.044868375	0.013246112	-3.787932204	-4.324051201
	14	4862	4	2.060921473	4.556054158	1.193739997	0.021138185	0.046729929	0.012243793	-3.856674179	-4.402736145
	15	5236	4	1.967089081	4.747278603	1.11	0.020175777	0.048691254	0.011422283	-3.903272552	-4.472189198
	16	5610	4	1.886264462	5.033767145	1.062182308	0.019346786	0.051629672	0.01089445	-3.94522898	-4.519501806
	17	5984	4	1.798820094	5.248618496	1.000237358	0.018449898	0.05383333	0.010259101	-3.992696432	-4.579590049
	18	6358	4	1.716263196	5.445507534	0.941169161	0.01760314	0.055852756	0.009653258	-4.039678011	-4.640459767
	19	6732	4	1.651891641	5.714964942	0.899911856	0.016942902	0.05861649	0.009230096	-4.077906298	-4.685285837
	20	7106	4	1.552329138	5.814311043	0.833698771	0.015921723	0.05963545	0.00855097	-4.140070906	-4.761710506
	21	7480	4	1.484347684	6.001768265	0.785912721	0.015224459	0.061558137	0.008060845	-4.184851972	-4.820736913
	22	7854	4	1.370797514	5.962896085	0.713685874	0.014059813	0.061159438	0.007320038	-4.264434681	-4.917139743
	23	8228	4	1.298156959	6.114561149	0.670904818	0.013314763	0.062715016	0.006881247	-4.318881843	-4.978955381
	24	8602	4	1.204221978	6.126029103	0.616015723	0.012351303	0.062832638	0.006318268	-4.393993681	-5.06431017
	25	8976	4	1.140260388	6.20324409	0.574354108	0.011695271	0.063624607	0.005890959	-4.448570732	-5.134336538
	26	9350	4	1.110761019	6.359747766	0.522925825	0.011392706	0.065229813	0.005363476	-4.474781995	-5.22814303
	27	9724	4	1.086332046	6.725495304	0.509866112	0.011142146	0.068981163	0.005229527	-4.497020452	-5.253434492
	28	10098	4	1.033692603	6.758558009	0.470398392	0.01060224	0.069320277	0.00482472	-4.546689935	-5.334002679
	29	10472	4	0.973062573	6.853928519	0.444336791	0.009980378	0.07029846	0.004557414	-4.607134268	-5.390999843
	30	10846	4	0.912612321	6.96293518	0.425711878	0.00936036	0.071416505	0.004366385	-4.671271488	-5.433819882
IM1-ax					IM2-eq						
slope	-0.000149086	-3.082275871	y-intercept		slope	-0.000186251	-3.453753695	y-intercept			
slope uncertainty	1.42783E-06	0.009017708	y-intercept uncertainty		slope uncertainty	1.19623E-06	0.007555009	y-intercept uncertainty			
R2 value	0.997438341	0.025316091	s(y)		R2 value	0.998846312	0.021209745	s(y)			
F	10902.41839	28	degrees of freedom		F	24241.99545	28	degrees of freedom			
regression ss	6.987408535	0.017945325	residual ss		regression ss	10.90534151	0.012595892	residual ss			

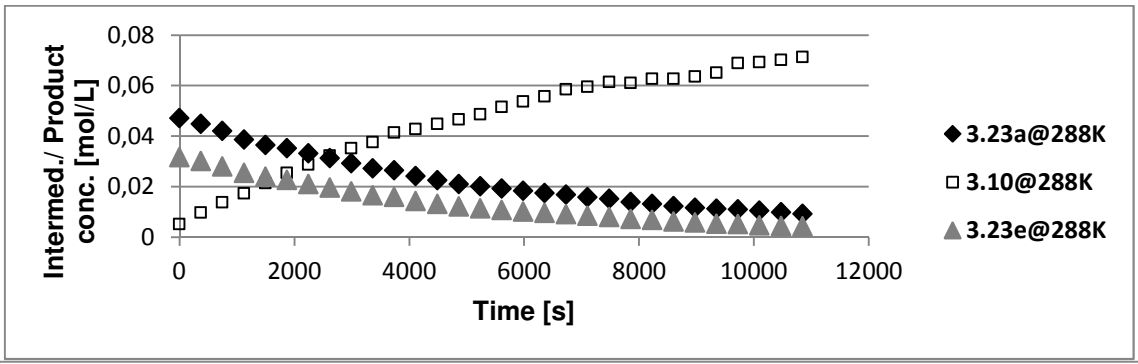

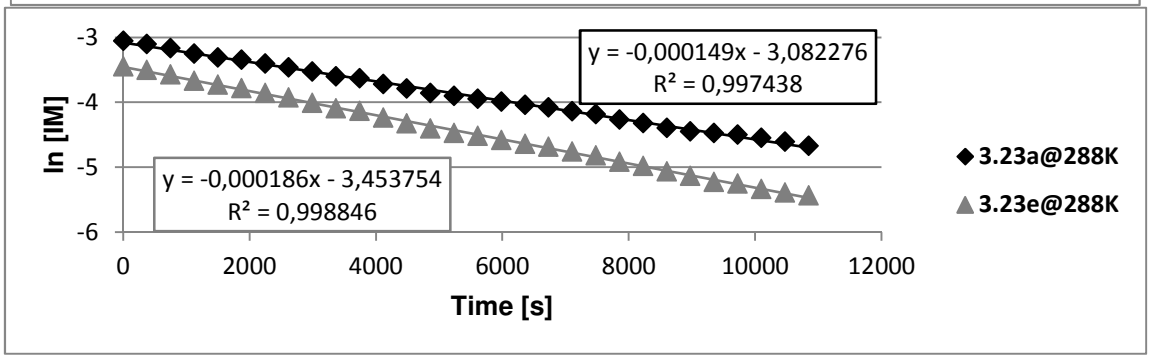

Kinetic data for compounds **3.23a** and **3.23e** at 288 K ([COT] = 0.04615 mol/L)

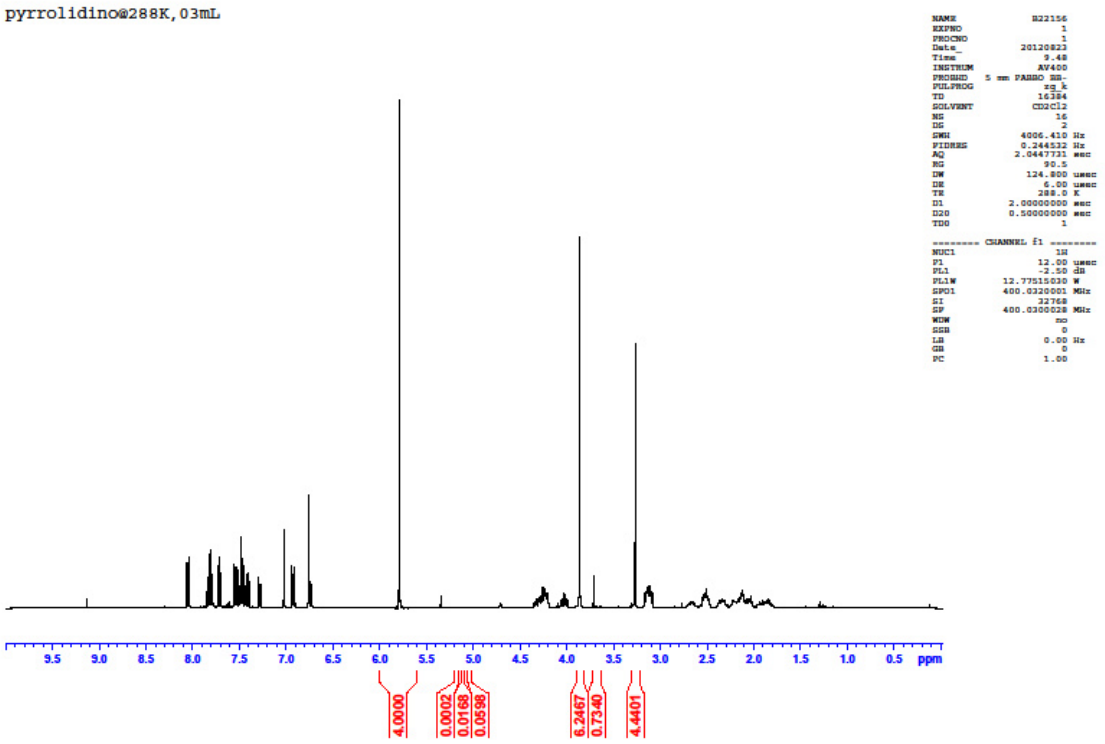

EXPERIMENT B4B	T = 288 K			phc0 69.760	sr 2.82						
FOLDER B22156				phc1 -14.106							
INTEGRALS normalised							INTEGRALS			LN OF INTEGRALS	
standard (COT)	error IM1 (noise)	corrected by avg error	error IM2 (noise)	corrected by avg error	P-CH3	IM2-CH3 eq	corrected by avg error			corrected by avg error	
6.0-5.6 ppm	5.2-5.125 ppm	5.15-5.06 ppm	5.1-5.016 ppm	3.895-3.820 ppm	3.73-3.64 ppm	3.31-3.225 ppm	IM1-CH3	P-CH3	IM2-CH3	IM1-CH3 OTf ax	IM2-CH3 OTf eq
4	0.000185	0.016751	0.059804	6.24666	0.73405	4.44008	6.214926873	0.651538468	4.336902046	1.826953959	1.467160279
4	0.004599193	0.031609615	0.074578697	6.033990483	1.400315881	4.259288602	6.002257355	1.317804349	4.156110649	1.792135624	1.424579697
4	0.014306737	0.039879793	0.075218316	5.202289991	1.924743964	3.65119078	5.170556864	1.842232432	3.548012827	1.642980393	1.26638768
4	0.010479345	0.045558815	0.080003632	5.271778366	2.625920386	3.605980269	5.240045239	2.543408854	3.502802316	1.656330132	1.25356331
4	0.014742975	0.054023223	0.082906149	5.010836071	3.249005163	3.359702467	4.979102944	3.166493631	3.256524514	1.605249743	1.180660527
4	0.025487679	0.062538621	0.08571588	4.425961534	3.674603134	2.945476315	4.394228406	3.592091602	2.842298361	1.480291954	1.044613007
4	0.021670636	0.066615308	0.087103855	4.367205595	4.308788131	2.812252311	4.335472468	4.226276598	2.709074357	1.466830593	0.996607011
4	0.025362537	0.068973239	0.089126856	3.98336967	4.765806645	2.552534739	3.951636543	4.683295113	2.449356785	1.374129808	0.895825453
4	0.025998293	0.073897084	0.088964887	3.843465088	5.256150111	2.369323292	3.811731961	5.173638578	2.266145338	1.338083669	0.818080299
4	0.02673812	0.072937705	0.090163033	3.415568874	5.500162958	2.101909972	3.383835747	5.417651426	1.998732019	1.219009902	0.692512989
4	0.028001536	0.078565887	0.094361077	3.384208371	6.128468839	2.013049882	3.352475244	6.045957307	1.909871929	1.209698952	0.647036187
4	0.029943604	0.080122128	0.097374497	3.088146756	6.436204439	1.835959678	3.056413628	6.353692906	1.732781724	1.117242212	0.54972805
4	0.031628445	0.08651644	0.10452215	2.911378545	6.849353759	1.694562982	2.879645417	6.766842227	1.591385028	1.057667168	0.464604724
4	0.030865117	0.089232998	0.106468742	2.776508267	7.194123254	1.56083525	2.74477514	7.111611722	1.457657297	1.009699155	0.376830556
4	0.034251987	0.089527141	0.106223377	2.517302908	7.380562734	1.4123769	2.485569781	7.298051201	1.309198947	0.910501921	0.269415459
4	0.037832358	0.091592617	0.109764205	2.300409228	7.444917869	1.259885535	2.2686761	7.362406337	1.156707582	0.819196446	0.145577678
4	0.037038811	0.088622614	0.103342553	2.108056335	7.581418533	1.144208685	2.076323208	7.498907	1.041030731	0.730598641	0.04021131
4	0.042217118	0.098668597	0.113505159	2.036748221	7.996633292	1.084811487	2.005015094	7.91412176	0.981633533	0.695651589	-0.018537224
4	0.040267932	0.096265947	0.114189201	1.90737664	8.223747485	0.999184578	1.875643513	8.141235952	0.896006624	0.628951808	-0.109807473
4	0.038221202	0.100327498	0.11569664	1.87062831	8.682579954	0.950321433	1.838895183	8.600068422	0.847143479	0.609164947	-0.165885202
4	0.04631161	0.103307061	0.121429173	1.69437052	8.686866419	0.858536585	1.662637393	8.604354886	0.755358632	0.508405133	-0.280562633
4	0.041073359	0.102929914	0.118066459	1.649349862	9.085220097	0.817165257	1.617616735	9.002708565	0.713987304	0.480953915	-0.336890099
4	0.038117287	0.095639257	0.111806726	1.469031357	8.861449307	0.731610311	1.437298229	8.778937774	0.628432357	0.362765122	-0.464526883
4	0.04442639	0.103034112	0.122297504	1.416436732	9.230915445	0.691881783	1.384703605	9.148403913	0.58870383	0.325486113	-0.529832058
4	0.043552977	0.107585479	0.124086369	1.382530319	9.533955862	0.650945205	1.350797192	9.451444329	0.547767251	0.300694931	-0.601904806
4	0.041223615	0.104411672	0.123559049	1.294580651	9.648571954	0.60776279	1.262847523	9.566060421	0.504584837	0.23336911	-0.684019293
4	0.043559136	0.104442231	0.121694836	1.183491648	9.511171233	0.553803769	1.151758521	9.4286597	0.450625815	0.141289923	-0.797117962
4	0.047570833	0.112405045	0.128066041	1.167905702	9.908255672	0.52364707	1.136172574	9.82574414	0.420469117	0.127665223	-0.866384247
4	0.041991707	0.102882087	0.122194206	1.047548667	9.676957789	0.477239639	1.01581554	9.594446256	0.374061685	0.015691777	-0.983334562
4	0.044328278	0.106482841	0.123105334	0.98565367	9.686999387	0.440807772	0.953920543	9.604487855	0.337629818	-0.047174899	-1.085805196
	average	average	average								
	0.031733127	0.082511532	0.103177954								

Experiment B4B	NMR entry	Time [sec]	Std COT 5.8 ppm, Integral=4	Integral IM1-CH3 (3.9 ppm)	Integral P-CH3 (3.7 ppm)	Integral IM2-CH3 (3.3 ppm)	[OTf IM1]	[P]	[OTf IM2]	LN [OTf IM1]	[OTf IM2]
Folder B22156	1	0	4	6.216066639	0.654522454	4.340547721	0.095623825	0.010068737	0.066772092	-2.347333273	-2.706470064
T = 288 K	2	374	4	5.888327252	1.294083924	4.07853051	0.090582101	0.019907324	0.062741394	-2.401498647	-2.768733852
0.3 mL Stk sol	3	748	4	5.171941929	1.845307174	3.551830663	0.079561707	0.028386975	0.054638995	-2.531222374	-2.907007457
0.05 mL Tf2O	4	1122	4	5.01503128	2.433743628	3.351755245	0.077147898	0.037439089	0.051561168	-2.562030948	-2.964986444
0.3 mL d2-DCM	5	1496	4	4.782335409	3.04115535	3.127475836	0.07356826	0.046783106	0.048111003	-2.6095416	-3.03424437
	6	1870	4	4.26185195	3.484225296	2.757089022	0.065561489	0.053598999	0.042413219	-2.724766811	-3.160295186
V(sample)= 0.65 mL	7	2244	4	4.206412092	4.10080205	2.62887794	0.064708639	0.063084005	0.040440906	-2.737860557	-3.20791349
n(COT) = 0.03 mmol	8	2618	4	3.775719412	4.474443641	2.339544779	0.05808315	0.068831858	0.035989997	-2.84587967	-3.324514235
c(COT) = 0.04615 mol/L	9	2992	4	3.654498718	4.960038755	2.172161178	0.056218372	0.07630193	0.033415079	-2.878511673	-3.398748
c(amide) = 0.09231 mol/L	10	3366	4	3.257396503	5.215192229	1.923866733	0.050109616	0.08022704	0.029595483	-2.993542349	-3.520133522
	11	3740	4	3.244564445	5.851461435	1.848650372	0.049912216	0.090014982	0.028438405	-2.997489489	-3.560014763
	12	4114	4	2.894340736	6.016514938	1.639394491	0.044524608	0.092554055	0.025219352	-3.111713247	-3.680143646
	13	4488	4	2.657931384	6.245536951	1.465319024	0.040887844	0.096077177	0.022541491	-3.196922462	-3.792397624
	14	4862	4	2.523089575	6.537239999	1.336040016	0.038813528	0.100564542	0.020552749	-3.248986434	-3.88476058
	15	5236	4	2.297065556	6.745011769	1.21	0.035336525	0.103760764	0.018559092	-3.342838143	-3.986795458
	16	5610	4	2.180994501	7.077933743	1.111707671	0.033550965	0.108882214	0.01710177	-3.394689641	-4.068573331
	17	5984	4	2.039517252	7.365422906	1.024080265	0.031374574	0.113304756	0.015753768	-3.461757468	-4.150675699
	18	6358	4	1.931069723	7.622308235	0.945287412	0.029706289	0.117256508	0.014541671	-3.516396497	-4.230736865
	19	6732	4	1.847143739	8.016427615	0.884125543	0.028415228	0.123319378	0.013600798	-3.560830085	-4.297626816
	20	7106	4	1.773405235	8.293788501	0.816939754	0.027280884	0.127586113	0.012567257	-3.601569047	-4.376660534
	21	7480	4	1.60532684	8.307669995	0.729387563	0.024695278	0.127799657	0.011220412	-3.701143232	-4.490020659
	22	7854	4	1.530731916	8.52082106	0.674021472	0.023547759	0.131078631	0.010368697	-3.748724609	-4.568963918
	23	8228	4	1.411451466	8.61913438	0.618638139	0.021712828	0.132591017	0.009516717	-3.829852023	-4.654705373
	24	8602	4	1.279896877	8.4609348	0.540598199	0.01968908	0.13015738	0.008316202	-3.927691097	-4.789549583
	25	8976	4	1.252478442	8.768560462	0.504584265	0.019267293	0.134889688	0.007762188	-3.949346265	-4.858491034
	26	9350	4	1.198789752	9.083124022	0.477622425	0.018441382	0.139728725	0.007347425	-3.993158098	-4.913405372
	27	9724	4	1.156822745	9.463182724	0.456107903	0.01779579	0.145575294	0.00701646	-4.028793373	-4.959496475
	28	10098	4	1.107368406	9.57469036	0.410689004	0.017035017	0.147290653	0.006317766	-4.072484211	-5.064389639
	29	10472	4	1.024469843	9.666847402	0.381130814	0.015759761	0.148708336	0.005863062	-4.150295355	-5.139083226
	30	10846	4	0.97659801	9.81914426	0.350907665	0.015023333	0.151051169	0.00539813	-4.198150771	-5.221702759
IM1-ax					IM2-eq						
slope	-0.000176742	-2.371944217	y-intercept		slope	-0.000238256	-2.702934712	y-intercept			
slope uncertainty	1.89201E-06	0.010723695	y-intercept uncertainty		slope uncertainty	1.5935E-06	0.009031765	y-intercept uncertainty			
R2 value	0.997143284	0.028638642	s(y)		R2 value	0.998882955	0.024120183	s(y)			
F	8726.307383	25	degrees of freedom		F	22355.47198	25	degrees of freedom			
regression ss	7.157071529	0.020504296	residual ss		regression ss	13.00603877	0.014544581	residual ss			

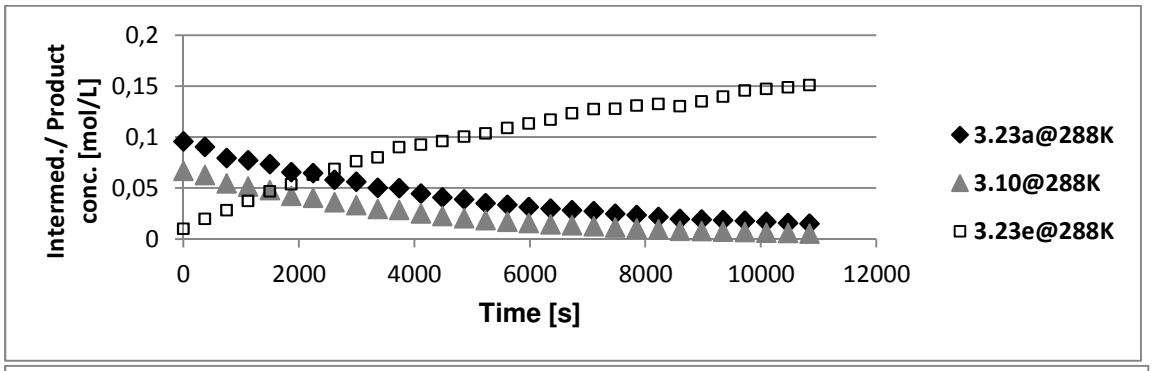

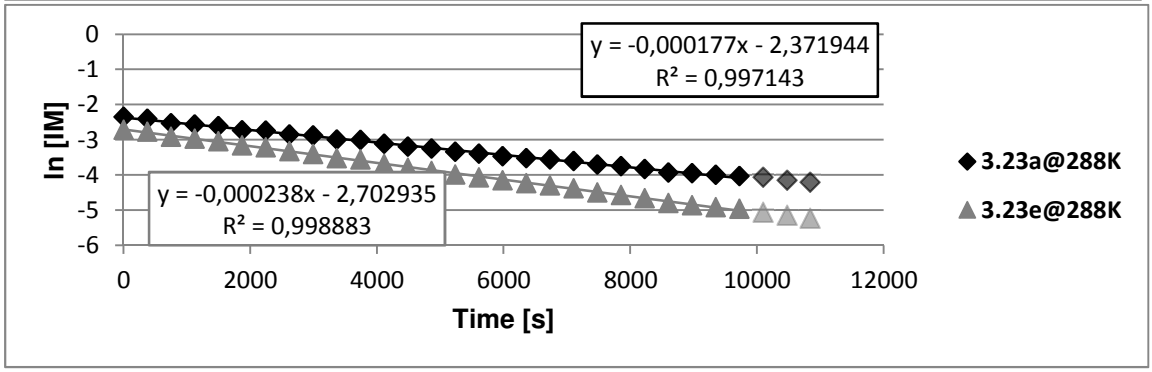

Kinetic data for compounds **3.23a** and **3.23e** at 288 K ([COT] = 0.06154 mol/L)

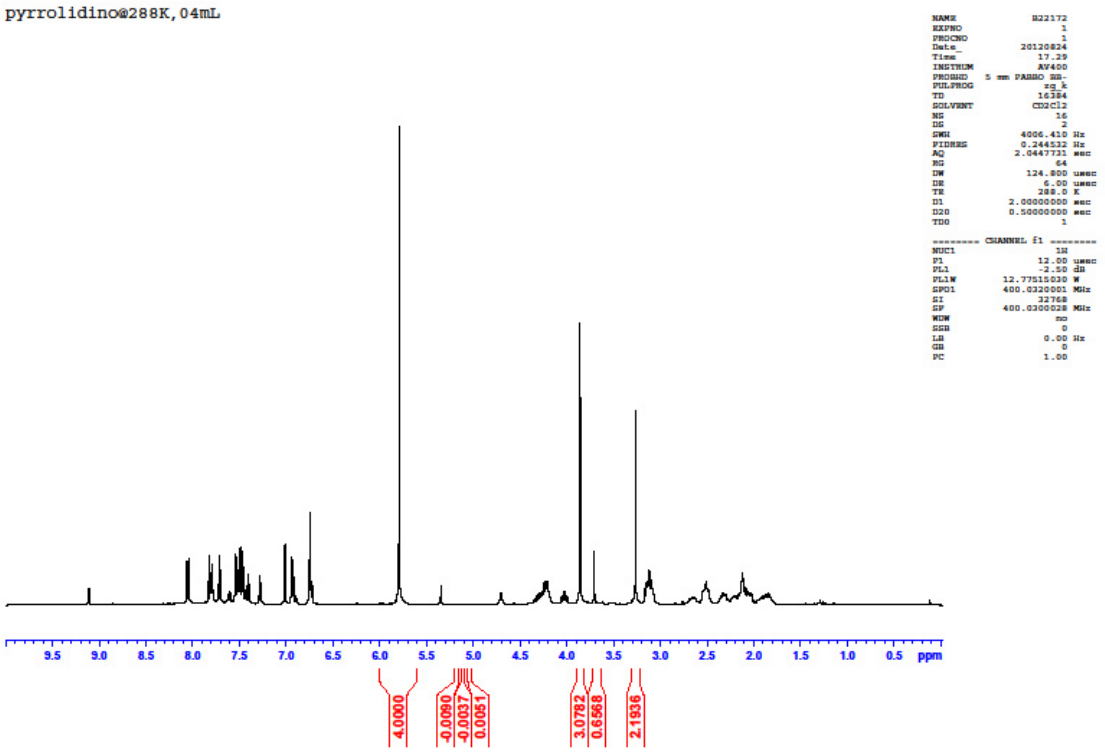

EXPERIMENT B4C	T = 288 K			phc0 63.408	sr 2.82						
FOLDER B22172				phc1 -6.002							
INTEGRALS normalised							INTEGRALS			LN OF INTEGRALS	
standard (COT)	error IM1 (noise)	corrected by avg error	error IM2 (noise)	corrected by avg error	P-CH3	IM2-CH3 eq	corrected by avg error			corrected by avg error	
6.0-5.6 ppm	5.2-5.125 ppm	5.15-5.06 ppm	5.1-5.016 ppm	3.895-3.820 ppm	3.73-3.64 ppm	3.31-3.225 ppm	IM1-CH3	P-CH3	IM2-CH3	IM1-CH3 OTf ax	IM2-CH3 OTf eq
4	-0.008962	-0.003695	0.005069	3.07821	0.656838	2.19355	3.075027242	0.629163887	2.156752753	1.12331376	0.768603735
4	-0.010395313	-0.000379245	0.009069951	3.057535504	1.056777014	2.131757802	3.054352746	1.029102901	2.094960555	1.116567703	0.739534725
4	-0.005854594	0.004264371	0.012565077	2.676166486	1.411170241	1.847120545	2.672983728	1.383496128	1.810323298	0.98319535	0.593505447
4	0.002789532	0.012041838	0.018176552	2.427815354	1.740099904	1.645290679	2.424632595	1.712425792	1.608493431	0.885680006	0.475297984
4	-0.005214278	0.011800099	0.019740343	2.499913146	2.125498153	1.638409232	2.496730387	2.097824041	1.601611985	0.914982031	0.471010613
4	-0.004235299	0.014995684	0.023618732	2.328970151	2.442258086	1.49934628	2.325787392	2.414583973	1.462549032	0.844058645	0.380180826
4	-0.003283402	0.017306327	0.02725456	2.167520193	2.735066661	1.369913266	2.164337434	2.707392548	1.333116019	0.77211428	0.287519073
4	-0.001854242	0.019993826	0.029765032	2.01993917	3.005490863	1.249831732	2.016756412	2.97781675	1.213034484	0.701490484	0.193125058
4	-0.000582675	0.021907578	0.032767632	1.880896104	3.256425262	1.140219542	1.877713345	3.228751149	1.103422294	0.630054731	0.098416527
4	0.001946316	0.023947528	0.034024372	1.621604005	3.365608975	0.998823655	1.618421246	3.337934862	0.962026408	0.481451135	-0.038713378
4	0.000876233	0.02623815	0.036591137	1.628409906	3.722485409	0.951072394	1.625227148	3.694811296	0.914275146	0.485647589	-0.089623718
4	0.00186837	0.027955415	0.039425867	1.514701472	3.917803902	0.860129403	1.511518714	3.89012979	0.823332156	0.413114916	-0.194395568
4	0.002252661	0.029013697	0.040731198	1.412067824	4.114048577	0.782489943	1.408885066	4.086374464	0.745692696	0.342798658	-0.293441699
4	0.003636494	0.030085673	0.041895843	1.238196986	4.166244096	0.695322755	1.235014228	4.138569983	0.658525508	0.21108249	-0.417752022
4	0.003763316	0.032575883	0.042959242	1.234381907	4.47004653	0.646628015	1.231199149	4.442372418	0.609830767	0.207988612	-0.494573791
4	0.004617934	0.033150934	0.043286864	1.099415982	4.529870821	0.578602039	1.096233224	4.502196708	0.541804792	0.091879961	-0.612849505
4	0.004989518	0.034191574	0.044010682	1.029437846	4.67375403	0.527515134	1.026255088	4.646079917	0.490717887	0.025916339	-0.711885885
4	0.026155201	0.049033134	0.053724883	0.93691536	4.556196912	0.4885326	0.933732602	4.528522799	0.451735353	-0.068565175	-0.794658773
4	0.011618081	0.037059332	0.045595255	0.859409115	4.605850929	0.407023804	0.856226357	4.578176816	0.370226557	-0.155220502	-0.993640146
4	0.00641377	0.036897907	0.045578923	0.886036272	5.132021636	0.404151656	0.882853513	5.104347523	0.367354409	-0.124595989	-1.001428206
4	0.006727832	0.036815164	0.045916015	0.830338907	5.234596171	0.368665061	0.827156149	5.206922058	0.331867814	-0.189761788	-1.10301854
4	0.006752828	0.037868436	0.047349929	0.779149758	5.327480814	0.336728068	0.775967	5.299806701	0.299930821	-0.253645286	-1.204203428
4	0.006974113	0.039104109	0.048192933	0.732927266	5.430291095	0.309040621	0.729744508	5.402616982	0.272243374	-0.315060796	-1.301058856
4	0.008951175	0.038258236	0.047348934	0.642880581	5.245030785	0.274580204	0.639697823	5.217356673	0.237782956	-0.446759366	-1.43639697
4	0.008418226	0.04011517	0.04843217	0.650508838	5.589102788	0.260826587	0.647326079	5.561428675	0.22402934	-0.434905125	-1.495978255
4	0.007720119	0.039439804	0.048382094	0.584004934	5.481583558	0.236705918	0.580822176	5.453909446	0.19990867	-0.543310635	-1.609894666
4	0.008682223	0.040892704	0.049691655	0.578417883	5.709246232	0.220832171	0.575235125	5.681572119	0.184034924	-0.55297641	-1.692629736
4	0.008754205	0.041099288	0.049818353	0.54801015	5.768359801	0.203535789	0.544827391	5.740685688	0.166738542	-0.607286248	-1.79132831
4	0.008848939	0.041379917	0.050192633	0.51690432	5.821391146	0.189483217	0.513721562	5.793717034	0.152685969	-0.666073869	-1.879371955
4	-0.006892526	0.016865849	0.022741564	0.459867165	5.901277295	0.219404732	0.456684407	5.873603183	0.182607484	-0.783762702	-1.700416325
	average	average	average								
	0.003182758	0.027674113	0.036797247								

Experiment B4C	NMR entry	Time [sec]	Std COT 5.8 ppm, Integral=4	Integral IM1-CH3 (3.9 ppm)	Integral P-CH3 (3.7 ppm)	Integral IM2-CH3 (3.3 ppm)	[OTf IM1]	[P]	[OTf IM2]	LN [OTf IM1]	[OTf IM2]
Folder B22172	1	0	4	3.075347851	0.630878113	2.158938607	0.063085636	0.012941413	0.044287027	-2.763262181	-3.117063482
T = 288 K	2	374	4	3.069259949	1.035858696	2.107316392	0.062960752	0.021248915	0.043228084	-2.765243724	-3.141264912
0.4 mL Stk sol	3	748	4	2.641631488	1.368508933	1.790648192	0.054188667	0.02807268	0.036732163	-2.915283484	-3.304102525
0.05 mL Tf2O	4	1122	4	2.284086857	1.613176195	1.515216471	0.046854235	0.033091621	0.031082141	-3.060713878	-3.471121884
0.2 mL d2-DCM	5	1496	4	2.430122288	2.04263355	1.55993367	0.049849909	0.041901223	0.031999439	-2.998738617	-3.442036897
	6	1870	4	2.267195616	2.354520141	1.426808224	0.046507739	0.048299056	0.029268593	-3.068136542	-3.531240259
V(sample)= 0.65 mL	7	2244	4	2.099506288	2.626895593	1.294124747	0.043067872	0.053886385	0.026546812	-3.144977982	-3.628845603
n(COT) = 0.04 mmol	8	2618	4	1.95600643	2.888663336	1.177433081	0.040124212	0.059256114	0.024153077	-3.215775339	-3.723343484
c(COT) = 0.06154	9	2992	4	1.800447916	3.096139434	1.058574654	0.036933188	0.06351214	0.021714895	-3.298644722	-3.829756861
c(amide) = 0.12308	10	3366	4	1.522437284	3.139770739	0.90489366	0.031230263	0.064407164	0.018562385	-3.466367671	-3.986618043
	11	3740	4	1.572830374	3.576015514	0.885671426	0.032263994	0.073355998	0.018168073	-3.433803416	-4.008089445
	12	4114	4	1.421623833	3.658499948	0.774288777	0.029162244	0.075048029	0.015883244	-3.534880435	-4.142490576
	13	4488	4	1.307469644	3.791681557	0.691502065	0.026820561	0.077780028	0.014185012	-3.618586498	-4.255569339
	14	4862	4	1.129715123	3.784898502	0.601399483	0.023174223	0.077640885	0.012336708	-3.764714701	-4.395176066
	15	5236	4	1.127693107	4.068100932	0.56	0.023132745	0.08345031	0.011438794	-3.76650615	-4.470744696
	16	5610	4	1.021725241	4.195598283	0.50460976	0.02095899	0.086065706	0.010351228	-3.865187586	-4.570650098
	17	5984	4	0.96089244	4.349585377	0.459245651	0.019711107	0.089224495	0.009420659	-3.926572999	-4.664850223
	18	6358	4	0.815990253	3.95609969	0.392360039	0.01673868	0.081152792	0.008048612	-4.090033067	-4.822255591
	19	6732	4	0.817082788	4.368389771	0.353721826	0.016761092	0.089610235	0.007256014	-4.088695055	-4.925924676
	20	7106	4	0.838650338	4.848174985	0.349231432	0.017203514	0.09945223	0.007163901	-4.062641618	-4.938700646
	21	7480	4	0.793978623	4.997458405	0.319180715	0.016287148	0.10251453	0.00654746	-4.117378939	-5.028678029
	22	7854	4	0.722469182	4.933534371	0.278857765	0.014820251	0.101203235	0.005720302	-4.211760712	-5.163733629
	23	8228	4	0.680200286	5.034880433	0.253403598	0.013953175	0.103282181	0.005198152	-4.272048183	-5.259452012
	24	8602	4	0.585271922	4.772413866	0.216586073	0.012005878	0.097898116	0.004442902	-4.422358914	-5.41644744
	25	8976	4	0.590053818	5.06831108	0.203122884	0.012103971	0.103967955	0.004166727	-4.414221726	-5.480624339
	26	9350	4	0.538264024	5.0531553	0.184715123	0.011041589	0.103657059	0.003789123	-4.506086287	-5.575620715
	27	9724	4	0.553896623	5.469501121	0.177951621	0.011362266	0.1121977	0.003650381	-4.477457408	-5.612923754
	28	10098	4	0.520750173	5.485588155	0.159862829	0.010682322	0.112527698	0.003279319	-4.539165065	-5.720119349
	29	10472	4	0.491135991	5.537461212	0.146475035	0.010074836	0.113591788	0.003004691	-4.597714419	-5.807580473
	30	10846	4	0.435608318	5.60074279	0.174584876	0.008935779	0.114889904	0.003581318	-4.717691991	-5.632024457
IM1-ax					IM2-eq						
slope	-0.000181804	-2.784898517	y-intercept		slope	-0.00026803	-3.065977325	y-intercept			
slope uncertainty	3.46363E-06	0.021875219	y-intercept uncertainty		slope uncertainty	2.8121E-06	0.015331419	y-intercept uncertainty			
R2 value	0.98993943	0.061411949	s(y)		R2 value	0.997365109	0.040220811	s(y)			
F	2755.142385	28	degrees of freedom		F	9084.536359	24	degrees of freedom			
regression ss	10.39081957	0.105599968	residual ss		regression ss	14.69617831	0.038825127	residual ss			

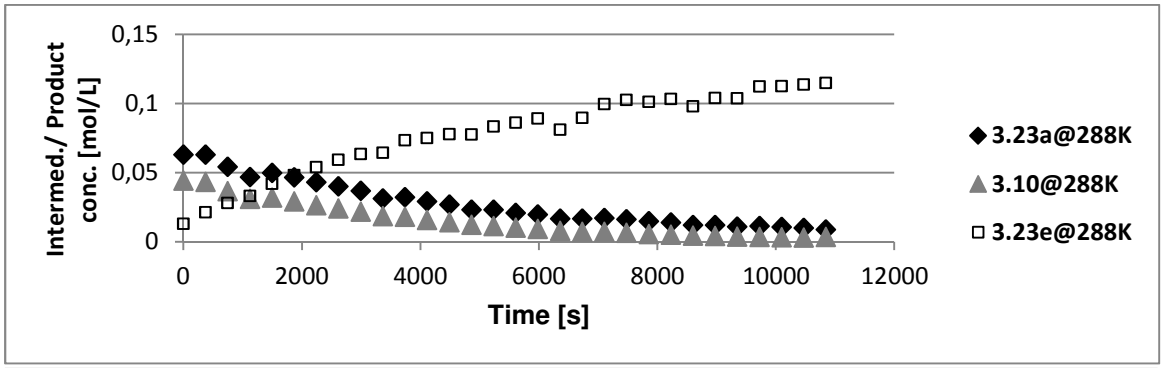

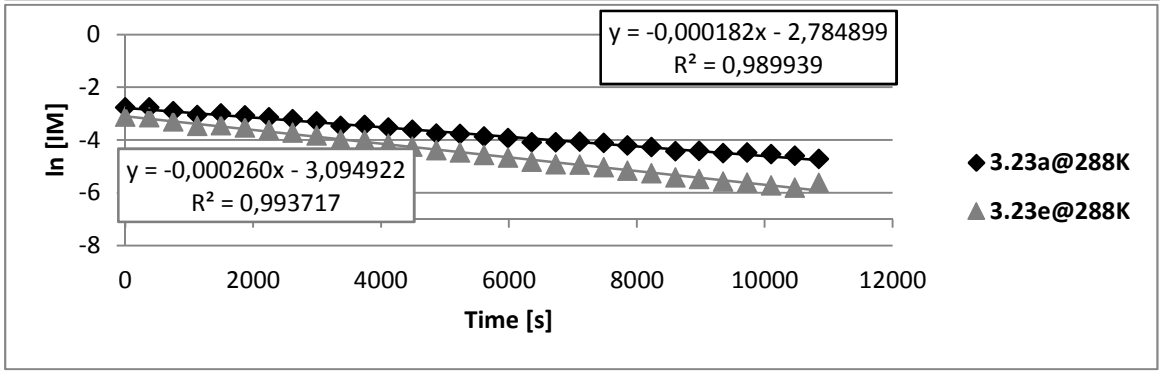

Kinetic data for compounds **3.23a** and **3.23e** at 291 K ([COT] = 0.03077 mol/L)

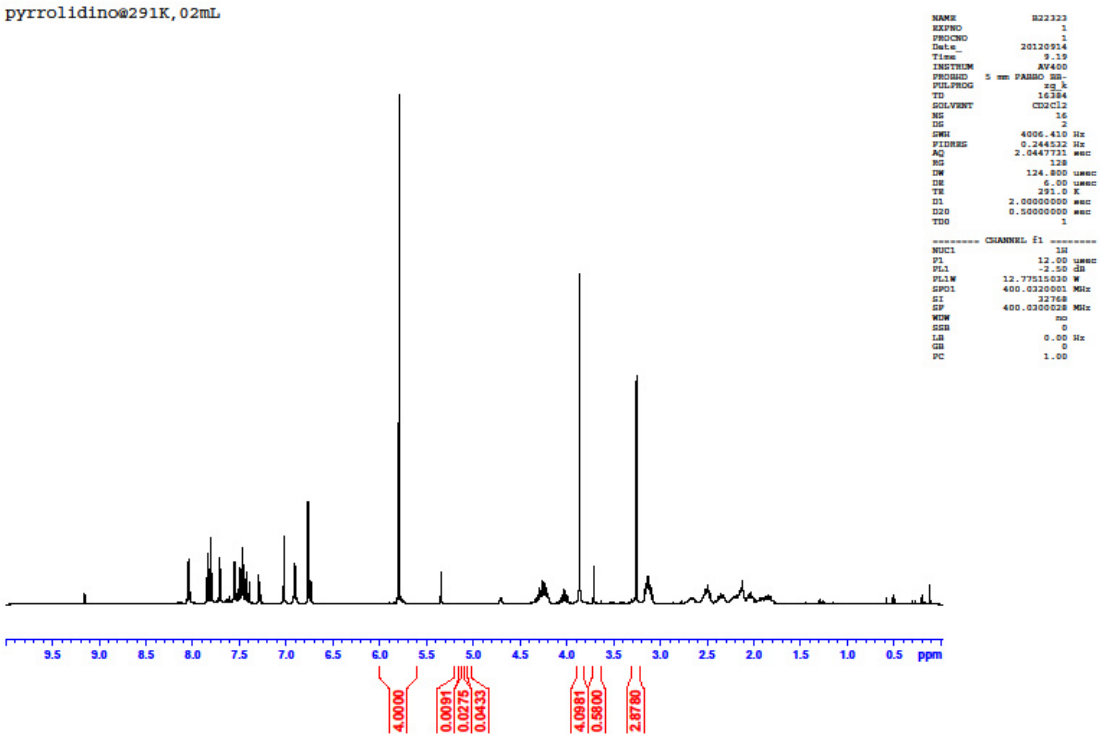

EXPERIMENT B5	T = 291 K			phc0 68.238	sr 2.82						
FOLDER B22323				phc1 -14.140							
INTEGRALS normalised							INTEGRALS			LN OF INTEGRALS	
standard (COT)	error IM1 (noise)	error P (noise)	error IM2 (noise)	IM1-CH3 ax	P-CH3	IM2-CH3 eq	corrected by avg error			corrected by avg error	
6.0-5.6 ppm	5.2-5.125 ppm	5.15-5.06 ppm	5.1-5.016 ppm	3.895-3.820 ppm	3.73-3.64 ppm	3.31-3.225 ppm	IM1-CH3	P-CH3	IM2-CH3	IM1-CH3 OTf ax	IM2-CH3 OTf eq
4	0.009097	0.027456	0.043323	4.09809	0.580024	2.87803	4.082366043	0.522691127	2.807557348	1.406676733	1.032314834
4	0.012843484	0.037785671	0.054044393	3.776038075	1.132962768	2.647267188	3.760314119	1.075629895	2.576794536	1.324502496	0.946546198
4	0.012151088	0.042441964	0.05983078	3.565279594	1.724645284	2.490877648	3.549555637	1.667312411	2.420404996	1.266822423	0.88393488
4	0.01373372	0.046867964	0.064098051	3.194632084	2.241526125	2.177716931	3.178908127	2.184193252	2.107244279	1.156537782	0.745381065
4	0.017183226	0.055024188	0.068909271	2.963436446	2.734708722	1.999790752	2.947712489	2.677375849	1.9293181	1.081029442	0.657166625
4	0.020068096	0.05767174	0.072370436	2.606275369	3.12498699	1.715254271	2.590551412	3.067654117	1.644781619	0.951870753	0.497607621
4	0.020379591	0.061166785	0.07656252	2.400464173	3.573191014	1.549237091	2.384740216	3.515858141	1.478764439	0.869090194	0.3912069
4	0.019722231	0.065575074	0.079415829	2.24887908	3.993368924	1.421575353	2.233155123	3.936036051	1.351102701	0.803415439	0.300921074
4	0.020475447	0.065706003	0.080716512	2.004173712	4.303933339	1.24059739	1.988449755	4.246600466	1.170124738	0.687355317	0.157110357
4	0.021999421	0.069605052	0.083514672	1.87897771	4.680694182	1.134120633	1.863253753	4.623361309	1.063647981	0.622324289	0.061704491
4	0.023365152	0.075104416	0.088476641	1.716583809	4.974227848	1.01089024	1.700859852	4.916894975	0.940417588	0.531133919	-0.06143126
4	0.025270042	0.075893867	0.091262455	1.54544231	5.203098441	0.894420712	1.529718354	5.145765568	0.82394806	0.425083636	-0.193647785
4	0.023850013	0.076716423	0.091330938	1.434160212	5.478652688	0.807756094	1.418436255	5.421319815	0.737283442	0.349555036	-0.304782872
4	0.028051287	0.079281453	0.09306232	1.295174334	5.670401142	0.719177511	1.279450377	5.613068269	0.648704859	0.246430593	-0.432777429
4	0.026212985	0.08066892	0.094638551	1.212853756	5.911052817	0.653883872	1.197129799	5.853719944	0.58341122	0.179926858	-0.538862989
4	0.011542578	0.044379626	0.05131613	0.972048029	6.05838757	0.660930041	0.956324072	6.001054697	0.590457389	-0.044658436	-0.526857806
4	0.002651944	0.042220047	0.051399382	0.939524261	6.533345568	0.6386882	0.923800304	6.476012695	0.568215548	-0.079259352	-0.565254446
4	0.009532119	0.042772747	0.051864796	0.82343321	6.48272086	0.57651306	0.807709254	6.425387987	0.506040408	-0.21355312	-0.681138755
4	0.003470796	0.042936803	0.052299785	0.783640303	6.809415043	0.549998596	0.767916346	6.75208217	0.479525944	-0.264074476	-0.734957279
4	0.004615871	0.040687135	0.051490413	0.707012	6.892448042	0.512754584	0.691288043	6.835115169	0.442281932	-0.369198692	-0.815807746
4	0.006540651	0.040309479	0.050288785	0.639215081	6.904747197	0.478100709	0.623491124	6.847414324	0.407628057	-0.47242075	-0.897400145
4	0.015536219	0.061729907	0.073519113	0.663365703	7.013809232	0.379507724	0.647641746	6.956476359	0.309035072	-0.434417597	-1.174300506
4	0.013896277	0.059576198	0.072781056	0.606507771	7.075773087	0.353319992	0.590783814	7.018440214	0.28284734	-0.526305125	-1.262847962
4	0.015475382	0.062140104	0.074187643	0.569170589	7.171213972	0.32944366	0.553446632	7.113881099	0.258971008	-0.59158995	-1.351039163
4	0.014241467	0.061529899	0.072629729	0.531506553	7.273321343	0.309838744	0.515782596	7.215988469	0.239366092	-0.662069928	-1.429761135
4	0.014146675	0.059592466	0.073511353	0.498979095	7.336722544	0.290916433	0.483255139	7.279389671	0.220443781	-0.727210528	-1.512112579
4	0.018200608	0.060401444	0.072728503	0.462819168	7.314520139	0.273847299	0.447095211	7.257187265	0.203374647	-0.804983707	-1.592705449
4	0.015249301	0.064171308	0.076927341	0.449473161	7.544194316	0.262036761	0.433749205	7.486861443	0.191564109	-0.835288782	-1.652532754
4	0.015581384	0.060384737	0.074810562	0.409610647	7.431472924	0.245898748	0.39388669	7.374140051	0.175426096	-0.931691999	-1.740537428
4	0.016634648	0.060188774	0.072868601	0.389429481	7.502034497	0.236973357	0.373705524	7.444701623	0.166500705	-0.984287161	-1.792755734
	average	average	average								
	0.015723957	0.057332873	0.070472652								

Experiment B5	NMR entry	Time [sec]	Std COT 5.8 ppm, Integral=4	Integral IM1-CH3 (3.9 ppm)	Integral P-CH3 (3.7 ppm)	Integral IM2-CH3 (3.3 ppm)	[OTf IM1]	[P]	[OTf IM2]	LN [OTf IM1]	LN [OTf IM2]
Folder B22323	1	0	4	4.082366043	0.522691127	2.807557348	0.041871468	0.005361069	0.02879618	-3.173150645	-3.547512544
T = 291 K	2	374	4	3.760314119	1.075629895	2.576794536	0.038568288	0.011032377	0.026429323	-3.255324882	-3.63328118
0.2 mL Stk sol	3	748	4	3.549555637	1.667312411	2.420404996	0.036406609	0.017101068	0.024825287	-3.313004955	-3.695892498
0.05 mL Tf2O	4	1122	4	3.178908127	2.184193252	2.107244279	0.032605001	0.022402542	0.021613302	-3.423289597	-3.834446314
0.4 mL d2-DCM	5	1496	4	2.947712489	2.677375849	1.9293181	0.030233704	0.027460952	0.019788373	-3.498797936	-3.922660754
	6	1870	4	2.590551412	3.067654117	1.644781619	0.026570422	0.031463906	0.016869977	-3.627956625	-4.082219757
V(sample)= 0.65 mL	7	2244	4	2.384740216	3.515858141	1.478764439	0.024459485	0.036060985	0.015167194	-3.710737184	-4.188620478
n(COT) = 0.02 mmol	8	2618	4	2.233155123	3.936036051	1.351102701	0.022904728	0.04037061	0.01385781	-3.776411939	-4.278906304
c(COT) = 0.03077	9	2992	4	1.988449755	4.246600466	1.170124738	0.020394866	0.043555965	0.012001579	-3.892472061	-4.422717021
c(amide) = 0.06154	10	3366	4	1.863253753	4.623361309	1.063647981	0.019110773	0.047420276	0.010909483	-3.957503089	-4.518122887
	11	3740	4	1.700859852	4.916894975	0.940417588	0.017445153	0.050430953	0.00964555	-4.04869346	-4.641258638
	12	4114	4	1.529718354	5.145765568	0.82394806	0.015689811	0.052778402	0.008450961	-4.154743742	-4.773475163
	13	4488	4	1.418436255	5.421319815	0.737283442	0.014548428	0.05560467	0.007562071	-4.230272342	-4.884610251
	14	4862	4	1.279450377	5.613068269	0.648704859	0.013122896	0.05757137	0.00665355	-4.333396785	-5.012604807
	15	5236	4	1.197129799	5.853719944	0.58341122	0.012278561	0.060039654	0.005983854	-4.399900521	-5.118690368
	16	5610	4	0.956324072	6.001054697	0.590457389	0.009808697	0.061550818	0.006056125	-4.624485814	-5.106685184
	17	5984	4	0.923800304	6.476012695	0.568215548	0.009475112	0.066422304	0.005827997	-4.65908673	-5.145081824
	18	6358	4	0.807709254	6.425387987	0.506040408	0.008284405	0.065903063	0.005190288	-4.793380498	-5.260966133
	19	6732	4	0.767916346	6.75208217	0.479525944	0.007876262	0.069253856	0.004918338	-4.843901854	-5.314784657
	20	7106	4	0.691288043	6.835115169	0.44	0.007090311	0.070105498	0.004536338	-4.949026071	-5.395635124
	21	7480	4	0.623491124	6.847414324	0.407628057	0.006394941	0.070231646	0.004180905	-5.052248128	-5.477227523
	22	7854	4	0.647641746	6.956476359	0.309035072	0.006642646	0.071350259	0.00316967	-5.014244975	-5.754127884
	23	8228	4	0.590783814	7.018440214	0.28284734	0.006059473	0.071985802	0.002901071	-5.106132504	-5.84267534
	24	8602	4	0.553446632	7.113881099	0.258971008	0.005676518	0.072964707	0.002656179	-5.171417328	-5.930866541
	25	8976	4	0.515782596	7.215988469	0.239366092	0.00529021	0.074011988	0.002455098	-5.241897306	-6.009588513
	26	9350	4	0.483255139	7.279389671	0.220443781	0.004956587	0.074662273	0.002261018	-5.307037906	-6.091939957
	27	9724	4	0.447095211	7.257187265	0.203374647	0.004585707	0.074434551	0.002085946	-5.384811085	-6.172532827
	28	10098	4	0.433749205	7.486861443	0.191564109	0.004448821	0.076790242	0.001964809	-5.41511616	-6.232360132
	29	10472	4	0.39388669	7.374140051	0.175426096	0.004039964	0.075634096	0.001799287	-5.511519378	-6.320364806
	30	10846	4	0.373705524	7.444701623	0.166500705	0.003832973	0.076357823	0.001707742	-5.564114539	-6.372583112
IM1-ax					IM2-eq						
slope	-0.000239289	-3.15991834	y-intercept		slope	-0.000307826	-3.497778252	y-intercept			
slope uncertainty	2.3243E-06	0.007150755	y-intercept uncertainty		slope uncertainty	3.65762E-06	0.011252734	y-intercept uncertainty			
R2 value	0.998774957	0.014545999	s(y)		R2 value	0.998167967	0.022890205	s(y)			
F	10598.87475	13	degrees of freedom		F	7082.943181	13	degrees of freedom			
regression ss	2.24257438	0.002750619	residual ss		regression ss	3.711189566	0.0068115	residual ss			

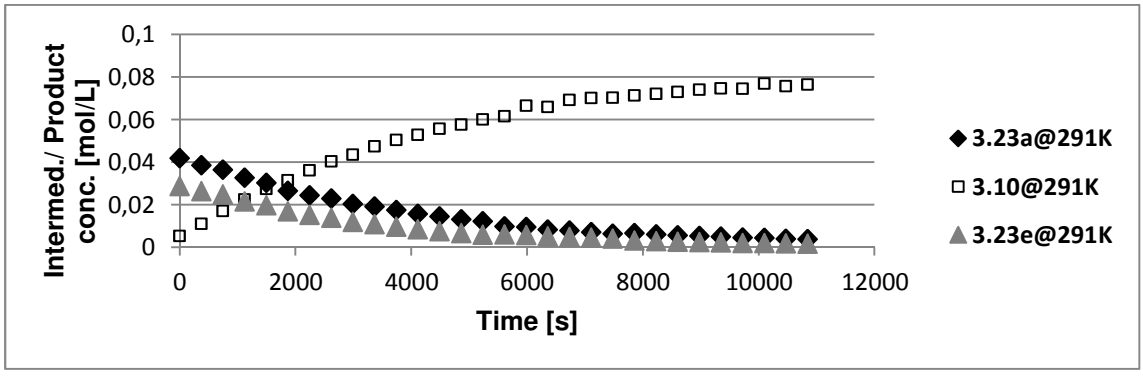

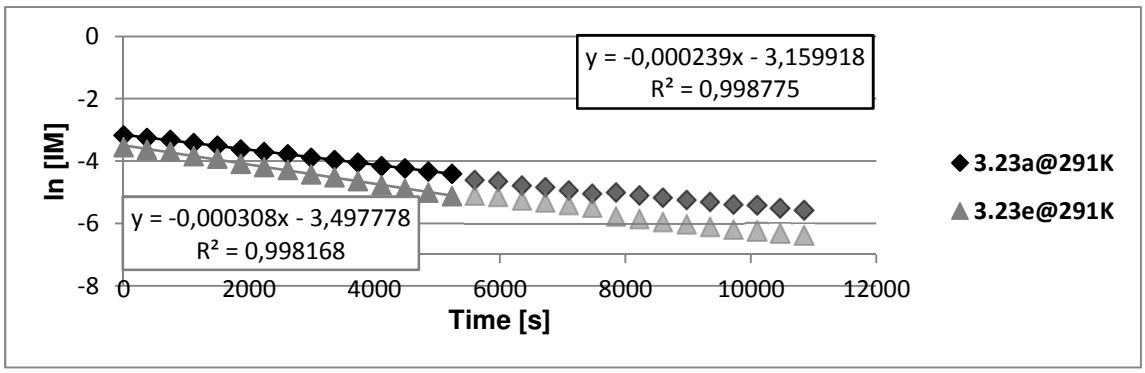

Kinetic data for compounds **3.23a** and **3.23e** at 294 K ([COT] = 0.03077 mol/L)

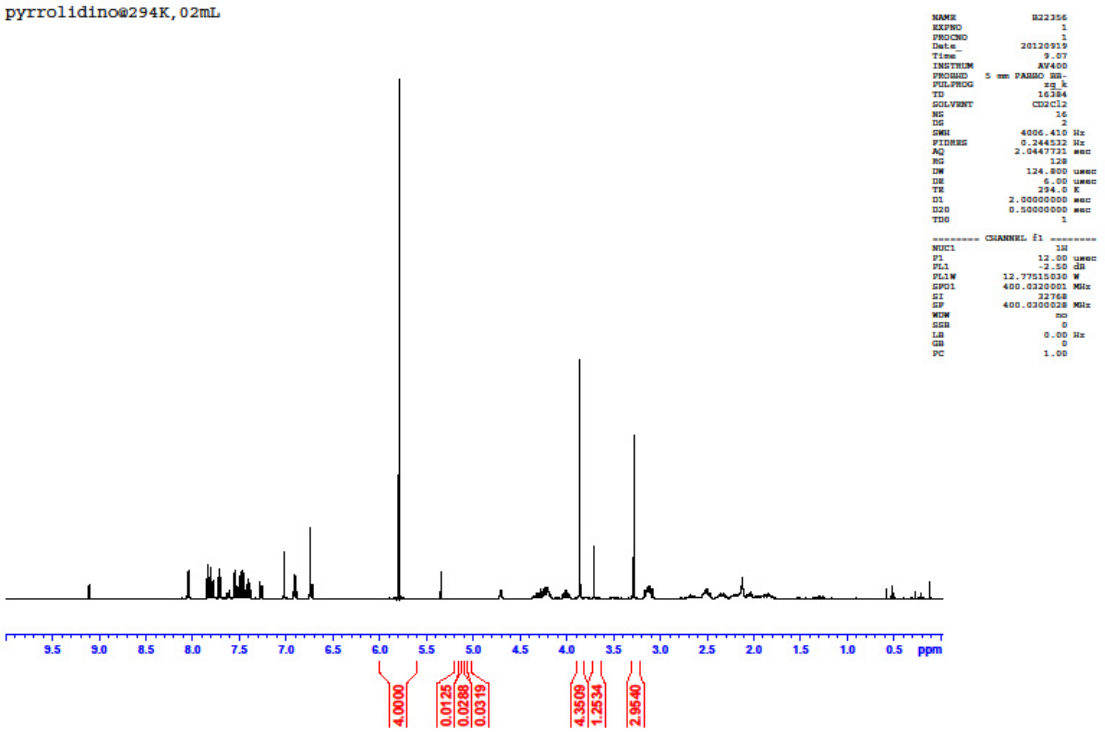

EXPERIMENT B6	T = 294 K			phc0 72.248	sr 2.82						
FOLDER B22356				phc1 -12.622							
INTEGRALS normalised							INTEGRALS			LN OF INTEGRALS	
standard (COT)	error IM1 (noise)	error P (noise)	error IM2 (noise)	IM1-CH3 ax	P-CH3	IM2-CH3 eq	corrected by avg error			corrected by avg error	
6.0-5.6 ppm	5.2-5.125 ppm	5.15-5.06 ppm	5.1-5.016 ppm	3.895-3.820 ppm	3.73-3.64 ppm	3.31-3.225 ppm	IM1-CH3	P-CH3	IM2-CH3	IM1-CH3 OTf ax	IM2-CH3 OTf eq
4	0.012482	0.028778	0.031855	4.35092	1.25336	2.95403	4.325310485	1.194304308	2.893203547	1.464483926	1.062364382
4	0.016906791	0.037884785	0.039043153	3.770107851	2.240465735	2.53911356	3.744498336	2.181410044	2.478287107	1.320287652	0.907567639
4	0.018373193	0.041097381	0.045607083	3.267927014	3.146949613	2.158638106	3.2423175	3.087893921	2.097811653	1.176288352	0.740894731
4	0.017320554	0.045104939	0.048284232	2.758249191	3.838964654	1.777815762	2.732639676	3.779908962	1.716989309	1.005268056	0.540572355
4	0.02287412	0.056073223	0.059794863	2.337126648	4.430825202	1.470839793	2.311517133	4.37176951	1.41001334	0.837904077	0.343599165
4	0.021827523	0.057413914	0.060053212	2.073867623	5.149131268	1.28037214	2.048258109	5.090075576	1.219545687	0.716989729	0.198478402
4	0.027718313	0.06068202	0.063432617	1.775967092	5.61027943	1.071952553	1.750357577	5.551223738	1.0111261	0.559820097	0.01106466
4	0.024777151	0.06026207	0.062844773	1.556590992	6.102428221	0.923863756	1.530981477	6.043372529	0.863037302	0.425909018	-0.147297365
4	0.023244374	0.058783031	0.060477664	1.333220821	6.408196188	0.779197804	1.307611306	6.349140496	0.718371351	0.268202042	-0.330768642
4	0.02208808	0.05832499	0.060578007	1.124583424	6.532104767	0.647221456	1.098973909	6.473049075	0.586395003	0.094376935	-0.53376165
4	0.02763517	0.062072638	0.062581131	0.9694952	6.703936985	0.552468351	0.943885686	6.644881293	0.491641898	-0.057750216	-0.710004678
4	0.026597478	0.06195945	0.063522014	0.849729044	6.963179538	0.482884645	0.824119529	6.904123846	0.422058191	-0.1934397	-0.86261208
4	0.029065361	0.064466861	0.066544967	0.757858959	7.153794871	0.418751439	0.732249445	7.094739179	0.357924986	-0.311634052	-1.027431851
4	0.030554717	0.065792931	0.064791008	0.672507287	7.374004523	0.368332363	0.646897773	7.314948832	0.30750591	-0.435566999	-1.179260972
4	0.029407555	0.064168332	0.063925679	0.595268268	7.561857929	0.322002431	0.569658753	7.502802237	0.261175978	-0.562717777	-1.342560853
4	0.030889965	0.068405682	0.069234274	0.537293381	7.707951051	0.288544361	0.511683866	7.648895359	0.227717908	-0.670048293	-1.479647662
4	0.025116508	0.060452384	0.061381961	0.478744025	7.778934075	0.262075905	0.45313451	7.719878383	0.201249452	-0.791566265	-1.603210085
4	0.030078303	0.067264432	0.067332805	0.444645878	7.911506605	0.228768649	0.419036363	7.852450913	0.167942195	-0.869797577	-1.784135434
4	0.029130812	0.064794348	0.066165035	0.395898792	7.841941659	0.20972606	0.370289277	7.782885968	0.148899607	-0.993470748	-1.904482982
4	0.026811787	0.061450525	0.06205796	0.363387596	7.960855289	0.192243253	0.337778081	7.901799597	0.1314168	-1.085366164	-2.029381331
4	0.029058746	0.061434928	0.064585745	0.340717165	8.016422557	0.177519256	0.31510765	7.957366865	0.116692803	-1.154840952	-2.148210414
4	0.027946234	0.065382279	0.067063331	0.323400666	8.113074347	0.160856794	0.297791151	8.054018655	0.100030341	-1.211362874	-2.30228173
4	0.028686958	0.065500858	0.066069894	0.296573081	8.081707903	0.150452563	0.270963567	8.022652212	0.089626109	-1.305770907	-2.412108604
4	0.02816406	0.062122223	0.065765773	0.278797509	8.131651464	0.143529476	0.253187994	8.072595773	0.082703023	-1.373623007	-2.492499122
4	0.026272845	0.059966179	0.060534365	0.253795799	8.163300891	0.143143813	0.228186284	8.104245199	0.082317359	-1.477592949	-2.497173265
4	0.025289279	0.060238032	0.063417467	0.25501775	8.176766589	0.131040802	0.229408235	8.117710898	0.070214349	-1.472252177	-2.656202593
4	0.02820365	0.064190832	0.066345069	0.238182538	8.212053896	0.122640043	0.212573024	8.152998204	0.06181359	-1.548469709	-2.783632042
4	0.028672056	0.065410792	0.068184245	0.232659272	8.225145077	0.115744062	0.207049757	8.166089386	0.054917609	-1.574796142	-2.901921238
4	0.028018315	0.064368199	0.064130183	0.225794479	8.270944903	0.119370064	0.200184964	8.211889212	0.058543611	-1.608513517	-2.837983313
4	0.025073544	0.057824498	0.059190089	0.223725629	8.293066747	0.119968991	0.198116115	8.234011055	0.059142538	-1.618901983	-2.827804849
	average	average	average								
	0.025609515	0.059055692	0.060826453								

Experiment B6	NMR entry	Time [sec]	Std COT 5.8 ppm, Integral=4	Integral IM1-CH3 (3.9 ppm)	Integral P-CH3 (3.7 ppm)	Integral IM2-CH3 (3.3 ppm)	[OTf IM1]	[P]	[OTf IM2]	LN [OTf IM1]	LN [OTf IM2]
Folder B22356	1	0	4	4.325310485	1.194304308	2.893203547	0.044363268	0.012249581	0.029674624	-3.115343452	-3.517462996
T = 294 K	2	374	4	3.744498336	2.181410044	2.478287107	0.038406071	0.022373996	0.025418965	-3.259539726	-3.672259739
0.2 mL Stk sol	3	748	4	3.2423175	3.087893921	2.097811653	0.03325537	0.031671499	0.021516555	-3.403539027	-3.838932647
0.05 mL Tf2O	4	1122	4	2.732639676	3.779908962	1.716989309	0.028027774	0.038769266	0.017610587	-3.574559322	-4.039255023
0.4 mL d2-DCM	5	1496	4	2.311517133	4.37176951	1.41001334	0.023708461	0.044839783	0.014462037	-3.741923302	-4.236228213
	6	1870	4	2.048258109	5.090075576	1.219545687	0.021008301	0.052207208	0.012508474	-3.862837649	-4.381348977
V(sample)= 0.65 mL	7	2244	4	1.750357577	5.551223738	1.0111261	0.017952834	0.056937051	0.010370783	-4.020007282	-4.568762718
n(COT) = 0.02 mmol	8	2618	4	1.530981477	6.043372529	0.863037302	0.015702767	0.061984858	0.008851886	-4.15391836	-4.727124743
c(COT) = 0.03077	9	2992	4	1.307611306	6.349140496	0.718371351	0.013411733	0.065121018	0.007368095	-4.311625336	-4.91059602
c(amide) = 0.06154	10	3366	4	1.098973909	6.473049075	0.586395003	0.011271809	0.066391907	0.006014458	-4.485450444	-5.113589028
	11	3740	4	0.943885686	6.644881293	0.491641898	0.009681121	0.068154332	0.005042607	-4.637577594	-5.289832056
	12	4114	4	0.824119529	6.904123846	0.422058191	0.008452719	0.070813297	0.00432891	-4.773267078	-5.442439458
	13	4488	4	0.732249445	7.094739179	0.357924986	0.007510438	0.072768375	0.003671117	-4.89146143	-5.607259229
	14	4862	4	0.646897773	7.314948832	0.30750591	0.006635015	0.075026992	0.003153986	-5.015394378	-5.759088351
	15	5236	4	0.569658753	7.502802237	0.261175978	0.0058428	0.076953742	0.002678795	-5.142545155	-5.922388231
	16	5610	4	0.511683866	7.648895359	0.227717908	0.005248171	0.07845217	0.002335627	-5.249875672	-6.05947504
	17	5984	4	0.45313451	7.719878383	0.201249452	0.00464765	0.079180219	0.002064149	-5.371393644	-6.183037463
	18	6358	4	0.419036363	7.852450913	0.167942195	0.004297916	0.080539972	0.001722527	-5.449624955	-6.363962812
	19	6732	4	0.370289277	7.782885968	0.148899607	0.003797934	0.079826467	0.001527214	-5.573298126	-6.48431036
	20	7106	4	0.337778081	7.901799597	0.1314168	0.003464477	0.081046125	0.001347898	-5.665193542	-6.609208709
	21	7480	4	0.31510765	7.957366865	0.116692803	0.003231954	0.081616059	0.001196879	-5.734668331	-6.728037793
	22	7854	4	0.297791151	8.054018655	0.100030341	0.003054345	0.082607385	0.001025978	-5.791190252	-6.882109108
	23	8228	4	0.270963567	8.022652212	0.089626109	0.002779183	0.08228567	0.000919265	-5.885598286	-6.991935982
	24	8602	4	0.253187994	8.072595773	0.082703023	0.002596865	0.082797924	0.000848257	-5.953450386	-7.072326501
	25	8976	4	0.228186284	8.104245199	0.082317359	0.002340431	0.083122542	0.000844302	-6.057420327	-7.077000643
	26	9350	4	0.229408235	8.117710898	0.070214349	0.002352964	0.083260655	0.000720165	-6.052079555	-7.236029971
	27	9724	4	0.212573024	8.152998204	0.06181359	0.002180291	0.083622585	0.000634001	-6.128297087	-7.36345942
	28	10098	4	0.207049757	8.166089386	0.054917609	0.00212364	0.083756857	0.000563272	-6.154623521	-7.481748616
	29	10472	4	0.200184964	8.211889212	0.058543611	0.00205323	0.08422661	0.000600462	-6.188340896	-7.417810691
	30	10846	4	0.198116115	8.234011055	0.059142538	0.002032011	0.084453507	0.000606605	-6.198729361	-7.407632227
IM1-ax					IM2-eq						
slope	-0.000393275	-3.129671234	y-intercept		slope	-0.000465784	-3.515680898	y-intercept			
slope uncertainty	3.84565E-06	0.011831189	y-intercept uncertainty		slope uncertainty	3.1954E-06	0.009830693	y-intercept uncertainty			
R2 value	0.998758493	0.024066892	s(y)		R2 value	0.999388554	0.019997503	s(y)			
F	10458.14219	13	degrees of freedom		F	21248.07462	13	degrees of freedom			
regression ss	6.057516102	0.007529799	residual ss		regression ss	8.497108056	0.005198702	residual ss			

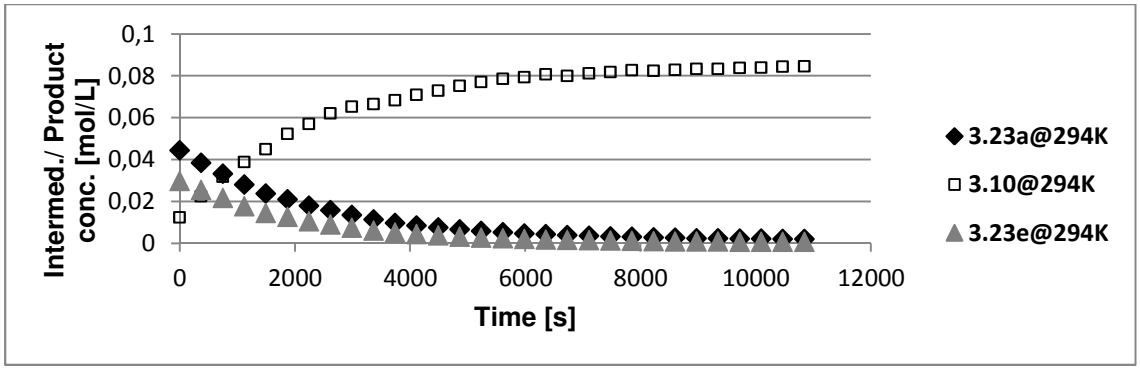

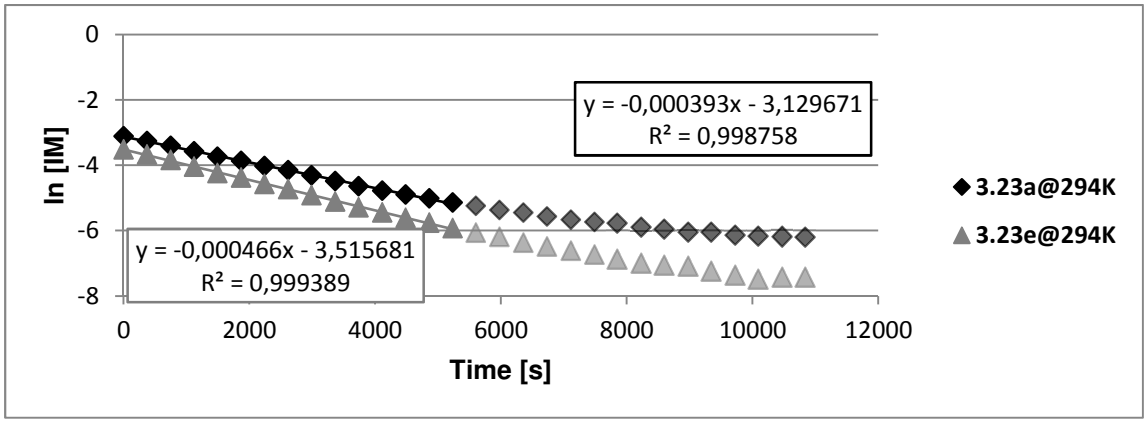

T [K]	1/T [K]	k_{IM1}	k_{IM2}	ln k_{IM1}	ln k_{IM2}	ln (k_{IM1}/T)	ln (k_{IM2}/T)				
294	0.003401361	0.000393	0.000466	-7.841700946	-7.671324924	-13.52528071	-13.35490469				
291	0.003436426	0.000239	0.000308	-8.339047006	-8.085410775	-14.01237027	-13.75873404				
288	0.003472222	0.000149	0.000186	-8.811564252	-8.589763884	-14.47452473	-14.25272436				
285	0.003508772	0.000094	0.000127	-9.272215776	-8.971323472	-14.92470496	-14.62381265				
282	0.003546099	0.000055	0.00008	-9.808177373	-9.433483923	-15.45008444	-15.07539099				
279	0.003584229	0.000034	0.00005	-10.28915003	-9.903487553	-15.92036182	-15.53469933				
IM1-axial	slope	-13363.16879	37.59743847	y-intercept	EA_{IM1-ax}	ln A_{IM1-ax}		IM1-ax	slope	-13076.80808	30.94002623
	slope uncertainty	117.3191971	0.409687657	y-intercept uncertainty	111.1 ± 1.0 kJ/mol	37.6			slope uncertainty	116.9461346	0.408384894
	R2 value	0.999691791	0.017949464	s(y)					R2 value	0.999680192	0.017892387
	F	12974.20463	4	degrees of freedom	$\Delta S^{\ddagger}$ = R(ln A-ln (ekB/h)-ln T				F	12503.50456	4
	regression ss	4.180071539	0.001288733	residual ss	$\Delta S_{IM1-ax}^{\ddagger}$(298K) = 17.6 ± 1.0 kJ/mol				regression ss	4.002840694	0.00128055
IM2-equatorial	slope	-12176.22852	33.73772501	y-intercept	EA_{IM2-eq}	ln A_{IM2-eq}		IM2-eq	slope	-11898.37787	27.10966769
	slope uncertainty	181.4271724	0.633557637	y-intercept uncertainty	101.2 ± 1.5 kJ/mol	33.74			slope uncertainty	279.5227789	0.970881287
	R2 value	0.999112735	0.02775778	s(y)					R2 value	0.998347043	0.031985028
	F	4504.233709	4	degrees of freedom	$\Delta S^{\ddagger}$ = R(ln A-ln (ekB/h)-ln T				F	1811.9287	3
	regression ss	3.470486722	0.003081977	residual ss	$\Delta S_{IM2-eq}^{\ddagger}$(298K) = 8.0 ± 1.6 kJ/mol				regression ss	1.853679216	0.003069126

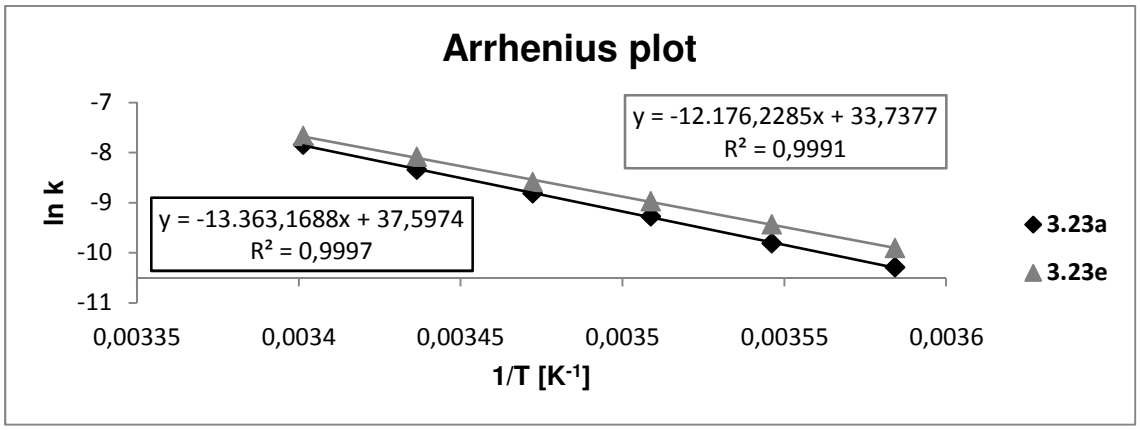

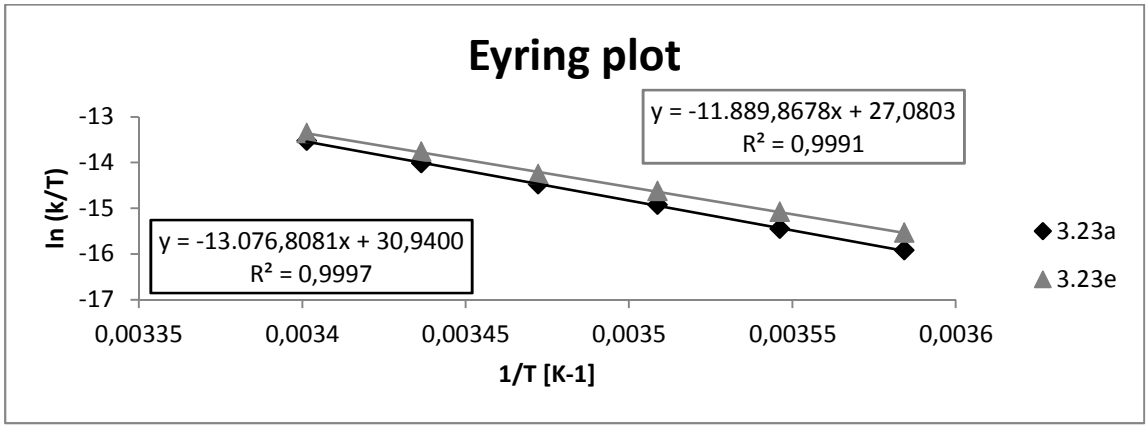

X-Ray crystal analysis for structure **3.122**

Table 1. Crystal data and structure refinement for jam_luka (**3.122**).

Identification code	jam_luka	
Empirical formula	C15 H12 F3 N O3 S2	
Formula weight	375.38	
Temperature	123(2) K	
Wavelength	0.71073 Å	
Crystal system	Triclinic	
Space group	P-1	
Unit cell dimensions	a = 6.6086(6) Å	α= 84.369(9)°.
	b = 7.8680(12) Å	β= 81.556(11)°.
	c = 16.054(2) Å	γ = 68.753(17)°.
Volume	768.66(17) $Å^3$	
Z	2	
Density (calculated)	1.622 Mg/m^3	
Absorption coefficient	0.394 mm^{-1}	
F(000)	384	
Crystal size	0.18 x 0.18 x 0.03 mm^3	
Theta range for data collection	3.12 to 27.00°.	
Index ranges	-8<=h<=8, -10<=k<=10, -20<=l<=20	
Reflections collected	4578	
Independent reflections	4578 [R(int) = 0.0000]	
Completeness to theta = 26.00°	99.6 %	
Absorption correction	Semi-empirical from equivalents	
Max. and min. transmission	1.00000 and 0.96486	
Refinement method	Full-matrix least-squares on F^2	
Data / restraints / parameters	4578 / 0 / 219	
Goodness-of-fit on F^2	0.933	
Final R indices [I>2sigma(I)]	R1 = 0.0481, wR2 = 0.1010	
R indices (all data)	R1 = 0.0722, wR2 = 0.1074	
Largest diff. peak and hole	0.714 and -0.465 e.$Å^{-3}$	

Table 2. Atomic coordinates (x 10^4) and equivalent isotropic displacement parameters ($Å^2$x 10^3) for jam_luka (**3.122**). U(eq) is defined as one third of the trace of the orthogonalised U^{ij} tensor.

	x	y	z	U(eq)
S(1)	6790(1)	3754(1)	2044(1)	21(1)
S(2)	-1068(1)	-2469(1)	2591(1)	19(1)
F(1)	2505(3)	-2882(3)	3245(1)	35(1)
F(2)	-412(3)	-987(3)	3876(1)	35(1)
F(3)	243(3)	-3876(3)	4059(1)	32(1)
O(1)	-804(3)	-952(3)	2072(1)	31(1)
O(2)	69(4)	-4247(3)	2251(2)	33(1)
O(3)	-3254(3)	-2196(3)	2987(1)	28(1)
N(1)	4085(4)	2122(3)	2462(2)	19(1)
C(1)	5074(5)	2758(4)	1798(2)	19(1)
C(2)	2619(4)	1165(4)	2460(2)	18(1)
C(3)	6238(5)	3233(4)	3115(2)	19(1)
C(4)	4702(5)	2397(4)	3231(2)	18(1)
C(5)	3898(5)	1897(4)	4034(2)	25(1)
C(6)	4737(5)	2247(4)	4707(2)	27(1)
C(7)	6310(5)	3070(4)	4584(2)	28(1)
C(8)	7066(5)	3596(4)	3785(2)	26(1)
C(9)	4836(5)	2625(4)	906(2)	19(1)
C(10)	2789(5)	3134(4)	622(2)	24(1)
C(11)	2672(5)	2971(4)	-218(2)	27(1)
C(12)	4554(5)	2338(4)	-774(2)	26(1)
C(13)	6572(5)	1889(5)	-504(2)	28(1)
C(14)	6722(5)	2016(4)	342(2)	23(1)
C(15)	389(5)	-2563(4)	3484(2)	23(1)

Table 3. Bond lengths [Å] and angles [°] for jam_luka (**3.122**).

S(1)-C(1)	1.701(3)
S(1)-C(3)	1.745(3)
S(2)-O(1)	1.436(2)
S(2)-O(3)	1.439(2)
S(2)-O(2)	1.445(2)
S(2)-C(15)	1.823(3)
F(1)-C(15)	1.331(3)
F(2)-C(15)	1.339(3)
F(3)-C(15)	1.337(3)
N(1)-C(1)	1.320(4)
N(1)-C(4)	1.414(4)
N(1)-C(2)	1.427(3)
C(1)-C(9)	1.481(4)
C(2)-H(2A)	0.9800
C(2)-H(2B)	0.9800
C(2)-H(2C)	0.9800
C(3)-C(8)	1.372(4)
C(3)-C(4)	1.379(4)
C(4)-C(5)	1.397(4)
C(5)-C(6)	1.378(4)
C(5)-H(5)	0.9500
C(6)-C(7)	1.394(5)
C(6)-H(6)	0.9500
C(7)-C(8)	1.387(4)
C(7)-H(7)	0.9500
C(8)-H(8)	0.9500
C(9)-C(14)	1.387(4)
C(9)-C(10)	1.397(4)
C(10)-C(11)	1.383(4)
C(10)-H(10)	0.9500
C(11)-C(12)	1.380(4)
C(11)-H(11)	0.9500
C(12)-C(13)	1.375(4)
C(12)-H(12)	0.9500
C(13)-C(14)	1.392(4)
C(13)-H(13)	0.9500
C(14)-H(14)	0.9500
C(1)-S(1)-C(3)	91.04(15)
O(1)-S(2)-O(3)	115.41(14)
O(1)-S(2)-O(2)	115.78(15)
O(3)-S(2)-O(2)	114.30(14)
O(1)-S(2)-C(15)	103.50(14)
O(3)-S(2)-C(15)	102.55(14)
O(2)-S(2)-C(15)	102.63(14)
C(1)-N(1)-C(4)	112.8(2)
C(1)-N(1)-C(2)	126.8(3)
C(4)-N(1)-C(2)	120.3(3)
N(1)-C(1)-C(9)	125.9(3)
N(1)-C(1)-S(1)	113.6(2)
C(9)-C(1)-S(1)	120.4(2)
N(1)-C(2)-H(2A)	109.5
N(1)-C(2)-H(2B)	109.5
H(2A)-C(2)-H(2B)	109.5
N(1)-C(2)-H(2C)	109.5
H(2A)-C(2)-H(2C)	109.5
H(2B)-C(2)-H(2C)	109.5
C(8)-C(3)-C(4)	121.5(3)
C(8)-C(3)-S(1)	128.7(3)
C(4)-C(3)-S(1)	109.7(2)
C(3)-C(4)-C(5)	121.7(3)
C(3)-C(4)-N(1)	112.7(3)
C(5)-C(4)-N(1)	125.6(3)
C(6)-C(5)-C(4)	116.9(3)
C(6)-C(5)-H(5)	121.5
C(4)-C(5)-H(5)	121.5
C(5)-C(6)-C(7)	120.9(3)
C(5)-C(6)-H(6)	119.5
C(7)-C(6)-H(6)	119.5
C(8)-C(7)-C(6)	121.7(3)
C(8)-C(7)-H(7)	119.2
C(6)-C(7)-H(7)	119.2
C(3)-C(8)-C(7)	117.2(3)
C(3)-C(8)-H(8)	121.4
C(7)-C(8)-H(8)	121.4
C(14)-C(9)-C(10)	119.9(3)
C(14)-C(9)-C(1)	118.1(3)
C(10)-C(9)-C(1)	122.0(3)
C(11)-C(10)-C(9)	119.3(3)
C(11)-C(10)-H(10)	120.4
C(9)-C(10)-H(10)	120.4
C(12)-C(11)-C(10)	120.5(3)
C(12)-C(11)-H(11)	119.7
C(10)-C(11)-H(11)	119.7
C(13)-C(12)-C(11)	120.5(3)
C(13)-C(12)-H(12)	119.8
C(11)-C(12)-H(12)	119.8
C(12)-C(13)-C(14)	119.8(3)
C(12)-C(13)-H(13)	120.1
C(14)-C(13)-H(13)	120.1
C(9)-C(14)-C(13)	120.0(3)
C(9)-C(14)-H(14)	120.0
C(13)-C(14)-H(14)	120.0
F(1)-C(15)-F(3)	107.5(2)
F(1)-C(15)-F(2)	107.0(2)
F(3)-C(15)-F(2)	107.2(3)
F(1)-C(15)-S(2)	111.7(2)
F(3)-C(15)-S(2)	111.8(2)
F(2)-C(15)-S(2)	111.5(2)

Symmetry transformations used to generate equivalent atoms:

Table 4. Anisotropic displacement parameters ($Å^2 x\ 10^3$) for jam_luka (**3.122**). The anisotropic displacement factor exponent takes the form: $-2\pi^2[\ h^2 a^{*2} U^{11} + ... + 2\ h\ k\ a^*\ b^*\ U^{12}\ ]$

	U^{11}	U^{22}	U^{33}	U^{23}	U^{13}	U^{12}
S(1)	24(1)	22(1)	21(1)	1(1)	-5(1)	-11(1)
S(2)	17(1)	18(1)	21(1)	-2(1)	-4(1)	-3(1)
F(1)	16(1)	33(1)	58(1)	-1(1)	-8(1)	-8(1)
F(2)	39(1)	26(1)	39(1)	-12(1)	-11(1)	-5(1)
F(3)	37(1)	30(1)	34(1)	10(1)	-16(1)	-16(1)
O(1)	34(1)	26(1)	26(1)	6(1)	-2(1)	-5(1)
O(2)	36(1)	24(1)	36(2)	-13(1)	-8(1)	-2(1)
O(3)	15(1)	34(1)	35(1)	1(1)	-5(1)	-8(1)
N(1)	16(1)	15(1)	23(1)	-3(1)	-2(1)	-3(1)
C(1)	18(2)	13(2)	22(2)	0(1)	1(1)	-1(1)
C(2)	10(1)	23(2)	19(2)	4(1)	-3(1)	-4(1)
C(3)	27(2)	12(2)	15(2)	1(1)	-5(1)	-2(1)
C(4)	21(2)	13(2)	15(2)	-2(1)	-6(1)	4(1)
C(5)	26(2)	18(2)	25(2)	0(2)	0(2)	-2(1)
C(6)	35(2)	16(2)	17(2)	0(1)	-4(2)	5(2)
C(7)	39(2)	16(2)	21(2)	-5(1)	-9(2)	2(2)
C(8)	31(2)	17(2)	29(2)	-4(2)	-8(2)	-2(2)
C(9)	27(2)	12(2)	16(2)	1(1)	-7(1)	-4(1)
C(10)	26(2)	19(2)	22(2)	-1(1)	-3(1)	-3(1)
C(11)	30(2)	24(2)	24(2)	-1(2)	-12(2)	-2(2)
C(12)	41(2)	19(2)	16(2)	0(1)	-6(2)	-7(2)
C(13)	31(2)	29(2)	20(2)	-6(2)	4(2)	-8(2)
C(14)	23(2)	23(2)	22(2)	-2(1)	-1(1)	-7(1)
C(15)	19(2)	16(2)	32(2)	-2(2)	-5(1)	-4(1)

Table 5. Hydrogen coordinates ($x\ 10^4$) and isotropic displacement parameters ($Å^2 x\ 10^3$) for jam_luka (**3.122**).

	x	y	z	U(eq)
H(2A)	2564	916	1879	27
H(2B)	1155	1911	2707	27
H(2C)	3132	9	2792	27
H(5)	2821	1340	4112	30
H(6)	4237	1922	5264	32
H(7)	6880	3276	5059	34
H(8)	8113	4183	3704	32
H(10)	1490	3587	1002	29
H(11)	1285	3297	-414	33
H(12)	4454	2210	-1348	31
H(13)	7861	1494	-894	33
H(14)	8114	1687	533	27

Table 6. Torsion angles [°] for jam_luka (**3.122**).

C(4)-N(1)-C(1)-C(9)	177.8(3)
C(2)-N(1)-C(1)-C(9)	0.8(5)
C(4)-N(1)-C(1)-S(1)	-0.7(3)
C(2)-N(1)-C(1)-S(1)	-177.7(2)
C(3)-S(1)-C(1)-N(1)	1.9(2)
C(3)-S(1)-C(1)-C(9)	-176.7(2)
C(1)-S(1)-C(3)-C(8)	179.4(3)
C(1)-S(1)-C(3)-C(4)	-2.6(2)
C(8)-C(3)-C(4)-C(5)	0.7(5)
S(1)-C(3)-C(4)-C(5)	-177.5(2)
C(8)-C(3)-C(4)-N(1)	-179.1(3)
S(1)-C(3)-C(4)-N(1)	2.7(3)
C(1)-N(1)-C(4)-C(3)	-1.4(3)
C(2)-N(1)-C(4)-C(3)	175.8(2)
C(1)-N(1)-C(4)-C(5)	178.9(3)
C(2)-N(1)-C(4)-C(5)	-4.0(4)
C(3)-C(4)-C(5)-C(6)	-1.1(4)
N(1)-C(4)-C(5)-C(6)	178.7(3)
C(4)-C(5)-C(6)-C(7)	0.2(4)
C(5)-C(6)-C(7)-C(8)	1.1(5)
C(4)-C(3)-C(8)-C(7)	0.7(5)
S(1)-C(3)-C(8)-C(7)	178.4(2)
C(6)-C(7)-C(8)-C(3)	-1.5(5)
N(1)-C(1)-C(9)-C(14)	-131.8(3)
S(1)-C(1)-C(9)-C(14)	46.6(4)
N(1)-C(1)-C(9)-C(10)	49.8(5)
S(1)-C(1)-C(9)-C(10)	-131.7(3)
C(14)-C(9)-C(10)-C(11)	1.9(5)
C(1)-C(9)-C(10)-C(11)	-179.7(3)
C(9)-C(10)-C(11)-C(12)	-0.9(5)
C(10)-C(11)-C(12)-C(13)	-1.1(5)
C(11)-C(12)-C(13)-C(14)	2.2(5)
C(10)-C(9)-C(14)-C(13)	-0.9(5)
C(1)-C(9)-C(14)-C(13)	-179.3(3)
C(12)-C(13)-C(14)-C(9)	-1.1(5)
O(1)-S(2)-C(15)-F(1)	-61.9(2)
O(3)-S(2)-C(15)-F(1)	177.7(2)
O(2)-S(2)-C(15)-F(1)	58.9(2)
O(1)-S(2)-C(15)-F(3)	177.6(2)
O(3)-S(2)-C(15)-F(3)	57.2(2)
O(2)-S(2)-C(15)-F(3)	-61.6(2)
O(1)-S(2)-C(15)-F(2)	57.7(2)
O(3)-S(2)-C(15)-F(2)	-62.7(2)
O(2)-S(2)-C(15)-F(2)	178.5(2)

Symmetry transformations used to generate equivalent atoms:

Crystal structure of jam luka (**3.122**)

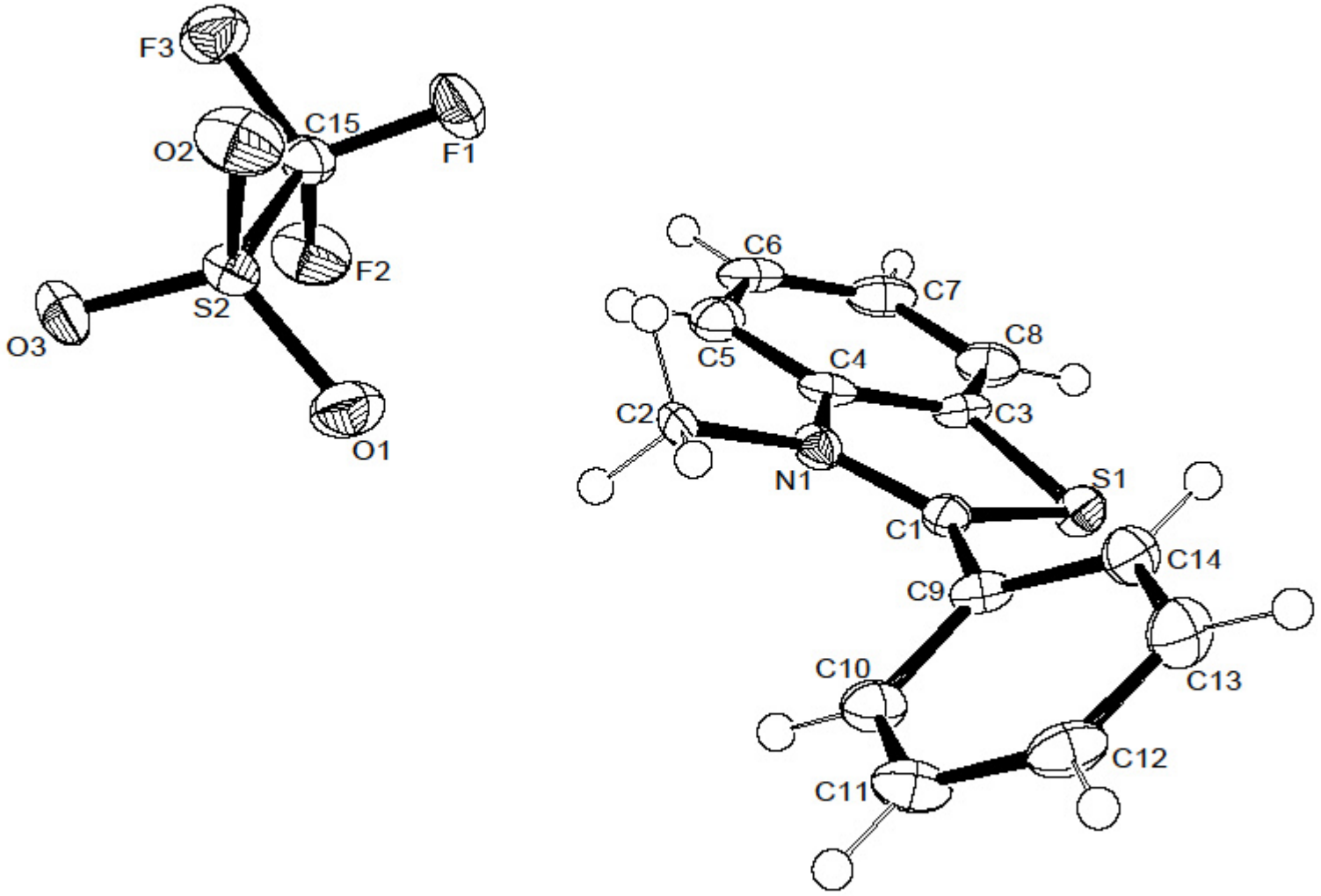

X-Ray crystal analysis for structure **3.132**

Table 1. Crystal data and structure refinement for lukactry2 (**3.132**).

Identification code	lukactry2	
Empirical formula	C15 H15 F3 N2 O4 S	
Formula weight	376.35	
Temperature	123(2) K	
Wavelength	1.54180 Å	
Crystal system	Monoclinic	
Space group	$P2_1/n$	
Unit cell dimensions	a = 8.1236(2) Å	α = 90°.
	b = 13.4733(4) Å	β= 100.775(3)°.
	c = 14.4823(4) Å	γ = 90°.
Volume	1557.17(7) $Å^3$	
Z	4	
Density (calculated)	1.605 Mg/m^3	
Absorption coefficient	2.411 mm^{-1}	
F(000)	776	
Crystal size	0.24 x 0.20 x 0.12 mm^3	
Theta range for data collection	7.60 to 69.50°.	
Index ranges	-9<=h<=9, -9<=k<=16, -17<=l<=17	
Reflections collected	4190	
Independent reflections	2527 [R(int) = 0.0137]	
Completeness to theta = 69.50°	86.4 %	
Absorption correction	Semi-empirical from equivalents	
Max. and min. transmission	1.00000 and 0.73248	
Refinement method	Full-matrix least-squares on F^2	
Data / restraints / parameters	2527 / 0 / 229	
Goodness-of-fit on F^2	1.039	
Final R indices [I>2sigma(I)]	R1 = 0.0372, wR2 = 0.1043	
R indices (all data)	R1 = 0.0394, wR2 = 0.1065	
Largest diff. peak and hole	0.362 and -0.329 e.$Å^{-3}$	

Table 2. Atomic coordinates (x 10^4) and equivalent isotropic displacement parameters ($Å^2$x 10^3) for lukactry2 (**3.132**). U(eq) is defined as one third of the trace of the orthogonalised U^{ij} tensor.

	x	y	z	U(eq)
S(1)	-1078(1)	2504(1)	8566(1)	20(1)
F(3)	-1611(2)	699(1)	7873(1)	37(1)
F(2)	-2260(2)	902(1)	9229(1)	47(1)
F(1)	321(2)	795(1)	9101(1)	49(1)
O(3)	-647(2)	2830(1)	9532(1)	31(1)
O(1)	813(2)	4331(1)	5936(1)	32(1)
O(4)	-2754(2)	2743(1)	8099(1)	30(1)
O(2)	202(2)	2653(1)	8012(1)	34(1)
N(2)	-603(2)	2847(1)	5555(1)	19(1)
N(1)	2365(2)	2934(1)	6288(1)	21(1)
C(10)	2586(2)	-164(1)	6693(1)	27(1)
C(14)	-2019(2)	1224(1)	5565(1)	24(1)
C(12)	-487(2)	-256(1)	6119(1)	24(1)
C(2)	2467(2)	1891(1)	6404(1)	21(1)
C(5)	3906(2)	3526(1)	6553(1)	27(1)
C(7)	-767(2)	2976(1)	4495(1)	24(1)
C(1)	971(2)	3450(1)	5977(1)	22(1)
C(8)	3964(2)	1430(1)	6746(1)	27(1)
C(4)	-578(2)	1768(1)	5785(1)	20(1)
C(11)	1019(2)	292(1)	6338(1)	23(1)
C(13)	-1963(2)	197(1)	5745(1)	26(1)
C(9)	4006(2)	393(2)	6881(1)	30(1)
C(3)	971(2)	1331(1)	6175(1)	20(1)
C(6)	-2078(2)	3352(1)	5861(1)	26(1)
C(15)	-1160(2)	1153(1)	8692(1)	26(1)

Table 3. Bond lengths [Å] and angles [°] for lukactry2 (**3.132**).

S(1)-O(4)	1.4389(13)
S(1)-O(2)	1.4409(14)
S(1)-O(3)	1.4458(14)
S(1)-C(15)	1.8322(19)
F(3)-C(15)	1.323(2)
F(2)-C(15)	1.333(2)
F(1)-C(15)	1.328(2)
O(1)-C(1)	1.195(2)
N(2)-C(4)	1.490(2)
N(2)-C(6)	1.515(2)
N(2)-C(7)	1.526(2)
N(2)-C(1)	1.542(2)
N(1)-C(1)	1.333(2)
N(1)-C(2)	1.417(2)
N(1)-C(5)	1.473(2)
C(10)-C(9)	1.360(3)
C(10)-C(11)	1.420(2)
C(10)-H(10)	0.9500
C(14)-C(4)	1.367(2)
C(14)-C(13)	1.408(3)
C(14)-H(14)	0.9500
C(12)-C(13)	1.363(3)
C(12)-C(11)	1.413(3)
C(12)-H(12)	0.9500
C(2)-C(8)	1.373(2)
C(2)-C(3)	1.416(2)
C(5)-H(5A)	0.9800
C(5)-H(5B)	0.9800
C(5)-H(5C)	0.9800
C(7)-H(7A)	0.9800
C(7)-H(7B)	0.9800
C(7)-H(7C)	0.9800
C(8)-C(9)	1.410(3)
C(8)-H(8)	0.9500
C(4)-C(3)	1.409(2)
C(11)-C(3)	1.419(2)
C(13)-H(13)	0.9500
C(9)-H(9)	0.9500
C(6)-H(6A)	0.9800
C(6)-H(6B)	0.9800
C(6)-H(6C)	0.9800
O(4)-S(1)-O(2)	115.11(9)
O(4)-S(1)-O(3)	115.09(8)
O(2)-S(1)-O(3)	115.27(9)
O(4)-S(1)-C(15)	102.76(8)
O(2)-S(1)-C(15)	103.73(8)
O(3)-S(1)-C(15)	102.24(8)
C(4)-N(2)-C(6)	110.61(13)
C(4)-N(2)-C(7)	109.29(13)
C(6)-N(2)-C(7)	108.55(13)
C(4)-N(2)-C(1)	116.73(13)
C(6)-N(2)-C(1)	106.89(13)
C(7)-N(2)-C(1)	104.37(13)
C(1)-N(1)-C(2)	125.73(14)
C(1)-N(1)-C(5)	115.64(15)
C(2)-N(1)-C(5)	118.60(14)
C(9)-C(10)-C(11)	120.26(17)
C(9)-C(10)-H(10)	119.9
C(11)-C(10)-H(10)	119.9
C(4)-C(14)-C(13)	119.13(16)
C(4)-C(14)-H(14)	120.4
C(13)-C(14)-H(14)	120.4
C(13)-C(12)-C(11)	121.07(16)
C(13)-C(12)-H(12)	119.5
C(11)-C(12)-H(12)	119.5
C(8)-C(2)-C(3)	120.45(17)
C(8)-C(2)-N(1)	121.32(16)
C(3)-C(2)-N(1)	118.21(14)
N(1)-C(5)-H(5A)	109.5
N(1)-C(5)-H(5B)	109.5
H(5A)-C(5)-H(5B)	109.5
N(1)-C(5)-H(5C)	109.5
H(5A)-C(5)-H(5C)	109.5
H(5B)-C(5)-H(5C)	109.5
N(2)-C(7)-H(7A)	109.5
N(2)-C(7)-H(7B)	109.5
H(7A)-C(7)-H(7B)	109.5
N(2)-C(7)-H(7C)	109.5
H(7A)-C(7)-H(7C)	109.5
H(7B)-C(7)-H(7C)	109.5
O(1)-C(1)-N(1)	127.68(17)
O(1)-C(1)-N(2)	115.50(15)
N(1)-C(1)-N(2)	116.67(15)
C(2)-C(8)-C(9)	119.67(17)
C(2)-C(8)-H(8)	120.2
C(9)-C(8)-H(8)	120.2
C(14)-C(4)-C(3)	122.08(16)
C(14)-C(4)-N(2)	119.68(15)
C(3)-C(4)-N(2)	118.14(14)
C(12)-C(11)-C(3)	118.78(16)
C(12)-C(11)-C(10)	122.43(17)
C(3)-C(11)-C(10)	118.77(16)
C(12)-C(13)-C(14)	120.61(16)
C(12)-C(13)-H(13)	119.7
C(14)-C(13)-H(13)	119.7
C(10)-C(9)-C(8)	121.39(17)
C(10)-C(9)-H(9)	119.3
C(8)-C(9)-H(9)	119.3
C(4)-C(3)-C(2)	122.27(16)
C(4)-C(3)-C(11)	118.32(16)
C(2)-C(3)-C(11)	119.41(15)
N(2)-C(6)-H(6A)	109.5
N(2)-C(6)-H(6B)	109.5
H(6A)-C(6)-H(6B)	109.5
N(2)-C(6)-H(6C)	109.5
H(6A)-C(6)-H(6C)	109.5
H(6B)-C(6)-H(6C)	109.5
F(3)-C(15)-F(1)	107.96(15)
F(3)-C(15)-F(2)	107.64(16)
F(1)-C(15)-F(2)	107.32(17)
F(3)-C(15)-S(1)	112.25(13)
F(1)-C(15)-S(1)	110.98(13)
F(2)-C(15)-S(1)	110.48(13)

Symmetry transformations used to generate equivalent atoms:

Table 4. Anisotropic displacement parameters ($Å^2 x\ 10^3$) for lukactry2 (**3.132**). The anisotropic displacement factor exponent takes the form: $-2\pi^2[h^2 a^{*2} U^{11} + ... + 2 h k a^* b^* U^{12}]$

	U^{11}	U^{22}	U^{33}	U^{23}	U^{13}	U^{12}
S(1)	18(1)	21(1)	22(1)	-2(1)	2(1)	0(1)
F(3)	47(1)	32(1)	31(1)	-14(1)	6(1)	-6(1)
F(2)	71(1)	29(1)	49(1)	1(1)	33(1)	-7(1)
F(1)	48(1)	29(1)	61(1)	-7(1)	-16(1)	15(1)
O(3)	39(1)	28(1)	25(1)	-7(1)	-1(1)	1(1)
O(1)	31(1)	20(1)	41(1)	-3(1)	-2(1)	1(1)
O(4)	22(1)	32(1)	34(1)	0(1)	-1(1)	5(1)
O(2)	28(1)	35(1)	40(1)	-4(1)	14(1)	-7(1)
N(2)	17(1)	22(1)	19(1)	-1(1)	3(1)	3(1)
N(1)	17(1)	24(1)	21(1)	-1(1)	3(1)	-1(1)
C(10)	34(1)	25(1)	23(1)	3(1)	8(1)	8(1)
C(14)	21(1)	27(1)	23(1)	-1(1)	4(1)	1(1)
C(12)	35(1)	20(1)	20(1)	0(1)	9(1)	-1(1)
C(2)	22(1)	24(1)	18(1)	0(1)	6(1)	3(1)
C(5)	19(1)	30(1)	32(1)	-3(1)	4(1)	-4(1)
C(7)	28(1)	27(1)	18(1)	1(1)	3(1)	-1(1)
C(1)	21(1)	23(1)	22(1)	-1(1)	2(1)	-1(1)
C(8)	20(1)	33(1)	27(1)	2(1)	3(1)	3(1)
C(4)	21(1)	22(1)	19(1)	-1(1)	5(1)	1(1)
C(11)	29(1)	24(1)	16(1)	0(1)	7(1)	3(1)
C(13)	29(1)	28(1)	22(1)	-3(1)	7(1)	-8(1)
C(9)	26(1)	34(1)	29(1)	5(1)	5(1)	12(1)
C(3)	22(1)	24(1)	15(1)	-1(1)	6(1)	4(1)
C(6)	21(1)	27(1)	30(1)	-2(1)	8(1)	7(1)
C(15)	29(1)	22(1)	26(1)	-3(1)	3(1)	1(1)

Table 5. Hydrogen coordinates ($x\ 10^4$) and isotropic displacement parameters ($Å^2 x\ 10^3$) for lukactry2 (**3.132**).

	x	y	z	U(eq)
H(10)	2642	-860	6799	32
H(14)	-3045	1536	5293	28
H(12)	-472	-950	6234	29
H(5A)	4644	3407	6101	40
H(5B)	4482	3333	7183	40
H(5C)	3616	4232	6551	40
H(7A)	199	2671	4290	36
H(7B)	-807	3685	4341	36
H(7C)	-1799	2655	4174	36
H(8)	4966	1807	6892	32
H(13)	-2962	-184	5606	31
H(9)	5048	76	7108	35
H(6A)	-3125	3062	5522	38
H(6B)	-2057	4063	5721	38
H(6C)	-2008	3258	6539	38

Table 6. Torsion angles [°] for lukactry2 (**3.132**).

C(1)-N(1)-C(2)-C(8)	-178.77(17)
C(5)-N(1)-C(2)-C(8)	-0.7(2)
C(1)-N(1)-C(2)-C(3)	-0.1(2)
C(5)-N(1)-C(2)-C(3)	178.03(15)
C(2)-N(1)-C(1)-O(1)	173.88(18)
C(5)-N(1)-C(1)-O(1)	-4.3(3)
C(2)-N(1)-C(1)-N(2)	-10.8(2)
C(5)-N(1)-C(1)-N(2)	171.03(14)
C(4)-N(2)-C(1)-O(1)	-166.48(15)
C(6)-N(2)-C(1)-O(1)	-42.1(2)
C(7)-N(2)-C(1)-O(1)	72.80(19)
C(4)-N(2)-C(1)-N(1)	17.6(2)
C(6)-N(2)-C(1)-N(1)	142.00(15)
C(7)-N(2)-C(1)-N(1)	-103.10(16)
C(3)-C(2)-C(8)-C(9)	-0.7(3)
N(1)-C(2)-C(8)-C(9)	177.95(16)
C(13)-C(14)-C(4)-C(3)	0.9(3)
C(13)-C(14)-C(4)-N(2)	177.12(15)
C(6)-N(2)-C(4)-C(14)	46.9(2)
C(7)-N(2)-C(4)-C(14)	-72.51(18)
C(1)-N(2)-C(4)-C(14)	169.40(15)
C(6)-N(2)-C(4)-C(3)	-136.68(15)
C(7)-N(2)-C(4)-C(3)	103.87(16)
C(1)-N(2)-C(4)-C(3)	-14.2(2)
C(13)-C(12)-C(11)-C(3)	0.9(2)
C(13)-C(12)-C(11)-C(10)	-177.45(17)
C(9)-C(10)-C(11)-C(12)	179.07(17)
C(9)-C(10)-C(11)-C(3)	0.7(3)
C(11)-C(12)-C(13)-C(14)	0.3(3)
C(4)-C(14)-C(13)-C(12)	-1.2(3)
C(11)-C(10)-C(9)-C(8)	1.1(3)
C(2)-C(8)-C(9)-C(10)	-1.1(3)
C(14)-C(4)-C(3)-C(2)	179.97(16)
N(2)-C(4)-C(3)-C(2)	3.7(2)
C(14)-C(4)-C(3)-C(11)	0.3(2)
N(2)-C(4)-C(3)-C(11)	-175.99(14)
C(8)-C(2)-C(3)-C(4)	-177.20(16)
N(1)-C(2)-C(3)-C(4)	4.1(2)
C(8)-C(2)-C(3)-C(11)	2.5(2)
N(1)-C(2)-C(3)-C(11)	-176.23(14)
C(12)-C(11)-C(3)-C(4)	-1.2(2)
C(10)-C(11)-C(3)-C(4)	177.24(15)
C(12)-C(11)-C(3)-C(2)	179.13(15)
C(10)-C(11)-C(3)-C(2)	-2.4(2)
O(4)-S(1)-C(15)-F(3)	57.81(15)
O(2)-S(1)-C(15)-F(3)	-62.40(15)
O(3)-S(1)-C(15)-F(3)	177.42(13)
O(4)-S(1)-C(15)-F(1)	178.73(14)
O(2)-S(1)-C(15)-F(1)	58.51(16)
O(3)-S(1)-C(15)-F(1)	-61.66(15)
O(4)-S(1)-C(15)-F(2)	-62.35(15)
O(2)-S(1)-C(15)-F(2)	177.44(14)
O(3)-S(1)-C(15)-F(2)	57.26(15)

Symmetry transformations used to generate equivalent atoms:

Crystal structure of lukactry2 (**3.132**)

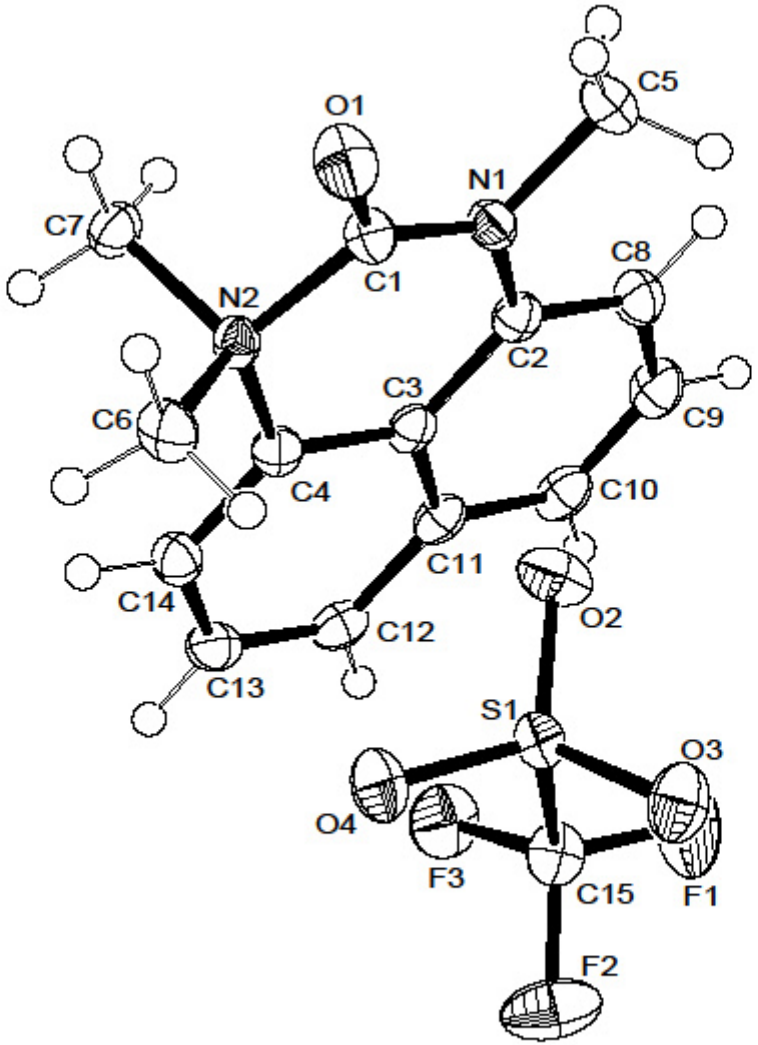

X-Ray crystal analysis for structure **3.133**

Table 1. Crystal data and structure refinement for jamluka288 (**3.133**).

Identification code	jamluka288	
Empirical formula	C19 H25 F3 N2 O5 S	
Formula weight	450.47	
Temperature	123(2) K	
Wavelength	0.71073 Å	
Crystal system	Monoclinic	
Space group	P21/c	
Unit cell dimensions	a = 12.1311(4) Å	□= 90°.
	b = 15.0080(5) Å	□= 111.048(4)°.
	c = 12.4296(5) Å	□ = 90°.
Volume	2111.99(13) $Å^3$	
Z	4	
Density (calculated)	1.417 Mg/m^3	
Absorption coefficient	0.213 mm^{-1}	
F(000)	944	
Crystal size	0.30 x 0.20 x 0.20 mm^3	
Theta range for data collection	3.23 to 28.00°.	
Index ranges	-16<=h<=15, -19<=k<=19, -16<=l<=15	
Reflections collected	10360	
Independent reflections	5040 [R(int) = 0.0264]	
Completeness to theta = 27.00°	99.8 %	
Absorption correction	Semi-empirical from equivalents	
Max. and min. transmission	1.00000 and 0.95618	
Refinement method	Full-matrix least-squares on F^2	
Data / restraints / parameters	5040 / 0 / 280	
Goodness-of-fit on F^2	1.034	
Final R indices [I>2sigma(I)]	R1 = 0.0488, wR2 = 0.1052	
R indices (all data)	R1 = 0.0725, wR2 = 0.1194	
Largest diff. peak and hole	0.359 and -0.321 $e.Å^{-3}$	

Table 2. Atomic coordinates (x 10^4) and equivalent isotropic displacement parameters ($Å^2$x 10^3) for jamluka288 (**3.133**). U(eq) is defined as one third of the trace of the orthogonalised U^{ij} tensor.

	x	y	z	U(eq)
S(1)	-2735(1)	1475(1)	-185(1)	25(1)
F(1)	-696(1)	680(1)	832(1)	52(1)
F(2)	-1848(1)	-12(1)	-644(1)	48(1)
F(3)	-959(1)	1161(1)	-876(1)	45(1)
O(1)	4014(1)	3505(1)	319(1)	29(1)
O(2)	4801(1)	4231(1)	-831(1)	27(1)
O(3)	-3245(1)	934(1)	470(1)	41(1)
O(4)	-2165(1)	2275(1)	386(1)	39(1)
O(5)	-3450(1)	1588(1)	-1378(1)	41(1)
N(1)	3048(1)	4667(1)	-655(1)	22(1)
N(2)	3284(1)	5199(1)	1579(1)	20(1)
C(1)	1974(2)	4228(1)	-680(2)	22(1)
C(2)	1340(2)	3775(2)	-1663(2)	29(1)
C(3)	318(2)	3291(2)	-1748(2)	32(1)
C(4)	-47(2)	3278(2)	-831(2)	29(1)
C(5)	556(2)	3759(1)	188(2)	23(1)
C(6)	1603(2)	4250(1)	290(2)	20(1)
C(7)	2166(2)	4703(1)	1354(2)	21(1)
C(8)	1714(2)	4699(1)	2216(2)	26(1)
C(9)	682(2)	4217(2)	2091(2)	30(1)
C(10)	130(2)	3746(1)	1110(2)	27(1)
C(11)	2904(2)	5401(2)	-1483(2)	35(1)
C(12)	4032(2)	4130(1)	-438(2)	23(1)
C(13)	4867(2)	2780(2)	585(2)	38(1)
C(14)	4223(2)	1946(2)	684(2)	34(1)
C(15)	3304(3)	1691(2)	-453(2)	55(1)
C(16)	3677(2)	2036(2)	1616(2)	44(1)
C(17)	4279(2)	4834(1)	2596(2)	24(1)

C(18)	3140(2)	6184(1)	1697(2)	26(1)
C(19)	-1498(2)	795(2)	-218(2)	30(1)

Table 3. Bond lengths [Å] and angles [°] for jamluka288 (**3.133**).

S(1)-O(5)	1.4337(16)
S(1)-O(4)	1.4381(16)
S(1)-O(3)	1.4381(16)
S(1)-C(19)	1.827(2)
F(1)-C(19)	1.330(2)
F(2)-C(19)	1.328(3)
F(3)-C(19)	1.335(2)
O(1)-C(12)	1.335(2)
O(1)-C(13)	1.455(3)
O(2)-C(12)	1.208(2)
N(1)-C(12)	1.384(3)
N(1)-C(1)	1.451(2)
N(1)-C(11)	1.474(3)
N(2)-C(7)	1.483(2)
N(2)-C(18)	1.501(3)
N(2)-C(17)	1.502(2)
N(2)-H(1N)	0.87(2)
C(1)-C(2)	1.368(3)
C(1)-C(6)	1.431(3)
C(2)-C(3)	1.407(3)
C(2)-H(2)	0.9500
C(3)-C(4)	1.363(3)
C(3)-H(3)	0.9500
C(4)-C(5)	1.413(3)
C(4)-H(4)	0.9500
C(5)-C(10)	1.416(3)
C(5)-C(6)	1.434(3)
C(6)-C(7)	1.425(3)
C(7)-C(8)	1.368(3)
C(8)-C(9)	1.405(3)
C(8)-H(8)	0.9500
C(9)-C(10)	1.360(3)
C(9)-H(9)	0.9500
C(10)-H(10)	0.9500
C(11)-H(11A)	0.9800
C(11)-H(11B)	0.9800
C(11)-H(11C)	0.9800
C(13)-C(14)	1.505(3)
C(13)-H(13A)	0.9900
C(13)-H(13B)	0.9900
C(14)-C(15)	1.501(3)
C(14)-C(16)	1.533(3)
C(14)-H(14)	1.0000
C(15)-H(15A)	0.9800
C(15)-H(15B)	0.9800
C(15)-H(15C)	0.9800
C(16)-H(16A)	0.9800
C(16)-H(16B)	0.9800
C(16)-H(16C)	0.9800
C(17)-H(17A)	0.9800
C(17)-H(17B)	0.9800
C(17)-H(17C)	0.9800
C(18)-H(18A)	0.9800
C(18)-H(18B)	0.9800
C(18)-H(18C)	0.9800
O(5)-S(1)-O(4)	114.64(10)
O(5)-S(1)-O(3)	115.37(10)
O(4)-S(1)-O(3)	114.85(11)
O(5)-S(1)-C(19)	103.83(10)
O(4)-S(1)-C(19)	102.98(10)
O(3)-S(1)-C(19)	102.77(10)
C(12)-O(1)-C(13)	119.65(16)
C(12)-N(1)-C(1)	116.39(16)
C(12)-N(1)-C(11)	116.74(16)
C(1)-N(1)-C(11)	116.34(16)
C(7)-N(2)-C(18)	112.45(15)
C(7)-N(2)-C(17)	112.29(15)
C(18)-N(2)-C(17)	111.34(16)
C(7)-N(2)-H(1N)	107.8(14)
C(18)-N(2)-H(1N)	107.0(14)
C(17)-N(2)-H(1N)	105.5(14)
C(2)-C(1)-C(6)	121.15(18)
C(2)-C(1)-N(1)	117.28(17)
C(6)-C(1)-N(1)	121.56(17)
C(1)-C(2)-C(3)	121.46(19)
C(1)-C(2)-H(2)	119.3
C(3)-C(2)-H(2)	119.3
C(4)-C(3)-C(2)	119.1(2)
C(4)-C(3)-H(3)	120.4
C(2)-C(3)-H(3)	120.4
C(3)-C(4)-C(5)	121.5(2)
C(3)-C(4)-H(4)	119.2
C(5)-C(4)-H(4)	119.2
C(4)-C(5)-C(10)	119.75(18)
C(4)-C(5)-C(6)	119.96(18)
C(10)-C(5)-C(6)	120.29(18)
C(7)-C(6)-C(1)	127.08(17)
C(7)-C(6)-C(5)	116.17(17)
C(1)-C(6)-C(5)	116.75(17)
C(8)-C(7)-C(6)	122.16(18)
C(8)-C(7)-N(2)	116.82(18)
C(6)-C(7)-N(2)	121.02(16)
C(7)-C(8)-C(9)	120.49(19)
C(7)-C(8)-H(8)	119.8
C(9)-C(8)-H(8)	119.8
C(10)-C(9)-C(8)	119.92(19)
C(10)-C(9)-H(9)	120.0
C(8)-C(9)-H(9)	120.0
C(9)-C(10)-C(5)	120.90(19)
C(9)-C(10)-H(10)	119.5
C(5)-C(10)-H(10)	119.5
N(1)-C(11)-H(11A)	109.5
N(1)-C(11)-H(11B)	109.5
H(11A)-C(11)-H(11B)	109.5
N(1)-C(11)-H(11C)	109.5
H(11A)-C(11)-H(11C)	109.5
H(11B)-C(11)-H(11C)	109.5
O(2)-C(12)-O(1)	125.77(19)
O(2)-C(12)-N(1)	125.75(19)
O(1)-C(12)-N(1)	108.42(16)
O(1)-C(13)-C(14)	106.98(17)
O(1)-C(13)-H(13A)	110.3
C(14)-C(13)-H(13A)	110.3
O(1)-C(13)-H(13B)	110.3
C(14)-C(13)-H(13B)	110.3
H(13A)-C(13)-H(13B)	108.6
C(15)-C(14)-C(13)	111.5(2)
C(15)-C(14)-C(16)	110.9(2)
C(13)-C(14)-C(16)	111.5(2)
C(15)-C(14)-H(14)	107.5
C(13)-C(14)-H(14)	107.5
C(16)-C(14)-H(14)	107.5
C(14)-C(15)-H(15A)	109.5
C(14)-C(15)-H(15B)	109.5
H(15A)-C(15)-H(15B)	109.5
C(14)-C(15)-H(15C)	109.5
H(15A)-C(15)-H(15C)	109.5
H(15B)-C(15)-H(15C)	109.5
C(14)-C(16)-H(16A)	109.5
C(14)-C(16)-H(16B)	109.5
H(16A)-C(16)-H(16B)	109.5
C(14)-C(16)-H(16C)	109.5
H(16A)-C(16)-H(16C)	109.5
H(16B)-C(16)-H(16C)	109.5
N(2)-C(17)-H(17A)	109.5
N(2)-C(17)-H(17B)	109.5
H(17A)-C(17)-H(17B)	109.5

N(2)-C(17)-H(17C)	109.5
H(17A)-C(17)-H(17C)	109.5
H(17B)-C(17)-H(17C)	109.5
N(2)-C(18)-H(18A)	109.5
N(2)-C(18)-H(18B)	109.5
H(18A)-C(18)-H(18B)	109.5
N(2)-C(18)-H(18C)	109.5
H(18A)-C(18)-H(18C)	109.5
H(18B)-C(18)-H(18C)	109.5
F(2)-C(19)-F(1)	106.84(19)
F(2)-C(19)-F(3)	106.70(17)
F(1)-C(19)-F(3)	107.89(18)
F(2)-C(19)-S(1)	111.82(15)
F(1)-C(19)-S(1)	111.54(15)
F(3)-C(19)-S(1)	111.78(15)

_____

Symmetry transformations used to generate equivalent atoms:

Table 4. Anisotropic displacement parameters ($Å^2 x\ 10^3$) for jamluka288 (**3.133**). The anisotropic displacement factor exponent takes the form: $-2p^2[\ h^2a^{*2}U^{11} + ... + 2\ h\ k\ a^*\ b^*\ U^{12}\ ]$

	U^{11}	U^{22}	U^{33}	U^{23}	U^{13}	U^{12}
S(1)	23(1)	29(1)	24(1)	4(1)	9(1)	0(1)
F(1)	37(1)	78(1)	35(1)	5(1)	7(1)	25(1)
F(2)	63(1)	31(1)	58(1)	-5(1)	31(1)	0(1)
F(3)	47(1)	51(1)	54(1)	2(1)	37(1)	-2(1)
O(1)	24(1)	28(1)	41(1)	11(1)	20(1)	8(1)
O(2)	24(1)	37(1)	27(1)	-1(1)	16(1)	-1(1)
O(3)	39(1)	44(1)	49(1)	17(1)	28(1)	5(1)
O(4)	36(1)	34(1)	45(1)	-11(1)	13(1)	-4(1)
O(5)	36(1)	51(1)	28(1)	6(1)	3(1)	2(1)
N(1)	19(1)	29(1)	20(1)	3(1)	9(1)	1(1)
N(2)	18(1)	25(1)	19(1)	-1(1)	10(1)	-1(1)
C(1)	15(1)	26(1)	23(1)	1(1)	6(1)	2(1)
C(2)	25(1)	39(1)	24(1)	-4(1)	9(1)	0(1)
C(3)	24(1)	36(1)	32(1)	-10(1)	5(1)	0(1)
C(4)	17(1)	29(1)	37(1)	-2(1)	7(1)	0(1)
C(5)	18(1)	24(1)	28(1)	1(1)	8(1)	2(1)
C(6)	16(1)	21(1)	22(1)	3(1)	6(1)	3(1)
C(7)	18(1)	23(1)	25(1)	3(1)	10(1)	0(1)
C(8)	25(1)	32(1)	24(1)	-2(1)	12(1)	-4(1)
C(9)	25(1)	40(1)	30(1)	2(1)	17(1)	-2(1)
C(10)	21(1)	28(1)	36(1)	3(1)	13(1)	-3(1)
C(11)	32(1)	43(1)	27(1)	13(1)	8(1)	1(1)
C(12)	23(1)	27(1)	20(1)	-4(1)	10(1)	-2(1)
C(13)	27(1)	33(1)	60(2)	11(1)	23(1)	11(1)
C(14)	35(1)	29(1)	41(1)	7(1)	18(1)	7(1)
C(15)	79(2)	37(1)	48(2)	-7(1)	21(2)	-6(2)
C(16)	49(2)	44(1)	44(1)	11(1)	24(1)	9(1)
C(17)	20(1)	30(1)	23(1)	1(1)	8(1)	0(1)
C(18)	25(1)	23(1)	34(1)	1(1)	15(1)	2(1)
C(19)	33(1)	35(1)	27(1)	2(1)	14(1)	2(1)

Table 5. Hydrogen coordinates ($x\ 10^4$) and isotropic displacement parameters ($Å^2 x\ 10^3$) for jamluka288 (**3.133**).

	x	y	z	U(eq)
H(2)	1594	3787	-2302	35
H(3)	-111	2978	-2435	39
H(4)	-723	2937	-878	34
H(8)	2100	5025	2904	31
H(9)	371	4219	2692	35
H(10)	-550	3403	1041	33
H(11A)	3683	5611	-1442	52
H(11B)	2474	5892	-1292	52
H(11C)	2459	5188	-2264	52
H(13A)	5527	2899	1318	46
H(13B)	5193	2715	-36	46
H(14)	4815	1452	922	41
H(15A)	2661	2128	-665	83
H(15B)	2990	1100	-389	83
H(15C)	3660	1679	-1046	83
H(16A)	4279	2246	2334	66
H(16B)	3378	1456	1748	66
H(16C)	3025	2465	1363	66
H(17A)	4110	4934	3301	36
H(17B)	5016	5136	2660	36
H(17C)	4358	4193	2490	36
H(18A)	2533	6412	994	40
H(18B)	3891	6484	1815	40
H(18C)	2901	6298	2358	40
H(1N)	3500(19)	5122(14)	986(18)	22(5)

Table 6. Torsion angles [°] for jamluka288 (**3.133**).

C(12)-N(1)-C(1)-C(2)	-79.2(2)
C(11)-N(1)-C(1)-C(2)	64.5(2)
C(12)-N(1)-C(1)-C(6)	99.5(2)
C(11)-N(1)-C(1)-C(6)	-116.8(2)
C(6)-C(1)-C(2)-C(3)	-1.9(3)
N(1)-C(1)-C(2)-C(3)	176.79(19)
C(1)-C(2)-C(3)-C(4)	0.2(3)
C(2)-C(3)-C(4)-C(5)	1.9(3)
C(3)-C(4)-C(5)-C(10)	178.4(2)
C(3)-C(4)-C(5)-C(6)	-2.4(3)
C(2)-C(1)-C(6)-C(7)	-179.0(2)
N(1)-C(1)-C(6)-C(7)	2.3(3)
C(2)-C(1)-C(6)-C(5)	1.4(3)
N(1)-C(1)-C(6)-C(5)	-177.24(17)
C(4)-C(5)-C(6)-C(7)	-178.94(18)
C(10)-C(5)-C(6)-C(7)	0.3(3)
C(4)-C(5)-C(6)-C(1)	0.7(3)
C(10)-C(5)-C(6)-C(1)	179.96(18)
C(1)-C(6)-C(7)-C(8)	178.1(2)
C(5)-C(6)-C(7)-C(8)	-2.3(3)
C(1)-C(6)-C(7)-N(2)	-2.3(3)
C(5)-C(6)-C(7)-N(2)	177.27(17)
C(18)-N(2)-C(7)-C(8)	-65.8(2)
C(17)-N(2)-C(7)-C(8)	60.7(2)
C(18)-N(2)-C(7)-C(6)	114.6(2)
C(17)-N(2)-C(7)-C(6)	-118.91(19)
C(6)-C(7)-C(8)-C(9)	2.0(3)
N(2)-C(7)-C(8)-C(9)	-177.55(18)
C(7)-C(8)-C(9)-C(10)	0.3(3)
C(8)-C(9)-C(10)-C(5)	-2.3(3)
C(4)-C(5)-C(10)-C(9)	-178.8(2)
C(6)-C(5)-C(10)-C(9)	1.9(3)
C(13)-O(1)-C(12)-O(2)	-10.7(3)
C(13)-O(1)-C(12)-N(1)	172.02(18)
C(1)-N(1)-C(12)-O(2)	146.60(19)
C(11)-N(1)-C(12)-O(2)	3.0(3)
C(1)-N(1)-C(12)-O(1)	-36.1(2)
C(11)-N(1)-C(12)-O(1)	-179.65(17)
C(12)-O(1)-C(13)-C(14)	-140.26(19)
O(1)-C(13)-C(14)-C(15)	66.3(3)
O(1)-C(13)-C(14)-C(16)	-58.3(3)
O(5)-S(1)-C(19)-F(2)	-64.99(17)
O(4)-S(1)-C(19)-F(2)	175.18(15)
O(3)-S(1)-C(19)-F(2)	55.55(17)
O(5)-S(1)-C(19)-F(1)	175.44(16)
O(4)-S(1)-C(19)-F(1)	55.62(18)
O(3)-S(1)-C(19)-F(1)	-64.01(18)
O(5)-S(1)-C(19)-F(3)	54.56(18)
O(4)-S(1)-C(19)-F(3)	-65.27(17)
O(3)-S(1)-C(19)-F(3)	175.10(15)

Symmetry transformations used to generate equivalent atoms:

Crystal structure of jamluka288 (**3.133**)

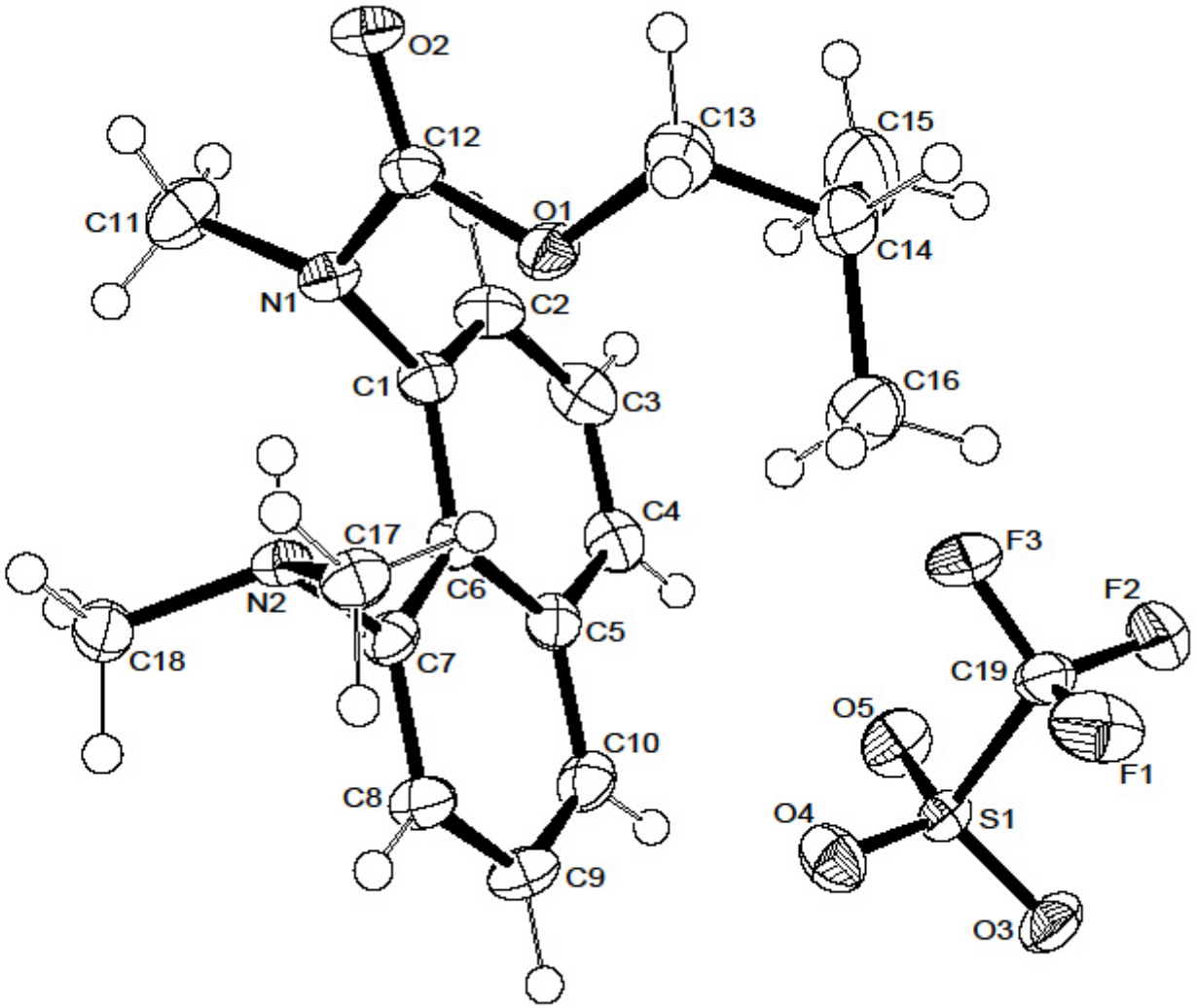

Superelectrophiles

DOI: 10.1002/ange.201202990

Superelectrophilic Amidine Dications: Dealkylation by Triflate Anion**

Luka S. Kovacevic, Christopher Idziak, Augustinas Markevicius, Callum Scullion, Michael J. Corr, Alan R. Kennedy, Tell Tuttle, and John A. Murphy**

Superelectrophilic behavior was first observed through activation of electrophiles in superacidic media,[1,2] but the existence of this type of behavior in other media is now of great interest.[2–5] Berkessel and Thauer suggested[3] that superelectrophilic activation could play a role in biology, specifically in the unusual enzymatic reduction of carbon dioxide to methane by certain methanogens.[6]

The key step in this enzymatic transformation involved the reduction of methenyltetrahydromethanopterin **1** to **2** by dihydrogen, mediated by an iron-containing hydrogenase. It was proposed that strong activation of **1** is needed within the enzyme for the hydrogenation to **2** to occur and that this would involve protonation of **1** to form a much more electrophilic species, that is, either the amidine dication **3** or **4**. It remained to be determined whether full protonation of **1** (as shown in Scheme 1) or a hydrogen-bonding interaction of **1** with an acidic group represents the necessary activation for the spontaneous hydrogenation to give **2**. Amidine dications have also been proposed as intermediates in synthetic transformations,[4,5] including the hydrolysis of amidines.[7] Salts **5** and **6**, the first fully characterized examples of amidine dications, were good methylating agents for the methylation of triethylamine **9** and had reactivity similar to dimethyl sulfate.[8] However, in a competition experiment involving a mixture of **5** and methyl triflate (MeOTf), and an amine as a nucleophile, MeOTf reacted completely and the salt **5** remained untouched, thus showing that MeOTf was the stronger methylating agent. This result is not surprising considering that the pK_a of triflic acid is -13[9] and that of $MeOSO_3H$, which is similar to that of sulfuric acid, is approximately -3,[9] thus suggesting that triflate anion is a better leaving group than the $MeOSO_3^-$ anion by a factor of approximately 10^{10}.

Herein, we report the design of amidine dications for the superelectrophilic cleavage of N–Me bonds and other N–R bonds. Methyl-transfer reactions involving MeN groups are central to life, an example being the conversion of homocysteine **11** into methionine **12**, which is a key amino acid and the precursor of *S*-adenosylmethionine **13**—the methyl-transfer agent routinely used by nature (Scheme 2).[10]

Two types of enzyme catalyze this transformation of homocysteine into methionine,[11] and the cobalamin-independent methionine synthase is the more remarkable. The

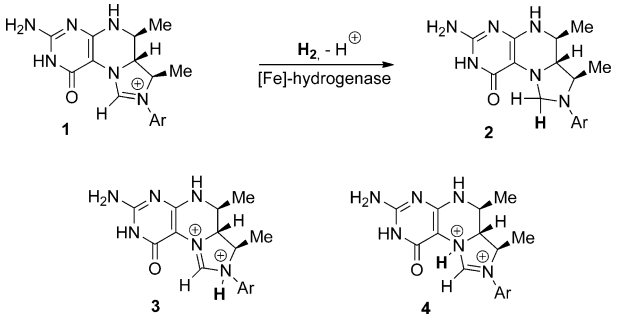

Scheme 1. Proposed amidine salts[3] in the reduction of **1** to **2**.

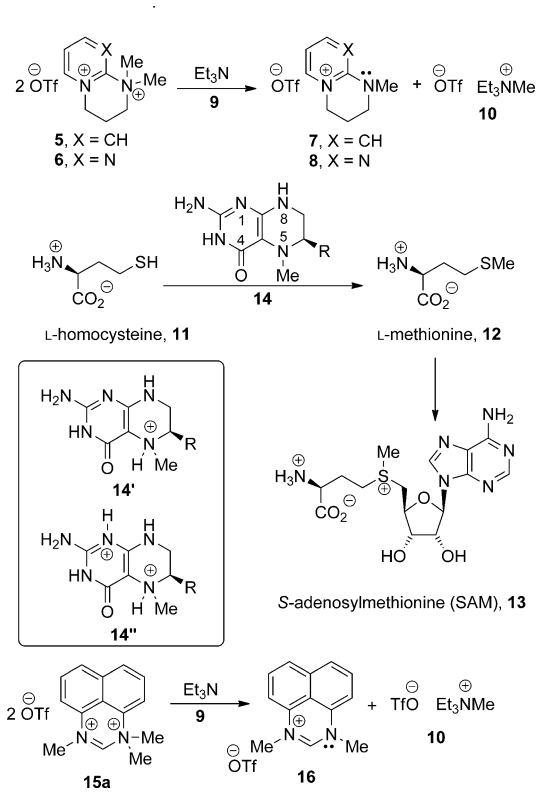

Scheme 2. Methyl-transfer reactions. Tf = trifluoromethanesulfonyl.

[*] L. S. Kovacevic, C. Idziak, A. Markevicius, C. Scullion, M. J. Corr, Dr. A. R. Kennedy, Dr. T. Tuttle, Prof. Dr. J. A. Murphy
WestCHEM, Department of Pure and Applied Chemistry
University of Strathclyde
295 Cathedral Street, Glasgow G1 1XL (United Kingdom)
E-mail: tell.tuttle@strath.ac.uk
john.murphy@strath.ac.uk

[**] We thank the EPSRC and the University of Strathclyde for funding and the EPSRC National MS Service Centre for mass spectra.

Supporting information for this article is available on the WWW under http://dx.doi.org/10.1002/anie.201202990.

methyl-transfer agent is the tetrahydrofolate **14**. An important question concerns the level of activation that could be achieved for the Me–N bond in tertiary amine **14**,[12,13] a moiety that would normally be expected to be completely unreactive to methyl transfer. The current hypothesis is that cation **14′** (a conjugate acid of **14** with protonation at N^5) is attacked by a zinc-bound thiolate of homocysteine.[13] However, double protonation, as in **14″**, might lead to significantly enhanced reactivity, thus allowing attack by thiol **11** rather than by the corresponding thiolate. But how reactive could a Me–N_{sp^3} bond be?

We envisioned that amidine dications[8] could be used for exploring the limits of synthetic, as opposed to enzymatic, activation toward alkylation.[14,15] An important driving force for the methyl transfers from **5** and **6**, may be that the demethylation reveals a nitrogen lone pair, which can delocalize over the heteroaromatic ring, in the respective products **7** and **8**. Herein, we introduce a new type of amidine dication which was designed to be more reactive in demethylation reactions (Scheme 3). Salt **15a** should undergo demethylation to afford amidinium salt **16**. The lone pair of the demethylated

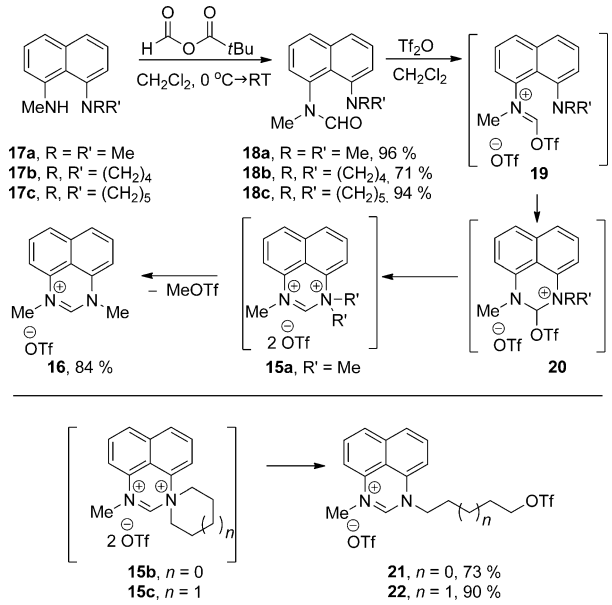

Scheme 3. Preparation and reactions of amidine dications **15**.

nitrogen atom is appropriately placed for extensive delocalization, which can be reflected in both the reaction kinetics and thermodynamics. The initial challenge was to explore the reactivity of **15**. In the preparation of target salt **15a**, formylation of **17a** afforded **18a** (Scheme 3). Treatment of the resulting formamide with triflic anhydride[15] did not give salt **15a**, but instead gave the expected product of demethylation of salt **15a**, that is, **16**, exclusively in 84% yield upon isolation. The completely selective formation of **16** and the absence of product arising from demethylation of the sp^2-hybridized nitrogen atom in **15a** supported our thinking that the electrons in the scissile C–N bond would be stabilized through their conjugation with the adjoining π system in the transition state of this reaction. To study the novel cleavage reactions further, two other substrates were prepared, the pyrrolidine **18b** and the piperidine **18c**.

If these substrates underwent analogous C–N bond cleavage reactions with triflate ion, then a product containing a triflate ester should be formed. The reaction of **18b** and **18c** with triflic anhydride in anhydrous dichloromethane again did not lead to the respective salts **15b** and **15c**, but instead gave the alkyl triflates **21** (73%) and **22** (90%) in very good yield, thus confirming the hypothesized substitution reaction involving triflate anion. These reactions must proceed by S_N2 mechanisms (see below) because the carbon atom at which substitution occurs in **15a–c** is a methylene or a methyl carbon atom and because the reactions afford a single product in high yield (no alkene resulting from elimination from **15b** and **15c** was observed). The increased reactivity of these systems, relative to **5**, is remarkable. The formation of an alkyl triflate in essentially quantitative yield, as described herein, means that the amidine cation **16** is approximately 100-fold better as a leaving group than triflate ion.[14b,c] To determine the mechanism of demethylation, we carried out a computational investigation on the reactive species outlined in Scheme 3.

The initial reaction of **18a** with triflic anhydride to form salt **19** (R = R′ = Me), which contains both a triflate substituent and a triflate counterion, was calculated as being exothermic ($\Delta G = -3.5$ kcal mol^{-1}). Calculations of the subsequent steps in the reaction show that they can occur either in the presence or in the absence of the triflate counterion (blue curve and red curve in Figure 1, respectively). The intermediate, **20**, which is formed in a facile reaction, is strongly favored thermodynamically relative to **19**. The counterion has little effect on the energetics of the step that forms intermediate **20**, which contains a tetrahedral triflate-bearing carbon atom. Calculations on a reaction involving direct abstraction of the methyl group by the sulfonyl oxygen atom of the triflate substituent *via* a 6-membered cyclic transition state derived from **20** suggest that it is not feasible. Instead, the triflate substituent spontaneously dissociates from the central carbon atom to be placed in the alignment necessary to cleave the C–N bond (see below).

However, in the subsequent step, the dissociation of the triflate moiety to form the planar dicationic species (**15a**), the counterion plays a stabilizing role; the presence of the counterion leads to a slight lowering of the barrier to dissociation as well as to a decrease in the endothermicity of the reaction to 5.8 kcal mol^{-1} (compared with 6.4 kcal mol^{-1}, which is the value calculated when no counterion is present, see Figure 1). Despite the presence of the counterion, the formation of **15a** is thermodynamically disfavored, and the reverse reaction (that is, **15a**→**20**) occurs with a very small barrier (0.5 kcal mol^{-1}). Therefore, the lifetime of **15a** is extremely short and, consistent with the experimental results, is unlikely to be observed. Conversely, the transformation of **20** into **16** is a strongly exothermic reaction (−21.9 kcal mol^{-1}) with an accessible barrier (20.9 kcal mol^{-1}; see Figure 1). For the transformation of **20** into **16**, the inclusion of the triflate counterion was found to play an important role in lowering the barrier to demethylation. However, the demethylation

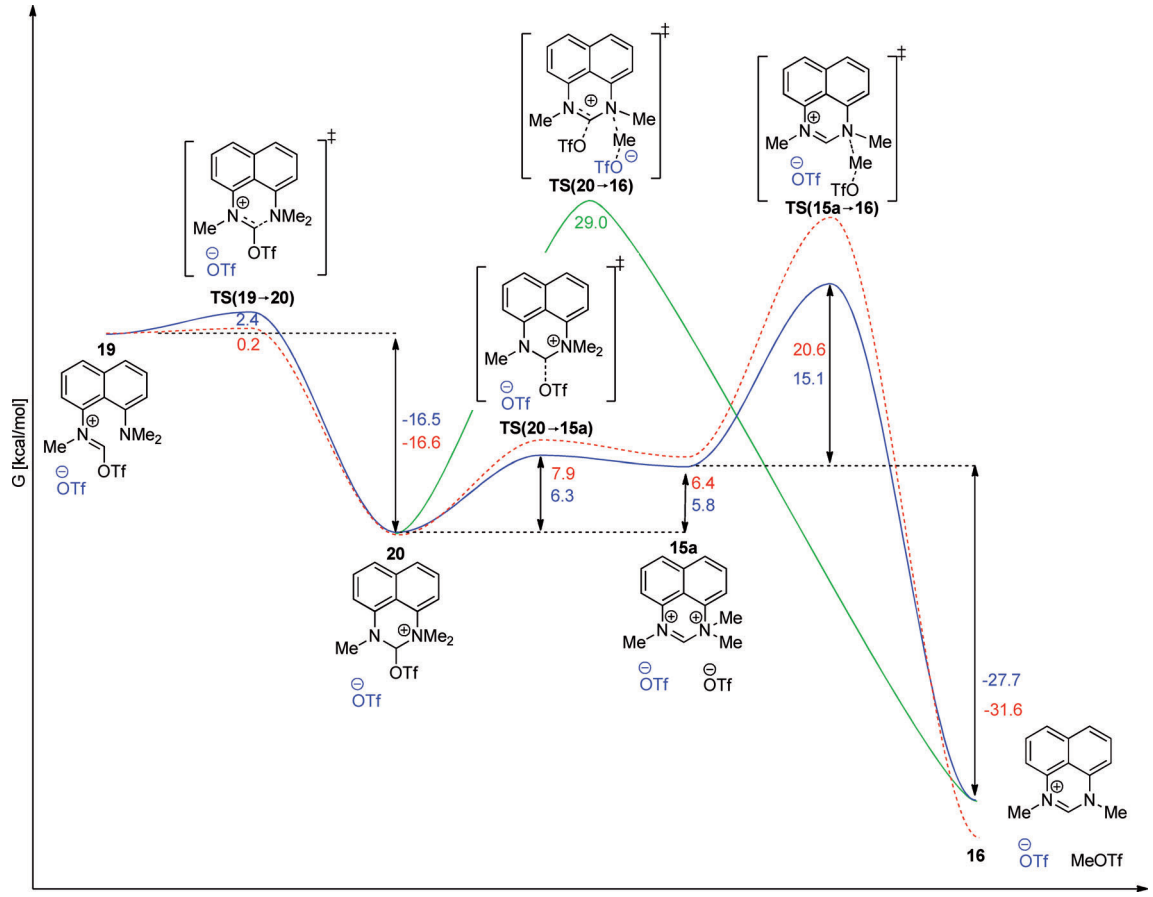

Figure 1. Free Energy (ΔG) profile for the formation of **16** from **19**, (R = Me) via the salt **15a**. Free energies are given in kcal mol^{-1}. Density functional theory (DFT) was used to characterize the respective minima (reactants, intermediates) and first order saddle points (transition states, TS's) on the potential energy surface. All structures were optimised in the solvent phase at the M06/6-311G level of theory.[16,17] The solvation model chosen for the study was the conductor-like polarizable continuum model (CPCM), using dichloromethane as the solvent. The red path corresponds to the calculated energy profile when the triflate counterion is not included in the computations, and the blue path is the energy profile with the counterion (also colored in blue) included; the green path represents a concerted E2 elimination pathway, which involves participation of both triflate moieties.

(formation of **16**) is only able to occur after the dissociation of the triflate substituent (this triflate moiety is colored in black in Figure 1) from the central tetrahedral carbon atom in **20** to form **15a** (see below). Whereas **15a** is unstable, relative to **20** or **16**, it represents a strongly bound reactant complex (ΔG = 18.2 kcal mol^{-1}) involving dissociated triflate anion for the subsequent demethylation reaction. The methyl group is then transferred to the triflate anion via a classical S_N2 transition state (Figure 2). The product **16** could also form through an alternative reaction pathway that occurs without the predissociation of the triflate substituent from **20** to form **15a**—the concerted attack of the triflate counterion (shown in blue in Figure 1) on the methyl group with a concomitant dissociation of the triflate substituent (**TS(20→16)**, green line, Figure 1], that is, an E2 reaction. The transition state for this pathway, which would lead directly to the product (**16**), was calculated and the associated activation free energy is ΔG^{*} = 29.0 kcal mol^{-1}. This barrier is too high to make the associated mechanism plausible for the formation of **16** under the experimental conditions. Moreover, the competing process—dissociation to form **15a**, followed by a subsequent S_N2

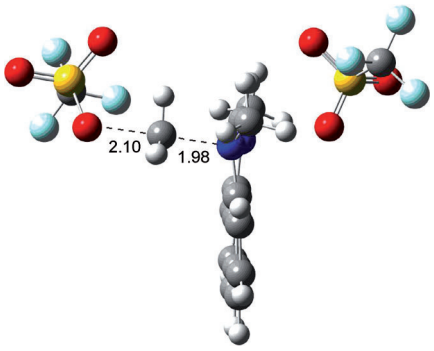

Figure 2. Geometry for **TS(15a→16)**. Distances are given in Å.

demethylation reaction to form **16**—has a significantly lower barrier and hence would be kinetically more favored (see the Supporting Information for similar results that were obtained from calculations on **18b**).

It is obvious that these amidine salts **15a–c** are extremely reactive. To demonstrate conclusively that this method, that is, reacting an amide with triflic anhydride[5] in the presence of

an amine, can lead to the isolation of a fully characterizable amidine salt and not involve dealkylative S_N2 reactions, we chose the precursor amide **23** (Scheme 4). When **23** was treated with triflic anhydride in CH_2Cl_2 it led to salt **24** being isolated in 91% yield and fully characterised by X-ray crystallography.[18]

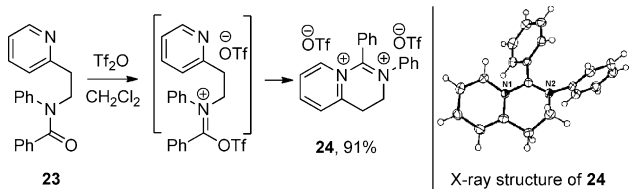

Scheme 4. Preparation of amidine salt **24**. For the crystal structure, thermal ellipsoids are shown at 50% probability.

In conclusion, we have shown that when incorporated into novel dicationic amidine salts, $C–N_{sp^3}$ bonds can be strongly activated for cleavage, to an extent where even triflate anion can act as the dealkylating nucleophile. The demonstration of this synthetic form of activation suggests that tertiary amines in other settings could be similarly activated. Substrate **14** (Scheme 2) is an interesting example, whereupon formation of salt **14″** might lead to methyl transfer. Even if salt formation does not occur, substrate **14** has numerous heteroatoms that may interact with methionine synthase through hydrogen bonds that, cumulatively, could contribute to its activation for demethylation.

Received: April 18, 2012
Revised: June 12, 2012
Published online: July 13, 2012

Keywords: cations · methionine · methyl transfer · nucleophilic substitution · superelectrophiles

[1] a) D. M. Brouwer, A. A. Kiffen, *Recl. Trav. Chim. Pays Bas* **1973**, *92*, 689; b) G. A. Olah, A. Germain, H. C. Lin, D. A. Forsyth, *J. Am. Chem. Soc.* **1975**, *97*, 2928–2929; c) G. A. Olah, *Angew. Chem.* **1993**, *105*, 805–827; *Angew. Chem. Int. Ed. Engl.* **1993**, *32*, 767–788; d) G. Rasul, G. K. Surya Prakash, G. A. Olah, *J. Org. Chem.* **1994**, *59*, 2552–2556.

[2] a) G. A. Olah, D. A. Klumpp, *Superelectrophiles and Their Chemistry*, Wiley, Hoboken, NJ, **2008**; b) D. A. Klumpp, *Beilstein J. Org. Chem.* **2011**, *7*, 346–363.

[3] A. Berkessel, R. K. Thauer, *Angew. Chem.* **1995**, *107*, 2418–2421; *Angew. Chem. Int. Ed. Engl.* **1995**, *34*, 2247–2250. At the time of the proposal, the enzyme was thought to be free of redox-active metal. Recent findings (Ref. [6]) show the presence of iron in a unique cofactor, but activation of **1** is still required to form **2**.

[4] a) M. G. Banwell, B. D. Bissett, S. Busato, C. J. Cowden, D. C. R. Hockless, J. W. Holman, R. W. Read, A. W. Wu, *J. Chem. Soc. Chem. Commun.* **1995**, 2551–2553; b) A. B. Charette, P. Chua, *Tetrahedron Lett.* **1997**, *38*, 8499–8502; c) A. B. Charette, P. Chua, *Synlett* **1998**, 163; d) A. B. Charette, P. Chua, *J. Org. Chem.* **1998**, *63*, 908–909; e) A. Yokoyama, T. Ohwada, K. Shudo, *J. Org. Chem.* **1999**, *64*, 611–617; f) A. B. Charette, S. Mathieu, J. Martel, *Org. Lett.* **2005**, *7*, 5401–5404; g) M. Movassaghi, M. D. Hill, *J. Am. Chem. Soc.* **2006**, *128*, 14254–14255; h) M. Movassaghi, M. D. Hill, *J. Am. Chem. Soc.* **2006**, *128*, 4592–4593; i) M. Movassaghi, M. D. Hill, O. K. Ahmad, *J. Am. Chem. Soc.* **2007**, *129*, 10096–10097; j) S. L. Cui, J. Wang, Y.-G. Wang, *J. Am. Chem. Soc.* **2008**, *130*, 13526–13527; k) E. L. Zins, P. Milko, D. Schroeder, J. Aysina, D. Ascenzi, J. Zabka, C. Alcaraz, S. D. Price, J. Roithova, *Chem. Eur. J.* **2011**, *17*, 4012–4020.

[5] A. B. Charette, M. Grenon, *Can. J. Chem.* **2001**, *79*, 1694–1703 showed formation of an amidine salt, but it could not be isolated.

[6] For reviews, see a) M. J. Corr, J. A. Murphy, *Chem. Soc. Rev.* **2011**, *40*, 2279–2292; b) S. Shima, U. Ermler, *Eur. J. Inorg. Chem.* **2011**, 963–972.

[7] a) M. W. Anderson, R. C. F. Jones, J. Saunders, *J. Chem. Soc. Perkin Trans. 1* **1986**, 205–209; b) S. Limatibul, J. W. Watson, *J. Org. Chem.* **1971**, *36*, 3803–3804.

[8] a) M. J. Corr, K. F. Gibson, A. R. Kennedy, J. A. Murphy, *J. Am. Chem. Soc.* **2009**, *131*, 9174–9175; b) M. J. Corr, M. Roydhouse, K. F. Gibson, S.-Z. Zhou, A. R. Kennedy, J. A. Murphy, *J. Am. Chem. Soc.* **2009**, *131*, 17980–17985.

[9] *Ionization Constants of Organic Acids in Solution* (Eds.: E. P. Serjeant, B. Dempsey), IUPAC Chemical Data Series No. 23, Oxford, **1979**.

[10] *DNA Methylation: Basic Mechanisms* (Eds.: W. Doerfler, P. Böhm), Springer, Berlin, **2006**.

[11] a) R. G. Matthews, *Acc. Chem. Res.* **2001**, *34*, 681–699; b) R. G. Matthews in *Chemistry and Biochemistry of B_{12}* (Ed.: R. Bannerjee), Wiley, New York, **1999**, pp. 681–706.

[12] R. E. Taurog, R. G. Matthews, *Biochemistry* **2006**, *45*, 5092–5102.

[13] a) B. P. Callahan, R. Wolfenden, *J. Am. Chem. Soc.* **2003**, *125*, 310–311; b) E. Hilhorst, T. B. R. A. Chen, A. S. Iskander, U. K. Pandit, *Tetrahedron* **1994**, *50*, 7837–7848.

[14] For alternative extremely reactive alkylating agents, see: a) T. Kato, E. Stoyanov, J. Geier, H. Grützmacher, C. A. Reed, *J. Am. Chem. Soc.* **2004**, *126*, 12451–12457. b) H. Shima, R. Kobayashi, T. Nabeshima, N. Furukawa, *Tetrahedron Lett.* **1996**, *37*, 667–670; c) H. Naka, T. Maruyama, S. Sato, N. Furukawa *Tetrahedron Lett.* **1999**, *40*, 345–348.

[15] Alternative amine dealkylations, a) B. H. Wolfe, A. H. Libby, R. S. Alawar, C. J. Foti, D. L. Comins, *J. Org. Chem.* **2010**, *75*, 8564–8570; b) J. H. Cooley, E. J. Evain, *Synthesis* **1989**, 1–7; c) H. A. Hageman, *Org. React.* **1953**, *7*, 198; d) J. von Braun, *Chem. Ber.* **1900**, *33*, 1438.

[16] Y. Zhao, D. G. Truhlar, *Theor. Chem. Acc.* **2008**, *120*, 215–241.

[17] W. J. Hehre, R. Ditchfield, J. A. Pople, *J. Chem. Phys.* **1972**, *56*, 2257–2261.

[18] CCDC 881667 (**24**) contains the supplementary crystallographic data for this paper. These data can be obtained free of charge from The Cambridge Crystallographic Data Centre via www.ccdc.cam.ac.uk/data_request/cif.

